

ADVERTIMENT. L'accés als continguts d'aquesta tesi queda condicionat a l'acceptació de les condicions d'ús estableties per la següent llicència Creative Commons:  http://cat.creativecommons.org/?page_id=184

ADVERTENCIA. El acceso a los contenidos de esta tesis queda condicionado a la aceptación de las condiciones de uso establecidas por la siguiente licencia Creative Commons:  <http://es.creativecommons.org/blog/licencias/>

WARNING. The access to the contents of this doctoral thesis it is limited to the acceptance of the use conditions set by the following Creative Commons license:  <https://creativecommons.org/licenses/?lang=en>



Departament de Pediatria, d'Obstetrícia i Ginecologia, i Medicina Preventiva i Salut Pública

Facultat de Medicina

Universitat Autònoma de Barcelona

Diagnòstic dels trastorns genètics de la substància blanca cerebral i identificació de noves malalties mitjançant tècniques de seqüenciació massiva

Tesi doctoral

Agustí Rodríguez-Palmero Seuma

Per optar al grau de Doctor en Medicina per la Universitat Autònoma de Barcelona

Directors: Dra. Aurora Pujol Onofre

Dr. Alfons Macaya Ruiz

Dr. Guillem Pintos Morell (del 24.01.2017 fins al 21.09.2020)

Tutor: Dr. Alfons Macaya Ruiz

Febrer 2022

A vosaltres, Pau i Èlia, que m'ompliu de felicitat i m'impulseu
dia a dia per intentar ser millor

A tu, Laia, que m'acompanyes en aquest viatge

Ítaca (Konstantino Kavafis)

Quan surts per fer el viatge cap a Ítaca,
has de pregar que el camí sigui llarg,
ple d'aventures, ple de coneixences.

Els Lestrígons i els Cíclops,
l'aïrat Posidó, no te n'esfereixis:
són coses que en el teu camí no trobaràs,
no, mai, si el pensament se't manté alt, si una
emoció escollida
et toca l'esperit i el cos alhora.

Els Lestrígons i els Cíclops,
el feroç Posidó, mai no serà que els topis
si no els portes amb tu dins la teva ànima,
si no és la teva ànima que els dreça davant teu.

Has de pregar que el camí sigui llarg.
Que siguin moltes les matinades d'estiu
que, amb quina delectança, amb quina joia!
entraràs en un port que els teus ulls ignoraven;
que et puguis aturar en mercats fenicis
i comprar-hi les bones coses que s'hi exhibeixen,
corals i nacres, mabres i banussos
i delicats perfums de tota mena:
tanta abundor com puguis de perfums delicats;
que vagis a ciutats d'Egipte, a moltes,
per aprendre i aprendre dels que saben.

Sempre tingues al cor la idea d'Ítaca.
Has d'arribar-hi, és el teu destí.
Però no forcis gens la travessia.
És preferible que duri molts anys
i que ja siguis vell quan fondegis a l'illa,
ric de tot el que hauràs guanyat fent el camí,
sense esperar que t'hagi de dar riqueses Ítaca.

Ítaca t'ha donat el bell viatge.
Sense ella no hauries pas sortit cap a fer-lo.
Res més no té que et pugui ja donar.

I si la trobes pobra, no és que Ítaca t'hagi enganyat.
Savi com bé t'has fet, amb tanta experiència,
ja hauràs pogut comprendre què volen dir les Ítaques.

ÍNDEX

ÍNDEX DE FIGURES I TAULES	6
ACRÒNIMS I ABREVIATURES	8
AGRAÏMENTS	10
RESUM	15
SUMMARY	19
I. INTRODUCCIÓ	23
1. Introducció Històrica	24
2. Biologia de la mielina	31
2.1 Els oligodendròcits (ODs) i el procés de mielinització	33
2.2 Suport energètic en el metabolisme axonal	40
3. Definició: trastorns genètics de la substància blanca cerebral (GWMDs)	41
4. Generalitats dels trastorns genètics de la substància blanca cerebral (GWMDs)	44
4.1 Formes clíniques de presentació	44
4.2 Classificació dels GWMDs.....	46
4.3 Tractament dels GWMDs.....	48
5. El diagnòstic dels GWMDs	52
5.1 Estudis de Neuroimatge.....	53
5.2 Estudis genètics en el procés diagnòstic dels GWMDs	58
II. JUSTIFICACIÓ I HIPÒTESI	69
III. OBJECTIUS.....	71
IV. MATERIAL I MÈTODES	73
1. Reclutament de pacients	74
2. Seqüenciació dels exomes, captura i classificació de les variants	75
3. Mètode de priorització basat en l'Interactoma	76
4. Anàlisi dels resultats dels estudis WES/WGS	78

V. RESULTATS.....	79
Article 1. Diagnosis of genetic white matter disorders by singleton whole-exome and genome sequencing using interactome-driven prioritization	80
Article 2. Biallelic <i>PI4KA</i> variants cause a novel neurodevelopmental síndrome with hypomyelinating leukodystrophy.....	139
Article 3. <i>DLG4</i> -related synaptopathy: a new rare brain disorder	167
VI. DISCUSSIÓ.....	189
1. Elevat rendiment diagnòstic mitjançant l'estudi de casos índex.....	191
2. Escurçament de temps per obtenir un diagnòstic genètic.....	200
3. Implicacions del diagnòstic en el maneig dels pacients	200
4. Identificació de nous gens associats a GWMDs, descripció de noves malalties	201
5. Descripció de nous fenotips, diagnòstic de formes atípiques, malalties ultra rares o de molt recent descripció i fenotips complexos	205
6. Proposta de protocol d'estudi dels GWMDs.....	209
7. Limitacions del treball	212
8. El futur dels trastorns genètics de la substància blanca cerebral	212
VII. CONCLUSIONS	216
VIII. BIBLIOGRAFIA.....	220
IX. ANNEX. Altres publicacions amb participació del doctorand fruit del present treball .	240
Altres publicacions de nous gens identificats en aquest projecte	241
Article A1. Bi-allelic variants in the mitochondrial RNase P subunit <i>PRORP</i> cause mitochondrial tRNA processing defects and pleiotropic multisystem presentations	241
Article A2. Impairment of the mitochondrial one-carbon metabolism enzyme <i>SHMT2</i> causes a novel brain and heart developmental syndrome	241
Altres publicacions de nous fenotips identificats en aquest projecte	242
Article A3. <i>POLR3A</i> variants with striatal involvement and extrapyramidal movement disorder.....	242
Article A4. <i>HNRNPH1</i> -related syndromic intellectual disability: Seven additional cases suggestive of a distinct syndromic neurodevelopmental syndrome.....	242
Publicació de validació funcional d'una variant intrònica	243
Article A5. A novel hypomorphic splice variant in <i>EIF2B5</i> gene is associated with mild ovarioleukodystrophy	243

ÍNDEX DE FIGURES I TAULES

Figura 1. Il·lustracions de Golgi i Cajal, de preparacions histològiques tenyides amb els mètodes de l'època	27
Figura 2. Pío del Río-Hortega, descobridor del “tercer element”: els oligodendròcits i la micròglia.....	28
Figura 3. Pío del Río Hortega. Il·lustracions del còrtex i substància blanca cerebrals, tenyits amb el procediment del carbonat de plata d'Hortega	28
Figura 4. Procés normal de mielinització en els primers dos anys de vida	30
Figura 5. Procés de formació de l'embolcall de mielina i disposició dels oligodendròcits en relació amb els axons, els astròcits i capil·lars vasculars.....	35
Figura 6. Factors implicats en el procés de mielinització	37
Figura 7. Representació de possibles mecanismes que relacionen l'activitat axonal amb el procés de mielinització	38
Figura 8. Imatge esquemàtica de l'acoblament metabòlic de les cèl·lules glials i l'axó	41
Figura 9. Tractament amb HSCT en pacients amb leucodistròfia metacromàtica (MLD)	50
Figura 10. Distribució de l'affectació de la substància blanca i característiques particulars d'alguns dels principals GWMDs.....	57
Figura 11. Taxa diagnòstica del WES en diferents grups de patologies	67
Figura 12. Mètode de priorització de variants basat en l'interactoma.....	77
Figura 13. Protocol diagnòstic utilitzat per l'estudi de la cohort de pacients amb GWMDs	78

Taula 1. Principals estudis publicats de cohorts de pacients estudiades mitjançant WES/WGS	196
Figura 14. Família reportada en la descripció d'una nova malaltia mitocondrial multisistèmica associada a variants patogèniques en el gen <i>PRORP</i>	204
Figura 15. Estudi de RM d'un dels casos amb variants patogèniques a <i>DEGS1</i>	205
Figura 16. Imatges de RM cranial del pacient amb afectació predominant estriatal i variants patogèniques en el gen <i>POLR3A</i>	206
Figura 17. Estudi de RM d'alguns pacients identificats amb malalties que rarament associen una afectació de substància blanca i ultra rares	208
Figura 18. Proposta d'algoritme diagnòstic dels GWMDs en el nostre entorn	211

ACRÒNIMS I ABREVIATURES

ACMG	<i>American College of Medical Genetics and Genomics</i>
AGS	<i>Aicardi-Goutières Syndrome</i>
AxD	<i>Alexander Disease</i>
CMA	<i>Chromosomal microarray</i>
CNV	<i>Copy Number Variant</i>
ELA	Asociación Española contra la Leucodistrofia
GWMD	<i>Genetic White Matter Disorders</i>
HDLS	<i>Hereditary Diffuse Leukoencephalopathy with axonal Spheroids</i>
HEMS	<i>Hypomyelination of Early Myelinating Structures</i>
HSCT	<i>Haematopoietic Stem-cell Transplantation</i>
H-ABC	Hypomyelination with Atrophy of the Basal Ganglia and Cerebellum
IPP	Interaccions proteïna-proteïna
iPSC	Cèl·lules mare pluripotents induïdes
JAK	Janus Kinase
KD	<i>Krabbe disease</i>
LBSL	<i>Leukodystrophy with Brain stem and Spinal cord involvement and Lactate elevation</i>
LBTL	<i>Leukodystrophy with Brain stem and Thalamus involvement and Lactate elevation</i>
LP (variant)	<i>Likely Pathogenic</i>
MLC	<i>Megalencephalic Leukodystrophy with subcortical Cysts</i>
NGS	<i>Next-generation Sequencing</i>

NDD	<i>Neurodevelopmental Disorders</i>
P (variant)	<i>Pathogenic</i>
PEATs	Potencials Evocats Auditius de Tronc
PEVs	Potencials Evocats Visuals
PI	Fosfatidilinositols
RM	Ressonància Magnètica
RNASET2	<i>RNAse T2-deficient leukoencephalopathy</i>
SNC	Sistema Nerviós Central
SNP	Sistema Nerviós Perifèric
SNV	<i>Single Nucleotide Variant</i>
TC	Tomografia Computada
TDAH	Trastorn per Dèficit d'Atenció amb Hiperactivitat
TEA	Trastorn de l'Espectre Autista
TND	Trastorn del neurodesenvolupament
VUS (variant)	<i>Variant of Unknown Significance</i>
VWMD	<i>Vanishing White Matter Disease</i>
WES	<i>Whole Exome Sequencing</i>
WGS	<i>Whole Genome Sequencing</i>
X-ALD	<i>X-linked Adrenoleukodystrophy</i>

AGRAÏMENTS

Aquesta tesi doctoral és fruit de la col·laboració d'un gran nombre de professionals de diversa índole: metges, biòlegs, bioinformàtics, bioquímics, tècnics de laboratori, assessors genètics, infermeres i administratius, entre d'altres. Sense la vostra aportació, mai no hauríem pogut aconseguir els resultats obtinguts en els diferents treballs aquí presentats. Per tant, no puc deixar d'agrair-vos la vostra participació i compromís.

En primer lloc, voldria agrair a la Dra. Aurora Pujol, codirectora d'aquesta tesi doctoral i directora del laboratori de malalties Neurometabòliques de l'Institut d'Investigació Biomèdica de Bellvitge (IDIBELL), la confiança depositada en mi en acollir-me en el seu grup d'investigació i permetre'm formar part d'aquest viatge. Ella és la persona que ha liderat i coordinat el projecte del qual aquesta tesi en forma part, a més dels estudis que se n'han derivat. Gràcies per permetre'm participar en aquest treball, per introduir-me en el camp de la genòmica i sobretot per ajudar-me a entendre el paper fonamental que juguem els clínics en el procés diagnòstic basat en els estudis genòmics. Gràcies per haver estat una font d'inspiració, per haver-me guiat durant aquest procés i haver-me encoratjat a seguir endavant des del primer moment. També agrair la teva exigència sempre, que considero imprescindible per haver pogut arribar fins aquí.

Agrair també l'ajuda que m'han donat sempre tots els professionals del laboratori de malalties Neurometabòliques d'IDIBELL. Em vau acollir molt bé des d'un principi i m'heu fet sentir un més, tot i les dificultats que representa integrar-se com a clínic en un equip format per professionals de ciències bàsiques. Gràcies, Edgard i Àgatha, per la paciència infinita que heu demostrat a l'hora d'aclarir-me conceptes genètics, per la inspiració, per la vostra disponibilitat sempre, per la vostra inestimable col·laboració en tots els treballs recollits en aquesta tesi i per la revisió final d'aquesta. També pel que he après de vosaltres a nivell humà. Gràcies a la Montse per haver-me ajudat en tot el que he necessitat durant aquests anys, per fer-me costat i per la valuosa feina de coordinació. Sense la teva tasca, tot això no hauria funcionat! Gràcies també a la resta de l'equip del laboratori: Stéphane, Nathalie,

Valentina, Laura, Leire, Cris, Juanjo... Heu estat sempre generosos, propers i heu demostrat tots una gran professionalitat, fent un paper fonamental cadascú des de la vostra expertesa, el que permet que l'engranatge del laboratori funcioni i resulti en estudis de gran qualitat científica. Gràcies per explicar-me el que és una poyata, una *pipeline* informàtica o el pLI. Suerte Valentina con tu tesis, que ha avanzado en paralelo con ésta, y también en lo que venga después! Carlos... gràcies pel teu bon humor sempre. Espero que ens puguem seguir reunint per gaudir d'esmorzars o dinars-berenars amb qualsevol excusa en el futur, i preferiblement sense mascaretes!

En segon lloc, vull agrair a l'Alfons Macaya, també codirector d'aquesta tesi i cap de secció de Neuropediatria de l'hospital de la Vall d'Hebrón. És la persona que va pensar en mi per aquest projecte, després que li hagués expressat el meu interès per fer recerca i la possibilitat de fer la tesi doctoral, ¡Contigo empezó todo!. Sempre he pensat que ets un model de neuropediatre a seguir, per l'equilibri que has aconseguit entre la tasca assistencial i el lideratge d'un grup de recerca. També per les qualitats personals, les que demostres amb els pacients i també amb els companys de professió. Igualment gràcies per la teva inestimable orientació, participació i revisió de les publicacions principals d'aquesta tesi. Per altra banda, agrair la formació que em vàreu proporcionar ja fa uns anys, juntament amb el Dr. Roig i la resta de l'equip de neuropediatria de la Vall d'Hebron (Mireia, Miquel, Susana) un cop finalitzada la meva residència de pediatria. Aquells anys vaig aprendre el que sé de neurologia pediàtrica, però també una forma de treballar i com gaudir d'aquesta branca de la pediatria tan especial. També un agraïment a l'Eli Vázquez, neuroradiòloga de l'Hospital Vall d'Hebron, que ha revisat els estudis de resonància d'una bona part dels pacients inclosos en aquesta tesi.

Agrair també al tercer codirector d'aquesta tesi, fins a la seva jubilació, el Dr. Guillem Pintos. Tu vas ser qui em va transmetre, des de la meva arribada com a resident a l'Hospital Germans Trias i Pujol, la passió pel camp de les "malalties rares". Gràcies pels consells, per l'estímul continu i per la teva proximitat.

Naturalment, un agraïment (i també una disculpa) per la meva família més propera: els meus fills Pau i Èlia i la meva dona Laia. Per tots aquells moments en els quals no he pogut estar al

100% amb vosaltres, Pau i Èlia, donada la manca crònica de son que he patit en els darrers cinc anys. Per les vegades que m'he adormit explicant-vos un conte al vespre o m'he vist forçat a fer una “breu” becaina després de dinar mentre miràvem alguna pel·lícula de dibuixos animats. També evidentment a tu, Laia, a qui he robat temps d'estar junts massa sovint en els darrers mesos, i que has hagut de suportar-me en moments de certs nervis, mal humor i també desencís.

Als meus pares, que van marxar massa aviat, i a qui sovint trobo a faltar. Ells van ser un gran exemple de bondat, ètica, esforç i, ben segur, els primers responsables de què hagi arribat fins aquí. També per descomptat als meus germans, que han fet de model on emmirallarm-me per la meva condició de germà petit. Heu estat sempre els meus referents, millors consellers i un exemple de treball i superació. Ah! I gràcies també a vosaltres per haver revisat aquest document.

Als meus amics, els de sempre del Col·legi Claver, alguns dels quals m'han fet companyia des dels inicis d'escola primària. Tot i la distància i la manca de contacte en algunes èpoques, sempre us tinc ben presents. També als que han vingut després, els de la facultat de Medicina de la UdL, amb els que hem passat molts bons moments des que ens vam anar coneixent a la biblioteca. Sempre és un plaer compartir rialles amb vosaltres. Sou genials.

Als meus companys de feina del Servei de Pediatria de l'Hospital Germans Trias i Pujol, els que hi són actualment i els que hi han passat. Són molts anys els que hem compartit i us heu convertit en la meva “família laboral”. A les meves companyes de la unitat de Neurologia Pediàtrica: Laura, Elisenda i Elena, amb qui fem un equip fantàstic. A la Núria de consultes, pel seu paper d'infermera, gestora de cas, psicòloga i quasi-mare en alguns moments. Els teus consells sempre ajuden (i els moments de riure també, clar!). A les secretàries de consultes, per la paciència a l'hora de gestionar les agendes, recordatoris i bona predisposició a ajudar-me sempre en el que ha estat necessari. També en general a tot el personal de l'hospital, que facilita d'una manera o altra la meva feina i fa el dia a dia més amable.

Agrair també a totes aquelles persones que en un moment o altre m'han inspirat, m'han estimulat a seguir endavant i han participat d'alguna manera en la meva formació personal

o com a neuropediatre. Entre ells, especial menció al Dr. Esquerda i la Dra. Anna M^a Casanovas, responsables de l'assignatura de Neurobiologia allà per l'any 1995 a la Universitat de Lleida (UdL). Recordo gaudir-la enormement, i ara crec que amb vosaltres va començar el meu interès per l'aprenentatge d'aquest òrgan tan fonamental, com complex i inabordable, que és el cervell.

Aquesta tesi és fruit de cinc anys de feina intensa, que he mirat de compaginar de la millor manera amb l'activitat amb els pacients a l'hospital i la vida familiar, que s'ha "complicat" en els darrers anys. No ha estat fàcil, però crec que l'esforç ha valgut la pena i aquest ha estat un procés d'aquells que deixen empremta per tota la vida. M'ha permès créixer des del punt de vista professional i introduir-me en el món de la investigació, que ha mantingut desperta la meva curiositat durant aquests anys i al que espero poder seguir dedicant un temps a partir d'ara.

Aquest treball és un exemple més de la importància de la col·laboració entre diferents hospitals i centres de recerca, tant en l'àmbit nacional com internacional. El món tecnològic actual facilita enormement aquesta tasca i ofereix un ventall de possibilitats que són imprescindibles per aconseguir un avenç en el coneixement, sobretot en el camp de les malalties rares. Així, no vull oblidar-me dels professionals que han col·laborat en aquest projecte enviant les dades clíniques, estudis de neuroimatge, mostres dels pacients i també intercanviant informació i impressions en múltiples ocasions. Són un nombrós grup de metges que pertanyen als següents centres hospitalaris: H. Vall d'Hebrón, H. Universitario de Donostia, H. Niño Jesús, H. Sant Joan de Déu, H. Bellvitge, Complejo Hospitalario de Navarra, Hospital Clínico San Borja Arriarán (Chile), Complejo asistencial Universitario de Burgos, H. Germans Trias i Pujol, Institut de Bioquímica Clínica, H. Universitario Lucus Augusti, H. Universitario Fundación de Alcorcón, H. Universitario Basurto, H. Prof. Dr. Juan P. Garrahan (Argentina), Kennedy Krieger Institute, H Universitario de Guadalajara, H La Fe, H. Virgen de la Arrixaca, H. Marqués de Valdecilla, H. Virgen de la Macarena, H. Universitario Río Hortega, H. Gregorio Marañón, H. Puerta de Hierro, H. Infanta Cristina, H. Reina Sofía de Córdoba, H. Virgen de la Luz, H. Can Misses. També els col·laboradors d'arreu del món que han participat en els Articles 2 i 3 d'aquesta tesi, i en els altres treballs publicats durant aquests anys en el context d'aquest projecte.

També un agraïment per les organitzacions que han permès el finançament d'aquest projecte i tants altres: CIBERER: ACCI14-759 i ACCI19-759, URDCat program: PERIS SLT002/16/00174, La Marató de TV3: 345/C/2014, Fondo de Investigación Sanitaria: FIS PI14/00581 i Hesperia Foundation.

Per últim, un agraïment especial pels pacients i les famílies. Sou els protagonistes principals d'aquesta història, aquells que patiu trastorns que sovint resulten massa durs i a qui mirem d'aportar una mica de llum, per aconseguir que algun dia la vostra vida sigui una mica més fàcil. Gràcies sempre per la vostra col·laboració. Agrair també a l'Asociación Española contra la Leucodistrofia (ELA), que sempre ha col·laborat amb nosaltres amb una eficiència encomiable.

RESUM

Els trastorns genètics de la substància blanca cerebral (en anglès, *Genetic White Matter Disorders*; GWMDs) són un conjunt de malalties que afecten predominantment a la producció o manteniment de la mielina del sistema nerviós central. Les manifestacions clíniques apareixen freqüentment durant la infància, tot i que poden iniciar-se a qualsevol edat, i principalment són motores, però també cognitiu-conductuals, epilèptiques, oculars o endocrinològiques, entre d'altres.

El diagnòstic genètic molecular d'aquestes malalties és fonamental per poder oferir a les famílies un assessorament genètic adequat, informació en relació amb el pronòstic i opcions de tractament específiques. Però l'abordatge utilitzat fins fa pocs anys, basat en la clínica, el patró d'afectació a la ressonància magnètica, els estudis metabòlics i genètics dirigits permeten arribar a un diagnòstic en menys de la meitat dels pacients.

Les tècniques de seqüenciació massiva (en anglès, *Next-Generation Sequencing*; NGS), incloent-hi la seqüenciació de l'exoma i del genoma complets (*Whole Exome Sequencing* (WES) i *Whole Genome Sequencing* (WGS), respectivament), han demostrat en estudis realitzats principalment en trios (analitzant conjuntament les dades genòmiques del pacient i els seus progenitors), ser una eina amb un alt rendiment diagnòstic en diversos grups de patologies de base genètica.

Els objectius d'aquest treball han estat: establir la utilitat clínica dels estudis WES/WGS mitjançant l'anàlisi únicament de casos índex (no trio) amb GWMDs, identificar nous gens implicats en la fisiopatologia d'aquests trastorns i descriure noves formes de presentació clínica.

En aquest estudi vam recollir pacients pediàtrics i adults amb un quadre clínic i patró de ressonància magnètica cranial coherents amb un GWMD, definit com una afectació simètrica difusa o de tractes anatòmics específics de la substància blanca cerebral, en

absència de complicacions perinatals, vasculars o que suggereixin un procés autoimmune. Els pacients van ser identificats en unitats de neurologia i neuropediatría de diversos hospitals terciaris de tota Espanya des de gener de 2015 fins a desembre de 2019, i havien estat estudiats prèviament mitjançant les proves complementàries habituals (estudis de ressonància magnètica, metabòlics, neurofisiològics i genètics com aCGH (*microarray-based Comparative Genomic Hybridization*), seqüenciació de gens específics o panells NGS amb diversos gens), sense haver pogut arribar a un diagnòstic específic. Vam recollir la informació clínica, les imatges de ressonància magnètica i les mostres dels pacients en el laboratori de Malalties Neurometabòliques de l’Institut d’Investigació Biomèdica de Bellvitge (IDIBELL). No vam realitzar un filtratge estricte de casos per part d’un neuroradiòleg expert en leucodistròfies, tot i que sí que hi va haver una revisió per part del doctorand com a neuropediatre en el moment de la inclusió. A més, molts dels casos van ser evaluats per un equip de neuròlegs pediàtrics i d’adults en el context del projecte URDCat, emmarcat dins del Pla Estratègic de Recerca i Innovació en Salut (PERIS) 2016-2020.

Vam analitzar tots els casos índex mitjançant WES i posteriorment, en aquells en els que no havíem pogut assolir un diagnòstic, per WGS. Per a l’anàlisi de les dades genètiques obtingudes vam utilitzar un algoritme computacional dissenyat per la Dra. Àgatha Schlüter al mateix laboratori d’IDIBELL, que prioritza les variants genètiques tenint en compte la informació clínica codificada en termes HPO (*Human Phenotype Ontology*) i informació referent a les interaccions físiques i funcionals de les proteïnes de l’organisme. Vam avaluar en equip les variants genètiques resultants, amb la participació del doctorand com a neuropediatre, per mirar d’analitzar la possible relació causal amb el fenotip del pacient. Les vam classificar d’acord amb els criteris publicats per l’*American College of Medical Genetics and Genomics* (ACMG). En els casos amb variants genètiques no descrites prèviament, vam realitzar estudis funcionals i metabòlics per tal de validar-les, mitjançant tècniques de qPCR, Western-blot, immunofluorescència i assajos enzimàtics, entre d’altres. Els nous gens candidats identificats es van verificar a través de la detecció d’altres famílies en consorcis internacionals (GeneMatcher i PhenomeCentral).

En aquest estudi vam incloure 126 famílies i vam poder establir el diagnòstic molecular en 91 d’elles (72% dels casos) (**article 1 d’aquesta tesi**). A més, vam identificar 7 gens candidats,

fenotips nous, atípics, i cinc famílies amb diagnòstic dual (identificació de més d'un gen implicat en el fenotip clínic). Els gens identificats més freqüentment van ser *EIF2B5* (malaltia de la substància blanca evanescent), *POLR3A* (síndrome 4H), *RNASEH2B* (síndrome d'Aicardi-Goutières) i *PLP1* (malaltia de Pelizaeus Merzbacher). Aquest estudi va evidenciar la gran heterogeneïtat genètica d'aquest grup de trastorns (57 gens identificats entre els 91 casos diagnosticats). A més, cal remarcar que la meitat d'aquests gens no s'havien associat clàssicament al concepte de leucodistròfia i, per tant, poden no estar inclosos en els panells de gens. Un altre aspecte important a destacar és la rapidesa diagnòstica que va permetre l'ús de les tecnologies NGS (entre quatre i dotze mesos habitualment) en comparació amb l'"odissea diagnòstica" d'anys d'evolució i nombroses proves complementàries realitzades prèviament en la majoria d'aquests pacients.

Un dels gens candidats nous associats a malaltia de la substància blanca cerebral que es descriu en aquest treball és *PI4KA*, que té un rol important en el metabolisme dels fosfatidilinositols (PI) a la membrana cel·lular (**article 2 d'aquesta tesi**). Vam recollir dades de deu pacients amb variants bial·lèliques en aquest gen i vam poder descriure l'espectre fenotípic associat, que comprèn des d'una malaltia hipomielinitzant greu, que pot associar-se a alteracions estructurals del cervell (en forma d'hipoplàsia del tronc de l'encèfal i del cerebel o polimicrogíria), fins a una paraparèisia espàstica pura. A més, alguns pacients presenten trastorns immunològics, gastrointestinals o anomalies genito-urinàries. L'estudi funcional mitjançant Western-Blot i immunofluorescència va demostrar nivells reduïts de *PI4KA* en fibroblasts derivats dels pacients, i els estudis d'immunofluorescència i lipidòmica van indicar una activitat disminuïda de *PI4KA* en fibroblasts i cèl·lules sanguínies.

La identificació d'una pacient portadora d'una variant patogènica en el gen *DLG4*, va permetre que el doctorand coordinés l'estudi fenotípic i genotípic d'una cohort de 53 pacients amb variants d'herència dominant/*de novo* en aquest gen, que codifica per la proteïna postsinàptica PSD-95 (**article 3 d'aquesta tesi**). El quadre clínic es caracteritza per una discapacitat intel·lectual en grau variable, un trastorn de l'espectre autista (TEA), epilepsia i trastorns del moviment en alguns d'ells. L'hàbit marfanoide, que prèviament havia estat suggerit com un tret característic associat a *DLG4*, només es descrivia en nou dels individus (23%) i, malgrat algunes característiques comunes, no es va poder definir un

fenotip dismòrfic característic d'aquest trastorn. Cal destacar que alguns d'aquests pacients presentaven anomalies de la substància blanca cerebral, en forma d'atròfia, retard de la mielinització o hiperintensitats periventriculars, i signes clínics d'afectació de via piramidal o inclús una paraparèisia espàstica. Per tant, aquest treball exemplifica la gran heterogeneïtat fisiopatològica dels GWMDs i evidencia que els trastorns sinàptics també poden tenir una forma de presentació compatible amb l'espectre fenotípic de GWMD-paraparèisia espàstica hereditària.

Finalment, vam poder participar en la descripció d'un nou GWMD produït per variants bial·lèliques en el gen *PRORP*, que s'associen a sordesa neurosensorial, insuficiència ovàrica primària, retard del desenvolupament i canvis de la substància blanca cerebral. També en la descripció d'un nou fenotip associat a *POLR3A*, amb predomini de clínica extrapiroamidal i afectació estriatal, i en la caracterització fenotípica de pacients amb variants en el gen *HNRNPH1*.

Aquesta tesi mostra la utilitat clínica dels estudis de WES i WGS realitzats en cas índex (no trio) en els GWMDs, i reflexa com aquests estudis possibiliten la identificació de nous gens candidats i nous fenotips clínics. Reforça a més la necessitat d'implantar-los en estadis inicials del procés diagnòstic, per poder identificar l'etiològia tan aviat com sigui possible, i poder oferir un assessorament genètic adequat i tractaments específics abans que l'afectació neurològica estigui ja massa avançada. Finalment, posa de manifest la importància de la col·laboració entre centres assistencials i d'investigació, i de la participació dels clínics en el procés diagnòstic basat en la NGS.

SUMMARY

Genetic white matter disorders (GWMDs) are a heterogeneous group of diseases that predominantly affect the production and maintenance of myelin in the central nervous system. Clinical manifestations frequently develop during childhood, although the onset can be at any age. They are mainly motor, but also cognitive, behavioural, epileptic, ophthalmologic or endocrinologic, among others.

Molecular genetic diagnosis of these diseases is essential to provide families with adequate genetic counselling, prognosis information and possible treatment options. However, the diagnostic approach used until a few years ago, based on clinical manifestations, magnetic resonance imaging (MRI), metabolic and targeted genetic studies leaves approximately half of GWMD patients without a genetic diagnosis.

Next-Generation Sequencing (NGS) techniques, including Whole-Exome Sequencing (WES) and Whole-Genome Sequencing (WGS), in studies conducted mainly in trios (analysing together probands' and their unaffected parent's genomic data), showed a high diagnostic yield in diverse disease groups.

This work aimed to establish the clinical utility of WES and WGS for the study of index cases with GWMDs (not trio), the identification of new genes involved in the pathophysiology of white matter disorders and new phenotypes.

For this study, we included paediatric and adult patients with clinical and MRI patterns consistent with a GWMD, defined as symmetrical diffuse or with specific anatomical tract involvement of the cerebral white matter, in the absence of perinatal or vascular complications or a clinical picture suggestive of an autoimmune process. Patients were identified at child and adult neurology units from several tertiary hospitals around Spain from January 2015 to December 2019. The referring physicians had not been able to establish a molecular diagnosis despite applying standard-of-care paraclinical studies (including mainly MRI, metabolic, neurophysiological, and genetic studies such as aCGH (microarray-based Comparative Genomic Hybridization), targeted Sanger sequencing or

NGS gene panels). Clinical information, MRIs, and samples were collected at the Neurometabolic Diseases laboratory of Bellvitge Biomedical Research Institute (IDIBELL). Although strict filtering of cases by a neuroradiologist focused on leukodystrophies was not performed, the doctoral student reviewed the information before inclusion. In addition, many cases were evaluated before inclusion by a team of experienced paediatric and adult neurologists under the URDCat initiative for undiagnosed neurological disorders, within the Strategic Plan for Research and Innovation in Health (PERIS) 2016-2020.

We analysed all the cases by WES and subsequently, in the remaining negative cases, by WGS. For the genomic data analysis, we used a computational algorithm designed by Dr. Àgatha Schlüter at IDIBELL's Neurometabolic Diseases laboratory, which prioritized variants taking into account clinical information encoded in HPO terms (Human Phenotype Ontology) and information on the physical and functional interactions of the body's proteins. Our team evaluated the genetic variants obtained, with the participation of the doctoral student to evaluate their association with the clinical phenotype. The variants were classified according to the American College of Medical Genetics and Genomics (ACMG) criteria. We performed functional and metabolic studies to validate unreported variants using qPCR, Western blot, immunofluorescence and enzymatic assay techniques, among others. The new candidate genes were verified by identifying additional families in international consortia (GeneMatcher and PhenomeCentral).

We included 126 families in the study, and we were able to establish the molecular diagnosis in 91 (72%) of them (**article 1 of this thesis**). We also identified seven candidate genes, new or atypical phenotypes, and five families with dual diagnosis (identification of more than one gene involved in the family's clinical phenotype). The most frequently identified diagnoses were *EIF2B5* (vanishing white matter disease), *POLR3A* (4H syndrome), *RNASEH2B* (Aicardi-Goutières syndrome), and *PLP1* (Pelizaeus Merzbacher disease). This study evidenced the significant genetic heterogeneity of this group of disorders (57 genes identified among the 91 diagnosed cases). In addition, half of the identified genes were not classically associated with the concept of leukodystrophy and therefore they may be not included in gene panels. It is also remarkable the short time-to-diagnosis allowed by WES/WGS studies (usually

between four and twelve months) in comparison to the previous "diagnostic odyssey" of years and numerous complementary tests performed on many of these patients.

One of the new candidate genes associated with white matter disorders identified in this work is *PI4KA*, which plays an important role in the phosphatidylinositol metabolism at the cell membrane (**article 2 of this thesis**). We collected ten patients with biallelic variants in this gene and were able to describe the associated phenotypic spectrum, ranging from a severe hypomyelinating disease associated with structural abnormalities of the brain (brainstem and cerebellar hypoplasia or polymicrogyria), to pure spastic paraparesis. In addition, some patients had immunological problems, gastrointestinal disorders, or associated genitourinary abnormalities. Western blot and immunofluorescence functional studies demonstrated reduced levels of *PI4KA* in patients' fibroblasts, and immunofluorescence and lipidomic studies, indicated decreased *PI4KA* activity in fibroblasts and blood cells.

The identification of a patient carrying a mutation in the *DLG4* gene allowed the doctoral student to coordinate the phenotypic and genotypic study of a cohort of 53 patients with dominant/*de novo* inheritance variants in this gene, which encodes the post-synaptic protein PSD-95 (**article 3 of this thesis**). The clinical picture was characterized by intellectual disability of variable severity, autism spectrum disorder, epilepsy, and movement disorders in some of them. Marfanoid habitus, which was previously suggested to be a characteristic feature of *DLG4*-related phenotypes, was found in only nine individuals (23%), and despite some overlapping features, a distinct facial dysmorphism could not be established. It should be noted that some of these patients had cerebral white matter atrophy, delayed myelination, periventricular hyperintensities, and clinical manifestations suggestive of pyramidal involvement or even spastic paraparesis. Therefore, this work exemplifies the great pathophysiological heterogeneity of GWMDs and shows that synaptic disorders may also present with a phenotype compatible with GWMD-hereditary spastic paraparesis spectrum.

Finally, we were able to contribute to the description of a new GWMD produced by biallelic variants in the *PRORP* gene, which are associated with neurosensory deafness, primary

ovarian failure, developmental delay and cerebral white matter abnormalities. We participated also in the description of a new phenotype associated with *POLR3A*, with a predominance of extrapyramidal manifestations and striatal involvement, and the phenotypic characterization of patients with variants in the *HNRNPH1* gene.

This thesis provides evidence of the clinical utility of singleton (not trio) WES and WGS studies in GWMDs and how it enables the identification of new candidate genes and new clinical phenotypes. It also reinforces the need to implement these studies in the early stages of the diagnostic process, to provide adequate genetic counselling and enable an early treatment before the advancement of neurological degeneration. Finally, it highlights the importance of collaboration between clinical and research centres, and the participation of clinicians in the diagnostic process based on NGS.

I. INTRODUCCIÓ

1. Introducció Històrica

El cervell humà ha fascinat els investigadors i acadèmics des de fa segles. Així i tot, després de milers d'anys d'investigació havent assolit nombrosos avenços, el coneixement de moltes de les seves funcions encara és força limitat. Actualment, està en marxa el projecte BRAIN, en el que durant un període de quinze anys, 500 laboratoris de tot el món i milers de científics, tracten de determinar un mapa del cervell per mirar de comprendre millor com s'organitza el seu funcionament (Yuste and Bargmann, 2017).

En el segle V aC, Alcmeó de Crotona va reconèixer que el cervell era l'òrgan fonamental de la sensació i la cognició, i ho va reflectir a través de les següents paraules:

"La seu de les sensacions és al cervell. Conté la facultat de govern. Tots els sentits estan connectats d'alguna manera amb el cervell; en conseqüència, ells són incapços d'actuar si el cervell està alterat o canvia la seva posició, ja que això atura els passatges a través dels quals actuen els sentits. Aquesta capacitat del cervell per sintetitzar sensacions fa que també sigui la seu del pensament: l'emmagatzematge de percepcions dóna memòria i creença, i quan aquestes s'estabilitzen, s'obté coneixement".

Ell va ser el primer que va emprar la dissecció com a eina d'investigació, i mitjançant aquesta tècnica va identificar els nervis òptics, suggerint que s'encarregaven de portar llum al cervell (Gross, 2013). Així i tot, el concepte que el cervell és l'òrgan encarregat del control de les sensacions i la cognició es va posar en dubte posteriorment, en temps de la Grècia clàssica i l'imperi Romà, quan van aparèixer dues teories oposades: la teoria encefalocèntrica, que considerava que era el cervell que se n'encarregava, i la teoria cardiocèntrica, defensada per personalitats com Aristòtil entre d'altres, que proposava que era el cor l'encarregat de controlar aquestes funcions. Galè de Pèrgam (129-213 dC) va estudiar les conseqüències de les lesions en diferents parts del sistema nerviós. D'aquesta manera, va demostrar que el cervell era l'encarregat del control del moviment, el va identificar com a òrgan relacionat amb la cognició i, per tant, també amb les malalties mentals. Va ser el primer a realitzar estudis sistemàtics del sistema nerviós central (SNC) des del punt de vista anatòmic i fisiològic, fent descripcions molt acurades de la seva anatomia macroscòpica, incloent-hi el

trajecte de nou parells cranials, la diferenciació de nervis motors i sensitius, o la identificació de la medul·la espinal com una estructura contigua al cervell (Gross, 2013).

El Renaixement italià va ser una època en la qual ciència i art van convergir per impulsar el coneixement de l'anatomia en general i la del cervell en particular. Andreas Vesalius (1514-1564), considerat el pare de l'anatomia moderna, va publicar en el 1543 la seva gran obra *De Humani Corporis Fabrica*, en la que probablement diversos deixebles del conegut pintor Tiziano van col·laborar-hi amb les seves il·lustracions. Un dels coneixements que hi va aportar va ser la descripció per primera vegada de la diferenciació entre la substància blanca i grisa del cervell humà.

Marcello Malpighi (1628–1694), va ser pioner en la utilització de la microscòpia per l'estudi anatòmic del cos humà. Va dedicar especial atenció a examinar el còrtex cerebral i el va descriure com una conformació de petites glàndules o "glòbuls". No obstant això, no va ser fins a la segona meitat del segle XIX, amb el desenvolupament de tècniques de fixació i tincions específiques, quan aquesta tecnologia va adquirir importància per l'estudi del SNC. En gran part, això va ser possible gràcies a Camilo Golgi (1843-1926), que en el 1873 va descobrir el mètode de la *reazione nera* (reacció negra), que permetia la tinció amb bona qualitat de diverses cèl·lules alhora, però en nombre relativament reduït, amb el que es podien estudiar millor les connexions entre elles. Amb aquesta tècnica va aconseguir visualitzar per primera vegada les cèl·lules nervioses amb les seves diferents parts (cos neuronal, dendrites i axó) (Figura 1A). Malgrat això, Golgi va ser un gran defensor de la teoria reticular, que considerava que les neurones eren nodes que formaven part d'una xarxa nerviosa, un continu, que explicava els aspectes holístics de les funcions cerebrals.

Rudolf Virchow (1821-1902) va identificar unes cèl·lules diferents de les neurones, situades a les parets dels ventricles cerebrals. Les va anomenar glia o *Nervenkitt* ("massilla nerviosa") i les va descriure en un dels llibres científics més destacables del segle XIX, anomenat *Patologia Cel·lular* (1858). Va considerar que formaven una mena de teixit conjuntiu, que tenia capacitat de patir inflamació, i que ell va anomenar mielina, procedent del terme grec "myelos" (medul·la).

Pocs anys després, Santiago Ramón i Cajal (1852-1934) va adoptar la tècnica de la *reazione nera* de Golgi i va fer-hi diverses modificacions, que li van permetre dur a terme els seus estudis de microanatomia del SNC. Les seves descripcions van suposar un salt important en el coneixement i, per molts, el naixement de la neurociència moderna. En aquests estudis va poder identificar que les neurones eren unitats independents des del punt de vista anatòmic, fisiològic i metabòlic, en el que es va anomenar teoria neuronal. Aquesta, era contraposada a la reticular defensada per Golgi i, tot i aquesta confrontació conceptual en referència a l'estructuració del SNC, els avenços en el coneixement desenvolupats per aquests dos autors van suposar que en el 1906 Golgi i Cajal compartissin el Premi Nobel de Fisiologia i Medicina.

Cajal també va formular la llei de la polaritat dinàmica de les neurones, segons la qual, aquestes transmeten els impulsos elèctrics unidireccionalment, des del cos neuronal fins a l'extrem del seu axó. Va poder identificar que les neurones tenen diferents formes, característiques segons la seva localització. A més, va determinar l'existència d'altres tipus cel·lulars en el cervell, com són els astròcits, i també un “tercer element” que no va poder identificar adequadament, donat que quedava poc tenyit amb les tècniques d’impregnació que utilitzava.

Va descriure magistralment la morfologia dels astròcits i la seva relació amb les neurones i els vasos sanguinis (Figura 1B), anomenant-les cèl·lules aracniformes (per la forma d’aranya) o cèl·lules de Deiters, considerant que Otto Friedrich Karl Deiters (1834-1863) n’era el descobridor. A més, també va formular teories sobre el desenvolupament i funcionalitat del sistema nerviós central, els mecanismes de plasticitat neuronal i dels processos de degeneració i regeneració.

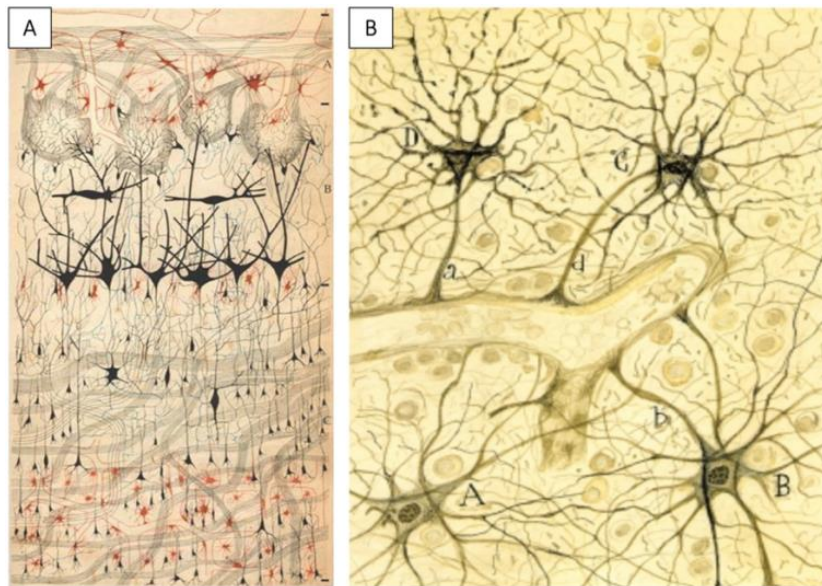


Figura 1. Il·lustracions de Golgi i Cajal, de preparacions histològiques tenyides amb els mètodes de l'època. **A)** Primera il·lustració realitzada per Golgi en el 1875, d'una preparació histològica amb el seu mètode de tinció de la “reazione nera”. Dibuix d'una secció vertical del bulb olfactori d'un gos. **B)** Dibuix de Santiago Ramón i Cajal que mostra els astròcits a la substància blanca del càortex cerebral d'un cervell humà adult (A-D), amb els peus perivasculars (a, b, d). Mètode d'or.

Pío del Río Hortega (1882-1945) va ser un deixeble de l'escola espanyola de Santiago Ramón y Cajal, que va revolucionar l'estudi de la neuròglia a partir de la millora de les tècniques d'impregnació metàl·lica aplicades per Golgi i Cajal. Mitjançant la utilització de carbonat de plata amoniacial (Del Río Hortega P, 1918), va poder identificar que el “tercer element” al que feia referència Cajal, corresponia en realitat a dos tipus cel·lulars: la micròglia, provenint del mesoderm i els oligodendròcits (ODs), d'origen ectodèrmic (Del Río Hortega, 1920, 1921) (Figura 2).

Va evidenciar que els ODs es troben propers a les fibres nervioses mielinitzades, amb processos en espiral al voltant de l'axó, i va establir un paral·lelisme amb les cèl·lules de Schwann del sistema nerviós perifèric, arribant a l'encertada conclusió que les dues estan relacionades amb la formació dels embolcalls de mielina. També va predir la seva implicació en el trofisme neuronal, afirmant que “realitzen funcions de suport, aïllament i nutrició relacionades amb la conducció nerviosa” i va predir el paper dels ODs en mecanismes de plasticitat dels circuits neuronals, tal com s'ha evidenciat en estudis recents (Fields, 2008; Lee *et al.*, 2012).

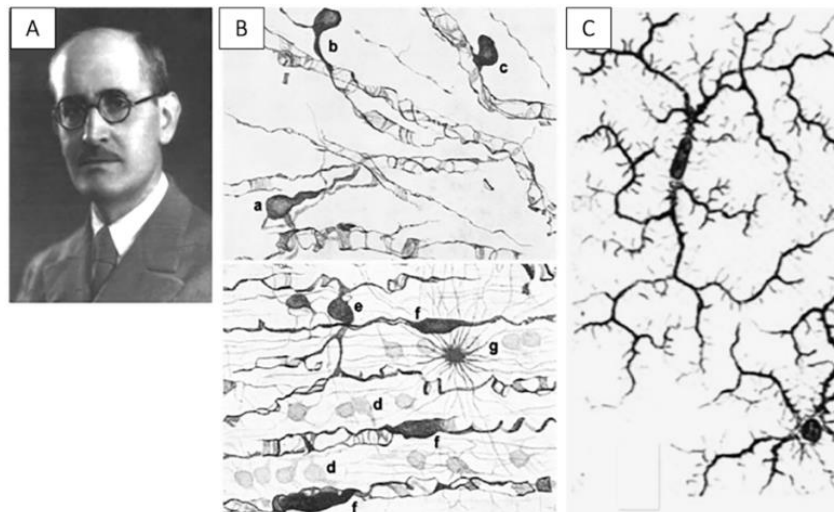


Figura 2. Pío del Río-Hortega, descubridor del “tercer elemento”: els oligodendròcits i la micròglia. (A) Retrat de Pío del Río-Hortega. (B) Representació dels oligodendròcits. (C) Representació de la micròglia. Adaptat de (de Castro, 2019).

En el 1928 va publicar la primera descripció sistemàtica dels ODs (Del Río Hortega, 1928) i va identificar l'existència d'una diversitat de cèl·lules oligodendroglials, que s'ha confirmat posteriorment a través d'estudis de microscòpia electrònica, immunohistoquímica i estudis genètics (Butt, 2012) (Figura 3). A més, va suggerir que hi havia una correlació entre el calibre de l'axó, la distància internodal i el gruix de la beina de mielina.

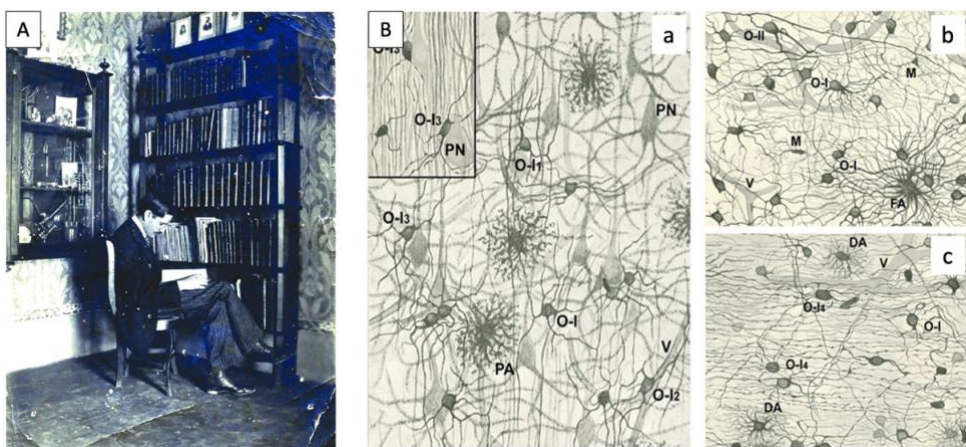


Figura 3. Pío del Río Hortega. Il·lustracions del còrTEX i substància blanca cerebrals, tenyits amb el procediment del carbonat de plata d'Hortega. (A) Pío del Río Hortega en el seu estudi a la casa familiar de Valladolid, 1910. (B) Representacions del còrTEX cerebral (a) i la substància blanca cerebral (b, c), en les que s'aprecien els oligodendròcits tipus I (O-I), tipus II (O-II), els astròcits protoplàsmics (PA), fibrosos (FA) i nans (DA), les cèl·lules microglials (M) i la seva disposició en relació amb les neurones piramidals (PN) i els vasos sanguinis (V). Adaptat de (Pérez-Cerdá *et al.*, 2015).

Per altra banda, va demostrar que la micròglia té una funció rellevant en la resposta al dany cerebral, fagocitant elements nocius o restes cel·lulars, i va indicar que «si hi ha neuronofàgia, creiem que només les cèl·lules de la micròglia ho fan, ja que la seva capacitat per migrar i fagocitar està fora de tot dubte». A més, va interessar-se per la neuropatologia i va ser una figura rellevant en l'estudi dels tumors del SNC.

En els inicis del segle XX, a partir d'estudis de tinció de la mielina realitzats en fetus i nounats, Paul Flechsig va descriure com el procés de mielinització del cervell segueix un patró espacial i temporal orquestrat de forma precisa (Flechsig Of Leipsic, 1901; Flechsig, 1920) (Figura 4). Així, en les fases més inicials es produeix la mielinització del tronc de l'encèfal, que conté estructures vitals pel control del sistema cardiocirculatori, la respiració i els mecanismes de succió-deglució, però també de les àrees primàries motores i sensitives (incloent-hi inputs de vies visuals i auditives) i els seus tractes corresponents. Posteriorment, es mielinitzen les àrees encarregades de tasques més complexes i finalment les encarregades de funcions intel·lectuals superiors.

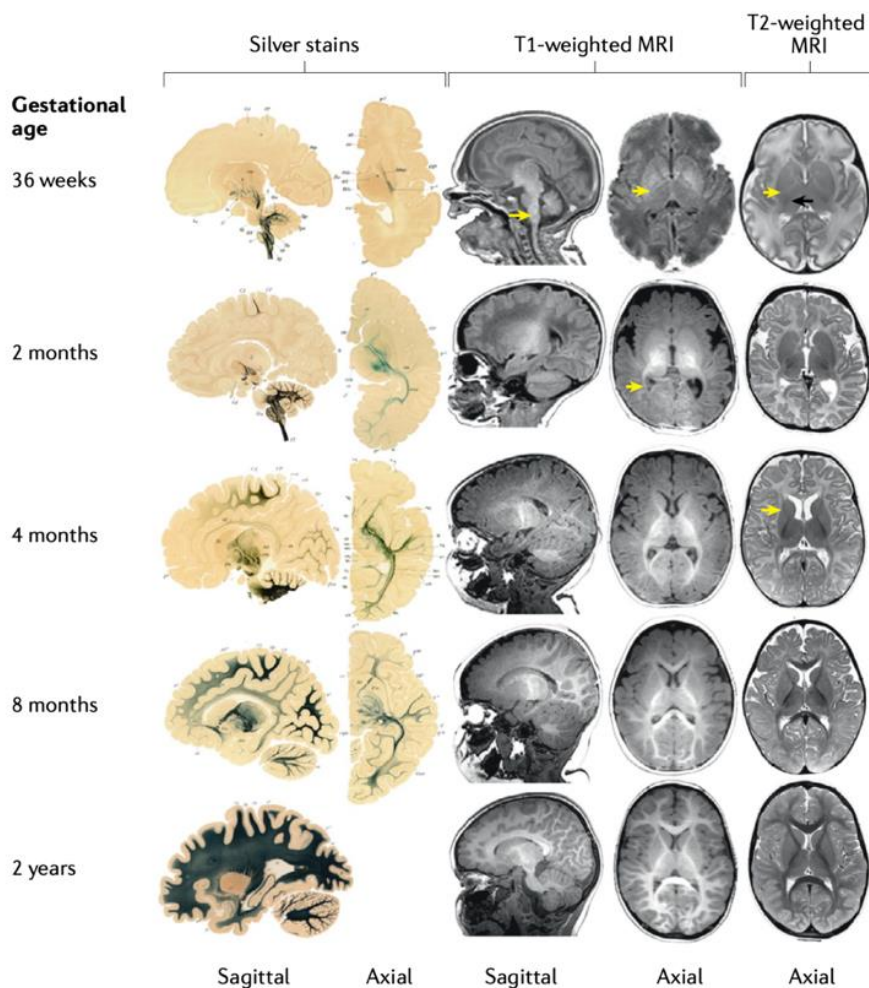


Figura 4. Procés normal de mielinització en els primers dos anys de vida. Talls de cervell preparats per Flechsig amb tinció de plata i correspondència amb imatges de ressonància magnètica, potenciades en T1 i T2, en les que podem apreciar la progressió normal de la mielinització del SNC. En un nounat se s'aprecia la mielinització del tronc de l'encèfal (fletxa groga llarga), la substància blanca cerebel·losa central i els tractes corticoespinals, així com el braç posterior de la càpsula interna (fletxa groga curta). Als dos mesos d'edat, la mielinització ha augmentat en els lòbul occipitals (radiació òptica, fletxa groga) i parietals, i l'espleni del cos callós. A partir dels quatre-cinc mesos, la mielinització transcorre en direcció frontal i, a partir dels 5-6 mesos, en la direcció temporal. La mielina està present en el braç anterior de la càpsula interna des dels 3-4 mesos (fletxa groga) i al genoll del cos callós a partir dels cinc mesos. A partir dels sis mesos, la mielinització avança als lòbul frontals. Posteriorment, progrésa cap a les regions subcorticals, fins a estar més o menys completa cap als dos anys de vida. De (Wolf *et al.*, 2021).

En el 1949, Huxley va evidenciar la importància de la mielina per promoure l'impuls saltatori i d'aquesta manera permetre la conducció de l'impuls nerviós a major velocitat, a més de reduir el consum axonal d'energia (Huxley and Stämpfli, 1949).

La primera descripció d'un trastorn de la substància blanca cerebral familiar ja l'havien fet de forma independent Pelizaeus (Pelizaeus, 1899) i Merzbacher (Merzbacher, 1910), referint-s'hi com una “esclerosi difusa” crònica progressiva, per diferenciar-la de l'esclerosi múltiple, caracteritzada en els anys 1860 per Jean-Martin Charcot. El primer esment al concepte de leucodistròfia el va fer Bielschowsky l'any 1928, en un text referent a la leucodistròfia metacromàtica (Bielschowsky and Henneberg, 1928).

Durant els anys setanta, l'aparició de la tomografia computada (TC) va permetre visualitzar la substància blanca i, per tant, les leucoencefalopaties *in vivo*. Però no va ser fins als anys vuitanta, amb l'aplicació clínica de la ressonància magnètica (RM) cranial, quan es va desenvolupar de forma important el camp de la neuroimatge. La RM cranial va permetre caracteritzar patrons d'afectació distintius entre les diferents malalties, obrint la possibilitat a l'establiment d'una sospita diagnòstica (van der Knaap *et al.*, 1991). Va possibilitar la descripció de patrons corresponents a noves entitats clíniques, com la leucoencefalopatia megalencefàlica amb quists subcorticals (*Megalencephalic Leukodystrophy with subcortical Cysts; MLC*) (van der Knaap *et al.*, 1995), la malaltia de la substància blanca evanescent (*Vanishing White Matter Disease; VWMD*) (van der Knaap *et al.*, 1997), la hipomielinització amb atròfia dels ganglis basals i cerebel (*Hypomyelination with Atrophy of the Basal Ganglia and Cerebellum; H-ABC*) (van der Knaap *et al.*, 2002), la leucoencefalopatia amb afectació

del tronc de l'encèfal i medul·la espinal amb elevació de lactat (*Leukoencephalopathy with Brain stem and Spinal cord Involvement and Lactate elevation; LBSL*) (van der Knaap *et al.*, 2003), la hipomielinització, hipodòncia i hipogonadisme hipogonadotrófic (síndrome 4H) (Wolf *et al.*, 2005) i la hipomielinització de les primeres estructures mielinitzants (*Hypomyelination of Early Myelinating Structures; HEMS*) (Steenweg *et al.*, 2012). Així, es va desenvolupar un sistema de classificació de les leucodistròfies en funció de les característiques de la neuroimatge (Schiffmann, 2009).

També, gràcies als estudis genètics de lligament (*linkage analysis*), determinant regions d'interès i seqüençant dels gens coneguts en aquestes, es van identificar els primers gens associats a leucodistròfies, com és el cas de *PLP1* (*Pelizaeus Merzbacher Disease; PMD*) (Hudson *et al.*, 1989), *ARSA* (*Metachromatic Leukodystrophy; MLD*) (Polten *et al.*, 1991), *ASPA* (malaltia de Canavan) (Kaul *et al.*, 1993), *GALC* (*Krabbe Disease; KD*) (Sakai *et al.*, 1994) i *ABCD1* (*X-linked Adrenoleukodystrophy; X-ALD*) (Mosser *et al.*, 1993).

Tot i aquests avenços, l'any 2010, el 50% dels pacients que patien una leucodistròfia no tenien un diagnòstic molecular específic (Bonkowsky *et al.*, 2010). En els darrers anys, l'aplicació de la tecnologia de seqüenciació massiva de nova generació (en anglès, *Next-Generation Sequencing (NGS)*), ha permès incrementar de forma exponencial les descripcions de noves bases moleculars en el camp de les leucodistròfies, des que l'any 2011 es va identificar el primer defecte genètic mitjançant aquesta tècnica: variants en dominància en el gen *CSF1R* causants de la leucoencefalopatia hereditària difusa amb esferoides (*Hereditary Diffuse Leukoencephalopathy with axonal Spheroids; HDLS*) (Rademakers *et al.*, 2011).

2. Biologia de la mielina

Les capacitats mentals són la característica més distintiva de l'ésser humà i venen determinades per una complexa arquitectura cel·lular que és resultant de centenars de milions d'anys d'evolució. El cervell humà està format per uns 100.000 milions de neurones i cada una d'elles té entre 10.000 i 20.000 connexions amb altres neurones i cèl·lules glials

(Nave and Werner, 2021). En el cervell dels mamífers, la substància blanca està formada bàsicament per projeccions axonals i les cèl·lules glials associades (oligodendròcits, astròcits, micròglia i cèl·lules NG2), que s'estima que es troben en un nombre similar al de neurones (von Bartheld *et al.*, 2016). Les projeccions axonals permeten la propagació dels potencials d'acció des del cos neuronal fins al terminal de l'axó, situat a mil·límetres o inclús metres de distància, com en el cas de les neurones de projecció, en les quals pot representar més del 99% de la seva massa cel·lular. Aquestes dades posen de manifest la importància de les connexions neuronals (i, per tant, de la mielina com a component fonamental d'aquestes) en l'organització de les funcions cerebrals i com permeten l'extraordinari repertori de capacitats neuroconductuals humanes. Les cèl·lules glials col·laboren en el funcionament d'aquests circuits cerebrals realitzant funcions fonamentals i específiques, tant durant el desenvolupament del SNC, com al llarg de la resta de la vida: serveixen de suport estructural, afavoreixen i regulen la ràpida comunicació a través de la mielinització i el suport metabòlic axonal, mantenen el microambient del cervell, participen en processos de plasticitat i reparació, i en l'intercanvi i processament d'informació amb altres tipus cel·lulars.

Els trastorns genètics de la substància blanca cerebral (en anglès, *Genetic White Matter Disorders*, GWMDs) són aquelles malalties de base genètica en les quals s'afecta de forma predominant el procés de mielinització i manteniment de la mielina (Helman *et al.*, 2020, Vanderver *et al.*, 2020b; Kaur *et al.*, 2021; Shukla *et al.*, 2021). Altres malalties com l'esclerosi múltiple cursen també amb una afectació predominant de la substància blanca del SNC, però en aquest cas de base immunitària. A més, en processos com la leucomalàcia periventricular, en les lesions de la medul·la espinal, en malalties neurodegeneratives com l'Alzheimer o inclús en trastorns psiquiàtrics, també hi ha un component d'afectació de la substància blanca (Fields, 2008). Per tant, el coneixement dels mecanismes implicats en la formació, manteniment i regeneració de la mielina és determinant en la recerca de tractaments d'un gran ventall de malalties que afecten el SNC.

2.1 Els oligodendròcits (ODs) i el procés de mielinització

Els ODs són les cèl·lules del SNC encarregades de la producció de mielina i s'estima que cada un d'ells participa en la mielinització de fins a 60 axons. Provenen de la diferenciació de les cèl·lules precursores dels oligodendròcits (OPCs), que durant el període embrionari proliferen, migren des de les zones germinals del cervell anterior i es distribueixen pel parènquima cerebral en onades successives. La majoria es diferencien en ODs madurs, un cop establertes les connexions neuronals, iniciant el procés de mielinització ja en el segon trimestre de la gestació. Aquest, progressa de forma molt important al llarg dels primers 2-3 anys (Figura 4, pàgines 29-30), però no es completa fins a la tercera dècada de la vida. Com s'ha descrit en l'apartat anterior, evoluciona en sentit ascendent i de la part posterior cap a la part anterior del cervell, en un procés perfectament orquestrat.

Una proporció de les OPCs romanen “a l'espera” durant la vida adulta (OPCs de l'adult ó cèl·lules NG2). Aquestes, poden diferenciar-se a ODs madurs per promoure canvis en la mielinització desencadenats per l'experiència, participant, per tant, en processos de plasticitat cerebral i aprenentatge, però també en la regeneració de la mielina en resposta a un procés lesiu (Hughes, 2021). Així, la mielinització és un procés dinàmic, que respon a les necessitats, adaptant-se a l'activitat neuronal, tal com descriu l'anomenada teoria de la “mielinització adaptativa” (Bechler *et al.*, 2015; Nave and Werner, 2021). Per tant, podem parlar d'una mielinització intrínseca, genèticament determinada, que es produeix principalment en el període fetal i primers anys de vida, i una segona etapa que ve determinada per l'experiència i permet regular finament la funcionalitat de la xarxa neuronal modulant la comunicació entre les neurones i les cèl·lules glials (Stadelmann *et al.*, 2019).

Per dur a terme la mielinització, els ODs han d'augmentar de forma molt important l'àrea de superfície de la seva membrana, formant extensions que embolcallen els axons múltiples vegades. Aquest és un procés complex, en el que els mecanismes de polimerització/despolimerització de l'actina juguen un paper fonamental (Stadelmann *et al.*, 2019; Brown and Macklin, 2020). La beina de mielina creix en sentit radial, però també longitudinalment al llarg de l'axó, el que determina l'agrupament dels canals de sodi entre les beines de mielina successives, en uns espais que s'estrenyen fins a conformar els nodes

de Ranvier (petits espais d'un μm , desproveïts de l'embolcall de mielina, que permeten la propagació del potencial d'acció de forma saltatòria i ràpida al llarg de l'axó). Posteriorment, es produeix un procés d'extrusió del citoplasma dels embolcalls i es completa d'aquesta manera la formació de la mielina compacta. Queden però els canals citoplasmàtics, que permeten la comunicació del cos de l'oligodendròcit amb les diferents capes de mielina i amb el compartiment axonal, facilitant la distribució de metabòlits. També romanen unes espirals anomenades bucles paranodals en els extrems de la beina, pròxims als nodes de Ranvier, i un espai periaxonal que recorre l'axó per sota de la beina de mielina (Wolf *et al.*, 2021) (Figura 5A).

Els oligodendròcits formadors de mielina, els astròcits i les cèl·lules ependimàries dels ventricles estan altament interconnectats mitjançant les unions comunicants (en anglès, *gap junctions*), conformant el que s'ha anomenat sinciti panglial. Els astròcits tenen projeccions que connecten amb els vasos sanguinis, a través de les quals obtenen nutrients de la circulació capil·lar, que distribueixen a través d'aquestes unions comunicants a la resta de cèl·lules glials i als axons. A més, també a través d'aquestes unions, els astròcits contacten amb les cèl·lules ependimàries dels ventricles, en el que representa una via de drenatge fonamental pel manteniment de l'homeòstasi del SNC. Les unions comunicants estan conformades per l'associació de dues connexines (proteïnes transmembrana): els astròcits expressen Cx30 i Cx43, i els oligodendròcits, Cx32, Cx47 i Cx29. Com a exemple de la importància d'aquestes estructures, les variants patogèniques en el gen que codifica per la Cx47 s'associen a la malaltia de *Pelizaeus Merzbacher-like disease* (PMLD) i les de la Cx43 s'associen a la *Oculodentodigital Dysplasia* (ODDD) (Figura 5B).

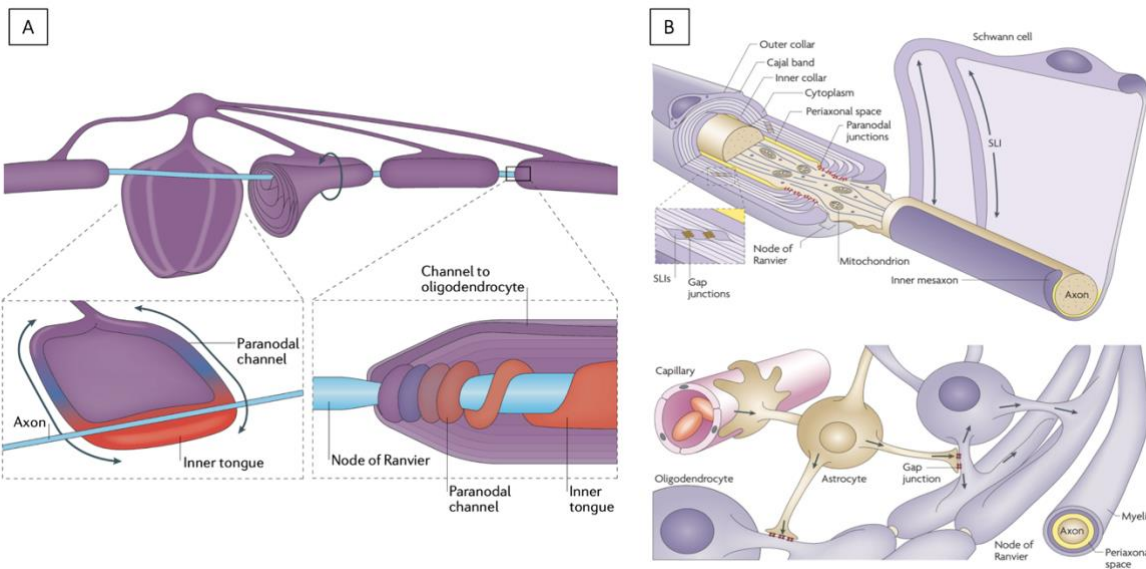


Figura 5. Procés de formació de l'embolcall de mielina i disposició dels oligodendròcits en relació amb els axons, els astròcits i capil·lars vasculars. **(A)** Representació de l'estensió de la membrana dels oligodendròcits i procés d'embolcallament de l'axó. Posterior formació de la mielina compacta deixant els bucles paranodals, que són espais no compactats fonamentals per a la transmissió de metabòlits. **(B)** Representació esquemàtica de la interrelació i alta connectivitat entre els oligodendròcits i les beines de mielina amb els astròcits a través de les unions comunicants, i amb els capil·lars vasculars. Adaptat de (Wolf et al., 2021) i (Nave, 2010).

Durant el període en què la mielinització és més intensa, es requereixen una gran quantitat de lípids, que representen el 75% del pes sec de la beina de mielina. Els més abundants són els àcids grassos de cadena llarga saturats, els glucoesfingolípids i el colesterol. Aquests, són sintetitzats en part pel mateix oligodendròcit, però també s'incorporen fonamentalment des dels astròcits, des de les neurones de l'entorn i de l'ambient extracel·lular (Hughes, 2021). També s'han de sintetitzar les proteïnes de membrana que conformen l'estructura de la beina.

Tot i que els oligodendròcits són els principals encarregats de la producció de mielina, aquest és un procés complex en el qual intervenen altres tipus cel·lulars i factors (Figura 6):

- L'activitat de l'axó promou la proliferació i diferenciació de les OPCs i és fonamental perquè es produeixi una mielinització completa (Figura 7). A més, hi ha evidència recent que l'activitat neuronal desencadenada per l'experiència induceix canvis en la mielinització que modelen la dinàmica dels circuits neuronals i d'aquesta manera conforma, per tant, un mecanisme de plasticitat cerebral (Mount and Monje, 2017).

- Els astròcits es diferencien abans que els ODs i produeixen substàncies essencials per la seva supervivència i diferenciació, com el factor de creixement derivat de plaquetes α (PDGF α). Tenen prolongacions que contacten amb els capil·lars sanguinis, formant part de la barrera hematoencefàlica, a través de les quals capten nutrients per donar suport metabòlic a altres cèl·lules glials i als axons. A més, proveeixen grans quantitats de lípids als ODs per la producció de mielina i alliberen substàncies que regulen el procés de mielinització, facilitant o inhibint la formació de la beina (Wolf *et al.*, 2021).
- La micròglia promou la mielinització via factor de creixement insulinoide 1 (IGF-1) durant el període neonatal, tal com s'ha descrit en estudis realitzats en ratolins (Wlodarczyk *et al.*, 2017). A més, també secreta el factor neurotròfic derivat del cervell (BDNF), que afavoreix la remielinització, i el factor de necrosi tumoral α (TNF α), la interleucina 6 (IL-6), el factor de creixement de fibroblasts 2 (FGF2), la interleucina 1 β (IL-1 β) i l'interferó γ (IFN γ), que estimulen la proliferació i diferenciació de les OPCs. Per contra, també sembla participar en processos de fagocitosi de la mielina, eliminant beines en formació, de manera similar al que succeeix amb la poda sinàptica. Inclús, a través de la regulació de l'activitat sinàptica o de la matriu extracel·lular, també poden influir en la formació o pèrdua de mielina (Hughes, 2021).
- Les cèl·lules endotelials dels vasos sanguinis interactuen amb els OPCs i permeten la seva migració durant el desenvolupament del SNC, en un procés dependent de l'expressió del receptor acoblat a proteïna G, GPR124 (Tsai *et al.*, 2016). Els perícits produeixen LAMA2, que pot estimular la diferenciació de les OPCs (De La Fuente *et al.*, 2017).
- Finalment, les hormones tiroidals són essencials per la diferenciació dels OPCs i, per tant, per la correcta mielinització. Això es posa de manifest en els pacients amb variants patogèniques en el gen *SLC16A2*, que codifica per una proteïna

transportadora de l'hormona tiroidal. La seva pèrdua de funció ocasiona la síndrome Allan-Herndon-Dudley, que s'associa un important retard de la mielinització. A més, altres factors també són essencials, com el Fe, folat i vitamina B12 (Wolf *et al.*, 2021).

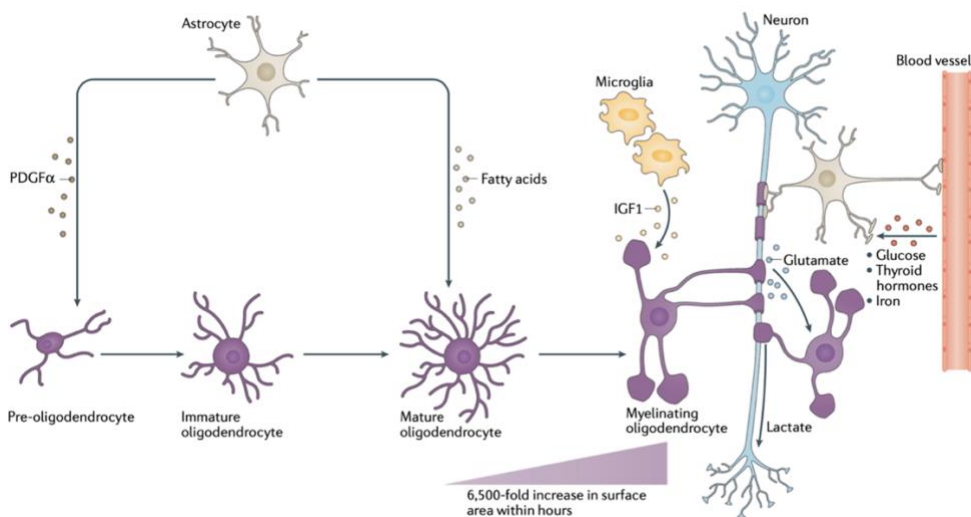


Figura 6. Factors implicats en el procés de mielinització. A més dels oligodendròcits, els astròcits i les cèl·lules microglials també participen en el procés de mielinització. Els astròcits promouen la maduració dels oligodendròcits a través de l'alliberació de PDGF α . Alhora, proveeixen d'àcids grisosos requerits per la mielinització als oligodendròcits ja madurs. L'activitat axonal també estimula la producció de mielina, com fa també la micròglia a través de la producció d'IGF-1. A més, les hormones tiroïdals i alguns micronutrients són indispensables en aquest procés. De (Wolf *et al.*, 2021).

Per tant, el procés de mielinització està altament regulat i depèn de diferents components cel·lulars i molècules de senyalització extracel·lular, que modulen l'activitat de diverses vies de senyalització a l'interior de l'oligodendròcit, com la via dels fosfatidilinositols (PI), la PI3K-AKT-mTOR i l'ERK/MAPK (Figura 7). La proteïna FAM126A (també coneguda com a *hyccin*), participa en la síntesi de PI regulant la síntesi de PtdIns(4)P, i el seu defecte s'associa a la malaltia hipomielinitzant amb cataracta congènita (*Hypomyelination with Congenital Cataracts; HCC*) (Biancheri *et al.*, 2011). Una altra proteïna d'aquesta via, que forma un complex amb FAM126A i amb TTC7, és la fosfatidilinositol 4-kinassa alfa (PI4KA), i és objecte d'estudi a l'article 2 d'aquesta tesi doctoral, en el que es demostra l'associació també amb una leucodistròfia hipomielinitzant (Verdura and Rodríguez-Palmero *et al.*, 2021). La proteïna DEGS1 (delta 4-desaturase, sphingolipid 1) per la seva banda, potencia l'activació d'AKT, i la seva hipofunció s'associa també a una malaltia hipomielinitzant, tal com es va

evidenciar en una publicació que inclou dos pacients de la cohort objecte d'estudi d'aquesta tesi, en col·laboració amb altres grups de recerca (veure secció Discussió) (Pant *et al.*, 2019).

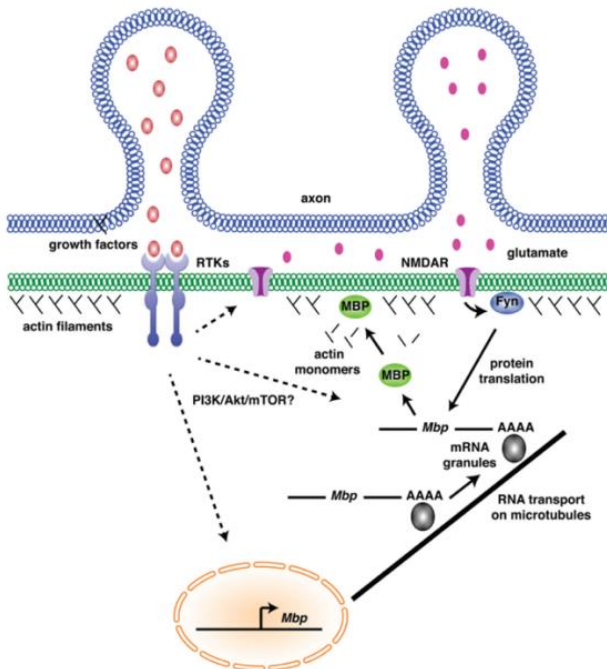


Figura 7. Representació de possibles mecanismes que relacionen l'activitat axonal amb el procés de mielinització. L'activitat elèctrica neuronal s'associa a l'alliberació de factors com Neuregulin-1 (Nrg1) i Brain-Derived Neurotrophic Factor (BDNF), que activen la transcripció de gens de mielina probablement via de senyalització PI3K/Akt/mTOR. A més, promouen l'expressió de receptors NMDA per glutamat, l'activació dels quals afavoreix la producció de MBP, que desencadenà el desacoblament dels filaments d'actina i permet la propagació de la membrana i l'embolcallament de l'axó. De (Hughes and Appel, 2016).

Com s'ha descrit prèviament, les beines de mielina són estructures fonamentalment lipídiques, però també contenen proteïnes fonamentals en la seva estructura. La proteïna bàsica de la mielina (MBP), organitza una xarxa a la superfície de la membrana citosòlica dels oligodendròcits. Actua com una “cremallera”, afavorint l’extrusió del citosol i compactació de les membranes. La 2',3'-cíclic nucleòtid-3' fosfodiesterasa (CNP1), interactua amb el citoesquelet d'actina i realitza una força oposada a la proteïna MBP, per mantenir oberts els canals citoplàsmics. Aquests, són especialment abundants durant el desenvolupament i són bàsics pel creixement de la beina de mielina, permetent la connexió del cos oligodendroglial (on se sintetitza principalment la membrana) amb les diferents capes de la mielina. En etapes posteriors, també permeten la transmissió de metabòlits entre l'oligodendròcit i

l’espai periaxonal. La Proteïna proteolipídica (PLP) és la més abundant de la mielina i contribueix a l’adhesió de les membranes externes entre elles. A més, també en formen part de la beina un seguit de molècules d’adhesió que mantenen la unió a l’axó (Wolf *et al.*, 2021).

Com hem vist prèviament, la mielina és un dels components principals del SNC dels animals vertebrats. Aquestes són les funcions principals en les quals participa:

- **Conducció d’impuls saltatori.** Permet la ràpida transmissió d’informació de forma eficient, amb una reducció del consum energètic de l’axó. Això succeeix gràcies a la conducció saltatòria dels impulsos nerviosos a través dels canals de Na dependents de voltatge agrupats en els nodes de Ranvier, en els que es regenera el potencial d’acció. Aquest mecanisme de conducció permet una major capacitat de processament i complexitat funcional del SNC (Tasaki, 1939; Hartline and Colman, 2007, Cohen *et al.*, 2020a).
- **Suport metabòlic a l’axó** (veure apartat 2.2). L’aïllament de l’axó per part de la beina de mielina comporta, per contra, una dificultat d'accés a l'espai extracel·lular ric en nutrients. Per tant, les cèl·lules glials i la mielina han d'afavorir la transmissió d'aquests metabòlits a l'espai axonal. Per altra banda, el fet que l'axó estigui distanciat del soma neuronal, fa que necessiti el suport de la maquinària enzimàtica de les cèl·lules glials per metabolitzar aquests nutrients.
- **Plasticitat del SNC.** La formació de nova mielina, engruiximent o aprimament de la beina, o la destrucció d'aquesta, són canvis mitjançant els quals l'activitat axonal determina la funcionalitat dels diferents circuits cerebrals, en un mecanisme que participa en la plasticitat cerebral i, per tant, en processos d'aprenentatge (mielinització adaptativa) (Chang *et al.*, 2016; Mount and Monje, 2017).
- **Barrera física entre els axons**, per tal d'evitar l'acoblament dels impulsos elèctrics entre axons adjacents (Nave and Werner, 2021).

- **Eliminació de radicals oxidatius.** Enzims com la superòxid dismutasa citoplàsmica (SOD1), superòxid dismutasa mitocondrial (SOD2), glutatió peroxidases i la catalasa peroxisomal s'encarreguen d'aquesta funció. La formació de gotes lipídiques glials (en anglès, *lipid droplets*) protegeix les neurones del dany oxidatiu (Bailey *et al.*, 2015; Nave and Werner, 2021).

El gruix i longitud de les beines de mielina són proporcionals al diàmetre dels axons a la substància blanca. A la substància grisa, els axons estan menys mielinitzats, probablement perquè aquí la seva funció és el suport metabòlic fonamentalment. Els ODs també estan especialitzats segons l'àrea del cervell en la qual estan localitzats (Wolf *et al.*, 2021).

2.2 Suport energètic en el metabolisme axonal

Un cop la mielinització ha estat completada, la funció principal de les cèl·lules glials passa a ser la de donar suport energètic per permetre la correcta propagació dels impulsos elèctrics i el transport axonal, a més de la participació en processos dinàmics de la mielinització i mecanismes de reparació (Fünfschilling *et al.*, 2012; Lee *et al.*, 2012). La circulació capil·lar és la principal font de substrats d'energia, però a la substància blanca subcortical té aproximadament la meitat de la densitat espacial que a la substància grisa cortical (Hirrlinger and Nave, 2014). Aquest fet, juntament amb l'extrema longitud dels axons, fan que el metabolisme axonal es vegi compromès, donat que els enzims glucolítics són sintetitzats en el soma neuronal (Hirrlinger and Nave, 2014). Aquest problema queda resolt mitjançant la utilització dels enzims de les cèl·lules glials per obtenir l'energia necessària per realitzar les funcions axonals. Els astròcits capten els nutrients dels capil·lars sanguinis a través de les seves extensions que envolten els capil·lars, i els transmeten a altres cèl·lules glials i a l'axó a través de les unions comunicants. També tenen capacitat per acumular glucogen, que poden degradar en condicions de baixa glucosa (Hirrlinger and Nave, 2014). El lactat i piruvat resultants del procés de glucòlisi en els ODs o astròcits, són transferits a l'axó a través dels canals citoplasmàtics situats a les capes de mielina i dels transportadors monocarboxílics (MCT1 i MCT2). A l'axó, s'incorporen al cicle d'àcids tricarboxílics per proporcionar energia

necessària per al correcte funcionament (Fünfschilling *et al.*, 2012; Lee *et al.*, 2012). Alhora, l'OD testa els requeriments energètics de l'axó a través dels receptors NMDA de la capa interna de mielina, que s'activen amb el glutamat que allibera l'axó amb la seva activitat. En resposta a aquest estímul, l'OD expressa nous transportadors GLUT1 per incorporar més glucosa i activar la glucòlisi (Stadelmann *et al.*, 2019; Wolf *et al.*, 2021) (Figura 8). A més, l'OD participa en la hidròlisi de N-acetilaspartat (NAA) neuronal mitjançant l'aspartatacilasa i en la regulació de l'homeòstasi a través de la recaptació d'ions (Moffett *et al.*, 2007; Morrison *et al.*, 2013; Saab *et al.*, 2013).

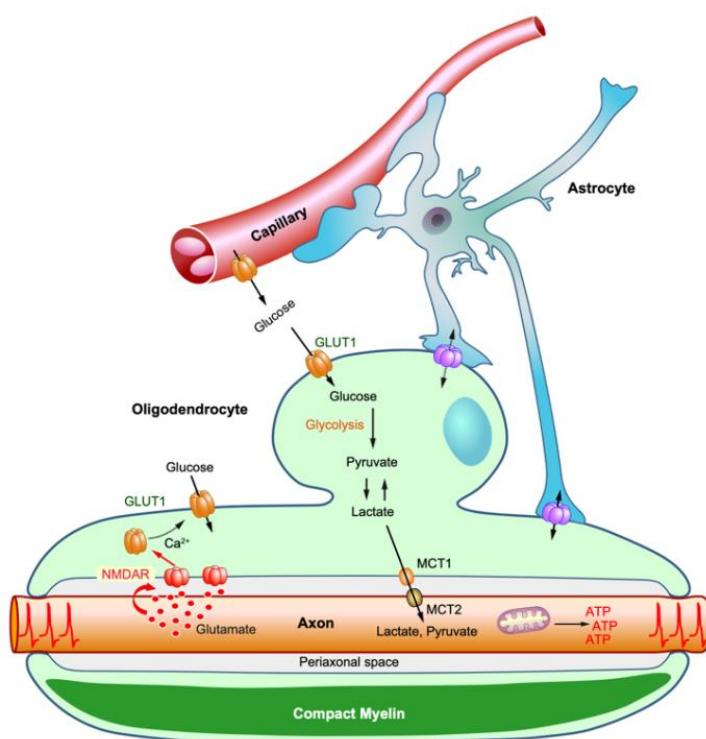


Figura 8. Imatge esquemàtica de l'acoblament metabòlic de les cèl·lules glials i l'axó. L'OD capta la glucosa des de l'espai extracel·lular i l'astròcit des dels capil·lars sanguinis, mitjançant els transportadors GLUT1. Aquesta és transformada en lactat, que es transfereix a l'axó des del mateix OD a través dels transportadors MCT1 i MCT2 o des de l'astròcit en el node de Ranvier. Alhora, les cèl·lules glials estan connectades per les unions comunicants que permeten el transport de metabòlits entre elles. L'activitat axonal produeix l'alliberament de glutamat a l'espai periaxonal, que activa l'expressió de receptors GLUT1 per incrementar la captació de glucosa per part de l'OD. De (Stadelmann *et al.*, 2019).

3. Definició: trastorns genètics de la substància blanca cerebral (GWMDs)

El concepte “leucodistròfia” té el seu origen en les arrels gregues leuco=blanc, dis=manca de, i tràfia=creixement. El va emprar per primera vegada Bielschowsky l'any 1928

(Bielschowsky and Henneberg, 1928), per fer referència a aquells trastorns hereditaris i progressius que es caracteritzaven per una degeneració de la substància blanca cerebral identificada en els estudis anatòmopatològics. Durant els anys vuitanta, es considerava que les leucodistròfies eren malalties genètiques, progressives, que implicaven primàriament la mielina de forma directa o a través de l'afectació dels ODs (Morell, 1984; Seitelberger, 1984). Aquesta definició es va mantenir durant molts anys fins que en el 2015, en un article de consens d'un conjunt d'experts en GWMDs, promogut pel consorci GLIA, es proposà un sistema de classificació incloent un llistat d'unes 30 leucodistròfies “clàssiques”, mentre que la resta de malalties genètiques de la substància blanca es definien com a leucoencefalopaties genètiques (Vanderver *et al.*, 2015). Es consideraven pròpiament leucodistròfies aquells que complien les següents característiques:

- Eren malalties hereditàries de la substància blanca cerebral, amb afectació o no del sistema nerviós perifèric.
- Aquelles que tenien en comú la presència d'anomalies de la mielina pròpiament o de les cèl·lules glials. La neuropatologia es caracteritzava primordialment per l'afectació dels oligodendròcits, astròcits i altres cèl·lules no-neuronals, sense incloure aquelles malalties en les quals l'afectació primària es produeix a les neurones en el còrtex cerebral o altres estructures de la substància grisa.
- Els trastorns del sistema nerviós central adquirits i aquells en els quals l'afectació de la substància blanca apareix en el context d'una malaltia sistèmica, tampoc formaven part d'aquesta categoria.

Aquesta definició admetia que no tots els trastorns de la substància blanca cerebral són progressius, sinó que alguns poden mantenir-se estables en el temps o evolucionar favorablement, tant clínicament com radiològicament. A més, acceptava que les leucodistròfies no tenen el seu origen en els oligodendròcits-mielina únicament, sinó també en altres cèl·lules no-neuronals. No obstant això, en moltes de les malalties de la substància blanca cerebral el coneixement de la fisiopatologia és limitat o aquesta pot ser complexa, amb diversos mecanismes intervenint a l'hora. Per aquest motiu, en molts casos la

diferenciació entre les leucodistròfies clàssiques i les leucoencefalopaties genètiques pot resultar difícil d'establir (Salsano, 2015).

En els darrers anys, la utilització dels estudis WES/WGS ha comportat un increment exponencial en el nombre de gens relacionats amb una afectació predominant de la substància blanca, evidenciant que molts d'ells no estan involucrats directament en els mecanismes de mielinització (com succeeix per exemple amb alguns gens constitutius (*housekeeping genes*)), tot i que produeixen quadres clínics que, per altra banda, complirien la definició de leucodistròfia (Salsano, 2015). Aquests aspectes han conduït al fet que darrerament s'hagi proposat incloure en aquest concepte tots aquells trastorns genètics que afecten principalment la substància blanca cerebral, sense tenir en compte quina és l'estructura o el mecanisme principal i quina sigui la seva evolució (Kevelam *et al.*, 2016; van der Knaap and Bugiani, 2017).

En aquest treball hem utilitzat el concepte “trastorns genètics de la substància blanca cerebral” (en anglès, *Genetic White Matter Disorders*; GWMDs), fent referència a un grup heterogeni de malalties amb un patró de ressonància magnètica suggestiu d’etiologia genètica, que comprèn tant les leucodistròfies com les leucoencefalopaties genètiques (Vanderver *et al.*, 2020b). Es tracta d'un concepte equivalent a la darrera definició proposada de leucodistròfia, però hem preferit evitar aquest terme considerant que pot portar a confusió per haver estat objecte de canvis al llarg de la història, ser imprecís i seguir en constant debat en l'actualitat (Bielschowsky and Henneberg, 1928; Kevelam *et al.*, 2016; van der Knaap and Bugiani, 2017; van der Knaap *et al.*, 2019). Aquests conceptes han de diferenciar-se de “leucoencefalopatia”, que és més genèric i engloba no només els trastorns hereditaris, sinó també aquells que apareixen en context de toxicitat, trastorns immunològics, infecciosos o per dany vascular.

4. Generalitats dels trastorns genètics de la substància blanca cerebral (GWMDs)

Els GWMDs són un conjunt de trastorns molt heterogenis, en els que hi ha implicats mecanismes fisiopatològics molt diversos. La incidència de cada una de les malalties és baixa individualment, però en conjunt s'ha estimat que pot arribar a 1/4733 nadons vius (Soderholm *et al.*, 2020). En un estudi observacional la incidència es va establir en 1/7663 (Bonkowsky *et al.*, 2010), mentre que en altres treballs s'ha calculat en 1.2-2/100.000 nadons vius (Heim *et al.*, 1997; Vanderver *et al.*, 2012).

4.1 Formes clíniques de presentació

L'edat d'inici de les manifestacions clíniques dels GWMDs és molt variable en la majoria dels casos, podent aparèixer des del període fetal fins a la vida adulta. Així i tot, aquesta és una dada que pot ser rellevant per establir una sospita diagnòstica, donat que sol haver-hi una edat característica per moltes de les malalties. Per exemple, l'AGS o la PMD s'inician habitualment al naixement o primers mesos de vida, la KD entre els 6 i 12 mesos, la MLD entre el primer i segon any, mentre que l'X-ALD sol fer-ho entre els 4 i els 10 anys de vida (Bonkowsky and Keller, 2021). En general, les formes hipomielinitzants solen manifestar-se més precoçment (inclusivament en el període neonatal) i cursar amb un retard psicomotor des dels primers mesos de vida, mentre que en les no-hipomielinitzants l'edat d'inici és més variable i quan aquesta és en edats més avançades, poden manifestar-se com una regressió motora.

La presentació clínica en nounats i lactants sol ser en forma d'encefalopatia o retard psicomotor, amb hipotonía inicialment. En l'evolució s'evidencia una afectació predominantment motora, amb espasticitat d'extremitats, tot i que també hi ha manifestacions cognitives acompanyants en la majoria dels casos. A més, pot haver-hi clínica extrapiramidal, en forma de distonia o discinesies principalment, atàxia (característica habitual en la VWMD o la leucodistròfia 4H) o manifestacions oftalmològiques, com nistagme, cataractes o estrabisme. Amb la progressió de la malaltia, l'afectació motora pot

comprometre funcions vitals com són la masticació, deglució i en alguns casos la respiració. Per altra banda, en les formes d'inici més tardà, en l'adolescència i vida adulta, la clínica sol ser més insidiosa i sovint predominen les manifestacions conductuals o psiquiàtriques (van der Knaap *et al.*, 2019; Bonkowsky and Keller, 2021).

Algunes malalties poden cursar amb trets característics, neurològics o extraneurològics, alguns dels quals poden ser claus per obtenir un diagnòstic:

- L'aparició de descompensacions agudes en context de traumatisme o quadre febril és característica de les malalties mitocondrials o la VWMD.
- Els episodis repetits de meningitis recurrents o la limfocitosi persistent en el líquid cefalorraquídi són freqüents a l'AGS.
- L'epilèpsia és prominent a l'AxD, la KD, la MLC, trastorns per acumulació d'àcid siàlic, malalties peroxisomals i a l'acidúria L-2-hidroxiglutàrica. De tota manera, és una manifestació freqüent en general, que està present gairebé en la meitat dels casos de GWMDs.
- La presència d'hipotonía, nistagme rotatori, titubeig cefàlic i en alguns casos estridor, és un quadre clínic suggestiu de la PMD.
- La neuropatia perifèrica és típica de la KD, la MLD o de les malalties mitocondrials, entre d'altres.
- La macrocefàlia és característica de la MLC, la malaltia de Canavan i l'AxD, mentre que la microcefàlia és típica de l'AGS i la leucoencefalopatia amb deficiència d'ARNasa T2 (RNASET2).
- Un canvi de coloració de la pell i l'aparició d'insuficiència adrenal són suggestius de l'X-ALD.
- Els trastorns de la dentició, l'hipogonadisme hipogonadotòfic i la miopia progressiva són característics de les leucodistròfies relacionades amb l'ARN polimerasa III (leucodistròfia 4H).

Pel que fa al pronòstic, per norma general aquest sol ser pitjor en les formes de presentació més precoces que les de l'adolescent o de l'adult. La majoria de malalties tenen un curs progressiu o inclús fatal, però en els darrers anys s'han descrit formes que es mantenen

estables o lentament progressives, com pot succeir en la leucodistròfia megalencefàlica amb quists subcorticals (MLC) tipus 1 i 2, associades a variants en *MLC1* i *HEPACAM*, respectivament (Hamilton *et al.*, 2018), la leucodistròfia amb afectació del tronc cerebral i medul·la espinal i elevació de lactat (LBSL), associada a *DARS2* o la leucoencefalopatia amb afectació talàmica i del tronc de l'encèfal amb hiperlactacidèmia (LTBL), associada a *EARS2* (Lynch *et al.*, 2017; Köhler *et al.*, 2018). Inclús en d'altres pot haver-hi una millora evident amb el pas dels anys, com s'ha reportat recentment en el cas de la leucodistròfia hipomielinitzant 19, produïda per variants en heterozigosi en el gen *TMEM63A* (Yan *et al.*, 2019). També cal destacar que pacients amb una mateixa malaltia poden presentar un curs clínic molt variable, inclús encara que el patró de RM pugui resultar similar, com succeeix en diversos trastorns hipomielinitzants. En resum, podem dir que tot i que resulta difícil establir el pronòstic en molts pacients amb GWMDs, hi ha factors que poden ser orientatius, com són el diagnòstic molecular concret (en aquelles malalties amb evolució més homogènia), l'edat d'inici, la severitat a la presentació, la severitat de la variant genètica i el grau d'afectació a la RM cranial (van der Knaap *et al.*, 2019).

4.2 Classificació dels GWMD

Els trastorns genètics de la substància blanca cerebral poden classificar-se tenint en compte diferents criteris:

- a) Segons el patró d'affectació en els estudis de neuroimatge (Schiffmann and van der Knaap, 2009; Parikh *et al.*, 2015):
 - Hipomielinitzants: aquells que es caracteritzen per una absència o disminució en la producció de mielina. L'estudi de RM mostra una substància blanca lleument hiperintensa de forma difusa en les seqüències potenciades en T2 i hipo-, iso- o hiperintensa en T1.
 - Trastorns No-Hipomielinitzants: aquesta categoria agruparia el que anteriorment s'havia anomenat trastorns desmielinitzants (destrucció de la mielina prèviament formada) i dismielinitzants (desenvolupament anòmal de la

mielina). Es caracteritzen per una hiperintensitat més accentuada en T2 i hipointensitat en les seqüències potenciades en T1. Segons la localització predominant de l'afectació, aquests alhora poden classificar-se en:

- i. Frontal.
- ii. Parieto-occipital.
- iii. Difusa.
- iv. Periventricular.
- v. Tronc de l'encèfal-cerebel.

b) Segons el procés metabòlic principalment implicat (van der Knaap *et al.*, 2019):

- a. Lisosomals.
- b. Peroxisomals.
- c. Mitocondrials.
- d. Trastorns del metabolisme d'aminoàcids i àcids orgànics.
- e. Trastorns de la reparació de l'ADN.
- f. Vasculopaties genètiques.
- g. Defectes de traducció.
- h. Defectes de l'homeòstasi de l'aigua i ions.

c) Segons els estudis d'anatomia patològica (van der Knaap and Bugiani, 2017):

- a. Oligodendròcits-mielina
- b. Astrocitopaties.
- c. Leuco-axonopaties.
- d. Microgliopaties.
- e. Leuco-vasculopaties.

Cal tenir present que en molts dels GWMDs els mecanismes fisiopatològics no són ben coneguts en l'actualitat o les dades d'anatomia patològica són escasses, especialment en aquelles malalties que han estat reportades més recentment. Per tant, aquestes classificacions poden estar subjectes a modificacions segons l'evolució del coneixement. En altres casos la fisiopatologia pot ser complexa i afectar diferents estructures de forma simultània, i per això la inclusió en un grup o un altre pot resultar en certa manera arbitrària.

4.3 Tractament dels GWMDs

En l'actualitat hi ha un gran ventall de possibilitats terapèutiques a considerar en els pacients amb un GWMD. De tota manera, poques han demostrat poder modificar la història natural d'aquestes malalties de forma significativa, així que la majoria s'orienten a la millora de la qualitat de vida dels pacients. L'aplicació en els darrers anys de les tècniques de seqüenciació massiva ha permès la identificació de nous trastorns de la substància blanca cerebral i avançar en el coneixement de la seva fisiopatologia, el que representa un pas fonamental en el desenvolupament de noves estratègies terapèutiques.

El maneig d'aquests pacients ha de ser multidisciplinari, amb una coordinació dels diferents especialistes realitzada habitualment pel pediatre o el neuropediatre. L'equip de rehabilitació ha d'intervenir en el tractament de l'espasticitat i la correcció postural, per aconseguir la millora funcional dels pacients i evitar l'aparició de deformitats. Aquests objectius s'assoleixen mitjançant la fisioteràpia, la teràpia ocupacional i la col·locació d'ortesi o equipament que pugui ajudar a evitar contractures i úlceres per pressió. L'espasticitat pot requerir tractament amb fàrmacs com el baclofèn per via oral o intratecal, injeccions de toxina botulínica o tècniques com la rizotomia dorsal selectiva. A més, és imprescindible que els rehabilitadors i fisioterapeutes participin en la formació dels cuidadors del pacient, per mantenir un correcte posicionament, realitzar exercicis d'estirament o aprendre a identificar possibles complicacions que puguin sorgir al llarg de l'evolució de la malaltia.

Un altre aspecte fonamental és la prevenció i tractament de les infeccions, a través d'una correcta pauta de vacunació, tractaments antibiòtics profilàctics, un maneig adequat dels problemes respiratoris, de la disfunció de bufeta o la instauració d'alimentació per gastrostomia quan sigui necessari, per evitar sobreinfeccions respiratòries. També és important el manteniment d'un bon estat nutricional, el tractament de la disfunció intestinal, de la sialorrea, de la irritabilitat, de les crisis epilèptiques, el maneig adequat del dolor i considerar la introducció de sistemes augmentatius de la comunicació (Adang *et al.*, 2017). No s'ha d'oblidar la importància de la figura del treballador social, dels psicòlegs que puguin donar suport al pacient i els seus familiars, i de l'equip de cures pal·liatives, segons les necessitats de cada cas.

A més d'aquestes mesures genèriques, algunes malalties poden precisar el maneig d'alguns aspectes concrets (van der Knaap *et al.*, 2019):

- Tractament amb suplements d'hidrocortisona per la síndrome d'Addison associada a l'X-ALD o Adrenomieloneuropatia.
- La realització d'una colecistectomia en pacients amb MLD, que tenen tendència a disfunció de la vesícula biliar, i també a l'aparició de pòlips i càncer.
- Prevenció dels traumatismes craneals i maneig adequat dels processos infecciosos que poden desencadenar una descompensació a la VWMD.
- Tractament hormonal substitutiu a la leucodistròfia 4H i tractament de la disfunció ovàrica que pot aparèixer en ovarioleucodistròfies relacionades amb variants patogèniques en els gens que codifiquen per proteïnes del complex eIF2B i en el gen AARS2, principalment.
- Maneig dels problemes immunològics que poden aparèixer associats a l'AGS.

Entre els tractaments encaminats a millorar la història natural de les malalties, cal destacar l'àcid quenodesoxicòlic per la xantomatosi cerebrotendinosa (CTX) i el trasplantament de cèl·lules mare hematopoètiques (HSCT), que ha demostrat la seva eficàcia en el tractament de la forma cerebral de X-ALD, la MLD i la KD (van der Knaap *et al.*, 2019; Bonkowsky and Keller, 2021; Bradbury and Ream, 2021) (Figura 9). En els pacients amb KD, si el trasplantament es realitza en els primers trenta dies de vida, el pronòstic funcional i la supervivència són millors que en aquells realitzats més tard (Duffner *et al.*, 2009). Així i tot, donat el retard en l'inici de l'efecte del trasplantament en el cervell, aquesta opció no és efectiva en el tractament de les formes ràpidament progressives (Page *et al.*, 2019). En la MLD cal tenir present que el HSCT no corregeix l'afectació del sistema nerviós perifèric, que influeix significativament en les dificultats motrius. Pel que fa a l'X-ALD, el pronòstic és millor si el pacient té màxim un símptoma neurològic i una puntuació de Loes per RM menor de 9 (Loes *et al.*, 1994). En el cas de la leucoencefalopatia hereditària difusa amb esferoides (HDLS), associada a variants patogèniques en el gen *CSF1R* (que codifica per una citocina que controla la producció, diferenciació i funció dels macròfags i micròglia), el HSCT pot aportar cèl·lules microglials. Per tant, aquesta és una opció terapèutica raonable, que s'ha dut a terme en casos puntuals amb bona resposta, tot i que l'experiència és encara molt

limitada actualment (Eichler *et al.*, 2016). D'altra banda, cal tenir present que el HSCT comporta un risc de mortalitat que se situa al voltant d'un 20%, que cal sospesar amb els possibles beneficis segons l'estat clínic del pacient en el moment del trasplantament.

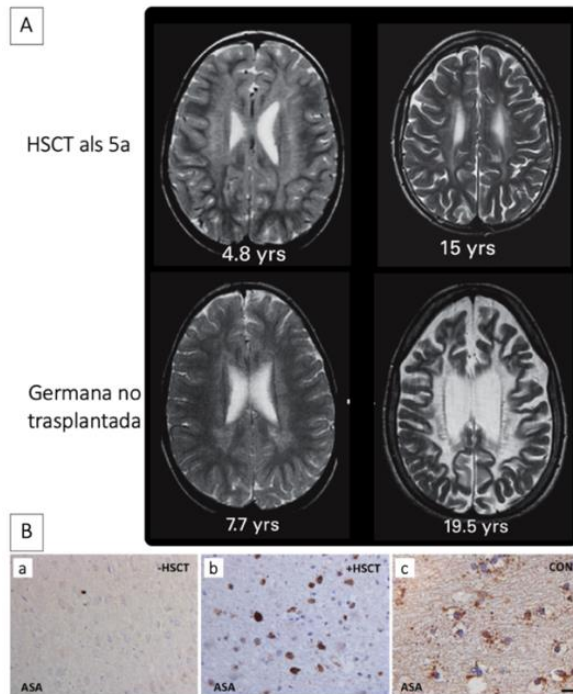


Figura 9. Tractament amb HSCT en pacients amb leucodistròfia metacromàtica (MLD). A. Evolució de l'afectació de la substància blanca cerebral en estudis de RM cranial d'un pacient amb MLD que va ser transplantat als 5 anys, en comparació amb l'evolució de la seva germana no transplantada. B. Expressió d'arilsulfatasa A (ASA) a la substància blanca de pacients amb MLD. Es mostra l'absència d'immunoreactivitat a la substància blanca d'un patient no tractat (a), mentre que es detecta la presència de cèl·lules positives per ASA en un patient tractat amb HSCT, tot i que es limita a cèl·lules morfològicament compatibles amb els macròfags (b). En un control, la tinció està present en tots els tipus de cèl·lules (c). Adaptat de (Krägeloh-Mann *et al.*, 2013) i (Wolf *et al.*, 2020).

Una alternativa a l'HSCT seria la teràpia gènica *ex-vivo*, en la que el trasplantament és autòleg, de cèl·lules modificades genèticament mitjançant vectors lentivirals que induceixen l'expressió del gen d'interès. D'aquesta manera s'elimina la possibilitat de rebuig empelt contra l'hoste i la necessitat de buscar un donant compatible. Aquesta opció ha estat emprada en l'X-ALD i en la MLD, amb resultats favorables pel que fa a increment de l'activitat enzimàtica i evolució funcional en aquesta última (Sessa *et al.*, 2016; Fumagalli *et al.*, 2022). En la MLD també s'han fet estudis per avaluar la teràpia gènica *in vivo*, a través d'un vector viral que s'administra intracerebralment, tot i que els resultats no han estat satisfactoris

(Helman *et al.*, 2015). La tecnologia CRISPR-Cas9 (*clustered regularly interspaced palindromic repeats*- CRISPR-associated protein 9), que permet una edició genètica de precisió per eliminar variants patogèniques o silenciar gens, és una opció terapèutica prometedora, i recentment s'ha publicat un estudi preclínic emprant aquesta tecnologia en cèl·lules de pacients amb MLD (Antony *et al.*, 2022).

Els oligonucleòtids antisentit per silenciar variants amb efecte dominant negatiu s'han estudiat en models de ratolins amb malaltia d'Alexander, PMD, malaltia de Canavan i també per corregir l'efecte d'un splicing anòmal en un model animal d'HEMS (Tantzer 2018). Els tractaments amb microARN, que poden regular l'expressió dels gens, també s'han estudiat en ratolins amb PMD i han demostrat un increment la mielinització i la supervivència (Elitt *et al.*, 2020).

La millora en el coneixement dels mecanismes fisiopatològics d'alguns d'aquests trastorns ha conduït al desenvolupament de tractaments dirigits a la via molecular implicada. Els exemples més coneguts en aquest camp serien la dieta baixa en fenilalanina per la fenilcetonúria o l'àcid quenodesoxicòlic per la xantomatosi cerebrotendinosa. A més, recentment s'ha proposat la utilització dels inhibidors de la quinasa Janus (*Janus Kinase; JAK*), que bloquegen la senyalització de l'interferó tipus I, millorant l'afectació neurològica en pacients amb AGS (Vanderver *et al.*, 2020a). En aquesta mateixa síndrome s'està investigant també el tractament amb inhibidors de la transcriptasa reversa. En la VWMD s'està estudiant el tractament amb guanabenz i en la leucodistròfia associada a *DEGS1*, identificada en context del present treball, també s'està investigant el possible tractament amb fingolimod (FTY720), que va demostrar eficàcia en el model de peix zebra reduint el desequilibri dihidroceramides/ceramides, augmentant el nombre d'oligodendròcits mielinitzants i propiciant una millora en la funció motora (Pant *et al.*, 2019). En el cas de l'X-ALD, l'oli de Lorenzo permet normalitzar els nivells d'àcids grassos de cadena molt llarga en plasma, però no la progressió de la malaltia. Una altra estratègia que està en estudi actualment per la MLD i la KD és la teràpia de reducció de substrat (Hawkins-Salsbury *et al.*, 2015).

El tractament enzimàtic substitutiu administrat per via intratecal, donat que no pot travessar la barrera hematoencefàlica per via intravenosa, és una opció per les malalties lisosomals que poden tenir afectació de la substància blanca cerebral (Fabry, Gaucher, MPS I, II, VI i malaltia de Pompe). En un estudi realitzat en pacients amb MLD, l'administració d'arilsulfatasa A recombinant per via intratecal va aconseguir un efecte dosi-dependènt de millora de la funció motriu i també a nivell bioquímic (Dali *et al.*, 2020).

5. El diagnòstic dels GWMDs

El diagnòstic dels GWMDs en l'actualitat es fonamenta en tres pilars bàsics: l'estudi del patró d'afectació de la substància blanca en les proves de neuroimatge, els estudis metabòlics per la identificació de malalties potencialment tractables i la tecnologia de seqüenciació massiva (NGS) (Parikh *et al.*, 2015).

Les tècniques de diagnòstic basades en la tecnologia NGS estan suposant una revolució en els darrers anys i un canvi de paradigma en l'abordatge diagnòstic. Aquestes, poden permetre assolir un increment de la taxa de diagnòstic, que és bàsic no només per optimitzar el maneig dels pacients, sinó també per conèixer millor l'espectre fenotípic associat a determinats gens i per l'estudi de nous mecanismes moleculars implicats en la fisiopatologia dels GWMDs. Així, aquest és el primer pas necessari per poder desenvolupar teràpies específiques, obrint d'aquesta manera el camí a la medicina genòmica personalitzada (Boycott *et al.*, 2017). El Consorci Internacional de Recerca en Malalties Rares (*International Rare Diseases Research Consortium; IRDiRC*) va establir com a objectiu a assolir entre 2017 i 2027 la següent declaració (Austin *et al.*, 2018):

"All patients coming to medical attention with a suspected rare disease will be diagnosed within one year if their disorder is known in the medical literature; all currently undiagnosable individuals will enter a globally coordinated diagnostic and research pipeline".

A més, segons quina sigui la sospita clínica, pot precisar-se la realització d'estudis neurofisiològics (inclosos EMG/VC, PEVs, PEATs), una evaluació oftalmològica completa o la

realització d'una punció lumbar (en l'AGS és característica la limfocitosi i l'elevació d'INF- α i neopterina p.ex.) entre d'altres, que poden ajudar a completar el fenotip dels pacients i concretar les possibilitats diagnòstiques. En alguns pacients, el quadre clínic o les troballes de neuroimatge poden ser suficientment característics i permetre una orientació diagnòstica (Schiffmann and van der Knaap, 2009; Parikh *et al.*, 2015), però en molts altres l'afectació és més inespecífica, i és en aquests últims en els quals els estudis WES/WGS són valuosos per arribar a un diagnòstic definitiu. En aquests darrers casos, la caracterització fenotípica completa també és fonamental per l'anàlisi i interpretació dels resultats obtinguts en els estudis WES/WGS.

Per altra banda, en els darrers anys diversos estats dels EUA i països com Holanda, han incorporat el cribatge neonatal de l'X-ALD, tal com ha recomanat recentment l'*US Health and Human Services Advisory Committee on Heritable Disorders in Newborns and Children* (<https://www.hrsa.gov/advisory-committees/heritable-disorders/rusp/index.html>). La identificació precoç de l'X-ALD permet la realització d'un trasplantament de cèl·lules hematopoètiques i evitar així una discapacitat significativa o inclús una mort prematura. A més, pot permetre la prevenció de les crisis adrenals. Alguns estats dels EUA, també han iniciat el cribatge de la malaltia de Krabbe (Bonkowsky and Keller, 2021).

5.1 Estudis de Neuroimatge

La ressonància magnètica cranial continua essent l'estudi principal en un pacient amb sospita d'un GWMD. Permet identificar i determinar el patró d'affectació de la substància blanca cerebral, que en alguns casos pot ser característic d'una malaltia específica (Schiffmann and van der Knaap, 2009). Així, la seva incorporació a la clínica durant els anys vuitanta i noranta, va permetre el reconeixement clínic de diverses formes de leucodistròfia. Malgrat això, aquesta valoració té certes limitacions i la seva sensibilitat i especificitat depenen en gran manera de l'entrenament i expertesa del neuroradiòleg, donat que la interpretació és subjectiva en molts casos. Per altra banda, l'especificitat del patró de RM ve determinada també pel moment evolutiu de la malaltia, amb el que una mínima afectació

en estadis inicials pot no ser informativa i, per altra banda, l'afectació extensa en fases molt avançades pot ser també poc específica.

En l'avaluació de la RM cranial en un pacient amb un possible GWMD, cal seguir una metodologia ben establerta i descrita en diverses publicacions (Schiffmann and van der Knaap, 2009; Parikh *et al.*, 2015). En primer lloc, cal determinar si les característiques de l'afectació de la substància blanca són suggestives d'un procés hipomielinitzant o un procés des/dismielinitzant. Com s'ha detallat prèviament (veure apartat 1 i 2.1), la mielinització del SNC s'estableix de forma molt important en els primers dos anys de vida i segueix una evolució ben determinada (Barkovich *et al.*, 1988; Barkovich, 2007). En els estudis de RM, quan la substància blanca no està encara mielinitzada, els temps de relaxació en T1 i T2 són llargs, i mostra un senyal més baix en T1 i més alt en les imatges potenciades en T2. Aquests temps de relaxació s'escurcen amb la mielinització, de forma més ràpida en T1 i més gradualment en T2. Per aquest motiu, les seqüències T1 són especialment útils per demostrar la presència de mielina en els primers 6-8 mesos de vida, mentre que les seqüències T2 reflecteixen millor la quantitat de mielina dipositada i permeten valorar com es completa el procés (Wolf *et al.*, 2021). En un individu adult sa, la substància blanca mielinitzada té un T1 i T2 més curt que la substància grisa. Per tant, es mostra com un senyal més alt que la substància grisa en les imatges potenciades en T1 i un senyal més baix a les imatges potenciades en T2.

En els processos hipomielinitzants, l'afectació de la substància blanca és habitualment difusa, amb una alteració de senyal en T2 habitualment més tènue que en les malalties desmielinitzants, que recorda al que s'observa en la neuroimatge normal d'un lactant petit. Per la seva banda, en les imatges potenciades en T1, la substància blanca resulta hipo-, iso- o hiperintensa respecte a la substància grisa, segons quin sigui el grau de mielinització. Un aspecte fonamental és la diferenciació d'un patró d'hipomielinització permanent, d'un retard de la mielinització, en el que hi ha una mielinització alentida, però que progressa en el temps. Aquest darrer és inespecífic i pot aparèixer en molts pacients amb un retard del desenvolupament. En aquests casos, el patró de la substància blanca pot ser menys homogeni o perxejat, i pot acompañar-se d'atròfia cerebral o anomalies de senyal de ganglis basals i tàlem, que poden ser indicatives d'un trastorn neuronal degeneratiu, com és

el cas de la lipofuscinosi neuronal ceroidea, la malaltia de Menkes o la síndrome d'Alpers, entre d'altres. Per tant, per establir una hipomielinització, és necessària la realització de dues RM amb un interval de temps significatiu. Aquesta pot definir-se com un patró de dèficit de la mielinització que no canvia en dues ressonàncies magnètiques realitzades amb almenys sis mesos de diferència en un nen major d'un any. En general, es pot establir que si hi ha un patró de dèficit de mielinització sever en nens de més de dos anys, és molt poc probable que evolucioni en el temps i podem establir un trastorn hipomielinitzant (Schiffmann and van der Knaap, 2009; Steenweg *et al.*, 2010; Harting *et al.*, 2020; Wolf *et al.*, 2021).

En segon lloc, és important determinar si les anomalies de la substància blanca cerebral són confluents, o aïllades i multifocals. En la majoria de les leucodistròfies el patró d'afectació sol ser bilateral, confluent i simètric, mentre que en els trastorns adquirits o de base immunològica soLEN ser més multifocals. Malgrat això, hi ha diverses excepcions a aquesta norma, com algunes malalties mitocondrials, l'acidúria L-2-hidroxiglutàrica, la LBSL, les mucopolisacaridoses, la galactosèmia, les anomalies cromosòmiques o alguns casos de HDLS o AxD, on pot haver-hi una afectació asimètrica. Al contrari, l'affectació de substància blanca posthipòxica, tòxica o associada a HIV, pot ser bilateral i simètrica (Schiffmann and van der Knaap, 2009).

En tercer lloc, la localització predominant de l'affectació (frontal, parieto-occipital, periventricular, subcortical, difusa o de fossa posterior) pot ajudar a orientar les possibles causes moleculars (Schiffmann and van der Knaap, 2009; Parikh *et al.*, 2015) (Figura 10).

Finalment, altres característiques de la neuroimatge poden ser suggestives de diagnòstics concrets (Figura 10):

- La rarefacció difusa de la substància blanca és característica de la VWMD, mentre que els quists ben definits a l'interior de la substància blanca anòmala poden veure's a les malalties mitocondrials, a l'AxD (de predomi frontals) i a la MLC (característicament temporals).
- La inflamació de la substància blanca anormal és una característica de la MLC, la VWMD o l'AxD, principalment.

- La captació de contrast pot ser suggestiva de malalties com l'X-ALD, malalties mitocondrials o l'AxD.
- La presència de dipòsits de calci és característica de l'AGS o la malaltia de Cockayne, per exemple. En l'estudi de RM cranial s'identifiquen mitjançant la seqüència eco gradient en T2 o seqüències per susceptibilitat magnètica (SWI), tot i que de vegades pot ser necessària la realització d'una TC cranial per la seva confirmació.
- En alguns casos de GWMDs, s'evidencia una afectació destacable de la substància grisa acompañant, que pot ser en forma de displàsia cortical com en el cas de les malalties peroxisomals o algunes distròfies musculars, o en forma d'atròfia cortical com en el cas d'AGS, probablement associada a degeneració axonal i pèrdua neuronal secundària. En els trastorns degeneratius amb afectació predominantment neuronal, l'atròfia cortical s'aprecia habitualment més precoçment i és més severa que la dels trastorns primaris de la substància blanca.
- L'afectació del tronc de l'encèfal i medul·la és característica de malalties mitocondrials o AxD, entre d'altres.
- En el context d'un trastorn hipomielinitzant, el senyal baix dels tàlems laterals en T2 orienta a una leucodistròfia 4H, l'atròfia del putamen a una malaltia H-ABC, mentre que l'alteració de senyal de la part lateral del cap del caudat és patognomònica de la leucodistròfia hipomielinitzant 14, associada a variants en el gen *UFM1* (Hamilton *et al.*, 2017).

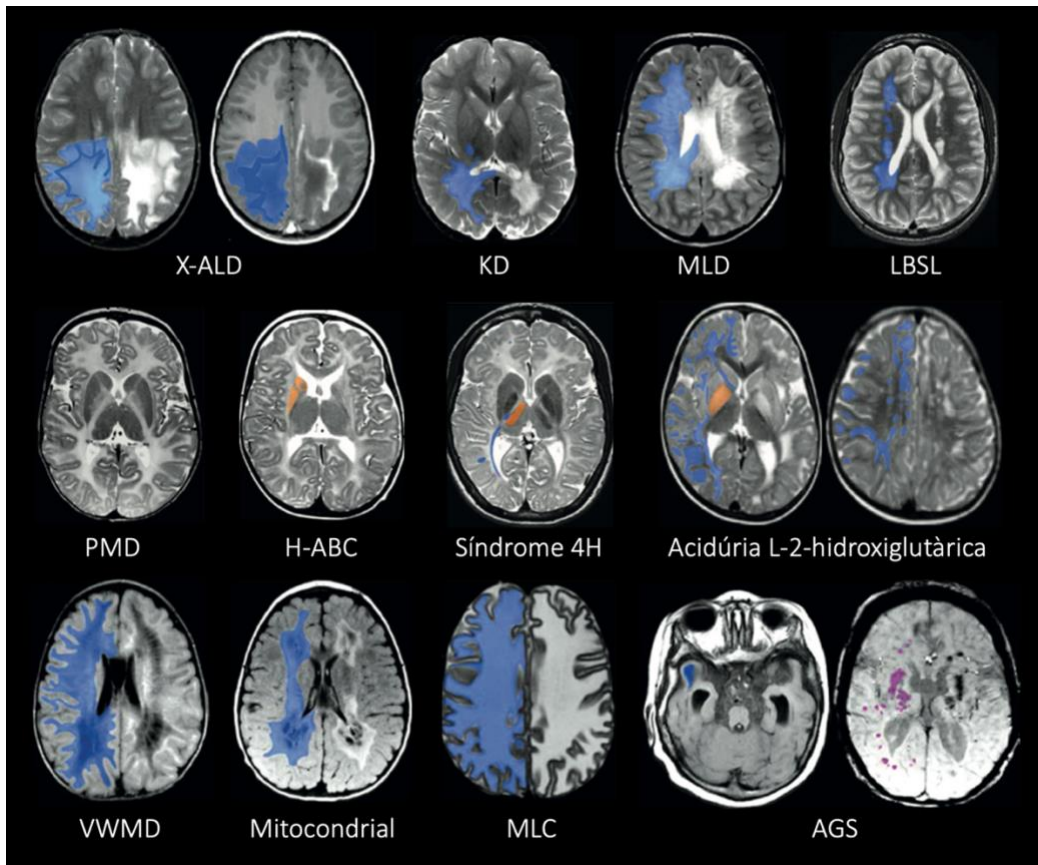


Figura 10. Distribució de l'affectació de la substància blanca i característiques particulars d'alguns dels principals GWMDs. X-ALD, adrenoleucodistròfia lligada al cromosoma X: afectació de substància blanca de predomini posterior, amb un realç en anell amb l'administració de contrast. KD, malaltia de Krabbe: afectació de la substància blanca periventricular posterior i de la substància grisa profunda. MLD, leucodistròfia metacromàtica: afectació de la substància blanca periventricular de forma difusa, amb patró tigrat característic. LBSL, leucodistròfia amb afectació del tronc de l'encéfal, medul·la i elevació de lactat: afectació no homogènia de la substància blanca periventricular. PMD, malaltia de Pelizaeus-Merzbacher: hipomielinització difusa. H-ABC, hipomielinització amb atròfia de ganglis basals i cerebel: patró d'hipomielinització amb atròfia del putamen. Síndrome 4H: hipomielinització amb senyal baix en T2 dels tàlems laterals. Acidúria L-2-hidroxiglutàrica: afectació multifocal de la substància blanca de predomini subcortical. VWMD, malaltia de la substància blanca evanescent: afectació difusa de la substància blanca amb rarefacció d'aquesta. Malalties Mitocondrials: la presència de quists ben definits a la substància blanca afecta és característica d'aquests trastorns. MLC, leucodistròfia amb megalencefàlica i quists subcorticals: presència d'inflamació difusa de la substància blanca. AGS, síndrome d'Aicardi-Goutières: és característica la presència de quists subcorticals temporals i dipòsits de calci que s'aprecien a les seqüències per susceptibilitat magnètica (SWI). Adaptat de (van der Knaap *et al.*, 2019).

5.2 Estudis genètics en el procés diagnòstic dels GWMDs

5.2.1 Història dels estudis genètics. Aproximació diagnòstica “clàssica”

L'any 1953, Watson i Crick van determinar l'estructura de l'ADN basant-se en la cristal·lografia fonamental de l'ADN i el treball de difració de raigs X de Rosalind Franklin. En el 1977, Frederick Sanger i els seus col·laboradors van desenvolupar la seqüenciació basada en el mètode de terminació de cadena, que consisteix en la incorporació selectiva de dideoxinucleòtids que finalitzen la cadena per part de l'ADN-polimerasa durant la replicació *in vitro* de l'ADN; aquest és el mètode més utilitzat per a la detecció de variants d'un sol nucleòtid (*Single Nucleotide Variants*; SNVs) i considerat *Gold Standard* fins a l'actualitat (Wright *et al.*, 2018).

Posteriorment, l'any 1986, es va generar el primer seqüenciador automàtic d'ADN, en el que va suposar l'inici d'una etapa amb un gran desenvolupament de les plataformes de seqüenciació. Per altra banda, a principis dels anys noranta va aparèixer la tecnologia FISH (*fluorescence in situ hybridisation*), que permetia identificar delecions submicroscòpiques de 40-300 kb a les regions adjacents als telòmers.

L'aproximació diagnòstica “clàssica” emprada fins a l'actualitat, basada en la realització de proves complementàries de forma seqüencial, inclou bàsicament dos tipus de proves des del punt de vista genètic: estudis dirigits d'alta resolució per un gen concret (seqüenciació Sanger) i estudis citogenètics (cariotip, amb una resolució de 5-7 Mb, i cariotip molecular basat en tecnologia de *microarrays* genòmics, amb resolució de 50-100 kb). Malgrat aquests desenvolupaments, sovint resulta difícil arribar a un diagnòstic molecular en els pacients amb un GWMD, per diferents motius:

- La freqüent inespecificitat del quadre clínic i patró d'afectació en l'estudi de RM.
- La gran heterogeneïtat genètica associada als GWMDs.
- La gran variabilitat fenotípica associada a molts dels gens implicats, que pot venir determinada per l'heterogeneïtat de locus i al·lèlica, la presència de variants genètiques en un o més altres locus (modificadors) i per factors ambientals (Wright *et al.*, 2018).

5.2.2 Estudis genòmics. Seqüenciació de nova generació

L'any 1990 es va iniciar un projecte ambiciós internacional que tenia com a objectiu determinar la seqüència de parells de bases que conformen l'ADN humà i la identificació i mapatge dels gens que s'hi inclouen: era el Projecte del Genoma Humà, que no es va completar fins al 14 d'abril de l'any 2003, en el que va suposar el projecte col·laboratiu de biologia més gran desenvolupat fins al moment (Abdellah *et al.*, 2004). Es va calcular que el cost de la seqüenciació completa en aquella època va ser de més de 2 bilions de dòlars. Aquest projecte va establir les bases pel desenvolupament de la tecnologia *Next-Generation Sequencing* (NGS), que permet la seqüenciació massiva en paral·lel de milions de seqüències simultàniament en un marge de temps curt, i posteriorment l'aparició de plataformes de seqüenciació comercials a partir de l'any 2005. En els darrers anys, amb les millors tècniques i l'abaratiment de costos de forma progressiva, estem vivint l'expansió d'aquesta tecnologia des del camp de la recerca al de la pràctica clínica, amb un cost de la seqüenciació d'un genoma complet que pot ser, actualment en el nostre entorn, menor a 1.000 euros.

L'any 2012, l'*American College of Medical Genetics and Genomics* (ACMG), va publicar unes guies fent referència a les situacions en què s'hauria de considerar la realització d'un estudi WES o WGS, en les que s'establien els següents punts principals (ACMG Board of Directors, 2012):

- En aquells pacients amb sospita d'un trastorn genètic, però en els quals el fenotip no és identifiable.
- En pacients en els quals la presentació clínica correspon a una síndrome amb múltiples causes genètiques possibles.
- En pacients en els quals s'han testat els gens que poden correspondre al fenotip, però no s'ha pogut determinar una causa molecular.

5.2.2.1 Tècnica de la seqüenciació massiva i metodologia diagnòstica

El procés d'un estudi de seqüenciació massiva comença amb l'extracció de l'ADN de les cèl·lules de l'individu, habitualment de glòbuls blancs de sang perifèrica. Posteriorment, aquest ADN es fragmenta i es prepara la llibreria, que en el cas del WES inclou un procés d'enriquiment per capturar únicament la informació de totes les regions que codifiquen proteïnes, així com les regions limítrofes amb els introns (Mardis, 2008; Ansorge, 2009). Finalment, els fragments d'ADN d'entre 50 i 150 parells de bases de llargària, són alineats i es comparen amb una seqüència referència de genoma humà mitjançant eines bioinformàtiques (Thiffault and Lantos, 2016). En aquesta tècnica, cada nucleòtid de l'ADN del pacient se seqüencia entre 50 i 150 vegades de mitjana (segons la cobertura), per tal d'assegurar la precisió de l'estudi.

Les variants resultants són classificades segons la seva freqüència, tipus i conseqüència d'acord amb els predictors *in silico*, patró d'erència, reports previs de patogenicitat i associació establecida amb el fenotip del pacient. En el cas de les malalties minoritàries, únicament es tenen en compte aquelles variants que tenen una baixa o nul·la freqüència a la població general. Per seleccionar variants que puguin causar les manifestacions clíniques del pacient, la informació clínica es codifica en termes HPO (*Human Phenotype Ontology*), un sistema que atribueix un codi numèric a les diferents característiques del pacient, per tal d'homogeneïtzar i estandarditzar la informació i que aquesta sigui intel·ligible per les plataformes bioinformàtiques (Robinson *et al.*, 2008; Köhler *et al.*, 2014; Haendel *et al.*, 2018)

L'any 2015, l'*American College of Medical Genetics and Genomics-Association for Molecular Pathology* (ACMG-AMP) va desenvolupar unes guies per la interpretació de les variants genètiques, que van suposar un gran salt qualitatiu a l'hora d'analitzar els resultats dels estudis genòmics, tot i que encara s'estan redefinint en l'actualitat. En elles s'estableixen uns criteris que permeten establir el grau d'evidència de patogenicitat de cada una de les variants, classificant-les en: patogèniques (*Pathogenic*, P; 95% de probabilitat), probablement patogèniques (*Likely Pathogenic*, LP; 90% de probabilitat), variants de significat incert (*variants of Unknown Significance*, VUS; 50% de probabilitat), probablement

benignes (*Likely Benign*, LB) i benignes (*Benign*, B) (Richards *et al.*, 2015b; Amendola *et al.*, 2016).

En molts dels casos, un cop establertes les variants candidates, és necessari revisar la informació clínica descrita prèviament associada als gens identificats en bases de dades com poden ser OMIM, Orphanet o DECIPHER, per valorar la correlació amb el fenotip del pacient. En aquest punt, els clínics tenen un paper determinant a l' hora d'establir el diagnòstic definitiu. També és fonamental revisar si la (o les) variants identificades representen una explicació completa del fenotip del pacient o solament parcial, el que justificaria buscar una altra variant que pugui ser responsable de la resta de manifestacions. En estudis previs, la detecció de més d'una malaltia genètica responsable del quadre clínic del pacient s'ha calculat en un 5% de casos aproximadament (Wright *et al.*, 2015; Posey *et al.*, 2017). En altres ocasions, caldrà reavaluar la clínica i les proves complementàries realitzades fins al moment o considerar la realització de nous estudis bioquímics o metabòlics per confirmar la relació causal. A més, en el cas d'estudis de cas índex (no trio), caldrà determinar si la (o les) variants identificades en el proband estan presents també en els progenitors o altres familiars afectats per determinar el patró d'herència (estudi de cosegregació). Els estudis de seqüenciació massiva tenen una molt bona sensibilitat i resulten especialment útils per la detecció de variants en heterozigosi i en mosaic, en comparació amb la seqüenciació per Sanger (Cheng *et al.*, 2014). Per aquest motiu, es considera que en l'actualitat no és necessària la validació mitjançant aquesta tècnica de les variants identificades en estudis de NGS (Beck *et al.*, 2016).

Les variants de significat incert i aquelles patogèniques en gens encara no associats a malaltia en humans, requeriran la realització d'estudis funcionals i la identificació d'altres pacients mitjançant plataformes com GeneMatcher (<https://genematcher.org/>) o MatchMaker Exchange (<https://www.matchmakerexchange.org/>) per determinar la seva patogenicitat. Aquestes plataformes permeten l'intercanvi d'informació clínica i genètica amb altres professionals d'arreu del món, el que és fonamental per definir noves entitats clíniques, avançar en el coneixement i en l'assistència dels pacients amb malalties genètiques (ACMG Board Of Directors, 2017).

5.2.2.2 Panells, WES o WGS?

El genoma humà conté 3,2 bilions de parells de bases, que s'organitzen de tal manera que constitueixen al voltant de 20.000 gens. Només un 1-2% del genoma codifica per proteïnes i és el que anomenem exoma, tot i que es calcula que al voltant d'un 85% de les variants conegeudes actualment o potencialment causants de malaltia, estan localitzades en aquestes regions.

Segons quina sigui la malaltia a estudiar, el context en el qual es realitza l'estudi (recerca o aplicació clínica) i els recursos disponibles, podem optar per la realització de diferents tècniques de seqüenciació. Així, en alguns casos en els quals el fenotip del pacient pugui resultar de variants en un grup reduït de gens ben definits, podríem optar per la realització d'un panell de gens, en el qual s'analitzen únicament els associats al fenotip en qüestió. Aquests poden incloure de dos a dos mil gens segons el disseny i la seva anàlisi és més fàcil, més ràpida i evita la possibilitat de troballes incidentals. Per altra banda, però, en molts trastorns neurològics la sensibilitat d'aquesta prova es veu reduïda per l'heterogeneïtat genètica i la ràpida descripció de noves entitats, el que ocasiona que aquests panells puguin quedar desfasats en poc temps. En altres situacions, optarem per la seqüenciació de tots els exons dels més de 4.000 gens associats a malalties monogèniques actualment (exoma clínic) o la seqüenciació de l'exoma o genoma complets (WES o WGS respectivament), que permeten la identificació de variants en gens no associats prèviament a patologia. En general, podem afirmar que els estudis que cobreixen més gens tenen més sensibilitat, però menys especificitat, requereixen un major coneixement per la seva anàlisi i augmenten les possibilitats de troballes genètiques incidentals (no relacionades amb el fenotip que motiva l'estudi) i, per tant, de conflictes ètics. Així i tot, l'estudi WGS té avantatges respecte a WES i la resta de tècniques:

- Cobertura més homogènia de les regions exòniques, especialment de les regions riques en GC (Belkadi *et al.*, 2015; Meienberg J, Bruggmann R, Oexle K, 2016). A més, WGS té menys dispersió en la distribució de la cobertura de l'al·lel, permetent una major precisió a l'hora de detectar posicions en heterozigosi en comparació amb WES (Lelieveld *et al.*, 2015).

- Capacitat d'identificar variants en regions intròniques i intergèniques.
- Disminució d'artefactes de la PCR en la preparació de llibreries.
- Millor capacitat per la detecció de variants de nombre de còpies (CNVs), donat que aquelles que són més petites de tres exons amb freqüència no es detecten a través de WES (Gambin *et al.*, 2017). És inclús millor que WES i aCGH per la detecció de CNVs i reordenaments cromosòmics balancejats (Dong *et al.*, 2018; Bertoli-Avella *et al.*, 2021).
- Les dades de WGS poden analitzar-se per detectar expansions de triplets (Dolzhenko *et al.*, 2017).
- WGS inclou l'ADN mitocondrial, i permet la identificació de variants en el mateix (Calvo *et al.*, 2012; Meienberg J, Bruggmann R, Oexle K, 2016).
- Possibilitat d'utilitzar protocols que permetin produir un genoma amb fase, el que pot ser útil per diferenciar quan les variants en el cas d'un trastorn d'erència recessiva estan en cis- o trans-, sense precisar l'estudi d'altres membres de la família per determinar-ho (Mostovoy *et al.*, 2016).
- Reducció del temps per obtenir resultats. Això resulta especialment interessant en pacients crítics, en els quals establir un diagnòstic pot ajudar a la presa de decisions. En aquest context, el resultat d'un estudi WGS ultra ràpid el podem determinar en un termini de pocs dies (Saunders *et al.*, 2012; Petrikin *et al.*, 2015; Willig *et al.*, 2015; Meng *et al.*, 2017; Gu *et al.*, 2020; Stark and Ellard, 2022).

Per tots aquests motius, el rendiment diagnòstic de WGS ha demostrat ser més alt que el d'altres tècniques com serien aCGH i WES en l'estudi de pacients amb discapacitat intel·lectual severa (Gilissen *et al.*, 2014), trastorns del neurodesenvolupament (Soden *et al.*, 2014; Stavropoulos *et al.*, 2016), encefalopatia epilèptica precoç (Ostrander *et al.*, 2018) o nounats ingressats en una unitat de crítics (Saunders *et al.*, 2012; Willig *et al.*, 2015), i probablement en un futur pròxim serà la tècnica de diagnòstic genètic d'elecció.

5.2.2.3 Limitacions dels estudis NGS

Els estudis de NGS permeten la seqüenciació simultània d'una gran quantitat d'informació genètica i, precisament per aquest motiu, una de les grans dificultats que comporten és la seva interpretació. En un estudi WES, podem trobar de l'ordre de 20.000 a 25.000 variants genètiques per individu respecte al genoma de referència, mentre que en un estudi WGS, aquesta xifra pot arribar als 4-5 milions. La majoria d'aquestes variants són comunes a la població general i benignes. Per això, per l'estudi de malalties rares caldrà un procés de filtratge per seleccionar aquelles que siguin poc freqüents a la població general, deletèries i que puguin associar-se al fenotip del pacient.

En el cas de l'exoma clínic o l'estudi WES, que són les tècniques més utilitzades a la pràctica clínica en l'actualitat, hi ha limitacions metodològiques ben conegudes. Aquestes comprenen dificultats per la identificació de variants del nombre de còpies, de variants estructurals (grans insercions, delecions, inversions, translocacions), d'expansions de triplets, per la identificació de variants del genoma mitocondrial, una cobertura desigual de regions exòniques i evidentment escassa cobertura de les intròniques, l'aparició d'artefactes de la PCR durant la preparació de la llibreria i una profunditat de seqüenciació desigual. En el cas de l'exoma clínic, a més, la limitació intrínseca del fet que no permet la identificació de nous gens que puguin associar-se a patologia (Meienberg J, Bruggmann R, Oexle K, 2016). A més, la interpretació d'aquests estudis depèn de la qualitat de les bases de dades poblacionals que s'utilitzen com a referència de freqüència de les variants a la població general (com són GnomAD o 1000 genomes project) i de la fiabilitat dels predictors *in silico*. Per altra banda, els informes clínics d'aquests estudis habitualment se centren en aquelles variants que afecten gens associats a malaltia minoritària. Així i tot, al voltant d'un 70% dels gens i regions reguladores tenen una funció desconeguda en l'actualitat, pel que les seves variants no es reporten habitualment, tot i que podrien també ser causants de malaltia o influir en el fenotip del pacient (Quintana-Murci, 2016; Boycott *et al.*, 2017).

La seqüenciació d'una gran quantitat de gens de forma simultània comporta també la capacitat de detectar variants genètiques no associades al motiu de consulta del pacient, però que poden tenir implicacions per la salut de l'individu o la família, amb el consegüent

conflicte ètic. L'ACMG va establir un llistat de malalties accionables que havien de ser reportades en cas que es detectessin variants patogèniques o probablement patogèniques (Green *et al.*, 2013; Kalia *et al.*, 2017; McGurk *et al.*, 2021). Aquesta situació és especialment complexa en el cas de pacients pediàtrics, donat que no tenen competència legal per prendre decisions (Bick *et al.*, 2019). A més, cal tenir present que aquests estudis poden desvetllar consanguinitat familiar o conflictes de paternitat.

Finalment, cal considerar que, tot i que el cost econòmic de la tècnica ha disminuït de forma significativa en els darrers anys, la interpretació dels resultats representa una important càrrega de treball per l'equip bioinformàtic, genetistes i també, en molts dels casos, dels professionals clínics que hauran d'establir la correlació amb el fenotip del patient. Per tant, l'anàlisi dels resultats comporta uns recursos que també haurien de tenir-se en compte a l'hora d'avaluar la relació cost-benefici d'aquesta tecnologia.

5.2.2.4 Aproximació diagnòstica mitjançant WES o WES seguint estratègia d'estudi del cas índex o trio?

La majoria d'estudis publicats utilitzen l'estratègia d'anàlisi per trios, el que significa seqüenciar el cas índex i els dos progenitors, i analitzar les dades obtingudes conjuntament. D'aquesta manera s'eliminen fàcilment les variants rares benignes familiars, es facilita la identificació de variants *de novo* i permet determinar la fase de les variants en trastorns recessius o d'*imprinting*. Es considera que l'anàlisi de trios permet reduir en 10 vegades el nombre de variants a considerar i d'aquesta manera reduir el temps d'anàlisi, augmentant en un 50% el rendiment diagnòstic de l'estudi (Fitzgerald *et al.*, 2015; Wright *et al.*, 2015, 2018).

En 2016, l'estudi WGS costava aproximadament tres vegades més que un WES, i era per tant equivalent a un estudi WES trio. Però la facilitat més gran d'anàlisi del trio, conjuntament amb les limitacions en el coneixement actuals, que dificulten la interpretació de variants en regions no codificant, fan que actualment WES trio pugui superar al WGS. Malgrat això,

aquesta situació molt probablement canviarà en un futur pròxim, el que potenciarà la utilització de WGS.

5.2.2.5 Aplicació dels estudis de seqüenciació massiva en el procés diagnòstic de pacients amb diferents grups de patologia

En l'actualitat hi ha projectes a gran escala que estan avaluant la utilitat clínica del WES/WGS, com són l'*Undiagnosed Diseases Network* (UDN) (Splinter *et al.*, 2018) i el *100.000 Genomes Project* (Barwell *et al.*, 2018). En el cas de l'UDN, impulsat des del *National Institutes of Health* (NIH), es va publicar un estudi que recollia dades de 382 pacients amb una avaluació completa, incloent-hi un 40% amb simptomatologia neurològica. El rendiment diagnòstic global va ser del 35%, quinze pacients van diagnosticar-se a través de la revisió clínica, mentre que el rendiment diagnòstic dels estudis WES i WGS va establir-se en un 28 i 19%, respectivament. El diagnòstic d'aquests pacients va conduir a canvis en el tractament en un 21%, a canvis en el procés diagnòstic en un 37% i a un consell genètic específic en un 36%. A més, aquest protocol d'estudi va permetre identificar 31 noves síndromes (Splinter *et al.*, 2018). Per altra banda, en el *100.000 Genomes Project*, el rendiment diagnòstic mig del WGS va ser del 25%, arribant al 40-55% en grups de patologies com és la discapacitat intel·lectual. Va permetre descriure tres malalties noves i 19 noves associacions pendents de confirmar, mentre que van calcular que en un 25% dels casos el diagnòstic va conduir a decisions clíniques rellevants pels pacients o les seves famílies. Un 15% dels diagnòstics corresponien a variants en regions no codificant o del genoma mitocondrial, expansions de triplets, canvis estructurals o en regions amb baixa cobertura a l'exoma, el que reforçava el valor del genoma (Smedley *et al.*, 2021). En un altre estudi, incloent-hi pacients amb trastorns del neurodesenvolupament, el rendiment diagnòstic va ser del 45% i l'obtenció d'un diagnòstic va comportar canvis en el maneig clínic en un 49% dels pacients (Soden *et al.*, 2014).

El rendiment de WES en estudis realitzats en diferents grups de patologies varia entre el 10 i el 70% (Yang *et al.*, 2014; Vissers *et al.*, 2017; Wright *et al.*, 2018) (Figura 11; Taula 1, pàgina 196). En una meta-anàlisi incloent 20.068 pacients pediàtrics amb probables trastorns

genètics, el rendiment diagnòstic va ser del 36% mitjançant WES i 41% per WGS, amb un rendiment de WGS en casos prèviament negatius per WES, del 29% (Clark *et al.*, 2018). En aquest estudi es va evidenciar un augment significatiu de rendiment diagnòstic mitjançant l'estudi de casos trio. Un altre estudi, incloent-hi 1.007 pacients amb diferents tipus de patologia (principalment neurològica, però també malformativa, esquelètica o muscular entre d'altres) estudiats per WGS, va mostrar un rendiment diagnòstic del 21,1%, sense diferències significatives entre els casos estudiats només en cas índex i els trios, tot i que l'estudi trio va permetre disminuir el nombre de sospites diagnòstiques associades a variants VUS (Bertoli-Avella *et al.*, 2021).

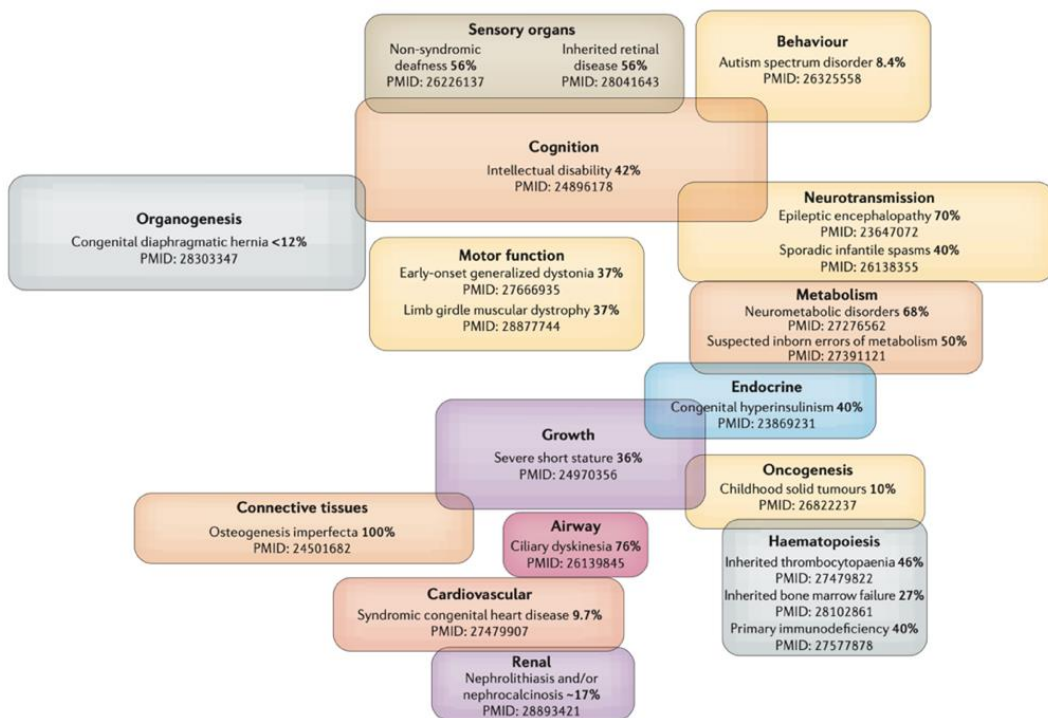


Figura 11. Taxa diagnòstica del WES en diferents grups de patologies. De l'article (Wright *et al.*, 2018).

La utilitat clínica directa de la implantació d'aquesta tecnologia és particularment evident en el cas de l'estudi de cohorts de pacients en estat crític, ingressats en unitats de cures intensives neonatales i pediàtriques. En aquests casos, obtenir un diagnòstic a temps per poder prendre decisions en relació amb el maneig dels pacients és fonamental i s'ha reportat una resposta fins i tot en solament 13 hores (Owen *et al.*, 2021). Fins al moment, s'han publicat més de 20 estudis incloent al voltant de 1500 pacients en aquest context clínic i s'ha

reportat un rendiment diagnòstic global de WES/WGS del 37%. El més important, però, és el fet que aquests diagnòstics comporten un canvi en el maneig (evitar proves complementàries o procediments quirúrgics, iniciar tractaments específics en alguns casos o instauració de mesures pal·liatives) en un 20-100% dels pacients diagnosticats (Willig *et al.*, 2015; Farnaes *et al.*, 2018; Stark and Ellard, 2022).

Finalment, diversos estudis han demostrat que la implantació dels estudis de seqüenciació massiva en el procés diagnòstic dels pacients pot comportar una optimització en el cost-benefici, tenint en compte que l'abordatge diagnòstic "clàssic" representa un cost molt elevat pel sistema sanitari (Sabatini *et al.*, 2016; Tan *et al.*, 2017). Per tant, en diversos treballs s'ha plantejat la possibilitat d'implantar WGS com a estudi de primer nivell en el procés diagnòstic de pacients amb sospita de malaltia genètica d'erència mendeliana (Stavropoulos *et al.*, 2016; Farnaes *et al.*, 2018; Lionel *et al.*, 2018).

II. JUSTIFICACIÓ I HIPÒTESI

Els GWMDs són un conjunt de trastorns heterogeni, caracteritzats per l'afectació selectiva de la substància blanca cerebral, en els quals s'han identificat més de cent causes genètiques. El quadre clínic i el patró d'afectació en els estudis de neuroimatge, són inespecífics en una proporció considerable dels casos. Com a resultat, l'abordatge diagnòstic "clàssic" dels GWMDs emprat fins els darrers anys, basat en els estudis genètics dirigits a partir de la sospita clínica, permet assolir el diagnòstic molecular en només la meitat dels pacients (van der Knaap *et al.*, 1999; Bonkowsky *et al.*, 2010; Steenweg *et al.*, 2010; Vanderver *et al.*, 2012; Kevelam *et al.*, 2016).

Els estudis basats en la tecnologia NGS han esdevingut una eina eficaç pel diagnòstic molecular de malalties rares, especialment en aquelles amb una gran heterogeneïtat genètica. En els darrers anys, s'han publicat diversos treballs que han demostrat la seva utilitat en aquest context (Fogel *et al.*, 2014; van de Warrenburg *et al.*, 2016; Splinter *et al.*, 2018; Smedley *et al.*, 2021) (veure Taula 1 a la secció Discussió). Pel que fa als GWMDs, durant els anys que ha durat aquesta tesi també s'han publicat treballs que reporten el bon rendiment dels panells de gens (Cohen *et al.*, 2020b), el WES (Vanderver *et al.*, 2016) i el WGS (Helman *et al.*, 2020). Així i tot, aquests estudis inclouen únicament població pediàtrica i la majoria han estat realitzats mitjançant l'anàlisi de trios (estudiant conjuntament les dades de seqüenciació del cas índex i els dos progenitors).

Per tant, en aquesta tesi doctoral, plantegem les següents hipòtesis de treball:

1. Els estudis WES i WGS duts a terme en casos índex de qualsevol edat amb GWMDs, interpretats mitjançant una eina computacional de creació pròpia, que prioritza les variants genètiques integrant la informació clínica i de bases de dades d'interacció física i funcional de les proteïnes de l'organisme, permeten assolir un alt percentatge de diagnòstics.
2. Les tècniques WES i WGS permeten escurçar el temps necessari per aconseguir un diagnòstic, respecte a l'abordatge diagnòstic "clàssic".
3. Els estudis WES i WGS permeten identificar nous gens associats a trastorns de la substància blanca cerebral i nous fenotips clínics.

III. OBJECTIUS

1. Determinar la utilitat clínica dels estudis WES i WGS en casos d'index de qualsevol edat amb GWMDs, interpretats mitjançant una eina computacional de creació pròpia, que prioritza les variants genètiques integrant la informació clínica i de bases de dades d'interacció física i funcional de les proteïnes de l'organisme.
 - a. Valorar la rendibilitat diagnòstica dels estudis WES, inclosa la reanàlisi periòdica de les dades obtingudes, i del WGS.
 - b. Comparar els resultats de la nostra estratègia diagnòstica amb l'estratègia diagnòstica "clàssica" i amb altres estudis publicats que valoren el rendiment de WES i WGS, la majoria dels quals han estat basats en l'anàlisi de trios.
 - c. Comparar el temps necessari per assolir un diagnòstic mitjançant WES/WGS amb el temps d'evolució de la malaltia al llarg de l'abordatge "clàssic" (abans de la inclusió a l'estudi).
 - d. Determinar els canvis en el maneig clínic que poden comportar els diagnòstics establerts mitjançant aquesta estratègia.
2. Identificar nous gens candidats implicats en els GWMDs. Trobar altres casos a través de plataformes de compartició de dades genotípiques i fenotípiques (GeneMatcher i PhenomeCentral), i realitzar la validació mitjançant estudis funcionals.
3. Identificar nous fenotips clínics, aportant coneixement de l'espectre de formes de presentació que poden associar-se als gens de substància blanca.
4. Proposar un protocol diagnòstic dels GWMDs incorporant les tecnologies NGS, que pugui ser aplicable a la pràctica clínica habitual hospitalària. Aquest protocol estarà fonamentat en els resultats obtinguts en aquest projecte i la informació d'altres publicacions en aquest camp.

IV. MATERIAL I MÈTODES

1. Reclutament de pacients

Aquest projecte arrenca l'any 2015, quan des del laboratori de malalties Neurometabòliques d'IDIBELL vam començar a recollir pacients de totes les edats amb sospita clínica d'una malaltia genètica de la substància blanca cerebral. Eren pacients amb una RM cranial que mostrava una hiperintensitat difusa en T2 o bilateral incloent tractes anatòmics específics consistents amb una malaltia genètica, que no havien pogut ser diagnosticats mitjançant l'estrategia diagnòstica habitual basada en la clínica, els estudis de neuroimatge, bioquímics, metabòlics i genètics (incloent-hi estudis dirigits segons la sospita clínica, cariotip, aCGH o panells de gens). Els estudis paraclínics realitzats abans de la seva inclusió a l'estudi eren els que va considerar el metge referent en cada cas. Es van excloure tots aquells pacients amb una història clínica o neuroimatge suggestives d'una complicació perinatal, vascular o d'una malaltia autoimmunitària.

La informació clínica i els estudis de neuroimatge van ser remesos des de diferents hospitals terciaris d'arreu del territori espanyol, des de gener de 2015 fins a desembre de 2019. No es va realitzar un procés de filtratge de casos per part d'un neuroradiòleg expert en leucodistròfies en el moment de la seva inclusió a l'estudi. El doctorand, com a neuropediatre, va recollir les dades clíniques i els estudis realitzats prèviament i va revisar les imatges de les RM cranials i medul·lars disponibles. També va coordinar l'intercanvi d'informació amb els metges referents de cada cas, tant per completar les característiques clíniques imprescindibles per a la interpretació dels resultats, com per sol·licitar noves mostres per la realització d'estudis funcionals. El doctorand va codificar la informació recollida, tant la referent a la clínica, com la que es desprèn dels estudis bioquímics i de les característiques de les RM, en termes HPO, per incloure'ls a l'anàlisi de priorització de variants. Va classificar el patró d'afectació de la substància blanca per RM d'acord amb publicacions anteriors que fan referència a aquest tema (Schiffmann and van der Knaap, 2009; Parikh *et al.*, 2015). Els estudis de RM d'alguns casos seleccionats van ser revisats conjuntament amb la Dra. Élida Vázquez (Hospital Universitari Vall d'Hebrón).

Una part dels casos van ser seqüenciats a través del projecte URDCat (*The Undiagnosed Rare Diseases Program of Catalonia*), emmarcat dins del Pla Estratègic de Recerca i Innovació en

Salut (PERIS) 2016-2020, impulsat i finançat per la Generalitat de Catalunya, amb la finalitat d'implementar la medicina personalitzada basada en la genòmica en malalties minoritàries neurològiques no diagnosticades. El doctorand va participar com a gestor de casos en aquest projecte, des de gener de 2017 fins a desembre de 2019, revisant i introduint a la plataforma la informació clínica dels pacients. Els casos estudiats a través d'aquest projecte, van ser avaluats per un comitè d'experts, que s'encarregava de prioritzar els més adequats per estudi WES/WGS.

Els pares o tutors legals de cada pacient van firmar un consentiment informat per escrit per la realització dels estudis i les publicacions que se n'han derivat. El comitè d'ètica de l'IDIBELL va aprovar l'estudi (nombre CEIC PR076/14).

2. Seqüenciació dels exomes, captura i classificació de les variants

Per a l'anàlisi WES, la captura es va fer amb el SeqCap EZ Human Exome Kit v3.0 (Roche Nimblegen, EUA) amb seqüències aparellades de 100 parells de bases (pb) de llargada, i per a WGS, es va fer amb llibreries sense amplificació per PCR amb seqüències aparellades de 150 pb, generades en una plataforma HiSeq2000-4000 (Illumina, Inc. EUA) al Centre Nacional d'Anàlisi Genòmica (CNAG-CRG Barcelona, Espanya). Es van identificar variants d'un sol nucleòtid i insercions/deleccions (indels) utilitzant les guies GATK (Van der Auwera *et al.*, 2013) i es van anotar a través del programari Annovar (Wang *et al.*, 2010). Les variacions del nombre de còpies (CNVs) es van analitzar mitjançant el paquet R ExomeDepth (Plagnol *et al.*, 2012).

Vam filtrar les variants d'un sol nucleòtid i insercions/deleccions (indels) segons el mode d'herència compatible amb la història familiar, freqüència al·lèlica inferior a 0.01 d'acord amb les bases de dades poblacionals GnomAD (gnomAD, <https://gnomad.broadinstitute.org/>) i 1000 Genomes Project (<https://www.internationalgenome.org/>), impacte deleteri de la variant d'acord amb els predictors computacionals (CADD, Mutation Taster, SIFT, Polyphen2 hvar, entre d'altres), reports previs de patogenicitat i associació establerta amb el fenotip del pacient. Les variants candidates van ser classificades d'acord amb els criteris ACMG/AMP de patogenicitat

(Richards *et al.*, 2015b; Amendola *et al.*, 2016). Vam considerar resolt un cas si una o ambdues variants es classificaven com a patogèniques o probablement patògenes, o si una d'elles es classificava com a VUS, però els estudis de segregació eren compatibles, i els resultats clínics i de resonància magnètica eren específics i altament suggestius per a la malaltia en qüestió. Vam revisar també les troballes incidentals en tots els pacients d'acord amb els criteris publicats (Kalia *et al.*, 2017).

3. Mètode de priorització basat en l'Interactoma

El mètode de priorització de variants va ser dissenyat i posat a punt per la Dra. Àgatha Schlüter, en el laboratori de malalties Neurometabòliques d'IDIBELL. Es va utilitzar un enfocament basat en dinàmica de xarxes, tal com s'ha aplicat anteriorment (Novarino *et al.*, 2014), en dos passos principals: (1) càlcul d'una mètrica fenotípica mitjançant comparacions de fenotips entre el pacient i les bases de dades de malalties humanes existents (coneixement previ) i (2) propagació iterativa d'aquesta puntuació fenotípica dins d'una xarxa proteïna-proteïna (Figura 12). Per al primer pas, es van extreure més de 300.000 associacions de gens-HPO de les bases de dades OMIM i HPO (Robinson *et al.*, 2008; Köhler *et al.*, 2017). La mètrica fenotípica es va propagar a proteïnes adjacents dins de la xarxa humana global construïda amb interaccions físiques i funcionals proteïna-proteïna (IPP). Per a un interactoma físic, es van integrar IPP de cinc bases de dades a gran escala: la xarxa BioPlex 3.0 (Huttlín *et al.*, 2017), el conjunt de dades Lit-BM-13 (Rolland *et al.*, 2014), els conjunts de dades HI Yeast-Two-Hybrid HI-I-05 i HI-II-14 (Rual *et al.*, 2005; Rolland *et al.*, 2014) i el Human Reference Interactome (HuRI), descarregat de <http://www.interactome-atlas.org> (Luck *et al.*, 2020). Per a un interactoma funcional, es van integrar les interaccions HumanNet-CF v.2 (Hwang *et al.*, 2019), les connexions entre gens entrelaçant els substrats-productes del metaboloma de les bases de dades KEGG (Kanehisa *et al.*, 2014) i RECON (Brunk *et al.*, 2018), i connexions de senyalització de la base de dades Signor 2.0 (Licata *et al.*, 2020). La fusió de les bases de dades físiques i funcionals va donar lloc a un interactoma humà global amb 20.146 proteïnes i 696.301 connexions. En resum, l'algoritme prioritza els gens associats (coneiguts) i candidats amb més bona associació a la clínica del pacient. Quan

es tracta d'un gen candidat, el mètode el selecciona a través de les seves connexions veïnals amb gens coneguts de malalties que s'associen millor amb els termes HPO del cas particular que s'estudia, classifica les variants segons l'impacte deleteri i genera una taula amb el rànquing d'aquestes. Un exemple paradigmàtic és el nou gen candidat *DEGS1*, que vam identificar i validar funcionalment l'any 2019 (Pant *et al.*, 2019). Aquest gen es va prioritzar perquè interacciona funcionalment en xarxa amb altres enzims d'esfingolípids causants de malalties amb termes HPO similars als del pacient, com ARSA, GALC, FA2H o ACER3. El mateix passa amb *PI4KA* (Verdura and Rodríguez-Palmero *et al.*, 2021); aquest gen es va prioritzar, ja que interactua amb altres gens que causen trastorns de la substància blanca com *FAM126A*, *PIK3CA*, *PIK3C2A* o *OCRL*.

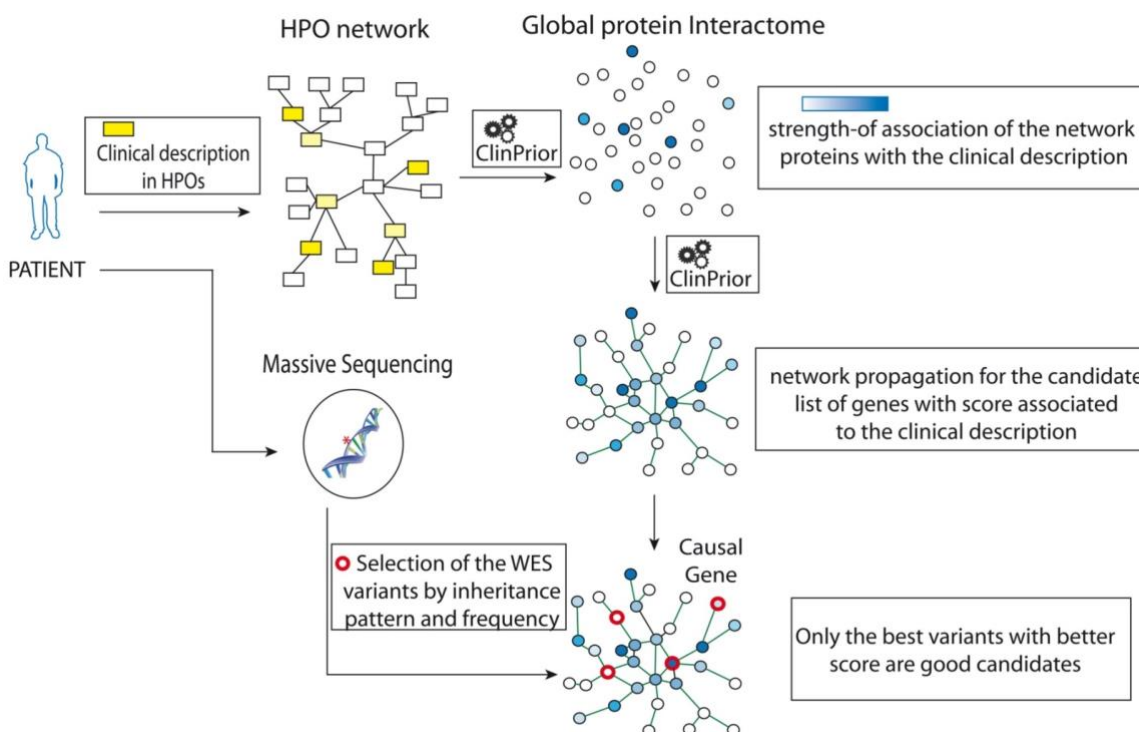


Figura 12. Mètode de prioritzacíó de variants basat en l'interactoma. Aquest és un nou algoritme creat per la Dra. Àgatha Schlüter al laboratori de malalties Neurometabòliques d'IDIBELL. Recull la informació clínica del pacient, prèviament estandardizada en termes HPO (Human Phenotype Ontology) per part del doctorand, i estableix una classificació d'associació amb proteïnes de l'interactoma. En un segon pas, es realitza una propagació per identificar proteïnes relacionades i per establir un llistat de possibles gens candidats associats a la descripció clínica. Finalment, es confronta aquesta informació amb el resultat de l'anàlisi del WES/WGS per identificar variants amb una baixa freqüència poblacional i patró d'herència compatible entre els gens resultants de la propagació i s'estableix un rànquing de variants.

4. Anàlisi dels resultats dels estudis WES/WGS

L'anàlisi dels resultats dels estudis de seqüenciació realitzats l'ha dut a terme principalment la Dra. Àgatha Schlüter, amb l'ajuda del Dr. Edgard Verdura. El doctorand també ha participat en l'anàlisi d'alguns casos a través de la plataforma del projecte URDCat.

Les variants candidates per cada pacient van ser estudiades conjuntament per part de l'equip del laboratori, i el doctorand va analitzar la correlació amb el fenotip clínic de cada cas, amb ajuda de la Dra Valentina Vélez (neuròloga d'adults) quan va ser necessari, a partir de la revisió de les descripcions prèvies recollides a la literatura i de la informació de bases de dades com OMIM, Orphanet, ClinVar, HGMD i Varsome (Figura 13).

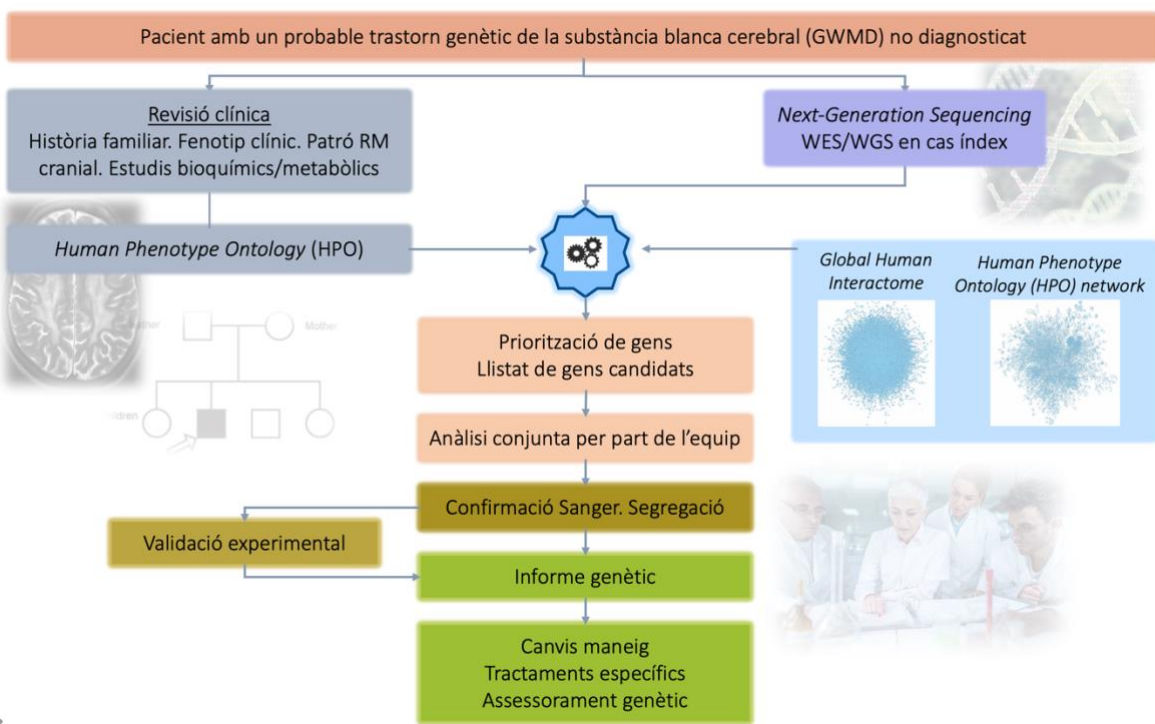


Figura 13. Protocol diagnòstic utilitzat per l'estudi de la cohort de pacients amb GWMDs. Procés d'anàlisi dut a terme al laboratori de malalties Neurometabòliques d'IDIBELL, per la identificació de variants genètiques dels pacients remesos amb una malaltia genètica de la substància blanca cerebral (GWMD). Implica la caracterització del fenotip clínic, bioquímic i alteracions de RM dels pacients, i codificació en termes HPO. Per altra banda, l'anàlisi de la seqüenciació de l'exoma o genoma complets del proband. Posteriorment, prioritació de les variants obtingudes a partir de la informació clínica i la informació de bases de dades amb informació de les interaccions físiques i funcionals de les proteïnes humanes. L'anàlisi de les variants prioritaries i correlació amb el fenotip del pacient s'estableix en reunions col-laboratives entre els neuròlegs, biòlegs i bioinformàtics del laboratori. Les variants potencialment implicades es confirmen per seqüenciació Sanger i es realitza l'estudi de segregació. Aquelles variants de significat incert (VUS) o en gens nous (no associats prèviament a GWMDs) es validen funcionalment. Finalment, s'elabora un informe que es tramet al metge referent de cada pacient, que informa a la família i considera els canvis en el maneig o una estratègia de tractament dirigida en cada cas.

V. RESULTATS

Article 1. Diagnosis of genetic white matter disorders by singleton whole-exome and genome sequencing using interactome-driven prioritization

Schlüter A*, Rodríguez-Palmero A*, Verdura E*, Vélez-Santamaría V, Ruiz M, Fourcade S, Planas-Serra L, Martínez JJ, Guilera C, Girós M, Artuch R, Yoldi ME, O'Callaghan M, García-Cazorla A, Armstrong J, Redin C, Mandel JL, Conejo D, Sierra-Córcoles C, Beltran S, Gut M, Vázquez E, del Toro M, Troncoso M, Pérez-Jurado LA, Gutiérrez-Solana LG, López de Munain A, Casanovas C, Aguilera-Albesa S, Macaya A, Pujol A#, on behalf of the GWMD working group

* Autors que han contribuït per igual en aquest treball

Revista: Neurology 2022 Jan 10; 10.1212/WNL.00000000000013278

Factor d'impacte (quartil per especialitat): 9.901 (Q1)

Participació del doctorand: aquest treball té una coautoría amb la Dra. Àgatha Schlüter i el Dr. Edgard Verdura. El doctorand ha revisat la informació clínica de tots els pacients inclosos, codificant-la en termes HPO i ha coordinat l'intercanvi d'informació amb els metges referents. Ha participat també en l'anàlisi d'alguns dels exomes i genomes, i directament en l'escriptura del manuscrit i en el disseny de les figures i taules. Aquest treball no es preveu que s'utilitzi en cap més tesi doctoral.

Resum de l'article 1

Introducció

- Cohort de 126 pacients de totes les edats amb sospita clínica d'un GWMD però etiologia desconeguda, tot i haver-se realitzat un abordatge diagnòstic "clàssic" (incloent-hi estudis de neuroimatge, bioquímics, metabòlics i genètics (estudis dirigits, aCGH o panells de gens)). En tots ells es va fer un estudi WES en casos índex, i en 16 casos que no havien pogut ser diagnosticats, es va dur a terme posteriorment un estudi WGS. Les dades genètiques van ser analitzades mitjançant un algoritme de priorització basat en l'interactoma i el fenotip dels pacients codificat en termes HPO.
- 80% de pacients inclosos havien iniciat el quadre clínic en edat pediàtrica.

Resultats

- En una primera revisió, el rendiment diagnòstic de l'estudi WES realitzat en el cas índex va ser del 59% (74/126). La reanàlisi anual va permetre identificar un diagnòstic en 12 casos més, amb el que el rendiment global del WES va ser del 68%. Posteriorment, l'estudi WGS fet en 16 pacients va permetre un diagnòstic en cinc d'ells, amb el qual el rendiment global va arribar al 72% (91/126 casos).
- La utilització d'estudis WES i WGS va permetre obtenir un diagnòstic en pocs mesos en la majoria dels casos, respecte a la mitjana de 6,3 anys d'evolució clínica dels pacients abans d'incorporar-se a l'estudi.
- Identificació de set gens candidats associats a un GWMD (*DEGS1* (Pant *et al.*, 2019), *PI4KA* (Verdura and Rodríguez-Palmero *et al.*, 2021), *PRORP* (Hochberg *et al.*, 2021)), nous fenotips i quadres clínics atípics.
- Gens més freqüentment identificats en aquesta cohort de pacients: *EIF2B5*, *POLR3A*, *RNASEH2B* i *PLP1*.
- Gran heterogeneïtat genètica: 57 gens diferents en els 91 casos diagnosticats. La meitat dels casos diagnosticats amb variants en gens que no corresponen a leucodistròfies "clàssiques".

- Implicacions relacionades amb un tractament o amb canvis en el maneig en 29/91 (32%) casos diagnosticats. Identificació de troballes incidentals en dos casos (gens *MYBPC3* i *SMAD3*).

Conclusions

- La nostra estratègia diagnòstica, estudiant únicament casos índex (no trios), permet assolir un elevat rendiment diagnòstic (72%). Els estudis computacionals utilitzats, la participació directa de clínics en el procés diagnòstic i la realització d'estudis funcionals són factors que poden justificar aquest elevat rendiment diagnòstic.
- La utilització de tècniques de seqüenciació massiva en el diagnòstic dels GWMD, permet escurçar el temps necessari per establir un diagnòstic, el que possibilita un assessorament genètic i la instauració de tractaments específics precoçment. A més, permet evitar la realització de múltiples proves complementàries innecessàries en aquests pacients. Això, juntament amb l'anàlisi de cas índex (no trio) en la nostra estratègia diagnòstica, pot reduir el cost econòmic del procés diagnòstic.
- Identificació de set gens nous candidats associats a GWMDs i nous fenotips clínics.
- Creació d'una xarxa d'interactoma expandida a partir dels resultats obtinguts en el present estudi, que pot ser útil per a la identificació de nous gens implicats en els trastorns genètics de la substància blanca cerebral en treballs futurs.

NOTA: algunes de les taules del material suplementari no estan incloses en aquesta tesi (eTable 8-11). El material suplementari complet de l'article està disponible en el següent enllaç: <http://links.lww.com/WNL/B741>

Neurology Publish Ahead of Print
DOI: 10.1212/WNL.0000000000013278

Diagnosis of Genetic White Matter Disorders by Singleton Whole-Exome and Genome Sequencing Using Interactome-Driven Prioritization

Author(s):

Agatha Schlüter, PhD^{1,2}; Agustí Rodríguez-Palmero, MD^{1,2,3}; Edgard Verdura, PhD^{1,2}; Valentina Vélez-Santamaría, MD^{1,4}; Montserrat Ruiz, PhD^{1,2}; Stéphane Fourcade, PhD^{1,2}; Laura Planas-Serra, MSc^{1,2}; Juan José Martínez, MSc^{1,2}; Cristina Guilera, MSc^{1,2}; Marisa Girós, PhD⁵; Rafael Artuch, MD^{2,6}; María Eugenia Yoldi, MD⁷; Mar O'Callaghan, MD, PhD^{2,6}; Angels García-Cazorla, MD, PhD^{2,6}; Judith Armstrong, PhD^{2,8}; Itxaso Martí, MD, PhD^{9,10,11,12}; Elisabet Mondragón Rezola, MD, PhD^{10,12,13}; Claire Redin, PhD¹⁴; Jean Louis Mandel, MD, PhD^{14,15,16}; David Conejo, MD¹⁷; Concepción Sierra-Córcoles, MD¹⁸; Sergi Beltran, PhD¹⁹; Marta Gut, PhD¹⁹; Elida Vázquez, MD²⁰; Mireia del Toro, MD, PhD^{2,21}; Mónica Troncoso, MD, PhD²²; Luis A. Pérez-Jurado, MD, PhD^{2,23,24}; Luis G. Gutiérrez-Solana, MD, PhD²⁵; Adolfo López de Munain, MD, PhD^{10,11,12,13}; Carlos Casasnovas, MD, PhD^{1,4}; Sergio Aguilera-Albesa, MD, PhD⁷; Alfons Macaya, MD, PhD^{2,21,26}; Aurora Pujol, MD, PhD^{1,2,27} on behalf of GWMD working group

This is an open access article distributed under the terms of the Creative Commons Attribution-NonCommercial-NoDerivatives License 4.0 (CC BY-NC-ND), which permits downloading and sharing the work provided it is properly cited. The work cannot be changed in any way or used commercially without permission from the journal.

Neurology® Published Ahead of Print articles have been peer reviewed and accepted for publication. This manuscript will be published in its final form after copyediting, page composition, and review of proofs. Errors that could affect the content may be corrected during these processes.

Equal Author Contributions:

These authors contributed equally to this work: Agatha Schlüter, Agustí Rodríguez-Palmero, Edgard Verdura

Corresponding Author:

Aurora Pujol
apujol@idibell.cat

Affiliation Information for All Authors: 1. Neurometabolic Diseases Laboratory, Bellvitge Biomedical Research Institute (IDIBELL), 08908 L'Hospitalet de Llobregat, Barcelona, Spain; 2. Center for Biomedical Research on Rare Diseases (CIBERER), ISCIII, Spain; 3. Pediatric Neurology Unit, Department of Pediatrics. Hospital Universitari Germans Trias i Pujol, Universitat Autònoma de Barcelona, Spain; 4. Neuromuscular Unit, Neurology Department, Hospital Universitari de Bellvitge, Universitat de Barcelona, Hospitalet de Llobregat, Spain; 5. Secció d'Errors Congènits del Metabolisme-IBC, Servei de Bioquímica i Genètica Molecular, Hospital Clínic, IDIBAPS, CIBERER, Barcelona, Spain; 6. Institut de Recerca Pediàtrica-Hospital Sant Joan de Déu (IRP-HSJD), Barcelona, Spain; 7. Pediatric Neurology Unit, Department of Pediatrics, Navarra Health Service, Navarrabiomed Research Foundation, Pamplona, Spain; 8. Molecular and Genetics Medicine Section, Hospital Sant Joan de Déu, Barcelona, Spain; 9. Department of Neuropediatrics, Hospital Universitario Donostia, San Sebastián, Spain; 10. Biodonostia Health Research Institute (Biodonostia HRI), San Sebastián, Spain; 11. University of the Basque Country (UPV-EHU), San Sebastian, Spain; 12. Centro de Investigación Biomédica en Red para Enfermedades Neurodegenerativas (CIBERNED), Carlos III Health Institute, Madrid, Spain; 13. Department of Neurology, Hospital Universitario Donostia, San Sebastián, Spain; 14. Département de Médecine translationnelle et Neurogénétique, IGBMC, CNRS UMR 7104/INSERM U964/Université de Strasbourg, Illkirch, France; 15. Laboratoire de Diagnostic Génétique, Hôpitaux Universitaires de Strasbourg, Strasbourg, France; 16. Chaire de Génétique Humaine, Collège de France, Illkirch, France; 17. Complejo asistencial universitario de Burgos, Burgos, Spain; 18. Department of Paediatric Neurology, Complejo Hospitalario Jaén, Jaén, Spain; 19. CNAG-CRG, Centre for Genomic Regulation (CRG), Barcelona Institute of Science and Technology (BIST), Barcelona, Spain; 20. Department of Pediatric Radiology, Hospital Materno-Infantil Vall d'Hebrón, Barcelona, Spain; 21. Pediatric Neurology Department, Vall d'Hebron University Hospital, Universitat Autònoma de Barcelona, Spain; 22. Pediatric Neurology, Hospital Clínico San Borja Arriarán, Central Campus Universidad de Chile, Chile; 23. Genetics Service, Hospital del Mar Research Institute (IMIM), Barcelona, Spain; 24. Department of Experimental and Health Sciences, Universitat Pompeu Fabra, Barcelona, Spain; 25. Department of Paediatric Neurology, Children's University Hospital Niño Jesús, Madrid, Spain; 26. Pediatric Neurology Research Group, Vall d'Hebron Research Institute, Universitat Autònoma de Barcelona, Barcelona, Spain; 27. Catalan Institution of Research and Advanced Studies (ICREA), Barcelona, Catalonia, Spain.

Contributions:

Agatha Schlüter: Drafting/revision of the manuscript for content, including medical writing for content; Major role in the acquisition of data; Study concept or design; Analysis or interpretation of data

Agustí Rodríguez-Palmero: Drafting/revision of the manuscript for content, including medical writing for content; Major role in the acquisition of data; Study concept or design; Analysis or interpretation of data

Edgard Verdura: Drafting/revision of the manuscript for content, including medical writing for content; Major role in the acquisition of data; Study concept or design; Analysis or interpretation of data

Valentina Vélez-Santamaría: Drafting/revision of the manuscript for content, including medical writing

for content; Major role in the acquisition of data; Analysis or interpretation of data
Montserrat Ruiz: Drafting/revision of the manuscript for content, including medical writing for content;
Major role in the acquisition of data
Stéphane Fourcade: Drafting/revision of the manuscript for content, including medical writing for content
Laura Planas-Serra: Major role in the acquisition of data
Juan José Martínez: Major role in the acquisition of data
Cristina Guilera: Major role in the acquisition of data
Marisa Girós: Major role in the acquisition of data
Rafael Artuch: Major role in the acquisition of data
María Eugenia Yoldi: Major role in the acquisition of data
Mar O'Callaghan: Major role in the acquisition of data
Angels García-Cazorla: Major role in the acquisition of data; Analysis or interpretation of data
Judith Armstrong: Major role in the acquisition of data
Itxaso Martí: Major role in the acquisition of data
Elisabet Mondragón Rezola: Major role in the acquisition of data
Claire Redin: Major role in the acquisition of data; Analysis or interpretation of data
Jean Louis Mandel: Major role in the acquisition of data; Analysis or interpretation of data
David Conejo: Major role in the acquisition of data
Concepción Sierra-Córcoles: Major role in the acquisition of data
Sergi Beltran: Major role in the acquisition of data; Analysis or interpretation of data
Marta Gut: Major role in the acquisition of data
Elida Vázquez: Major role in the acquisition of data
Mireia del Toro: Major role in the acquisition of data
Mónica Troncoso: Major role in the acquisition of data
Luis A. Pérez-Jurado: Drafting/revision of the manuscript for content, including medical writing for content; Analysis or interpretation of data
Luis G. Gutiérrez-Solana: Major role in the acquisition of data; Analysis or interpretation of data
Adolfo López de Munain: Major role in the acquisition of data; Analysis or interpretation of data
Carlos Casasnovas: Major role in the acquisition of data; Analysis or interpretation of data
Sergio Aguilera-Albesa: Drafting/revision of the manuscript for content, including medical writing for content; Major role in the acquisition of data; Analysis or interpretation of data
Alfons Macaya: Drafting/revision of the manuscript for content, including medical writing for content; Major role in the acquisition of data; Study concept or design; Analysis or interpretation of data
Aurora Pujol: Drafting/revision of the manuscript for content, including medical writing for content; Major role in the acquisition of data; Study concept or design; Analysis or interpretation of data

Number of characters in title: 130

Abstract Word count: 324

Word count of main text: 3161

References: 48

Figures: 4

Tables: 1

Supplemental: CARE Checklists

Search Terms: [155] Leukodystrophies

Acknowledgements: We thank patients and families for their collaboration, and the European Leukodystrophy Association ELA-Spain for its support. This study was funded by the URDCat program (PERIS SLT002/16/00174) from the Autonomous Government of Catalonia, Centre for Biomedical Research on Rare Diseases (CIBERER, ACCI19-759), The Hesperia Foundation (Royal House of Spain), and CNAG's call "300 exomes to elucidate rare diseases" to AP, the Instituto de Salud Carlos III and Fondo Europeo de Desarrollo Regional (FEDER), Unión Europea, una manera de hacer Europa (FIS PI20/00758) to CC, La Marató de TV3 Foundation (202006-30) to CC and AP, and the AWS Cloud Credits for Research program to AS. This study has also been funded by Instituto de Salud Carlos III through the programs Miguel Servet (CPII16/00016) to SF, Sara Borrell (CD19/00221) to EV, and Rio Hortega, CM18/00145 to VV co-funded by the European Social Fund (ESF, investing in your future). MR was funded by the Center for Biomedical Research on Rare Diseases, an initiative of the Instituto de Salud Carlos III. Several authors of this publication are members of the European Reference Network for Rare Neurological Diseases - Project ID No 739510: AM, MdT. We thank the CERCA Program/Generalitat de Catalunya for institutional support.

Study Funding: URDCat program (PERIS SLT002/16/00174) from the Autonomous Government of CataloniaCentre for Biomedical Research on Rare Diseases (CIBERER, ACCI19-759) The Hesperia Foundation (Royal House of Spain)CNAG's call "300 exomes to elucidate rare diseases" to the Instituto de Salud Carlos III and Fondo Europeo de Desarrollo Regional (FEDER), Unión Europea, una manera de hacer Europa (FIS PI20/00758) La Marató de TV3 Foundation (202006-30) AWS Cloud Credits for Research program.Instituto de Salud Carlos III through the programs Miguel Servet (CPII16/00016) to SF Sara Borrell (CD19/00221) to EV, Rio Hortega, CM18/00145 to VV co-funded by the European Social Fund (ESF, investing in your future). MR was funded by the Center for Biomedical Research on Rare Diseases, an initiative of the Instituto de Salud Carlos III. European Reference Network for Rare Neurological Diseases - Project ID No 739510: AM, MdT.

Disclosures: The authors report no disclosures relevant to the manuscript.

ABSTRACT

Background and Objectives: Genetic white matter disorders (GWMD) are of heterogeneous origin, with more than a hundred causal genes identified to date. Classical targeted approaches achieve a molecular diagnosis in only half of all patients. Here we aim to determine the clinical utility of singleton whole-exome sequencing and whole-genome sequencing (sWES-WGS) interpreted with a phenotype- and interactome-driven prioritization algorithm to diagnose GWMD patients, while identifying novel phenotypes and candidate genes.

Methods: A case series of patients of all ages with undiagnosed GWMD despite extensive standard-of-care paraclinical studies were recruited between April 2017 and December 2019 in a collaborative study at the Bellvitge Biomedical Research Institute (IDIBELL) and neurology units of tertiary Spanish hospitals. We ran sWES and WGS and applied our interactome-prioritization algorithm, based on the network expansion of a seed group of GWMD-related genes, derived from the HPO terms of each patient.

Results: We received 126 patients (101 children and 25 adults), with ages ranging from 1 month to 74 years. We obtained a first molecular diagnosis by singleton WES in 59% of cases, which increased to 68% after annual reanalysis and reached 72% after WGS was performed in 16 of the remaining negative cases. We identified variants in 57 different genes among 91 diagnosed cases, with the most frequent being *RNASEH2B*, *EIF2B5*, *POLR3A* and *PLP1*; and a dual diagnosis underlying complex phenotypes in six families, underscoring the importance of genomic analysis to solve these cases. Finally, we discovered 9 candidate genes causing novel diseases, and propose additional putative novel candidate genes for yet-to-be discovered GWMD.

Discussion: Our strategy enables a high diagnostic yield and is a good alternative to trio WES/WGS for GWMD. It shortens the time to diagnosis compared to the classical targeted approach, thus optimizing appropriate management. Furthermore, the interactome-driven prioritization pipeline enables the discovery of novel disease-causing genes and phenotypes, and predicts novel putative candidate genes, shedding light on etiopathogenic mechanisms that are pivotal for myelin generation and maintenance.

INTRODUCTION

The advent of next-generation sequencing (NGS) in clinical applications (especially targeted sequencing panels and whole-exome sequencing) has increased the diagnostic yield of hereditary neurological diseases with high genetic heterogeneity and low mutational burden^{1–4}. Genetic white matter disorders (GWMD) are a heterogeneous group of diseases with an MRI pattern suggestive of a genetic etiology, encompassing both leukodystrophies and genetic leukoencephalopathies^{5,6}. The classical combined MRI, biochemical, and target gene-based approach leaves approximately half of GWMD patients without a genetic diagnosis^{7–10}. In these undiagnosed cases, trio WES (whole-exome sequencing) followed by WGS (whole-genome sequencing) allowed a diagnosis in 62% of the cases in a recent study on a cohort of 71 pediatric patients^{4,11}.

Despite continuous advances, the analysis of NGS data poses the challenge of variant selection and interpretation, which is especially relevant for singleton exomes, or when there is no possibility to perform family cosegregation/linkage studies. WES genotypes yield approximately 500-1,000 variants per individual, after filtering by frequency below 1% and deleteriousness. Hence, establishing a prioritization system based on the patient's phenotype^{12,13} or gene interaction networks^{14–17} may prove useful to improve rapid selection of candidate variants.

Here, we describe 126 families with patients displaying GWMD analyzed by singleton WES-WGS (sWES-WGS). We interpret genetic data by integrating standardized phenotypic data in HPO (Human Phenotype Ontology) terms, as well as interaction and functional network information to facilitate the identification of causal genes and enable novel disease-gene discovery.

MATERIALS AND METHODS

Patient Recruitment

Study participants were identified at child and adult neurology units from several tertiary hospitals around Spain from April 2017 to December 2019. They were pediatric and adult patients with clinical and MRI patterns consistent with a GWMD defined as symmetrical, confluent white matter involvement, in absence of perinatal or vascular complications or suggestive of an autoimmune process. A molecular diagnosis could not be established by the referring physicians despite applying standard-of-care paraclinical studies (including mainly MRI, metabolic, neurophysiological and genetic studies such as aCGH, targeted Sanger sequencing, or NGS gene panels). Clinical information, MRIs and samples were collected by the Neurometabolic Diseases laboratory of Bellvitge Biomedical Research Institute (IDIBELL) and although strict filtering of cases by a neuroradiologist focused on leukodystrophies was not performed, re-evaluation by a team of experienced child and adult neurologists and neuroradiologists under the URD-Cat initiative for neurological undiagnosed disorders, was made before inclusion. This clinical team was driving the diagnostic process and exchanged information with the referring clinicians when required, both prior and post-variant calling. MRI pattern was classified according to previous published articles^{18,19}.

Standard Protocol Approvals, Registrations, and Patient Consents

Written informed consent for genetic testing and publication was obtained by the parents or legal guardians of each patient at each site. The ethics committee of IDIBELL approved the study with CEIC n. PR076/14.

See Supplemental Methods for NGS, variant calling and classification, functional validation and the interactome-driven gene prioritization method.

Data Availability

Data not provided in the article because of space limitations may be shared (anonymized) at the request of any qualified investigator for purposes of replicating procedures and results.

RESULTS

Clinical data

We recruited 126 families with an undiagnosed GWMD. Based on cranial MRI findings, 86 cases (68%) were classified as non-hypomyelinating, whereas 40 of the cases showed a hypomyelinating picture. The index cases were 50 females and 76 males, with ages ranging from 1 month to 74 years (median 10.3 years). The age at onset ranged from the first month of life to 72 years (median one year); age was lower than 18 years in 101 cases (80%) and higher in 25. The median evolution of disease before WES testing was 6.3 years (1 month - 34 years), and it was longer than 10 years in 37% of patients. Consanguinity was reported in 18 families (14%). Clinical characteristics, MRI patterns, studies performed and sWES-WGS results of every patient are summarized in **Table 1** and **eTable 1**.

Diagnostic Yield of WES and WGS in a cohort of GWMD patients

All the patients were initially studied by WES. The first diagnostic rate was 74/126 (59%), which increased to 86/126 cases (68%) after a subsequent reanalysis 12-24 months later. The reasons for this increase in yield were attributed to i) variants not initially identified because

of filtering issues (3 cases); ii) variants located in noncoding regions (3 cases); iii) pipeline update/technical issues (2 cases); and iv) newly reported disease-causing genes (3 cases). Next, we performed WGS in 16 of the remaining 38 negative cases, prioritized by availability of DNA from proband and parents, and solved 5 more cases involving intronic variants or 3'UTR variants.

Furthermore, this approach allowed us to identify 9 novel candidate genes, for which we gathered additional patients with very similar phenotypes through collaboration with international Leukodystrophy Reference Centers and the platform GeneMatcher²⁰. We functionally validated and reported two novel disease genes (*DEGS1*²¹ and *PI4KA*²²) in two families each, whereas the other 5 validated cases are currently in preparation. Two more candidate genes are awaiting additional patients while functional studies are on-going.

Overall, we obtained a positive genetic diagnosis in 91 out of 126 GWMD cases (72%) (**Figure 1, eFigure 1, eTables 1 and 2**). The diagnostic rates by age group were 77% in those with onset before 3 years, 73% in those with onset between 3 and 18 years and 60% in the adult-onset group (**Figure 1D**). Considering the MRI pattern, the diagnostic rate was 57/86 (66%) in the non-hypomyelinating group and 34/40 (85%) in those with hypomyelination. Following the classification proposed in Vanderver *et al.*⁵, 46 (51%) of the diagnosed families had variants in genes associated with "canonical or classic leukodystrophies", and the remaining 45 (49%) had variants in genes associated with "genetic leukoencephalopathies".

For the 33 cases that remained undiagnosed after WES/WGS, we noted a trend towards adulthood onset (30% of unsolved cases were adults *versus* 16% of adults in solved cases), cystic lesions on MRI (12% of undiagnosed cases *versus* 5% in solved cases), and absence of consanguinity (97% non consanguineous in unsolved *versus* 82% in solved cases).

Although genetic heterogeneity in our cohort was very high, some genes were found to be more frequently mutated, including *EIF2B5*, *POLR3A*, and *RNASEH2B*, in six families each,

and *PLP1* variants in five families (**eTable 3**). New phenotypes were identified in two cases, atypical forms of presentation in seven, and six more cases were complex, blended phenotypes with variants in more than one gene (**Figure 2, eTable 4 and eResults for clinical summaries**). Moreover, several cases with variants in the classical spastic paraplegia genes *SPG11* and *CYP2U1* presented clear white matter involvement as shown in **Figure 3**.

According to the ACMG/AMP guidelines^{23–25}, 86 out of the 91 diagnosed cases were classified as definitively diagnosed with pathogenic or likely pathogenic variants. In 14 of these 86 cases, the functional validation converted VUS variants into pathogenic or likely pathogenic variants. We analysed the impact of 8 variants on splicing using either cDNA sequencing (from RNA derived from PBMC or fibroblasts), and/or minigene splicing assay²⁶ (n=3). The minigene assays were instrumental to confirm the pathogenic role of an intronic variant in MLC1 (c.597+37C>G), gene not expressed in PBMC nor fibroblasts, and another intronic variant in EIF2B5 (c.1156+13G>A), which lead to a mild form of ovarioleukodystrophy²⁶. Importantly, we also performed targeted lipidomics, which proved a pathogenic role for variants in genes related to lipid metabolism such as *ACER3*, *DEGS1*²¹ and *PI4KA*²², together with qRT-PCR, Western blots, or immunofluorescence as required (**eTable 5**). In other cases which were not amenable to experimental validation (5 remaining until 91), we reported out VUSs highly compatible with the clinical, MRI picture and segregation and were considered solved by expert assessment.

Among the 91 cases diagnosed, 60 harbored biallelic mutations (31 homozygous; 16 of them in consanguineous families), 22 in an autosomal dominant mode (12 *de novo*) and 7 X-linked (5 of them *de novo*), whereas two cases had mutations in more than one gene with different inheritance patterns (one with AD and AR inheritance; one AD and X-linked) (**eFigure 1**). Segregation by Sanger was performed in all but 8 patients due to the unavailability of parental samples. We found several variants more than once in our patients: i) the *RNASEH2B* p.Ala177Thr variant in 6 independent families (frequency: 0.001306 in gnomAD

(v2.1.1))²⁷; ii) the *EIF2B5* p. Leu106Phe variant (frequency: 0.00004943 in gnomAD (v2.1.1)) in 2 independent families, and the *EIF2B5* p.Arg113His variant (frequency: 0.00001647 in gnomAD (v2.1.1))²⁸ in 5 families, and iii) the *SPG11* frameshift variant p.Met245Valfs*2 twice independently (frequency: 0.0001071 in gnomAD (v2.1.1))²⁹.

Of note, in addition to SNVs and indels, we detected a pathogenic copy number variant (CNV) in four cases (4.4%) by WES (**eTable 6**): a 6930 Kb 1p36 heterozygous deletion in LNF-36 and validated by aCGH (eFigure 2), a 117 Kb duplication in 5q including *HNRNPH1* and *RUFY1* genes in LNF-105³⁰, a 60.4 Kb duplication containing *LMNB1* in LNF-34, and a 21.3 Kb homozygous deletion encompassing *TANGO2* in LNF-97³¹. We validated the last three CNVs by Q-PCR (**eTable 6**). We also identified a uniparental disomy of maternal origin of chromosome 6 in LNF-68, harboring a loss-of-function homozygous variant in a novel candidate gene that was highly ranked by our prioritization method (in preparation).

An added value of our study is that 73 of the 123 identified variants had not been previously reported in the literature, Human Gene Mutation Database (HGMD, public access), or ClinVar databases (**eTable 7**).

Management implications of a positive diagnosis

Importantly, diagnosis allowed us to improve the clinical management in 29 cases (**eTable 1**). In 22 of them, it led to the consideration of a specific treatment option for the disease, such as hematopoietic stem cell transplant (HSCT) for Krabbe disease (LNF-18, SPG-72) and hereditary diffuse leukoencephalopathy with spheroids (LNF-6, LNF-16, LNF-70, LMSR), dietary management for phenylketonuria (LNF-40.4) or pyridostigmine for myasthenic syndrome caused by *GFPT1* (LNF-88). In other cases, diagnosis led to an improvement in patient follow-up, such as screening for the appearance of tumors in *PTEN* (LNF-109) or preventative measures for head trauma and infections in patients with vanishing white matter disease. Finally, we identified and reported incidental findings (according to Kalia SS *et al.*³²) in two patients: a pathogenic variant in the *MYBPC3* gene (p.Trp792ValfsTer41) in SPG-14

and in *SMAD3* (Loeys-Dietz syndrome) (p.Val363ThrfsTer3) in LNF-48. In both cases, cardiological follow-up will ensue, with cranial magnetic resonance angiography and orthopedic controls in the second case.

GWMD expanded network

Starting with a seed list of 843 genes that are causative or associated of GWMD according to OMIM, we built a protein interactome network based on the principle that physical and functional interacting genes may account for related biological processes and cause similar diseases. We developed a prioritization method that identifies the most likely disease-causing genes associated with each patient's phenotype (standardized in Human Phenotype Ontology (HPO)³³ terms) using a global protein human interactome network built with functional and physical interactions, represented by 20.146 genes (see **Supplemental Methods and Results (eTables 8-11)**)¹⁴. We applied this prioritization tool to the respective clinical description in HPOs of the 843 proteins associated with GWMD to build a GWMD interactome or expanded network, resulting in 1530 proteins and 18288 interactions (**Figure 4**). To evaluate the functional signature of these 1530 proteins, we performed an enrichment analysis of the Gene Ontology (GO) terms (**eTables 8-10**). In line with the hypothesis that genes associated with similar diseases may converge towards specific biological pathways, major modules emerged, which are involved in the pathophysiology of GWMD abnormalities: i) the mitochondrial oxidative phosphorylation (OXPHOS) system (e.g., NADH-ubiquinone oxidoreductase Fe-S protein 1, *NDUFS1*), ii) the lysosome (e.g., the galactosylceramidase enzyme, *GALC*), iii) the peroxisome (peroxins) (e.g., peroxin 6, *PEX6*), iv) the metabolism of ribonucleotides (e.g., ribonuclease H2 subunit B, *RNASEH2B*), and v) the purine metabolism pathway with RNA polymerases I and III (e.g., RNA polymerase III subunit A, *POLR3A*). Among the 1530 proteins we identified (beside the 843 GWMD seed proteins): i) 587 proteins associated with disease but not yet with GWMD and ii) 100 novel candidates that were not previously associated with GWMD or any disease (**eTable 11**). Of particular

interest among these last 100 proteins, we highlight: i) the delta 4-desaturase sphingolipid 1 (DEGS1) in patients LNF-41 and LNF-42 (**Figure 4B**), causing Hypomyelinating Leukodystrophy 18 (HLD18, OMIM #615843)²¹ ii) the phosphatidylinositol 4-kinase alpha (PI4KA) recently associated with leukodystrophy and identified in patient LNF-107 and VH-3^{22,34} (**Figure 4C**), iii) the mitochondrial ribosome-associated GTPase 1 (*MTG1*) that plays a role in the regulation of mitochondrial ribosome assembly and translational activity (**Figure 4D**), and iv) the potassium voltage-gated channel subfamily A regulatory beta subunit 2 protein (*KCNAB2*) (**Figure 4E**). While Genematcher was key to find additional cases for *DEGS1* and *PI4KA* deficiencies, matches for putative candidates such as *MTG1* and *KCNAB2* are yet to be found.

DISCUSSION

This is the largest series of GWMD patients studied by WES/WGS reported to date and the first one including patients of all ages offering a global vision of the GWMD diagnosis throughout life. Here, we have proven the utility of sWES-WGS combined with a phenotypic and interactome-driven prioritization method, reaching a diagnostic yield of 72%. These results are superior to those recently reported by a reference genetic diagnostics company on 541 cases, with a WES diagnostic yield for leukodystrophies of 32% (including trio and singleton cases) and 22.6% when considering proband-only cases³⁵. In another report including 100 adult-onset leukodystrophy patients, the diagnostic rate was 26%³⁶. Our results are slightly better than those reported in another study including 71 pediatric cases^{4,11}. In Vanderver's report, a first trio WES allowed a definite diagnosis in 42% of cases⁴, while in a second phase of the study including the 41 negative cases, a molecular diagnosis was established in nine more cases by reanalysis and in five cases using WGS, representing 17% and 12%, respectively¹¹. We were able to increase diagnostic yield 24% (12/50) by WES reanalysis and 31% (5/16) by singleton WGS. However, in the referred study, previous expert filtering of cases led to a lower proportion of well-known or canonical leukodystrophy genes

in their cohort⁴ in comparison to ours (36% vs 51% in our cohort), which may have an impact on our higher diagnostic yield. Comparison between the results of these cohorts is difficult because of different study protocols and target population, which comprised a 20% of adult GWMD in our case versus a pediatric population-only in Vanderver's case⁴. It is likely that the use of trio WES/WGS would have improved our diagnostic yields, and most certainly would have ameliorated turn-around-times. Because of the very late implantation of clinical exomes (instead of WES) in our healthcare system and limited research funding resources we chose to apply singleton WES to help as many families as possible, since trio studies may cost double^{37,38} to three times higher in our healthcare system. The use of trio WES/WGS is however recommended when urgent diagnosis is required in ICU settings³⁹. Thus in our opinion, the decision to use a singleton or trio sequencing strategy should depend on the clinical urgency, the entities under study that determine the proportion of dominant *de novo* expected inheritances, the family characteristics and availability of DNA, and funding or structural resources needed to optimize the cost-benefit ratio in every setting³⁷.

Our study enabled identification of disorders caused by genes rarely associated with white matter involvement (*PTEN*, *GFPT1*⁴⁰ and *CAPNI*⁴¹), the diagnosis of certain cases with atypical presentation (*SCN8A*⁴², *SOX10*⁴³, *POLR3A*⁴⁴), the characterization of families harboring variants in more than one causative gene with blended phenotypes, the identification of genes only recently associated with disease (i.e., *PYCR2*⁴⁵ or *TMEM63A*⁴⁶) and the discovery of novel disease entities and candidate genes, which constitute important advantages over disease-specific panels or clinical exomes (**Figure 2, eTables 1 and 4, eResults for clinical summaries**). Further, in nine families (10%), we identified variants in genes associated primarily with hereditary spastic paraparesis (*SPG11*, *SPG7*, *SPAST*, *DDHD2*, *CAPNI* and *CYP2UI*) (Figure 3), underscoring the notion of a continuum of clinical spectrum, similarly to X-adrenoleukodystrophy, PMD/SPG2, metachromatic dystrophy (MLD) or Alexander disease⁴⁷. Moreover, half of the genes identified in this cohort are linked to genetic leukoencephalopathies, not classically considered

“leukodystrophy genes”. Since many of these genes are not included in multigene panels, the WES/WGS-derived diagnostic yield would be expected to be superior. As an example, the diagnostic yield of a leukodystrophies disease-gene panel containing 134 genes was 46% in a recent study⁴⁸.

Our report also exemplifies the genetic heterogeneity of GWMD (57 different genes among the 91 diagnosed cases), which supports that WES/WGS should be considered a first-tier diagnostic test when the clinical presentation and MRI pattern do not point to a specific diagnosis, in agreement with the recent randomized clinical trial on pediatric GWMD patients⁶. This would allow for gaining precious time, which is fundamental to establish appropriate genetic counseling and specific treatment when available, usually indicated only in the early stages of these very severe diseases. On average, our patients reached a positive diagnosis at 6 months after study inclusion, which stood in sharp contrast with the previous “diagnostic odyssey” of 10 years of disease evolution on average. Hence, reducing multiple unnecessary examinations with a low cost-benefit ratio, as it is the case for some metabolic studies in the context of a nonspecific neuroimaging, would entail significant economic savings for the healthcare system, which together with the continued lowering of WES/WGS costs, makes a clear case for the adoption of at least WES if not WGS, as a first-tier test for undiagnosed GWMD. However, first line metabolic tests that may identify potentially treatable cases should always be considered, prior or in parallel with WES/WGS.

Our study protocol has certain limitations. Paraclinical studies preceding inclusion are heterogeneous and depend on the availability of resources in the different participating centers. Additionally, we reported as diagnosed 5 cases harboring VUS using technically strict ACMG criteria, since these variants could not be functionally validated. However, these cases with VUS were carefully reviewed by expert clinicians and considered to explain the phenotypic presentation with very high probability, and were thus considered solved by

expert assessment. Finally, WGS studies were prioritized in only 16 of the remaining 38 negative cases (42%) because of limited DNA availability of parents to perform segregation and funding resources.

In summary, we provide evidence of the effectiveness of sWES-WGS analysis based on a phenotype- and interactome-driven prioritization algorithm to diagnose patients with GWMD and to identify new phenotypes and novel disease genes. Finally, we also provide a WM expanded interactome composed of known and putative new GWMD genes with the potential to aid in the validation of private mutations in genes found in single families and the identification of novel candidate genes. We believe that the utilization of advanced computational methods together with the integration of a functional genomics laboratory capable of experimental validation of VUSS and candidate genes, together with the direct implication of adult and pediatric neurologists in the process has been determining factors for this high diagnostic yield.

Supplement-<http://links.lww.com/WNL/B741>

References

1. Fogel BL, Lee H, Deignan JL, et al. Exome sequencing in the clinical diagnosis of sporadic or familial cerebellar ataxia. *JAMA Neurol.* 2014;71(10):1237-1246.
2. Gonzaga-Jauregui C, Harel T, Gambin T, et al. Exome Sequence Analysis Suggests that Genetic Burden Contributes to Phenotypic Variability and Complex Neuropathy. *Cell Rep.* 2015;12(7):1169-1183.
3. van de Warrenburg BP, Schouten MI, de Bot ST, et al. Clinical exome sequencing for cerebellar ataxia and spastic paraparesis uncovers novel gene-disease associations and unanticipated rare disorders. *Eur J Hum Genet.* 2016;24(10):1460-1466.

4. Vanderver A, Simons C, Helman G, et al. Whole exome sequencing in patients with white matter abnormalities. *Ann Neurol.* 2016;79(6):1031-1037.
5. Vanderver A, Prust M, Tonduti D, et al. Case definition and classification of leukodystrophies and leukoencephalopathies. *Mol Genet Metab.* 2015;114(4):494-500.
6. Vanderver A, Bernard G, Helman G, et al. Randomized Clinical Trial of First-Line Genome Sequencing in Pediatric White Matter Disorders. *Ann Neurol.* 2020;88(2):264-273.
7. van der Knaap MS, Breiter SN, Naidu S, Hart AA, Valk J. Defining and categorizing leukoencephalopathies of unknown origin: MR imaging approach. *Radiology.* 1999;213(1):121-133.
8. Köhler W, Curiel J, Vanderver A. Adulthood leukodystrophies. *Nat Rev Neurol.* 2018;14(2):94-105.
9. van der Knaap MS, Schiffmann R, Mochel F, Wolf NI. Diagnosis, prognosis, and treatment of leukodystrophies. *Lancet Neurol.* 2019;4422(19):962-972.
10. Bonkowsky JL, Nelson C, Kingston JL, Filloux FM, Mundorff MB, Srivastava R. The burden of inherited leukodystrophies in children. *Neurology.* 2010;75(8):718-725.
doi:10.1212/WNL.0b013e3181eee46b
11. Helman G, Lajoie BR, Crawford J, et al. Genome sequencing in persistently unsolved white matter disorders. *Ann Clin Transl Neurol.* 2020;7(1):144-152.
12. Köhler S, Vasilevsky NA, Engelstad M, et al. The Human Phenotype Ontology in 2017. *Nucleic Acids Res.* 2017;45(D1):D865-D876.
13. Boudellioua I, Kulmanov M, Schofield PN, Gkoutos G V., Hoehndorf R. DeepPVP: Phenotype-based prioritization of causative variants using deep learning. *BMC Bioinformatics.* 2019;20(1):65.
14. Novarino G, Fenstermaker AG, Zaki MS, et al. Exome sequencing links corticospinal motor neuron disease to common neurodegenerative disorders. *Science (80-).* 2014;343(6170):506-511.

15. Cornish AJ, David A, Sternberg MJE. PhenoRank: Reducing study bias in gene prioritization through simulation. *Bioinformatics*. 2018;34(12):2087-2095.
16. Vanunu O, Magger O, Ruppin E, Shlomi T, Sharan R. Associating genes and protein complexes with disease via network propagation. *PLoS Comput Biol*. 2010;6(1):e1000641.
17. Yang H, Robinson PN, Wang K. Phenolyzer: Phenotype-based prioritization of candidate genes for human diseases. *Nat Methods*. 2015;12(9):841-843.
18. Schiffmann R. An MRI-based approach to the diagnosis of white matter disorders. *Neurology*. 2009;72:750-759. doi:10.1212/01.wnl.0000343049.00540.c8
19. Parikh S, Bernard G, Leventer RJ, et al. A clinical approach to the diagnosis of patients with leukodystrophies and genetic leukoencephelopathies. *Mol Genet Metab*. 2015.
20. Sobreira N, Schiettecatte F, Valle D, Hamosh A. GeneMatcher: A Matching Tool for Connecting Investigators with an Interest in the Same Gene. *Hum Mutat*. 2015;36(10):928-930.
21. Pant D, Dorboz I, Schluter A, et al. Loss of the sphingolipid desaturase DEGS1 causes hypomyelinating leukodystrophy. *J Clin Invest*. 2019;129(3):1240-1256.
22. Verdura E, Rodríguez-Palmero A, Vélez-Santamaría V, et al. Biallelic PI4KA variants cause a novel neurodevelopmental syndrome with hypomyelinating leukodystrophy. *Brain*. Published online August 20, 2021. doi:10.1093/BRAIN/AWAB124
23. Richards S, Aziz N, Bale S, et al. Standards and guidelines for the interpretation of sequence variants: A joint consensus recommendation of the American College of Medical Genetics and Genomics and the Association for Molecular Pathology. *Genet Med*. 2015;17(5):405-424.
24. Amendola LM, Jarvik GP, Leo MC, et al. Performance of ACMG-AMP Variant-Interpretation Guidelines among Nine Laboratories in the Clinical Sequencing Exploratory Research Consortium. *Am J Hum Genet*. 2016;98(6):1067-1076.

25. Brandt T, Sack LM, Arjona D, et al. Adapting ACMG/AMP sequence variant classification guidelines for single-gene copy number variants. *Genet Med.* 2020;22(2):336-344.
26. Rodríguez-Palmero A, Schlüter A, Verdura E, et al. A novel hypomorphic splice variant in EIF2B5 gene is associated with mild ovarioleukodystrophy. *Ann Clin Transl Neurol.* 2020;7(9):1574-1579.
27. Crow YJ, Leitch A, Hayward BE, et al. Mutations in genes encoding ribonuclease H2 subunits cause Aicardi-Goutières syndrome and mimic congenital viral brain infection. *Nat Genet.* 2006;38(8):910-916.
28. Turón-Viñas E, Pineda M, Cusí V, et al. Vanishing White Matter Disease in a Spanish Population. *J Cent Nerv Syst Dis.* 2014;6:JCNSD.S13540.
29. Stevanin G, Azzedine H, Denora P, et al. Mutations in SPG11 are frequent in autosomal recessive spastic paraplegia with thin corpus callosum, cognitive decline and lower motor neuron degeneration. *Brain.* 2008;131(Pt 3):772-784.
30. Reichert SC, Li R, Turner S, et al. HNRNPH1 □related syndromic intellectual disability: Seven additional cases suggestive of a distinct syndromic neurodevelopmental syndrome. *Clin Genet.* 2020;98(1):91-98.
31. Mingirulli N, Pyle A, Hathazi D, et al. Clinical presentation and proteomic signature of patients with TANGO2 mutations. *J Inherit Metab Dis.* 2020;43(2):297-308.
32. Kalia SS, Adelman K, Bale SJ, et al. Recommendations for reporting of secondary findings in clinical exome and genome sequencing, 2016 update (ACMG SF v2.0): A policy statement of the American College of Medical Genetics and Genomics. *Genet Med.* 2017;19(2):249-255.
33. Köhler S, Doelken SC, Mungall CJ, et al. The Human Phenotype Ontology project: Linking molecular biology and disease through phenotype data. *Nucleic Acids Res.* 2014;42:D966-74.
34. Salter CG, Cai Y, Lo B, et al. Biallelic PI4KA variants cause neurological, intestinal

35. Zou F, Zuck T, Pickersgill CD, et al. A Comprehensive and Dynamic Approach for Genetic Testing for Patient with Leukodystrophy Demonstrates a Genetic Etiology in 33% of Cases (P4.6-054). *Neurology*. 2019;92(15 Supplement):P4.6-054.
36. Lynch DS, Rodrigues Branda de Paiva A, Zhang WJ, et al. Clinical and genetic characterization of leukoencephalopathies in adults. *Brain*. 2017;140(5):1204-1211.
37. Tan TY, Lunke S, Chong B, et al. A head-to-head evaluation of the diagnostic efficacy and costs of trio versus singleton exome sequencing analysis. *Eur J Hum Genet*. 2019;27(12):1791-1799.
38. Richards J, Korgenski EK, Taft RJ, Vanderver A, Bonkowsky JL. Targeted leukodystrophy diagnosis based on charges and yields for testing. *Am J Med Genet Part A*. 2015;167A(11):2541-2543.
39. Kingsmore SF, Cakici JA, Clark MM, et al. A Randomized, Controlled Trial of the Analytic and Diagnostic Performance of Singleton and Trio, Rapid Genome and Exome Sequencing in Ill Infants. *Am J Hum Genet*. 2019;105(4):719-733.
40. Senderek J, Müller JS, Dusl M, et al. Hexosamine biosynthetic pathway mutations cause neuromuscular transmission defect. *Am J Hum Genet*. 2011;88(2):162-172.
41. Gan-Or Z, Bouslam N, Birouk N, et al. Mutations in CAPN1 Cause Autosomal-Recessive Hereditary Spastic Paraparesis. *Am J Hum Genet*. 2016;98(5):1038-1046.
42. Gardella E, Møller RS. Phenotypic and genetic spectrum of SCN8A-related disorders, treatment options, and outcomes. *Epilepsia*. 2019;60(Suppl 3):S77-S85.
43. Bondurand N, Dastot-Le Moal F, Stanchina L, et al. Deletions at the SOX10 gene locus cause Waardenburg syndrome types 2 and 4. *Am J Hum Genet*. 2007;81(6):1169-1185.
44. Harting I, Al-Saady M, Krägeloh-Mann I, et al. POLR3A variants with striatal involvement and extrapyramidal movement disorder. *Neurogenetics*. 2020;21(2):121-

45. Nakayama T, Al-Maawali A, El-Quessny M, et al. Mutations in PYCR2, Encoding Pyrroline-5-Carboxylate Reductase 2, Cause Microcephaly and Hypomyelination. *Am J Hum Genet.* 2015;96(5):709-719. doi:10.1016/j.ajhg.2015.03.003
46. Yan H, Helman G, Murthy SE, et al. Heterozygous Variants in the Mechanosensitive Ion Channel TMEM63A Result in Transient Hypomyelination during Infancy. *Am J Hum Genet.* 2019;105(5):996-1004.
47. Müller vom Hagen J, Karle KN, Schüle R, Krägeloh-Mann I, Schöls L. Leukodystrophies underlying cryptic spastic paraparesis: Frequency and phenotype in 76 patients. *Eur J Neurol.* 2014;21(7):983-988.
48. Cohen L, Manín A, Medina N, et al. Argentinian clinical genomics in a leukodystrophies and genetic leukoencephalopathies cohort: Diagnostic yield in our first 9 years. *Ann Hum Genet.* 2020;84(1):11-28.

TABLE AND FIGURE LEGENDS

Table 1. Main clinical features of the 126 index cases.

	nº cases	(%)
Sex		
Female	50	40
Male	76	60
Age at onset		
<3 years	86	68
3-18 years	15	12
>18 years	25	20
Consanguinity		
Yes	18	14
Main clinical features		
Motor symptoms		
Pyramidal	94	74
Extrapyramidal	34	27
Hypotonia	15	12
GDD/ID/cognitive decline	91	72
ASD/behaviour/psychiatric manif.	21	16
Cerebellar	42	33
Epilepsy	36	28
Ophthalmologic	55	43
Predominant MRI pattern		
Hypomyelination	40	31
Non-hypomyelination		
Periventricular	49	39
Diffuse	19	15
Frontal	12	9
Multifocal	3	2
Parieto-Occipital	2	1
Cerebellar	2	1
Complementary exams		
Metabolic studies	116	92
Neurophysiologic studies	99	78
Karyotype/aCGH/NGS panel	65	51
Targeted genetic studies	65	51
TOTAL cases	126	

Figure 1. Diagnostic process diagram and diagnostic yield (A) Number of cases included in the study and diagnostic process. (B) Global, WES and WGS diagnostic yield. (C) Percentage of diagnosis in the first WES analysis, obtained by WES reanalysis and by WGS. (D) Diagnostic percentage according to age.

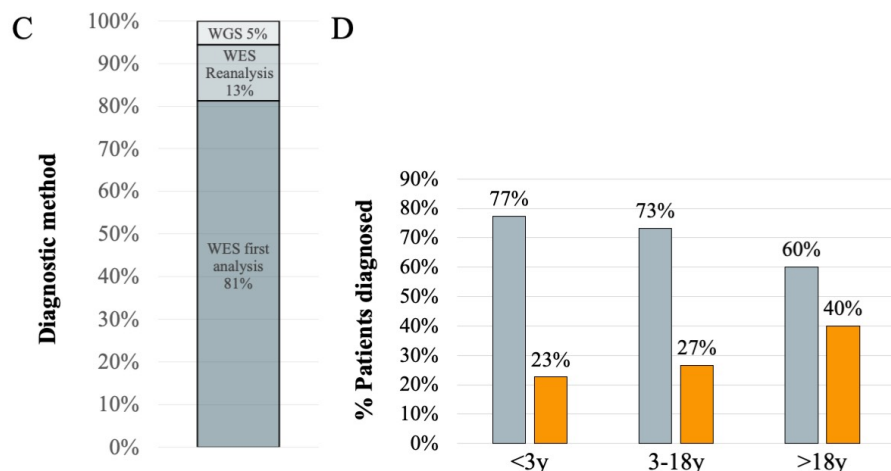
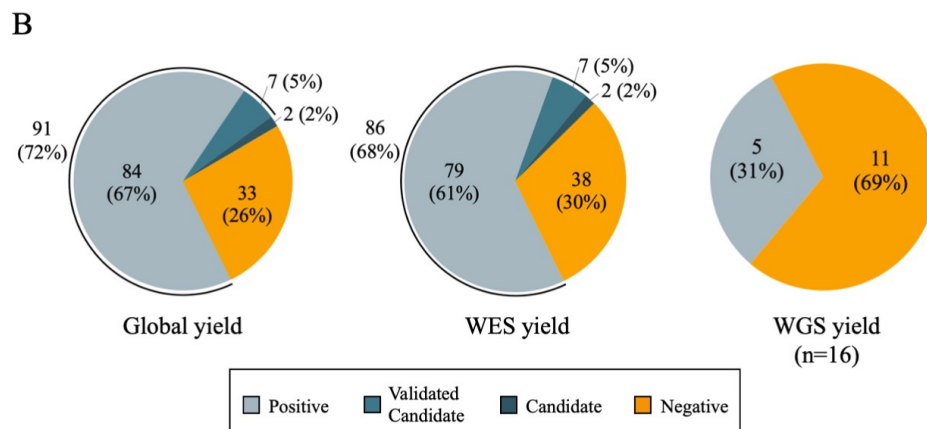
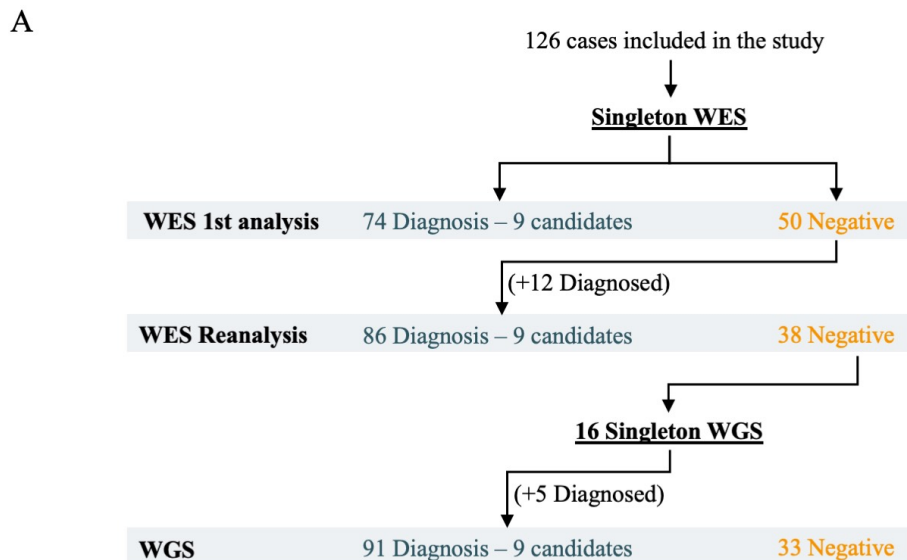


Figure 2. MRI findings in patients with new/atypical and blended phenotypes. (A) LNF-48, 5 years. *PARS2*; p.Arg186Gly / p.Lys187Arg (COMP HTZ). Periatrial WM hyperintensity (red arrows) with frontal-parietal atrophy, ventriculomegaly and thin corpus callosum (arrowheads) (axial T2-FLAIR, sagittal T1-weighted images). (B) LNF-29, 10 months. *PNPT1*; p.Ala507Ser (HMZ). Bilateral periatrial and temporal anterior subcortical WM hyperintensities (red arrows) with temporal cystic lesions (arrowheads) (axial T2 and coronal T2-FLAIR-weighted images). (C) LNF-47, 2 years. *POLR3A*; c.1771-7C>G / p.Leu1129= (COMP HTZ). Optic radiation mild WM hyperintensity (red arrows), striatal atrophy and hyperintensity (arrowheads) and superior cerebellar peduncles hyperintense signal (asterisks) (axial T2 images). (D) LNF-85, 48 years. *PSEN1*; p.Thr350Ile (HTZ). MRI showed diffuse WM hyperintensities (red arrows) with corpus callosum and cortical atrophy (arrowheads) (axial T2 and sagittal T1 FLAIR images). (E) LNF-88, 13 years. *GFPT1*; p.Asp296Val (HMZ). Axial T2 hyperintensities involving deep cerebral WM (red arrows), cerebellar peduncles (white arrows) and middle blade of corpus callosum (arrowheads), sparing subcortical WM (axial T2 and sagittal T1-weighted images). (F) LNF-114, 5 months. *SCN8A*; p.Val409Met (HTZ). Important myelination delay, thin corpus callosum and signs of cerebral and cerebellar atrophy (axial and sagittal T1-weighted images). (G) SPG-25, 44 years. *SOX10*; p.Tyr83Asp (HTZ). Periventricular WM signal abnormality, sparing U fibers (red arrows), and thin isthmus of the corpus callosum (arrowhead) (axial T2-FLAIR and sagittal T1 weighted images). (H) LNF-40.0, 13 years. *CYP2U1*; p.Arg178Thr (HMZ) and LNF-40.4, 15 years. *PAH*; p.Thr380Met (HMZ). Periventricular WM hyperintensities (red arrows) (axial T2 weighted images). (I) LNF-56, 15 years. *POLR3A*; p.Cys724Tyr/ p.Pro705Ala (COMP HTZ) and *CACNA1A*; p.Tyr546Ter (HTZ). Periventricular symmetric heterogeneous WM hyperintensities (red arrows) and hypointensity in globus pallidus (arrowheads), thalamic anterolateral nuclei (asterisks), optic radiations and pyramidal tracts, with mild atrophy of the cerebellar superior vermis (white arrow) (axial T2 and sagittal T1-

weighted images). (J) LNF-89.3, 15 years. *CP*; p. Gly868GlufsTer26 (HMZ)/*NDUFS1*; p.Ser701Asn (HTZ). Periventricular symmetric T2 hyperintensity with cystic degeneration and pyramidal tract involvement (red arrows) and corpus callosum atrophy. Accumulation of paramagnetic material in the *substancia nigra* (asterisks) (axial T2-FLAIR and axial SWI).

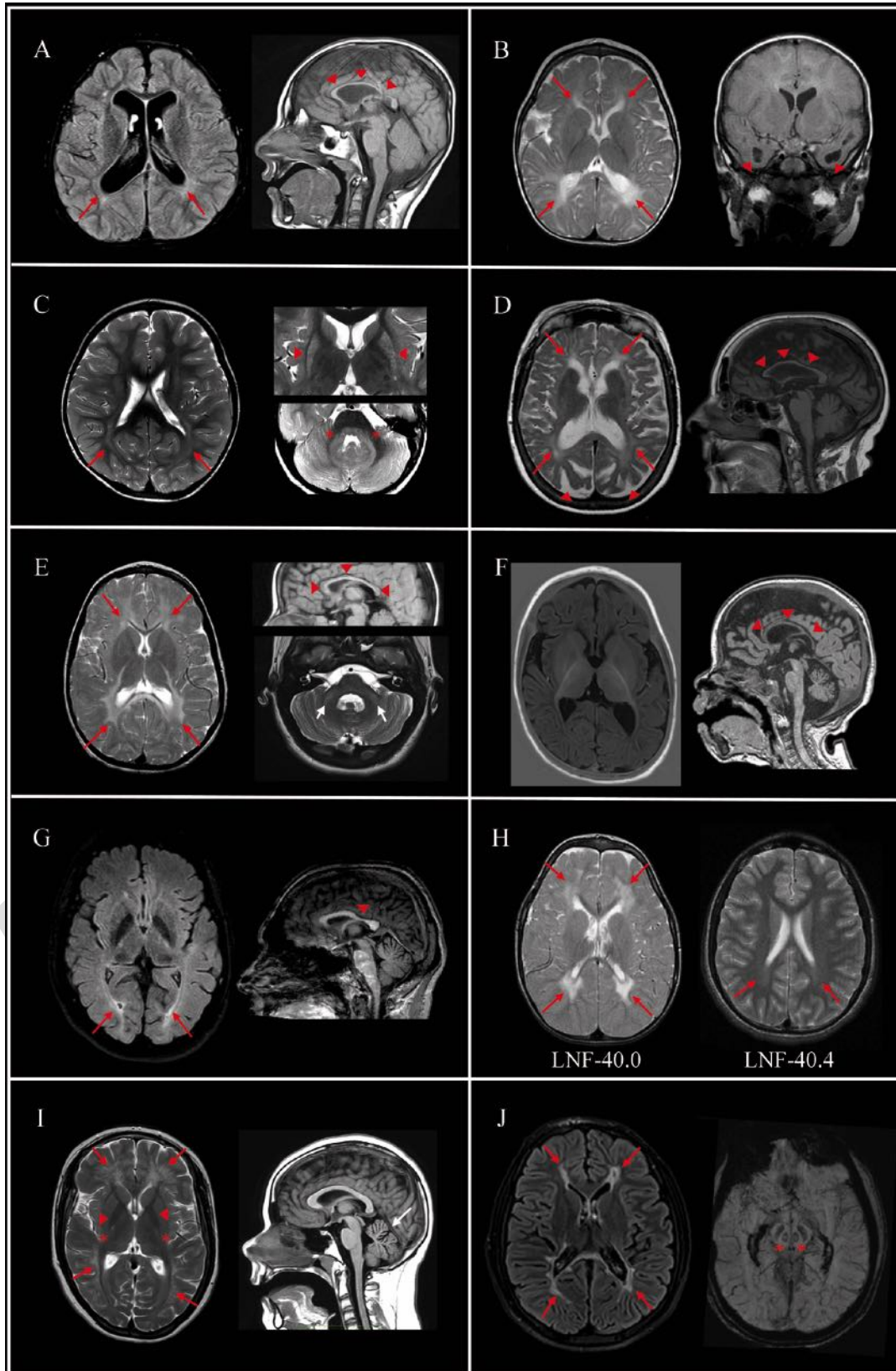


Figure 3. MRI images of selected cases with variants in hereditary spastic paraparesis (HSP) genes and white matter involvement. T2 hyperintensity in the bilateral periventricular white matter (axial T2 images (A and D); axial T2-FLAIR images (B and C).

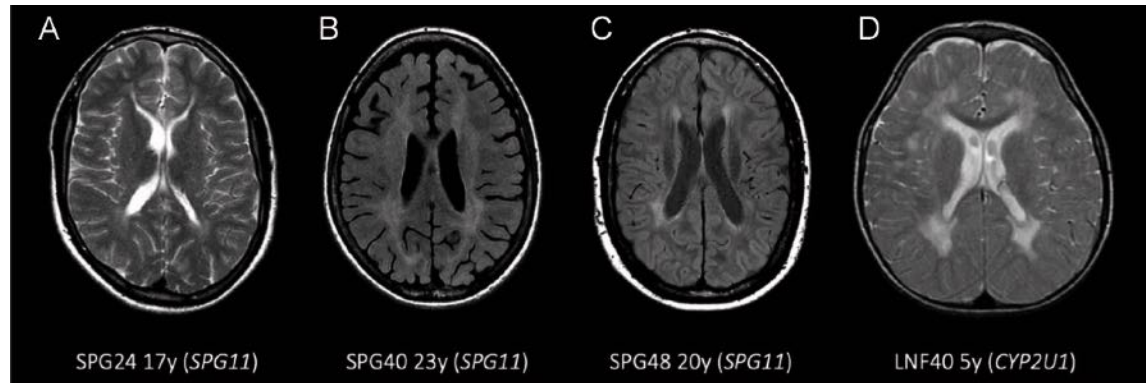
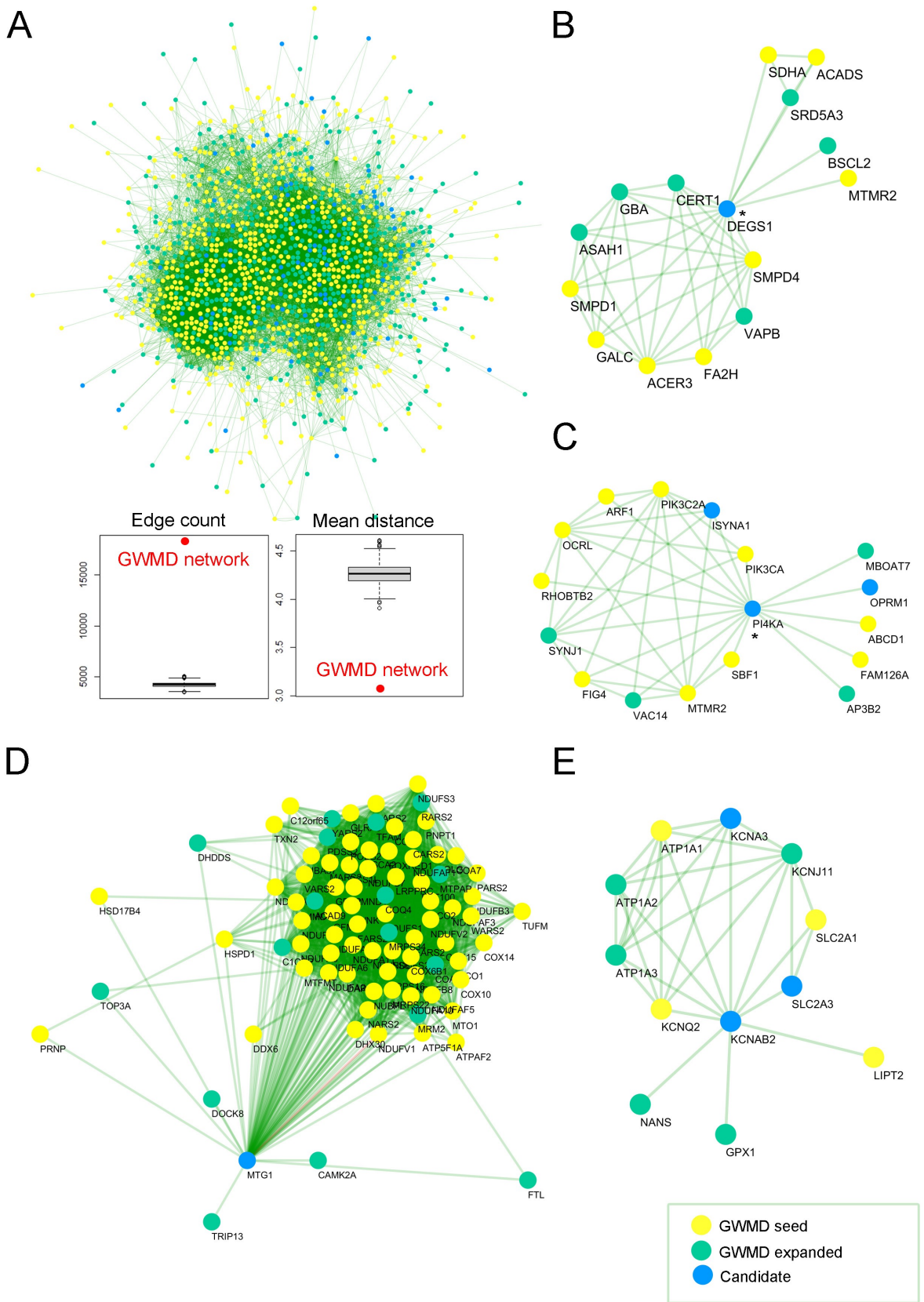


Figure 4. GWMD expanded interactome. (A.a) The GWMD seeds + expanded network was generated by the network prioritization tool, resulting in 1530 proteins. The seed genes known to be mutated in GWMD are shown in yellow circles, disease genes not previously associated with GWMD are shown in green, and new GWMD candidates are shown in blue. Comparison of statistical connectivity strength 525 of the GWMD expanded network with 1000 permutations of randomly selected proteins from the global human network. Red dots denote the value of the metric on the GWMD expanded network constituted by 1530 proteins. Box and whisker plots denote matched null distributions (i.e., 1000 permutations). (A.b) Within-group edge count (i.e., number of edges between members of the query set). (A.c) Mean distance is the average path length in the network obtained by calculating the shortest paths between all pairs of proteins. (B, C, D and E) Zoom in the network for specific putative candidates as illustrative example of the GWMD expanded network potentiality: (A) delta 4-desaturase, sphingolipid 1 (*DEGS1*); (B) phosphatidylinositol 4-kinase alpha (*PI4KA*); (D) mitochondrial ribosome-associated GTPase 1 (*MTG1*); and (E) potassium voltage-gated channel subfamily A regulatory beta subunit 2 (*KCNAB2*) protein. * indicates recently associated with leukodystrophy.

White Matter expanded network. Available in NDEx repository at
<https://public.ndexbio.org/#/network/fd5fc166-9ecc-11eb-9e72-0ac135e8bacf?accesskey=a75ac048b59aca2c9310c04a6f1d96ea34052231d9204f284c5e1d420fc2ca26>



Appendix 2: Coinvestigators

Name	Location	Contribution
Hugo A. Arroyo, MD	H. Garrahan (Argentina)	Major role in the acquisition of data
Andrés Barrios, MD	H. San Borja Arriarán (Chile)	Major role in the acquisition of data
Andrea Campo, MD	H. Virgen Macarena, Sevilla (Spain)	Major role in the acquisition of data
Tamara Castillo, MD	H. Donostia, Donostia (Spain)	Major role in the acquisition of data
Rosario Cazorla, MD	H. Puerta de Hierro, Madrid (Spain)	Major role in the acquisition of data
María Asunción García, MD	H. Alcorcón, Madrid (Spain)	Major role in the acquisition of data
Ainhoa García, MD	H. Cruces, Bilbao (Spain)	Major role in the acquisition of data
Antonio Hedrera, MD	H. Central de Asturias, Oviedo (Spain)	Major role in the acquisition of data
Juan Hernández, MD	H. Universitario de Guadalajara, Guadalajara (Spain)	Major role in the acquisition of data
Nathalie Launay, MD	IDIBELL, Barcelona (Spain)	Major role in the acquisition of data
Maria Lorenzo, MD	H. Infanta Cristina, Madrid (Spain)	Major role in the acquisition of data
Concepción Miranda, MD	H. Gregorio Marañón, Madrid (Spain)	Major role in the acquisition of data
Fermín Moreno, MD	H. Donostia, Donostia (Spain)	Major role in the acquisition of data
Amaia Muñoz, MD	H. Donostia, Donostia (Spain)	Major role in the acquisition of data
Juan Narbona, MD	Clínica U. Navarra, Pamplona (Spain)	Major role in the acquisition of data
Mª Socorro Pérez, MD	H. Marqués de Valdecilla, Santander (Spain)	Major role in the acquisition of data
Maria Antonia Ramos, MD	H. Virgen del Camino, Pamplona (Spain)	Major role in the acquisition of data
Miquel Raspall-Chaure, MD	H. Vall d'Hebron, Barcelona (Spain)	Major role in the acquisition of data
Manel Roig-Quilis, MD	H. Vall d'Hebron, Barcelona (Spain)	Major role in the acquisition of data
Miguel Ángel Urtasun, MD	H. Donostia, Donostia (Spain)	Major role in the acquisition of data
María Esther Vázquez, MD	H. Lucus Augusti, Lugo (Spain)	Major role in the acquisition of data
Juan Francisco Vázquez, MD	H. La Fe, Valencia (Spain)	Major role in the acquisition of data

Supplemental Results

Illustrative Clinical Cases

MRI images are displayed in Figure 2 in the main text.

a) Novel phenotypes

LNF-48: a 13-year-old male patient and his 9-year-old sister, born from nonconsanguineous parents after uneventful pregnancies and deliveries. Both presented global developmental delay with hypotonia evolving to spastic paraparesis with ataxia and were able to walk with assistance at the last examination. They also had erratic ocular movements and bimanual stereotypies, but none of them had seizures. MRI showed periatrial T2 WM hyperintensity with frontoparietal atrophy and a thin corpus callosum. Metabolic studies were normal. Both patients were compound heterozygous for missense variants in *PARS2* (p.Arg186Gly) and (p.Lys187Arg), classified as likely pathogenic according to the ACMG criteria^{1,2}, and segregation studies were consistent with an autosomal recessive mode of inheritance. Although developmental delay, spasticity, predominantly anterior cortico-subcortical atrophy and a thin corpus callosum had been reported in association with *PARS2*, the few cases reported to date had presented a severe seizure disorder, most of them with hyperlactatemia and MRI findings of basal ganglia abnormalities or hypomyelination³. Therefore, this family expands the clinical phenotype associated with *PARS2*.

LNF-105: a 11-year-old male harbouring a duplication encompassing both the *HNRNPH1* and *RUFY1* genes (5q53.3(178950829-179067861)x3). The phenotype was reported in a previous publication⁴.

b) Atypical phenotypes

LNF-29: two brothers aged 14 and 7 years, born from nonconsanguineous parents after an uneventful pregnancy and delivery. Both had shown severe global developmental delay with hypotonia since the first months of life, which had evolved to spastic-dystonic tetraparesis. They also had microcephaly, nystagmus and erratic ocular movements, and the older brother also presented generalized and myoclonic seizures between 3 months and 3 years of age. MRI showed bilateral periatrial and temporal anterior subcortical T2 WM hyperintensities, WM volume loss, a thin corpus callosum and cysts in the anterior temporal regions. They harbor one variant in homozygosity in the *PNPT1* gene (p.Ala507Ser), classified as pathogenic. The MRI pattern in these two brothers, resembling RNASET2, Aicardi-Goutières syndrome or a congenital CMV infection, has been reported recently to be associated with mutations in *PNPT1*⁵.

LNF-47: a 4-year-old male compound heterozygous variants in *POLR3A* (p.Leu1129= and c.1771-7C>G) clinical and radiological phenotype reported in a previous publication⁶.

LNF-77: biallelic heterozygous variants *in trans* were found in *POLR1C*, a gene associated with POLR3-related leukodystrophy and Treacher Collins syndrome.

Although it has been suggested that mutations in these two diseases act via different mechanisms (impairment of the assembly and nuclear import of POLR3 in leukodystrophy cases), one of the variants present in this patient (p.Arg279Gln) had previously been described exclusively in Treacher Collins syndrome cases to date and had been shown to impair nucleolar targeting⁷. Given that our patient did not show any features of Treacher Collins syndrome, we propose that pathogenic variants already described in Treacher Collins syndrome cases may also cause leukodystrophy, at least when found in compound heterozygosity with another causative mutations.

LNF-85: a 64-year-old woman presented cognitive decline and pyramidal signs starting at 48 years of age. She had no previous remarkable family or personal history. MRI showed diffuse T2 WM hyperintensities with cortical and cerebellar atrophy. We identified the variant (p.Thr350Ile) in heterozygosis in *PSEN1*, a gene that has been associated with Alzheimer disease but also with spastic paraparesis⁸. Although white matter hyperintensities have been identified as a core feature in autosomal dominant forms of Alzheimer's disease⁹, the pattern in this case resembled leukodystrophy.

LNF-88: two sisters, aged 15 and 16 years, who were born from consanguineous parents and presented a clinical picture with predominant progressive spastic paraparesis since the first year of life with proximal weakness, dysarthria and cognitive deficits. MRI of both sisters performed at 2 and 12 years old in one and at 3 and 15 years old in the other, showed nonprogressive T2 WM hyperintensities in predominantly deep cerebral WM, the inner layer of the corpus callosum and the middle cerebellar peduncles, sparing the periventricular and subcortical cerebral WM and the outer layers of the corpus callosum.

EMG revealed a myopathic pattern. We identified a missense variant in *GFPT1* (p.Asp296Val) in homozygosity, a gene that is mainly associated with myasthenic syndromes but has also been reported very recently to cause a leukoencephalopathy¹⁰ that shows an MRI pattern overlapping with our two cases (**Figure 2, F**).

LNF-114: a male patient, currently 3 years old, with no remarkable family or perinatal history, who presented neonatal seizures since the first minutes of life and hyperekplexia-like episodes in response to sounds. He also had global developmental delay; global hypotonia; and phenotypic abnormalities consisting of a long face, prominent forehead, low hairline, low-set and dysplastic ears, bilateral inguinal and abdominal hernias, arthrogryposis, and bone dysplasia with bilateral hip luxation. MRI performed at 5 months showed an important myelination delay, thin corpus callosum and signs of cerebral and cerebellar atrophy. WES revealed a *de novo* heterozygous missense variant in *SCN8A* (p.Val409Met). Previously reported manifestations associated with *SCN8A* did not include bone dysplasia, dysmorphic traits or giant hernias. Severe myelination delay is not a frequent feature, although it has been reported in two patients previously¹¹. Similarly, hyperekplexia-like episodes have been described in a single patient¹².

SPG-2: a 76-year-old male patient with spastic paraparesis and upper limb hyperreflexia and dysarthria with onset at 40 years of age. He was born at full term to nonconsanguineous parents after an unremarkable pregnancy and delivery. His development was considered normal during childhood. He had two older healthy siblings. MRI performed at clinical onset showed bands of periventricular WM hyperintensities on T2 and FLAIR sequences. He was homozygous for a pathogenic variant (c.1605+5G>A)

in *CAPN1* that had been previously described to result in exon skipping, generating a frameshifted transcript¹³. The presence of white matter abnormalities had been reported previously in only one case of spastic paraplegia 76 (OMIM # 616907)¹⁴

SPG-25: a family with 4 affected generations (the index case (male) and his mother, grandmother, sister and nephew) with predominant ataxia beginning in youth, slow saccades, nystagmus, cephalic tremor, dysarthria, dysphagia, and demyelinating neuropathy with motor, sensitive and autonomic involvement. Brain MRI showed diffuse WM signal abnormalities compatible with hypomyelination without cerebellar atrophy. WES revealed a heterozygous missense novel variant (p.Tyr83Asp) in *SOX10* that was firstly classified as a VUS according to ACMG criteria, but cosegregation studies in this family including three affected members were consistent. *SOX10* mutations are known to cause Waardenburg syndrome with Hirschsprung disease (OMIM # 613266) and a more severe phenotype, including peripheral demyelinating neuropathy, central dysmyelinating leukodystrophy, Waardenburg syndrome and Hirschsprung disease (PCWH) (OMIM # 609136)¹⁵. In this family, there are predominant neurological manifestations but are not associated with Hirschsprung or Waardenburg syndrome, thus expanding the clinical spectrum associated with *SOX10* variants.

c) Cases with dual diagnoses

LNF40: a family with 3 affected siblings (13, 21 and 20 years old) who were born from consanguineous parents of Palestinian origin and presented global developmental delay and spasticity starting in the first two years of life. A metabolic neonatal screening study was not performed in the country of origin. MRI showed confluent symmetric

periventricular T2 hyperintensities in LNF40.0 and LNF40.3 and delayed myelination in LNF40.4. We identified a previously unreported, homozygous VUS variant (p.Arg178Thr) in *CYP2U1* in the first two siblings (SPG56, OMIM: 615030), while LNF40.4 harbored a homozygous pathogenic variant in *PAH* (p.Thr380Met), already described as causing phenylketonuria, which was biochemically confirmed after the molecular report was handed. Segregation analysis was compatible in this family.

LNF-56: a 15-year-old female patient who presented moderate intellectual disability, ADHD, behavioral abnormalities (obsessions, mood disorder, emotional lability, visual hallucinations), absence and myoclonic seizures beginning at thirteen years old. She also showed nystagmus, strabismus and instability starting in the first years of life. MRI showed periventricular heterogeneous T2 WM hyperintensities and hypointensity in the globus pallidus, thalamic anterolateral nuclei, dentate nuclei, optic radiations and pyramidal tracts, with mild atrophy of the cerebellar superior vermis. WES analysis identified two variants in *POLR3A* in compound heterozygosity, classified as pathogenic (p.Cys724Tyr) and likely pathogenic (p.Pro705Ala), as well as a heterozygous loss-of-function variant in *CACNA1A* (p.Tyr546Ter) that was revealed to be *de novo* after the segregation study. The patient's clinical picture could be more related to the variant in *CACNA1A*, but the radiological pattern was more consistent with *POLR3A*.

LNF-89: two siblings, 21 and 18 years old, who presented with microcytic and hypochromic anemia with low plasma and urinary copper, low ceruloplasmin and high plasmatic ferritin. Hepatic MRI showed iron overload, which, together with the biochemical abnormalities found, was fully compatible with aceruloplasminemia. Cranial MRI showed accumulation of paramagnetic material in the *substantia nigra* and red nuclei on SWI in both, but also periventricular symmetric T2 hyperintensity with necrosis and cystic degeneration and pyramidal tract involvement and corpus callosum atrophy in

LNF89.3, who also manifested a global developmental delay since the first months of life with spastic paraparesis and dysarthria. Taking into account that neurological manifestations in aceruloplasminemia usually appear during adulthood and consist of chorea, dystonia, tremors or ataxia related to iron accumulation in the basal ganglia, thalamus and dentate nucleus, a WES study was performed and allowed identification of a homozygous variant (p.Gly868GlufsTer26) in the *CP* gene in both brothers, confirming aceruloplasminemia, but also a *NDUFS1* missense homozygous VUS variant in LNF89.3 (p.Ser701Asn), probably accounting for the neurological manifestations in this patient.

SPG-62: a 7-year-old patient with global developmental delay that progressed to mild cognitive impairment and autism spectrum disorder. At 2 ½ years, he presented a convulsive status epilepticus with respiratory depression and Todd's paralysis of the right side of the body and later seizures in the context of fever, for which he was treated with valproic acid. Beginning at 3.5 years of age, he developed progressive spastic paraparesis. He also had dysarthria and strabismus. His older brother had a delayed language acquisition. MRI showed a mild myelination delay. WES revealed a pathogenic variant in *ATP1A3* (p.Pro775Leu) in heterozygosity, which has been reported in ClinVar in several patients with neurodevelopmental disorders, as well as a hemizygous variant in *NEXMIF* (p.Pro789Leu). The clinical phenotype of the patient was compatible with these two genes^{16,17}.

GWMD expanded network validation

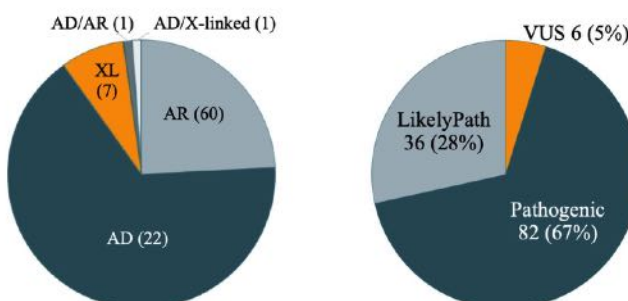
To assess whether there was greater connectivity in the GWMD expanded network than in the global network, we calculated i) the number of edges between protein pairs and ii) the average path length in the GWMD network by calculating the shortest paths between

all protein pairs. We then compared these statistics for 1000 permutations of a randomly selected set of 1530 proteins derived from the global network. Next, we calculated the Z scores to describe how far the measures of the GWMD expanded network deviate from the expected mean (μ) to finally obtain that the GWMD expanded network is significantly much more cohesive than expected by chance ($P<1E-25$).

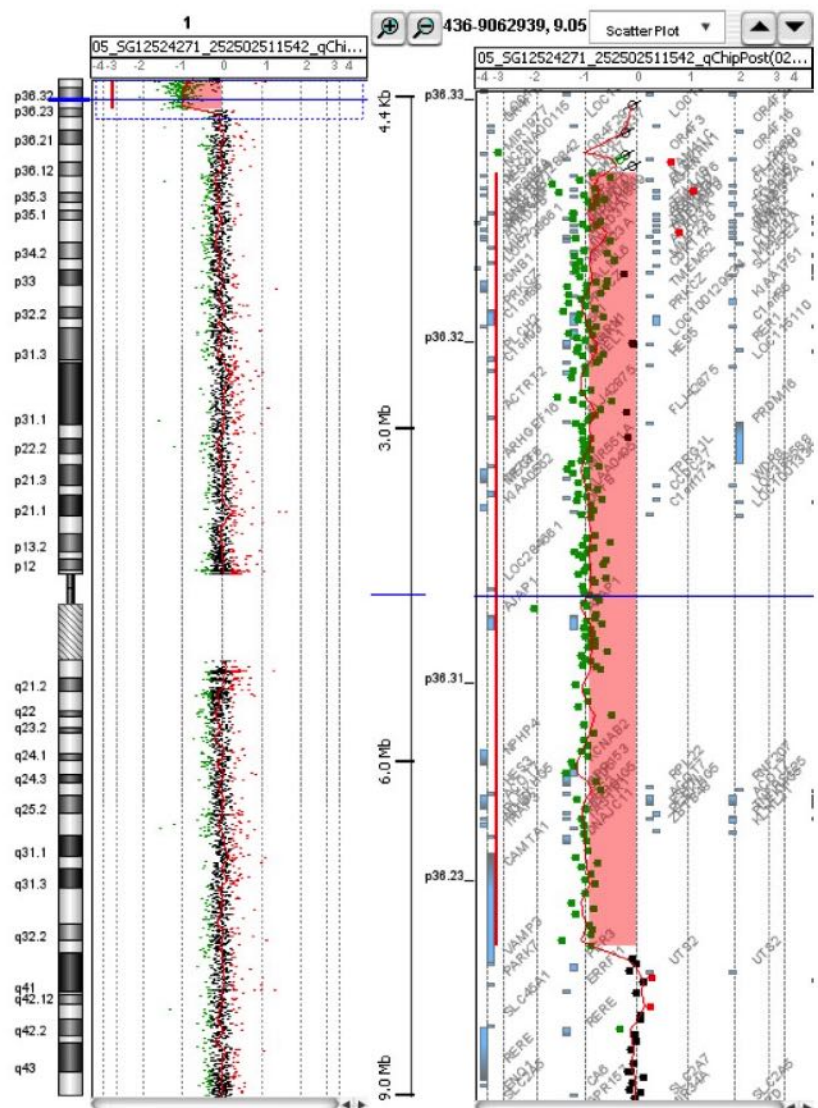
Among the 1530 proteins conforming to the expanded GWMD network, there were 100 candidates that were not previously associated with diseases, providing reasonable functional candidates for further research (eTable 6). To evaluate the possible disease association of the new gene candidates, we analyzed their gene constraints, including loss-of-function intolerance (pLI) or missense variation intolerance (missense Z-score). Among the 100 new candidates, we found 26 proteins extremely loss-of-function intolerant with a $pLI \geq 0.9$ (the closer pLI is to one, the more LoF-intolerant the gene appears to be. $pLI \geq 0.9$ was considered extremely LoF intolerant, such as nuclear receptor binding SET domain protein 2 (*NSD2*), and 8 missense variation intolerant proteins with a Z-score ≥ 3.08 (i.e. with probability $P<0.001$), such as GA binding protein transcription factor subunit alpha (*GABPA*).

eFigure Legends

eFigure 1. Inheritance pattern of the diagnosed cases and distribution of variant classification.



eFigure 2. 1p36 deletion array-CGH. Detail of the molecular karyotype showing the terminal 7.6 Mb deletion identified in the short arm of chromosome 1 in case LNF-45. arr[GRCh37] 1p36.33p36.23(757093_7686264)x1.



eTable legends

eTable 1. Clinical table. Clinical manifestations, main complementary exams and genes identified in diagnosed cases. Specific therapeutic options.

eTable 2. ACMG criteria for the classification of identified variants

eTable 3. List of identified genes, OMIM nomenclature and numbers of cases identified in our cohort.

eTable 4. Atypical cases. Patients with new phenotypes, atypical forms of presentation and blended phenotypes in families with more than one gene associated with the phenotype.

eTable 5. Cases with functionally validated variants.

eTable 6. Cases with experimentally validated CNV variants.

eTable 7. New variants. Table with the 73 novel variants indentified in our cohort.

eTable 8. Enrichment of GO terms of molecular function in the GWMD network.

Top 50 molecular function (MF) GO terms enriched in the GWMD network integrating proteins by using hypergeometric distribution function statistical analysis.

eTable 9. Enrichment of GO terms of biological process in the GWMD network. Top 50 biological process (BP) GO terms enriched in the GWMD network integrating proteins by using a hypergeometric distribution function statistical analysis.

eTable 10. Enrichment of GO terms of cellular compartment in the GWMD network. Top 50 cellular compartment (CC) GO terms enriched in the GWMD network integrating proteins by using a hypergeometric distribution function statistical analysis.

eTable 11. Candidate genes in the GWMD network. One hundred candidate genes predicted by the prioritization tool to be associated with GWMD.

eTable 1. Clinical table. Clinical manifestations, main complementary exams and genes identified in diagnosed cases. Specific therapeutic options.

Patient ID	Sex, current age	Age at onset	Family history	Motor symptoms	Cognitive-Behavior	Ataxia	Epilepsy	Head Growth	Ophthalmologic	MRI involvement	Others / Investigation findings	Gene	Diagnostic technique	Specific therapeutic / management options	
LNF-1	F, 33 y	4 y	YES (sister)	Pyramidal signs Wheelchair (19 y)	GDD / ID	YES	YES	N	Myopia magna	Hypomyelination	Dysarthria, dysmetria Hypogonadotropic hypogonadism Dysphagia	<i>POLR3A</i>	WES	Hypogonadism management	
LNF-6	F, 40 y	27 y	YES (mother and sister)	Pyramidal and Extrapyramidal signs, weakness	N	NO	Macrocephaly	N		Frontal T2 WM HI	Suprasellar insufficiency Episodic dystonic movements	<i>CSF1R</i>	WES	HSCT	
LNF-15	M, 7 y	3 m	NO	Hypotonia	GDD-ID	Instability	YES, neonatal focal seizures	Macrocephaly	Nystagmus	Hypomyelination, Subarachnoid space enlargement in FT areas	(3m) Irritability, opisthotonus Lumbosacral hernivertebral, kyphosis, sparse hair; absent osteo-tendinous reflexes	<i>TMEM63A</i>	WES (Re-analysis)	NO	
LNF-16	M, 45 y	28 y	NO	Pyramidal signs	Manic depressive	NO	NO	Optic neuritis		Thin CC	Abnormal VEPs, BAEPs	Motor apraxia Language disorder	<i>CSF1R</i>	WES	HSCT
LNF-18	F, 19 y	18 m	Consanguinity	Pyramidal signs Lower limb weakness Wheelchair (3 y)	GDD-ID	NO	YES, clonic seizures	N	Nystagmus, optic nerve atrophy	Frontal T2 WM HI	Periorbito-occipital, posterior arm of internal capsules, brainstem and cerebellar peduncles	Irritability Denyelinating PNP Low GALC activity	<i>GALC</i>	WES	HSCT
LNF-19	F, 18 y	3 y	NO	Pyramidal signs Lower limb weakness Wheelchair (10 y)			YES, generalized myoclonic	YES		T2 WM HI					
LNF-20	F, 26 y	4 y	NO	Athetosis	GDD / ID	YES	NO	Normal	N	Diffuse T2 WM HI Cystic lesions	Hypomyelination Thin CC	Relapses: lethargic, dizziness, headache, weakness (fever)	<i>EFB5</i>	WES	Avoidance of head trauma
LNF-23	F, 25 y	2 y	NO		GDD-ID Manic depressive psychosis	YES	NO	N	N	Cerebellar atrophy	Hypomyelination Thalamus T2 hypointensity Enlarged ventricles CC and brainstem atrophy	Severe dysphagia Urinary incontinence	<i>POLR3B</i>	WES	NO
LNF-28	M, 23 y	<6 m	Consanguinity	Rigid-akineti c syndrome	GDD-ID	Instability	YES, epileptic encephalopathy	N	Nystagmus Strabismus Microphthalmia Congenital bilateral cataract Upgaze limitation	Hypomyelination Mild brain atrophy Thin CC	Dysmorphic traits Abn. VLCFA Abn. ERG, VEPs, BAEPs	<i>PEX11b</i>	WES	NO	

LNF-29	M, 4 y	<6 m	YES (brother)	Spastic-dystonic tetraparesis	GDD LDD	NO	NO	Microcephaly	Erect movements Nystagmus	Periventricular and subcortical temporal anterior T2 WM HI Temporal cystic lesions WM and CC atrophy MRS periventricular decrease NAA	Ataxia	<i>PNPPT1</i>	WES (Re-analysis)	NO
LNF-30	F, 21 y	4 y	NO	Spastic-dystonic tetraparesis	Normal	NO	NO	Microcephaly	Instability	Posterior T2 WM HI	<i>TUBB4A</i>	WES	NO	
LNF-31	F, 27 y	17 y	NO	Spastic tetraparesis	Behavioral disorder Dysthymia	NO	YES, generalized	Microcephaly	Periventricular, inferior colliculi, dentate nuclei and cerebellar hemispheres T2 WM HI (progressive) Cystic lesions Cervical medullar atrophy	Episode: headache, weakness in the right limbs and urinary incontinence	<i>EF2B5</i>	WES	Avoidance of head trauma	
LNF-32	F, 3 y	10 m	NO	Spastic-dystonic tetraparesis	GDD-ID	NO	NO	Microcephaly	Hyponyelination White matter atrophy. Cephalocephaly	Startle response. Irritability Dysarthria CSF neopterin increase Abn. SSEP, VEPs	<i>RNASEH2B</i>	WES	JAK1 and JAK2 inhibitors Monitoring of immuno-mediated manifestations	
LNF-33	M, 14 y	2 y	Consanguinity	Spastic-dystonic tetraparesis Orofacial and arms dystonia	Language regression	YES	NO	Microcephaly	Periventricular T2 WM HI with cerebellar, CC and posterior medullar involvement	Difuse T2 WM HI Cerebellar and medulla atrophy	<i>DARS2</i>	WES (Re-analysis)	NO	
LNF-34	M, 50 y	30 y	NO	Spastic paraparesis	N	YES	NO	Microcephaly	Difuse T2 WM HI Urinary incontinence	<i>LMNB1</i>	WES	NO		
LNF-36	M, 5 y	<12 m	NO	Hypotonia	GDD-ID	YES	NO	Microcephaly	Hyponyelination T2 HI pyramidal bulbs Cortico-subcortical atrophy. Thin CC	Dysmorphic traits Adrenal insufficiency Hepatomegaly Abn. VLCFA Denyelinating PNP Abn. BAEPs	<i>PEX6</i>	WES	NO	
LNF-37	F, 32 y	26 y	NO	Pyramidal signs Dystonia Lower limb paresthesia	N	Instability	NO	Microcephaly	Periventricular, cerebellar peduncles and pons/tuberance T2 WM HI Cerebral and medullar atrophy Thin CC	Precocious menopause Abn. SSEP, VEPs	<i>EF2B5</i>	WES	POF treatment Avoidance of head trauma	
LNF-40.0 and 40.3	M, 10 y	10 m	Consanguinity YES (affected sister and brother)	Spastic-dystonic tetraparesis	GDD-ID	NO	YES	Microcephaly Nystagmus	Periventricular WM HI WM, CC and BS atrophy	Dysphagia, Dysarthria	<i>CYP2U1</i>	WES	NO	

LNF-40.4 (brother)	M, 16 y	< 1 m	Consanguinity YES (affected sister and brother)	Spasticity	GDD-ID	YES	NO	N	N	Hyponyelination Short CC	Increased pl Phe	P4H	WES	Dietary treatment
LNF-41	F, 1.5 y (exitus)	NN	Consanguinity	Spastic tetraparesis	GDD	NO	NO	IHG	Nystagmus	Hyponyelination Mild ventriculomegaly	Ponto-statual delay NN myoclonus Denyelinating PNP Abn. SSEP, VEPs, BAEPs	DEGS1	WES	Fingolimod (under investigation)
LNF-42	F, 5 y	NN	NO	Spastic tetraparesis	GDD / ID	NO	YES	Microcephaly / IHG	Congenital nystagmus Oculogyric crisis	Hyponyelination CC, BG and cerebellar atrophy	Hypodontia Articular contractures Cachexia	DEGS1	WES	Fingolimod (under investigation)
LNF-43	M, 12 y	6 y	NO	Spastic paraparesis	N	NO	NO	Normal	Normal	Diffuse T2 WM HI	EFZB5	WES	Avoidance of head trauma	
LNF-45	F, 5 y	<1 m	NO	Pyramidal signs	GDD	NO	YES	NN clonic and myoclonic Pharmacoresistant epilepsy	N	Nystagmus	Dysmorphic traits Dehydration episodes Anemia, thrombocytopenia Abn. BAEPs	lp36 del	WES	NO
LNF-47	M, 4 y	6 m	NO	Pyramidal and Extrapyramidal	GDD / ID	YES	NO	Normal	Normal	Subcortical T2 WM HI as well as in centrum semiovale, corona radiata, optic radiation and also in dentate nuclei and superior and inferior cerebellar peduncles Striatal necrosis	Increased mitochondria in muscle biopsy Decreased activity of complex I, II, III	POLR3A	WES (Re-analysis)	NO
LNF-48.0	M, 9 y	6 m	YES (brother affected)	Pyramidal signs	GDD	YES	NO	N	Erratic movements	Stereotypies Abnormal SSEP Abnormal VEPs	PARS2	WES	NO	
LNF-51	M, 3 y	6 m	NO	Spastic paraparesis	GDD	NO	NO	N	N	Multifocal, parietal T2 WM HI Cystic lesions Restricted diffusion T-O	NDUFS1	WES	NO	
LNF-56	F, 16 y	11 m	NO	Behaviour disorder	GDD	YES	YES	N	Nystagmus Strabismus	Hyperlactemia	POLR34 CACNA1A	WES	Hypogonadism management Acetazolamide (CACNA1A)	
LNF-57	M, 7 y	5 y	NO	NO	NO	NO	YES	N	Generalized	Periventricular WM HI, anterior predominance	GFAP	WES	NO	

LNF-66	F, 1 y	5 m	NO	Hypotonia Dyskinetic movements	GDD	NO	YES	Microcephaly	No visual tracking	Bilateral capsulo-thalamic focal T2 HI Delayed myelination Mild CC atrophy (5m)	Pigiocephaly Low pl uric acid and homocysteine Abn. VEPs Normal cardiological study	<i>TPA4</i>	WES	WES	NO
LNF-69	M, 3 y	4 m	Consanguinity	Spastic tetraparesis	GDD	NO	NO	N	Nystagmus	Hypomyelination Bilateral hippocampus atrophy	Opiostethosis Ponto-statalur delay Gastroesophageal reflux Denyelinating PNP	<i>RNASEH2B</i>	WES	WES	JAK1 and JAK2 inhibitors Monitoring of immuno-mediated manifestations
LNF-70	F, 41 y	38 y	NO	Pyramidal signs	Cognitive decline Behaviour disorder	NO	NO	N	N	Frontal T2 WM HI		<i>CSF1R</i>	WES	WES	HSCT
LNF-71	M, 6 y	1 y	Consanguinity NO	Motor clumsiness	ID	YES	NO	NO	N	Periventricular T2 WM HI. Involvement of U fibers in frontal areas	Tremor Normal metabolic study (plasma, urine, CSF) OXPHOS (ms) normal	<i>EF2BS GFMI</i>	WES (Re-analysis)	WES (Re-analysis)	Avoidance of head trauma
LNF-72	F, 3 y	4 m	NO	Pyramidal and Extrapyramidal	GDD	NO	NO	Microcephaly , strabismus	Hypometropia	Periventricular T2 WM HI	Hip dysplasia CSF increased lactate OXPHOS N (muscle)	<i>MSTO1</i>	WES (Re-analysis)	WES (Re-analysis)	NO
LNF-76	F, 3 y	4 m	Consanguinity YES (sister)	Pyramidal and Extrapyramidal	GDD / ID	NO	YES	Microcephaly / Insufficient head growth	Eratic movements	Diffuse T2 WM HI Thin CC	Stable response Irritability Ponto-statalur delay	<i>TREX1</i>	WES (Re-analysis)	WES (Re-analysis)	JAK1 and JAK2 inhibitors Monitoring of immuno-mediated manifestations
LNF-77	M, 21 y	3 y	NO	Spastic-dystonic tetraparesis Motor apraxia	ID	YES	NO	N	Upgaze limitation Slow saccades Hypometropia	Hypomyelination	Dysmetria, tremor Abn. BAEPs, VERs Ms biopsy: subsarcoplasmal normal mitochondria	<i>POLR1C</i>	WES	WES	NO
LNF-80	F, 5 y	4 m	NO	Spastic tetraparesis	GDD, ID	NO	NO	Microcephaly	N	Diffuse T2 WM HI, anterior predominance White matter atrophy Thin CC	Ponto-statalur delay 25 leucocytes in CSF (MN predominance)	<i>RNASEH2B</i>	WES	WES	JAK1 and JAK2 inhibitors Monitoring of immuno-mediated manifestations
LNF-81	M, 5 y	<6 m	NO	Hypotonia Choreoathetosis. Dystonia	GDD LDD	YES	YES	Microcephaly palpebral myoclonus	Nystagmus	Hypomyelination Anterior cortical atrophy CC atrophy	Ponto-statalur delay Feeding difficulties GI dysmotility OXPHOS (ms); complex II deficiency	<i>PYCR2</i>	WES	WES	NO
LNF-83	M, 1.6 y	4 m	NO	Spastic-dystonic tetraparesis	GDD	NO	NO	IHG	Strabismus	Hypomyelination Thin CC		<i>SLC16A2</i>	WES	WES	NO

L.NF-84	M, 74 y	72 y	Consanguinity	Pyramidal signs	Cognitive decline	NO	NO	N	Bilateral lens subluxation (73 y)	Periventricular T2 WM HI	Increased urine methylmalonic acid	<i>MMUT DSTYK</i>	WES	Dietary treatment
L.NF-85	F, 61 y	48 y	NO	Pyramidal signs	Cognitive decline	Instability	NO	N	Periventricular T2 WM HI	Cerebral and cerebellar atrophy	Neurogenic bladder	<i>PSEN1</i>	WES	NO
L.NF-86	F, 30 y	2 y	NO	Pyramidal and Extrapyramidal	N	YES	NO	Normal	Periventricular Cerebellar WM involvement	Dysarthria, tremor	Dysplastic toenails	<i>DARS2</i>	WGS	NO
L.NF-87	M, 7 y	3 m	NO	Spasticity	ID	NO	YES	Macrocephaly	Hypomyelination Diffuse cerebral atrophy	Delayed dentition. Drooling Abn. BAEPs, VEPs	<i>TMEM63A</i>	WES (Re-analysis)	NO	
L.NF-88	F, 12 y	6 m	Consanguinity YES (sister)	Pyramidal Proximal weakness	GDD / ID	NO	NO	Normal	Periventricular T2 WM HI	EMG myopathic Abnormal SSEP Abnormal BAEPs	<i>GFP71</i>	WES	Pyridostigmine	
L.NF-89.3	M, 16 y	<1 m	Consanguinity YES (brother)	Spastic paraparesis	GDD-ID LDD Memory problems	YES	NO	Microcephaly	Periventricular T2 WM HI SWI, pallid and dentate nuclei hypointensity CC atrophy	Microcytic and hypochromic anemia. Low Cu pl, low Cu u, low ceruloplasmin. Low IST and High ferritin. Hepatic MRI: iron overload. Normal echocardiogram	<i>CP NDUFS1</i>	WES	Iron chelating treatment	
L.NF-90	M, 10 m	6 m	Consanguinity	Spastic-dystonic tetraparesis Hypokinesia	GDD	NO	NO	IHG	Poor eye contact Upgaze episodes	Hypomimia Thin CC	10m: somnolent episode with fever Frequent febrile episodes	<i>RNASEH2B</i>	WES	JAK1 and JAK2 inhibitors Monitoring of immun-mediated manifestations
L.NF-91	M, 4 y	1 y	NO	Hypotonia	N	YES	NO	Normal	Hypomyelination	Dysmetria Delayed dentition	<i>POLR3B</i>	WGS	NO	
L.NF-92	F, 9 y	1 y	NO	Hypotonia Motor clumsiness	LDL	NO	NO	N	Subcortical bifrontal and periaural WM lesions Superior vermis atrophy	Dysmorphic traits	<i>USP7</i>	WES (Re-analysis)	NO	
L.NF-93	M, 2 y	<6 m	NO	N	Spastic-dystonic tetraparesis	GDD	NO	NO	Progressive macrocephaly	Diffuse T2 WM HI. Temporal cysts	<i>MLC1</i>	WGS	NO	
L.NF-94	M, 4 y	3 m	NO	Spastic-dystonic tetraparesis	GDD-ID LDD	NO	NO	N	Hypomyelination MRS: diminished NAA. Mild increase choline	Drooling Dysarthria	<i>PLP1</i>	WES	NO	
L.NF-95	M, 9 y	11 m	NO	Spastic-dystonic tetraparesis	Spastic-dystonic tetraparesis	YES Absences, clonic	N	N	(11m) Frono-temporal T2 WM HI, anterior predominance (6y) Improvement	<i>RNASEH2B</i>	WES	JAK1 and JAK2 inhibitors Monitoring of immun-mediated manifestations		

LNF-96	M, 12 y	6 m	NO	Hypotonia	GDD / ID Behavior (ASD)	NO	YES	Normal	Normal	Periventricular T2 WM HI	Prematurity (34w), IUGR (birthweight 1350g). Thrombopenia. Dysmorphic traits: prominent ears Ingual and umbilical hernias Acute encephalopathy with hemiparesis, VI and VII nerve paresis (7yo)	SON	WES (Re-analysis)	NO	
LNF-97	F, 4 y	6 m	NO	Pyramidal and Extrapyramidal	GDD / ID	NO	NO	Normal	Strabismus	Periventricular T2 WM HI	Episodic drooling. Dystonic postures Upper limb myoclonus Absences	TANGO2	WES	NO	
LNF-104	F, 46 y	22 y	NO	Pyramidal signs	Cognitive decline	NO	YES	Normal	Normal	Periventricular T2 WM HI	Urinary incontinence Relapses	EF2B5	WES	Avoidance of head trauma	
LNF-105	M, 11 y	6 m	NO	Spastic tetraparesis	GDD-ID	YES	YES	Microcephaly	Nystagmus Strabismus	Periventricular T2 WM HI	Dysmetria, intentional tremor Hypogonadism. Micropenis Overweight Cryptorchidism. Posterior urethral valves Increased lactate	HNRNPH1	WES	NO	
LNF-106	M, 7 y	1 y	YES (brother)	Pyramidal	GDD / ID	NO	NO	Normal	Normal	Periventricular T2 WM HI	Hyponyelination	Peripheral neuropathy	PLP1	WES	NO
LNF-107	F, 3 y	NN	NO	Pyramidal and Extrapyramidal	GDD	NO	YES	Normal	Normal	Periventricular T2 WM HI	Hyponyelination C hypoplasia Pontocerebellar hypoplasia	P4KA	WES	NO	
LNF-109	F, 5 y	1 y	NO	Pyramidal signs	Psychiatric / ASD	NO	NO	Macrocephaly	Normal	Periventricular T2 WM HI	Hyponyelination	PTEN	WES	NO	
LNF-110	M, 9 y	6 m	NO	Pyramidal signs	GDD / ID	YES	YES	Normal	Strabismus	Hyponyelination	Scanning speech Dysphagia Drooling	PLP1	WES	NO	
LNF-112	F, 13 y	4 m	NO	Pyramidal signs	GDD / ID	NO	NO	Congenital nystagmus Strabismus	Normal	Bilateral hip subluxation Scoliosis Abnormal SSEP Abnormal BAEPs	Hyponyelination	GJC2	WES	NO	
LNF-114	M, 1,3 y	< 1 m	NO	Hypotonia	GDD / ID	NO	YES	Normal	NN abnormal ocular movements	Hyponyelination Thin CC	Dysmorphic traits: long face, prominent forehead, low-set and dysmorphic ears Ingual and umbilical hernias Bone dysplasia, arthrogryposis Adducted thumbs	SCN8A	WES	NO	
LNF-115	F, 10 y	4 m	Consanguinity	Pyramidal signs	GDD / ID Behavior	NO	YES	Microcephaly	Normal	Hyponyelination Thin CC	OXP105 (fibroblast): hyperactivity in all complexes and citrate synthase, indicating mitochondrial proliferation. Referred to citrate synthase, it suggests mild complex II deficiency.	SPAT45	WES	NO	
LNF-116	M, 4 y	<6 m	YES (uncle)	Spastic tetraparesis	GDD	NO	NO	N	Nystagmus	Hyponyelination	Dysarthria Abnormal VEPs	PLP1	WES	NO	

LNF-118	M, 35 y	12 m	NO	Pyramidal and Extrapyramidal	GDD / ID	YES	NO	Normal	Ophthalmoparesis is Slow saccades Vertical gaze difficulties	Hypomyelination BG hypointensity	Scanned speech, dysdiadochokinesia Hypogonadism. Obesity	<i>POLR3A</i>	WES	Hypogonadism management
LNF-120	F, 12 y	12 m	NO	Pyramidal	Normal	NO	NO	Normal	Periventricular T2 WM HI	Abnormal SSEP	<i>RNASEH2B</i>	WES	JAK1 and JAK2 inhibitors Monitoring of immunemediated manifestations	
LNF-121	M, 5 y	4 m	NO	Pyramidal and Extrapyramidal	GDD / ID	NO	NO	Normal	Nystagmus	Periventricular T2 WM HI Cerebellar atrophy	Contractures	<i>SESECS</i>	WES	NO
LNF-126	M, 3 y	NN	NO	Pyramidal and Extrapyramidal	GDD / ID	NO	YES	Microcephaly	N	EEG: multifocal paroxysmal activity	<i>HECW2</i>	WGS	NO	
LNF-128	M, 10 m	4 m	NO	NO	GDD	NO	YES	N	Periventricular T2 WM HI frontal predominance Cystic lesions Putaminal and caudate involvement	Thin CC	<i>GFAP</i>	WES	NO	
LNF-130	M, 2 y	2 y	NO	Spastic-dystonic tetraparesis	GDD	NO	NO	N	Diffluse T2 WM HI Thin CC	T2 WM HI frontal subcortical predominance Cystic lesions Anterior CC involvement 8yo: brainstem and cerebellar involvement	<i>PLP1</i>	WES	NO	
VH-1	M, 8 y	10 m	YES (mother, grandfather)	Pyramidal signs	GDD-ID	NO	YES	Focal seizures	Macrocephaly	Nystagmus	Neuroblastoma Def alpha1AT	<i>GFAP</i>	WES	NO
VH-2	M, 5 y	4 m	NO	Pyramidal signs	N	YES	NO	N	Nystagmus	Hypomyelination Mild cerebellar atrophy	Dysarthria, dysmetria IUGR Abn BAEPs, VEPs	<i>GJC2</i>	WES	NO
VH-3	M, 14 m	NN	NO	Hypotonia	GDD	NO	YES	Microcephaly / Insufficient head growth	Nystagmus	Hypomyelination Thin CC	Axonal sensory neuropathy, startle, low weight, recurrent infections, AA neutropenia, NN anemia, cryptorchidism	<i>P4KA</i>	WES	NO
SPG-2	M, 71 y	40 y	YES (brother)	Spastic paraparesis	N	NO	NO	N	Periventricular T2 WM HI	Cerebral atrophy	Dysarthria	<i>C4PN1</i>	WES	NO
SPG-14	M, 45 y	15 y	YES (sister)	Pyramidal	Normal	YES	NO	Normal	Periventricular T2 WM HI	Congenital hip luxation Psoriasis	<i>POLR3A</i> (Reanalysis)	WES	NO	
SPG-20	F, 36 y	28 y	NO	Spastic paraparesis	N	NO	NO	N	Periventricular T2 WM HI	Frontal T2 WM HI	<i>SPG11</i>	WES	NO	
SPG-21	M, 51 y	39 y	NO	Pyramidal	GDD / ID	YES	NO	Normal	Abnormal extraocular mov. Ptosis	Dysarthria	<i>SPG7</i>	WGS	NO	

SPG-24	M, 18 y	18 y	NO	Spastic paraparesis	ID	NO	N	N	Periventricular T2 WM HI	ADHD	<i>SPG11</i>	WES	NO	
SPG-25	M, 42 y	18 y	YES (mother, grandmother)	N	Spastic paraparesis	YES	NO	N	Nystagmus	Demyelinating polyneuropathy Pes cavus	<i>SOX10</i>	WES	NO	
SPG-40	F, 25 y	15 y	NO	Spastic paraparesis Distal weakness	N	NO	NO	N	Periventricular T2 WM HI	Peripheral neuropathy	<i>SPG11</i>	WES	NO	
SPG-48	M, 21 y	2 y	NO	Spasticity	GDD Attention disorder	NO	NO	N	Periventricular T2 WM HI	Mild atrophy Thin CC	Abn. VEPs	<i>SPG11</i>	WES	NO
SPG-61	F, 6 y	2 y	Consanguinity	Spastic tetraparesis	GDD-ID	NO	NO	Microcephaly	Periventricular T2 WM hyperintensities Thin CC	Scoliosis Enuresis	<i>DHD2</i>	WES	NO	
SPG-62	M, 4 y	1 y	NO	Spastic paraparesis	ID ASD	NO	YES	Strabismus Disc pallor	Periventricular T2 WM HI	ASD. Short attention span Dysarthria	<i>ATP1A3</i> <i>NEXMHF</i>	WES	NO	
SPG-69	F, 13 y	1 y	Consanguinity	Spastic paraparesis	N	NO	NO	Normal	Periventricular T2 WM HI posterior	Dysmetria, dysdiadochokinesia	<i>ACER3</i>	WES	NO	
SPG-72	F, 21 y	18 y	YES (brother)	Spastic paraparesis	N	YES	NO	Normal	Periventricular T2 WM HI posterior	Sensory-motor polyneuropathy	<i>GALC</i>	WES	HSCT	
SPG-73	M, 18 y	2 y	NO	Pyramidal	Language disorder	NO	NO	Normal	Periventricular T2 WM HI	Predominance	<i>SPAST</i>	WES	NO	
SPG-106	M, 3 y	4 m	NO	Spastic-dystonic tetraparesis	GDD	NO	NO	Microcephaly	Congenital nystagmus	IUGR (3rd trimester) Thin CC	<i>SCLC6A2</i>	WES	NO	
CPR	F, 4 y	12 m	NO	Pyramidal and Extrapyramidal	GDD / ID	YES	NO	Normal	Hypomyelination	Swallowing difficulties. Choking Pontostriatal delay Increased T3	<i>TUBB4A</i>	WES	NO	
GLA	M, 2m	NN	NO	Hypotonia	GDD	NO	YES			Abnormal wide anterior fontanel Glomerulocystic kidney disease, bilateral pelvic ectasia				
LMSR	F, 24 y	23 y	YES (father)	Pyramidal	Cognitive decline	NO	NO	Normal	Abnormal gyration pattern Colpocephaly	Liver insufficiency, cholestasis Perimembranous VSD Hypertransaminasemia, hyperammonemia, hyperbilirubinemia Abnormal VLCFA, diminished plasmalogens	<i>PEX2</i>	WES	NO	
								Frontal			<i>CSFR</i>	WES	HSCT	

Abn-abnormal; ASD-autism spectrum disorder; BAEPs-brainstem auditory evoked potentials; CC-corpus callosum; CSF-cerebrospinal fluid; F-female; F-s-fibritile seizures; GDD-global developmental delay; ID-intellectual disability; HG-hypoglycemia; IS-infantile spasms; LDD-language developmental delay; M-male; N-normal; NN-neonatal; ON-optic nerve; OXPHOS-oxidative phosphorylation; SSEP-somatosensory evoked potentials; VEPs-visual evoked potentials; VSD-ventricular septal defect; WM-white matter

Table 2. ACMG criteria for the classification of identified variants

cTable 3. List of identified genes, OMIM nomenclature and numbers of cases identified in our cohort.

Gene	Associated condition in OMIM	Inheritance	Nº of families
<i>EIF2BS</i>	Leukoencephalopathy with vanishing white matter (CACH)	AR	6
<i>POLR3A</i>	Leukodystrophy, hypomyelinating, with or without oligodontia and/or hypogonadotropic hypogonadism 4H syndrome	AR	6
<i>RNASEH2B</i>	Aicardi-Goutières syndrome	AR	6
<i>PLP1</i>	Pelizaeus-Merzbacher disease	X-linked	5
<i>CSF1R</i>	Leukoencephalopathy, diffuse hereditary, with spheroids	AD	4
<i>SPG11</i>	Spastic paraplegia 11	AR	4
<i>GFAP</i>	Alexander disease	AD	3
<i>DARS2</i>	Leukoencephalopathy with brain stem and spinal cord involvement and lactate elevation	AR	2
<i>DEGS1</i>	Leukodystrophy, hypomyelinating, 18	AR	2
<i>GALC</i>	Krabbe disease	AR	2
<i>GJC2</i>	Leukodystrophy, hypomyelinating, 2	AR	2
<i>NDUFS1</i>	Mitochondrial complex I deficiency	AR	2
<i>PI4KA</i>		AR	2
<i>POLR3B</i>	Leukodystrophy, hypomyelinating, 8, with or without oligodontia and/or hypogonadotropic hypogonadism	AR	2
<i>SLC16A2</i>	Allan-Herndon-Dudley syndrome	AR	2
<i>TMEM63A</i>	Leukodystrophy, hypomyelinating, 19, transient infantile	AD	2
<i>TUBB4A</i>	Leukodystrophy, hypomyelinating, 6	AR	2
<i>1p36 deletion</i>	Chromosome 1p36 deletion syndrome	AD	1
<i>ACER3</i>	Leukodystrophy, progressive, early childhood-onset	AR	1
<i>ATP1A3</i>	Alternating hemiplegia of childhood 2 // CAPOS syndrome	AD	1
<i>CACNA1A</i>	Episodic ataxia, type 2 // Epileptic encephalopathy, early infantile, 42	AD	1
<i>CAPN1</i>	Spastic paraplegia 76, autosomal recessive	AR	1
<i>CP</i>	Aceruloplasminemia	AR	1
<i>CYP2U1</i>	Spastic paraplegia 56	AR	1
<i>DDHD2</i>	Spastic paraplegia 54	AR	1
<i>DSTYK</i>	Spastic paraplegia 23	AR	1
<i>GFM1</i>	Combined oxidative phosphorylation deficiency 1	AR	1
<i>GFPT1</i>	Myasthenia, congenital, 12, with tubular aggregates	AR	1
<i>HECW2</i>	Neurodevelopmental disorder with hypotonia, seizures, and absent language	AD	1
<i>HNRNPH1</i>		AD	1
<i>ITPA</i>	Epileptic encephalopathy, early infantile, 35	AR	1
<i>LMNB1</i>	Leukodystrophy, adult-onset, autosomal dominant	AD	1
<i>MLC1</i>	Megalencephalic leukoencephalopathy with subcortical cysts	AR	1
<i>MMUT</i>	Methylmalonic aciduria, mut(0) type	AR	1
<i>MSTO1</i>	Myopathy, mitochondrial, and ataxia	AD/AR	1
<i>NEXMIF</i>	Mental retardation, X-linked 98	X-linked	1
<i>PAH</i>	Phenylketonuria	AR	1
<i>PARS2</i>	Epileptic encephalopathy, early infantile, 75	AR	1
<i>PEX2</i>	Peroxisome biogenesis disorder 5A (Zellweger)	AR	1
<i>PEX6</i>	Peroxisome biogenesis disorder 4A (Zellweger)	AR	1
<i>PEX11B</i>	Peroxisome biogenesis disorder 14B	AR	1
<i>PNPT1</i>	Combined oxidative phosphorylation deficiency 13	AR	1
<i>POLR1C</i>	Leukodystrophy, hypomyelinating, with or without oligodontia and/or hypogonadotropic hypogonadism 4H syndrome	AR	1
<i>PSEN1</i>	Alzheimer disease, type 3	AD	1
<i>PTEN</i>	Macrocephaly/autism syndrome	AD	1
<i>PYCR2</i>	Leukodystrophy, hypomyelinating, 10	AR	1
<i>SCN8A</i>	Epileptic encephalopathy, early infantile, 13	AD	1
<i>SEPSECS</i>	Pontocerebellar hypoplasia type 2D	AR	1
<i>SLC16A2</i>	Allan-Herndon-Dudley syndrome	X-linked	1
<i>SON</i>	ZTTK syndrome	AD	1
<i>SOX10</i>	PCWH syndrome	AD	1
<i>SPAST</i>	Spastic paraplegia 4, autosomal dominant	AD	1
<i>SPATA5</i>	Epilepsy, hearing loss, and mental retardation syndrome	AR	1
<i>SPG7</i>	Spastic paraplegia 7, autosomal recessive	AR	1
<i>TANGO2</i>	Metabolic encephalomyopathic crises, recurrent, with rhabdomyolysis, cardiac arrhythmias, and neurodegeneration	AR	1
<i>TREX1</i>	Aicardi-Goutières Goutieres syndrome	AR	1
<i>USP7</i>	Hao-Fountain syndrome	AD	1

eTable 4. Atypical cases. Patients with new phenotypes, atypical forms of presentation and blended phenotypes in families with more than one gene associated with the phenotype.

NEW PHENOTYPES							Comments			
Patient	Sex, current age (y)	Age at Onset	Family history	Main Clinical Features	MRI	Relevant Investigation findings	Gene	Inheritance	ACMG classif.	
LNF-48.0	M, 13	6mo	YES (affected sister)	PS, GDD>ID, ataxia, erratic ocular movements, stereotypies	Periventricular Thin CC	Abnormal SSEP Abnormal VEPs	<i>PARS2</i>	AR	LP / LP	
LNF-105	M, 15	5mo	NO	PS, GDD>ID, ataxia, epilepsy, microcephaly, Strabismus, optic disc pallor, nystagmus	Periventricular Cysts Cerebellar atrophy	Hyperlactacidemia	<i>HNRNPH1</i>	AD	P	
ATYPICAL PHENOTYPES										
LNF-29.0	M, 9	4mo	YES (affected brother)	PS-EPS, GDD>ID, microcephaly, nystagmus, erratic ocular mov	Periventricular Cystic lesions	CSF NT:3-ortomelitdopa and neopterin elevation	<i>PNP1</i>	AR (XL)	P	
LNF-47	M, 8	6mo	NO	PS-EPS, GDD>ID, ataxia	Striatal necrosis Mild subcortical T2 hyperintensity as well as in centrum semiovale, corona radiata, optic radiation and also in dentate nuclei and superior and inferior cerebellar peduncles	Increased mitochondria in muscle biopsy Decreased activity of complex I, II, III	<i>POLR3A</i>	AR	P / P	
LNF-85	F, 64	48y	NO	PS, CD, ataxia, neurogenic bladder	Periventricular		<i>PSEN1</i>	AD	VUS	
LNF-88.0	M, 16	6mo	YES (affected sister) Consanguinity	PS, GDD>ID	Periventricular	EMG myopathic Abnormal SSEP Abnormal BAEPs Ms biopsy: multifocal bodies	<i>GFP1</i>	AR	LP	
LNF-114	M, 3	NN	NO	Hypotonia, GDD>ID, epilepsy NN abnormal ocular movements Hyperkplexia-like episodes Abnormal phenotype, inguinal hernias, arthrogryposis, bone dysplasia, bilateral hip luxation	Delayed myelination Thin CC	OXPHOS (fibroblast): hyperactivity in all complexes but citrate synthase too, which indicates mitochondrial proliferation. Referred to citrate synthase, it suggests mild complex II deficiency.	<i>SCN8A</i>	AD	P	
SPG-2	M, 76	40y	YES (affected brother)	PS, Dysarthria	Periventricular		<i>CANPI</i>	AR	P	
SPG-25	M, 46	18y	YES (three generations)	Ataxia, nystagmus Pes cavus, hypopallestesia, hyporeflexia (ankle)	Diffuse	NO	<i>SOX10</i>	AD	LP	

BLENDED PHENOTYPES

LNF-40.0	M, 15	10mo	YES (two brothers and sister affected) Consanguinity	PS-EPS, GDD/ID, epilepsy, nystagmus, dysphagia, dysarthria	Periventricular Delayed myelination	<i>PAH</i> <i>CYP2U1</i>	AR	P LP
LNF-56	F, 20	11mo	NO	GDD/ID, behaviour disorder, ataxia, epilepsy, nystagmus, strabismus Obesity, amenorrhea, hypertrichosis	Periventricular	Mildly increased CSF lactate	<i>POLR3A</i> <i>CACNA1A</i>	AR P
LNF-71	M, 6	1y	NO	GDD/ID, ataxia	Periventricular Mega cisterna magna	Normal metabolic study (plasma, urine, CSF) OXPHOS (ms) normal	<i>EIF2B5</i> <i>GFM1</i>	AR P / P
LNF-84	M, 74	72y	NO	PS, cognitive decline, instability Bilateral lens subluxation	Periventricular	Increased urine methylmalonic acid Dysphagia Osteopenia	<i>MMUT</i> <i>DSTYK</i>	AR P / P
LNF-89.3	M, 20	NN	YES (two brothers) Consanguinity	PS, GDD/ID, ataxia, microcephaly	Periventricular	Mycrocytic and hypochromic anemia. Low plCu, uCu and ceruloplasmin. Low IST and High ferritin. Hepatic MRI: iron overload. Normal echocardiogram	<i>CP</i> <i>NDUFS1</i>	AR VUS
SPG-62	M, 8	12mo	NO	PS, GDD/ID, ASD, epilepsy, dysarthria, short attention span	Periventricular	Focal EEG abnormalities	<i>ATP1A3</i> <i>NEXMIF</i>	XL AD P LP

CD, cognitive decline; CSF, cerebro-spinal fluid; EPS, extrapyramidal signs; F, female; GDD, global developmental delay; ID, intellectual disability; LP, likely-pathogenic; M, male; mo, months; P, Pathogenic; PS, pyramidal signs; SNHL, sensoryneural hearing lossVUS, variant of unknown significance; XL, X-linked; Y, years

eTable 5. Cases with functionally validated variants.

ID	Gene	Inheritance	Chromosome start/has	Ref	Type	Nomenclature	Functional testing performed	Description
LNF-37	<i>ELF2BS</i>	Compound Heterozygous	3 18385831	G A	splicing	Elf2bs:NM_003907.2:c.155+3G>A	cDNA and minigene analysis	Targeted lipidomics analysis towards sphingolipids detecting dihydroceramide and ceramide demonstrated increased reaction substrate and decreased product. ¹⁰
LNF-41	<i>DEGS1</i>	Homozygous	1 224377798	AT A	frameshift deletion	DEGS1:NM_003676.3:c.604delNP_003667.1:p.(Ty202thrfsTer8)	targeted lipidomes	Targeted lipidomics analysis towards sphingolipids detecting dihydroceramide and ceramide demonstrated increased reaction substrate and decreased product. ¹⁰
LNF-42	<i>DEGS1</i>	Compound Heterozygous	1 224377714	G C	nonsynonymous SNV	DEGS1:NM_003676.3:c.518G>c.NP_003667.1:p.(Ag173Pro)	targeted lipidomes	Targeted lipidomics analysis towards sphingolipids detecting dihydroceramide and ceramide demonstrated increased reaction substrate and decreased product. ¹⁰
LNF-42	<i>DEGS1</i>	Compound Heterozygous	1 224377794	A AT	frameshift insertion	DEGS1:NM_003676.3:c.601dupNP_003667.1:p.(Ty701leufsTer7)	targeted lipidomes	Targeted lipidomics analysis towards sphingolipids detecting dihydroceramide and ceramide demonstrated increased reaction substrate and decreased product. ¹⁰
LNF-47	<i>POLR3A</i>	Compound Heterozygous	10 79743720	G T	Exon 1 Splicing	POLR3A:NM_007055.3:c.338T>A;NP_008936.2:p.(Uu1129x)	cDNA analysis	Sanger sequencing of PBMC cDNA revealed that p.Leu1129L synonymous variant resulted into skipping of POLR3A's exon 26 (93 pb, in-frame), which corresponds to a functional domain of MSTO1 exon 4
LNF-72	<i>MSTO1</i>	Compound Heterozygous	1 15581130	G A	splicing	MSTO1:NM_00125532.1:c.365+48G>A	cDNA analysis	Sanger sequencing of PBMC cDNA revealed that c.366G>A variant resulted into skipping of MSTO1 exon 4 (69 pb, in-frame), which corresponds to a functional domain of MSTO1
LNF-73	<i>MLC1</i>	Compound Heterozygous	22 50515233	G C	splicing	MLC1:NM_015166.3:c.597+37G>G	minigene analysis	Minigene splicing assay revealed that c.597+37G>G resulted into the creation of 2 novel mRNA isoforms which include 159 and 168 bp of MLC1's exon 7 (in-frame insertions), containing 2 stop codons resulting in transcripts targeted by NMD.
LNF-107	<i>PI4K4</i>	Compound Heterozygous	22 21098918	C T	nonsynonymous SNV	PI4K4:NM_058004.3:c.345G>A;NP_477352.3:p.(Pro87SerTer36)	targeted lipidomes	A targeted lipidomics analysis is detecting phosphatidylinositol (PI) and its phosphorylated forms (PIP and PIP2) was performed. All of the patients showed a significantly decreased PIP/PIP2 ratio compared to age-matched controls, indicating decreased PI4KA activity in these patients. Moreover, Western Blot with an antibody anti-PI4KA (12411-I-AP) Protein blot corroborated low protein levels. Finally, immunofluorescence detecting decreased reaction product with an antibody anti-PI(4)P ² (Z-P004, Echelon Biosciences Inc.) was performed as described in Verdura et al. Brain in Press.
LNF-107	<i>PI4K4</i>	Compound Heterozygous	22 21119188	A AG	frameshift insertion	PI4K4:NM_058004.3:c.262dupNP_477352.3:p.(Pro87SerTer36)	targeted lipidomes	A targeted lipidomics analysis is detecting phosphatidylinositol (PI) and its phosphorylated forms (PIP and PIP2) was performed. All of the patients showed a significantly decreased PIP/PIP2 ratio compared to age-matched controls, indicating decreased PI4KA activity in these patients. Moreover, Western Blot with an antibody anti-PI4KA (12411-I-AP) Protein blot corroborated low protein levels. Finally, immunofluorescence detecting decreased reaction product with an antibody anti-PI(4)P ² (Z-P004, Echelon Biosciences Inc.) was performed as described in Verdura et al. Brain in Press.
LNF-10	<i>PLP1</i>	Hemizygous	X 103031928	G A	splicing	PLP1:NM_000333.3:c.4+3G>A	qRT-PCR	qRT-PCR using PBMC cDNA from this patient revealed a strongly reduced quantity of PLP1 mRNA compared to controls, confirming a loss of function effect from variant c.4+3G>A
LNF-107	<i>PLP1</i>	Compound Heterozygous	22 21119188	A AG	frameshift insertion	PLP1:NM_000333.3:c.4+3G>A	targeted lipidomes	Minigene splicing assay revealed that variant c.32+3G>G results into skipping of SEPSIC's exon 1, which contains the ATG start codon, and thus results into a loss of function. This skipping was also confirmed in PBMC's cDNA from a patient carrying the same variant in homozygosis.
LNF-121	<i>SEPSIC5</i>	Homozygous	4 25161875	T C	splicing	SEPSIC5:NM_016955.3:c.114+3A>G	cDNA and minigene analysis	Sanger sequencing of cDNA analysis from fibroblasts revealed that c.762+61G>C results into skipping of PLP1's exon 7 (63 pb, in-frame, deleting 21 amino acids located in a strongly conserved region of PLP1).
LNF-130	<i>PLP1</i>	Hemizygous	X 103044333	T G	splicing	PLP1:NM_000333.3:c.762+61>G	cDNA analysis	A targeted lipidomics analysis is detecting phosphatidylinositol (PI) and its phosphorylated forms (PIP and PIP2) was performed. All of the patients showed a significantly decreased PIP/PIP2 ratio compared to age-matched controls, indicating decreased PI4KA activity in these patients. Moreover, Western Blot with an antibody anti-PI4KA (12411-I-AP) Protein blot corroborated low protein levels. Finally, immunofluorescence detecting decreased reaction product with an antibody anti-PI(4)P ² (Z-P004, Echelon Biosciences Inc.) was performed as described in Verdura et al. Brain in Press.
VH-3	<i>PI4K4</i>	Homozygous	22 21068803	C G	nonsynonymous SNV	PI4K4:NM_058004.3:c.577G>C;NP_477352.3:p.(Gly1925Arg)	targeted lipidomes	Sanger sequencing of PBMC cDNA revealed that variant c.613R>A-G results into skipping of STG11's exon 24 (134 pb), resulting into an out-of-frame transcript targeted by NMD.
SPG-20	<i>SPG11</i>	Compound Heterozygous	15 44862719	T C	splicing	SPG11:NM_001160227.1:c.613R>A-G	cDNA analysis	Sanger sequencing of fibroblast cDNA revealed that c.286+83A>G results into creation of a transcript which includes a 75 bp pseudogene located in SPG7's intron 2. This in-frame pseudogene includes at least two codon stops. Western Blot showed reduced levels of SPG7, confirming a loss of function effect. ⁴¹
SPG-21	<i>SPG7</i>	Compound Heterozygous	16 89577833	A G	splicing	SPG7:NM_003119.3:c.286+85A>G	cDNA analysis	A targeted lipidomics analysis is on sphingolipids demonstrated a similar lipid profile published. Edvardson et al. ⁴¹ Moreover, qPCR analysis of the ACER3 gene showed reduced expression compared to 4 controls.
SPG-69	<i>ACER3</i>	Homozygous	11 76727730	G T	nonsynonymous SNV	ACER3:NM_013397.5:c.631G>t;NP_060837.3:p.(Gly211Cys)	targeted lipidomes	

eTable 6. Cases with experimentally validated CNV variants.

ID	Genes	Inheritance	Chr	Start base	End base	Type	Nomenclature	CNV validation
LNF-34	<i>LMNB1</i>	Heterozygous	5	126112000	126172800	duplication	5q23.2(126112000-126172800)x3	Q-PCR was carried out to measure the relative copy number of the human LMNB1 gene (exon 1 - exon 1, exon 4 - exon 4, and exon 7 - exon 7) compared to the human FGF1 (exon 4- exon 4) or ELOVL7 (exon 4- exon 4) gene. LNF34.0 exhibits 1.5-fold increase copy number of the LMNB1 gene compared to the parents and 7 healthy individuals.
LNF-45	<i>Ip36</i>	Heterozygous	1	757093	7686264	deletion	1p36.33p36.23(757093_7686264)x1	The deletion in 1p36.1 has been validated by array-CGH with the qChip Post microarray performed in Qgenomics (http://www.qgenomics.com/), which revealed a deletion of approximately 7.6 Mb long in heterozygous (eFigure2).
LNF-97	<i>TANGO2</i>	Homozygous	22	20030879	20052185	deletion	22q11.21(20030879-20052185)x0	Q-PCR was carried out to measure the relative copy number of the human TANGO2 gene (exon 1, exon 5, and exon 9) relative to the human ARVCF or ZDHHC8 genes. LNF-97.0 exhibited 2.0-fold decreased levels of TANGO2 gene compared to 11 healthy individuals, parents showed 1.5-fold decrease levels of this gene.
LNF-105	<i>HNRNPH1</i>	Heterozygous	5	178950829	179067861	duplication	5q53.3(178950829-179067861)x3	Q-PCR was carried out to measure the relative copy number of the human HNRNPH1 gene (intron 5 - exon 6 and exon 9 - intron 9) relative to the human C5ORF60 gene. LNF-105.0 exhibited 1.5-fold increased levels of HNRNPH1 gene compared to parents and 10 healthy individuals, demonstrating that it was a de novo CNV ²⁶ .

eTable 7. New variants. Table with the 73 novel variants identified in our cohort.

Case	Inheritance	Gene	Chromosome	Start base	Ref.	Alt.	Nomenclature
LNF-1	compound hetozygous	<i>POLR3A</i>	10	79760778	C	T	POLR3A:NM_007055.3:c.2343G>A:NP_008986.2:p.(Gly812Ser)
LNF-1	compound hetozygous	<i>POLR3A</i>	10	79767546	A	G	POLR3A:NM_007055.3:c.1988T>C:NP_008986.2:p.(Ile663Thr)
LNF-6	heteozygous	<i>CSF1R</i>	5	149441340	T	C	CSF1R:NM_001288705.2:c.1699A>G:NP_001275634.1:p.(Thr567Ala)
LNF-15	heteozygous	<i>TMEM63A</i>	1	226041470	C	T	TMEM63A:NM_014698.2:c.1657G>A:NP_055513.2:p.(Gly553Ser)
LNF-16	heteozygous	<i>CSF1R</i>	5	149441339	G	A	CSF1R:NM_001288705.2:c.1700C>T:NP_001275634.1:p.(Thr567Met)
LNF-18	homzygous	<i>GALC</i>	14	88450739	C	G	GALC:NM_000153.3:c.581G>C:NP_000144.2:p.(Gly194Ala)
LNF-20	homzygous	<i>POLR3B</i>	12	106895121	T	C	POLR3B:NM_018082.5:c.3005T>C:NP_060552.4:p.(Ile1002Thr)
LNF-23	compound hetozygous	<i>POLR3A</i>	10	79778956	G	A	POLR3A:NM_007055.3:c.1253C>T:NP_008986.2:p.(Ala418Val)
LNF-28	homzygous	<i>PEX11B</i>	1	145518171	CA	C	PEX11B:NM_001184795.1:c.233del:NP_001171724.1:p.(Asn78IlefsTer42)
LNF-32	compound hetozygous	<i>RNASEH2B</i>	13	51517465	G	T	RNASEH2B:NM_001142279.2:c.445G>T:NP_001135751.1:p.(Glu149Ter)
LNF-37	compound hetozygous	<i>EIF2BS</i>	3	183855994	A	G	EIF2BS:NM_003907.2:c.725A>G:NP_003898.2:p.(Tyr242Cys)
LNF-37	compound hetozygous	<i>EIF2BS</i>	3	183858531	G	A	EIF2BS:NM_003907.2:c.1156<13G>A
-40.0 & LNF-44	homzygous	<i>CYP2U1</i>	4	108866168	G	C	CYP2U1:NM_183075.2:c.533G>C:NP_898898.1:p.(Arg178Thr)
LNF-41	homzygous	<i>DEGS1</i>	1	224377798	AT	A	DEGS1:NM_003676.3:c.604del:NP_003667.1:p.(Tyr202TrfsTer8)
LNF-42	compound hetozygous	<i>DEGS1</i>	1	224377714	G	C	DEGS1:NM_003676.3:c.518G>C:NP_003667.1:p.(Arg173Pro)
LNF-42	compound hetozygous	<i>DEGS1</i>	1	224377794	A	AT	DEGS1:NM_003676.3:c.601dup:NP_003667.1:p.(Tyr201LeufsTer7)
LNF-47	compound hetozygous	<i>POLR3A</i>	10	79743720	G	T	POLR3A:NM_007055.3:c.3387C>A:NP_008986.2:p.(Leu1129=)
LNF-48	compound hetozygous	<i>PARS2</i>	1	55224279	T	C	PARS2:NM_152268.3:c.556A>G:NP_689481.2:p.(Arg186Gly)
LNF-48	compound hetozygous	<i>PARS2</i>	1	55224275	T	C	PARS2:NM_152268.3:c.560A>G:NP_689481.2:p.(Lys187Arg)
LNF-56	compound hetozygous	<i>POLR3A</i>	10	79764608	G	C	POLR3A:NM_007055.3:c.2113C>G:NP_008986.2:p.(Pro705Ala)
LNF-56	heteozygous	<i>CACNA1A</i>	19	13423516	G	GT	CACNA1A:NM_001127221.1:c.1637dup:NP_001120693.1:p.(Tyr546Ter)
LNF-57	heteozygous	<i>GFAP</i>	17	42992614	C	T	GFAP:NM_002055.4:c.2416>A:NP_002046.1:p.(Ala81Thr)
LNF-66	compound hetozygous	<i>ITPA</i>	20	3199198	T	TCAGC	ITPA:NM_03453.3:c.333_336dup:NP_258412.1:p.(Tyr113SerfsTer47)
LNF-69	compound hetozygous	<i>RNASEH2B</i>	13	51517505	A	C	RNASEH2B:NM_001142279.2:c.485A>C:NP_001135751.1:p.(Lys162Thr)
LNF-70	heteozygous	<i>CSF1R</i>	5	149435607	A	G	CSF1R:NM_001288705.2:c.2536T>C:NP_001275634.1:p.(Trp846Arg)
LNF-72	compound hetozygous	<i>MSTO1</i>	1	155583446	A	G	MSTO1:NM_001256532.1:c.1389>A>G
LNF-72	compound hetozygous	<i>MSTO1</i>	1	155581130	G	A	MSTO1:NM_001256532.1:c.366<48G>A
LNF-80	compound hetozygous	<i>RNASEH2B</i>	13	51517496	G	T	RNASEH2B:NM_001142279.2:c.476G>T:NP_001135751.1:p.(Ser159Ile)
LNF-81	compound hetozygous	<i>PYCR2</i>	1	226110025	A	C	PYCR2:NM_001271681.1:c.197T>G:NP_001258610.1:p.(Leu66Arg)
LNF-83	hemizygous	<i>SLC16A2</i>	X	73641674	G	T	SLC16A2:NM_006517.4:c.202G>T:NP_0065082.2:p.(Glu68Ter)
LNF-84	homzygous	<i>MMUT</i>	14	73678582	C	T	PSEN1:NM_007318.2:c.1049C>T:NP_015557.2:p.(Thr350Ile)
LNF-85	heteozygous	<i>PSEN1</i>	6	49425727	G	A	MMUT:NM_000255.3:c.430C>T:NP_000246.2:p.(Arg144Cys)
LNF-86	compound hetozygous	<i>DARS2</i>	1	173797450	T	C	DARS2:NM_018122.5:c.228>217>C
LNF-86	compound hetozygous	<i>DARS2</i>	1	173822598	C	T	DARS2:NM_018122.5:c.1456C>T:NP_060592.2:p.(Leu486Phe)
LNF-87	heteozygous	<i>TMEM63A</i>	1	226041427	C	A	TMEM63A:NM_014698.2:c.1700G>T:NP_055513.2:p.(Gly567Val)
LNF-88	homzygous	<i>GFPT1</i>	2	69575425	T	A	GFPT1:NM_001244710.1:c.887A>T:NP_001231639.1:p.(Asp296Val)
LNF-89	homzygous	<i>NDUF51</i>	2	206988991	C	T	NDUF51:NM_005006.6:c.2102G>A:NP_004997.4:p.(Ser701Asn)
LNF-91	compound hetozygous	<i>POLR3B</i>	12	106807883	C	A	POLR3B:NM_018082.5:c.1101<3145C>A
LNF-92	heteozygous	<i>USP7</i>	16	9002201	T	C	USP7:NM_003470.2:c.1268A>G:NP_003461.2:p.(Asp423Gly)
LNF-93	compound hetozygous	<i>MLC1</i>	22	50515233	G	C	MLC1:NM_015166.3:c.597<37C>G
LNF-93	compound hetozygous	<i>MLC1</i>	22	50523919	A	G	MLC1:NM_015166.3:c.-195T>C
LNF-94	hemizygous	<i>PLP1</i>	X	103040672	C	T	PLP1:NM_000533.3:c.166C>T:NP_000524.3:p.(Gln56Ter)
LNF-105	heteozygous	<i>HNRNPH1</i>	5	178950829			SqS3.3(178950829-179067861)x3
LNF-106	hemizygous	<i>PLP1</i>	X	103041532	C	T	PLP1:NM_000533.3:c.330C>T:NP_000524.3:p.(Gly110=)
LNF-107	compound hetozygous	<i>PI4KA</i>	22	2109818	C	T	PI4KA:NM_058004.3:c.3454G>A:NP_477352.3:p.(Glu1152Lys)
LNF-107	compound hetozygous	<i>PI4KA</i>	22	21119188	A	AG	PI4KA:NM_058004.3:c.2624dup:NP_477352.3:p.(Pro876SerfsTer36)
LNF-109	heteozygous	<i>PTEN</i>	10	89717611	TC	T	PTEN:NM_000314.4:c.638del:NP_000305.3:p.(Pro213LeufsTer8)
LNF-110	hemizygous	<i>PLP1</i>	X	103031928	G	A	PLP1:NM_000533.3:c.4+1G>A
LNF-114	heteozygous	<i>SCN8A</i>	12	52099291	G	A	SCN8A:NM_014191.3:c.1225G>A:NP_055006.1:p.(Val409Met)
LNF-115	heteozygous	<i>SPATAS5</i>	4	123949435	G	A	SPATAS5:NM_145207.2:c.1964G>A:NP_660208.2:p.(Arg655Gln)
LNF-116	hemeizygous	<i>PLP1</i>	X	103043441	T	C	PLP1:NM_000533.3:c.696<27C
LNF-121	homzygous	<i>SEPSECS</i>	4	25161875	T	C	SEPSECS:NM_016955.3:c.114+3A>G
LNF-126	homzygous	<i>HECW2</i>	2	197065797	C	T	HECW2:NM_020760.3:c.204G>A
LNF-128	heteozygous	<i>GFAP</i>	17	42988611	C	T	GFAP:NM_002055.4:c.1120G>A:NP_002046.1:p.(Glu374Lys)
LNF-130	hemizygous	<i>PLP1</i>	X	103044333	T	G	PLP1:NM_000533.3:c.762+6T>G
VH-2	compound hetozygous	<i>GJC2</i>	1	228345743	T	G	GJC2:NM_020435.3:c.284T>G:NP_065168.2:p.(Leu95Arg)
VH-3	homozygous	<i>PI4KA</i>	22	21066803	C	G	PI4KA:NM_058004.3:c.5773G>C:NP_477352.3:p.(Gly1925Arg)
SPG-14	compound hetozygous	<i>POLR3A</i>	10	79785447	C	T	POLR3A:NM_007055.3:c.2516>A:NP_008986.2:p.(Gly84Glu)
SPG-20	compound hetozygous	<i>SPG11</i>	15	44856746	T	A	SPG11:NM_001160227.1:c.6811A>T:NP_001153699.1:p.(Lys2271Ter)
SPG-21	compound hetozygous	<i>SPG7</i>	16	89623308	T	C	SPG7:NM_003119.3:c.2195T>C:NP_003110.1:p.(Leu732Pro)
SPG-21	compound hetozygous	<i>SPG7</i>	16	89577853	A	G	SPG7:NM_003119.3:c.286<483>A>G
SPG-24	compound hetozygous	<i>SPG11</i>	15	44876685	C	T	SPG11:NM_001160227.1:c.5193G>A:NP_001153699.1:p.(Trp1731Ter)
SPG-25	heteozygous	<i>SOX10</i>	22	38379545	A	C	SOX10:NM_006941.3:c.247T>G:NP_008872.1:p.(Tyr83Asp)
SPG-40	compound hetozygous	<i>SPG11</i>	15	44859637	C	CA	SPG11:NM_001160227.1:c.6399dup:NP_001153699.1:p.(Glu2134Ter)
SPG-40	compound hetozygous	<i>SPG11</i>	15	44912518	C	A	SPG11:NM_001160227.1:c.2704G>T:NP_001153699.1:p.(Glu902Ter)
SPG-61	homzygous	<i>DDHD2</i>	8	38103267	C	T	DDHD2:NM_001164232.1:c.856C>T:NP_001157704.1:p.(Gln286Ter)
SPG-62	hemizygous	<i>NEXMIF</i>	X	73962026	G	A	NEXMIF:NM_00108537.2:c.2366C>T:NP_001008537.1:p.(Pro789Leu)
SPG-69	homzygous	<i>ACER3</i>	11	76727750	G	T	ACER3:NM_018367.5:c.631G>T:NP_060837.3:p.(Gly111Cys)
SPG-72	compound hetozygous	<i>GALC</i>	14	88450776	C	G	GALC:NM_000153.3:c.544G>C:NP_000144.2:p.(Ala182Pro)
SPG-72	compound hetozygous	<i>GALC</i>	14	88454813	C	G	GALC:NM_000153.3:c.250G>C:NP_000144.2:p.(Asp84His)
SPG-106	hemizygous	<i>SLC16A2</i>	X	73744432	GTTG	G	SLC16A2:NM_006517.4:c.817_819del:NP_006508.2:p.(Leu273del)
GLA	homzygous	<i>PEX2</i>	8	77895633	T	C	PEX2:NM_001172087.1:c.782A>G:NP_001165558.1:p.(His261Arg)
LMSR	heteozygous	<i>CSF1R</i>	5	149434890	G	A	CSF1R:NM_001288705.2:c.2564C>T:NP_001275634.1:p.(Pro855Leu)

Neurology®

Diagnosis of Genetic White Matter Disorders by Singleton Whole-Exome and Genome Sequencing Using Interactome-Driven Prioritization

Agatha Schlüter, Agustí Rodríguez-Palmero, Edgard Verdura, et al.

Neurology published online January 10, 2022

DOI 10.1212/WNL.0000000000013278

This information is current as of January 10, 2022

Updated Information & Services

including high resolution figures, can be found at:
<http://n.neurology.org/content/early/2022/01/10/WNL.0000000000013278.full>

Subspecialty Collections

This article, along with others on similar topics, appears in the following collection(s):

Leukodystrophies

<http://n.neurology.org/cgi/collection/leukodystrophies>

Permissions & Licensing

Information about reproducing this article in parts (figures, tables) or in its entirety can be found online at:

http://www.neurology.org/about/about_the_journal#permissions

Reprints

Information about ordering reprints can be found online:

<http://n.neurology.org/subscribers/advertise>

Neurology ® is the official journal of the American Academy of Neurology. Published continuously since 1951, it is now a weekly with 48 issues per year. Copyright Copyright © 2022 The Author(s). Published by Wolters Kluwer Health, Inc. on behalf of the American Academy of Neurology.. All rights reserved. Print ISSN: 0028-3878. Online ISSN: 1526-632X.



Article 2. Biallelic PI4KA variants cause a novel neurodevelopmental syndrome with hypomyelinating leukodystrophy

Edgard Verdura E*, Rodríguez-Palmero A*, Vélez-Santamaría V, Planas-Serra L, de la Calle I, Raspall-Chaure M, Roubertie A, Benkirane M, Saettini F, Pavinato L, Mandrile G, O'Leary M, O'Heir E, Barredo E, Chacón A, Michaud V, Goizet C, Ruiz M, Schlüter A, Rouvet I, Sala J, Fossati Ch, Iascone M, Canonico F, Marcé-Grau A, de Souza P, Adams DR, Casasnovas C, Rehm HL, Mefford HC, Gutiérrez-Solana LG, Brusco A, Koenig M, Macaya A, Pujol A.

*Autors que han contribuït per igual en aquest treball

Revista: Brain. 2021 Oct 22;144(9):2659-2669. doi: 10.1093/brain/awab124

Factor d'impacte (quartil per especialitat): 13.501 (Q1)

Participació del doctorand: aquest treball té una coautoría amb el Dr. Edgard Verdura. El doctorand ha participat en el disseny conceptual de l'estudi, ha revisat la informació clínica i estudis de neuroimatge de tots els pacients inclosos i ha contactat amb els metges referents dels pacients. Ha participat en l'anàlisi d'alguns dels exomes. Ha escrit la part clínica del manuscrit i ha participat en el disseny de les figures i taules. Aquest treball no es preveu que s'utilitzi en cap més tesi doctoral.

Resum de l'article 2

Introducció

- Prèviament a aquesta publicació, s'havien descrit únicament tres fetus d'una mateixa família portadors de variants patogèniques en el gen *PI4KA*. Presentaven polimicrogíria bilateral, hipoplàsia/displàsia del cerebel i anomalies dels nuclis olivars i dentats, així com contractures articulars i superposicions digitals (Pagnamenta *et al.*, 2015).

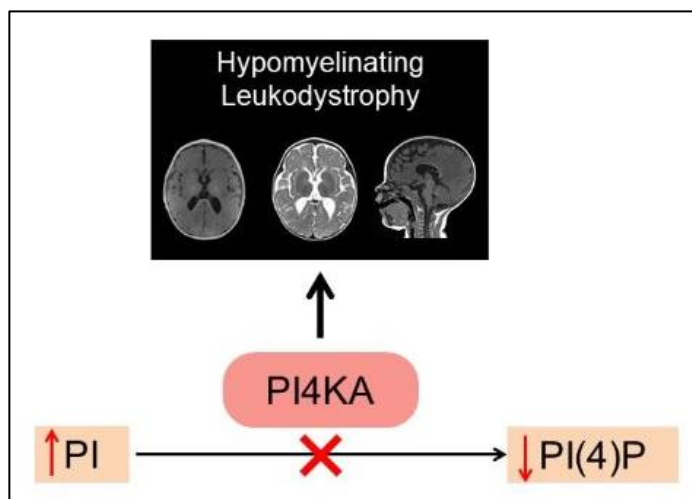
Resultats

- Identificació de 10 pacients amb variants genètiques bial·lèliques en el gen *PI4KA*. Un cas identificat a la nostra cohort de pacients amb GWMDs, dos a la de paraparèssies espàstiques hereditàries, un més identificat a través del projecte URDCat i la resta recollits a través de la plataforma GeneMatcher (Sobreira *et al.*, 2015).
- Segons el quadre clínic, diferenciació de dos grups principals de pacients:
 - Aquells amb un trastorn del neurodesenvolupament des del primer any de vida, associat amb una leucodistròfia hipomielinitzant, retard de la mielinització o anomalies estructurals cerebrals (polimicrogíria, hipoplàsia/atròfia del tronc cerebral i cerebel). A més, poden presentar crisis epilèptiques d'aparició en el primer any de vida, atàxia i trastorns del moviment. També manifestacions immunològiques, gastrointestinals i anomalies genitourinàries.
 - Pacients amb una paraparèsi espàstica hereditària predominant.
- Majoria de variants de canvi de sentit, la meitat de les quals estan agrupades en els dominis catalític i “cradle”.
- Els estudis de western blot i immunofluorescència van evidenciar uns nivells més baixos de PI4KA en fibroblasts dels pacients, i els estudis d'immunofluorescència i de lipidòmica dirigida van demostrar una activitat disminuïda de PI4KA.

Conclusions

- Descripció d'un nou GWMD, associat a variants patogèniques bial·lèliques en el gen *PI4KA*. L'espectre fenotípic comprèn des d'un trastorn global del neurodesenvolupament amb una leucodistròfia hipomielinitzant o anomalies del desenvolupament del SNC fins a una paraparèisia espàstica pura.
- Associació de trastorns immunològics, manifestacions gastrointestinals (com la malaltia de Crohn precoç) i anomalies genitourinàries en alguns dels pacients.
- Importància de la via dels fosfatidilinositzols (PI) en el desenvolupament del SNC i el procés de mielinització.

Resum gràfic de l'article





Biallelic PI4KA variants cause a novel neurodevelopmental syndrome with hypomyelinating leukodystrophy

Edgard Verdura,^{1,2,†} Agustí Rodríguez-Palmero,^{1,3,†} Valentina Vélez-Santamaría,^{1,4} Laura Planas-Serra,^{1,2} Irene de la Calle,¹ Miquel Raspall-Chaure,^{5,6} Agathe Roubertie,^{7,8} Mehdi Benkirane,⁹ Francesco Saettini,¹⁰ Lisa Pavinato,¹¹ Giorgia Mandrile,¹² Melanie O'Leary,¹³ Emily O'Heir,¹³ Estibaliz Barredo,¹⁴ Almudena Chacón,¹⁴ Vincent Michaud,^{15,16} Cyril Goizet,^{16,17} Montserrat Ruiz,^{1,2} Agatha Schlüter,^{1,2} Isabelle Rouvet,¹⁸ Julia Sala-Coromina,^{5,6} Chiara Fossati,¹⁹ Maria Iascone,²⁰ Francesco Canonico,²¹ Anna Marcé-Grau,⁵ Precilla de Souza,²² David R. Adams,^{22,23} Carlos Casasnovas,^{1,2,4} Heidi L. Rehm,¹³ Heather C. Mefford,²⁴ Luis González Gutierrez-Solana,^{2,25} Alfredo Brusco,^{11,26} Michel Koenig,⁹ Alfons Macaya^{5,6} and Aurora Pujol^{1,2,27}

[†]These authors contributed equally to this work.

Phosphoinositides are lipids that play a critical role in processes such as cellular signalling, ion channel activity and membrane trafficking. When mutated, several genes that encode proteins that participate in the metabolism of these lipids give rise to neurological or developmental phenotypes. PI4KA is a phosphoinositide kinase that is highly expressed in the brain and is essential for life.

Here we used whole exome or genome sequencing to identify 10 unrelated patients harbouring biallelic variants in PI4KA that caused a spectrum of conditions ranging from severe global neurodevelopmental delay with hypomyelination and developmental brain abnormalities to pure spastic paraparesis. Some patients presented immunological deficits or genito-urinary abnormalities. Functional analyses by western blotting and immunofluorescence showed decreased PI4KA levels in the patients' fibroblasts. Immunofluorescence and targeted lipidomics indicated that PI4KA activity was diminished in fibroblasts and peripheral blood mononuclear cells.

In conclusion, we report a novel severe metabolic disorder caused by PI4KA malfunction, highlighting the importance of phosphoinositide signalling in human brain development and the myelin sheath.

1 Neurometabolic Diseases Laboratory, Bellvitge Biomedical Research Institute (IDIBELL), L'Hospitalet de Llobregat, 08908, Barcelona, Catalonia, Spain

2 Centre for Biomedical Research in Network on Rare Diseases (CIBERER), Instituto de Salud Carlos III, 28029, Madrid, Spain

3 Pediatric Neurology Unit, Department of Pediatrics, Hospital Universitari Germans Trias i Pujol, Universitat Autònoma de Barcelona, Catalonia, Spain

4 Neuromuscular Unit, Neurology Department, Hospital Universitari de Bellvitge, Universitat de Barcelona, L'Hospitalet de Llobregat, Barcelona, Spain

5 Neurology Research Group, Vall d'Hebron Research Institute, Universitat Autònoma de Barcelona, Barcelona, Spain

6 Department of Paediatric Neurology, Vall d'Hebron University Hospital, Barcelona, Spain

- 7 Département de Neuropédiatrie, Hôpital Gui de Chauliac Pôle Neurosciences Tête et Cou, Montpellier, France
 8 INSERM U1051, Institut des Neurosciences de Montpellier, Montpellier, France
 9 Laboratoire de Génétique de Maladies Rares EA7402, Institut Universitaire de Recherche Clinique, Université de Montpellier, CHU Montpellier, CEDEX 5, 34295 Montpellier, France
 10 Paediatric Hematology Department, Fondazione MBBM, University of Milano Bicocca, Monza, Italy
 11 Department of Medical Sciences, University of Torino, 10126 Torino, Italy
 12 Thalassemia Centre and Medical Genetics Unit, San Luigi Gonzaga University Hospital, Orbassano, Italy
 13 Center for Mendelian Genomics, Program in Medical and Population Genetics, Broad Institute of MIT and Harvard, Cambridge, MA, USA
 14 Neuropediatric Department, Hospital Universitario Gregorio Marañón, Madrid, Spain
 15 Molecular Genetics Laboratory, Bordeaux University Hospital, Bordeaux, Aquitaine, France
 16 INSERM U1211, Rare Diseases Laboratory: Genetics and Metabolism, University of Bordeaux, Talence, Aquitaine, France
 17 Reference Center for Rare Neurogenetic Diseases, Department of Medical Genetics, University Hospital Centre Bordeaux Pellegrin Hospital Group, Bordeaux, Aquitaine, France
 18 Cellular Biotechnology Department and Biobank, Hospices Civils de Lyon, CHU de Lyon, Lyon, France
 19 Department of Paediatrics, Fondazione MBBM, Monza, Italy
 20 Molecular Genetics Laboratory, USSD LGM, Papa Giovanni XXIII Hospital, Bergamo, Italy
 21 Department of Neuroradiology, University of Milan-Bicocca, San Gerardo Hospital, ASST di Monza, Monza, Italy
 22 Office of the Clinical Director, National Human Genome Research Institute, NIH, Bethesda, MD, USA
 23 Undiagnosed Diseases Program, The Common Fund, NIH, Bethesda, MD, USA
 24 Division of Genetic Medicine, Department of Paediatrics, University of Washington, Seattle, WA 98195, USA
 25 Pediatric Neurology, Hospital Infantil Universitario Niño Jesús, Madrid, Spain
 26 Medical Genetics Unit, Città della Salute e della Scienza, University Hospital, 10126 Turin, Italy
 27 Catalan Institution of Research and Advanced Studies (ICREA), Barcelona, Catalonia, Spain

Correspondence to: Prof Aurora Pujol, MD, PhD
 Neurometabolic Diseases Laboratory, IDIBELL
 Hospital Duran i Reynals, Gran Via 199
 08908 L'Hospitalet de Llobregat
 Barcelona, Spain
 E-mail: apujol@idibell.cat

Keywords: PI4KA; phosphoinositol; inborn errors of metabolism; hypomyelinating leukodystrophy; spastic paraplegia

Abbreviation: PI = phosphatidylinositol

Introduction

Phosphoinositide lipids at the plasma membrane, which are important determinants of membrane identity, play roles in cell signalling, controlling cell shape and motility and thus also affect the interaction of cells with their environment.¹ Phosphoinositide metabolism at the plasma membrane begins with the phosphorylation of phosphatidylinositol (PI) to PI(4)P, which is later further phosphorylated to PI(4,5)P₂ and PI(3,4,5)P₃. This first step is catalysed by phosphatidylinositol 4 kinase A (PI4KA, MIM *600286) and is regulated by FAM126A and TTC7, which are subunits of the same complex.^{2,3} Animal models in which PI4KA homologues are inactivated show profound abnormalities: downregulation of Pi4ka expression in zebrafish leads to multiple developmental defects affecting the brain, heart, trunk and most prominently the loss of pectoral fins, while the Pi4ka orthologue knockout is lethal in flies, mice and yeast.^{4–7}

It is intriguing that pathogenic variants in FAM126A, a gene that encodes another partner of the PI4KA/TTC7/FAM126A protein complex, cause hypomyelinating leukodystrophy [hypomyelination and congenital cataracts(HCC); MIM #610532], with the main pathogenic mechanism of which is defective PI(4)P production in oligodendrocytes, a process coregulated by the myelin basic protein (MBP).^{2,8}

Notably, mutations in other genes that encode proteins that are involved in PI metabolism are associated with neurodevelopmental disorders. For instance, variants in the PIK3CA, PIK3R2, AKT3, and FIG4 genes have been linked to the development of polymicrogyria, which can be associated or not with megalencephaly and capillary malformation,^{5,9–12} and PI4K2A variants have been associated with intellectual disability and epilepsy.¹³

In this study, we identified 10 patients from unrelated families carrying biallelic variants in PI4KA that caused a spectrum of conditions ranging from severe global neurodevelopmental delay with hypomyelination/delayed myelination and developmental brain abnormalities to pure spastic paraplegia. Analysis of protein structure by 3D modelling and functional studies using western blotting, immunofluorescence and targeted lipidomic studies of the PI4KA pathway in patient cells were performed to confirm the pathogenicity of the identified variants.

Materials and methods

Genetic studies and variant assessment

We identified PI4KA variants in probands by whole-exome or whole-genome sequencing in clinical diagnostic or research

settings. Candidate variants were validated by Sanger sequencing and tested for co-segregation in all family members except for Patient 5's mother (unavailable). The Genome Aggregation Database (gnomAD v.2.1.1; <https://gnomad.broadinstitute.org/>; accessed 30 November 2020) was used to determine variant frequency in control populations. Variants were annotated with ANNOVAR. High-quality variants with an effect on the coding sequence or splice site regions with a frequency lower than 0.01 were retrieved from public databases (gnomAD and in-house databases). The functional impact of variants was analysed with various prediction tools, including PolyPhen-2, M-CAP, CADD, MutationTaster and LRT pred. Sequence alignment was performed using ClustalOmega (<https://www.ebi.ac.uk/tools/msa/clustalo/>; accessed 30 November 2020) with sequences extracted from NCBI databases. The PI4KA complex (6bq1 template from the RCSB PDB database)³ was visualized with PyMOL version 2.2.3 (<https://www.pymol.org/>; accessed 30 November 2020).

Patient recruitment

We obtained genotypic and phenotypic information from patients with probable pathogenic PI4KA variants (after *in silico* criteria), from different hospitals identified with GeneMatcher.¹⁴ All patients were analysed by the neurologists and/or clinical geneticists of their respective referral centre, who determined the para-clinical analyses to be performed in each case. We reviewed clinical information related to neurodevelopment, growth parameters, neurological manifestations, behaviour, dysmorphology, and the results of other exams. Hypomyelination was diagnosed when neuroimaging evidenced mildly elevated hyperintensity of most cerebral white matter in T₂-weighted images and mild hypointensity, isointensity or mild hyperintensity relative to the cortex in T₁-weighted images.¹⁵ Blood samples were obtained using standard methods. Written informed consent for genetic testing and publication of the clinical information, including clinical pictures, was obtained from the parents or legal guardians of each patient according to the Declaration of Helsinki.

The research project was approved by the Clinical Research Ethics Committees of IDIBELL Institute (Patients 1 and 9, PR076/14), VHIR Institute [Patient 2, PR(AG)223/2017], CHU Bordeaux (Patient 4, Comité de Protection des Personnes Bordeaux—Outre Mer III), the Broad Institute (Patient 5, Partners IRB Protocol #:2016P001422), the University of Washington (Patient 6, #28853), Città della Salute e della Scienza University Hospital (Patient 7, n. 0060884), the Comitato Etico Brianza (Patient 8; Monza, Italy; PID-GENMET), the IIGM Institute (Patient 10, Comité de Ética de la Investigación con Medicamentos, CEIM) and the Montpellier Local Ethics Committee (Patient 3).

Western blotting

Human fibroblasts were homogenized in RIPA buffer (150 mM NaCl, 1% Nonidet™ P40, 0.5% sodium deoxycholate, 0.1% SDS, and 50 mM Tris, pH 8.0), sonicated for 1 min at 4°C, centrifuged for 10 min at 1000g mixed with 4× NuPAGE LDS Sample Buffer (Invitrogen) and heated for 5 min at 100°C. Protein concentrations were quantified using a BCA protein assay kit (Thermo Fisher Scientific). Twenty-five micrograms of each protein sample was subjected to polyacrylamide gel electrophoresis for 30 min at 100 V and for 1 h at 120 V in NuPAGE MOPS SDS Running Buffer (Invitrogen) supplemented with 5 mM sodium bisulfite (Ref. 243973, Sigma-Aldrich). The proteins were transferred to nitrocellulose membranes. After blocking with 5% bovine serum albumin (BSA, Sigma-Aldrich) in 0.05% TBS-Tween (TBS-T) for 1 h at room temperature, the membranes were incubated with primary

antibodies for 2 h at room temperature. Following incubation with secondary antibodies for 1 h at room temperature, the proteins were detected with the Chemidoc™ Touch Imaging System (Bio-Rad). The bands were quantified with ImageLab (Bio-Rad). The primary antibodies that were used were anti-PI4KA (12411-1-AP Proteintech) and anti-β-Actin (A2228, Sigma). The secondary antibodies that were used were polyclonal goat anti-mouse (P0447, Dako Cytomation) and polyclonal goat anti-rabbit (P0448, Dako Cytomation). The unmodified full-length blot is shown in Supplementary Fig. 3.

Immunofluorescence

A total of 150 000 cells were seeded on coverslips in wells containing 2 ml of 10% formalin and fixed in for 30 min at room temperature. To permeabilize and block the cells, the coverslips were incubated for 20 min at room temperature in blocking buffer (1% BSA, 0.2% powdered milk, 2% NCS, 0.1 M glycine, and 0.1% Triton™ X-100). The cells were immunostained with primary antibodies for 2 h at room temperature. Following incubation with secondary antibodies for 1 h at room temperature, the slides were mounted using Mowiol®. Confocal images were acquired using a Leica TCS SL laser scanning confocal spectral microscope (Leica Microsystems) and analysed with ImageJ (NIH, USA). The primary antibodies that were used were anti-PI4KA (12411-1-AP, Proteintech) and anti-PI(4)P (Z-P004, Echelon Biosciences Inc.). The secondary antibodies that were used were Alexa Fluor® 555-conjugated goat anti-rabbit IgG (A-21428, Invitrogen) and Alexa Fluor® 488-conjugated goat anti-mouse IgG (A-11001, Invitrogen).

Lipidomics analysis

Peripheral blood mononuclear cells (PBMCs) were isolated from whole blood using standard methods. Quantification of phosphoinositide species was performed at ATK-Analytics Innovation and Discovery using 200 µg of TCA-precipitated PBMCs as the starting material. Lipids were extracted and derivatized using TMS-Diazomethane prior to mass spectrometry, as described previously.^{16,17} PI 17:0 and 20:4 and PI(4)P 17:0 and 20:4 (LM1502, LM1901, Avanti Polar Lipids) were used in parallel as internal standards. The results were analysed using MassLynx software.

Statistical analysis

Statistical significance was assessed using Student's t-test when two groups were compared, and P < 0.05 was considered significant.

Data availability

The authors confirm that the data supporting the findings of this study are available within the article and its *Supplementary material*.

Results

Gene discovery and variant assessment

In the framework of a research project aiming to end the diagnostic odyssey in patients with neurogenetic diseases (URD-Cat, Undiagnosed Rare Diseases Consortium of Catalonia), we performed whole-exome sequencing and identified biallelic variants in PI4KA in two patients (Patients 1 and 2) affected with hypomyelinating leukodystrophy. Patient 1 was a compound heterozygote for a missense variant and a loss-of-function variant (p.Glu1152Lys, p.Pro876SerfsTer36), while Patient 2 harboured a

homozygous missense variant (p.Gly1925Arg) located close to the PI4KA catalytic site, suggesting possible consanguinity. Through GeneMatcher,¹⁴ we recruited eight additional patients from independent families carrying biallelic variants in PI4KA with compatible phenotypes (Figs 1 and 2). Accordingly, the pLI value of PI4KA was 0.00031, and the pRec value was 1, indicating that biallelic deleterious variants in this gene are pathogenic.¹⁸ All identified variants were ultra-rare with minor allele frequencies (MAF) <0.00001 in the Genome Aggregation Database (gnomAD) (Supplementary Table 1). Eight patients were compound heterozygous, while two [Patient 2, p.(Gly1925Arg) and Patient 8, p.(Asp1854Asn)] were homozygous. Twelve of the identified variants were missense variants, one was an in-frame deletion of one amino acid, and the remaining four variants were predicted to result in loss-of-function. All missense/in-frame variants affected conserved amino acids and were predicted to be deleterious by various prediction tools (Table 1 and Supplementary Fig. 1). PI4KA contains an α -solenoid domain, a dimerization domain, and a 'cradle' domain (which contains three contact surfaces with TTC7, with which PI4KA interacts directly), as well as a catalytic domain at the C-terminus that is responsible for phosphorylation activity and is anchored at the cell membrane.^{2,3} Interestingly, 7 of 13 conserved missense/in-frame variants were clustered near the active site of PI4KA in the catalytic and 'cradle' domains (Fig. 1C and Supplementary Fig. 2). All patients harbouring one loss-of-function variant were compound heterozygotes with a missense or in-frame variant, with no patients harbouring two loss-of-function variants. Patients 4 and 9 shared one of the truncating variants (p.Thr2053SerfsTer4) but displayed discordant phenotypes. Patient 9, who carried an in-frame variant near the catalytic domain of the second allele had a milder presentation, showing spastic paraparesis with an age of onset of 17. Patient 4 harboured a missense variant in the α -solenoid domain and presented with severe hypomyelinating leukodystrophy with onset at 1 year of age.

Clinical features

We studied 10 patients harbouring biallelic, ultrarare and probably deleterious variants after *in silico* predictions in PI4KA. Table 1 outlines the main clinical features of the patients, and the Supplementary material includes the patients' clinical summaries and demographics. Weight, length and cranial circumference were all normal at birth, while at the last examination (median age 7 years; 3–42 years), three patients (Patients 1, 2 and 6) had low weight, four (Patients 1, 3, 6 and 8) had short height and four (Patients 2, 3, 6 and 8) had a head circumference less than two standard deviations (SD) below the mean. The median age of disease onset was 2 years (birth to 17 years).

Based on neurological involvement, patients in this cohort fall into two main groups.

Group 1

Patients with developmental encephalopathy with hypomyelinating leukodystrophy/delayed myelination and structural brain anomalies (Patients 1–8). These patients presented global developmental delay in the first 12 months of life; in five of these patients, clinical manifestations started in the neonatal period, mainly seizures and/or severe hypotonia. At the last examination (3–19 years of age), all of the patients presented moderate-to-severe intellectual disability, except for Patient 5, in whom intellectual disability was mild. Four patients were non-verbal, and four had not achieved ambulation, with Patient 3 being non-ambulatory even at the age of 13 years. Axial hypotonia with limb spasticity and pyramidal signs were present in all patients except Patient 2, in whom severe global hypotonia predominated and a neurophysiological

study performed at 11 months of age showed axonal sensory neuropathy. Six patients had cerebellar ataxia, and five presented a movement disorder, including tremor in two patients, dystonia in two patients, choreoathetosis in one patient and stereotypies in another patient. There were no formal diagnoses of behavioural disorders, but two patients showed hyperexcitable behaviour. Six patients developed epileptic seizures, which appeared in the neonatal period in four patients and were very frequent initially but became less frequent later. Patient 6 remained without seizures after stopping antiepileptic treatment at 18 months of age. Seizures were generalized, focal and myoclonic, and in Patient 1, episodes suggestive of infantile spasms were described at 3.5 months of age. In Patients 1–3, seizures usually appeared to be associated with fever or microbial infections and could evolve into status epilepticus. The EEG results of Patients 1 and 2 showed multifocal epileptiform discharges, with paracentral predominance being observed in Patient 1, which improved over time, and slow background activity. In Patient 4, frontotemporal spike-wave discharges were reported, and in Patient 8, bilateral frontal anomalies evolved into marked abnormalities of background activity and frequent diffuse spike and spike-wave discharges; however, in the other three patients, interictal EEG was normal.

Other clinical features included nystagmus in four patients, strabismus in two patients, and myopia and bilateral iris and retinal coloboma in one patient. Sensorineural hearing loss was reported in one patient. Four patients had feeding difficulties in early childhood, and two required nasogastric tube feeding during the first weeks of life. Patients 2, 3, 5 and 8 had immunological problems, including hypogammaglobulinaemia in three patients and lymphopaenia and autoimmune neutropaenia in one patient each. It is worth noting that symptoms of bowel dysfunction (vomiting, diarrhoea, constipation or gastroesophageal reflux disease) were reported in Patients 3, 5, 7 and 8. Finally, Patients 2, 6 and 8 presented abnormalities of the genito-urinary system, such as cryptorchidism, renal cysts and duplication of the collecting system.

Group 2

Patients with predominant spastic paraparesis (Patients 9 and 10). These patients presented a milder phenotype characterized by progressive spastic paraparesis with onset at 2 and 17 years and pes cavus. One showed mild intellectual disability, and the other patient had normal cognition. Patient 9 received a diagnosis of Crohn's disease with a stenosing-inflammatory pattern and corticosteroid-dependent course at 21 years of age.

Brain MRI findings

The MRI images of all the patients are shown in Fig. 2. Group 1 patients showed a pattern of marked, diffuse supratentorial and infratentorial hypomyelination associated with white matter atrophy and a thin corpus callosum (Patients 1–4), incomplete/delayed myelination (Patients 5–7) and bilateral perisylvian polymicrogyria (Patient 8). The corpus callosum was dysplastic in Patients 3, 5 and 6. In Patients 1, 4 and 6, there was brainstem and cerebellar hypoplasia/atrophy, which remained unchanged up to age 2 in Patient 1. In addition, there was a component of cerebellar atrophy that progressed in successive controls in Patients 3, 4 and 7 (inferior lobe). The severity of myelin involvement correlated with clinical manifestations, which were more severe in Patients 1–3. In contrast, cerebral neuroimaging in the clinically milder patients (Patients 9 and 10) was normal, except for an arachnoid cyst of the posterior fossa in Patient 9, which was considered an unrelated finding. However, in these patients (and in Patients 1–3), cranial MRI revealed cervical spinal cord atrophy.

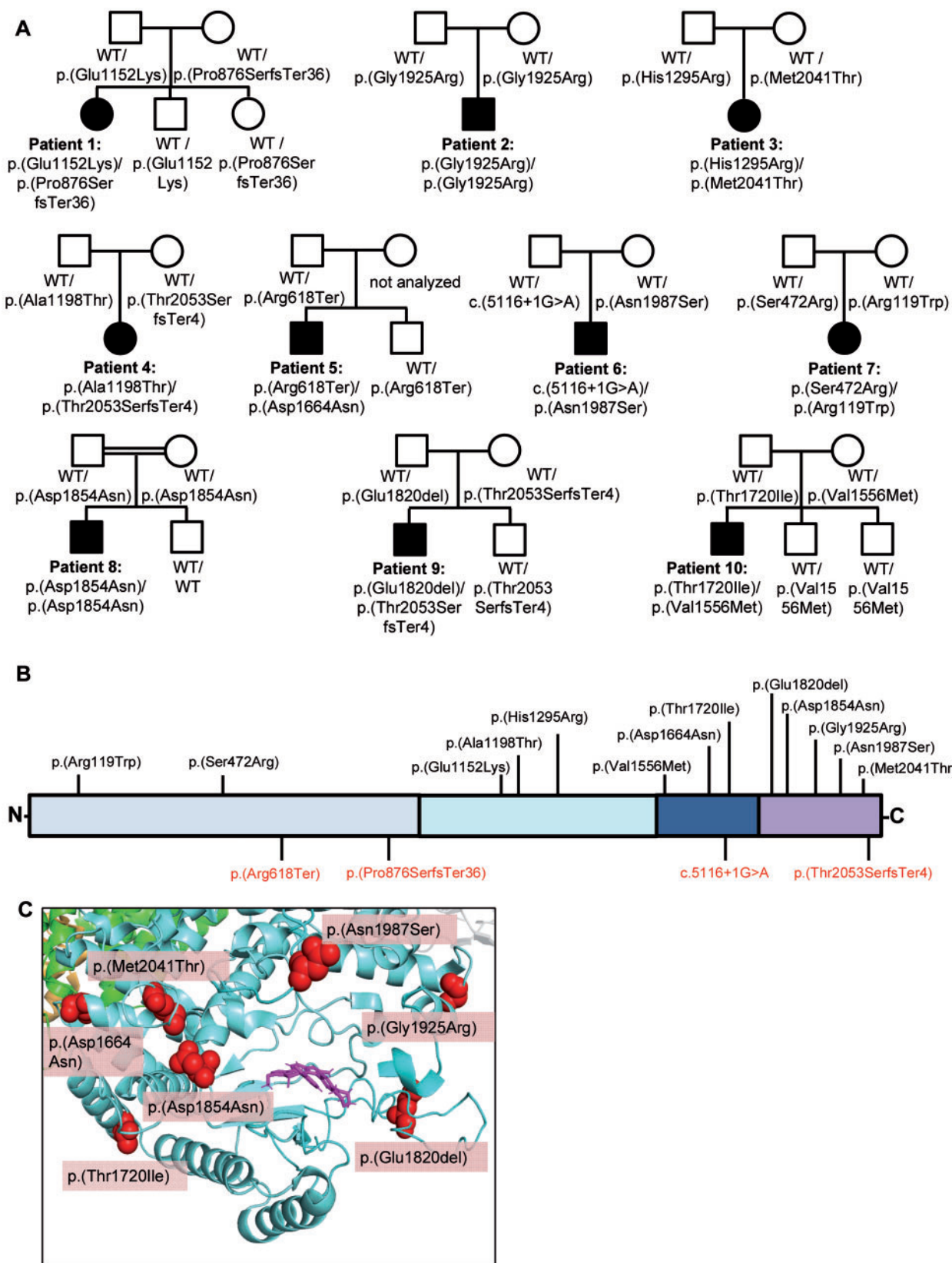


Figure 1 PI4KA variant features. (A) Family trees. Square = male; circle = female; filled symbols = affected individuals; open symbols = unaffected carriers; WT = wild-type allele. (B) Structure of PI4KA protein and the mutations identified in this study. Top: Missense/in-frame variants. Bottom: Loss-of-function variants. Light blue = α -solenoid domain; cyan = dimerization domain; dark blue = 'cradle' domain; dark purple = catalytic domain. (C) 3D representation of the PI4KA catalytic domain. Blue = PI4KA; green = TTC7B; pink = A1, PI4KA inhibitor occupying the ATP-binding space in the catalytic domain. The red balls represent the location of the missense/in-frame variants found in our cohort. Note the clustering of missense/in-frame variants near the catalytic site of PI4KA.

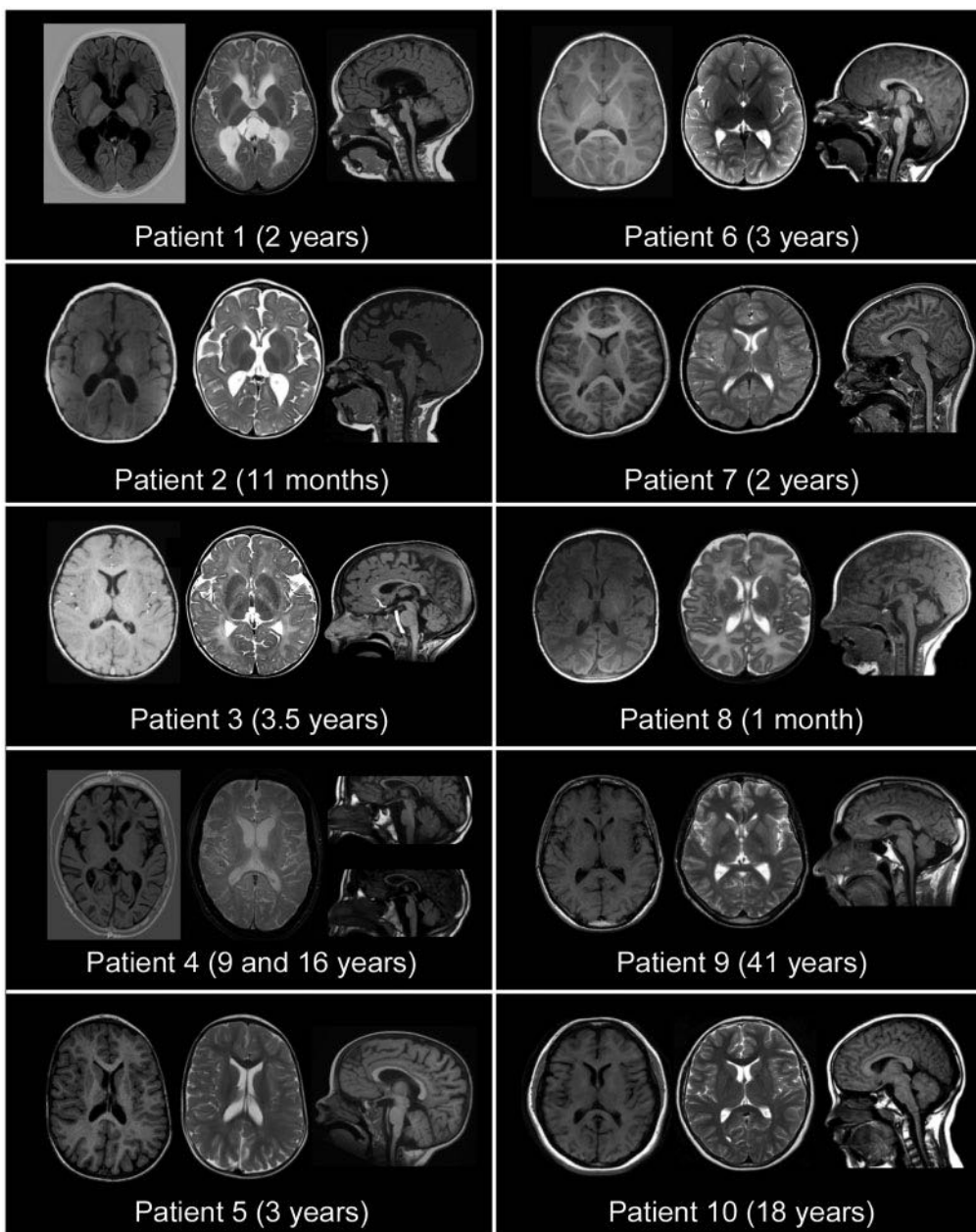


Figure 2 MRI features of patients harbouring biallelic PI4KA variants. Left: Axial T₁-weighted sequences. Middle: Axial T₂-weighted sequences. Right: Sagittal T₁-weighted sequences. Patients 1 and 2 exhibited diffuse hypomyelination, global white matter atrophy with posterior predominance, a thin corpus callosum and colpocephaly. Patient 1 also presented with brainstem and cerebellar hypoplasia. Patients 3 and 4 had diffuse hypomyelination with a thin corpus callosum and progressive cerebellar atrophy. Patient 4 also had brainstem atrophy. Patients 5–7 exhibited delayed myelination with mild ventriculomegaly. Patients 5 and 6 showed a dysplastic corpus callosum. Patient 6 had brainstem and cerebellar atrophy and Patient 7 exhibited atrophy of the cerebellar inferior lobe. Patient 8 showed bilateral perisylvian polymicrogyria. Patients 9 and 10 showed cervical spinal cord atrophy, and arachnoid cyst of the posterior fossa was observed in Patient 9, the images of whom were otherwise normal.

PI4KA activity *in vitro* and *in vivo*

We were able to obtain skin biopsies and/or blood samples from Patients 1, 3, 4, 9 and 10, and performed functional analysis of their variants. Western blot analysis showed that the expression of the PI4KA protein was strongly decreased in the fibroblasts of Patients 1, 3, 4, 9 and 10 compared to those of age-matched controls (Fig. 3B). This result was supported by immunofluorescence images (Fig. 3C and D). To evaluate the activity of PI4KA, we used an antibody against the head group of its reaction product, PI(4)P, as previously described.² Immunofluorescence revealed lower levels of PI(4)P in our patients' fibroblasts (Fig. 3C and D). Finally, we also

performed lipidomics analysis to quantify global phosphoinositide (PI, PIP and PIP₂) levels in Patients 1, 2, 9 and 10. All of the patients showed a significantly decreased PIP/PI ratio compared to age-matched control subjects, indicating decreased PI4KA activity in these patients (Fig. 3E).

Discussion

We describe here a novel neurological syndrome caused by biallelic mutations in the PI4KA gene. The clinical spectrum ranges from a neurodevelopmental disorder of neonatal onset associated

Table 1 Main clinical features of the 10 patients with biallelic PI4KA variants

General information	Patient 1	Patient 2	Patient 3	Patient 4	Patient 5	Patient 6	Patient 7	Patient 8	Patient 9	Patient 10
Gender	Female	Male	Female	Female	Male	Male	Female	Male	Male	Male
Ethnicity	Caucasian	Caucasian	Caucasian	Caucasian	Caucasian	Asian/Caucasian	Caucasian	Turkish	Caucasian	Latin American
Age of onset	Newborn	Newborn	6 months	1 year	Newborn	Newborn	Newborn	Newborn	17 years	2 years
Age at exam	3 years	13 years	19 years	10 years	6 years	6 years	11 years	5 years	40 years	18 years
Variant	c.2624dupC c.345G>A	c.5773G>C c.5773G>C	c.3884A>G c.6122T>C	c.3592G>A c.6156_6159delGACA	c.1852G>T c.4990C>A	c.5116+1G>A c.5960A>G	c.1414A>C c.355C>T	c.556G>A c.556G>A	c.5459_5461 delAAAG	c.4666G>A c.5159C>T
cdNA										
Protein	p.(Pro876SerfsTer36) p.(Glu1152Lys)	p.(Gly1925Arg) p.(Gly1925Arg)	p.(His1295Arg) p.(Met2041Thr)	p.(Ala198Thr) p.(Thr2053 SerfsTer4)	p.(Arg8618Ter) p.(Asp1664Asn)	p? p.(Asn1987Ser)	p.(Ser472Arg) p.(Arg119TP)	p.(Asp1854Asn) p.(Asp1854Asn)	p.(Val1556Met) p.(Thr1720Ile)	
Examination										
Weight (SD)	11.4 kg (-2.6)	10.5 kg (-2.4)	3.9 kg (-1)	49 kg (-1)	26.8 kg (1.23)	15.8 kg (-2.3)	40 kg (-0.4)	14.5 kg (-1.4)	64 kg (-0.9)	Not available
Height (SD)	92 cm (-3.8)	Not available	141 cm (-2.7)	169 cm (+0.8)	133.6 cm (0.7)	105.8 cm (-2)	148 cm (-0.6)	100 cm (-2)	171 cm (-1)	Not available
HC (SD)	48.5 cm (-1.4)	46.2 cm (-3.3)	52 cm (-2)	Not available	50 cm (0.5)	47 cm (-3.8)	52.3 cm (-1.9)	47 cm (-3.5)	56 cm (-0.3)	
Motor signs	Spastic tetraparesis	Spastic paraparesis	Spastic paraparesis	Spastic tetraparesis	Spastic tetraparesis	Spastic tetraparesis	Spastic tetraparesis	Spastic tetraparesis	Spastic tetraparesis	Spastic paraparesis
Ataxia	+	-	+	+	+	+	+	-	-	-
Epilepsy	++ (IS)	++	+	+	+	+	-	++	-	-
Additional features	Dystonia, choreoathetosis, hyperexcitability, nystagmus	Axonal sensory neuropathy, nystagmus, startle	Irritability (first months), tremor, very smiley, nystagmus	Tremor, nystagmus	Tremor, nystagmus	Hand flapping when excited	Stereotypic movements, ocular dyspraxia	Dystonia	No delay	Delayed
Development										
Gross motor	Severely delayed	Severely delayed	Severely delayed	Delayed	Delayed	Delayed	Delayed	Severely delayed	No delay	Delayed
Walking	Not achieved	Not achieved	Delayed	Delayed	4.5 years	5 years	Not achieved	Normal	15 months	
Language	None	None	Single words	None	Delayed	Delayed	None	Normal	Normal	Normal
Intellectual disability	Severe	Severe	Severe	Moderate	Severe	Severe	Severe	Severe	Mild	Mild
MRD description										
	Diffuse hypomyelination, WM atrophy, ventriculomegaly, thin CC, brainstem and cerebellar hypoplasia	Diffuse hypomyelination, WM atrophy, ventriculomegaly, thin CC	Diffuse hypomyelination, dysplastic thin CC, cerebellar atrophy with calcifications	Diffuse hypomyelination, dysplastic CC, cerebral, brainstem and cerebellar atrophy	Delayed myelination, dysplastic CC, brainstem and ventriculomegaly	Delayed myelination, dysplastic CC, brainstem and cerebellar atrophy	Delayed myelination, external hydrocephalus, cerebellar atrophy	Bilateral palsy, external hydrocephalus, cerebellar atrophy	Arachnoid cyst of the posterior fossa, cervical spinal cord atrophy	Cervical spinal cord atrophy

+ = present; - = absent; + + = severe; CC = corpus callosum; HC = head circumference; ID = intellectual disability; IS = infantile spasms; WM = white matter.

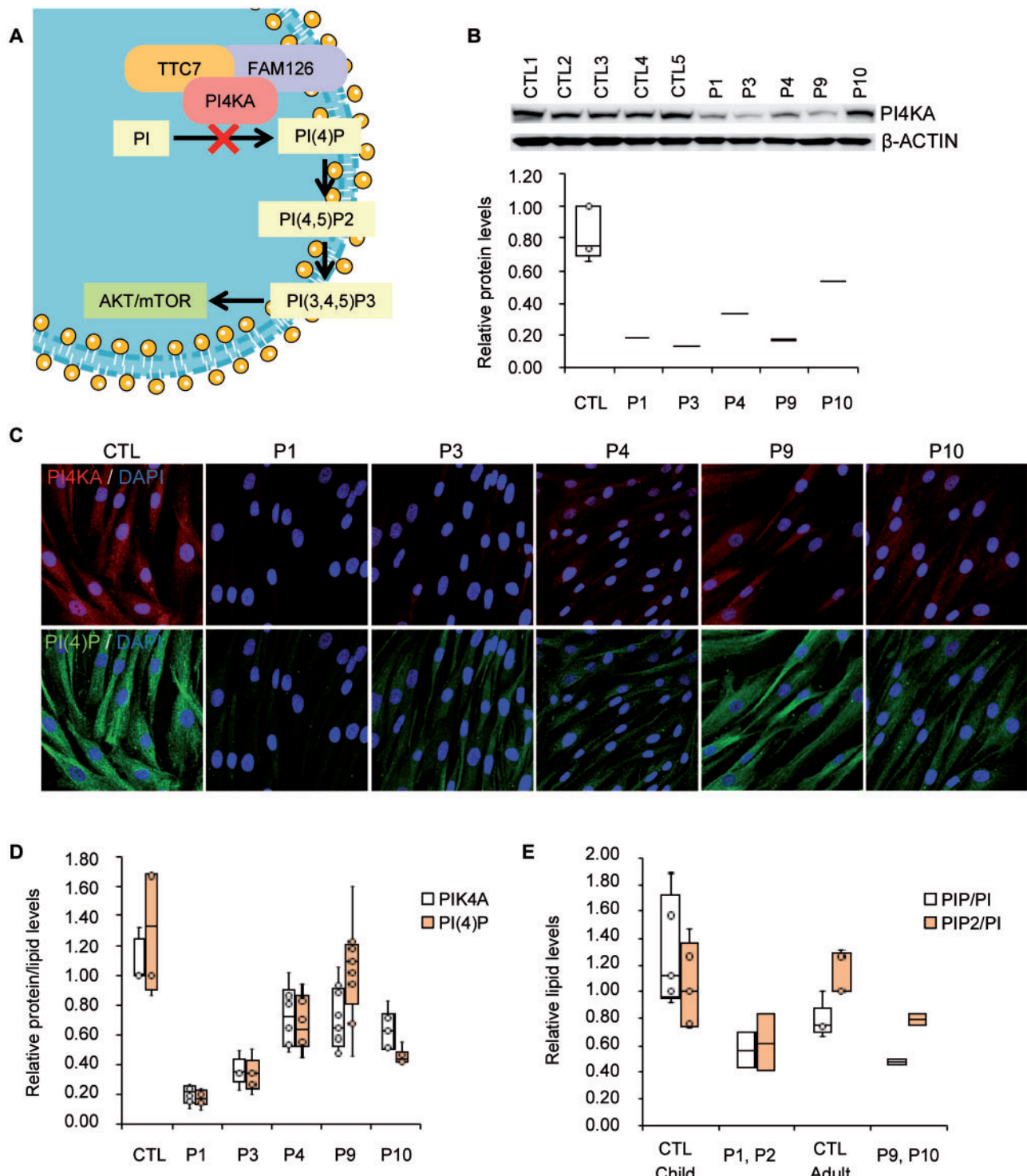


Figure 3 PI4KA activity evaluation. (A) Schematic representation of the PI4KA pathway. (B) Western blot of PI4KA protein and quantification. Patients' fibroblasts ($n = 5$) and controls (CTL, $n = 5$). (C) Immunofluorescence of PI4KA protein and the head group of the lipid PI(4)P and (D) its quantification on a minimum of 100 cells. Patient's fibroblasts ($n = 5$) and controls (CTL, $n = 4$). (E) Targeted lipidomics against phosphatidylinositol (PI), PIP and PIP2, in human PBMCs from control (CTL) children ($n = 5$), control adults ($n = 5$); and PI4KA deficient patients ($n = 4$). Data represented as mean \pm SD. * $P < 0.05$, ** $P < 0.01$, *** $P < 0.001$ (two-tailed Student's *t*-test). Box plot centre line corresponds to the median, lower and upper limits to the first and third quartiles (25th and 75th percentiles), respectively, and whiskers to $1.5 \times$ the interquartile range.

with severe hypomyelinating leukodystrophy with pontocerebellar hypoplasia (or even polymicrogyria in one case) to spastic paraparesis beginning in adolescence. This cohort illustrates how mutations in genes causing childhood leukodystrophies at the most severe end of the clinical spectrum, can also give rise to milder

presentations, such as juvenile or adult-onset spastic paraplegias. TUBB4A-related leukodystrophy, X-linked adrenoleukodystrophy, Pelizaeus-Merzbacher disease and Alexander disease are paradigmatic for this well-described phenomenon.^{19–24} Although in most cases recessive mutations in this gene will manifest as hypomyelinating

leukodystrophy, we propose the term 'PI4KA-spectrum' to describe the different neurological conditions associated with this gene.

Pyramidal tract involvement with increased limb muscle tone predominates in most of the patients in this cohort. Remarkably, Patient 2 shows severe global hypotonia with areflexia and abnormal nerve conduction studies, indicating peripheral nervous system involvement, which is in line with the neuropathy described in a mouse model with *Pi4ka* inactivation restricted to Schwann cells.²⁵ In comparison with patients with mutations in FAM126A (HCC), another member of the PI4KA/TTC7/FAM126A complex,² four of our patients had an earlier clinical onset in the neonatal period and were neurologically more severely affected. Furthermore, epilepsy appears to be more common than in HCC patients,²⁶ and immunological or gastrointestinal symptoms have not been reported in patients with HCC. On the other hand, it is striking that none of the patients in the present study developed cataracts, which suggests that their presence may be directly due to malfunction of FAM126A. Peripheral neuropathy is an invariable feature of HCC, whereas it was only observed in one of the patients reported here. Regarding neuroimaging, Patient 4 exhibited a hypomyelinating pattern with a more conspicuous periventricular T₂ hyperintensity, similar to the pattern described in patients with FAM126A mutations.²⁶ In contrast, the polymicrogyria and brainstem and cerebellar hypoplasia reported in our cohort have not been described in FAM126A patients.

Further differential diagnosis should be made with other diseases associated with hypomyelination, mainly PLP1 disorders, and specifically disorders that present with cerebellar atrophy or hypoplasia, such as Pol III-related disorders, 18q syndrome, TUBB4A- and RARS-associated hypomyelination and hereditary spastic paraparesis (both pure and complex forms). Disorders that cause pontocerebellar hypoplasia and myelination delay should also be taken into account.²⁷ The combination of severe developmental delay, motor impairment and early-onset seizures is a feature of developmental and epileptic encephalopathies (DEEs), and patients with these diseases often show posterior fossa anomalies, cerebral dysgenesis or delayed myelination. Hence, this group of diseases should also be considered.²⁸ Finally, other disorders associated with neuronal migration and polymicrogyria should be included in the differential diagnosis.^{29,30}

Previously, mutations in PI4KA were reported in three foetuses from a single family who showed bilateral polymicrogyria with hypoplasia/dysplasia of the cerebellum, olfactory and dentate nucleus abnormalities, joint contractures and overlapping fingers.³¹ All three foetuses were compound heterozygous for two loss-of-function variants: a premature stop variant [p.(Arg796Ter)] and a missense variant located in the active site that abrogated kinase activity [p.(Asp1854Asn)]. Therefore, the phenotypes presented by these foetuses may represent the most severe end of the phenotypic spectrum of diseases associated with PI4KA mutations since no abnormalities were detected during pregnancy in our cases. This suggests that our patients may retain higher residual PI4KA activity than previously reported patients.³¹ In support of this hypothesis, *Pi4ka* mouse models harbouring two complete loss-of-function alleles are embryonic lethal,⁵ while *pi4ka* knockdown zebrafish, which retain some *Pi4ka* activity, show multiple developmental abnormalities.⁴ Interestingly, the only patient in our study who shared a variant with the family reported by Pagnamenta et al.³¹ [p.(Asp1854Asn)] also developed polymicrogyria, suggesting that this variant may be specifically associated with this developmental brain anomaly. Furthermore, the fact that this variant in homozygosity leads to a milder phenotype than the foetuses in Pagnamenta et al.,³¹ who had the p.Asp1854Asn variant in compound heterozygous state with a stop codon variant, strongly suggests that this missense variant would not cause a

complete loss-of-function, and a certain degree of residual PI4KA activity is retained. Despite a clear enrichment of missense variants close to PI4KA's active site hence supporting the pathogenic role of these variants, we did not find a patient with two loss-of-function alleles, suggesting that the missense variants identified in this cohort may be hypomorphic. Patients 1, 4, 5 and 9 harboured loss-of-function variants (out-of-frame indels or stop variants) that were always in *trans* with missense variants located far from the active site [p.(Glu1152Lys), p.(Asp1664Asn), p.(Ala1198Thr)] or small in-frame mutations [Patient 9, p.(Glu1820del)], suggesting that the impairment of PI4KA activity resulting from these variants may have been less severe than that caused by other variants. Two patients harbouring the p.(Thr2053SerfsTer4) variant presented different phenotypes, indicating that p.(Ala1198Thr) (Patient 4) might be more deleterious than p.(Glu1820del) (Patient 9); however, phenotype-genotype correlation in a small cohort of patients poses a challenge.

Although the clinical manifestations presented by our cohort of patients were prominently neurological, five patients presented with an immune disorder and/or a history of recurrent infections. On the other hand, one patient suffered from Crohn's disease, whereas more non-specific manifestations, such as vomiting, diarrhoea, constipation or gastroesophageal reflux disease, were present in four patients. It is tempting to speculate that some of these extraneurological manifestations could be caused by disruption of the interactions between PI4KA and TTC7A, defects that have been associated with immunodeficiency and gastrointestinal manifestations.³²

The pathogenic effects of PI4KA mutations remain poorly understood. PI4KA and PI(4)P levels were significantly diminished in the fibroblasts of five patients. PI(4,5)P₂, a product of PI(4)P phosphorylation, is a substrate for the PI3K-AKT-mTOR pathway, which is critical for the myelination process.^{2,8} PIP levels were reduced in the PBMCs of four patients, and specifically PI(4)P was diminished as shown in fibroblasts of five patients, suggesting that their use as biomarkers for diagnosis and prognosis may be indicated. Moreover, and given the important role of PI(4)P in the transport of phosphatidylserine, a phospholipid abundantly found in myelin, to the plasma membrane,^{33,34} PI4KA malfunction may lead to disturbances in the brain cell membrane lipidome, resulting in aberrant myelination. Concordantly, PI4KA inhibition has been shown to significantly reduce phosphatidylserine levels in cultured cells by inhibiting its transport to the plasma membrane, a phenomenon also observed in Lenz-Majewski syndrome, a developmental condition that involves similar abnormalities in PI(4)P/phosphatidylserine metabolism.³⁵ Furthermore, inositol phospholipids are also important in processes such as actin remodelling and oligodendrocyte membrane polarization, which are essential for myelination. This process is similar to the actin polymerization-depolymerization sequence required for correct cell migration during brain development²⁵ and may underlie both the myelination and neurodevelopmental defects we describe (polymicrogyria and brainstem-cerebellar hypoplasia). Interestingly, mice with knockout of *Pi4k2a*, another kinase involved in PI(4)P formation from PI, develop late-onset features resembling hereditary spastic paraparesis, and the inhibition of PI4K activity disrupts the retrograde axonal transport of neurotrophins.³⁶ The alteration of axonal transport is one of the main processes involved in hereditary spastic paraparesia³⁷ and is also dependent on oligodendrocyte function.³⁸

Given that lipid metabolism defects appear to play an important role in the pathophysiology of PI4KA-associated disorders and other leukodystrophies and hereditary spastic paraparesias, therapeutic avenues for these patients could involve normalization of lipidic disturbances impacting myelination.^{39,40} Alternatively,

upregulation of PI4KA expression or treatment with drugs that specifically treat secondary deficiencies in interacting proteins (TTC7B and FAM126A) may prove helpful in alleviating symptoms in the most severe patients in the future.^{41,42}

In summary, we describe a novel inherited error of metabolism caused by PI4KA malfunction resulting in a broad phenotypic spectrum ranging from severe global neurodevelopmental delay associated with hypomyelinating leukodystrophy and/or brain developmental anomalies such as pontocerebellar hypoplasia/atrophy (or even polymicrogyria) in the most severe forms to spastic paraparesis in milder cases. The presence of immunological deficits, gastrointestinal manifestations or genito-urinary abnormalities may be helpful for the diagnosis of these patients.

Acknowledgements

We are grateful to the patients and their families. We also thank Cristina Guilera and Juanjo Martínez (Neurometabolic Disease Laboratory) and Lise Larrieu and Morgane Pointaux (Laboratoire de Génétique Moléculaire) for their excellent technical assistance; Eric Jeziorski for the initial referral of Patient 3; Lucia A. Baselli (Department of Pediatrics, Fondazione IRCCS Ca' Granda Ospedale Maggiore Policlinico, Milan), Gaia Kullman (Department of Child Neurology and Psychiatry, San Gerardo Hospital, University of Milan-Bicocca) and Silvia Maitz (Clinical Pediatric Genetic Unit, Pediatric Clinic, Fondazione MBBM, San Gerardo Hospital) for the initial referral of Patient 8; Alexis Traynor-Kaplan for help interpreting the lipidomics results; the University of Washington's School of Pharmacy's Mass Spectrometry Center; and the Cellular Biotechnology Department and Biobank, Hospices Civils de Lyon.

Funding

We thank the CERCA Program/Generalitat de Catalunya for institutional support. This study was supported by grants from the Hesperia Foundation, the Asociación Española contra las Leucodistrofias (ALE-ELA España), the Autonomous Government of Catalonia (SGR 2017SGR1206 and PERIS program URD-Cat SLT002/16/00174) and the Center for Biomedical Research on Rare Diseases (CIBERER) (ACCI19-759 to A.P.). This study was also funded by Fundació La Marató de TV3 (595/C/2020) as well as Instituto de Salud Carlos III (FIS PI20/00758 to C.C.) (co-funded by European Regional Development Fund. ERDF, a way to build Europe). This study was also funded by the Instituto de Salud Carlos III (Rio Hortega, CM18/00145 to V.V.; PFIS, FI18/00141 to L.P.; and Sara Borrell, CD19/00221 to E.V.), co-funded by European Social Fund. ESF investing in your future; the Ministerio de Ciencia e Innovación y Universidades (Juan de la Cierva, FJCI-2016-28811 to E.V.), and the Center for Biomedical Research on Rare Diseases (CIBERER to M.R.).

Sequencing and analysis of Patient 5 were performed by the Broad Institute of MIT and Harvard Center for Mendelian Genomics (Broad CMG) and were funded by the National Human Genome Research Institute, the National Eye Institute, the National Heart, Lung and Blood Institute grants UM1 HG008900 and R01 HG009141 and the Chan Zuckerberg Initiative to the Rare Genomes Project. This work was in part supported by the association 'Connaître les Syndromes Cérébelleux' (CSC). This research received funding specifically appointed to the Department of Medical Sciences from the Italian Ministry for Education, University and Research (Ministero dell'Istruzione, dell'università e della ricerca-MIUR) under the programme 'Dipartimenti di Eccellenza 2018-2022' Project code D15D18000410001. Whole-exome sequencing was performed as part of the Autism Sequencing Consortium and was supported by

the NIMH (MH111661). D.R.A. and A.P. are members of the Undiagnosed Disease Network International (UDNI).

Competing interests

The authors report no competing interests.

Supplementary material

[Supplementary material](#) is available at Brain online.

References

- Burke JE. Structural basis for regulation of phosphoinositide kinases and their involvement in human disease. *Mol Cell*. 2018; 71(5):653–673.
- Baskin JM, Wu X, Christiano R, et al. The leukodystrophy protein FAM126A (hyccin) regulates PtdIns(4)P synthesis at the plasma membrane. *Nat Cell Biol*. 2016;18(1):132–138.
- Lees JA, Zhang Y, Oh MS, et al. Architecture of the human PI4KIII α lipid kinase complex. *Proc Natl Acad Sci U S A*. 2017; 114(52):13720–13725.
- Ma H, Blake T, Chitnis A, Liu P, Balla T. Crucial role of phosphatidylinositol 4-kinase III α in development of zebrafish pectoral fin is linked to phosphoinositide 3-kinase and FGF signaling. *J Cell Sci*. 2009;122(Pt 23):4303–4310.
- Nakatsu F, Baskin JM, Chung J, et al. PtdIns4P synthesis by PI4KIII α at the plasma membrane and its impact on plasma membrane identity. *J Cell Biol*. 2012;199(6):1003–1016.
- Tan J, Oh K, Burgess J, Hipfner DR, Brill JA. PI4KIII α is required for cortical integrity and cell polarity during Drosophila oogenesis. *J Cell Sci*. 2014;127(Pt 5):954–966.
- Cutler NS, Heitman J, Cardenas ME. STT4 is an essential phosphatidylinositol 4-kinase that is a target of Wortmannin in *Saccharomyces cerevisiae*. *J Biol Chem*. 1997;272(44):27671–27677.
- Wolf NI, Ffrench-Constant C, van der Knaap MS. Hypomyelinating leukodystrophies - unravelling myelin biology. *Nat Rev Neurol*. 2021;17(2):88–103.
- Nellist M, Schot R, Hoogeveen-Westerveld M, et al. Germline activating AKT3 mutation associated with megalencephaly, polymicrogyria, epilepsy and hypoglycemia. *Mol Genet Metab*. 2015;114(3):467–473.
- Baulac S, Lenk GM, Dufresnois B, et al. Role of the phosphoinositide phosphatase FIG4 gene in familial epilepsy with polymicrogyria. *Neurology*. 2014;82(12):1068–1075.
- Rivière J-B, Mirzaa GM, O'Roak BJ, et al.; Finding of Rare Disease Genes (FORGE) Canada Consortium. De novo germline and postzygotic mutations in AKT3, PIK3R2 and PIK3CA cause a spectrum of related megalencephaly syndromes. *Nat Genet*. 2012;44(8):934–940.
- Poduri A, Evrony GD, Cai X, et al. Somatic activation of AKT3 causes hemispheric developmental brain malformations. *Neuron*. 2012;74(1):41–48.
- Alkhater RA, Scherer SW, Minassian BA, Walker S. PI4K2A deficiency in an intellectual disability, epilepsy, myoclonus, akathisia syndrome. *Ann Clin Transl Neurol*. 2018;5(12):1617–1621.
- Sobreira N, Schiettecatte F, Valle D, Hamosh A. GeneMatcher: A matching tool for connecting investigators with an interest in the same gene. *Hum Mutat*. 2015;36(10):928–930.
- Schiffmann R, Van Der Knaap MS. Invited Article: An MRI-based approach to the diagnosis of white matter disorders. *Neurology*. 2009;72(8):750–759.
- Traynor-Kaplan A, Kruse M, Dickson EJ, et al. Fatty-acyl chain profiles of cellular phosphoinositides. *Biochim Biophys Acta*. 2017;1862(5):513–522.

17. De La Cruz L, Traynor-Kaplan A, Vivas O, Hille B, Jensen JB. Plasma membrane processes are differentially regulated by type I phosphatidylinositol phosphate 5-kinases and RASSF4. *J Cell Sci.* 2020;133(2):jcs233254.
18. Karczewski KJ, Francioli LC, Tiao G, et al.; Genome Aggregation Database Consortium. The mutational constraint spectrum quantified from variation in 141,456 humans. *Nature.* 2020; 581(7809):434–443.
19. Casasnovas C, Verdura E, Vélez V, et al. A novel mutation in the GFAP gene expands the phenotype of Alexander disease. *J Med Genet.* 2019;56(12):846–849.
20. Elitt MS, Barbar L, Shick HE, et al. Suppression of proteolipid protein rescues Pelizaeus-Merzbacher disease. *Nature.* 2020; 585(7825):397–403.
21. Köhler W, Curiel J, Vanderver A. Adulthood leukodystrophies. *Nat Rev Neurol.* 2018;14(2):94–105.
22. van der Knaap MS, Schiffmann R, Mochel F, Wolf NI. Diagnosis, prognosis, and treatment of leukodystrophies. *Lancet Neurol.* 2019;18(10):962–972.
23. Kancheva D, Chamova T, Guergueltcheva V, et al. Mosaic dominant TUBB4A mutation in an inbred family with complicated hereditary spastic paraparesis. *Mov Disord.* 2015;30(6):854–858.
24. Di Bella D, Magri S, Benzoni C, et al. Hypomyelinating leukodystrophies in adults: Clinical and genetic features. *Eur J Neurol.* 2021;28(3):934–944.
25. Alvarez-Prats A, Bjelobaba I, Aldworth Z, et al. Schwann-cell-specific deletion of phosphatidylinositol 4-kinase alpha causes aberrant myelination. *Cell Rep.* 2018;23(10):2881–2890.
26. Biancheri R, Zara F, Rossi A, et al. Hypomyelination and congenital cataract: Broadening the clinical phenotype. *Arch Neurol.* 2011;68(9):1191–1194.
27. van Dijk T, Baas F, Barth PG, Poll-The BT. Poll-The BT. What's new in pontocerebellar hypoplasia? An update on genes and subtypes. *Orphanet J Rare Dis.* 2018;13(1):92.
28. Scheffer IE, Liao J. Deciphering the concepts behind "Epileptic encephalopathy" and "Developmental and epileptic encephalopathy". *Eur J Paediatr Neurol.* 2020;24:11–14.
29. Schiller S, Rosewich H, Grünwald S, Gärtner J. Inborn errors of metabolism leading to neuronal migration defects. *J Inherit Metab Dis.* 2020;43(1):145–155.
30. Juric-Sekhar G, Hevner RF. Malformations of cerebral cortex development: Molecules and mechanisms. *Annu Rev Pathol Mech Dis.* 2019;14:293–318.
31. Pagnamenta AT, Howard MF, Wisniewski E, et al. Germline recessive mutations in PI4KA are associated with perisylvian polymicrogyria, cerebellar hypoplasia and arthrogryposis. *Hum Mol Genet.* 2015;24(13):3732–3741.
32. Jardine S, Dhingani N, Muise AM. TTC7A: Steward of intestinal health. *Cell Mol Gastroenterol Hepatol.* 2019;7(3):555–570.
33. Chung J, Torta F, Masai K, et al. PI4P/phosphatidylserine countertransport at ORP5- and ORP8-mediated ER - Plasma membrane contacts. *Science.* 2015;349(6246):428–432.
34. Von Filseck JM, Čopić A, Delfosse V, et al. Phosphatidylserine transport by ORP/Osh proteins is driven by phosphatidylinositol 4-phosphate. *Science.* 2015;349(6246):432–436.
35. Sohn M, Ivanova P, Brown HA, et al. Lenz-Majewski mutations in PTDSS1 affect phosphatidylinositol 4-phosphate metabolism at ER-PM and ER-golgi junctions. *Proc Natl Acad Sci U S A.* 2016; 113(16):4314–4319.
36. Bartlett SE, Reynolds AJ, Weible M, Hendry IA. Phosphatidylinositol kinase enzymes regulate the retrograde axonal transport of NT-3 and NT-4 in sympathetic and sensory neurons. *J Neurosci Res.* 2002;68(2):169–175.
37. Lo Giudice T, Lombardi F, Santorelli FM, Kawarai T, Orlacchio A. Hereditary spastic paraparesis: Clinical-genetic characteristics and evolving molecular mechanisms. *Exp Neurol.* 2014;261: 518–539.
38. Edgar JM, McLaughlin M, Yool D, et al. Oligodendroglial modulation of fast axonal transport in a mouse model of hereditary spastic paraparesis. *J Cell Biol.* 2004;166(1):121–131.
39. Rickman OJ, Baple EL, Crosby AH. Lipid metabolic pathways converge in motor neuron degenerative diseases. *Brain.* 2019; 143(4):1073–1087.
40. Pant DC, Boespflug-Tanguy O, Pujol A, et al. Loss of the sphingolipid desaturase DEGS1 causes hypomyelinating leukodystrophy. *J Clin Invest.* 2019;129(3):1240–1256.
41. Jardine S, Anderson S, Babcock S, et al. Drug screen identifies leflunomide for treatment of inflammatory bowel disease caused by TTC7A deficiency. *Gastroenterol.* 2020;158(4): 1000–1015.
42. Wong M-T, Chen SS. Hepatitis C virus subverts human choline kinase- α to bridge phosphatidylinositol-4-kinase III β (PI4KIII β) and NS5A and upregulates PI4KIII β activation, thereby promoting the translocation of the ternary complex to the endoplasmic reticulum for viral replication. *J Virol.* 2017;91(16): e00355–17.

SUPPLEMENTARY MATERIAL

CASE REPORTS

Case 1

Patient 1 is a 6-year-old female who was born at term after an uneventful pregnancy. Her parents were not consanguineous, and she had a healthy sister and brother. She started having seizures in the neonatal period, and electroencephalogram (EEG) performed at 3.5 months showed multifocal acute waves over the central region of the right cerebral hemisphere in the midline and the right temporal regions. During the study, a total of 4 episodes of proximal stiffening of the limbs with a decrease in EEG activity were recorded. These episodes were highly suggestive of infantile spasms. Later, seizures appeared mainly in the context of infections, and they were myoclonic, focal and generalized with a tendency to evolve into status epilepticus. At 17 months of age, a slow background was the only notable EEG finding. The patient had repetitive respiratory infections, otitis and pneumonia. She had a severe neurodevelopmental delay, and physical exams at 9 months and 4 years of age showed horizontal nystagmus and severe spastic-dystonic tetraparesis with brisk deep tendon reflexes, bilateral ankle clonus and the Babinski sign. She also had choreiform movements and was unable to walk and communicate.

Magnetic resonance imaging (MRI) performed at 2 and 5 years of age showed diffuse severe hypomyelination with a thin corpus callosum, white matter atrophy with posterior predominance, colpocephaly and brainstem and cerebellum hypoplasia. Spectroscopy showed a decreased N-acetylaspartate peak. Visual evoked potentials (VEPs) were normal. The results of metabolic analysis of plasma, urine and cerebrospinal fluid (CSF) were normal except for a mild decrease in 5-hydroxyindoleacetic acid levels. Array-CGH data were also normal.

Case 2

Patient 2 is a 4-year-old male who was born by caesarean section at 32 weeks of gestation because of intrauterine growth restriction, oligohydramnios and maternal preeclampsia with HELLP (haemolysis, elevated liver enzyme levels, and low platelet levels) syndrome. His

parents were not consanguineous. His birth weight was 1260 gr, and his Apgar scores were 9/9/9. He had extreme neonatal hypotonia with feeding difficulties and bilateral cryptorchidism. He was diagnosed with neonatal anaemia that required transfusion of three red blood cell concentrates. He started having seizures during the second week of life, which occurred daily during the first 2 months despite several antiepileptic drug combinations. Afterwards, seizures usually appeared during febrile illness and could evolve into status epilepticus. The seizures involved facial congestion, tachycardia and upper limb and palpebral clonic movements. The patient was treated with levetiracetam, and clobazam was added during febrile episodes. He suffered recurrent bronchitis episodes and pneumococcal bacteremia at 2 years of age. Physical exam at 3 years of age showed acquired microcephaly (head circumference: 46.2 cm; -3.3 SD), failure to thrive, poor eye contact, pendular nystagmus, severe hypotonic tetraparesis with areflexia and a startle response to acoustic stimuli. Neurodevelopment was seriously delayed, with the patient exhibiting severe motor delay, no language acquisition and profound cognitive impairment.

Repeated EEG showed multifocal epileptic abnormalities with slowed background but were normal from ten months of age. A nerve conduction study performed at the age of 11 months showed axonal neuropathy. MRI at the age of 11 months showed severe diffuse hypomyelination with a thin corpus callosum, white matter atrophy and colpocephaly. The latencies of auditory evoked potentials (BAEPs) and VEPs were prolonged. The results of plasma and urine metabolic studies were all normal.

Case 3

Patient 3, a 13-year-old female, was born at 35 weeks and 5 days and had a birth weight of 2740 gr and a length of 44 cm. Her mother had been diagnosed with systemic lupus erythaematosus, had suffered a previous spontaneous miscarriage, and underwent treatment with acetylsalicylic acid during pregnancy. Delivery was normal (Apgar scores 10/10), but the patient developed transient neonatal hypocalcaemia. During the postnatal period, gastroesophageal reflux disease, as well as an atrial septal defect, was diagnosed. Axial hypotonia, bilateral nystagmus, and early episodes of eye deflection were noted. The patient often cried during the first months of life, and a developmental delay became apparent at 6 months. At that time, she presented with status epilepticus with repeated tonic seizures

following a febrile episode. Treatment with clonazepam, phenytoin, and valproic acid was started. Afterwards, she suffered seizures during infectious diseases. At 16 months of age, she developed truncal ataxia with slight spasticity and nystagmus, which became more evident in the lateral right gaze. At 23 months of age, cerebellar syndrome was evident. She began to stand up with support and to say some syllables. At 3 years of age, she presented acute neurological deterioration during a respiratory illness, with cerebellar worsening and choreo-dystonic movement. She had several episodes of acute otitis media and pneumonia, exhibited hypogammaglobulinemia with a low CD19+ B-cell count, and was administered immunoglobulin. On the most recent neurological examination at 7 years of age, she did not walk alone, spastic paraparesis with increased tone in the lower limbs and brisk reflexes in all four limbs was evident, and ataxia and dysmetria had slightly improved. She had a moderate intellectual disability and exhibited smiling behaviour. Growth was delayed, with the patient having a weight of 39 kg (-1 SD) and a height of 141 cm (-2.7 SD).

Initial MRI brain scan at 6 months of age showed signal alteration (T2W and FLAIR) in the posterior fossa and cerebellar calcifications. By age 3.5 years of age, MRI demonstrated diffuse hypomyelination with dysplastic, a thin corpus callosum and medulla, and progressive cerebellar atrophy with vermian predominance and calcifications. MRI spectroscopy pattern was normal. Karyotype analysis was normal. Extensive metabolic testing revealed no abnormalities. Muscle biopsy did not show any relevant findings. Mitochondrial respiratory chain enzyme levels were normal. The candidate genes *CCM1/2/3*, *COL4A1*, *COL4A2*, *MCP2*, *CDKL5*, *SCAI*, and *PDHA1* were sequenced without abnormal findings.

Case 4

Patient 4 is a 19-year-old female of French descent. She was born at 36 weeks after an unremarkable pregnancy. A severe developmental delay became evident very early, with the patient exhibiting little spontaneous movement and no communicative intent. She developed spastic paraparesis and suffered focal seizures with impaired awareness. On examination, there were no dysmorphic features. She had lateral gaze nystagmus, truncal ataxia, severe spasticity of the upper and lower limbs with brisk reflexes, bilateral Babinski signs and bilateral hand tremors. Currently, she is dependent on others for daily life activities, walks

with support, is capable of saying two words but unable to say a whole sentence. MRI showed diffuse hypomyelination with more conspicuous T2W and FLAIR periventricular hyperintensity, thinning of the corpus callosum and brainstem and cerebellar atrophy. Extensive metabolic and genetic test results were normal.

Case 5

Patient 5 is a 10-year-old fraternal twin male born at 35.5 weeks from an unrelated-donor egg. The prenatal period was uneventful. The neonatal period was notable for hypoglycemia, hypotonia, torticollis and jaundice. Poor head control and delayed milestones were observed in the first 6 months of age; oral feeding difficulties and emesis marked the first 18 months of age. The family history is significant for paternal 3rd cousin with Crohn's disease; father with loose joints, strabismus, hypotonia and generalized fatigue in early childhood period. Developmental milestones included the following: Rolling over at 9 months; sitting without support at 12 months; walking at 2 years, 9 months; and, speaking of first words at 24 months. Gait was abnormal due to generalized hypotonia, increased tone, and spasticity in bilateral lower extremities. Independent walking and running, both with a wide-based gait, required the use of supra malleolar orthotics. Gait gradually worsened over time. At 6 years of age, some left-leg dragging began. Stair ascention was possible using a side rail. Increasing spasticity prompted surgical intervention with bilateral selective percutaneous myofascial lengthening to both achilles tendons. Spasticity has continued to progress since that time. Currently, bilateral ankle-foot orthotics allow ambulation over short distances using a walker. Assistance is needed for bed to chair and sitting to standing transitions. No support is needed for toileting.

Physical exam at age of 5 revealed short palpebral fissures, an upturned nose, overfolded upper ear helix with ear asymmetry, keratosis pilaris, and ligamentous laxity. He had generalized hypotonia and lower extremity spasticity in his hips and ankles. He has a marked alternating hair color and texture pattern.

Clinical exam at 10 years of age revealed weight 26.8 kg, 15%ile, Z score -1.14, Height of 133.6 cm 24%ile, Z score - 0.71 and of BMI 15 kg/m² 17% Z score -0.97. The face is elongated with asymmetry, mid face hypoplasia, micrognathia, high arched palate, and overcrowded teeth. There is ear asymmetry with an overfolded upper ear helix. Neurological

exam revealed mild lateral asymmetry and lower extremities more affected than upper. Reflexes were brisk and complicated by bilateral hamstring contracture. Ophthalmological exam was normal. Speech evaluation revealed moderate to severe speech impairment related to low tone and diminished respiratory support for speech production in a co-articulatory manner. Audiological evaluation showed normal hearing sensitivity but abnormal brainstem auditory evoked response function; Neurodevelopmental evaluation revealed borderline intellectual functioning and impaired adaptive functioning. Functioning has decreased in the past three years, suggestive of progression.

Brain MRI showed progressive cerebral atrophy and delayed myelination that never reached completion. Patchy, diffuse T2 hyperintensities were noted bilaterally. Electroencephalography detected interictal epileptiform discharges in the right occipital and bilateral frontal regions. Repetitive nerve stimulation and needle electromyogram studies were normal and not indicative of a neuromuscular disorder. A radiographic skeletal survey detected osteopenia, which was confirmed by decreased bone mineral density on a DEXA scan. Extensive biochemical and mitochondrial studies in CSF, serum and urine were normal except for borderline-low decrease in CSF serine (normal in plasma and urine). The CSF neuropteran level was normal.

Other medical history includes constipation, epistaxis and three episodes of impetigo, and at 9 years and 8 months, a diagnosis of juvenile idiopathic arthritis was made. Given the normal platelet count and history of epistaxis, a platelet electron transmission microscopy study was performed and showed normal numbers of dense granules.

Case 6

Patient 6 is a 6-year-old boy born to Vietnamese and Caucasian parents. He was delivered at term by caesarean section due to breech presentation after an unremarkable pregnancy and had a birth weight of 2.63 kg (-1.2 SD). Congenital axial hypotonia was evident from birth. He had feeding difficulties and required a nasogastric tube for the first 6 weeks of life. Dysmorphic features were present, such as bilateral epicanthal folds, long palpebral fissures, a wide nose with antverted nares, a wide mouth, small widely spaced teeth, thin fingers, and a single palmar crease on the right hand. He was diagnosed with mild bilateral sensorineural

hearing loss. Bilateral cryptorchidism and minor cardiac and renal malformations were also present. Ophthalmological examination revealed bilateral iris and retinal coloboma and myopia. He had seizures 2 hours after birth that were unresponsive to treatment with phenobarbital and levetiracetam but relapsed after the first month of life when topiramate was added. He has not had any subsequent seizures. Anticonvulsant drugs were successfully withdrawn at 18 months of age, and he remained seizure-free. He had postnatal growth failure, and his development was severely delayed; he sat at 17 months of age and walked at 4.5 years of age, exhibiting a wide-based unsteady gait and frequent falls. He was diagnosed with a language disorder and did not learn to speak. He had a severe intellectual disability with no behavioural abnormalities except for hand flapping when excited. At the most recent examination at 6 years, he weighed 15.8 kg (-2.3 SD), was 105.8 cm tall (-2 SD), and had a head circumference of 47 cm (-2 to -3 SD). He had axial hypotonia and spastic tetraparesis with brisk reflexes and bilateral ankle clonus.

Initial brain MRI showed delayed myelination, although on his last MRI at 3 years of age, myelination was normal. This last study revealed a dysplastic corpus callosum and mild brainstem and cerebellar atrophy.

Case 7

Patient 7 is an 11-year-old girl, the only child of unrelated parents with unremarkable familiar history. She was born by caesarean section because of maternal hypertension at 37 weeks and 4 days after an uneventful pregnancy, and ultrasound and prenatal screening tests were normal. At birth, she had a weight of 3590 gr (1.7 SD), a length of 51 cm (1.48 SD), a head circumference of 36.5 cm (1.8 SD), and Apgar scores 9/10. She exhibited regular sleep with few nocturnal awakenings; otherwise, the neonatal period was normal. At 3 months, she started having episodes of redness of her face, fixed eyes, breathing cessation, hypertonia of the arms and legs, and unconsciousness for 30 seconds. Epilepsy was reasonably excluded by normal EEG. She was diagnosed with gastroesophageal reflux with a partial treatment response. Polysomnography showed hypoxemic events during sleep. Neurodevelopment was normal for the first months, and she sat at 7 months of age. A global delay became evident after that; she did not start to walk before 28 months of age, said her first words after three years of age, has difficulties with relationships, exhibits discontinuous eye contact and

requires speech therapy and physiotherapy support. At the most recent examination at 11 years of age, she presented stereotypic movement of the mouth, tongue and hands (opening-closing) and head (lateral rotation with lateral deviation of the gaze) and bruxism. Physical examination revealed plagiocephaly, a squared face, a high forehead, hypertelorism, epicanthal folds, a thin upper lip, a wide nasal root and anteverted nostrils with incisurae alae nasi. Microcephaly became evident, with the patient presenting a head circumference of 52.3 cm (-1.9 SD), weight of 40 kg (-0.44 SD) and length of 148 cm (-0.67 SD). Ophthalmological evaluation indicated ocular dyspraxia and strabismus. She presented axial hypotonia with spastic paraparesis, brisk deep tendon reflexes and bilateral Babinski signs. Currently, she is able to move a spoon to her mouth but she is not able to fill it. She is using a tablet with pictures for alternative communication. She has not achieved urinary or faecal continence.

Brain MRI at 12 months of age showed external hydrocephalus with remission in successive controls. MRI at 2 years of age showed hyperintensity of the white matter in the temporal and posterior regions and mild cerebellar atrophy (predominantly in the inferior lobe). PEVs revealed a slowing of the conduction. The candidate genes *FGFR2*, *FGFR3*, *TWIST*, *MECP2*, *CDKL5*, *FOXP1* and *MEF2C* were sequenced by Sanger sequencing with normal results.

Case 8

Patient 8 is a 5-year-old male patient who was born at 36 weeks of gestational age after an uneventful pregnancy. His birth weight was 2860 gr. His parents were first-degree cousins of Turkish origin. The mother reported one previous ectopic pregnancy and one previous abortion due to unspecified causes. A neurodevelopmental delay was evident since the first months, and he had severe neonatal hypotonia with suction problems in the first days of life, requiring a nasogastric tube for feeding. Bilateral cryptorchidism was noted. He started having seizures in the first week of life, and initial EEG showed symmetric delta theta activity with bilateral frontal focus. He had spontaneous cramping with disorganized motor skills. Ocular tracking and fixation were deficient. There was no grip and no hand-eye coordination.

At the age of 4 years, he is a watchful child who does not engage with gaze. He has predominantly axial hypotonus with appendicular spasticity mainly in the right limbs, and he does not maintain control of his head. Normal and symmetrical osteotendinous reflexes are

present. EEG at the age of 12 months showed poorly differentiated diffuse and symmetrical theta activity and unrecognizable background rhythm. He received levetiracetam and phenobarbital, and after the addition of clobazam at the age of 3 years, seizures stopped, but EEG continued exhibiting a 5 Hz background rhythm mixed with theta dysrhythmic activity and recurring spikes and spike-wave spread without physiological elements during sleep, during which spike-wave figures became more frequent with left predominance. The results of metabolic analysis of plasma, urine and cerebrospinal fluid were normal. MRI performed at 1 month of age showed bilateral perisylvian polymicrogyria. Metabolic studies performed in plasma, urine and cerebrospinal fluid (CSF) were normal

He was admitted several times due to non-hemolytic anaemia, requiring RBC transfusions. Recurrent vomiting and gastroesophageal reflux ended in hypovolemic shock requiring admission, and at two years of age, percutaneous endoscopic gastrostomy was performed. He had recurrent respiratory infections.

Case 9

Patient 9, a 42-year-old man, was born to nonconsanguineous parents of Spanish descent. He was born at term after an unremarkable pregnancy and delivery. He has two older healthy siblings. While his development was considered normal during childhood, he was always considered a clumsy boy who fell frequently. At the age of 17 years, he started to experience difficulties walking. He complained of weakness and stiffness of the lower limbs that worsened over the years and urinary urge, with no other neurological findings. Spastic paraparesis became evident, and he was widely studied. Brain MRI at age 35 showed an arachnoid cyst of the posterior fossa with a mild mass effect on both cerebellar hemispheres and cervical spinal cord atrophy, which was otherwise normal. Visual evoked potentials were compatible with central bilateral involvement, and auditory evoked potentials showed long latencies, indicating bilateral conduction involvement. At age 21, he was diagnosed with ileocolonic Crohn's disease with a stenosing-inflammatory pattern and a steroid-dependent course. He underwent treatment with azathioprine, which was discontinued due to digestive intolerance. At age 27, mercaptopurine was started, and clinical and biological remission of the disease was achieved. Staged biopsies of the colon described fragments of the colonic

mucosa with moderate inflammatory infiltrate and the presence of eosinophils in the lamina propria.

On the most recent neurological examination at 40 years of age, he had lateral gaze exhaustible nystagmus. Strength of the lower limbs (MRC: 3/5) was moderately decreased, and strength of the upper limbs was normal except for the bilateral *first interosseous*, *abductor pollicis brevis*, and *abductor digiti minimi* muscles, which were slightly weak (MRC: 4/5). The tone was increased, and deep tendon reflexes were globally brisk in all four limbs, with bilateral Hoffman's sign, clonus, and bilateral extensor plantar responses. He had distal hypopallesthesia in the lower limbs and decreased pin-prick sensation in his feet. He has a paraparetic gait and needs crutches to walk. He worked as a carpenter until 27 years of age, after which he received a disability grant. He has two healthy daughters aged 3 and 12.

Case 10

Patient 10, an 18-year-old male adolescent, is the descendant of nonconsanguineous Latin American parents. Her mother had two older boys from a prior marriage. He was born at term after an unremarkable pregnancy. His development was considered normal during the first year, and he started to walk at 15 months of age, but his parents worried about frequent falls and a tiptoe gait and visited a neuro-paediatrician, who made the diagnosis of spastic paraparesis at 2 years of age. He received treatment with carbidopa/levodopa with no response and botulinum toxin with slight improvement. At 17 years of age, physical exploration showed mild progression of spasticity, with lower limb hypertonia, hyperreflexia, and bilateral ankle clonus. The upper limbs had normal tone but brisk reflexes. He had bilateral cavus feet and contractures of the hips, knees, and ankles. He has mild cognitive impairment and performs poorly in school, lagging behind his peers. Cranial MRI was normal apart from atrophy of the cervical spinal cord. The results of karyotype analysis and metabolic tests were normal.

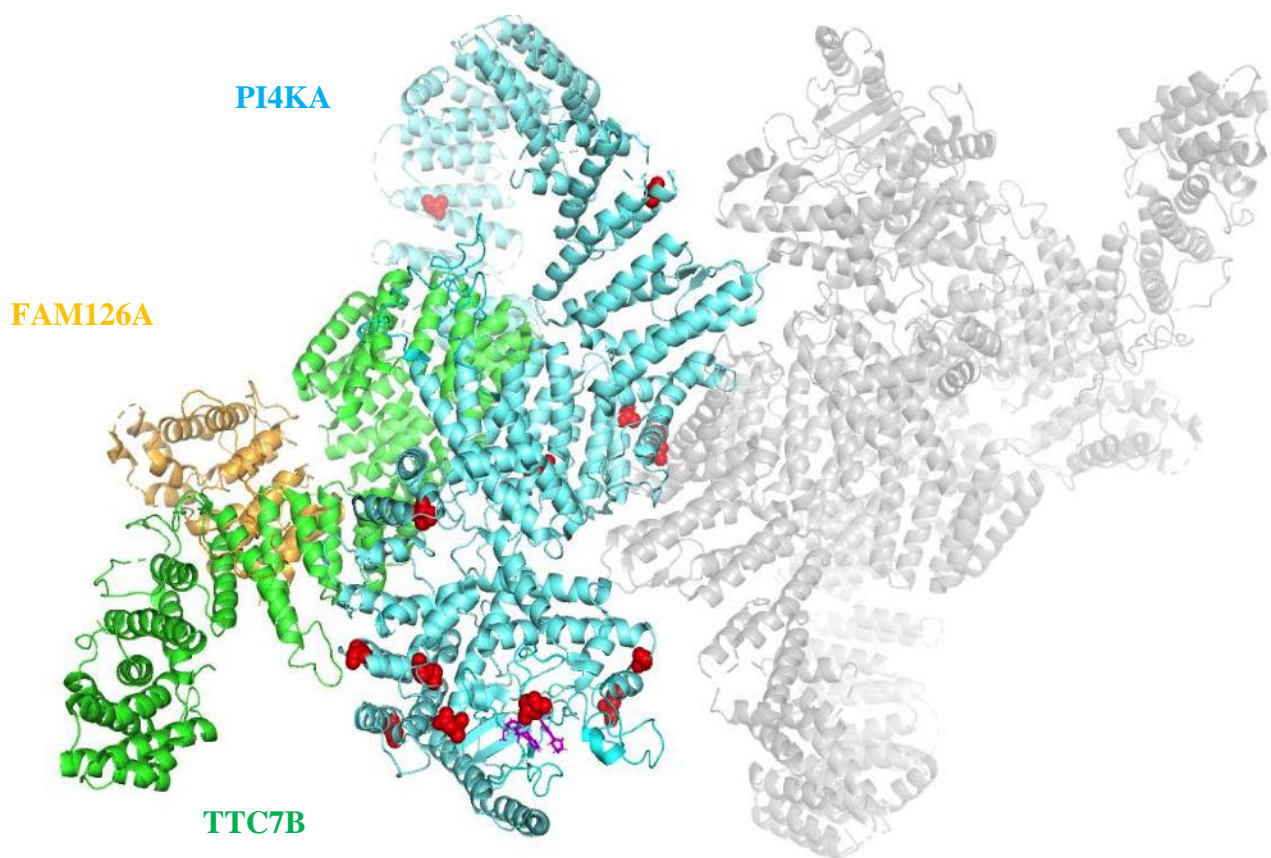
<u>Patient</u>	<u>Genomic position (hg19)</u>	<u>cDNA change (NM_058004)</u>	<u>Protein (NP_477352)</u> change	<u>Frequency in gnomAD v2.1.1 (#/total alleles)</u>	<u>Frequency in gnomAD v3 (#/total alleles)</u>	<u>PolyPhen-2 (score)</u>	<u>M-CAP (score)</u>	<u>Mutation Taster</u>	<u>LRT Pred</u>	<u>GERP (score)</u>	<u>CADD Score (Phred value)</u>
P7	chr22:21188862 G>A	c.355 C>T (exon 3)	p.(Arg119Trp)	2.39e-5 (6/251348)	0 (no carriers)	Probably Damaging (0.997)	D (0.044)	D	NA	1.67	23.7
P7	chr22:21158635 T>G	c.1414 A>C (exon 12)	p.(Ser472Arg)	3.98e-6 (1/251456)	0 (no carriers)	Possibly Damaging (0.899)	T (0.020)	D	D	5.08	23.0
P5	chr22:21155333 G>A	c.1852 C>T (exon 16)	p.(Arg618Ter)	1.01e-4 (22/218722)	7.68e-5 (11/143266)	NA	NA	A	D	4.55	39
P1	chr22:21119189 dupG	c.2624dupC (exon 22)	p.(Pro876Ser fsTer36)	3.99e-6 (1/250576)	0 (no carriers)	NA	NA	NA	NA	NA	32
P1	chr22:21098918 C>T	c.3454 G>A (exon 30)	p.(Glu1152Lys)	3.98e-6 (1/251262)	6.98e-6 (1/143346)	Probably Damaging (0.988)	D (0.064)	D	D	5.84	32
P4	chr22:21096917 C>T	c.3592 G>A (exon 31)	p.(Ala1198Thr)	0 (no carriers)	0 (no carriers)	Possibly Damaging (1.0)	D (0.087)	D	D	5.87	28.4
P3	chr22:21088699 T>C	c.3884 A>G (exon 33)	p.(His1295Arg)	0 (no carriers)	0 (no carriers)	Probably Damaging (1.0)	D (0.473)	D	D	5.17	25.7
P10	chr22:21083617 C>T	c.4666 G>A (exon 39)	p.(Val1556Met)	1.61e-4 (45/280184)	1.26e-4 (18/143320)	Possibly Damaging (0.743)	D (0.030)	D	D	5.15	23.7
P5	chr22:21080781 C>T	c.4990 G>A (exon 42)	p.(Asp1664Asn)	0 (no carriers)	0 (no carriers)	Possibly Damaging (1.0)	D (0.459)	D	D	4.88	32
P6	chr22:21075585 C>T	c.5116+1G>A (intron 43)	NA	0 (no carriers)	0 (no carriers)	NA	NA	D	NA	5.12	34
P10	chr22:21073068 G>A	c.5159 C>T (exon 44)	p.(Thr1720Ile)	0 (no carriers)	0 (no carriers)	Benign (0.001)	D (0.045)	D	D	4.9	22.2
P9	chr22:21068746_21068748delCTT	c.5459_5461delAAG (exon 47)	p.(Glu1820del)	0 (no carriers)	6.98e-6 (1/143164)	NA	NA	NA	NA	NA	NA

P8	chr22:21067580C>T	c.5560G>A (exon 48)	p.(Asp1854Asn) (4/209116)	1.91e-5 (1/ 152230)	6.57e-6 (1/ 152230)	Probably Damaging (1.0)	D (0.529)	D	D	4.69	32
P2	chr22:21066803 C>G	c.5773 G>C (exon 50)	p.(Gly1925Arg) (1/229730)	4.35e-6 (1/229730)	6.98e-6 (1/143174)	Probably Damaging (1.0)	D (0.679)	D	D	4.49	28.3
P6	chr22:21065110 T>C	c.5960 A>G (exon 52)	p.(Asn1987Ser) (17/250476)	6.79e-5 (17/250476)	0 (no carriers)	Probably Damaging (0.999)	D (0.062)	D	D	5.01	24.1
P3	chr22:21064247 A>G	c.6122 T>C (exon 53)	p.(Met2041 Thr) (no carriers)	0 (no carriers)	0 (no carriers)	Probably Damaging (1.0)	D (0.732)	D	D	5.26	27.2
P4, P9	chr22:21064210_21064213delTGTC	c.6156_6159del GACA (exon 53)	p.(Thi2053Ser fsTer4) (no carriers)	0 (no carriers)	0 (no carriers)	NA	NA	NA	NA	NA	NA

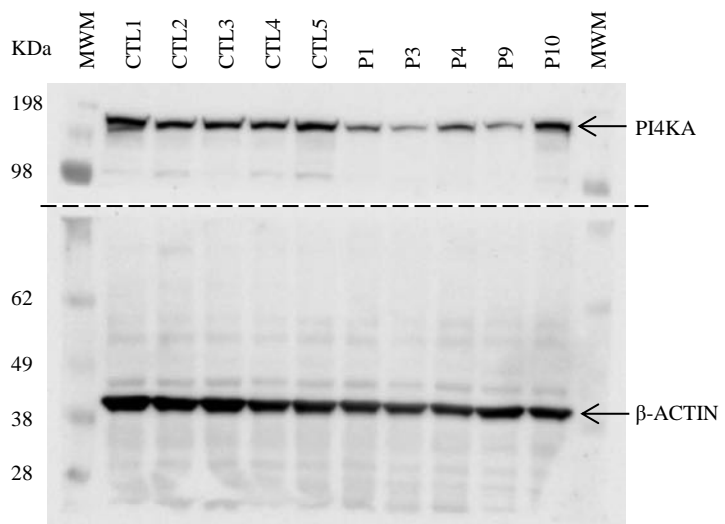
Supplemental Table 1: Features of PI4KA variants found in patients. NA: not assessed. Grey: Deleterious predictions.

	p.Arg119Trp	p.Ser472Arg	p.Glu1152Lys
MUT	EESTA W KGRGA	QSKTS R KVIIIA	NRYAGE E VYGM
H sapiens	EESTA R KGRGA	QSKT S KVIIIA	NRYAGE E VYGM
P troglodytes	EESTA R KGRGA	QSKT S KVIIIA	NRYAGE E VYGM
M musculus	EESTA R KGRGN	QSKT S KVIIIA	NRYAGE E VHGM
G gallus	EESSARKGRGL	QSKT S KVIIIA	NRYAGE E VSGM
X tropicalis	EESNSRKGKGT	QSKT S KVIIIA	NRYAGE E VAGM
D rerio	EESSE R KGREA	QSKT S KVIIIA	NRYAGE E VAGM
	 p.Ala1198Thr	 p.His1295Arg	 p.Val1556Met
MUT	MFKLT T MLIIS	PEVTP R YIWID	SPYLA M QLPAR
H sapiens	MFKLT A MLIIS	PEVTP H YIWID	SPYLA A QLPAR
P troglodytes	MFKLT A MLIIS	PEVTP H YIWID	SPYLA A QLPAR
M musculus	MFKLT A MLIIS	PEVTP H YIWID	SPYLA A QLPAR
G gallus	MFKLT A LALLIIS	PEVTP H YIWIE	SPHLA V QLPTR
X tropicalis	MFKLT A LALLIIS	PQVNPH H YIWID	SPHLA L QLPTR
D rerio	LFKMA A LLIIS	PDVT H YIWIE	APYLAL L QLPAR
	 p.Asp1664Asn	 p.Thr1720Ile	 p.Glu1820del
MUT	QALRY N KMGYV	LVEEI I GSLSG	SELEK - GLRCR
H sapiens	QALRY D KMGYV	LVEEI I GSLSG	SELEKE - GLRCR
P troglodytes	QALRY D KMGYV	LVEEI T SSLSG	SELEKE - GLRCR
M musculus	QALRY D KMGYV	LVEEI T GSLSG	SELEKE - GLQCR
G gallus	QALRY D KMGYV	LVEEI T GSLSG	SELEKE - GLRCR
X tropicalis	QALRY D KMGYV	LVEEI T GSLSG	SELEKE - GLSCR
D rerio	QALRY D KMGYV	MVEEI T HSLSG	SELEKE - GLRCP
	 p.Asp1854Asn	 p.Gly1925Arg	 p.Asn1987Ser
MUT	FKVGDNCRQDM	FTRQY R DESTL	SSPGGS S LGWEP
H sapiens	FKVGDDCRQDM	FTRQY G DESTL	SSPGGN N LGWEP
P troglodytes	FKVGDDCRQDM	FTRQY G DESTL	SSPGGN N LGWEP
M musculus	FKVGDDCRQDM	FTRQY G DESTL	SSPGGN N LGWEP
G gallus	FKVGDDCRQDM	FTRQY G DESTL	SSPGGN N LGWEP
X tropicalis	FKVGDDCRQDM	FTRQY G DESAL	SSPGGN N LGWEP
D rerio	FKVGDDCRQDM	FRNQY G DESTL	SSPGGN N LGWEP
	 p.Met2041Thr		
MUT	SLVTL T LDTGL		
H sapiens	SLVTL M LDTGL		
P troglodytes	SLVTL M LDTGL		
M musculus	SLVTL M LDTGL		
G gallus	SLVTL M LDTGL		
X tropicalis	SLVTL M LDTGL		
D rerio	SLVTL M LDTGL		

Supplemental Figure 1: Amino acid sequence alignments of PI4KApotein across several species.



Supplemental Figure 2: 3D representation of the PI4KA/TTC7B/FAM126A dimer.
Blue: PI4KA; green: TTC7B; orange: FAM126A; grey: opposite PI4KA/TTC7B/FAM126A heterocomplex; Pink: A1, PI4KA inhibitor occupying ATP binding space in the catalytic domain. Red balls represent missense/in-frame variants found in our cohort.



Supplemental Figure 3: Unmodified full-length blot used to make the images in Figure 3. Patients' fibroblasts (n=5) and controls (CTL, n=5). MWM, Molecular Weight Marker. The following antibodies were used; anti-PI4KA (12411-1-AP Proteintech) for human cells as validated in www.antibodypedia.com (AB_2268237) and anti- β -ACTIN (A2228, Sigma).

Article 3. *DLG4-related synaptopathy: a new rare brain disorder*

Rodríguez-Palmero A, Boerrigter MM, Gómez-Andrés D, Aldinger KA, Marcos-Alcalde I, Popp B, Everman DB, Lovgren AK, Arpin S, Bahrambeigi V, Beunders G, Bisgaard AM, Bjerregaard VA, Bruel AL, Challman TD, Cogné B, Coubes C, de Man SA, Denommé-Pichon AS, Dye TJ, Elmslie F, Feuk L, García-Miñaúr S, Gertler T, Giorgio E, Gruchy N, Haack TB, Haldeman-Englert CR, Haukanes BI, Hoyer J, Hurst ACE, Isidor B, Soller MJ, Kushary S, Kvarnung M, Landau YE, Leppig KA, Lindstrand A, Kleinendorst L, MacKenzie A, Mandrile G, Mendelsohn BA, Moghadasi S, Morton JE, Moutton S, Müller AJ, O'Leary M, Pacio-Míguez M, Palomares-Bralo M, Parikh S, Pfundt R, Pode-Shakked B, Rauch A, Repnikova E, Revah-Politi A, Ross MJ, Ruivenkamp CAL, Sarrazin E, Savatt JM, Schlüter A, Schönewolf-Greulich B, Shad Z, Shaw-Smith C, Shieh JT, Shohat M, Spranger S, Thiese H, Mau-Them FT, van Bon B, van de Burgt I, van de Laar IMBH, van Drie E, van Haelst MM, van Ravenswaaij-Arts CM, Verdura E, Vitobello A, Waldmüller S, Whiting S, Zweier C, Prada CE, de Vries BBA, Dobyns WB, Reiter SF, Gómez-Puertas P, Pujol A, Tümer Z.

Revista: *Genetics in Medicine* 2021 May;23(5):888-899. doi: 10.1038/s41436-020-01075-9

Factor d'impacte (quartil per especialitat): 8.90 (Q1)

Participació del doctorand: el doctorand ha participat en el disseny conceptual de l'estudi, ha revisat la informació clínica de tots els pacients inclosos i ha contactat amb els metges referents dels pacients. Ha escrit el manuscrit i ha participat en el disseny de les figures i taules. Aquest treball no es preveu que s'utilitzi en cap més tesi doctoral.

Resum de l'article 3

Introducció

- Revisió de dades fenotípiques i genotípiques de 53 pacients amb variants genètiques en heterozigosi en *DLG4*, que codifica per la proteïna postsinàptica PSD-95. Els pacients es van recollir a través de la revisió de la literatura i a través de les bases de dades GeneMatcher (Sobreira *et al.*, 2015) i Decipher (Firth *et al.*, 2009).
- Prèviament, s'havien reportat només 11 pacients amb variants en *DLG4* en heterozigosi, en diferents estudis. En un d'ells, se suggeria que l'hàbit marfanoid podia ser característic d'aquesta entitat.

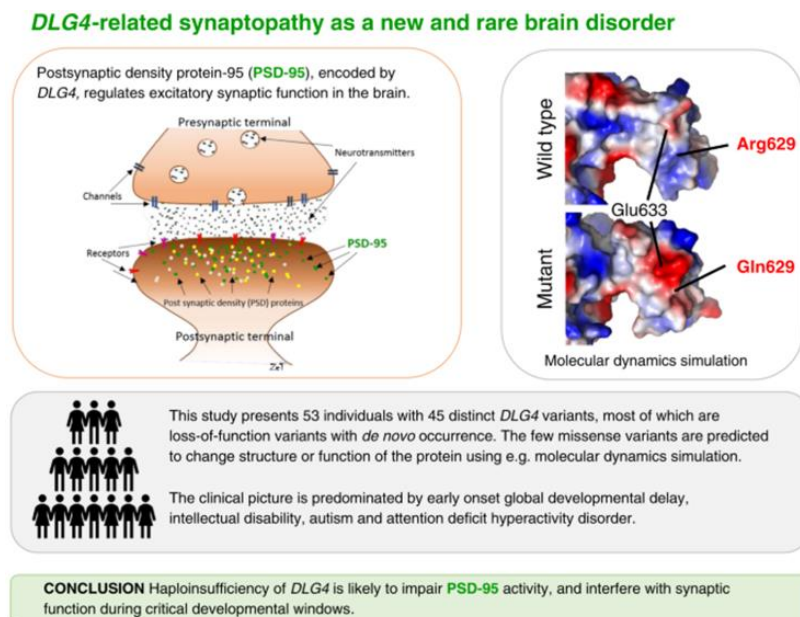
Resultats

- Descripció del fenotip clínic dels pacients, la majoria dels quals presentaven un retard global del desenvolupament, evident ja en els primers dos anys de vida, amb evolució a una discapacitat intel·lectual en el 98% dels casos. Un 57% mostrava simptomatologia de trastorn per déficit d'atenció amb hiperactivitat (TDAH), un 56% d'ells un trastorn de l'espectre autista (TEA) i un 53% epilepsia (tres casos en forma d'espasmes infantils i tres casos associada a una síndrome punta-ona contínua del son (POCS)). En un 39% dels pacients s'havia reportat una regressió en el seu desenvolupament.
- Altres manifestacions observades foren: trastorns del moviment (46%), manifestacions oftalmològiques (50%), hipotonía (53%), trets dismòrfics (38%; sense poder-se identificar un patró característic del trastorn). L'hàbit marfanoide estava present en només un 23% dels casos.
- Un dels pacients presentava espasticitat d'extremitats inferiors, dos retard de la mielinització i dos més, una hiperintensitat de la substància blanca periventricular.
- La majoria de variants genètiques eren de pèrdua de funció, mentre que només sis d'elles eren de canvi de sentit, localitzades en els dominis funcionals de la proteïna. Mitjançant modelització 3D, es va aportar evidència que aquestes variants de canvi de sentit provocaven canvis estructurals o funcionals de la proteïna resultant.

Conclusions

- La sinaptopatia *DLG4* es caracteritza per un retard del desenvolupament-discapacitat intel·lectual, trets autístics, un trastorn per déficit d'atenció amb hiperactivitat (TDAH), epilepsia o trastorns del moviment. L'hàbit marfanoide, que havia estat suggerit com característic d'aquest trastorn, està present en una petita proporció de pacients.
- Alguns pacients poden associar una afectació piramidal i presentar-se com una paraparèisia espàstica predominant. En altres hem identificat una afectació de la substància blanca cerebral, amb atròfia, retard de la mielinització o hiperintensitats periventriculars. Això posa en evidència com l'activitat neuronal i sinàptica regula la producció de la mielina i el seu manteniment.

Resum gràfic de l'article



NOTA: la taula completa que recull la informació detallada del fenotip dels pacients no està inclosa en aquesta tesi doctoral. Pot consultar-se en el següent enllaç: <https://www.nature.com/articles/s41436-020-01075-9#Sec12>

**ARTICLE**

DLG4-related synaptopathy: a new rare brain disorder

Agustí Rodríguez-Palmero et al.[#]

PURPOSE: Postsynaptic density protein-95 (PSD-95), encoded by *DLG4*, regulates excitatory synaptic function in the brain. Here we present the clinical and genetic features of 53 patients (42 previously unpublished) with *DLG4* variants.

METHODS: The clinical and genetic information were collected through GeneMatcher collaboration. All the individuals were investigated by local clinicians and the gene variants were identified by clinical exome/genome sequencing.

RESULTS: The clinical picture was predominated by early onset global developmental delay, intellectual disability, autism spectrum disorder, and attention deficit–hyperactivity disorder, all of which point to a brain disorder. Marfanoid habitus, which was previously suggested to be a characteristic feature of *DLG4*-related phenotypes, was found in only nine individuals and despite some overlapping features, a distinct facial dysmorphism could not be established. Of the 45 different *DLG4* variants, 39 were predicted to lead to loss of protein function and the majority occurred de novo (four with unknown origin). The six missense variants identified were suggested to lead to structural or functional changes by protein modeling studies.

CONCLUSION: The present study shows that clinical manifestations associated with *DLG4* overlap with those found in other neurodevelopmental disorders of synaptic dysfunction; thus, we designate this group of disorders as *DLG4*-related synaptopathy.

Genetics in Medicine (2021) 23:888–899; <https://doi.org/10.1038/s41436-020-01075-9>

INTRODUCTION

The human brain is formed by about 100 billion neurons that are highly interconnected through synapses, which regulate the brain circuit functions. The molecular structure of the synapse is highly complex, and its function is regulated by several proteins at different levels. In excitatory synapses, the postsynaptic submembrane space contains a multiprotein complex called the postsynaptic density (PSD), which has crucial roles in the structural organization and function of the synapses. It contains several scaffold proteins including PSD-95, encoded by *DLG4* (discs large MAGUK scaffold protein 4). PSD-95 belongs to the MAGUK (membrane-associated guanylate kinases) family and has 3 PDZ domains at the N-terminus, an SH3 (Src homology 3) domain and a guanylate kinase-like domain (GKLD). PSD-95 participates in synaptic maturation and dendritic morphology and regulates function of the glutamate receptors NMDA (N-methyl-D-aspartic acid) and AMPA (α -amino-3-hydroxy-5-methyl-4-isoxazolepropionic acid).¹ PSD-95 is also involved in the structural organization of the PSD through the interaction and stabilization of adhesion molecules, such as NLG1 (neuroigin 1); the voltage-gated, Shaker-type K⁺ (K_V1) channels are also key binding partners of PSD-95.¹ Notably, the PSD is a very dynamic structure and its composition (i.e., PSD-95 expression) and morphology are dependent on neuronal activity, which determines synaptic plasticity, essential for learning and memory processes.¹

DLG4 (encoding PSD-95) has three other paralogs (*DLG1* encoding SAP97; *DLG2* encoding PSD-93/Chapsyn-110; and *DLG3* encoding SAP-102), all of which are evolutionarily conserved and have diverse functions.² Homozygous *Dlg1* knockout mice (*Dlg1*^{-/-}) are embryonic lethal while the knockouts of other paralogs are viable. *Dlg3*^{-/-} animals do not show observable cognitive deficits, but in humans, truncating *DLG3* variants have been identified in individuals with X-linked intellectual disability with or without comorbidities (OMIM 300850).^{3,4} On the other hand, *Dlg2*^{-/-} mice show impairments in cognitive flexibility, learning, and attention²

and *DLG2* missense variants are associated with autism,⁵ and gross *DLG2* deletions are described in individuals with schizophrenia, autism, and bipolar disorder.^{6,7} The *Dlg4*^{-/-} mice show increased repetitive behaviors, abnormal communication, impaired motor coordination, increased stress reactivity, anxiety-related responses, and abnormal learning and working memory.^{2,8,9} On the other hand, male *Dlg4*^{+/+} mice present with hypersocial behavior with increased aggression and territoriality levels, while female mice show increased vocalization, and both genders show hypoactivity without motor deficits.¹⁰

In humans, pathogenic *DLG4* variants are rare, and to date only 11 individuals with a *DLG4* variant have been reported. Eight of these published individuals were identified as part of screening cohorts to find new candidate genes for ID ($n = 4$), cerebral visual impairment ($n = 1$), developmental disorders ($n = 1$), and schizophrenia and autism spectrum disorders ($n = 2$).^{11–15} The remaining three individuals were identified by Moutton et al. in a series of 64 individuals with ID and skeletal signs suggestive of Marfan syndrome (OMIM 154700) but do not meet the international criteria, termed Marfanoid habitus (MH).¹⁶

Here we report phenotype and genotype information on 53 individuals (including the 11 previously published cases, clinical features of whom are updated when possible) with heterozygous *DLG4* variants collected through an international collaboration. The effect of the missense variants on protein function was further investigated through structural modeling and molecular dynamics simulation studies. Our results establish *DLG4*-related synaptopathy as a new and rare brain disorder.

MATERIALS AND METHODS**Individuals included in this study**

We ascertained the genotype and phenotype information for 53 individuals with a variant in *DLG4* (Fig. 1, Table 1, Figs. S1, S2, Tables S1, S2). Eleven individuals were reported previously.^{11–17} Phenotypes of four of

[#]A full list of authors and their affiliations appears at the end of the paper.

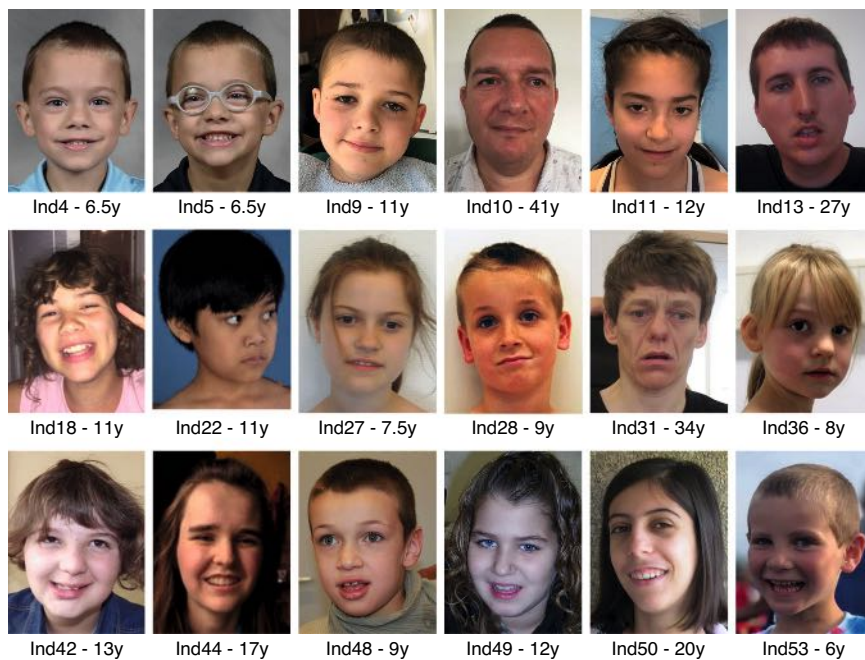


Fig. 1 Facial features of the individuals. Individuals 4 and 5 are twins, and individuals, 49 and 50 have the same *DLG4* variant. Ind individual.

these individuals have been updated, while further clinical information could not be obtained for seven individuals. The previously unreported individuals were identified through GeneMatcher (<http://genematcher.org/statistics/>)¹⁸ or the Database of Chromosomal Imbalance and Phenotype in Humans Using Ensembl Resources (DECIPHER, <https://decipher.sanger.ac.uk>).¹⁹ The clinical information of each individual was reviewed including neurodevelopment, growth parameters, neurological manifestations, behavior, dysmorphology, and MH by the local clinicians (Tables 1 and S1). The prevalence of each clinical manifestation related to the total number of cases for whom this information was available is shown in Table S2. The presence of ID was evaluated in individuals over 5 years old and ASD in those over 3 years old. Regression was defined as a loss of previously acquired skills. Statistical calculations were made using Pearson chi-squared test with Yates continuity correction. A heat map for clinical features was built by means of gplots package in R and hierarchical clustering was made according to binary distances (Fig. 2S).

Identification and evaluation of the variants

DLG4 variants were identified in the probands using massively parallel sequencing (next-generation sequencing; NGS) based technologies (exome/genome sequencing with or without employing virtual gene panels) in clinical diagnostic or research settings, and parental testing for the identified variant was performed when possible ($n = 48$). Pathogenicity of the identified *DLG4* variants was established according to American College of Medical Genetics and Genomics/Association for Molecular Pathology (ACMG/AMP) criteria (Table S3).^{20,21} The Genome Aggregation Database (gnomAD v.2.1.1; <https://gnomad.broadinstitute.org/>) was employed to check the presence of the variants in control populations. NMDEscPredictor tool²² (<https://nmdprediction.shinyapps.io/nmdescpredictor/>) was employed to predict whether the truncating variants escaped nonsense-mediated decay (NMD). SpliceAI²³ (<https://github.com/Illumina/SpliceAI>) a deep learning-based splice variant prediction tool was used to annotate the variants for their predict effect on splicing (Table S3). All the variants are described using the NM_001365.4 (GRCh37/hg19) transcript of *DLG4* (Fig. 2, Tables 2 and S3).

Structural modeling and molecular dynamics simulation of the missense variants

The 3D structure of the human PSD-95 protein (UniProtKB id: P78352–2, The UniProt Consortium 2019) was modeled using as templates the homologous structures present in the Protein Data Bank: 1KJW²⁴ and 2XKX²⁵ (Fig. 3). Models for the wild type protein and the Gly220Val, Asp229Val, Gly241Ser, Asp375Gly, Arg629Gln and Thr654Ile variants were

built using the SWISS-MODEL server (<https://swissmodel.expasy.org>), and their structural quality was within the range of that accepted for homology-based structure (Anolea/Gromos/QMEAN4).²⁶ Molecular dynamics simulation was carried out as described previously²⁷ and the details can be found in the Supplementary text.

RESULTS

Phenotypic spectrum

The phenotype information is shown in Tables 1 and S1 and the frequencies of clinical features in Table S2. There were no significant gender-specific differences in the clinical severity and the median age at last evaluation was 11 years (18 months–47 years). The mean age for initial clinical presentation was 1.3 years (4 months–5 years). Most individuals presented with the first symptoms in form of developmental delay before age two, except for five individuals with later clinical onset, including four who became symptomatic at age 3 years and one at age 5 years. Of 45 individuals, GDD was reported in 38 (84%) whereas specific motor developmental delay was present in six and predominant language delay in two individuals. Speech was completely absent at the last evaluation in eight individuals older than 3 years. Regression in motor development and/or language was observed in 17/43 individuals with an average age of onset of regression of 4 years (6 months–18 years). ID was present in 44/45 individuals (98%) (all of whom were older than 5 years of age at the last evaluation) and was classified as severe in 29%, moderate in 34%, mild in 29%, mild-moderate in 2% and unspecified in 4%. Of those older than 3 years with clinical information available, ASD manifestations were documented in 24/43 individuals. ASD was reported as a comorbidity in 15/26 (57%) individuals with moderate to severe ID but in only 3/10 (30%) individuals with mild ID ($p = 0.562$). Among the 12 individuals with language regression (with or without motor regression), ten individuals also had ASD, but not all the individuals with ASD had language regression. Attention deficit hyperactivity disorder (ADHD) features were present in 20/35 individuals and tended to occur more frequently in individuals with ASD (11/17, 64%) than in those without ASD (8/17, 47%; $p = 0.49$).

Table 1. Clinical features.

ID of the affected individual	Gender, current age	Age at onset	Development delay	Developmental regression	ID	Autism	Anxiety	ADHD	Abnormal movements	Behavior other	Muscle tone	Epilepsy (age onset)	Ophthalmological	Dysmorphic face	Skeletal	MH	MRI
1	M, 5 years	NI	+ (Motor)	NI	+	+	NI	NI	OCD Repetitive behaviors	-	-	Nystagmus	+	Joint laxity	NI	Normal	
2	M, 10 years	6 months	+ (Motor)	-	+ (Mild)	+	+	+	Tremors	Hallucinations Suicidal ideations Thoughts of harming others (sexually abused in childhood)	-	+ (9 years) General	Hyperopia	+	-	- Normal	
3	F, 15 years	5 years	-	-	+ (Mild)	+	+	+	Overfriendly	-	-	Myopia	+	Joint laxity Scoliosis	+	Normal	
4	M, 6.5 years	10 months	+ (GDD)	-	+ (Mild)	-	-	-	-	Hypotonia	-	Strabismus, hyperopia requiring surgery	NI	Joint laxity Hyperextensible knees requiring AFOs	+	Normal	
5	M, 6.5 years	9 months	+ (GDD)	-	+ (Mild)	-	+	-	-	Hypotonia	-	Strabismus, hyperopia requiring surgery	NI	Joint laxity Hyperextensible knees requiring AFOs	+	NA	
6	F, 16 years	1 years	+ (GDD)	+ (1–2 years)	+ (Severe)	+	-	-	Stereotypies Ataxia	-	-	Hypotonia	+ (15 years)	-	-	Normal	
7	M, 7 years	3 years	+ (GDD)	+ (4 years)	+ (Mild)	-	-	-	Hyperactivity Dyspraxia	-	-	Hypotonia	+ (15 years) Focal ESSE	-	-	Normal	
8	F, 2 years	NI	NI	NI	NA	NA	NA	NA	NI	NI	NI	NI	NI	NI	NI	Normal	
9	M, 11 years	6 months	+ (GDD)	+ (4 years)	+ (Severe)	+	+	+	Stereotypies Ataxia	Overfriendly High sensory needs	-	Hypotonia	+ (9 years) Focal	Strabismus Nystagmus	-	Joint laxity	- Hippocampal asymmetry (left cerebral and cerebellar atrophy, ventricular dilatation)
10	M, 36 years	NI	+ (GDD)	-	+ (Severe)	NI	+	NI	-	Obsessed with football and jigsaw puzzles Withdrawn behavior	-	+ General	-	-	NI	NI	
11	F, 11 years	3 years	+ (GDD)	-	+ (Severe)	-	-	+	-	-	+ (6 years) FS	Strabismus (alternating exotropia) Astigmatism	-	-	Normal		
12	M, 18 years	<1 year	+ (Motor)	+ (14 years)	Learning disorder—scattered cognitive abilities	+	-	+	Apraxia Tremor Stereotypies Tics	Catalonia (14 years)	-	-	-	-	-	Normal	
13	M, 28 years	3 months	+ (GDD)	-	+ (Moderate)	+	+	+	-	Aggressive, shy	-	Hypotonia	NI	+	-	NI	
14	M, 1.5 years	6 months	+ (GDD)	+ (6 months) motor	NA	NA	NA	NI	-	NI +(6 months) IS	-	-	-	-	NI	NI	
15	F, 4 years	NI	+ (Language)	+ (2 years) language	NA	+	NI	NI	No aggressive/ repetitive behavior	NI	NI	NI	NI	NI	NI	NI	
16	M, 12 years	15 months	+ (GDD)	-	+ (Mild)	NI	NI	NI	Episodes of whole body shaking	-	+ Focal	-	-	NI	NI	Normal	
17	M, 7 years	2 years	+ (GDD)	-	+ (Moderate)	-	-	+	+ (Mild)	Easy overstrained by external stimuli, played rather on his own in infancy	-	Hypotonia	-	+	Joint laxity	- Normal	

Table 1 continued

ID of the affected individual	Gender	Age at onset current age	Developmental delay	Developmental regression	ID	Autism	Anxiety	ADHD	Abnormal movements	Behavior other	Muscle tone	Epilepsy (age on set)	Ophthalmological	Dysmorphic face	Skeletal	MH	MRI
18	F, 12 years	NI	NI	NI	- (Mild)	+	NI	NI	Tantrums	NI	-	NI	NI	NI	NI	NI	NI
19	F, 3 years	NI	+ (GDD)	NI	NA	NI	NI	NA	NI	NI	Cortical blindness	+	NI	NI	NI	Normal	
20	F, 11 years	3 years	+ (GDD)	-	+ (Moderate)	+	-	OCD	Hyperactivity	Hypotonia + (9 years)	Myopia	NI	Joint laxity Scoliosis	-	Large perivascular space (left frontal)	NI	
21	M, 7 years	18 months	+ (GDD)	-	+ (Moderate)	+	NI	-	-	-	NI	-	Joint laxity Pectus anomaly	-	NA		
22	M, 11 years	3 years	+ (GDD)	+ (3 years)	+ (Severe)	+	-	-	-	-	-	NI	NI	NI	NI	NI	Vermis atrophy
23	NI	NI	NI	NI	NI	NI	NI	NI	NI	NI	NI	NI	NI	NI	NI	NI	Normal
24	M, 21 years	NI	NI	NI	+ (Moderate)	-	NI	NI	NI	NI	NI	NI	Strabismus	NI	NI	NI	
25	M, 4 years	6 months	+ (GDD)	-	NA	+	-	-	Self-injurious behavior	Hypotonia	NI	NI	NI	NI	NI	NI	
26	M, 7 years	6 months	+ (GDD)	-	+ (Moderate)	+	-	+	Behavioral outburst with frustration (can be physical)	Hypotonia + (6 months)	-	-	+	-	NI		
27	F, 10 years	6 months	+ (Motor)	-	+ (Moderate)	-	-	+	Social	-	Strabismus	+	Joint laxity Kyphosis Pes planus	-	Frontotemporal corticosubcortical atrophy with enlarged anterior peripheral liquor spaces	Normal	
28	M, 9 years	2 years	+ (GDD)	-	+ (Mild)	-	-	+	-	Tantrums	Toe walking (persist 9 years)	-	-	-	-	Thin corpus callosum (anterior predominance)	
29	F, 20 years	<1 year	+ (GDD)	+ (18 years) motor	+ (Severe)	+	+	Stereotypies	Two episodes of psychosis at 12 and 13 years of age respectively	Hypotonia	Amblyopia	-	Scoliosis	-	NI		
30	F, 23 years	6 months	+ (GDD)	-	+ (Moderate)	-	+	-	Withdrawn behavior	-	-	-	Cubitus valgus	-			
31	F, 34 years	1 year	+ (GDD)	+ (6 months) - 3 years	+ (Severe)	-	+	Dystonia Stereotypies Ataxia	Inappropriate laughing/ screaming spells	Dystonia + (1 year)	-	-	Scoliosis	-	NI	Vermis atrophy	
32	M, 5 years	<1 year	+ (GDD)	-	+ (Mild)	-	-	+ Stereotypies Ataxia	Easily frustrated, frequent use of dirty words	Hypotonia + (1.1 years)	Strabismus (exotropia)	-	-	-	NI	NI	
33	M, 16 years	<1 year	+ (GDD)	+ (2 years) language	+ (Severe)	+	NI	+	Impulsive	Hypotonia + (5 years) General Refractory	-	+	-	-	-	Periorbital bilateral T2 HI	
34	M, 18 years	<1 year	+ (GDD)	+ (22 months) language	+ (Moderate)	+	-	Behavioral outbursts	Hypotonia + (7 years) Focal	-	-	+	Scoliosis	-	Normal		
35	M, 11 years	NI	NI	NI	+ (Mild)	NI	+	NI	Stereotypies	Tantrums	NI	Cortical blindness	NI	NI	NI	Normal	
36	F, 8 years	<1 year	+ (GDD)	-	+ (Moderate)	-	+	NI	Depression and aggressive outbursts; bipolar disorder	NI	NI	NI	NI	NI	NI	Normal	
37	F, 47 years	NI	+ (motor)	NI	+ (Moderate)	+	NI	NI	Hyperactive, sensitive to high-pitched noises, loves playing with	Hypotonia	-	-	Joint laxity	-	Incomplete inversion of the left hippocampus		
38	M, 3.5 years	8 months	+ (GDD)	+ (18 months)	NA	+	NI	NA	-	-	-	-	-	-	-		

Table 1 continued

ID of the affected individual	Gender, current age	Age at onset	Developmental delay	Developmental regression	ID	Autism	Anxiety	ADHD	Abnormal movements	Behavior other	Muscle tone	Epilepsy (age on set)	Ophthalmological	Dysmorphic face	Skeletal	MH	MRI
water Head banging to fall asleep																	
39	F, 23 years	2 years	+ (GDD)	-	+ (Mild-moderate)	-	+	-	Ataxia	Social	NI	Yes 7 years Focal Refractory	-	NI	-	-	-
40	F, 13 years	6 months	+ (GDD)	+ (1 year)	+ (Severe)	-	-	+	Tics	Hypotonia	+ (4 months) IS, focal	-	-	-	-	Bilateral polymicrogyria (parieto-occipital) Cerebellar > cerebral atrophy	
41	M, 35 years	NI	+ (Language)	NI	+ (Moderate)	+	NI	NI	NI	NI	+ (14 years)	Strabismus	NI	Pectus anomaly Limited elbow extension	+ (Mild corticosubcortical atrophy)	NI	
42	F, 13 years	9 months	+ (GDD)	-	+ (Severe)	+	+	+	Stereotypies Aggressive and self-injurious behavior trichotillomania, pica, bruxism	-	+ (2 years)	Strabismus Hyperopia	+	-	NI	Normal	
43	F, 13 years	NI	+ (GDD)	+	+ (Mild)	NI	NI	+	Spasticity Dystonia Ataxia	Dystonia	+ Focal	Slow upgaze vertical saccades Visual-spatial difficult	-	Scoliosis	NI	Incomplete hippocampal inversion and ipsilateral dysmorphic temporal horn	
44	F, 19 years	NI	+ (GDD)	+ (7 years)	+ (Moderate)	+	+	NI	Tremors Stereotypies Ataxia	Period of hearing voices	Hypotonia	+ (8 years) Focal	Loss of peripheral fields Tracking difficulties	NI	Joint laxity Scoliosis Dolichostenomelia	+	Normal
45	F, 2 years	2 years	+ (GDD)	-	NA	NA	+	NA	Ataxia	Hypotonia	-	-	+	-	-	NI	
46	M, 23 years	3 years	+ (GDD)	-	+ (Mild)	-	+	-	Dystonia Withdrawn behavior	Dystonia	-	Nystagmus	-	Joint laxity Scoliosis Dolichostenomelia	+	Normal	
47	M, 6 years	<1 year	+ (GDD)	-	+ (Severe)	-	+	-	Stereotypies Ataxia	Inappropriately contact seeking and trusting, happy, smiling, laughing Hyperactive Repetitive behaviors	Hypotonia	-	-	-	-	Normal	
48	M, 18 years	9 months	+ (GDD)	-	+ (Severe)	-	-	+	Dystonia Stereotypies Ataxia	Very happy, distanceless, attention seeking	Hypotonia	+ (5 years) General Refractory	-	+	Joint laxity	-	Delayed myelination Reduced cholin concentration
49	F, 11 years	NI	NI	NI	+ (Moderate)	NI	+	NI	NI	NI	NI	Cortical blindness	NI	NI	NI	NI	Delayed myelination
50	F, 20 years	3 years	+ (GDD)	-	+ (Moderate)	-	-	-	Happy, affiliative obsessive behavior	-	+ (6.5 years) Focal	Hyperopia	+	+	+	+	Normal
51	M, 8.5 years	1 year	+ (GDD)	+ (8 years)	+ (Mild)	-	+	+	Phobias, social communication disorder	Hypotonia	-	-	+	-	-	Normal	
52	F, 8.5 years	1 year	+ (Motor)	-	+	+	-	+	-	-	+ (17 years) ESES	-	-	-	-	Normal	
53	M, 6 years	18 months	+ (GDD)	+ (2-5 years)	+ (Severe)	+	-	-	Stereotypies Ataxia	Excessive jumping	Hypotonia	+ (2 years) ESES	-	-	-	-	Normal

ADHD attention deficit-hyperactivity disorder, AFOs ankle-foot orthosis, CC corpus callosum, ESE electrical status epilepticus in sleep, F female, FS febrile seizures, GDD global developmental delay, ID intellectual disability, IS infantile spasms, M male, MH marfanoid habitus, MRI magnetic resonance image, NA not informed, OCD obsessive-compulsive disorder, WMH white matter hyperintensity.

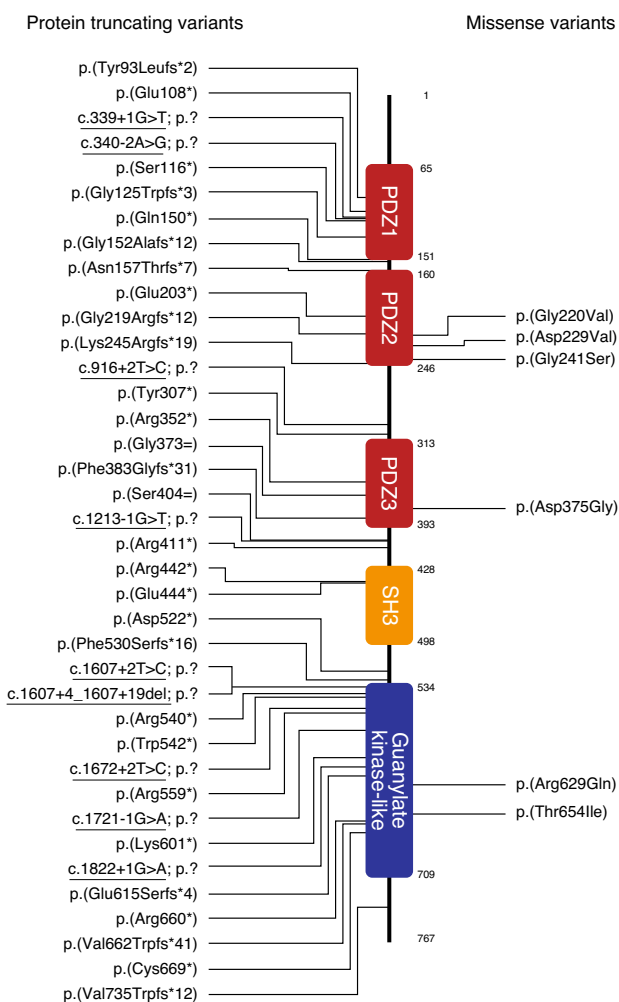


Fig. 2 *DLG4* variants shown on PSD-95. Among the 44 different variants, 6 were missense and two were synonymous while the remaining were predicted to be protein truncating variants. The missense variants were localized to the functional domains of the protein. Splice variants are underlined. PDZ1–3 domains (red) SH3 (light brown), GKLD (blue). All the variants are annotated using the *DLG4* transcript, NM_001365.4.

Epilepsy was reported in 25/47 individuals (53%) and classified as generalized epilepsy in five individuals and focal epilepsy in ten. The type of epilepsy was not specified in the remaining individuals. Two individuals were reported to have febrile seizures, three had infantile spasms and three individuals had an electroclinical presentation compatible with status epilepticus during slow-wave sleep (ESES). The mean age of epilepsy onset was 6 years (6 months–15 years). For six individuals, seizures were reported as refractory to pharmacologic treatment. Electroencephalography (EEG) information was available in 17 of the 25 individuals with epilepsy and showed focal abnormalities in 12 individuals (seven multifocal), generalized abnormalities in two and abnormal background in seven. Epilepsy tended to be more frequent in individuals with moderate/severe ID (18/26, 69%) than in those with mild ID (4/12, 33%; $p = 0.084$) and in those with autistic features (13/22, 59%) versus those without (8/19, 42%; $p = 0.44$). Of the individuals with epilepsy, 12 (50%) had regression in motor development and/or language, whereas it was present in 4/18 (22%) of those without epilepsy ($p = 0.13$).

Other neurological manifestations included hypotonia (23/43, 53%) and abnormal movements (19/41, 46%) such as stereotypies

($n = 12$), ataxia ($n = 9$), dystonia ($n = 4$) and tremor ($n = 3$). Significant facial dysmorphic features were reported in 15/39 individuals (38%), though establishing a characteristic gestalt was not possible as features were variable. Some of the more frequently observed common features were long face, thin eyebrows, thin upper lip and wide nasal bridge with a broad tip of nose (Fig. 1). Skeletal abnormalities were reported in 23/44 (41%) individuals.

Brain magnetic resonance imaging (MRI) was performed in 40 individuals and 13 (32%) were noted to have abnormalities (Fig. 1S). Abnormal MRI was found in 20% of the individuals with mild ID (2/10) and in 40% (9/22) of those with moderate/severe ID. The reported abnormalities include variable degrees of brain atrophy ($n = 5$), cerebellar atrophy ($n = 4$), thin corpus callosum, dysmorphic hippocampus ($n = 3$, two with incomplete hippocampal inversion [IHI]), delayed myelination ($n = 2$) and periventricular T2 white matter hyperintensity ($n = 2$).

Spectrum of the *DLG4* variants

Among the 53 individuals, 44 different variants were identified (Table 2, Fig. 2). Six variants were found more than once—three unrelated individuals each had the c.1054C>T, c.1324C>T, c.1618C>T and c.1978C>T variants. The c.340–2A>G variant was identified in monozygotic concordant twins, and the c.1587del variant was detected in a set of brothers, and after excluding nonpaternity, germline mosaicism in one of the parents was presumed as these variants were found to be de novo. Among the 48 individuals for whom parental studies were conducted, 43, including a monozygotic twin pair (ID-4 and ID-5), had de novo variants, and one individual inherited the variant (ID-22) from his mother with somatic mosaicism in buccal tissue (blood was not investigated and the percentage of mosaicism could not be obtained). One individual (ID-15) had a maternally inherited *DLG4* variant, but clinical information on the mother was not available.¹⁵

Among the 44 different variants, six were annotated as missense and two were predicted as synonymous while the remaining were predicted to be protein truncating variants: 15 nonsense variants, four single-nucleotide duplications, six single-nucleotide and one eight-nucleotide deletion, one indel and nine splice-site variants. Eight splice-site variants within the canonical splice sequences and the intronic variant (c.1607+4_1607+19del) were all expected to alter splicing (Fig. 2). All the duplications and deletions as well as the indel were frameshift variants. One of these variants, c.2203_2207delinsT (ID-53) was predicted to escape nonsense-mediated decay (NMD), while all the other protein truncating variants were predicted to be subject to degradation by NMD.

Two individuals had de novo variants annotated as synonymous. Individual 25 had the p.(Ser404=) (c.1212G>A) variant, which was at the last nucleotide of exon 11 and using SpliceAI it was predicted to cause a canonical splice donor loss with a probability of 63% with a new donor gain 4 bp downstream, which would result in a frameshift (p.[Val405Thrfs*17]). The other synonymous variant, p.(Gly373=) (c.1119C>T), identified in individual 22 was in the middle of exon 11 and SpliceAI predicted a donor gain with a probability of 44%. Further analyses with reverse transcriptase polymerase chain reaction (RT-PCR) revealed a deletion in the RNA transcript (r.1118_1212del) predicted to result in a frameshift, p.(Glu374Glnfs*11).

The missense variants were localized to the functional domains of the protein (three in the PDZ2 domain, one in the PDZ3 domain, and two in the Guanylate kinase-like domain). None of these variants were detected among the 125,748 exomes and 15,708 genomes from unrelated individuals in the gnomAD database, and they were all classified as pathogenic or likely pathogenic, except for two missense variants that were classified as variants of uncertain significance (VUS) according to

Table 2. *DLG4* variants and their predicted effects.

gDNA Chr17(GRCh37)	cDNA (NM_001365.4)	Exon/ intron	Predicted effect on PSD-95	PSD- 95 domain	Predicted coding effect	CADD score	Inheritance	ID of the affected individual
g.7107520dup	c.277dup	5	p.(Tyr93Leufs*2)	PDZ1	Frameshift	32	dn	1
g.7107344C>A	c.322G>T	6	p.(Glu108*)	PDZ1	Nonsense	40	dn	2
g.7107326C>A	c.339+1G>T	IVS6	p.?			35	uk	3
g.7107137T>C	c.340-2A>G	IVS6	p.?			34	dn	4 ^a
							dn	5 ^a
g.7107128G>C	c.347C>G	7	p.(Ser116*)	PDZ1	Nonsense	36	dn	6
g.7107103dup	c.372dup	7	p.(Gly125Trpfs*3)	PDZ1	Frameshift	32	dn	7
g.7107027G>A	c.448C>T	7	p.(Gln150*)	PDZ1	Nonsense	37	dn	8
g.7107020del	c.455del	7	p.(Gly152Alafs*12)		Frameshift	32	dn	9
g.7106909del	c.468del	8	p.(Asn157Thrfs*7)		Frameshift	31	dn	10
g.7106770C>A	c.607G>T	8	p.(Glu203*)	PDZ2	Nonsense	37	dn	11
g.7106629dup	c.654dup	9	p.(Gly219Argfs*12)	PDZ2	Frameshift	32	dn	12
g.7106624C>A	c.659G>T	9	p.(Gly220Val)	PDZ2	Missense	26.6	dn	13
g.7106597T>A	c.686A>T	9	p.(Asp229Val)	PDZ2	Missense	27.7	dn	14
g.7106562C>T	c.721G>A	9	p.(Gly241Ser) ^f	PDZ2	Missense	27.7	mat	15
g.7106549del	c.734delA	9	p.(Lys245Argfs*19)		Frameshift	32	dn	16
g.7106220A>G	c.916+2T>C	IVS10	p.?			33	dn	17
g.7100367A>T	c.921T>A	11	p.(Tyr307*)		Nonsense	36	dn	18
g.7100234G>A	c.1054C>T	11	p.(Arg352*)	PDZ3	Nonsense	37	dn	19
							dn	20
							Not mat ^b	21
g.7100169G>A	c.1119C>T	11	p.(Gly373=) ^c	PDZ3	Synonymous	13.7	dn	22
g.7100164T>C	c.1124A>G	11	p.(Asp375Gly) ^f	PDZ3	Missense	25.7	uk	23
g.7100134_7100141del	c.1147_1154del	11	p.(Phe383Glyfs*31)	PDZ3	Frameshift	33	dn	24
g.7100076C>T	c.1212G>A	11	p.(Ser404=) ^c		Synonymous	25.4	dn	25
g.7099895C>A	c.1213-1G>T	IVS11	p.?			35	Mat/ mosaic	26
g.7099876G>A	c.1231C>T	12	p.(Arg411*)		Nonsense	41	dn	27
g.7099645G>A	c.1324C>T	13	p.(Arg442*)	SH3	Nonsense	38	dn	28
							dn	29
							dn	30
g.7099639C>A	c.1330G>T	13	p.(Glu444*)	SH3	Nonsense	40	dn	31
g.7097682dup	c.1563dup	14	p.(Asp522*)		Frameshift	33	dn	32
g.7097658del	c.1587del		p.(Phe530Serfs*16)		Frameshift	28.2	Germline mosaicism ^d	33
							Germline mosaicism ^d	34
g.7097636A>G	c.1607+2T>C	IVS14	p.?			34	dn	35
g.7097619_7097634del	c.1607+4_1607 +19del	IVS14	p.?			16.38	dn	36
g.7097309G>A	c.1618C>T	15	p.(Arg540*)		Nonsense	44	uk	37
							dn	38
g.7097301C>T	c.1626G>A	15	p.(Trp542*)	GKLD	Nonsense	51	dn	39
g.7097302C>T	c.1625G>A						dn	40
g.7097161A>G	c.1672+2T>C	IVS16	p.?			34	uk	41
g.7097031G>A	c.1675C>T	17	p.(Arg559*)	GKLD	Nonsense	45	uk	42
g.7096904C>T	c.1721-1G>A	IVS17	p.?			35	dn	43
g.7096823T>A	c.1801A>T	18	p.(Lys601*)	GKLD	Nonsense	44	dn	44
g.7096801C>T	c.1822+1G>A	IVS18	p.?			35	dn	45
g.7096416del	c.1843del	19	p.(Glu615Serfs*4)	GKLD	Frameshift	33	dn	46

Table 2 continued

gDNA Chr17(GRCh37)	cDNA (NM_001365.4)	Exon/ intron	Predicted effect on PSD-95	PSD-95 domain	Predicted coding effect	CADD score	Inheritance	ID of the affected individual
g.7096373C>T	c.1886G>A	19	p.(Arg629Gln)/ p.(His608Argfs*14) ^e	GKLD	Missense/ frameshift	32	dn	47
g.7096298G>A	c.1961C>T	19	p.(Thr654Ile)	GKLD	Missense	26.7	dn	48
g.7096281G>A	c.1978C>T	19	p.(Arg660*)	GKLD	Nonsense	41	dn	49
						41	dn	50
g.7096275del	c.1984del	19	p.(Val662Trpfs*41)	GKLD	Frameshift	34	dn	51
g.7095310G>T	c.2007C>A	20	p.(Cys669*)	GKLD	Nonsense	40	dn	52
g.7094124_7094128delinsA	c.2203_2207delinsT	22	p.(Val735Trpfs*12)		Frameshift	34	dn	53

Combined Annotation Dependent Depletion (CADD) tool was used to score the deleteriousness of the variants (<https://cadd.gs.washington.edu/>) and Mutalyzer (<https://mutalyzer.nl>) was used to check sequence variant nomenclature according to the guidelines of the Human Genome Variation Society (Table S4).

cDNA complementary DNA, *del* deletion, *dn* de novo, *dup* duplication, *gDNA* genomic DNA, *GKLD* guanylate kinase-like domain, *IVS* intervening sequence (intron), *mat* maternal, *NA* not applicable, *uk* unknown.

^aIndividuals 4 and 5 are monozygotic twins.

^bThe variant was not maternal, father not available.

^cFurther analyses revealed a deletion in the RNA transcript (r.1118_1212del) predicted to result in frameshift, p.(Glu373Glnfs*11) in individual 22, and in individual 25 the variant was in the canonical splice sequence and predicted to affect splicing.

^dIndividuals 33 and 34 are brothers (the parents do not have the variant and germline mosaicism is suspected).

^ePrediction tools suggests that this substitution is a splice variant predicted to result in frameshift, p.(His608Argfs*14).

^fThese missense variants are classified as variants of unknown significance (VUS) according to American College of Medical Genetics and Genomics/Association for Molecular Pathology (ACMG/AMP) criteria, and even though protein studies suggest that they affect protein function, further functional studies are warranted to determine their pathogenicity.

ACMG/AMP criteria.^{20,21} Both of the latter variants were identified as part of a large screening study:¹⁵ p.(Gly241Ser) was maternally inherited (no phenotypic information on the mother is available), and the inheritance of p.(Asp375Gly) was not reported. All the missense variants were scored using SpliceAI tool and no splicing change was predicted for five of these. However, a new splice acceptor was predicted with 99% probability for the c.1886G>A, (p.(Arg629Gln) in ID-47), which would result in a frameshift, p.(His608Argfs*14). The family is contacted for verification of this finding.

Prediction of the structural and functional effect of missense *DLG4* variants using homology modeling

To study the functional implications of the six missense *DLG4* variants p.(Gly220Val), p.(Asp229Val), p.(Gly241Ser), p.(Asp375Gly), p.(Arg629Gln), and p.(Thr654Ile), a 3D model of the wild type PSD-95 was generated using standard homology modeling-based techniques (Fig. 3). Subsequently, models for the six PSD-95 mutants were generated using the wild type model as a template and subjected to 100 ns of unrestricted molecular dynamics (MD) simulation. The details of the results of the protein modeling and MD simulation can be found in the Supplementary material.

Three of the modeled missense substitutions [p.(Gly220Val), p.(Asp229Val), p.(Gly241Ser)] occur in the PDZ2 domain of PSD-95 (Fig. 3). The simulation studies suggest that all these substitutions alter the structure of the PDZ2 domain (Fig. 3b, c). Furthermore, the p.(Asp229Val) substitution is predicted to modify the kinase/phosphatase recognition motif, and the p.(Gly241Ser) substitution is predicted to modify the ubiquitylation recognition motif, both of which are likely to affect the protein function. Notably, modeling of the p.(Gly241Arg) variant, which is reported in a single individual in the gnomAD database and alters the same amino acid as the p.(Gly241Ser) variant (ID-15), did not suggest a structural effect on the protein structure supporting that this variant was likely benign (Fig. 3d; Supplementary material).

The Asp375 residue is located in a loop between two beta-sheets in the PDZ3 domain, which is enriched in negatively

charged amino acids (Asp374, Asp375, and Asp377), and it is probably involved in the interaction with other adjacent structures such as potassium channels²⁵ (Fig. 3e). The p.(Asp374Gly) substitution generated a decrease in the negative charge of the surface, which is likely to modify the nature of this interaction and affect its functionality.

The residues Arg629 and Thr654 are both located in the guanylate kinase-like domain (GKLD, Fig. 3f–g). The p.(Arg629Gln) substitution is likely to modify the surface charge and thereby may affect the interaction of PSD-95 with other proteins such as the potassium channels. The p.(Thr654Ile) substitution is likely to modify the guanosine monophosphate (GMP) binding site, as well as modify the structure of the putative active site. In addition, this substitution could modify a kinase/phosphatase recognition motif predicted in the rat.²⁸

Genotype–phenotype correlation

All the individuals share core clinical manifestations that mainly affect the central nervous system, although there is some variability regarding the severity of ID, epilepsy, and the presence of other associated features, such as movement disorders. Most of the individuals ($n=47$) had predicted loss of function (LoF) variants distributed throughout the protein, while only six had missense variants (two of which were classified as VUS), localized in the highly conserved regions of the functional protein domains (PDZ2, PDZ3, and GKLD). However, given the small sample size and some missing clinical information, it is difficult to make genotype–phenotype comparison. Among the individuals with truncating variants, one had a c.2203_2207delinsT (ID-53) variant, which was predicted to escape NMD. However, the clinical features of this individual were not specifically milder than those of the other individuals with truncating variants. Of note, in individuals with the same *DLG4* variant including two brothers (ID-33 and ID-34) we observed some variability in terms of the presence and severity of clinical manifestations and the MRI findings. The exception was the monozygotic twin brothers (ID-4 and ID-5) with almost identical symptoms.

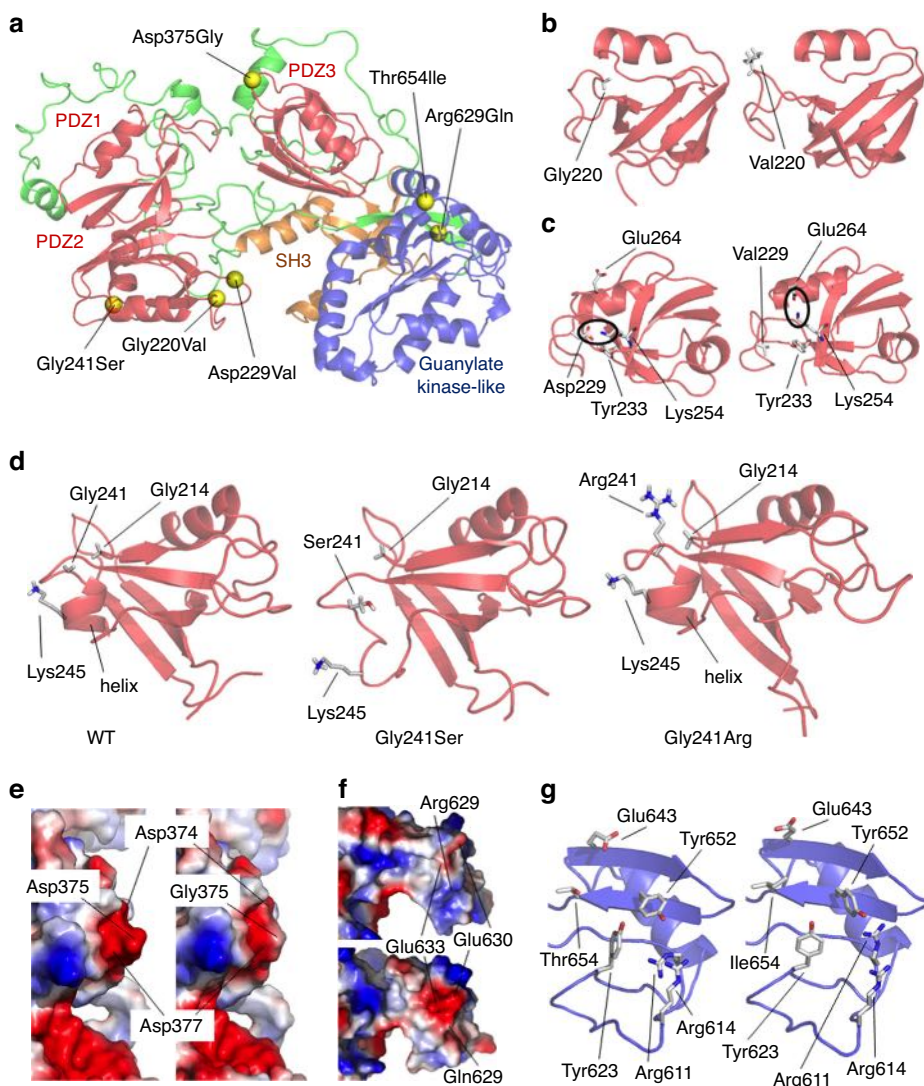


Fig. 3 Structural modeling of *DLG4* missense variants. (a) Structure model of human *DLG4* protein. Locations of domains PDZ 1, 2, and 3; SH3; and guanylate kinase-like (GK-LIKE) are labeled. Positions of variants p.(Gly220Val), p.(Asp229Val), p.(Gly241Ser), p.(Asp375Gly), p.(Arg629Gln), and p.(Thr654Ile) are shown as yellow spheres. (b) Structure of the wild type (left) and p.(Gly220Val) (right) at PDZ2 domain after molecular dynamics (MD) simulation. The positions of Gly220 and Val220 are indicated. (c) Structure of the wild type (left) and Asp229Val variant (right) PDZ2 domain after MD simulation. The positions of residues Asp229 (or Val229), Lys254, and Glu264 are indicated. Salt bridges are shown with black circles. (d) Structure of the PDZ2 domain of the wild type, Gly241Ser, and Gly241Arg variants after MD simulation. Locations of amino acids Gly241/Ser241/Arg241, Gly214, and Lys245 are labeled. The Gly241Ser substitution identified in individual 15 alters the structure of the PDZ2 domain, while the Gly241Arg substitution, which is reported in a single individual in the gnomAD database, does not suggest a structural effect supporting that this variant was likely benign. (e) Left: position of negatively charged residues Asp374, Asp375, and Asp377 in the surface of PDZ3 domain. Right: variant of Asp375 to Gly promotes a decrease in the local negative charge of the surface. (f) Surface of the wild type (upper panel) and Arg629Gln variant (lower panel) guanylate kinase-like domain after 100 ns of MD simulation. The positions of residues Arg629 (or Gln629) are indicated. Note the contribution of the Glu630 and Glu633 residues in the negatively charged patch in the surface of the variant protein. (g) Residues conserved in the guanylate kinase-like domain located in the homologous positions to those coordinating GMP binding in the yeast guanylate kinase enzyme²⁴ both in wild type (left) and Thr654Ile variant (right) proteins. PDZ1–3 domains (red) SH3 (light brown), GKLD (blue). Figures were generated using the PyMol Molecular Graphics System (<https://pymol.org/>; Schrödinger, LLC, Portland, OR).

DISCUSSION

This study includes the largest series of individuals harboring variants in *DLG4* published to date and demonstrates that the clinical phenotype is largely neurodevelopmental, with an early onset of symptoms and a clinical picture predominated by GDD/ID, ASD, ADHD, hypotonia, and epilepsy. Given that the synaptopathies are defined as brain disorders associated with synaptic dysfunction²⁹ and that the individuals presented in this study have clinical features overlapping those observed in

individuals with synaptopathies (cognitive disorders such as intellectual disability, motor dysfunction such as ataxia and dystonia, epilepsy and psychiatric diseases such as ASD and ADHD)^{29,30} we coin the phenotypes associated with *DLG4* variants as *DLG4*-related synaptopathy.

Postsynaptic disorders are relatively unknown. Among individuals with *DLG4*-related disorders, cognitive impairment and ASD predominate, as already described in the context of PSD-complex dysfunction in the hippocampus excitatory synapses in mice.^{31,32}

The present work also suggests a certain correlation between the degree of ID and the presence of ASD and epilepsy, these being more frequent in the context of moderate to severe ID. The physiopathology of epilepsy observed in *DLG4*-related synaptopathy is currently unknown, but it is plausible that variants of the functional domains of PSD-95 will affect the function of glutamate receptors (such as NMDA or AMPA) or K_v1 channels, which are known to be dysfunctional in epileptic disorders, and hereby lead to altered excitatory synaptic transmission.

Variants in genes encoding postsynaptic proteins of striatal medium spiny neurons (MSNs) have previously been associated with movement disorders.³³ Taking into account that PSD-95 has been identified in glutamatergic synapses of midbrain dopaminergic neurons³⁴ and the MSNs of the human neostriatum,³⁵ it is not surprising that some individuals with *DLG4* variants had an associated movement disorder. Most of the symptoms observed in *DLG4*-related disorder, may thus be explained by impaired synaptic plasticity due to the changes in the structural organization of the PSD. However, further research is warranted to understand the synaptic physiopathology in this disorder.

Brain abnormalities as detected by MRI are diverse and nonspecific. They mainly include cerebral and/or cerebellar atrophy, thinning of the corpus callosum, hippocampal dysmorphia (two individuals with incomplete hippocampal inversion [IHI]) and mild delayed myelination. Although IHI has been reported in the general population, it has been described more frequently in individuals with epilepsy and febrile status epilepticus.^{36,37} Therefore, taking into account that PSD-95 is highly expressed in the hippocampus and diminished activity alters the correct development of excitatory synapses (producing an excitatory/inhibitory imbalance) and modifies dendritogenesis during embryological development, IHI could represent a neuroimaging manifestation of the abnormal neurodevelopment provoked by *DLG4* variants. This possibility should be considered in future studies. In this series, careful review of the neuroimaging studies of the individuals has not been possible, so in some cases, this anomaly could have gone unnoticed. On the other hand, in five individuals (ID-9, 26, 28, 38, 41), there is some component of white matter atrophy, and it is associated with thinning of the corpus callosum in three of them. This is in agreement with an association between genetic variability in *DLG4* and white matter structure in the preterm neonatal brain as described previously.³⁸ Furthermore, corticosubcortical atrophy with anterior predominance is seen in two of the individuals (ID-26 and ID-28; Fig. 1S) and could be associated with the high expression of PSD-95 in the prefrontal cortex.³⁹

DLG4 variants have recently been associated with ID through identification of three individuals with de novo LoF variants in a cohort of 820 individuals with ID (0.37%)¹² and, subsequently, three LoF *DLG4* variants were identified in a cohort of 64 individuals with ID and MH (corresponding to 4.7% of the cohort). Considering the higher prevalence in this series compared with the larger series of ID individuals, the authors suggested that *DLG4* was a strong candidate gene in ID individuals with comorbid MH.¹⁶ In the present study, we could re-examine 38 individuals specifically for MH features, which were present only in 9, suggesting that MH is not a major clinical feature of *DLG4*-related synaptopathy. In a very recent study comprising 31,058 individuals, LoF variants of *DLG4* were identified in 15 individuals,⁴⁰ suggesting that incidence of this synaptopathy is about 0.05% among the individuals with ID.

DLG4 is likely to be intolerant to both missense and LoF variants ($Z = 4.93$ for missense and observed/expected (o/e) value = 0.06–0.24 for LoF variants, gnomAD database). All the variants described in this study meet criteria for classification as pathogenic or likely pathogenic, except for two of the missense variants, p.(Gly241Ser) and p.(Asp375Gly), which are classified as VUS. We included these variants as they were associated with ASD

in a previous study,¹⁵ and the modeling studies show an effect on the protein, acting in highly conserved regions of its functional domains. LoF variants reported in this study are distributed throughout the protein, whereas the missense variants are localized to the functional protein domains (PDZ1, PDZ3, GKLD). Structure modeling suggests that the missense variants affect structural conformation and/or protein function and are therefore likely to act as LoF variants. These modifications in highly conserved positions of the protein presumably alter its function, thereby affecting its interaction with other proteins, which is fundamental for synaptogenesis, functional dynamics, and plasticity. Modeling studies were helpful to predict the functional consequences of the missense variants and thus supported the pathogenicity classification. Furthermore, modeling of the p.(Gly241Arg) variant, which is reported in a single presumably unaffected individual in the gnomAD database and affects the same amino acid as the p.(Gly241Ser) variant we had identified in an affected individual, did not suggest a structural effect on the protein and was likely to be benign. However, further functional studies are warranted, especially for the VUS, to understand the effect of the missense variants on protein function. Apart from protein modeling we annotated the variants using an NMD and a splice variant prediction tool. Both synonymous variants p.(Gly373=) and p.(Ser404=) were predicted to affect splicing leading to frameshift, and this was verified with RT-PCR. Notably, the c.1886G>A substitution, which was initially annotated as a missense variant, p.(Arg629Gln), was predicted to result in a frameshift, p.(His608Argfs*14). Furthermore, one of the truncating variants, c.2203_2207delinsT, 100 bp upstream to the TGA stop codon, was suggested to escape NMD, but the prediction was not verified. These findings underline the importance of RNA based studies in clinical diagnosis to understand the consequences of the DNA variants.

This study has certain limitations. The individuals come from different centers and therefore have been clinically evaluated by professionals using different criteria. Employment of Human Phenotype Ontology (HPO, <https://hpo.jax.org>) terms to describe the phenotypic abnormalities as part of the clinical practice and research may help to overcome this limitation. Furthermore, the available clinical information is limited in several individuals, making it more difficult to extract detailed information (and percentages) on certain manifestations such as epilepsy. Finally, information on neuroimaging studies in all the individuals could have enabled a more comprehensive assessment of the presence of abnormalities in the development of the hippocampus and other brain structures. Studies of the cerebrospinal fluid might have enabled us to determine whether a characteristic neurotransmitter profile could serve as biomarker.

In conclusion, haploinsufficiency of *DLG4* is likely to impair PSD-95 activity, interfere with synaptic function during critical developmental windows and alter the synaptic plasticity necessary for the functional adaptation and modulation of learning and behavioral processes, leading to the neurodevelopmental disorder described in this group of individuals. We provide evidence that missense variants affecting the functional domains of PSD-95 can also cause a *DLG4*-related synaptopathy. A better understanding of the pathophysiology of synaptopathies could contribute to the development of new specific therapies in the future.

DATA AVAILABILITY

All data that are not already included in the supplementary material are available upon request.

Received: 16 October 2020; Revised: 12 December 2020; Accepted: 15 December 2020;

Published online: 17 February 2021

REFERENCES

- Sheng, M. & Kim, E. The postsynaptic organization of synapses. *Cold Spring Harb. Perspect. Biol.* **3**, a005678 (2011).
- Nithianantharajah, J. et al. Synaptic scaffold evolution generated components of vertebrate cognitive complexity. *Nat. Neurosci.* **16**, 16–24 (2013).
- Philips, A. K. et al. X-exome sequencing in Finnish families with Intellectual Disability - Four novel mutations and two novel syndromic phenotypes. *Orphanet J. Rare Dis.* **9**, 49 (2014).
- Tarpey, P. et al. Mutations in the DLG3 gene cause nonsyndromic X-linked mental retardation. *Am. J. Hum. Genet.* **75**, 318–324 (2004).
- Guo, H. et al. Inherited and multiple de novo mutations in autism/developmental delay risk genes suggest a multifactorial model. *Mol. Autism* **9**, 64 (2018).
- Xu, B., Roos, J. L., Levy, S., Van Rensburg, E. J., Gogos, J. A. & Karayiorgou, M. Strong association of de novo copy number mutations with sporadic schizophrenia. *Nat. Genet.* **40**, 880–885 (2008).
- Kirov, G. et al. De novo CNV analysis implicates specific abnormalities of postsynaptic signalling complexes in the pathogenesis of schizophrenia. *Mol. Psychiatry* **17**, 142–153 (2012).
- Feyder, M. et al. Association of mouse Dlg4 (PSD-95) gene deletion and human DLG4 gene variation with phenotypes relevant to autism spectrum disorders and Williams' syndrome. *Am. J. Psychiatry* **167**, 1508–1517 (2010).
- Coley, A. A. & Gao, W. J. PSD-95 deficiency disrupts PFC-associated function and behavior during neurodevelopment. *Sci. Rep.* **9**, 9486 (2019).
- Winkler, D. et al. Hypersocial behavior and biological redundancy in mice with reduced expression of PSD95 or PSD93. *Behav. Brain Res.* **352**, 35–45 (2018).
- Rauch, A. et al. Range of genetic mutations associated with severe non-syndromic sporadic intellectual disability: an exome sequencing study. *Lancet.* **380**, 1674–1682 (2012).
- Lelieveld, S. H. et al. Meta-analysis of 2,104 trios provides support for 10 new genes for intellectual disability. *Nat. Neurosci.* **19**, 1194–1196 (2016).
- Fitzgerald, T. W. et al. Large-scale discovery of novel genetic causes of developmental disorders. *Nature* **519**, 223–228 (2015).
- Bosch, D. G. M. et al. Novel genetic causes for cerebral visual impairment. *Eur. J. Hum. Genet.* **24**, 660–665 (2016).
- Xing, J. et al. Resequencing and association analysis of Six PSD-95-related genes as possible susceptibility genes for schizophrenia and autism spectrum disorders. *Sci. Rep.* **6**, 27491 (2016).
- Moutton, S. et al. Truncating variants of the DLG4 gene are responsible for intellectual disability with marfanoid features. *Clin. Genet.* **93**, 1172–1178 (2018).
- Baker, S. W. et al. Automated clinical exome reanalysis reveals novel diagnoses. *J. Mol. Diagn.* **21**, 38–48 (2019).
- Sobreira, N., Schietecatte, F., Valle, D. & Hamosh, A. GeneMatcher: a matching tool for connecting investigators with an interest in the same gene. *Hum. Mutat.* **36**, 928–930 (2015).
- Firth, H. V. et al. DECIPHER: Database of Chromosomal Imbalance and Phenotype in Humans Using Ensembl Resources. *Am. J. Hum. Genet.* **84**, 524–533 (2009).
- Richards, S. et al. Standards and guidelines for the interpretation of sequence variants: a joint consensus recommendation of the American College of Medical Genetics and Genomics and the Association for Molecular Pathology. *Genet Med* **17**, 405–424 (2015).
- Amendola, L. M. et al. Performance of ACMG-AMP variant-interpretation guidelines among nine laboratories in the Clinical Sequencing Exploratory Research Consortium. *Am. J. Hum. Genet.* **98**, 1067–1076 (2016).
- Coban-Akdemir, Z. et al. Identifying genes whose mutant transcripts cause dominant disease traits by potential gain-of-function alleles. *Am. J. Hum. Genet.* **103**, 171–178 (2018).
- Jaganathan, K. et al. Predicting splicing from primary sequence with deep learning. *Cell.* **176**, 535–548 (2019).
- McGee, A. W., Dakoji, S. R., Olsen, O., Bredt, D. S., Lim, W. A. & Prehoda, K. E. Structure of the SH3-guanylate kinase module from PSD-95 suggests a mechanism for regulated assembly of MAGUK scaffolding proteins. *Mol. Cell* **8**, 1291–1301 (2001).
- Fomina, S. et al. Self-directed assembly and clustering of the cytoplasmic domains of inwardly rectifying Kir2.1 potassium channels on association with PSD-95. *Biochim. Biophys. Acta* **1808**, 2374–2389 (2011).
- Benkert, P., Biasini, M. & Schwede, T. Toward the estimation of the absolute quality of individual protein structure models. *Bioinformatics* **27**, 343–350 (2011).
- Krab, L. C. et al. Delineation of phenotypes and genotypes related to cohesin structural protein RAD21. *Hum. Genet.* **139**, 575–592 (2020).
- Hornbeck, P. V., Zhang, B., Murray, B., Kornhauser, J. M., Latham, V. & Skrypek, E. PhosphoSitePlus, 2014: mutations, PTMs and recalibrations. *Nucleic Acids Res.* **43**, D512–D520 (2015).
- Grant, S. G. N. Synapse diversity and synaptome architecture in human genetic disorders. *Hum. Mol. Genet.* **28**, R219–R225 (2019).
- Tristán-Noguero, A. & García-Cazorla, Á. Synaptic metabolism: a new approach to inborn errors of neurotransmission. *J. Inherit. Metab. Dis.* **41**, 1065–1075 (2018).
- Zapata, J. et al. Epilepsy and intellectual disability linked protein Shrm4 interaction with GABA B Rs shapes inhibitory neurotransmission. *Nat. Commun.* **8**, 14536 (2017).
- Ung, D. C. et al. Ptchd1 deficiency induces excitatory synaptic and cognitive dysfunctions in mouse. *Mol. Psychiatry* **23**, 1356–1367 (2017).
- Abela, L. & Kurian, M. A. Postsynaptic movement disorders: clinical phenotypes, genotypes, and disease mechanisms. *J. Inherit. Metab. Dis.* **41**, 1077–1091 (2018).
- Jang, M. et al. Coexistence of glutamatergic spine synapses and shaft synapses in substantia nigra dopamine neurons. *Sci. Rep.* **5**, 14773 (2015).
- Morigaki, R. & Goto, S. Postsynaptic density protein 95 in the striosome and matrix compartments of the human neostriatum. *Front. Neuroanat.* **9**, 154 (2015).
- Gamss, R. P., Slasky, S. E., Bello, J. A., Miller, T. S. & Shinnar, S. Prevalence of hippocampal malrotation in a population without seizures. *Am. J. Neuroradiol.* **30**, 1571–1573 (2009).
- Chan, S. et al. Hippocampal malrotation is associated with prolonged febrile seizures: Results of the FEBSTAT study. *Am. J. Roentgenol.* **205**, 1068–1074 (2015).
- Krishnan, M. L. et al. Integrative genomics of microglia implicates DLG4 (PSD95) in the white matter development of preterm infant. *Nat. Commun.* **8**, 428 (2017).
- Ohnuma, T., Kato, H., Arai, H., Faull, R. L. M., McKenna, P. J. & Emson, P. C. Gene expression of PSD95 in prefrontal cortex and hippocampus in schizophrenia. *Neuroreport* **11**, 3133–3137 (2000).
- Kaplanis, J. et al. Evidence for 28 genetic disorders discovered by combining healthcare and research data. *Nature* **586**, 757–762 (2020).

FUNDING

Funding information can be found in Supplementary text 2.

ACKNOWLEDGEMENTS

We thank all the affected individuals and families for their collaboration. Several authors of this publication are members of the European Reference Network for Developmental Anomalies and Intellectual Disability (ERN-ITHACA) ITHACA (EU Framework Partnership Agreement ID: 3HP-HP-FPA ERN-01–2016/739516). We thank Jette Rasmussen for graphical assistance and Cristina Guilera and Juanjo Martínez for technical assistance.

AUTHOR CONTRIBUTIONS

Conceptualization: K.A.A., K.A.L., B.d.V., W.B.D., A.P., Z.T. Data curation: A.R.-P., M.M.B., D.G.-A., I.M.-A., B.P., P.G.-P., Z.T. Formal analysis: A.R.-P., M.M.B., D.G.-A., B.P., E.V., P.G.-P. Investigation: K.A.A., B.P., D.B.E., A.K.-L., S.A., V.B., G.B., A.-M.B., A.-L.B., T.D.C., B.C., C.C., S.A.d.M., A.-S.D.-P., T.J.D., F.E., L.F., S.G.-M., E.G., N.G., T.B.H., C.R.H.-E., B.I.H., J.H., A.C.E.H., B.I., M.J.-S., L.K., S.K., M.K., Y.E.L., K.A.L., A.L., A.M., G.M., B.A.M., S.M., J.E.M., S.M., A.J.M., M.C.O., M.P.-M., M.P.-B., S.P., R.P., B.P.-S., A.R., E.R., A.R.-P., M.J.R., C.A.L.R., E.S., J.M.S., A.S., B.S.-G., Z.S., C.S.-S., J.S., M.S., S.S., H.T., F.T.M.-T., B.v.B., I.v.d.B., I.M.B.H.v.d.L., E.v.D., M.M.v.H., C.M.v.R.-A., E.V., A.V., S.W., S.W., C.Z., C.E.P., B.B.A.d.V., W.B.D., S.F.R., P.G.-P., A.P., Z.T. Project administration: M.M.B., V.A.B., Z.T. Visualization: W.B.D., S.F.R., P.G.-P., Z.T. Writing—original draft: A.P., M.M.B., A.R.-P., Z.T. Writing—review & editing: A.R.-P., D.G.-A., K.A.A., B.P., D.B.E., A.K.-L., S.G.-M., T.G., L.K., G.M., M.C.O., M.P.-B., E.R., A.R.-P., J.M.S., F.T.M.-T., C.M.v.R.-A., C.E.P., S.F.R., P.G.-P., Z.T.

ETHICS DECLARATION

Informed written consent for genetic testing and publication of the clinical information including clinical pictures was obtained from the parents or the legal guardians of each individual according to the Declaration of Helsinki. The work carried out at the corresponding author's (Z.T.) institution has been approved by the Regional Ethical Committee, Capital Region of Denmark (H15007871).

COMPETING INTERESTS

The authors declare no competing interests.

ADDITIONAL INFORMATION

The online version of this article (<https://doi.org/10.1038/s41436-020-01075-9>) contains supplementary material, which is available to authorized users.

Correspondence and requests for materials should be addressed to Z.T.

Reprints and permission information is available at <http://www.nature.com/reprints>

Publisher's note Springer Nature remains neutral with regard to jurisdictional claims in published maps and institutional affiliations.

Agustí Rodríguez-Palmero^{1,2}, Melissa Maria Boerrigter^{3,4}, David Gómez-Andrés⁵, Kimberly A. Aldinger⁶, Íñigo Marcos-Alcalde^{7,8}, Bernt Popp^{9,10}, David B. Everman¹¹, Alycia Kern Lovgren¹², Stephanie Arpin¹³, Vahid Bahrambeigi^{11,14}, Gea Beunders¹⁵, Anne-Marie Bisgaard¹⁶, V. A. Bjerregaard³, Ange-Line Bruel¹⁷, Thomas D. Challman¹⁸, Benjamin Cogné^{19,20}, Christine Coubes²¹, Stella A. de Man²², Anne-Sophie Denommé-Pichon¹⁷, Thomas J. Dye^{23,24}, Frances Elmslie²⁵, Lars Feuk²⁶, Sixto García-Miñaur²⁷, Tracy Gertler²⁸, Elisa Giorgio²⁹, Nicolas Gruchy³⁰, Tobias B. Haack³¹, Chad R. Haldeman-Englert³², Bjørn Ivar Haukanes³³, Juliane Hoyer⁹, Anna C. E. Hurst³⁴, Bertrand Isidor^{19,20}, Maria Johansson Soller^{35,36}, Sulagna Kushary³⁷, Malin Kvarnung^{35,36}, Yuval E. Landau^{38,39,40}, Kathleen A. Leppig⁴¹, Anna Lindstrand^{35,36}, Lotte Kleinendorst⁴², Alex MacKenzie⁴³, Giorgia Mandrile⁴⁴, Bryce A. Mendelsohn⁴⁵, Setareh Moghadasi⁴⁶, Jenny E. Morton⁴⁷, Sébastien Moutton^{17,48}, Amelie J. Müller³¹, Melanie O'Leary¹², Marta Pacio-Míguez²⁷, María Palomares-Bralo²⁷, Sumit Parikh⁴⁹, Rolph Pfundt⁵², Ben Pode-Shakked^{40,51,52,53}, Anita Rauch⁵⁴, Elena Repnikova⁵⁵, Anya Revah-Politi^{36,56}, Meredith J. Ross⁵⁷, Claudia A. L. Ruivenkamp⁴⁶, Elisabeth Sarrazin⁵⁸, Juliann M. Savatt¹⁸, Agatha Schlüter¹, Bitten Schönewolf-Greulich³, Zahra Shad⁵⁹, Charles Shaw-Smith⁶⁰, Joseph T. Shieh⁶¹, Motti Shohat⁶², Stephanie Spranger⁶³, Heidi Thiese⁴¹, Frederic Tran Mau-Them¹⁷, Bregje van Bon⁵⁰, Ineke van de Burgt⁵⁰, Ingrid M. B. H. van de Laar⁶⁴, Esmée van Drie⁴², Mieke M. van Haelst⁴², Conny M. van Ravenswaaij-Arts¹⁵, Edgard Verdura¹, Antonio Vitobello¹⁷, Stephan Waldmüller³¹, Sharon Whiting⁴³, Christiane Zweier⁹, Carlos E. Prada^{24,65}, Bert B. A. de Vries⁵⁰, William B. Dobyns^{6,66,67}, Simone F. Reiter³³, Paulino Gómez-Puertas⁷, Aurora Pujol^{1,68,70} and Zeynep Tümer^{1,69,70} 

¹Neurometabolic Diseases Laboratory, Bellvitge Biomedical Research Institute (IDIBELL), L'Hospitalet de Llobregat, Barcelona, and Center for Biomedical Research on Rare Diseases (CIBERER), Madrid, Spain. ²Paediatric Neurology Unit, Hospital Universitari Germans Trias i Pujol, Universitat Autònoma de Barcelona, Barcelona, Spain. ³Kennedy Center, Department of Clinical Genetics, Copenhagen University Hospital, Rigshospitalet, Copenhagen, Denmark. ⁴Department of Gastroenterology and Hepatology, Radboud University Medical Center, Nijmegen, The Netherlands. ⁵Child Neurology Unit, Hospital Universitari Vall d'Hebron, Vall d'Hebron Research Institute (VHIR), Barcelona, Spain. ⁶Center for Integrative Brain Research, Seattle Children's Research Institute, Seattle, WA, USA. ⁷Molecular Modelling Group, Severo Ochoa Molecular Biology Centre (CBM SO, CSIC-UAM), Madrid, Spain. ⁸Bioscience Research Institute, School of Experimental Sciences, Francisco de Vitoria University, Pozuelo de Alarcón, Spain. ⁹Institute of Human Genetics, Friedrich-Alexander-Universität Erlangen-Nürnberg (FAU), Erlangen, Germany. ¹⁰Institute of Human Genetics, University of Leipzig Hospitals and Clinics, Leipzig, Germany. ¹¹Greenwood Genetic Center, Greenwood, SC, USA. ¹²Broad Center for Mendelian Genomics, Broad Institute of MIT and Harvard, Cambridge, MA, USA. ¹³Service de génétique, CHU de Tours, UMR 1253, iBrain, Université de Tours, Inserm, Tours, France. ¹⁴Graduate School of Biomedical Sciences, The University of Texas, MD Anderson Cancer Center UTHealth, Houston, TX, USA. ¹⁵Department of Genetics, University Medical Center Groningen, Groningen, The Netherlands. ¹⁶Center for Rett syndrome, Department of Pediatrics and Adolescent Medicine, Copenhagen University Hospital, Rigshospitalet, Denmark. ¹⁷INSERM UMR1231, GAD, University of Burgundy, FHU-TRANSLAD, CHU Dijon-Bourgogne, Dijon, France. ¹⁸Geisinger Autism & Developmental Medicine Institute, Lewisburg, PA, USA. ¹⁹Service de Génétique Médicale, CHU Nantes, Nantes, France. ²⁰Université de Nantes, CNRS, INSERM, l'institut du thorax, Nantes, France. ²¹Département de Génétique Médicale, Maladies rares et Médecine personnalisée, CHU Montpellier, France. ²²Department of Pediatrics, Amphia Hospital, Breda, The Netherlands. ²³Division of Neurology, Cincinnati Children's Hospital Medical Center, Cincinnati, OH, USA. ²⁴Department of Pediatrics, University of Cincinnati College of Medicine, Cincinnati, OH, USA. ²⁵South West Thames Regional Genetics Service, St George's University Hospitals, University of London, London, United Kingdom. ²⁶Science for Life Laboratory, Department of Immunology, Genetics and Pathology, Uppsala University, Uppsala, Sweden. ²⁷Institute of Medical and Molecular Genetics (INGEMM), La Paz University Hospital, Madrid, Spain. ²⁸Division of Neurology, Department of Pediatrics, Ann and Robert H. Lurie Children's Hospital of Chicago, Chicago, IL, USA. ²⁹Department of Medical Sciences, University of Turin, Torino, Italy. ³⁰Service de Génétique, CHU Caen Clemenceau, Biotargen, Univ Caen, France. ³¹Institute of Medical Genetics and Applied Genomics, University of Tübingen, Tübingen, Germany. ³²Mission Fullerton Genetics Center, Asheville, NC, USA. ³³Department of Medical Genetics, Haukeland University Hospital, Bergen, Norway. ³⁴Department of Genetics, University of Alabama at Birmingham, Birmingham, AL, USA. ³⁵Department of Clinical Genetics, Karolinska University Hospital, Stockholm, Sweden. ³⁶Department of Molecular Medicine and Surgery, Karolinska Institutet, Stockholm, Sweden. ³⁷Institute for Genomic Medicine, Columbia University Irving Medical Center, New York, NY, USA. ³⁸Leumit Health Care Services, Tel-Aviv, Israel. ³⁹Metabolic Disease Service, Schneider Children's Medical Center of Israel, Tel-Aviv, Israel. ⁴⁰Sackler Faculty of Medicine, Tel-Aviv University, Tel-Aviv, Israel. ⁴¹Genetic Services, Kaiser Permanente of Washington, Seattle, WA, USA. ⁴²Department of Clinical Genetics, Amsterdam UMC, University of Amsterdam, Amsterdam, The Netherlands. ⁴³Children's Hospital of Eastern Ontario, University of Ottawa, Ottawa, Canada. ⁴⁴Thalassemia Centre and Genetic Unit, San Luigi University Hospital, Orbassano, Italy. ⁴⁵Department of Pediatrics, Division of Medical Genetics, University of California, San Francisco, CA, USA. ⁴⁶Department of Clinical Genetics, Leiden University Medical Center, Leiden, The Netherlands. ⁴⁷West Midlands Regional Clinical Genetics Service and Birmingham Health Partners, Birmingham Women's and Children's Hospitals NHS Foundation Trust, Birmingham Women's Hospital, Birmingham, United Kingdom. ⁴⁸CPDPN, Pôle mère enfant, Maison de Santé Protestante Bordeaux Bagatelle, Talence, France. ⁴⁹Mitochondrial Medicine & Neurogenetics, Cleveland Clinic, Cleveland, OH, USA. ⁵⁰Department of Human Genetics, Radboud University Medical Center, Nijmegen, The Netherlands. ⁵¹Institute of Rare Diseases, Edmond and Lily Safra Children's Hospital, Sheba Medical Center, Tel-Hashomer, Israel. ⁵²Genomic Unit, Sheba Cancer Research Center, Sheba Medical Center, Tel-Hashomer, Israel. ⁵³Wohl Institute for Translational Medicine and Cancer Research Center, Sheba Medical Center, Tel-Hashomer, Israel. ⁵⁴Institute of Medical Genetics, University of Zurich, Schlieren, Switzerland. ⁵⁵Division of Clinical Laboratory Genetics & Genomics, Children's Mercy Hospital, Kansas City, MO, USA. ⁵⁶Precision Genomics Laboratory, Columbia University Irving Medical Center, New York, NY, USA. ⁵⁸Centre de Référence des Maladies rares neuromusculaires AOC, Hôpital Pierre Zobda Quitman, CHU Martinique, Fort de France, Martinique. ⁵⁹Cook Children's Medical Center Genetics, Fort Worth, TX, USA. ⁶⁰Department of Clinical Genetics, Royal Devon and Exeter NHS Foundation Trust, Exeter, United Kingdom. ⁶¹Institute for Human Genetics, University of California San Francisco, San Francisco, CA, USA. ⁶²Bioinformatics unit, Cancer Research Center, Sheba Medical Center and Sackler Medical Center, Tel Aviv University and Maccabi HMO, Tel Aviv, Israel. ⁶³Praxis fuer Humangenetik, Klinikum Bremen-Mitte, Bremen, Germany. ⁶⁴Department of Clinical Genetics, Erasmus MC, University Medical Center Rotterdam, Rotterdam, The Netherlands. ⁶⁵Division of Human Genetics, Cincinnati Children's Hospital Medical Center, Cincinnati, OH, USA. ⁶⁶Department of Pediatrics, University of Washington, Seattle, WA, USA. ⁶⁷Department of Neurology, University of Washington, Seattle, WA, USA. ⁶⁸Catalan Institution for Research and Advanced Studies (ICREA), Barcelona, Spain. ⁶⁹Department of Clinical Medicine, Faculty of Health and Medical Sciences, University of Copenhagen, Copenhagen, Denmark. ⁷⁰These authors share senior authorship: Aurora Pujol, Zeynep Tümer.

✉email: Zeynep.tumer@regionh.dk

SUPPLEMENTARY FIGURES

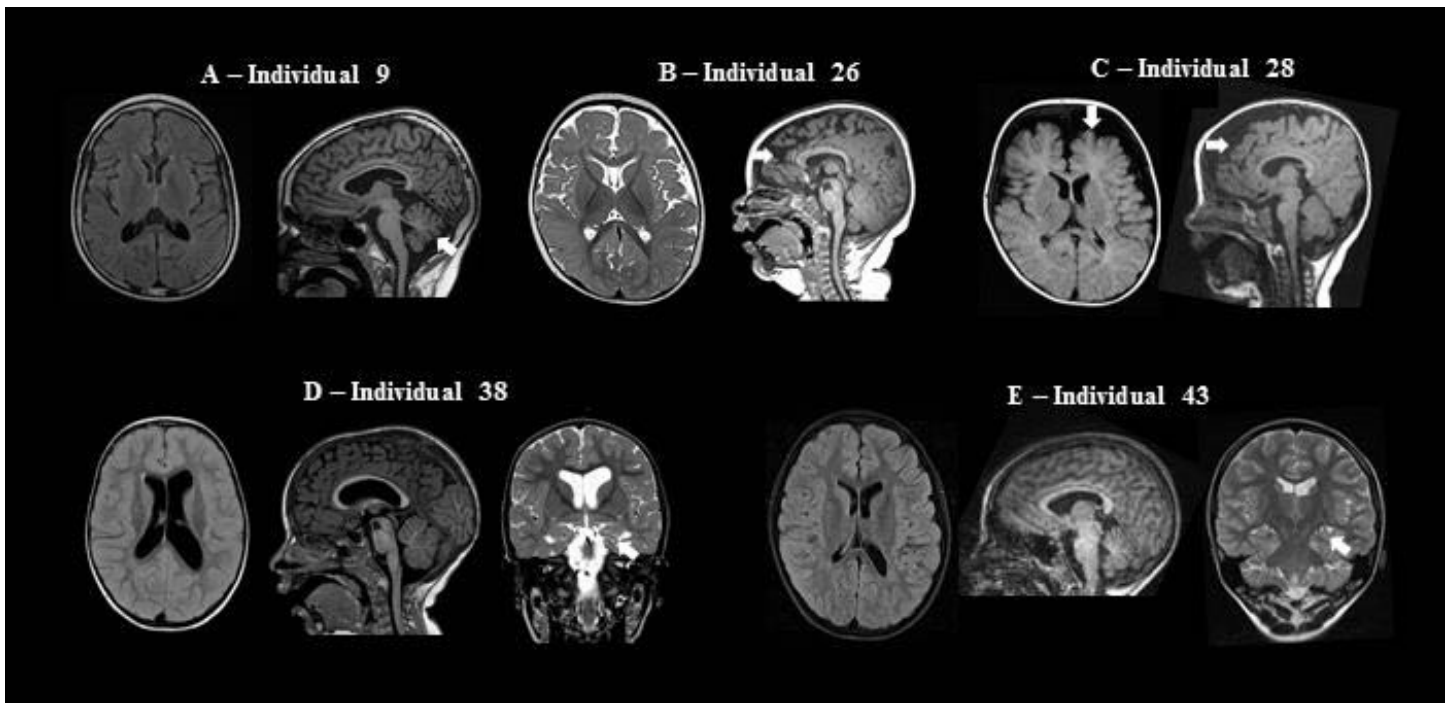


Figure S1 – MRI abnormalities identified in individuals with *DLG4* variants.

Images of individual 9 (**A**) show mild diffuse cerebral and cerebellar atrophy (arrow) with diffuse thinning of the corpus callosum. Individual 26 (**B**) and 28 (**C**) show marked frontotemporal cortical (arrow) and subcortical atrophy with enlarged anterior peripheral liquor spaces. Individual 26 (**B**) also has a dysmorphic corpus callosum (arrowhead) and a cavum septum pellucidum, whereas individual 28 (**C**) presents mild thinning of the anterior part of the corpus callosum (arrowhead). Individual 38 (**D**) and individual 43 (**E**) show incomplete inversion of the left hippocampus (arrow) with ipsilateral ventricle dilatation. Individual 38 (**D**) also presents diffuse thinning of the corpus callosum. MRI types: Axial T2-flair-weighted (A, B, D and E left image); Axial T1-weighted (C left image); Sagittal T1-weighted (A-C right, and D and E middle image); Coronal T2-weighted (D and E right image).

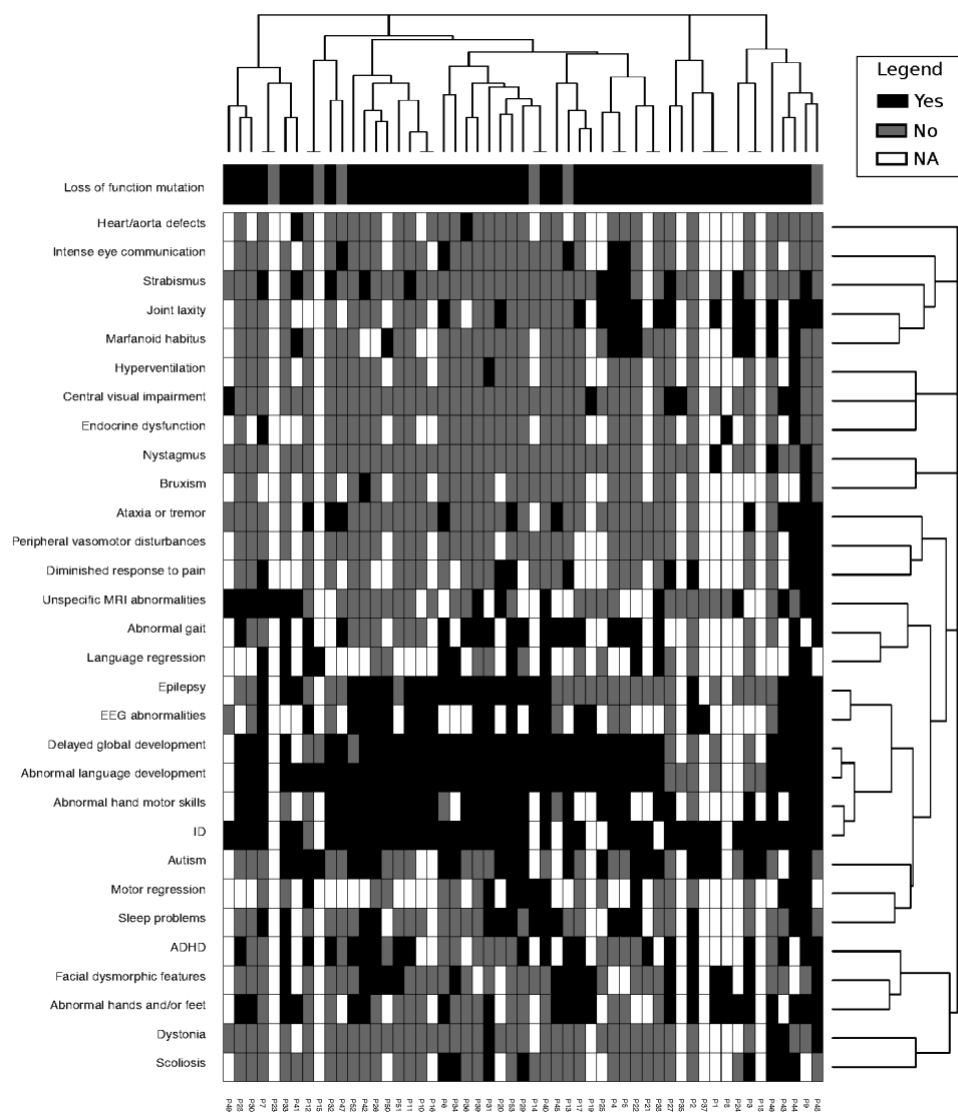


Figure S2 – Phenotype heat map

Heat map representing clinical manifestations (rows) of individuals with *DLG4* variants (columns). A black square indicates the presence of a manifestation in each individual and a gray square confirms its absence. White square represents that data are not available. A dendrogram above the heat map represents the binary similarities between individuals (the closer the junction to the bottom, the more similarity between two given individuals). Loss of functions (black) and missense variants (gray) are indicated by an additional panel below the heat map. Clinical manifestations are also ordered according to hierarchical clustering with the dendrogram shown in the right aspect of the figure. Heat map was built by means of gplots package in R and hierarchical clustering was made according to binary distances.

SUPPLEMENTARY TABLE

Supplementary Table 2 – Clinical features and their frequency in 53 individuals

Features	Total (n=53)	Percentage
Age at onset (mean)	1.3	
Current age (mean)	13.5	
Sex		
<i>Female</i>	23	43%
<i>Male</i>	29	55%
<i>Unknown</i>	1	2%
Global Developmental Delay	38/45	84%
<i>Regression</i>	17/43	39%
Intellectual disability	44/45	98%
<i>Mild</i>	13/45	29%
<i>Moderate</i>	15/45	34%
<i>Mild-Moderate</i>	1/45	2%
<i>Severe</i>	13/45	29%
<i>Unspecified</i>	2/45	4%
ASD	24/43	56%
ADHD	20/35	57%
Epilepsy	25/47	53%
<i>Severe/Refractory</i>	10/25	40%
Abnormal movements	19/41	46%
<i>Stereotypies</i>	12/41	29%
<i>Ataxia</i>	9/41	22%
<i>Dystonia</i>	4/41	10%
<i>Tremor</i>	3/41	7%
Hypotonia	23/43	53%
Ophthalmologic symptoms	23/46	50%
Anxiety	20/38	53%
Sleep problems	17/38	44%
Episodic vomiting	10/35	28%
Skeletal manifestations	23/44	52%
<i>Joint laxity</i>	16/44	36%
<i>Scoliosis</i>	9/44	20%
Facial Dysmorphology	15/39	38%
Marfanoid habitus	9/38	23%
MRI abnormalities	13/40	32%

STRUCTURAL MODELLING AND MOLECULAR DYNAMICS SIMULATION

Details of the methods

Structural modelling of DLG4 missense variants

The 3D structure of the human PSD-95 protein (UniProtKB id: P78352-2, The UniProt Consortium 2019) was modelled using as templates the homologous structures present in the Protein Data Bank: 1KJW (McGee *et al.*, 2001) and 2XKX (Fomina *et al.*, 2011) (Figure 4). Models for the wild type protein and the Gly220Val, Asp229Val, Gly241Ser, Asp375Gly, Arg629Gln and Thr654Ile variants were built using the SWISS-MODEL server (<https://swissmodel.expasy.org>), and their structural quality was within the range of that accepted for homology-based structure (Anolea/Gromos/QMEAN4) (Benkert *et al.*, 2011). Models were energy minimized using the GROMOS 43B1 force field implemented in DeepView (<https://spdbv.vital-it.ch/>), using 500 steps of steepest descent minimization followed by 500 steps of conjugate-gradient minimization.

Molecular Dynamics Simulation

Modelled structures were subjected to 100 ns of unrestrained Molecular Dynamics (MD) simulation using the AMBER18 molecular dynamics package (<http://ambermd.org/>; University of California-San Francisco, CA). 3D models were solvated with a periodic octahedral pre-equilibrated solvent box using the LeaP module of AMBER, with 12 Å as the shortest distance between any atom in the protein subdomain and the periodic box boundaries. Free MD simulation was performed using the PMEMD program of AMBER18 and the ff14SB force field (<http://ambermd.org/>), applying the SHAKE algorithm, a time step of 2 femtoseconds (fs) and a non-bonded cut-off of 12Å. Systems were initially relaxed over 10,000 steps of energy minimization, using 1,000 steps of steepest descent minimization followed by 9,000 steps of conjugate-gradient minimization. Simulations were then started with a 20 picoseconds (ps) heating phase, raising the temperature from 0 to 300 K in 10 temperature change steps, after each of which velocities were reassigned. During minimization and heating, the C α trace dihedrals were restrained with a force constant of 500 kcal mol $^{-1}$ rad $^{-2}$ and gradually released in an equilibration phase in which the force constant was progressively reduced to 0 over 200 ps. After the equilibration phase, 100 ns of unrestricted MD simulation were obtained for the structures. MD trajectories were analysed using VMD software (Humphrey *et al.*, 1996). Figures were generated using the PyMOL Molecular Graphics System (<https://pymol.org/>; Schrödinger, LLC, Portland, OR) (Figure 4).

Details of the results

To study the functional implications of the six missense *DLG4* variants p.(Gly220Val), p.(Asp229Val), p.(Gly241Ser), p.(Asp375Gly), p.(Arg629Gln) and p.(Thr654Ile), a 3D model of the wild type PSD-95 was generated using standard homology modelling-based techniques (Figure 4). Subsequently, models for the six PSD-95 mutants were generated using the wild type model as a template and subjected to 100 ns of unrestricted Molecular Dynamics (MD) simulation.

Three of the missense substitutions [p.(Gly220Val), p.(Asp229Val), p.(Gly241Ser)] occur in the PDZ2 domain of PSD-95. For the Gly220Val variant, substitution of a small amino acid (Gly220) by a larger one (Val220) leads to a conformational change of the PDZ2 domain. After 100 ns of molecular dynamics simulation, the loop where the mutated amino acid is located is repositioned to a location far from the core of the subdomain (Figure 4B).

In the wild type protein, the Asp229 residue forms a salt bridge with the adjacent Lys254 residue, and this interaction was stable during almost the entire simulation (Fig. 2C). The mutant Val229 variant on the other hand moved away from Lys254 which established a new salt bridge with Glu264. Consequently, the loop containing Val229 relocated away from the core domain modifying the structure of PDZ2. Notably, Tyr233 in the vicinity of Asp229 is a putative phosphorylation site (Hornbeck *et al.*, 2014) and Val229 would be predicted to modify the kinase/phosphatase recognition motif, potentially affecting the functionality of the protein.

Substitution of Gly with Ser at position 241 (Figure 4D) also suggested a structural change of the PDZ2 domain, although much less marked than the alteration in position 229 discussed above. In the wild type protein, Gly241 remained along the trajectory in a compact cluster with Gly214, with a distance between the C-alpha atoms of both amino acids around 4.25 Å. When Gly was replaced by Ser at position 241, the larger size of the serine residue caused the distance between Ser241 and Gly214 to oscillate reaching values up to 8.25 Å at specific events and values higher than 5.25 Å during more than 25% of the simulation time. These changes caused the disorganization of the small adjacent alpha-helix. In addition, the wild type Gly241 is part of the recognition motif for the ubiquitylation of the adjacent Lys245 residue in mouse (Wagner *et al.*, 2012; Hornbeck *et al.*, 2015) and replacement of Gly with Ser at position 241 is likely to alter the regulation of the ubiquitylation process. In gnomAD database, substitution of Gly241 with Arg was reported in heterozygote form in a single individual in Latino control population. We have also investigated the functional implication of this substitution and despite the larger size of the Arg, the structure of the protein did

not show a substantial change compared to wild-type protein and the adjacent alpha-helix was still in place, suggesting that this variant was likely benign.

Asp375 is located in a loop between two beta-sheets in the PDZ3 domain, which is enriched in negatively charged amino acids (Asp374, Asp375 and Asp377), and it is probably involved in the interaction with other adjacent structures such as potassium channels (Fomina *et al.*, 2011) (Figure 4E). The substitution of Asp by Gly at position 375 generated a decrease in the negative charge of the surface, which is likely to modify the nature of this interaction and affect its functionality.

The residues Arg629 and Thr654 are both located in the guanylate kinase-like domain (GKLD, Figure 4H). Arg629 is within a small alpha-helix and close to negative residues Glu630 and Glu633 (Figure 4F, above). Substitution of Arg with Gln at position 629 did not lead to an apparent change in the local structure after 100 ns of molecular dynamics, but a substantial difference in the distribution of surface charges was observed. In the wild type protein, the positive charge of Arg629 partially neutralized the negative charges of Glu630 and Glu633. However, substitution of Arg to Gln at position 629 resulted in the emergence of a negatively charged local patch (Figure 4F, below). This modification in surface charge may affect the interaction of PSD-95 with other proteins such as the potassium channels.

Thr654 is part of a group of amino acids, along with Arg611, Arg614, Tyr623, Glu643 and Tyr652, which occupy positions homologous to those forming the guanosine monophosphate (GMP) binding site in the yeast guanylate kinase enzyme (McGee *et al.*, 2001) (Figure 4G). In the yeast enzyme, the residue equivalent to Thr654 (Ser81 in yeast) binds the GMP guanine ring through a polar interaction. Substitution of Thr by Ile at this position would make such binding difficult, as well as modify the structure of the putative active site. In addition, the Ile654 would be expected to modify the kinase/phosphatase recognition motif for the phosphorylation of the nearby Tyr652 residue, predicted in the rat (Hornbeck *et al.*, 2015).

FUNDING INFORMATION

Sequencing and analysis of individual 53 were provided by the Broad Institute of MIT and Harvard Center for Mendelian Genomics (Broad CMG) and was funded by the National Human Genome Research Institute, the National Eye Institute, and the National Heart, Lung and Blood Institute grant UM1 HG008900 and in part by National Human Genome Research Institute grant R01 HG009141. T.B.H was supported by the Deutsche Forschungsgemeinschaft (DFG, German Research Foundation) – Projektnummer (418081722). The protein studies were supported by grants from the Spanish Ministry of Science, Innovation and Universities/State Research Agency RTC-2017-6494-1 and RTI2018-094434-B-I00 (MCIU/AEI/FEDER, UE) to P.G-P. as well as funds from the European JPIAMR-VRI network “CONNECT” to P.G-P. We thank CERCA Program/Generalitat de Catalunya for institutional support and Centro de Computación Científica CCC-UAM” for computational support. This study was supported by the Centre for Biomedical Research on Rare Diseases (CIBERER) [ACCI14-759], the URDCat program (PERIS SLT002/16/00174), the Hesperia Foundation and the Secretariat for Universities, Research of the Ministry of Business and Knowledge of the Government of Catalonia [2017SGR1206] to A.P. and by grants from the Dutch Organization for Health Research and Development, (ZON-MW grants 917–86–319 and 912–12–109 to B.B.A.d.V). C.Z. and B.P. were supported by grants from the German Research Foundation (DFG) (ZW 184-6/1, PO 2366/2-1). This publication was supported by the National Center for Advancing Translational Sciences, National Institutes of Health, through Grant Number UL1TR001873. The content is solely the responsibility of the authors and does not necessarily represent the official views of the NIH. We acknowledge the contribution of the DECIPHER Consortium. The DECIPHER (funding by the Wellcome Trust) study makes use of data generated by the DECIPHER community. A full list of centers who contributed to the generation of the data is available from decipher.sanger.ac.uk and via email from decipher@sanger.ac.uk.

VI. DISCUSSIÓ

Els trastorns genètics de la substància blanca cerebral (GWMDs) són un grup de malalties discapacitants, que es manifesten de forma diversa, però en les que predomina la simptomatologia motora. La majoria d'aquests trastorns s'inicien durant l'edat pediàtrica i molts d'ells són progressius. Establir un diagnòstic molecular és essencial per poder oferir a les famílies un assessorament genètic adequat, diagnòstic prenatal, informació en relació amb el pronòstic, possibles opcions de tractament, i facilitar l'accés als diferents serveis socials i associacions de pacients. A més, representa un pas fonamental per incrementar el coneixement dels diferents fenotips clínics i radiològics, per comprendre millor els mecanismes fisiopatològics implicats i facilitar així el desenvolupament de tractaments dirigits. Malauradament, la inespecificitat del quadre clínic i de l'afectació en els estudis de neuroimatge en molts dels casos, comporta que només es puguin diagnosticar la meitat mitjançant l'abordatge "clàssic", basat en l'orientació clínica a partir de la neuroimatge i els estudis bioquímics/metabòlics (van der Knaap *et al.*, 1999, 2019; Bonkowsky *et al.*, 2010; Vanderver *et al.*, 2016; Köhler *et al.*, 2018).

Durant el temps en el qual s'ha desenvolupat aquesta tesi doctoral, hi ha hagut un progrés important dels estudis genòmics, amb millors tècniques i un abaratiment del cost econòmic, que han permès la seva incorporació a la pràctica clínica habitual. La gran majoria dels estudis publicats fins al moment s'han basat en l'anàlisi de trios (analitzant les dades genètiques del cas índex i les dels seus progenitors simultàniament), el que facilita la identificació de variants patogèniques, especialment quan aquestes són *de novo* i en famílies amb consanguinitat. En canvi, en l'àmbit assistencial, l'estrategia utilitzada habitualment en el nostre entorn és la de l'anàlisi únicament de casos índex, donat que representa un cost econòmic que es calcula de dos a tres vegades menor que l'estrategia trio (Richards *et al.*, 2015a; Tan *et al.*, 2019). Per tant, era necessari establir el rendiment diagnòstic de l'estudi de casos índex en pacients amb GWMDs, tal com s'està duent a terme en l'àmbit assistencial. A més, quan s'avaluen pacients adults sovint no hi ha disponibilitat de mostres dels progenitors i l'estudi de cas índex és l'únic possible.

1. Elevat rendiment diagnòstic mitjançant l'estudi de casos índex

L'objectiu principal d'aquest treball era determinar la utilitat clínica dels estudis WES i WGS en casos índex amb GWMDs no diagnosticats, tot i haver-se realitzat un abordatge diagnòstic “clàssic” extens en la majoria dels pacients. **L'article 1 (Schlüter, Rodríguez-Palmero, Verdura et al., 2022)**, recull la sèrie més llarga de pacients amb GWMDs estudiada mitjançant WES i WGS publicada fins a l'actualitat. A més, inclou pacients de totes les edats (101 (80%) amb clínica d'inici en edat pediàtrica i 25 (20%) en edat adulta), oferint una visió global del diagnòstic dels GWMDs al llarg de la vida a Espanya (**les característiques de la cohort estan recollides a la taula 1 de l'article 1, pàgina 104**). El percentatge diagnòstic assolit és del 72%, superior al reportat en altres sèries de pacients amb GWMDs estudiades en la majoria de casos mitjançant estratègia trio, amb un cost econòmic probablement menor. Aquest alt rendiment representa que, donat que s'ha reportat que l'abordatge diagnòstic clàssic permet identificar aproximadament la meitat dels casos (Bonkowsky et al., 2010; Vanderver et al., 2016), la taxa de diagnòstic global dels GWMDs en l'actualitat podria situar-se al voltant del 80%.

L'estudi inicial mitjançant WES va permetre diagnosticar 74/126 famílies (59%), mentre que la reanàlisi periòdica anual va augmentar els diagnòstics a 86/126 (68%). Finalment, la realització de WGS en 16 dels 38 casos que quedaven negatius, va comportar el diagnòstic de cinc pacients més, arribant als 91 totals (**veure Figura 1 de l'article 1, pàgina 105**). Els gens identificats més freqüentment van ser *RNASEH2B*, *EIF2B5*, *POLR3A* i *PLP1*. En relació amb el patró de la neuroimatge, vam poder establir un diagnòstic en 57/86 (66%) de les formes no-hipomielinitzants i en 34/40 (85%) pacients amb trastorns hipomielinitzants.

La majoria dels diagnòstics eren de malalties autosòmiques recessives (60 casos), mentre que 22 eren autosòmiques dominants, 7 lligades a l'X i en dos casos vam identificar variants en més d'un gen amb patrons d'erència diferents (un amb herència AD i AR i l'altre AD i lligada a l'X). En quatre casos (4,4%) vam poder identificar canvis patogènics tipus CNV, una microdeleció 1p36 (LNF-36; **les característiques clíniques, radiològiques i diagnòstics de les famílies d'aquesta cohort poden consultar-se a la eTaula 1, material suplementari de l'article**

1, pàgines 122-129), una duplicació incloent els gens *HNRNPH1* i *RUFY1* (LNF-105), una duplicació que inclou *LMNB1* (LNF-34) i una deleció que comprèn el gen *TANGO2* (LNF-97).

Entre els pacients en els quals no vam poder assolir un diagnòstic, cal remarcar que hi ha una proporció més elevada de formes d'inici a l'edat adulta respecte als casos diagnosticats (30% contra 16%), de pacients amb alteracions quístiques en els estudis de neuroimatge (12% contra 5%) i menor proporció de famílies consanguínies (95% contra 82%). En relació amb el factor edat, el rendiment diagnòstic és més alt en població pediàtrica que en població adulta (77% en els d'inici de la clínica abans dels tres anys de vida, 73% en els de tres a divuit anys i 60% en els d'inici després dels divuit anys). Això pot venir determinat pel fet que les malalties d'inici en la vida adulta poden tenir més freqüentment una penetrància incompleta, el que dificulta l'anàlisi i interpretació de les dades genòmiques, donat que les variants genètiques causals poden trobar-se en un cert percentatge de població recollida com a "sana" en bases de dades poblacionals. A més, en aquesta franja d'edat hi ha una proporció major de malalties associades a causes poligèniques o variants somàtiques, i els factors ambientals juguen un paper probablement més important. Així i tot, el rendiment diagnòstic en la població adulta en aquesta cohort és molt elevat i supera el rendiment reportat en altres estudis (Lynch *et al.*, 2017; Wright *et al.*, 2018; Sainio *et al.*, 2022). Pel que fa a la major proporció d'anomalies quístiques entre els no diagnosticats, podria explicar-se pel fet que alguns d'aquests podrien correspondre a malalties mitocondrials no determinades, donat que tres d'aquests quatre casos s'han estudiat únicament per WES, o trastorns adquirits.

La comparació amb altres estudis de cohorts de GWMDs resulta difícil, donades les diferències pel que fa a les característiques poblacionals, criteris d'inclusió, aspectes tècnics i període de temps en el qual s'ha realitzat cadascun d'ells (amb el que implica de diferències en l'àmbit tecnològic i de coneixement). Aquest treball se suma a altres que han evidenciat que els estudis NGS representen una eina diagnòstica eficaç en diferents grups de patologies, especialment aquells amb una gran heterogeneïtat genotípica (veure Taula 1, pàgina 196).

A continuació, es fa referència als principals treballs de cohorts de pacients amb GWMDs estudiats mitjançant tècniques de seqüenciació massiva publicats fins a l'actualitat:

- En una cohort de 191 pacients pediàtrics amb GWMDs registrats en el *Myelin Disorders Bioregistry Project* (MDBP) i l'*Amsterdam Database of Unclassified Leucoencephalopathies*, es van diagnosticar 101 casos mitjançant la revisió de la clínica, la neuroimatge i els estudis bioquímics per part d'un grup d'experts. Dels restants, es van incloure 71 pacients pediàtrics per estudi WES en trios i es va arribar a un diagnòstic definitiu (amb variants patogèniques (P) o probablement patogèniques (LP)) en 25 casos (35%). Altrament, cinc casos més van ser considerats com probablement diagnosticats després de la identificació de variants VUS amb un fenotip clínic concordant, amb el que la taxa de diagnòstic total es va determinar en 42% (Vanderver *et al.*, 2016). Cal destacar que només 9 dels 25 casos amb diagnòstic definitiu corresponien a gens de leucodistròfia “clàssics”, mentre que la resta eren gens de leucoencefalopaties genètiques, d'acord amb la classificació establerta en una publicació de consens (Vanderver *et al.*, 2015). En una tercera fase de l'estudi, incloent-hi els 41 casos que encara persistien negatius, van establir un diagnòstic en 14 casos més: nou per reanàlisi de les dades del WES i cinc casos mitjançant WGS en trios, representant el 22% i el 12%, respectivament. Per tant, el rendiment conjunt dels estudis WES i WGS aplicats en aquesta cohort va ser d'un 62% (Helman *et al.*, 2020).

Comentari: en aquest treball, el filtratge de casos previ per part d'experts va comportar una menor proporció de gens de leucodistròfia “clàssica” o canònics en comparació amb la cohort presentada en **l'article 1 d'aquesta tesi doctoral** (36% versus 51%, respectivament), el que pot influir en el rendiment diagnòstic obtingut. De tota manera, el disseny de l'estudi d'aquesta tesi (sense un filtratge de casos per part d'experts en el camp dels GWMDs) probablement reflecteix millor la realitat del diagnòstic d'aquests trastorns, en què neuròlegs i neuroradiòlegs no especialitzats en aquest camp s'enfronten al repte diagnòstic que representen aquests pacients. Per altra banda, el rendiment reportat mitjançant l'estudi de reanàlisi del WES i WGS

en trios és inferior a l'obtingut en aquesta tesi en casos índex (24% (12/50) i 31% (5/16), respectivament).

- Un treball realitzat en una cohort de 100 pacients adults amb leucodistròfia estudiats per exoma dirigit va reportar una taxa diagnòstica del 26%. La realització posterior de WES en els casos negatius no va permetre identificar cap més diagnòstic (Lynch *et al.*, 2017).

Comentari: el rendiment diagnòstic en població adulta en aquesta tesi doctoral és del 60%, clarament superior.

- Una empresa de referència de diagnòstic genòmic dels EUA (GeneDx) va reportar en una comunicació, una sèrie de 541 casos de leucodistròfia, en la que el rendiment diagnòstic del WES va ser del 32%, incloent-hi estudi de trios i ànalisi de cas índex, i del 22,6% si es consideraven únicament aquests últims (Zou *et al.*, 2019).

Comentari: el menor rendiment diagnòstic respecte al reportat en aquesta tesi doctoral pot estar relacionat, almenys en part, amb el fet que en laboratoris de referència es disposa habitualment de menys informació clínica per l'anàlisi de les dades genòmiques i menys possibilitat d'intercanviar informació amb personal clínic. Per contra, s'ha reportat que els estudis realitzats en un entorn hospitalari o amb participació de clínics tenen habitualment un major rendiment diagnòstic (Clark *et al.*, 2018). A més, en els laboratoris de diagnòstic no es duu a terme habitualment la validació funcional de les variants VUS, el que també influeix probablement en el menor rendiment.

- En un article que feia referència a una cohort de 46 pacients, el rendiment diagnòstic d'un panell de gens (incloent-hi 134 gens) va ser del 41% (Cohen *et al.*, 2020b).

Comentari: en aquesta tesi doctoral, d'acord amb la classificació proposada per un comitè d'experts en trastorns de la substància blanca (Vanderver *et al.*, 2015), 46

(51%) dels diagnòstics obtinguts es poden classificar com a leucodistròfies i 45 (49%) com a leucoencefalopaties genètiques. Algunes d'aquestes últimes poden no estar incloses en els panells genètics de leucodistròfies, el que explica probablement per què el rendiment d'aquest tipus d'estratègia és més baix. A més, l'ús de panells de gens no permet la detecció de variants en gens candidats nous ni probablement algunes en gens de GWMDs descrits recentment (donat que els panells queden desfasats ràpidament).

- En un estudi prospectiu randomitzat controlat incloent 34 pacients, dut a terme en pacients pediàtrics amb un GWMD, es va demostrar que la utilització en primera línia de WGS té un rendiment diagnòstic superior al maneig clínic “clàssic” (56% versus 21%) i que permet escurçar el temps per assolir un diagnòstic (Vanderver *et al.*, 2020*b*).
- Finalment, molt recentment s'han publicat les dades de dues cohorts amb una alta taxa de consanguinitat:
 - En una cohort de 44 pacients de l'Iran, estudiats mitjançant un panell de gens (41 casos) i WES (tres casos) en probands, el rendiment diagnòstic va ser del 90% (Mahdieh *et al.*, 2021).
 - En una publicació d'un estudi realitzat a l'Índia incloent 104 famílies estudiades mitjançant aCGH i WES en cas índex, el rendiment diagnòstic va ser del 65% (Kaur *et al.*, 2021).

Comentari: respecte als dos darrers estudis presentats, cal destacar que l'elevada taxa de consanguinitat (82,5% i del 54,8%, respecte al 14% de consanguinitat en la cohort objecte d'estudi en aquesta tesi), facilita clarament la identificació de variants en l'anàlisi de panells i WES en casos índex. A més, en cap dels dos estudis no diagnostiquen cap malaltia amb patró d'erència AD (on l'anàlisi de trio facilita més la interpretació; mentre que en la nostra sèrie, un 24% dels diagnòstics són AD).

Estudi	N	Tècnica	Estratègia	Grup patologia	Rendiment Diagnòstic	Comentaris
(Yang <i>et al.</i> , 2013)	250	WES	Probands	Malalties genètiques (pediàtriques)	25%	80% fenotips neurològics
(Vissers <i>et al.</i> , 2017)	150	WES	Trios	Malalties genètiques (pediàtriques)	29,3%	Estratègia diagnòstica "clàssica": 7,3% diagnòstics
(Clark <i>et al.</i> , 2018) (meta-anàlisi)	20.068	CMA WES WGS	Probands Trios	Malalties genètiques (pediàtriques)	13% (CMA) 36% (WES) 40% (WGS)	
(Splinter <i>et al.</i> , 2018)	132	WES WGS	Probands Trios	Malalties genètiques	74%	40% patologia neurològica 21% canvis en tractament
(Lionel <i>et al.</i> , 2018)	103	WGS	Probands	Malalties genètiques	41%	
(Smedley <i>et al.</i> , 2021)	2.183	WGS	Probands Trios	Malalties genètiques	25%	25% canvis maneig clínic
(Bertoli-Avella <i>et al.</i> , 2021)	1.007	WGS	Probands Trios	Malalties genètiques	21,1%	Rendiment casos WES neg 14,5%
(Stranneheim <i>et al.</i> , 2021)	3219	WGS	Probands Trios	Malalties genètiques	40%	
(Shieh <i>et al.</i> , 2021)	50	WGS	Probands?	Malalties genètiques	40%	
(Sainio <i>et al.</i> , 2022)	100	Exoma clínic	Probands	Malalties genètiques (adults)	27%	
(Soden <i>et al.</i> , 2014)	119	WES WGS	Trios	TND	45%	Ràpid WGS: 11/15 famílies diagnosticades (73%)
(Gilissen <i>et al.</i> , 2014)	50	WGS	Trios	DI severa	42%	
(Srivastava <i>et al.</i> , 2014)	78	WES	Probands	TND	41%	Canvis maneig 100%
(Coutelier <i>et al.</i> , 2018)	319	Panell de gens	Probands	Atàxia cerebel-losa	22,6%	
(Zech <i>et al.</i> , 2020)	764	WES	Probands (81%) Trios (15%)	Distònia	19%	Canvis maneig 34%
(Schon <i>et al.</i> , 2021)	345	WGS	Probands (23%) Trios (42%)	Sospita mitocondrial	33%	
(Vanderver <i>et al.</i> , 2016)	71	WES	Trios	GWMDs	42%	
(Arai-Ichinoi <i>et al.</i> , 2016)	17	WES	Probands (53%) Trios (47%)	GWMDs hipomielinitzants	35%	
(Lynch <i>et al.</i> , 2017)	100	WES	Probands	GWMDs (adults)	26%	
(Helman <i>et al.</i> , 2020)	41	WGS	Trios	GWMDs	34%	
(Vanderver <i>et al.</i> , 2020b)	32	WGS	Trios	GWMDs	59%	Estudi Randomitzat Controlat
(Mahdиеh <i>et al.</i> , 2021)	44	Panell (n41) WES (n3)	Probands	GWMDs	90%	82,5% de famílies consang.
(Kaur <i>et al.</i> , 2021)	80	WES	Probands	GWMDs	66,67%	55% de famílies consang.

Taula 1. Principals estudis publicats de cohorts de pacients estudiades mitjançant WES/WGS. Inclou tant estudis realitzats en pacients amb malalties genètiques diverses (groc), pacients amb grups concrets de malalties neurològiques (taronja) i estudis realitzats en cohorts de pacients amb malalties genètiques de la substància blanca cerebral (GWMDs) (verd).

TND: Trastorns del Neurodesenvolupament.

Tot i l'elevat rendiment diagnòstic obtingut en aquesta tesi, cal remarcar que aquesta s'ha dut a terme en el context d'un projecte de recerca i no en l'àmbit clínic i, per tant, diversos factors fan que els resultats no siguin fàcilment extrapolables a la pràctica clínica habitual. Entre els aspectes que poden haver influït en aquest elevat rendiment diagnòstic, podríem destacar els següents:

- La interpretació de les dades dels pacients, obtingudes mitjançant un sistema bioinformàtic dissenyat en el mateix laboratori per la Dra. Àgatha Schlüter i en el context d'un equip especialitzat en leucodistròfies, són factors que poden haver contribuït a aquests bons resultats. Per aquest estudi, s'ha dissenyat un sistema de priorització que integra la informació clínica dels pacients en format HPO i de bases de dades que recullen informació de la interacció física i funcional de les proteïnes de l'organisme. A partir d'aquestes dades s'ha elaborat un interactoma ampliat, que ha permès la priorització de gens que prèviament no havien estat associats a GWMDs (veure secció Material i Mètodes, apartat 3).
- La implicació directa de professionals clínics (el doctorand com a neuropediatre i una neuròloga d'adults) en estreta col·laboració amb l'equip bioinformàtic encarregat de l'anàlisi de les dades genòmiques. Aquest entorn de treball ha afavorit l'intercanvi constant d'informació clínica i genètica, i la discussió de les variants prioritzaDES en reunions d'equip periòdiques. També hi ha hagut una comunicació fluida amb els metges referents de cada cas, que ha permès disposar d'informació clínica detallada de la majoria dels casos.

A més, convé subratllar que en alguns casos l'anàlisi del fenotip ha estat determinant per orientar l'estudi genòmic i poder identificar finalment variants intròniques no canòniques. En el pacient LNF-93, la presència d'una macrocefàlia progressiva i una RM que mostrava una hiperintensitat difusa de la substància blanca cerebral en T2 amb quists temporals, van orientar la cerca activa de variants a *MLC1*, on vam poder trobar la variant c.597 + 37C>G. En el cas LNF-37, el quadre clínic compatible amb una ovarioleucodistròfia amb hiperintensitats periventriculars i quists a la RM,

suggerien que la presència de variants als gens que codifiquen per proteïnes del complex eIF2B eren la possibilitat diagnòstica més probable, i així vam poder detectar la variant c.1156 + 13G>A a *EIF2B5*. En LNF-47, la presència d'hipodòncia va ser clau també per identificar una variant intrònica a *POLR3A* (c.1771 - 7C>G), responsable d'un fenotip clínic i radiològic particular, amb predomini de clínica extrapiroamidal i afectació estriatal a la neuroimatge (veure apartat 5 d'aquesta secció).

- Finalment, la possibilitat de realitzar en el context d'un estudi de recerca, els estudis funcionals adients per corroborar la patogenicitat de variants inicialment catalogades com a VUS en 14 dels 91 casos diagnosticats. Es va analitzar l'impacte de 8 variants sobre l'*splicing* mitjançant la seqüenciació d'ADNc (a partir d'ARN derivats de cèl·lules mononuclears de sang perifèrica o fibroblasts) o assaig de splicing de mini-gens (en tres casos). Els assajos de mini-gens van ser fonamentals per confirmar la patogenicitat de la variant intrònica en el gen *MLC1* (c.597 + 37C>G) (pacient LNF-93), gen no expressat en PBMC ni fibroblasts, una en el gen *SEPSECS* (c.114 + 3A>G) (LNF-121) i la variant intrònica a *EIF2B5* (c.1156 + 13G>A) (LNF-37). En aquest tercer cas, aquest estudi va permetre demostrar que aquesta variant genètica s'associava a la producció d'una proporció de proteïna normal i també proteïna anòmala resultant d'un splicing alterat. Això podria explicar el fenotip lleu amb inici a la vida adulta, en forma d'una ovarioleucodistròfia, que presentava la pacient reportada (Rodríguez-Palmero *et al.*, 2020) (**veure Annex, article A5**). En altres casos, es van realitzar estudis de lipidòmica dirigida, que van demostrar l'efecte deleteri de variants en gens relacionats amb el metabolisme lipídic (dos d'ells identificats per primera vegada): *ACER3*, *DEGS1* (Pant *et al.*, 2019) i *PI4KA* (Verdura and Rodríguez-Palmero *et al.*, 2021) (**article 2 d'aquesta tesi doctoral**) juntament amb qRT-PCR, Western-blot o immunofluorescència segons es va requerir.

Un altre objectiu era demostrar la superioritat de l'abordatge mitjançant NGS respecte a l'abordatge diagnòstic “clàssic” en els GWMDs. **L'article 1 d'aquesta tesi doctoral** descriu un alt rendiment diagnòstic en aquesta cohort de pacients que no havien pogut ser

diagnosticats mitjançant l'aproximació diagnòstica clàssica, demostrant aquesta superioritat dels estudis genòmics. La gran heterogeneïtat genètica d'aquests trastorns, les formes de presentació inespecífiques, incompletes o atípiques, i també amb fenotips clínics o radiològics nous, són els motius fonamentals que poden influir en aquesta superioritat diagnòstica de la tecnologia de seqüenciació massiva. També cal remarcar que la manca d'expertesa de la majoria dels neuròlegs i neuroradiòlegs en aquestes malalties dificulta l'establiment d'un diagnòstic de sospita clar basat en la clínica i exploracions de neuroimatge. De tota manera, l'estrategia diagnòstica "clàssica" segueix sent d'utilitat en molts casos, i la seva combinació amb els estudis genòmics probablement representa l'estrategia més eficient, com es descriu en el protocol d'estudi proposat a l'apartat 6 d'aquesta secció.

Probablement, l'ús de WES/WGS en trios podria haver permès assolir encara un millor rendiment diagnòstic en aquest treball i, sense dubte, hauria millorat els temps d'anàlisi de les dades genòmiques (Tan *et al.*, 2019). No obstant això, l'estudi de casos índex és l'utilitzat actualment en l'àmbit assistencial en el nostre entorn, i calia determinar-ne l'eficiència. A més, tenint en compte que en el moment de l'inici del treball els estudis d'exoma encara no s'havien estès pràcticament a l'àmbit clínic i la limitació dels recursos econòmics de la investigació, es va optar per la realització d'estudis WES/WGS només en cas índex. D'aquesta manera es va permetre la participació del nombre més gran de famílies possible. Tanmateix, en determinades situacions, com pot ser en el context de presa de decisions de maneig en pacients ingressats en una UCI, pot ser preferible la realització WES/WGS en trio, per tal d'aconseguir el màxim rendiment en el menor temps possible, tal com requereix aquest tipus de situacions (Petrikin *et al.*, 2015; Meng *et al.*, 2017; Kingsmore *et al.*, 2019; Stark and Ellard, 2022). En conclusió, la decisió d'emprar una estrategia de seqüenciació únicament del proband o de trio dependrà de la urgència clínica, del grup fenotípic a estudi, de les característiques familiars, de la disponibilitat d'ADN, i del finançament o recursos disponibles (Tan *et al.*, 2019).

2. Escurçament de temps per obtenir un diagnòstic genètic

És essencial destacar que les tècniques de seqüenciació massiva permeten establir un diagnòstic en un termini de temps clarament més curt que el que representa l'abordatge diagnòstic seqüencial. Això queda evidenciat quan es comparen els 4-12 mesos habituals per assolir un diagnòstic mitjançant l'estudi WES/WGS, amb els 6,3 anys d'evolució mitjana dels casos abans de la inclusió en aquest treball. És per això que a la literatura sovint s'ha anomenat a l'estratègia clàssica en la qual es realitzen diversos tipus de proves de forma seqüencial, com a "odissea diagnòstica" (Németh *et al.*, 2013; Bonkowsky and Keller, 2021). Aquest factor és determinant quan s'avalua la utilitat clínica, donat que el diagnòstic precoç permet oferir un assessorament genètic adequat a les famílies (sobretot tenint en compte que la gran majoria de pacients amb un GWMD són pediàtrics) i a més, la resposta als tractaments disponibles és molt més favorable quan aquests s'inicien abans que l'afectació de la substància blanca estigui massa avançada (Bonkowsky and Keller, 2021). També cal considerar que el menor temps necessitat per identificar l'etiologia redueix l'impacte del procés diagnòstic a nivell psicològic en el pacient i els seus familiars. Finalment, tal com s'ha comentat a l'apartat anterior, la situació en que aquesta diferència resulta més evident és en pacients en estat crític, quan l'anàlisi ultra ràpida de les dades genòmiques (en alguns casos inclús en menys de 24 hores) és determinant per poder escollir la millor actuació mèdica en cada cas (Petrikin *et al.*, 2015; Meng *et al.*, 2017; Kingsmore *et al.*, 2019; Stark and Ellard, 2022).

3. Implicacions del diagnòstic en el maneig dels pacients

Un aspecte fonamental a remarcar és el fet que, tot i que sovint s'assumeix que molts d'aquests trastorns no disposen d'un tractament curatiu, sí que hi ha mesures terapèutiques que poden implantar-se per tal d'optimitzar el maneig dels pacients. A més, en alguns casos hi ha tractaments que poden modificar el curs natural de la malaltia si s'instauren abans que l'afectació neurològica s'hagi desenvolupat. Aquest fet reforça la importància d'arribar a un diagnòstic molecular com més aviat millor (Bonkowsky and Keller, 2021). Així, a l'**article 1 de la present tesi** s'evidencia que establir un diagnòstic molecular pot comportar canvis

significatius en el maneig clínic en 29 dels 91 pacients diagnosticats (32%). En 22 d'ells, condueix a la consideració d'una opció de tractament específica per a la malaltia: el trasplantament de cèl·lules mare hematopoètiques (HSCT) per a la malaltia de Krabbe (pacients LNF-18, SPG-72) (**veure eTable 1 de l'article 1, pàgines 122-129**) i la leucoencefalopatia hereditària difusa amb esferoides (LNF-6, LNF-16, LNF-70, LMSR), el maneig dietètic de la fenilcetonúria (LNF-40), la piridostigmina per a la síndrome miastènica causada per *GFPT1* (LNF-88) i el tractament quelant del ferro per a l'aceruloplasminèmia (LNF-89). També pot afavorir el maneig de l'hipogonadisme en casos associats a *POLR3A* (LNF-1, LNF-56, LNF-118) i el tractament de la insuficiència ovàrica prematura associada a *EIF2B5* en LNF-37 (Rodríguez-Palmero *et al.*, 2020). La variant *CACNA1A* en LNF-56 pot comportar part de les manifestacions clíniques i, per tant, l'acetazolamida pot aportar beneficis clínics en aquest cas. En pacients diagnosticats d'AGS (LNF-32, LNF-69, LNF-76, LNF-80, LNF-90, LNF-95, LNF-120), es pot contemplar el tractament amb inhibidors de la quinasa Janus (JAK1/JAK2) així com el seguiment de les manifestacions immunomediades, mentre que en LNF-41 i LNF-42 (*DEGS1*), l'ús de fingolimod (Pant *et al.*, 2019) està actualment en estudi. En altres casos, el diagnòstic condueix a millorar el seguiment dels pacients, com ara la detecció de l'aparició de tumors en *PTEN* (LNF-109) o l'evitació de traumatismes cranials i infeccions en els pacients amb diagnòstic de VWMD. A més, es van revisar les troballes incidentals d'acord amb les recomanacions de l'ACMG (Kalia *et al.*, 2017), i es van identificar variants patogèniques en dos casos: una variant patògena en el gen *MYBPC3* (p.Trp792ValfsTer41) (pacient SPG-14) i una a *SMAD3* (síndrome de Loeys-Dietz) (p.Val363ThrfTer3) (LNF-48). En ambdós casos, això comporta un seguiment cardiològic, mentre que en el segon cas, indica la realització a més d'una RM angiogràfica cranial i controls ortopèdics.

4. Identificació de nous gens associats a GWMDs, descripció de noves malalties

Aquest estudi també ha permès la identificació de set nous gens associats a l'afectació de la substància blanca del cervell, tres dels quals han estat validats i publicats, mentre que els quatre restants estan en estudi actualment. En l'**article 2 d'aquesta tesi doctoral (Verdura**

and Rodríguez-Palmero *et al.*, 2021) es descriu un nou espectre fenotípic en 10 pacients amb variants bial·lèliques en el gen *PI4KA*, que poden originar des d'un retard psicomotor sever amb una leucodistròfia hipomielinitzant i alteracions estructurals del cervell (hipoplàsia del tronc de l'encèfal o del cerebel i polimicrogíria) (OMIM #616531), fins a una paraparèisia espàstica pura (OMIM #619621). Les formes severes es manifesten amb un retard global del desenvolupament ja des del primer any de vida. La majoria associen epilepsia, que pot aparèixer des del període neonatal. Les crisis són focals, mioclòniques, generalitzades o en forma d'espasmes infantils, i algunes d'elles apareixen en context de quadres infecciosos i poden ser perllongades. A més, alguns casos poden associar atàxia o un trastorn del moviment. Aquests pacients també poden presentar manifestacions no neurològiques: gastrointestinals (atrèsies intestinals múltiples o malaltia inflamatòria intestinal principalment, així com reflux gastro-esofàgic, restrenyiment, diarrea o vòmits), immunològiques (immunodeficiències combinades) i genitourinàries (criptorquìdia, quists renals o duplicació del sistema col·lector). En les formes clíniques lleus predomina la paraparèisia espàstica i pot associar-se també un trastorn cognitiu lleu (Salter *et al.*, 2021; Verdura and Rodríguez-Palmero *et al.*, 2021).

El gen *PI4KA* codifica per un enzim que participa en el metabolisme dels PI, fonamentals en processos de senyalització cel·lular, tràfic de membrana, regulació de canals iònics i també en processos de remodelació de l'actina, polarització de la membrana dels oligodendròcits i en la regulació de la composició lipídica de la seva membrana. Els processos de polimerització-despolimerització de l'actina intervenen en l'adaptació de la membrana de l'OD per embolcallar l'axó i també en la migració cel·lular durant el desenvolupament del cervell (Alvarez-Prats *et al.*, 2018). Per tant, la seva disfunció pot estar implicada en els defectes de la mielinització i les anomalies del SNC descrites en aquests pacients. A més, l'alteració del metabolisme dels PI desregula la via PI3K-AKT-mTOR, influeix en la polarització dels oligodendròcits i modifica els lípids de la seva membrana, el que també afecta la mielinització (Baskin *et al.*, 2016; Wolf *et al.*, 2021). Per altra banda, els ratolins *knock-out* per Pi4k2a, una altra cinasa implicada en la formació de PI(4)P a partir de PI, desenvolupen un quadre clínic similar a una paraparèisia espàstica hereditària i la inhibició de PI4K altera el transport axonal retrògrad de les neurotrofines, mecanisme implicat en les paraparèsies espàstiques i també depenen de l'activitat dels oligodendròcits (Bartlett *et al.*, 2002). Els

defectes de polarització a nivell intestinal s'han relacionat amb anomalies de la formació de la llum epitelial intestinal (Shewan *et al.*, 2011). Finalment, els PI actuen com a segons missatgers activant cascades de senyalització implicades en nombroses funcions de les cèl·lules immunitàries, des de la supervivència i el creixement cel·lular fins a l'adhesió i la migració cel·lular (Okkenhaug, 2013).

La majoria de les variants genètiques identificades en aquesta cohort són de canvi de sentit, i s'agrupen a prop del centre catalític o el domini “*cradle*”, alterant probablement a la funció catalítica de PI4KIIIα o a la formació del complex amb TTC7A o TTC7B (Salter, Cai, Lo and Helman *et al.*, 2021; Verdura and Rodríguez-Palmero *et al.*, 2021). Les variants de pèrdua de funció estan en heterozigosi composta amb una variant de canvi de sentit (*missense*) o sense canvi del marc de lectura (*in-frame*), i cap pacient té dues variants de pèrdua de funció. Curiosament, el pacient que presenta una polimicrogíria en l'estudi de neuroimatge, és homozigot per la variant p.(Asp1854Asn), que també està present en els tres fetus reportats amb polimicrogíria a les ressonàncies fetals en un estudi previ, tot i que en aquests casos la variant estava en heterozigosi composta amb una de pèrdua de funció (Pagnamenta *et al.*, 2015). Això suggereix que aquesta variant pot associar-se específicament a l'aparició d'aquesta malformació del desenvolupament cortical.

Les proves funcionals mitjançant *western blot* i immunofluorescència van mostrar una disminució dels nivells de PI4KA en els fibroblasts dels pacients. La immunofluorescència i els estudis de lipidòmica dirigida van indicar que l'activitat de PI4KA estava reduïda en fibroblasts i cèl·lules mononuclears de sang perifèrica dels pacients.

Un altre gen nou de malaltia de la substància blanca cerebral identificat en el context d'aquest projecte és *PRORP*, associat a la deficiència combinada de la fosforilació oxidativa 54, OMIM #619737) (Hochberg *et al.*, 2021) (**veure Annex, article A1**). Aquest gen codifica per la subunitat catalítica de la ribonucleasa P mitocondrial, una proteïna que participa en el processament de l'ARN mitocondrial. A través d'una col·laboració internacional vam poder participar en la descripció de quatre famílies amb un fenotip multisistèmic variable, que podia comprendre una pèrdua auditiva neurosensorial, una insuficiència ovàrica primària, un retard del desenvolupament o anomalies de la substància blanca cerebral

(Figura 14). En una de les famílies es descrivia també un pacient amb trets dismòrfics, acidosi làctica i una RM cranial amb heterotòpies nodulars periventriculars, un cos callós displàstic, pèrdua difusa de substància blanca subcortical i quists bilaterals congènits. Els estudis funcionals realitzats en fibroblastes de dues de les quatre famílies, van demostrar una disminució dels nivells de PRORP, una acumulació de transcrits mitocondrials no processats i una disminució dels nivells de proteïnes sintetitzades a nivell mitocondrial, que es recuperaven mitjançant la introducció d'ADNc de PRORP *wild-type*, així com una disminució del processament de mt-ARNt.

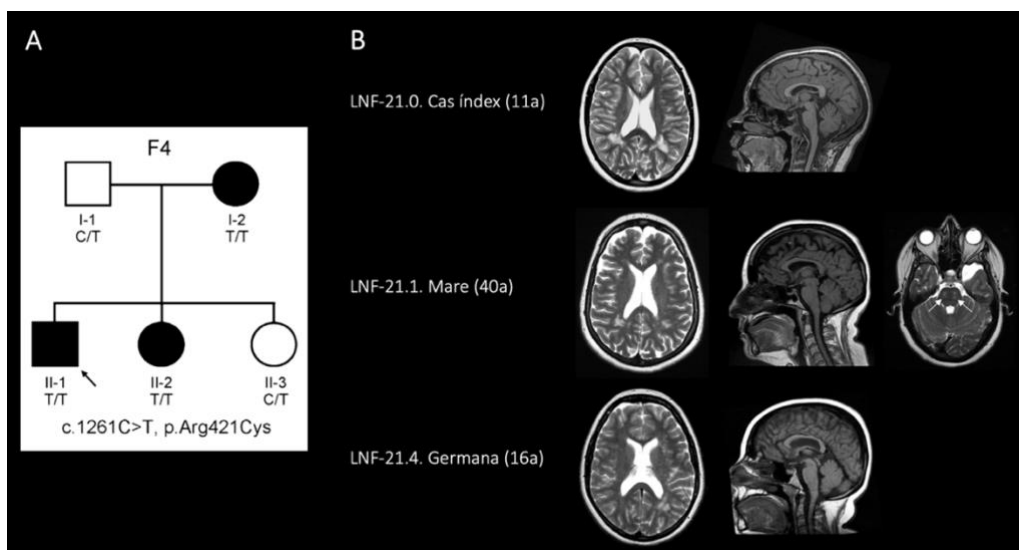


Figura 14. Família reportada en la descripció d'una nova malaltia mitocondrial multisistèmica associada a variants patogèniques en el gen *PRORP*. **A.** Arbre familiar amb tres pacients inclosos a l'estudi des d'IDIBELL (F4). **B.** Ressonància magnètica cranial del cas índex, la seva mare i la germana. Imatges axials potenciades en T2 que mostren lesions hiperintenses, nodulars, confluentes a la substància blanca periventricular i subcortical bilaterals, de predomini posterior. La mare afecta presenta també lesions hiperintenses al lemnisc medial i tracte tegmental central a la protuberància (fletxes). Adaptat de (Hochberg *et al.*, 2021).

En el context d'aquest projecte, també es van identificar dos pacients amb variants patogèniques en el gen *DEGS1*, que es van publicar conjuntament amb 17 casos més, per descriure una nova malaltia: la leucodistròfia hipomielinitzant tipus 18 (OMIM #618404) (Pant *et al.*, 2019). Els pacients inclosos presentaven un trastorn neurològic caracteritzat per un retard global del desenvolupament (o regressió del desenvolupament entre els 6-18 mesos), discapacitat intel·lectual en grau variable, tetraparèisia espàstic-distònica, epilepsia,

nistagme i un retard pondoestatural sever. Alguns dels pacients podien associar a més una neuropatia perifèrica. Els estudis de neuroimatge mostraven la presència d'hipomielinització, aprimament del cos callós, i atròfia talàmica i cerebel·losa progressives (Figura 15).

Els estudis funcionals van poder demostrar un augment de dihidroceramida i la proporció dihidroceramida/ceramida (DhCer/Cer) en fibroblasts i múscul dels pacients. Per altra banda, en un model de peix zebra es va poder evidenciar que el fingolimod, que inhibeix la ceramida sintasa en un pas previ a DEGS1, corregia les alteracions bioquímiques, millorava les alteracions motrius i augmentava el nombre d'oligodendròcits mielinitzants.

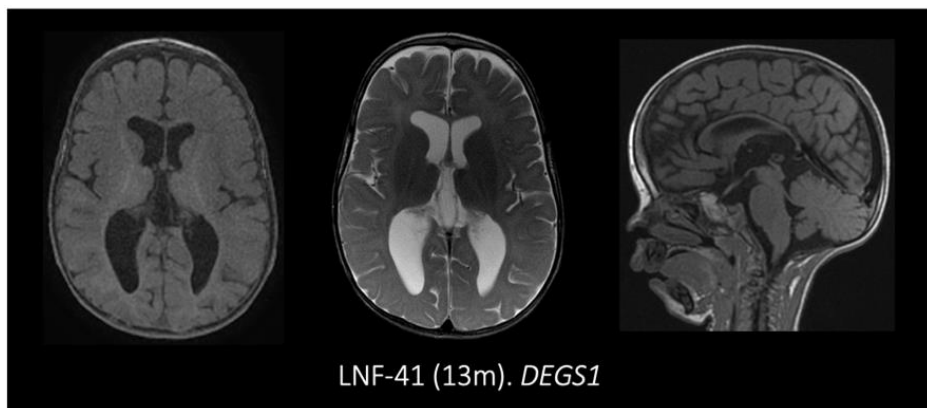


Figura 15. Estudi de RM d'un dels casos amb variants patogèniques a DEGS1. S'aprecia un patró d'hipomielinització amb una hipersenyal tènue difusa en la seqüència potenciada en T2 i també en T1, atròfia dels tàlems i un aprimament difús del cos callós.

5. Descripció de nous fenotips, diagnòstic de formes atípiques, malalties ultra rares o de molt recent descripció i fenotips complexos

La realització d'estudis WES/WGS permet identificar noves formes de presentació, quadres clínics incomplets o fenotips atípics, incrementant d'aquesta manera el coneixement del ventall fenotípic que pot associar-se a alguns dels gens de substància blanca.

Un dels pacients inclosos en la cohort objecte d'estudi en aquesta tesi presentava un fenotip clínic en el qual predominava una tetraparèisia espàstic-distònica amb bradicinèsia i atàxia. En l'estudi de neuroimatge s'apreciava una afectació estriatal bilateral amb lleu

hiperintensitat de les radiacions òptiques i dels peduncles cerebel·losos superiors (Figura 16). En aquest cas, el pacient presentava també hipodòncia, signe clínic que va guiar la reanàlisi del WES i va permetre detectar la presència de dues variants en el gen *POLR3A*, una de les quals era intrònica: c.1771-7C>G:p.? i c.3387C>A:p.(Leu1129Leu). Aquest pacient, juntament amb 8 casos més, va formar part d'un estudi en el qual es va descriure un nou fenotip clínic i radiològic associat a *POLR3A*. Els pacients presentaven una afectació clínica predominantment extrapiramidal, havent-se catalogat dos d'ells de parkinsonisme juvenil, i un patró en la RM caracteritzat per una hiperintensitat estriatal en T2 amb atròfia i una afectació també dels peduncles cerebel·losos superiors. Curiosament, tots els pacients presentaven en un dels alels una de les següents variants intròniques, c.1771-6C > G o c.1771-7C > G, en heterozigosi composta amb una altra variant del gen *POLR3A*. (Harting *et al.*, 2020) (**veure Annex, article A3**).

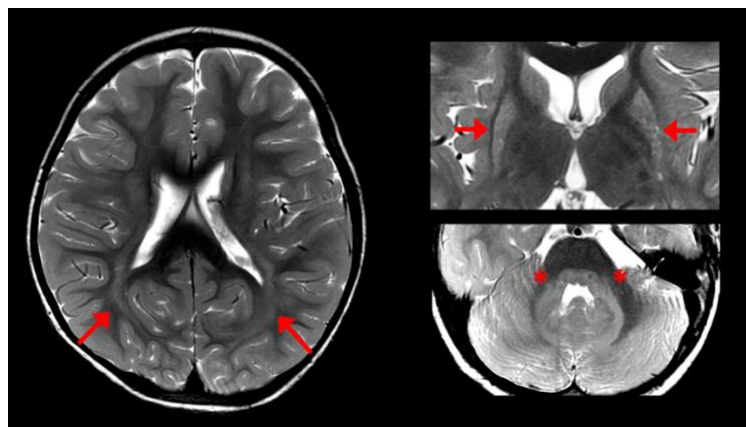


Figura 16. Imatges de RM cranial del pacient amb afectació predominant estriatal i variants patogèniques en el gen *POLR3A*. (LNF-47, 2 anys). S'aprecia lleu hiperintensitat de la substància blanca a les radiacions òptiques (fletxes), atròfia estriatal (fletxes curtes) i hiperintensitat dels peduncles cerebel·losos superiors (asteriscs) (Talls axials potenciatats en T2). Adaptat de (Harting *et al.*, 2020).

Vam poder participar en la descripció fenotípica de set pacients amb variants en el gen *HNRNPH1*. Les manifestacions clíiques incloïen trets facials dismòrfics distintius, augment de la incidència d'anomalies craneals, del paladar i cerebrals, així com malformacions genitourinàries i un augment de la incidència d'anomalies oftalmològiques. Per altra banda, en comparació amb els pacients amb discapacitat intel·lectual lligada a l'*X* associada a *HNRNPH2*, *tipus Bain* (MRXSB), presentaven una menor incidència d'epilèpsia i defectes

cardíacs. Això suggereix que les variants patògenes de *HNRNPH1* donen lloc a una causa sindròmica relacionada, però diferent, del quadre clínic associat a *HNRNPH2*. Els pacients amb variants que afecten el *nuclear localization sequence* (NLS), requerit per l'entrada de la proteïna al nucli de la cèl·lula per poder realitzar la seva funció, semblen associar-se a un fenotip clínic més sever (Reichert *et al.*, 2020) (veure Annex, article A4).

Un punt rellevant a destacar és la gran heterogeneïtat genètica que presenten els GWMDs, com demostra el fet que s'han identificat 57 gens diferents entre els 91 casos diagnosticats. La meitat dels diagnòstics corresponen a malalties classificades com a leucoencefalopaties genètiques d'acord amb la classificació proposada per un panell d'experts (Vanderver *et al.*, 2015), i no leucodistròfies clàssiques, el que pot justificar el menor rendiment dels panells de gens, que poden no incloure una proporció significativa d'aquests gens (Cohen *et al.*, 2020b). A més, en nou famílies (10%), s'han identificat variants en gens associats principalment a paraparèsia espàstica hereditària (*SPG11*, *SPG7*, *SPAST*, *DDHD2*, *CAPN1* i *CYP2U1*), subratllant la noció d'un espectre clínic continu d'aquests dos grups de malalties, de manera similar a l'X-ALD, PMD/SPG2, MLD o AxD (Müller vom Hagen *et al.*, 2014) (veure Figura 3 de l'article 1, pàgina 108).

L'article 3 d'aquesta tesi doctoral (Rodríguez-Palmero *et al.*, 2021) és un clar exemple del fet que alguns d'aquests pacients no haurien estat identificats mitjançant l'estudi de panells de gens. Aquesta publicació descriu les manifestacions clíniques i aspectes moleculars de 53 pacients amb variants en heterozigosi en el gen *DLG4*, que codifica per la proteïna postsinàptica PSD-95. El fenotip clínic dels es caracteritza fonamentalment per un retard del desenvolupament/discapacitat intel·lectual, trets autístics, trastorn per dèficit d'atenció amb hiperactivitat (TDAH), epilepsia (que en alguns pacients pot ser en forma d'espasmes infantils o punta-onà contínua del son (POCS)) o trastorns del moviment. Per tant, la forma de presentació clínica és similar a la d'altres sinaptopaties. Així i tot, resulta interessant el fet que en alguns d'ells associen signes de via piramidal i una afectació de la substància blanca cerebral, que pot ser en forma d'atròfia, retard de la mielinització o hiperintensitats periventriculars. Aquests trets són poc freqüents en els trastorns sinàptics i, per tant, dificulen clarament l'orientació clínica en aquests casos. Cal recordar que l'activitat sinàptica i la transmissió dels impulsos elèctrics a través de l'axó són un estímul fonamental

per la formació-manteniment de la mielina, el que pot explicar que en alguns d'aquests pacients pugui haver-hi anomalies de la substància blanca, encara que siguin habitualment menors. La majoria dels pacients tenen variants genètiques de pèrdua de funció, i només en sis casos les variants eren de canvi de sentit. En aquests casos, estudis realitzats mitjançant el modelatge de proteïnes suggerien canvis estructurals o funcionals a conseqüència de les variants genètiques.

A més, en aquest treball també hem pogut diagnosticar casos de malalties que infreqüentment s'associen un trastorn de la substància blanca cerebral, malalties ultra rares o de molt recent descripció. Per tant, casos que molt difícilment es podien haver orientat des del punt de vista clínic (Figura 17).

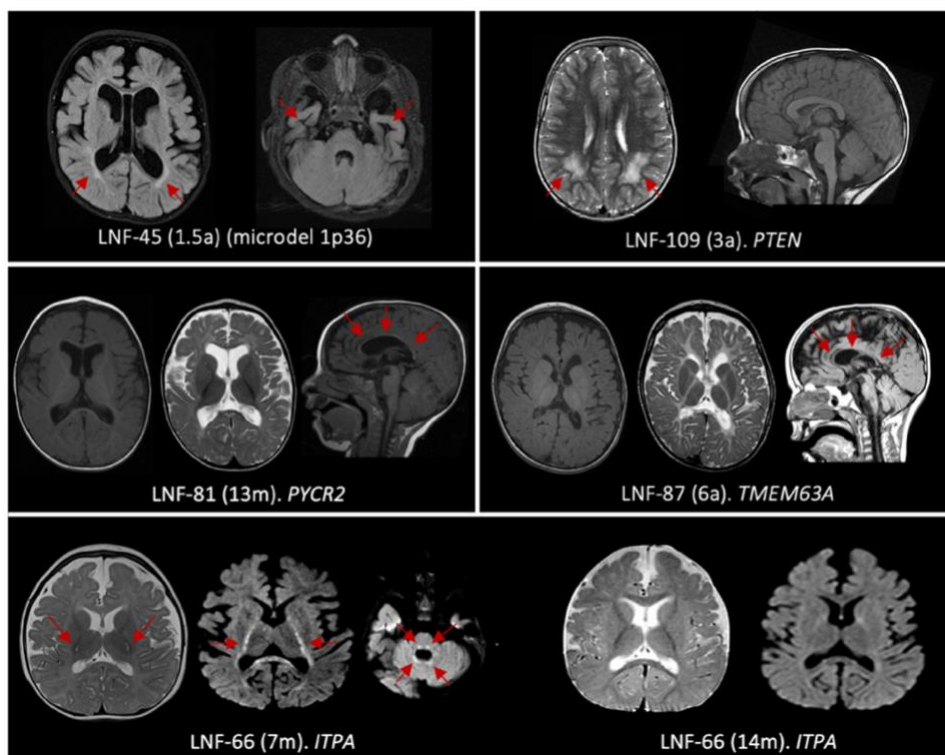


Figura 17. Estudi de RM d'alguns pacients identificats amb malalties que rarament associen una afectació de substància blanca i ultra rares. LNF-109. PTEN; p.Pro213LeufsTer8 (HTZ). Hiperintensitats periatrials bilaterals. També hiperintensitats nodulars bilaterals frontals de distribució més subcortical (T2 axial, T1 sagital). LNF-45. Síndrome de microdeleció 1p36. Hiperintensitat de la substància blanca periventricular, ventricle laterals dilatats amb persistència de *cavum septum pellucidum* i imatges pseudoquísticas a zones temporals anteriors, que corresponen en realitat a solcs amples per atròfia (T2-FLAIR axial). LNF-81 PYCR2; p.Arg125Trp/p.Leu66Arg (COMP HTZ). Hiperintensitat tènue de la substància blanca cerebral compatible amb hipomielinització, difusa, amb aprimament difús del cos callós i atròfia cortico-subcortical de predomini anterior (T1 i T2 axials, T1 sagital). LNF-87. TMEM63A. p.Gly567Val (HTZ). Hipomielinització generalitzada amb aprimament difús del cos callós i signes d'atròfia del tronc de l'encèfal i cerebel (T1 i T2 axials, T1-FLAIR sagital). LNF-66. ITPA; p.Tyr113SerfsTer46/p.Gly123SerfsTer104 (COMP HTZ). (7 m): hiperintensitat T2 de la via piramidal en el braç posterior de la càpsula interna (fletxes). L'estudi de difusió mostra un augment del senyal bilateral al braç posterior de la càpsula interna, radiacions òptiques i tronc de l'encèfal. (14 m): el seguiment mostra la resolució d'imatges hiperintenses però un augment de l'atròfia cerebral i persistent retard de la mielinització.

En 5 famílies (5,5%) es van identificar variants en més d'un gen, que vam considerar que contribuïen al fenotip dels pacients (**veure resums clínics d'aquests casos en el material suplementari, i Figura 2 de l'article 1, pàgines 116-118 i 107 respectivament**).

A més, en l'estudi d'aquesta cohort vam poder descriure 73 variants genètiques no reportades prèviament, el que és fonamental per facilitar el diagnòstic per part d'altres professionals d'arreu del món.

Finalment, amb la informació obtinguda en aquest treball, vam generar una xarxa d'interactoma ampliada que facilitarà la identificació de nous gens candidats de malalties de la substància blanca cerebral, expandint l'espectre mutacional i fenotípic, el que ajudarà a una millor comprensió de mecanismes fisiopatològics implicats en els trastorns de la formació i manteniment de la mielina (**Figura 4 de l'article 1, pàgina 110**).

6. Proposta de protocol d'estudi dels GWMDs

Els resultats d'aquest treball poden ser d'utilitat per considerar una proposta de protocol d'estudi dels GWMD en el nostre entorn, que guardaria similituds amb altres propostes recents aparegudes a la literatura (van der Knaap *et al.*, 2019) (Figura 18). La ressonància magnètica nuclear segueix tenint un paper fonamental en el procés diagnòstic, donat que permet sospitar que el pacient té un GWMD i a més, orientar el diagnòstic del pacient classificant les anomalies d'acord amb els patrons d'afectació descrits a la literatura (Schiffmann and van der Knaap, 2009; Parikh *et al.*, 2015). En alguns casos, el quadre clínic i el patró de la neuroimatge pot ser característics d'un diagnòstic concret, i pot conduir a la realització d'estudis metabòlics o genètics dirigits a aquesta sospita. Així i tot, en molts altres, el patró clínic és inespecífic o pot associar-se a diferents causes moleculars, i és en aquests en els que estaria indicada la realització en primera línia d'un estudi de seqüenciació massiva (preferiblement WES o WGS), tal com també s'ha suggerit en altres publicacions recents (Vanderver *et al.*, 2016, 2020b; van der Knaap *et al.*, 2019; Helman *et al.*, 2020). Això permetria guanyar un temps preciós, que és fonamental per establir un assessorament genètic adequat i un tractament específic si n'hi ha disponible, normalment indicat només

en estadis inicials d'aquestes malalties. A més, d'aquesta manera s'evitaria la realització de múltiples proves complementàries amb una baixa relació cost-benefici. Així i tot, sempre s'han de tenir en compte els estudis metabòlics de primera línia, essencials per poder identificar malalties potencialment tractables, i que haurien de considerar-se abans o en paral·lel amb el WES/WGS (van der Knaap *et al.*, 2019, Vanderver *et al.*, 2020*b*). En cas de no haver pogut trobar un diagnòstic molecular concret, caldria considerar la possibilitat de consultar centres experts en aquest grup de malalties o participar en estudis per la identificació de nous gens implicats en els GWMDs a través de consorcis internacionals.

En el cas dels GWMDs, que s'associen a un grup relativament restringit de gens, la realització de l'estudi WES (o preferiblement WGS) només en casos índex sembla raonable, tal com demostra el bon rendiment d'aquesta estratègia en la cohort presentada. En grups de malalties més inespecífiques (com la discapacitat intel·lectual) o fenotips més complexos que afecten diversos òrgans, el nombre de gens/variants a considerar sol ser més alt i caldria valorar si aquests casos pogués ser preferible l'estratègia trio.

La implantació sistemàtica de la tecnologia NGS en la pràctica clínica pot conduir en un futur pròxim a l'aproximació diagnòstica basada en el genotipatge inicial. A partir d'aquest, resultarà fonamental la interacció entre genetistes i clínics per determinar la correlació entre les possibles variants genètiques identificades i el fenotip del pacient (Srivastava *et al.*, 2014; Stessman *et al.*, 2014). Per tant, la implantació d'aquesta tecnologia, que obre un camp enorme de possibilitats, pot comportar una revolució completa del procés diagnòstic en el camp de les malalties minoritàries.

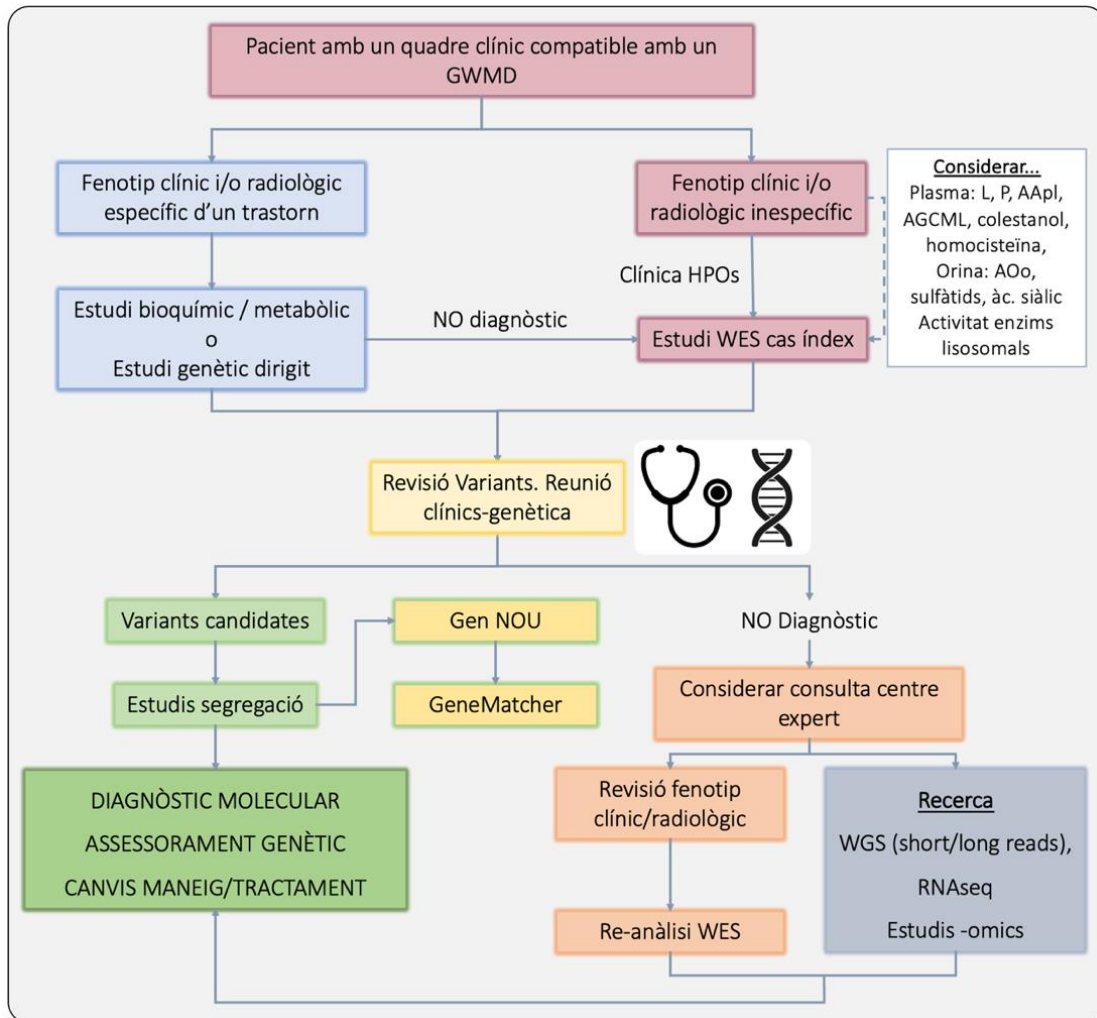


Figura 18. Proposta d'algoritme diagnòstic dels GWMDs en el nostre entorn. En els pacients amb un fenotip clínic i radiològic característic d'una malaltia concreta, es pot valorar la realització d'estudis bioquímics/metabòlics o genètics dirigits per mirar de confirmar aquesta sospita diagnòstica. En aquells amb un patró fenotípic inespecífic, hauria de considerar-se la realització d'un exoma clínic/WES/WGS com a primera línia de diagnòstic, basant l'anàlisi de variants en una caracterització completa del fenotip del pacient i patró d'erència sospitat. És fonamental l'intercanvi d'informació entre clínics i genetistes a l'hora d'interpretar els resultats. En casos amb estudi no informatiu, pot ser necessari l'assessorament per part d'un centre expert per revisar el fenotip clínic o un centre de recerca especialitzat per reavaluar el cas i considerar la realització d'altres tècniques d'estudi.

7. Limitacions del treball

El nostre protocol d'estudi té certes limitacions. En primer lloc, la seva naturalesa multicèntrica comporta que els estudis paraclínics realitzats abans de la inclusió dels pacients a l'estudi siguin heterogenis i depenguin de la disponibilitat de recursos en els diferents centres participants. En la majoria de casos, aquests havien estat exhaustius (estudis metabòlics en un 92% dels casos, diferents tipus d'estudis neurofisiològics en un 78%, estudis genètics no dirigits (aCGH, cariotip o panell de gens) en un 51% i estudis genètics dirigits en un altre 51%), però en d'altres eren més limitats (**veure Taula 1 de l'article 1, pàgina 104**). Cal esmentar que hem considerat com a diagnosticats 5 casos amb variants genètiques de significat incert seguint els criteris de l'ACMG, que no podien validar-se funcionalment. No obstant això, la revisió acurada del fenotip d'aquests pacients ens va dur a considerar que aquestes variants explicaven la presentació fenotípica amb una alta probabilitat i, per tant, es van considerar com a resolts. A més, els estudis WGS es van prioritzar només en 16 dels 38 casos negatius restants (42%) a causa de la disponibilitat limitada d'ADN dels pares per realitzar recursos de segregació i per motius de finançament. Posteriorment, hem pogut realitzar estudis WGS en aquests casos, que estan sent analitzats actualment.

Finalment, un aspecte important a considerar és el fet que aquest estudi ha estat realitzat en el marc d'un projecte de recerca, i, per tant, els resultats no són fàcilment extrapolables a la pràctica clínica habitual. De tota manera, evidencia l'elevada rendibilitat diagnòstica que pot permetre aquesta tecnologia, en un termini curt de temps en molts dels casos, i això ha de servir com a model per replantejar l'abordatge diagnòstic d'aquests pacients, tal com he proposat en l'apartat 6 d'aquesta secció.

8. El futur dels trastorns genètics de la substància blanca cerebral

Els darrers anys, hem viscut avenços rellevants en el camp del diagnòstic dels GWMDs, que han vingut fonamentalment de la mà de les noves tècniques genòmiques. Aquestes evolucionen ràpidament, s'incorporen progressivament a la pràctica clínica diària i estan

suposant un canvi de paradigma del procés diagnòstic, cada vegada més centrat en la genòmica. És per això que es necessita que els diferents professionals implicats en aquest procés (genetistes, assessors genètics i personal clínic) tinguin una formació específica en aquest camp, per tal de comprendre millor els avantatges i inconvenients d'aquestes tècniques, i la interpretació dels resultats que se'n desprenden. A més, és necessària la creació d'equips multidisciplinaris en l'àmbit hospitalari, que puguin participar en la interpretació dels resultats, compartir informació i alhora estar comunicats amb laboratoris de recerca que col·laborin en la validació de variants genètiques que ho requereixin.

El progressiu abaratiment dels costos dels estudis de seqüenciació massiva i els avenços en la interpretació de les variants en regions no codificant, probablement afavoriran la utilització de WGS a la pràctica clínica habitual, tenint en compte els avantatges que ofereix respecte als panells de gens o l'estudi de l'exoma (veure apartat 5.2.2.2) (Wright *et al.*, 2018). També s'imposarà probablement la seqüenciació de lectures més llargues (en anglès, *Long-Read Sequencing* o seqüenciació de tercera generació), que facilita la identificació de variants en regions complexes i la detecció de variants estructurals (Pollard *et al.*, 2018). Alhora, la millora de les tècniques bioinformàtiques d'anàlisi probablement comportarà una major automatització del procés d'interpretació de les variants. Per altra banda, la informació cada vegada més completa recollida en les diferents bases de dades genètiques poblacionals, permetrà una millor interpretació de les variants i la reducció de la proporció de variants VUS.

Un aspecte a desenvolupar és el millor coneixement dels mecanismes implicats en la interacció entre les variants genètiques, intervenint en l'expressió fenotípica de les malalties. Rarament, una única variant genètica és responsable del fenotip d'un pacient sinó que, per contra, l'efecte d'aquesta variant principal es veu influenciat per altres amb un efecte modest i moltes altres amb un efecte menor (principalment en regions no codificant del genoma). A més, l'expressió resultant d'aquest conjunt de factors genètics es veu influenciada per components ambientals que poden afectar la seva penetrància i expressivitat. La major comprensió d'aquestes interaccions ajudarà a conèixer els mecanismes que fonamenten la variabilitat fenotípica que presenten molts d'aquestes malalties. D'aquesta manera, a través de la integració de puntuacions de risc genètic,

podrem estratificar el pronòstic i personalitzar el maneig que requereix cada pacient (Wright *et al.*, 2018). El desenvolupament dels estudis multiòmics, que integren les dades obtingudes de la genòmica, transcriptòmica, epigenòmica, metabolòmica i proteòmica, son fonamentals per avançar en aquesta direcció i també permetran incrementar el rendiment diagnòstic i facilitaran el desenvolupament de tractaments dirigits.

El millor coneixement dels mecanismes fisiopatològics que està comportant la utilització dels estudis genòmics afavorirà la investigació en noves aproximacions terapèutiques, modulant processos metabòlics específics de cada malaltia, com per exemple oligonucleòtids antisentit o teràpies basades en cèl·lules mare. A més, és esperable que hi hagi un avenç en les tècniques d'edició genètica. Altrament, la utilització de línies cel·lulars o organoids derivats de cèl·lules mare pluripotents induïdes (iPSC), facilitaran el desenvolupament de fàrmacs per poder realitzar assajos clínics. En paral·lel, també caldrà dissenyar assaigs clínics i estudis multicèntrics que permetin conèixer millor la història natural dels diferents GWMDs, factors que poden influir-hi i biomarcadors per avaluar la resposta als nous tractaments.

L'evidència científica acumulada fins a l'actualitat suggerix que la instauració del tractament abans que es produueixi una afectació significativa de la substància blanca és fonamental per aconseguir una bona resposta al mateix (Adang *et al.*, 2017; Bonkowsky and Keller, 2021; Bradbury and Ream, 2021). Tenint en compte que moltes formes s'inicien ja en els primers mesos de vida, el desenvolupament de noves estratègies terapèutiques comportarà un major interès per incorporar algunes d'aquestes malalties a l'estudi de cribatge neonatal (Bonkowsky and Keller, 2021).

Per altra banda, en el camp de la neuroimatge també s'estan desenvolupant tècniques que podrien servir com a biomarcadors de l'evolució en el temps de la mielinització i determinar de forma més precisa la resposta a tractaments que puguin desenvolupar-se. Aquestes tècniques permeten quantificar la mielina de la substància blanca cerebral i avaluar la integritat de la seva microestructura. L'aigua retinguda intramielinica disminueix quan la substància blanca està totalment mielinitzada i pot mesurar-se a través de l'estudi dels temps de relaxació de la substància blanca en T1 i T2 (MacKay and Laule, 2016). També es

pot avaluar el grau de mielinització mesurant la relació del contingut lipídic i proteic. L'estudi dels paràmetres relatius a la ràtio de transferència de magnetització (*Magnetization Transfer Ratio; MTR*), els paràmetres de quantificació de la difusió o la valoració del g-ràtio, que mesura el gruix dels axons respecte al diàmetre de les beines de mielina, són altres tècniques que permeten la quantificació de la mielina. L'aproximació multimodal, combinant diversos d'aquests mètodes de RM, ha mostrat coherència respecte als estudis histològics pel que fa a la maduració de la mielina, caracteritzant adequadament la quantitat i qualitat d'aquesta i, per tant, podria ser d'utilitat en l'estudi dels trastorns hipomielinitzants (Steenweg *et al.*, 2016; Cercignani and Bouyagoub, 2018; Wolf *et al.*, 2021). Tot i que aquests avenços són esperançadors de cara al futur, actualment permeten quantificar la mielina normal, mentre que en malalties en les quals la seva composició química o estructura es veuen modificades, perden fiabilitat (Wolf *et al.*, 2021).

VII. CONCLUSIONS

1. L'estudi dels trastorns genètics de la substància blanca cerebral (GWMDs) mitjançant WES i WGS en cas índex (no trio), analitzats mitjançant un sistema de priorització basat en un nou algoritme computacional de creació pròpia, i complementat amb estudis funcionals, permet establir el diagnòstic molecular en un 72% dels casos d'una cohort de 126 pacients d'arreu la geografia nacional (**article 1**). L'algoritme utilitzat integra la informació clínica dels pacients (codificada en termes HPO) i de bases de dades amb informació de les interaccions físiques i funcionals de les proteïnes de l'organisme, per establir una priorització de les variants candidates per cada pacient.
 - 1.1. Aquest rendiment diagnòstic és superior al reportat en altres cohorts estudiades mitjançant WES/WGS en trios i també al de l'aproximació diagnòstica "clàssica", basada en la realització d'estudis genètics dirigits segons la sospita clínica.
 - 1.2. En els casos amb un estudi WES negatiu, la reanàlisi periòdica de les dades genòmiques i la realització de WGS permeten incrementar el percentatge de casos diagnosticats, amb un rendiment del 24% i del 31%, respectivament.
 - 1.3. La utilització de tècniques de seqüenciació massiva en els GWMDs permet escurçar el temps necessari per obtenir un diagnòstic, el que és fonamental per poder oferir a les famílies un assessorament genètic. A més, en aquesta cohort hem vist que pot comportar canvis en el maneig clínic o inclús tractaments específics en 1/3 dels pacients.
2. La realització dels estudis WES/WGS en casos índex pot permetre la reducció del cost del procés diagnòstic en els GWMDs en comparació amb l'estudi de trios. A més, l'aplicació d'estudis NGS evita la realització de múltiples proves complementàries que tenen un rendiment diagnòstic molt menor.
3. Els estudis WES/WGS, a diferència dels exomes clínics, permeten la identificació de nous gens associats a GWMDs, i en definitiva permeten el descobriment de noves malalties:

3.1. L'**article 2** d'aquesta tesi doctoral descriu un nou error congènit del metabolisme produït per variants bial·lèliques en el gen *PI4KA*:

3.1.1. L'espectre fenotípic comprèn des d'un trastorn global del neurodesenvolupament amb una leucodistròfia hipomielinitzant i anomalies del desenvolupament del SNC (hipoplàsia/atròfia ponto-cerebel·losa o polimicrogòria), fins a una paraparèisia espàstica pura. Alguns pacients presenten déficits immunològics, manifestacions gastrointestinals i anomalies genitourinàries associades.

3.1.2. La via metabòlica dels fosfatidilinositols és fonamental pel desenvolupament del SNC i per un correcte procés de mielinització.

3.2. La presència de variants bial·lèliques en el gen *PRORP*, relacionat amb el processament de l'ARNt mitocondrial, s'associa a una nova malaltia mitocondrial amb presentació variable, que pot manifestar-se principalment amb sordesa neurosensorial, insuficiència ovàrica primària, retard del desenvolupament i alteracions de la substància blanca cerebral (**Annex, article A1**).

4. Els estudis WES/WGS permeten identificar nous fenotips clínics, i també el diagnòstic de formes de presentació atípiques o produïdes probablement per l'efecte de variants en més d'un gen.

4.1. Les variants intròniques c.1771-6C > G o c.1771-7C > G en el gen *POLR3A*, s'associen a un nou fenotip en el qual predominen les manifestacions extrapiramidals, i que es caracteritza per una afectació estriatal i dels peduncles cerebel·losos superiors en l'estudi de neuroimatge (**Annex, article A3**).

4.2. Les variants en heterozigosi en el gen *HNRNPH1* s'associen a discapacitat intel·lectual amb trets dismòrfics diferencials, alteracions de la substància blanca cerebral, i més anomalies cardíacaques congènites, genitourinàries i oftalmològiques respecte als pacients amb variants a *HNRNPH2* (**Annex, article A4**).

4.3. Els trastorns genètics que poden associar anomalies de la substància blanca cerebral són molt diversos. L'**article 3** il·lustra el fenotip i genotip d'una cohort de pacients amb variants en heterozigosi en el gen *DLG4*, que codifica per la proteïna postsinàptica PSD-95:

- 4.3.1. En aquesta sinaptopatia, el quadre clínic es caracteritza principalment per un retard global del desenvolupament, discapacitat intel·lectual en grau variable, autisme, TDAH epilèpsia i un trastorn del moviment.
- 4.3.2. A més, els pacients poden associar anomalies de la substància blanca cerebral en forma d'atròfia, retard de la mielinització o hiperintensitats periventriculars. Això evidencia com l'activitat neuronal i sinàptica influeix en la producció i manteniment de la mielina.
5. Per totes aquestes troballes, concloc que els estudis d'exoma complet (o inclús genoma) haurien de considerar-se de primera línia en el procés diagnòstic quan la presentació clínica i el patró d'afectació de la substància blanca en els estudis de neuroimatge no permetin sospitar un diagnòstic concret.
6. Destaco la importància de la creació d'equips multidisciplinaris que participin en el procés diagnòstic mitjançant WES/WGS, amb col·laboració entre centres assistencials i d'investigació, i l'ús de plataformes de col·laboració internacional com GeneMatcher. La utilització de tècniques computacionals avançades, la participació directa dels neuròlegs i neuropediatres en el procés diagnòstic i la possibilitat de realitzar estudis funcionals per la validació de variants (**Annex, article A5**), incrementen considerablement el rendiment diagnòstic dels estudis NGS. Amb aquestes premisses, la creació d'Unitats multidisciplinàries de neurogenètica i genòmica serien la resposta que necessita la nostra sanitat a l'era de la medicina genòmica i personalitzada.

VIII. BIBLIOGRAFIA

Abdellah Z, Ahmadi A, Ahmed S, Aimable M, Ainscough R, Almeida J, et al. Finishing the euchromatic sequence of the human genome. *Nature* 2004; 4317011: 931–945.

ACMG Board of Directors. Points to consider in the clinical application of genomic sequencing. *Genet Med* 2012; 14: 759–761.

ACMG Board Of Directors. Laboratory and clinical genomic data sharing is crucial to improving genetic health care: a position statement of the American College of Medical Genetics and Genomics. *Genet Med* 2017; 197: 721–722.

Adang LA, Sherbini O, Ball L, Bloom M, Darbari A, Amartino H, et al. Revised consensus statement on the preventive and symptomatic care of patients with leukodystrophies. *Mol Genet Metab* 2017; 1221–2: 18–32.

Alvarez-Prats A, Bjelobaba I, Aldworth Z, Baba T, Abebe D, Kim YJ, et al. Schwann-Cell-Specific Deletion of Phosphatidylinositol 4-Kinase Alpha Causes Aberrant Myelination. *Cell Rep* 2018; 2310: 2881–2890.

Amendola LM, Jarvik GP, Leo MC, McLaughlin HM, Akkari Y, Amaral MD, et al. Performance of ACMG-AMP Variant-Interpretation Guidelines among Nine Laboratories in the Clinical Sequencing Exploratory Research Consortium. *Am J Hum Genet* 2016; 986: 1067–1076.

Ansorge WJ. Next-generation DNA sequencing techniques. *N Biotechnol* 2009; 254: 195–203.

Antony JS, Daniel-Moreno A, Lamsfus-Calle A, Raju J, Kaftancioglu M, Ureña-Bailén G, et al. A Mutation-Agnostic Hematopoietic Stem Cell Gene Therapy for Metachromatic Leukodystrophy. *Cris J* 2022; 51: 66–79.

Arai-Ichinoi N, Uematsu M, Sato R, Suzuki T, Kudo H, Kikuchi A, et al. Genetic heterogeneity in 26 infants with a hypomyelinating leukodystrophy. *Hum Genet* 2016; 1351: 89–98.

Austin CP, Cutillo CM, Lau LPL, Jonker AH, Rath A, Julkowska D, et al. Future of Rare Diseases Research 2017–2027: An IRDiRC Perspective. *Clin Transl Sci* 2018; 111: 21–27.

Van der Auwera GA, Carneiro MO, Hartl C, Poplin R, Del Angel G, Levy-Moonshine A, et al. From FastQ data to high confidence variant calls: the Genome Analysis Toolkit best practices pipeline. *Curr Protoc Bioinforma* 2013; 431110: 11.10.1-11.10.33.

Bailey AP, Koster G, Guillermier C, Hirst EMA, MacRae JI, Lechene CP, et al. Antioxidant Role for Lipid Droplets in a Stem Cell Niche of Drosophila. *Cell* 2015; 1632: 340–353.

Barkovich AJ. An approach to MRI of metabolic disorders in children. *J Neuroradiol* 2007; 342: 75–88.

Barkovich AJ, Kjos BO, Jackson DE, Norman D. Normal maturation of the neonatal and infant brain: MR imaging at 1.5 T. *Radiology* 1988; 1661 I: 173–180.

von Bartheld CS, Bahney J, Herculano-Houzel S. The search for true numbers of neurons and glial cells in the human brain: A review of 150 years of cell counting. *J Comp Neurol* 2016; 52418: 3865–3895.

Bartlett SE, Reynolds AJ, Weible M 2nd, Hendry IA. Phosphatidylinositol kinase enzymes regulate the retrograde axonal transport of NT-3 and NT-4 in sympathetic and sensory neurons. *J Neurosci Res* 2002; 682: 169–175.

Barwell JG, O'sullivan RBG, Mansbridge LK, Lowry JM, Dorkins HR. Challenges in implementing genomic medicine: the 100,000 Genomes Project. *J Transl Genet Genom* 2018; 213: <http://dx.doi.org/10.20517/jtgg.2018.17>.

Baskin JM, Wu X, Christiano R, Oh MS, Schauder CM, Gazzero E, et al. The leukodystrophy protein FAM126A (hyccin) regulates PtdIns(4)P synthesis at the plasma membrane. *Nat Cell Biol* 2016; 181: 132–138.

Bechler ME, Byrne L, Ffrench-Constant C. CNS Myelin Sheath Lengths Are an Intrinsic Property of Oligodendrocytes. *Curr Biol* 2015; 2518: 2411–2416.

Beck TF, Mullikin JC, Biesecker LG. Systematic Evaluation of Sanger Validation of NextGen SequencingVariants. *Clin Chem* 2016; 624: 647.

Belkadi A, Bolze A, Itan Y, Cobat A, Vincent QB, Antipenko A, et al. Whole-genome sequencing is more powerful than whole-exome sequencing for detecting exome variants. *Proc Natl Acad Sci U S A* 2015; 11217: 5473–5478.

Bertoli-Avella AM, Beetz C, Ameziane N, Rocha ME, Guatibonza P, Pereira C, et al. Successful application of genome sequencing in a diagnostic setting: 1007 index cases from a clinically heterogeneous cohort. *Eur J Hum Genet* 2021; 291: 141–153.

Biancheri R, Zara F, Rossi A, Mathot M, Cecile Nassogne M, Yalcinkaya C, et al. Hypomyelination and Congenital Cataract Broadening the Clinical Phenotype. *Arch Neurol* 2011; 689: 1191–4.

Bick D, Jones M, Taylor SL, Taft RJ, Belmont J. Case for genome sequencing in infants and children with rare, undiagnosed or genetic diseases. *J Med Genet* 2019; 5612: 783–791.

Bielschowsky M, Henneberg R. Über familiäre diffuse Sklerose (leukodystrophia cerebri progressiva hereditaria). *J Psychol Neurol* 1928; 36: 131–181.

Bonkowsky JL, Keller S. Leukodystrophies in Children: Diagnosis, Care, and Treatment. *Pediatrics* 2021; 1483: e2021053126.

Bonkowsky JL, Nelson C, Kingston JL, Filloux FM, Mundorff MB, Srivastava R. The burden of inherited leukodystrophies in children. *Neurology* 2010; 758: 718–725.

Boycott K, Rath A, Chong J, Hartley T, Alkuraya F, Baynam G, et al. International Cooperation to Enable the Diagnosis of All Rare Genetic Diseases. *Am J Hum Genet* 2017; 1005: 695–705.

Bradbury AM, Ream MA. Recent Advancements in the Diagnosis and Treatment of Leukodystrophies. *Semin Pediatr Neurol* 2021; 37: 100876.

Brown TL, Macklin WB. The Actin Cytoskeleton in Myelinating Cells. *Neurochem Res* 2020; 453: 684–693.

Brunk E, Sahoo S, Zielinski DC, Altunkaya A, Dräger A, Mih N, et al. Recon3D enables a three-dimensional view of gene variation in human metabolism. *Nat Biotechnol* 2018; 363: 272–281.

Butt AM. Structure and Function of Oligodendrocytes. In: Kettenmann H, Ransom BR, editor(s). *Neuroglia*. Oxford University Press; 2012. p. 62–73

Calvo SE, Compton AG, Hershman SG, Lim SC, Lieber DS, Tucker EJ, et al. Molecular diagnosis of infantile mitochondrial disease with targeted next-generation sequencing. *Sci Transl Med* 2012; 4118: 118ra10.

de Castro F. Cajal and the spanish neurological school: Neuroscience would have been a different story without them. *Front Cell Neurosci* 2019; 13May: 1–14.

Cercignani M, Bouyagoub S. Brain microstructure by multi-modal MRI: Is the whole greater than the sum of its parts? *Neuroimage* 2018; 182: 117–127.

Chang K-J, Redmond SA, Chan JR. Remodeling myelination: implications for mechanisms of neural plasticity. *Nat Neurosci* 2016; 192: 190–197.

Cheng AAY, Teo Y-YY, Ong RRT-H, AY C, YY T, RT O. Assessing single nucleotide variant detection and genotype calling on whole-genome sequenced individuals. *Bioinformatics* 2014; 3012: 1707–1713.

Clark MM, Stark Z, Farnaes L, Tan TY, White SM, Dimmock D, et al. Meta-analysis of the diagnostic and clinical utility of genome and exome sequencing and chromosomal microarray in children with suspected genetic diseases. *NPJ genomic Med* 2018; 31: 1–10.

Cohen CCH, Popovic MA, Klooster J, Weil MT, Möbius W, Nave KA, et al. Saltatory Conduction along Myelinated Axons Involves a Periaxonal Nanocircuit. *Cell* 2020; 1802: 311-322.e15.

Cohen L, Manín A, Medina N, Rodríguez-Quiroga S, González-Morón D, Rosales J, et al. Argentinian clinical genomics in a leukodystrophies and genetic leukoencephalopathies cohort: Diagnostic yield in our first 9 years. *Ann Hum Genet* 2020; 841: 11–28.

Coutelier M, Hammer MB, Stevanin G, Monin M-L, Davoine C-S, Mochel F, et al. Efficacy of Exome-Targeted Capture Sequencing to Detect Mutations in Known Cerebellar Ataxia Genes. *JAMA Neurol* 2018; 755: 591–599.

Dali CI, Sevin C, Krägeloh-Mann I, Giugliani R, Sakai N, Wu J, et al. Safety of intrathecal delivery of recombinant human arylsulfatase A in children with metachromatic leukodystrophy: Results from a phase 1/2 clinical trial. *Mol Genet Metab* 2020; 1311–2: 235–244.

Dolzhenko E, van Vugt JJFA, Shaw RJ, Bekritsky MA, Van Blitterswijk M, Narzisi G, et al. Detection of long repeat expansions from PCR-free whole-genome sequence data. *Genome Res* 2017; 2711: 1895–1903.

Dong Z, Wang H, Chen H, Jiang H, Yuan J, Yang Z, et al. Identification of balanced chromosomal rearrangements previously unknown among participants in the 1000 Genomes Project: implications for interpretation of structural variation in genomes and the future of clinical cytogenetics. *Genet Med* 2018; 207: 697–707.

Duffner PK, Caviness VSJ, Erbe RW, Patterson MC, Schultz KR, Wenger DA, et al. The long-term outcomes of presymptomatic infants transplanted for Krabbe disease: report of the workshop held on July 11 and 12, 2008, Holiday Valley, New York. *Genet Med* 2009; 116: 450–454.

Eichler FS, Li J, Guo Y, Caruso PA, Bjonnes AC, Pan J, et al. CSF1R mosaicism in a family with hereditary diffuse leukoencephalopathy with spheroids. *Brain* 2016; 139Pt 6: 1666–1672.

Elitt MS, Barbar L, Shick HE, Powers BE, Maeno-Hikichi Y, Madhavan M, et al. Suppression of proteolipid protein rescues Pelizaeus-Merzbacher disease. *Nature* 2020; 5857825: 397–403.

Farnaes L, Hildreth A, Sweeney N, Clark M, Chowdhury S, Nahas S, et al. Rapid whole-genome sequencing decreases infant morbidity and cost of hospitalization. *NPJ genomic Med* 2018; 3: 10.

Fields RD. White matter in learning, cognition and psychiatric disorders. *Trends Neurosci* 2008; 317: 361–370.

Firth H V., Richards SM, Bevan AP, Clayton S, Corpas M, Rajan D, et al. DECIPHER: Database of Chromosomal Imbalance and Phenotype in Humans Using Ensembl Resources. *Am J Hum Genet* 2009; 844: 524–33.

Fitzgerald TW, Gerety SS, Jones WD, Van Kogelenberg M, King DA, McRae J, et al. Large-scale discovery of novel genetic causes of developmental disorders. *Nature* 2015; 5197542: 223–8.

Flechsig Of Leipsic P. Developmental (Myelogenetic) Localisation of the Cerebral Cortex in the Human Subject. *Lancet* 1901; 1584077: 1027–1030.

Flechsig PE. Anatomie des menschlichen Gehirns und Rückenmarks auf myelogenetischer Grundlage. Thieme; 1920

Fogel BL, Lee H, Deignan JL, Strom SP, Kantarci S, Wang X, et al. Exome sequencing in the clinical diagnosis of sporadic or familial cerebellar ataxia. *JAMA Neurol* 2014; 7110: 1237–1246.

Fumagalli F, Calbi V, Natali Sora MG, Sessa M, Baldoli C, Rancoita PM V, et al. Lentiviral haematopoietic stem-cell gene therapy for early-onset metachromatic leukodystrophy: long-term results from a non-randomised, open-label, phase 1/2 trial and expanded access. *Lancet* 2022; 39910322: 372–383.

Fünfschilling U, Supplie LM, Mahad D, Boretius S, Saab AS, Edgar J, et al. Glycolytic oligodendrocytes maintain myelin and long-term axonal integrity. *Nature* 2012; 4857399: 517–21.

Gambin T, Akdemir Z, Yuan B, Gu S, Chiang T, Carvalho C, et al. Homozygous and hemizygous CNV detection from exome sequencing data in a Mendelian disease cohort. *Nucleic Acids Res* 2017; 454:

1633–1648.

Gilissen C, Hehir-Kwa JY, Thung DT, van de Vorst M, van Bon BWM, Willemsen MH, et al. Genome sequencing identifies major causes of severe intellectual disability. *Nature* 2014; 5117509: 344–347.

Green R, Berg J, Grody W, Kalia S, Korf B, Martin C, et al. ACMG recommendations for reporting of incidental findings in clinical exome and genome sequencing. *Genet Med* 2013; 157: 565–574.

Gross C. Some Revolutions in Neuroscience. *J Cogn Neurosci* 2013; 251: 4–13.

Gu S, Chen CA, Rosenfeld JA, Cope H, Launay N, Flanigan KM, et al. Truncating variants in UBAP1 associated with childhood-onset nonsyndromic hereditary spastic paraplegia. *Hum Mutat* 2020; 413: 632–640.

Haendel MA, Chute CG, Robinson PN. Classification, Ontology, and Precision Medicine. *N Engl J Med* 2018; 37915: 1452–1462.

Hamilton E, Tekturk P, Cialdella F, van Rappard D, Wolf N, Yalcinkaya C, et al. Megalencephalic leukoencephalopathy with subcortical cysts: Characterization of disease variants. *Neurology* 2018; 9016: E1395–E1403.

Hamilton EMC, Bertini E, Kalaydjieva L, Morar B, Dojčáková D, Liu J, et al. UFM1 founder mutation in the Roma population causes recessive variant of H-ABC. *Neurology* 2017; 8917: 1821–1828.

Harting I, Al-Saady M, Krägeloh-Mann I, Bley A, Hempel M, Bierhals T, et al. POLR3A variants with striatal involvement and extrapyramidal movement disorder. *Neurogenetics* 2020; 212: 121–33.

Hartline DK, Colman DR. Rapid Conduction and the Evolution of Giant Axons and Myelinated Fibers. *Curr Biol* 2007; 171: R29–R35.

Hawkins-Salsbury JA, Shea L, Jiang X, Hunter DA, Guzman AM, Reddy AS, et al. Mechanism-based combination treatment dramatically increases therapeutic efficacy in murine globoid cell leukodystrophy. *J Neurosci* 2015; 3516: 6495–6505.

Heim P, Claussen M, Hoffmann B, Conzelmann E, Gärtner J, Harzer K, et al. Leukodystrophy incidence in Germany. *Am J Med Genet* 1997; 714: 475–478.

Helman G, Van Haren K, Bonkowsky JL, Bernard G, Pizzino A, Braverman N, et al. Disease specific therapies in leukodystrophies and leukoencephalopathies. *Mol Genet Metab* 2015; 1144: 527–536.

Helman G, Lajoie BR, Crawford J, Takanohashi A, Walkiewicz M, Dolzhenko E, et al. Genome sequencing in persistently unsolved white matter disorders. *Ann Clin Transl Neurol* 2020; 71: 144–152.

Hirrlinger J, Nave KA. Adapting brain metabolism to myelination and long-range signal transduction. *Glia* 2014; 6211: 1749–61.

Hochberg I, Demain LAM, Richer J, Thompson K, Urquhart JE, Rea A, et al. Bi-allelic variants in the mitochondrial RNase P subunit PRORP cause mitochondrial tRNA processing defects and pleiotropic multisystem presentations. *Am J Hum Genet* 2021; 10811: 2195–2204.

Hudson LD, Puckett C, Berndt J, Chan J, Gencic S. Mutation of the proteolipid protein gene PLP in a human X chromosome-linked myelin disorder. *Proc Natl Acad Sci U S A* 1989; 8620: 8128–8131.

Hughes AN. Glial Cells Promote Myelin Formation and Elimination. *Front Cell Dev Biol* 2021; 9May: 1–16.

Hughes EG, Appel B. The cell biology of CNS myelination. *Curr Opin Neurobiol* 2016; 39: 93–100.

Hutlin EL, Bruckner RJ, Paulo JA, Cannon JR, Ting L, Baltier K, et al. Architecture of the human interactome defines protein communities and disease networks. *Nature* 2017; 5457655: 505–509.

Huxley AF, Stämpfli R. Evidence for saltatory conduction in peripheral myelinated nerve fibres. *J Physiol* 1949; 1083: 315–339.

Hwang S, Kim CY, Yang S, Kim E, Hart T, Marcotte EM, et al. HumanNet v2: Human gene networks for disease research. *Nucleic Acids Res* 2019; 47D1: D573–D580.

Kalia SS, Adelman K, Bale SJ, Chung WK, Eng C, Evans JP, et al. Recommendations for reporting of secondary findings in clinical exome and genome sequencing, 2016 update (ACMG SF v2.0): A policy statement of the American College of Medical Genetics and Genomics. *Genet Med* 2017; 192: 249–55.

Kanehisa M, Goto S, Sato Y, Kawashima M, Furumichi M, Tanabe M. Data, information, knowledge and principle: Back to metabolism in KEGG. *Nucleic Acids Res* 2014; 42: D199-205.

Kaul R, Gao GP, Balamurugan K, Matalon R. Cloning of the human aspartoacylase cDNA and a common missense mutation in Canavan disease. *Nat Genet* 1993; 52: 118–123.

Kaur P, do Rosario MC, Hebbar M, Sharma S, Kausthubham N, Nair K, et al. Clinical and genetic spectrum of 104 Indian families with central nervous system white matter abnormalities. *Clin Genet* 2021; 1005: 542–550.

Kevelam SH, Steenweg ME, Srivastava S, Helman G, Naidu S, Schiffmann R, et al. Update on leukodystrophies: A historical perspective and adapted definition. *Neuropediatrics* 2016; 476: 349–354.

Kingsmore SF, Cakici JA, Clark MM, Gaughran M, Feddock M, Batalov S, et al. A Randomized, Controlled Trial of the Analytic and Diagnostic Performance of Singleton and Trio, Rapid Genome and Exome Sequencing in Ill Infants. *Am J Hum Genet* 2019; 1054: 719–733.

van der Knaap MS, Barth PG, Gabreëls FJ, Franzoni E, Begeer JH, Stroink H, et al. A new leukoencephalopathy with vanishing white matter. *Neurology* 1997; 484: 845–855.

van der Knaap MS, Barth PG, Stroink H, van Nieuwenhuizen O, Arts WF, Hoogenraad F, et al. Leukoencephalopathy with swelling and a discrepantly mild clinical course in eight children. *Ann Neurol* 1995; 373: 324–334.

van der Knaap MS, Breiter SN, Naidu S, Hart AA, Valk J. Defining and categorizing leukoencephalopathies of unknown origin: MR imaging approach. *Radiology* 1999; 2131: 121–33.

van der Knaap MS, Bugiani M. Leukodystrophies: a proposed classification system based on pathological changes and pathogenetic mechanisms. *Acta Neuropathol* 2017; 1343: 351–382.

van der Knaap MS, Naidu S, Pouwels PJW, Bonavita S, van Coster R, Lagae L, et al. New syndrome characterized by hypomyelination with atrophy of the basal ganglia and cerebellum. *AJNR Am J Neuroradiol* 2002; 239: 1466–1474.

van der Knaap MS, Schiffmann R, Mochel F, Wolf NI. Diagnosis, prognosis, and treatment of leukodystrophies. *Lancet Neurol* 2019; 442219: 962–972.

van der Knaap MS, Valk J, de Neeling N, Nauta JJP. Pattern recognition in magnetic resonance imaging of white matter disorders in children and young adults. *Neuroradiology* 1991; 336: 478–493.

van der Knaap MS, van der Voorn P, Barkhof F, Van Coster R, Krägeloh-Mann I, Feigenbaum A, et al. A new leukoencephalopathy with brainstem and spinal cord involvement and high lactate. *Ann Neurol* 2003; 532: 252–258.

Köhler S, Doelken SC, Mungall CJ, Bauer S, Firth H V., Bailleul-Forestier I, et al. The Human Phenotype Ontology project: Linking molecular biology and disease through phenotype data. *Nucleic Acids Res* 2014; 42: D966-74.

Köhler S, Vasilevsky NA, Engelstad M, Foster E, McMurry J, Aymé S, et al. The Human Phenotype Ontology in 2017. *Nucleic Acids Res* 2017; 45D1: D865–D876.

Köhler W, Curiel J, Vanderver A. Adulthood leukodystrophies. *Nat Rev Neurol* 2018; 142: 94–105.

Krägeloh-Mann I, Groeschel S, Kehrer C, Opherk K, Nägele T, Handgretinger R, et al. Juvenile metachromatic leukodystrophy 10 years post transplant compared with a non-transplanted cohort. *Bone Marrow Transplant* 2013; 483: 369–375.

De La Fuente AG, Lange S, Silva ME, Gonzalez GA, Tempfer H, van Wijngaarden P, et al. Pericytes Stimulate Oligodendrocyte Progenitor Cell Differentiation during CNS Remyelination. *Cell Rep* 2017; 208: 1755–1764.

Lee Y, Morrison BM, Li Y, Lengacher S, Farah MH, Hoffman PN, et al. Oligodendroglia metabolically support axons and contribute to neurodegeneration. *Nature* 2012; 4877408: 443–448.

Lelieveld S, Spielmann M, Mundlos S, Veltman J, Gilissen C. Comparison of Exome and Genome Sequencing Technologies for the Complete Capture of Protein-Coding Regions. *Hum Mutat* 2015; 368: 815–822.

Licata L, Lo Surdo P, Iannuccelli M, Palma A, Micarelli E, Perfetto L, et al. SIGNOR 2.0, the SIGnaling Network Open Resource 2.0: 2019 update. *Nucleic Acids Res* 2020; 48D1: D504–D510.

Lionel AC, Costain G, Monfared N, Walker S, Reuter MS, Hosseini SM, et al. Improved diagnostic yield compared with targeted gene sequencing panels suggests a role for whole-genome sequencing as a first-tier genetic test. *Genet Med* 2018; 204: 435–443.

Loes DJ, Hite S, Moser H, Stillman AE, Shapiro E, Lockman L, et al. Adrenoleukodystrophy: a scoring method for brain MR observations. *AJNR Am J Neuroradiol* 1994; 159: 1761–1766.

Luck K, Kim DK, Lambourne L, Spirohn K, Begg BE, Bian W, et al. A reference map of the human binary protein interactome. *Nature* 2020; 5807803: 402–408.

Lynch DS, Rodrigues Brandao de Paiva A, Zhang WJ, Bugiardini E, Freua F, Tavares Lucato L, et al.

Clinical and genetic characterization of leukoencephalopathies in adults. *Brain* 2017; 140(5): 1204–1211.

MacKay AL, Laule C. Magnetic Resonance of Myelin Water: An in vivo Marker for Myelin. *Brain Plast* (Amsterdam, Netherlands) 2016; 21: 71–91.

Mahdieh N, Soveizi M, Tavasoli AR, Rabbani A, Ashrafi MR, Kohlschütter A, et al. Genetic testing of leukodystrophies unraveling extensive heterogeneity in a large cohort and report of five common diseases and 38 novel variants. *Sci Rep* 2021; 11(1): 3231.

Mardis ER. The impact of next-generation sequencing technology on genetics. *Trends Genet* 2008; 24(3): 133–141.

McGurk KA, Zheng SL, Henry A, Josephs K, Edwards M, de Marvao A, et al. Correspondence on 'ACMG SF v3.0 list for reporting of secondary findings in clinical exome and genome sequencing: a policy statement of the American College of Medical Genetics and Genomics (ACMG)' by Miller et al. *Genet Med* 2021; 23(1): 3600(21)05372–7.

Meienberg J, Bruggmann R, Oexle K MG. Clinical sequencing: is WGS the better WES? *Hum Genet* 2016; 135(3): 359–362.

Meng L, Pammi M, Saronwala A, Magoulas P, Ghazi AR, Vetrini F, et al. Use of Exome Sequencing for Infants in Intensive Care Units: Ascertainment of Severe Single-Gene Disorders and Effect on Medical Management. *JAMA Pediatr* 2017; 171(12): e173438.

Merzbacher L. Eine eigenartige familiär-hereditäre erkrankungsform (Aplasia axialis extracorticalis congenita). *Zeitschr Ges Neurol Psych* 1910; 31: 1–138.

Moffett JR, Ross B, Arun P, Madhavarao CN, Namboodiri AMA. N-Acetylaspartate in the CNS: from neurodiagnostics to neurobiology. *Prog Neurobiol* 2007; 81(2): 89–131.

Morell P. A correlative synopsis of the leukodystrophies. *Neuropediatrics* 1984; Suppl: 62–65.

Morrison BM, Lee Y, Rothstein JD. Oligodendroglia: Metabolic supporters of axons. *Trends Cell Biol* 2013; 23(12): 644–651.

Mosser J, Douar AM, Sarde CO, Kioschis P, Feil R, Moser H, et al. Putative X-linked adrenoleukodystrophy gene shares unexpected homology with ABC transporters. *Nature* 1993;

3616414: 726–730.

Mostovoy Y, Levy-Sakin M, Lam J, Lam E, Hastie A, Marks P, et al. A hybrid approach for de novo human genome sequence assembly and phasing. *Nat Methods* 2016; 137: 587–590.

Mount CW, Monje M. Wrapped to Adapt: Experience-Dependent Myelination. *Neuron* 2017; 954: 743–756.

Müller vom Hagen J, Karle KN, Schüle R, Krägeloh-Mann I, Schöls L. Leukodystrophies underlying cryptic spastic paraparesis: Frequency and phenotype in 76 patients. *Eur J Neurol* 2014; 217: 983–988.

Nave K-A. Myelination and support of axonal integrity by glia. *Nature* 2010; 4687321: 244–252.

Nave K-A, Werner HB. Ensheathment and Myelination of Axons: Evolution of Glial Functions. *Annu Rev Neurosci* 2021; 441: 197–219.

Németh AH, Kwasniewska AC, Lise S, Parolin Schnenberg R, Becker EBE, Bera KD, et al. Next generation sequencing for molecular diagnosis of neurological disorders using ataxias as a model. *Brain* 2013; 136Pt 10: 3106–3118.

Novarino G, Fenstermaker AG, Zaki MS, Hofree M, Silhavy JL, Heiberg AD, et al. Exome sequencing links corticospinal motor neuron disease to common neurodegenerative disorders. *Science* (80-) 2014; 3436170: 506–511.

Okkenhaug K. Signaling by the phosphoinositide 3-kinase family in immune cells. *Annu Rev Immunol* 2013; 31: 675–704.

Ostrander BEP, Butterfield RJ, Pedersen BS, Farrell AJ, Layer RM, Ward A, et al. Whole-genome analysis for effective clinical diagnosis and gene discovery in early infantile epileptic encephalopathy. *NPJ genomic Med* 2018; 3: 22.

Owen MJ, Niemi A-K, Dimmock DP, Speziale M, Nespeca M, Chau KK, et al. Rapid Sequencing-Based Diagnosis of Thiamine Metabolism Dysfunction Syndrome. *N Engl J Med* 2021; 38422: 2159–2161.

Page KM, Stenger EO, Connelly JA, Shyr D, West T, Wood S, et al. Hematopoietic Stem Cell Transplantation to Treat Leukodystrophies: Clinical Practice Guidelines from the Hunter's Hope Leukodystrophy Care Network. *Biol blood marrow Transplant J Am Soc Blood Marrow Transplant*

2019; 2512: e363–e374.

Pagnamenta AT, Howard MF, Wisniewski E, Popitsch N, Knight SJL, Keays DA, et al. Germline recessive mutations in PI4KA are associated with perisylvian polymicrogyria, cerebellar hypoplasia and arthrogryposis. *Hum Mol Genet* 2015; 2413: 3732–3741.

Pant D, Dorboz I, Schluter A, Fourcade S, Launay N, Joya J, et al. Loss of the sphingolipid desaturase DEGS1 causes hypomyelinating leukodystrophy. *J Clin Invest* 2019; 1293: 1240–1256.

Parikh S, Bernard G, Leventer RJ, van der Knaap MS, van Hove J, Pizzino A, et al. A clinical approach to the diagnosis of patients with leukodystrophies and genetic leukoencephalopathies. *Mol Genet Metab* 2015; 1144: 501–515.

Pelizaeus F. Über eine eigenartige familiäre Entwick-lungshemmung cornehmlich auf motorischem Gebiete. *Arch Psych* 1899; 31: 100.

Pérez-Cerdá F, Sánchez-Gómez MV, Matute C. Pío del Río hortega and the discovery of the oligodendrocytes. *Front Neuroanat* 2015; 9: 92.

Petrikin JE, Willig LK, Smith LD, Kingsmore SF. Rapid whole genome sequencing and precision neonatology. *Semin Perinatol* 2015; 398: 623–631.

Plagnol V, Curtis J, Epstein M, Mok KY, Stebbings E, Grigoriadou S, et al. A robust model for read count data in exome sequencing experiments and implications for copy number variant calling. *Bioinformatics* 2012; 2821: 2747–54.

Pollard MO, Gurdasani D, Mentzer AJ, Porter T, Sandhu MS. Long reads: their purpose and place. *Hum Mol Genet* 2018; 27R2: R234–R241.

Polten A, Fluharty AL, Fluharty CB, Kappler J, von Figura K, Gieselmann V. Molecular basis of different forms of metachromatic leukodystrophy. *N Engl J Med* 1991; 3241: 18–22.

Posey JE, Harel T, Liu P, Rosenfeld JA, James RA, Coban Akdemir ZH, et al. Resolution of Disease Phenotypes Resulting from Multilocus Genomic Variation. *N Engl J Med* 2017; 3761: 21–31.

Quintana-Murci L. Understanding rare and common diseases in the context of human evolution. *Genome Biol* 2016; 171: 1–14.

Rademakers R, Baker M, Nicholson AM, Rutherford NJ, Finch N, Soto-Ortolaza A, et al. Mutations in

the colony stimulating factor 1 receptor (CSF1R) gene cause hereditary diffuse leukoencephalopathy with spheroids. *Nat Genet* 2011; 442: 200–205.

Reichert SC, Li R, Turner S, van Jaarsveld RH, Massink MPG, van den Boogaard MH, et al. HNRNPH1-related syndromic intellectual disability: Seven additional cases suggestive of a distinct syndromic neurodevelopmental syndrome. *Clin Genet* 2020; 981: 91–98.

Richards J, Korgenski EK, Taft RJ, Vanderver A, Bonkowsky JL. Targeted leukodystrophy diagnosis based on charges and yields for testing. *Am J Med Genet Part A* 2015; 167A11: 2541–3.

Richards S, Aziz N, Bale S, Bick D, Das S, Gastier-Foster J, et al. Standards and guidelines for the interpretation of sequence variants: A joint consensus recommendation of the American College of Medical Genetics and Genomics and the Association for Molecular Pathology. *Genet Med* 2015; 175: 405–424.

Del Río Hortega P. Noticia de un nuevo y fácil método para la coloración de la neuroglia y el tejido conjuntivo. *Trab Lab Invest Biol* 1918; 15: 367–378.

Del Río Hortega P. Estudios sobre la neuroglía. La microglía y su transformación en células en bastoncito y cuerpos granuloadiposos. *Trab Lab Invest Biol* 1920; 18: 37–82.

Del Río Hortega P. La glía de escasas radiaciones (oligodendroglía). *Bol Real Soc Esp Hist Nat* 1921; 21: 63–92.

Del Río Hortega P. Tercera aportación al conocimiento morfológico e interpretación funcional de la oligodendroglíale. *Mem Real Soc Esp Hist Nat* 1928; 14: 5–122.

Robinson PN, Köhler S, Bauer S, Seelow D, Horn D, Mundlos S. The Human Phenotype Ontology: A Tool for Annotating and Analyzing Human Hereditary Disease. *Am J Hum Genet* 2008; 835: 610–615.

Rodríguez-Palmero A, Boerrigter MM, Gómez-Andrés D, Aldinger KA, Marcos-Alcalde I, Popp B, et al. DLG4-related synaptopathy: a new rare brain disorder. *Genet Med* 2021; 235: 888–899.

Rodríguez-Palmero A, Schlüter A, Verdura E, Ruiz M, Martínez JJ, Gourlaouen I, et al. A novel hypomorphic splice variant in EIF2B5 gene is associated with mild ovarioleukodystrophy. *Ann Clin Transl Neurol* 2020; 79: 1574–79.

Rolland T, Tasan M, Charlotteaux B, Pevzner SJ, Zhong Q, Sahni N, et al. A proteome-scale map of the

human interactome network. *Cell* 2014; 1595: 1212–1226.

Rual JF, Venkatesan K, Hao T, Hirozane-Kishikawa T, Dricot A, Li N, et al. Towards a proteome-scale map of the human protein-protein interaction network. *Nature* 2005; 4377062: 1173–8.

Saab AS, Tzvetanova ID, Nave KA. The role of myelin and oligodendrocytes in axonal energy metabolism. *Curr Opin Neurobiol* 2013; 236: 1065–1072.

Sabatini L, Mathews C, Ptak D, Doshi S, Tynan K, Hegde M, et al. Genomic Sequencing Procedure Microcosting Analysis and Health Economic Cost-Impact Analysis: A Report of the Association for Molecular Pathology. *J Mol Diagn* 2016; 183: 319–328.

Sainio MT, Aaltio J, Hyttinen V, Kortelainen M, Ojanen S, Paetav A, et al. Effectiveness of clinical exome sequencing in adult patients with difficult-to-diagnose neurological disorders. *Acta Neurol Scand* 2022; 1451: 63–72.

Sakai N, Inui K, Fujii N, Fukushima H, Nishimoto J, Yanagihara I, et al. Krabbe disease: isolation and characterization of a full-length cDNA for human galactocerebrosidase. *Biochem Biophys Res Commun* 1994; 1982: 485–491.

Salsano E. Leukodystrophy or genetic leukoencephalopathy? Nature does not make leaps. *Mol Genet Metab* 2015; 1144: 491–93.

Salter CG, Cai Y, Lo B, Helman G, Taylor H, Mccartney A, et al. Biallelic PI4KA variants cause neurological, intestinal and immunological disease. *Brain* 2021; 14412: 3597–3610.

Saunders C, Miller N, Soden S, Dinwiddie D, Noll A, Alnadi N, et al. Rapid whole-genome sequencing for genetic disease diagnosis in neonatal intensive care units. *Sci Transl Med* 2012; 4154: 154ra135.

Schiffmann R. An MRI-based approach to the diagnosis of white matter disorders. *Neurology* 2009; 72: 750–759.

Schiffmann R, van der Knaap MS. An MRI-based approach to the diagnosis of white matter disorders. *Neurology* 2009; 728: 750–59.

Schlüter A, Rodríguez-Palmero A, Verdura E, Vélez-Santamaría V, Ruiz M, Fourcade S, et al. Diagnosis of Genetic White Matter Disorders by Singleton Whole-Exome and Genome Sequencing Using Interactome-Driven Prioritization. *Neurology* 2022; 10.1212/WNL.0000000000013278.

Schon KR, Horvath R, Wei W, Calabrese C, Tucci A, Ibañez K, et al. Use of whole genome sequencing to determine genetic basis of suspected mitochondrial disorders: cohort study. *BMJ* 2021; 375: e066288.

Seitelberger F. Structural manifestations of leukodystrophies. *Neuropediatrics* 1984; Suppl: 53–61.

Sessa M, Lorioli L, Fumagalli F, Acquati S, Redaelli D, Baldoli C, et al. Lentiviral haemopoietic stem-cell gene therapy in early-onset metachromatic leukodystrophy: an ad-hoc analysis of a non-randomised, open-label, phase 1/2 trial. *Lancet (London, England)* 2016; 38810043: 476–487.

Shewan A, Eastburn DJ, Mostov K. Phosphoinositides in cell architecture. *Cold Spring Harb Perspect Biol* 2011; 38: a004796.

Shieh JT, Penon-Portmann M, Wong KHY, Levy-Sakin M, Verghese M, Slavotinek A, et al. Application of full-genome analysis to diagnose rare monogenic disorders. *NPJ genomic Med* 2021; 61: 77.

Shukla A, Kaur P, Narayanan DL, do Rosario MC, Kadavigere R, Girisha KM. Genetic disorders with central nervous system white matter abnormalities: An update. *Clin Genet* 2021; 991: 119–132.

Smedley D, Smith KR, Martin A, Thomas EA, McDonagh EM, Cipriani V, et al. 100,000 Genomes Pilot on Rare-Disease Diagnosis in Health Care - Preliminary Report. *N Engl J Med* 2021; 38520: 1868–1880.

Sobreira N, Schiettecatte F, Valle D, Hamosh A. GeneMatcher: A Matching Tool for Connecting Investigators with an Interest in the Same Gene. *Hum Mutat* 2015; 3610: 928–30.

Soden SE, Saunders CJ, Willig LK, Farrow EG, Smith LD, Petrikin JE, et al. Effectiveness of exome and genome sequencing guided by acuity of illness for diagnosis of neurodevelopmental disorders. *Sci Transl Med* 2014; 6265: 265ra168.

Soderholm HE, Chapin AB, Bayrak-Toydemir P, Bonkowsky JL. Elevated Leukodystrophy Incidence Predicted From Genomics Databases. *Pediatr Neurol* 2020; 111: 66–69.

Splinter K, Adams DR, Bacino CA, Bellen HJ, Bernstein JA, Cheattle-Jarvela AM, et al. Effect of Genetic Diagnosis on Patients with Previously Undiagnosed Disease. *N Engl J Med* 2018; 37922: 2131–39.

Srivastava S, Cohen JS, Vernon H, Barañano K, McClellan R, Jamal L, et al. Clinical whole exome sequencing in child neurology practice. *Ann Neurol* 2014; 764: 473–83.

Stadelmann C, Timmler S, Barrantes-Freer A, Simons M. Myelin in the Central Nervous System: Structure, Function, and Pathology. *Physiol Rev* 2019; 993: 1381–1431.

Stark Z, Ellard S. Rapid genomic testing for critically ill children: time to become standard of care? *Eur J Hum Genet* 2022; 302: 142–149.

Stavropoulos D, Merico D, Jobling R, Bowdin S, Monfared N, Thiruvahindrapuram B, et al. Whole Genome Sequencing Expands Diagnostic Utility and Improves Clinical Management in Pediatric Medicine. *NPJ genomic Med* 2016; 1: 15012.

Steenweg ME, Vanderver A, Blaser S, Bizzi A, De Koning TJ, Mancini GMS, et al. Magnetic resonance imaging pattern recognition in hypomyelinating disorders. *Brain* 2010; 133: 2971–82.

Steenweg ME, Wolf NI, Schieving JH, Fawzi Elsaied M, Friederich RL, Ostergaard JR, et al. Novel hypomyelinating leukoencephalopathy affecting early myelinating structures. *Arch Neurol* 2012; 691: 125–128.

Steenweg ME, Wolf NI, van Wieringen WN, Barkhof F, van der Knaap MS, Pouwels PJW. Quantitative MRI in hypomyelinating disorders: Correlation with motor handicap. *Neurology* 2016; 878: 752–758.

Stessman HA, Bernier R, Eichler EE. A genotype-first approach to defining the subtypes of a complex disease. *Cell* 2014; 1565: 872–877.

Stranneheim H, Lagerstedt-Robinson K, Magnusson M, Kvarnung M, Nilsson D, Lesko N, et al. Integration of whole genome sequencing into a healthcare setting: high diagnostic rates across multiple clinical entities in 3219 rare disease patients. *Genome Med* 2021; 131: 40.

Tan T, Dillon O, Stark Z, Schofield D, Alam K, Shrestha R, et al. Diagnostic Impact and Cost-effectiveness of Whole-Exome Sequencing for Ambulant Children With Suspected Monogenic Conditions. *JAMA Pediatr* 2017; 1719: 855–862.

Tan TY, Lunke S, Chong B, Phelan D, Fanjul-Fernandez M, Marum JE, et al. A head-to-head evaluation of the diagnostic efficacy and costs of trio versus singleton exome sequencing analysis. *Eur J Hum Genet* 2019; 2712: 1791–1799.

Tasaki I. The electro-saltatory transmission of the nerve impulse and the effect of narcosis upon the nerve fiber. *Am J Physiol Content* 1939; 1272: 211–227.

Thiffault I, Lantos J. The Challenge of Analyzing the Results of Next-Generation Sequencing in Children. *Pediatrics* 2016; 137s1: s4–s7.

Tsai HH, Niu J, Munji R, Davalos D, Chang J, Zhang H, et al. Oligodendrocyte precursors migrate along vasculature in the developing nervous system. *Science* (80-) 2016; 3516271: 379–84.

Vanderver A, Adang L, Gavazzi F, McDonald K, Helman G, Frank DB, et al. Janus Kinase Inhibition in the Aicardi–Goutières Syndrome. *N Engl J Med* 2020; 38310: 986–89.

Vanderver A, Bernard G, Helman G, Sherbini O, Boeck R, Cohn J, et al. Randomized Clinical Trial of First-Line Genome Sequencing in Pediatric White Matter Disorders. *Ann Neurol* 2020; 882: 264–273.

Vanderver A, Hussey H, Schmidt JL, Pastor W, Hoffman HJ. Relative incidence of inherited white matter disorders in childhood to acquired pediatric demyelinating disorders. *Semin Pediatr Neurol* 2012; 194: 219–223.

Vanderver A, Prust M, Tonduti D, Mochel F, Hussey HM, Helman G, et al. Case definition and classification of leukodystrophies and leukoencephalopathies. *Mol Genet Metab* 2015; 1144: 494–500.

Vanderver A, Simons C, Helman G, Crawford J, Wolf NI, Bernard G, et al. Whole exome sequencing in patients with white matter abnormalities. *Ann Neurol* 2016; 796: 1031–1037.

Verdura E, Rodríguez-Palmero A, Vélez-Santamaría V, Planas-Serra L, de la Calle I, Raspall-Chaure M, et al. Biallelic PI4KA variants cause a novel neurodevelopmental syndrome with hypomyelinating leukodystrophy. *Brain* 2021; 1449: 2659–69.

Vissers LE, van Nimwegen KJ, Schieving JH, Kamsteeg E-J, Kleefstra T, Yntema HG, et al. A clinical utility study of exome sequencing versus conventional genetic testing in pediatric neurology. *Genet Med* 2017; 199: 1055–63.

Wang K, Li M, Hakonarson H. ANNOVAR: functional annotation of genetic variants from high-throughput sequencing data. *Nucleic Acids Res* 2010; 3816: e164.

van de Warrenburg BP, Schouten MI, de Bot ST, Vermeer S, Meijer R, Pennings M, et al. Clinical exome sequencing for cerebellar ataxia and spastic paraplegia uncovers novel gene-disease associations and unanticipated rare disorders. *Eur J Hum Genet* 2016; 2410: 1460–1466.

Willig L, Petrikin J, Smith L, Saunders C, Thiffault I, Miller N, et al. Whole-genome sequencing for identification of Mendelian disorders in critically ill infants: a retrospective analysis of diagnostic and clinical findings. *Lancet Respir Med* 2015; 35: 377–387.

Włodarczyk A, Holtman IR, Krueger M, Yoge N, Bruttger J, Khorrooshi R, et al. A novel microglial subset plays a key role in myelinogenesis in developing brain. *EMBO J* 2017; 3622: 3292–3308.

Wolf NI, Breur M, Plug B, Beerepoot S, Westerveld ASR, van Rappard DF, et al. Metachromatic leukodystrophy and transplantation: remyelination, no cross-correction. *Ann Clin Transl Neurol* 2020; 72: 169–180.

Wolf NI, ffrench-Constant C, van der Knaap MS. Hypomyelinating leukodystrophies — unravelling myelin biology. *Nat Rev Neurol* 2021; 172: 88–103.

Wolf NI, Harting I, Boltshauser E, Wiegand G, Koch MJ, Schmitt-Mechelke T, et al. Leukoencephalopathy with ataxia, hypodontia, and hypomyelination. *Neurology* 2005; 648: 1461–1464.

Wright CF, Fitzgerald TW, Jones WD, Clayton S, McRae JF, Van Kogelenberg M, et al. Genetic diagnosis of developmental disorders in the DDD study: A scalable analysis of genome-wide research data. *Lancet* 2015; 3859975: 1305–1314.

Wright CF, FitzPatrick DR, Firth H V. Paediatric genomics: Diagnosing rare disease in children. *Nat Rev Genet* 2018; 195: 253–268.

Yan H, Helman G, Murthy SE, Ji H, Crawford J, Kubisiak T, et al. Heterozygous Variants in the Mechanosensitive Ion Channel TMEM63A Result in Transient Hypomyelination during Infancy. *Am J Hum Genet* 2019; 1055: 996–1004.

Yang Y, Muzny DM, Reid JG, Bainbridge MN, Willis A, Ward PA, et al. Clinical whole-exome sequencing for the diagnosis of mendelian disorders. *N Engl J Med* 2013; 36916: 1502–1511.

Yang Y, Muzny DM, Xia F, Niu Z, Person R, Ding Y, et al. Molecular findings among patients referred for clinical whole-exome sequencing. *Jama* 2014; 31218: 1870–1879.

Yuste R, Bargmann C. Toward a Global BRAIN Initiative. *Cell* 2017; 1686: 956–959.

Zech M, Jech R, Boesch S, Škorvánek M, Weber S, Wagner M, et al. Monogenic variants in dystonia:

an exome-wide sequencing study. Lancet Neurol 2020; 19(11): 908–918.

Zou F, Zuck T, Pickersgill CD, Zamora FM, Retterer K, Scuffins J, et al. A Comprehensive and Dynamic Approach for Genetic Testing for Patient with Leukodystrophy Demonstrates a Genetic Etiology in 33% of Cases (P4.6-054). Neurology 2019; 92(15 Supplement): P4.6-054.

IX. ANNEX. Altres publicacions amb participació del doctorand fruit del present treball

Altres publicacions de nous gens identificats en aquest projecte

Article A1. Bi-allelic variants in the mitochondrial RNase P subunit *PRORP* cause mitochondrial tRNA processing defects and pleiotropic multisystem presentations

Hochberg I, Demain LAM, Richer J, Thompson K, Urquhart JE, Rea A, Pagarkar W, **Rodríguez-Palmero A**, Schlüter A, Verdura E, Pujol A, Quijada-Fraile P, Amberger A, Deutschmann AJ, Demetz S, Gillespie M, Belyantseva IA, McMillan HJ, Barzik M, Beaman GM, Motha R, Ng KY, O'Sullivan J, Williams SG, Bhaskar SS, Lawrence IR, Jenkinson EM, Zambonin JL, Blumenfeld Z, Yalonetsky S, Oerum S, Rossmanith W; Genomics England Research Consortium, Yue WW, Zschocke J, Munro KJ, Battersby BJ, Friedman TB, Taylor RW, O'Keefe RT, Newman WG. Bi-allelic variants in the mitochondrial RNase P subunit PRORP cause mitochondrial tRNA processing defects and pleiotropic multisystem presentations. *Am J Hum Genet.* 2021; 25:S0002-9297(21)00379-7. doi: 10.1016/j.ajhg.2021.10.002. Epub ahead of print.
Factor d'impacte (quartil per especialitat): 10.5 (Q1)

Article A2. Impairment of the mitochondrial one-carbon metabolism enzyme *SHMT2* causes a novel brain and heart developmental syndrome.

García-Cazorla À, Verdura E, Juliá-Palacios N, Anderson EN, Goicoechea L, Planas-Serra L, Tsogtbaatar E, Dsouza NR, Schlüter A, Urreizti R, Tarnowski JM, Gavrilova RH; SHMT2 Working Group, Ruiz M, **Rodríguez-Palmero A**, Fourcade S, Cogné B, Besnard T, Vincent M, Bézieau S, Folmes CD, Zimmermann MT, Klee EW, Pandey UB, Artuch R, Cousin MA, Pujol A. *Acta Neuropathol.* 2020;140(6):971-975. doi: 10.1007/s00401-020-02223-w.
Factor d'impacte (quartil per especialitat): 17.088 (Q1)

Altres publicacions de nous fenotips identificats en aquest projecte

Article A3. *POLR3A* variants with striatal involvement and extrapyramidal movement disorder.

Harting I, Al-Saady M, Krägeloh-Mann I, Bley A, Hempel M, Bierhals T, Karch S, Moog U, Bernard G, Huntsman R, van Spaendonk RML, Vreeburg M, **Rodríguez-Palmero A**, Pujol A, van der Knaap MS, Pouwels PJW, Wolf NI. *Neurogenetics*. 2020;21(2):121-133. doi: 10.1007/s10048-019-00602-4.

Factor d'impacte (quartil per especialitat): 2.66 (Q2)

Article A4. *HNRNPH1*-related syndromic intellectual disability: Seven additional cases suggestive of a distinct syndromic neurodevelopmental syndrome.

Reichert SC, Li R, A Turner S, van Jaarsveld RH, Massink MPG, van den Boogaard MH, Del Toro M, **Rodríguez-Palmero A**, Fourcade S, Schlueter A, Planas-Serra L, Pujol A, Iascone M, Maitz S, Loong L, Stewart H, De Franco E, Ellard S, Frank J, Lewandowski R. *Clin Genet*. 2020; 98(1):91-98. doi: 10.1111/cge.13765.

Factor d'impacte (quartil per especialitat): 4.438 (Q1)

Publicació de validació funcional d'una variant intrònica

Article A5. A novel hypomorphic splice variant in *EIF2B5* gene is associated with mild ovarioleukodystrophy

Rodríguez-Palmero A, Schlüter A, Verdura E, Ruiz M, Martínez JJ, Gourlaouen I, Ka C, Lobato R, Casasnovas C, Le Gac G, Fourcade S, Pujol A. *Ann Clin Transl Neurol* 2020; 7(9): 1574-79.

Factor d'impacte (quartil per especialitat): 3.66 (Q2)

Bi-allelic variants in the mitochondrial RNase P subunit PRORP cause mitochondrial tRNA processing defects and pleiotropic multisystem presentations

Irit Hochberg,^{1,16,22} Leigh A.M. Demain,^{2,3,22} Julie Richer,⁴ Kyle Thompson,⁵ Jill E. Urquhart,^{2,3} Alessandro Rea,^{2,3} Waheeda Pagarkar,⁶ Agustí Rodríguez-Palmero,^{7,8} Agatha Schlüter,⁷ Edgard Verdura,⁷ Aurora Pujol,^{7,9} Pilar Quijada-Fraile,¹⁰ Albert Amberger,¹¹ Andrea J. Deutschmann,¹¹ Sandra Demetz,¹¹ Meredith Gillespie,⁴ Inna A. Belyantseva,¹² Hugh J. McMillan,¹³ Melanie Barzik,¹² Glenda M. Beaman,^{2,3} Reeya Motha,¹⁴ Kah Ying Ng,¹⁵ James O'Sullivan,^{2,3} Simon G. Williams,^{2,3} Sanjeev S. Bhaskar,^{2,3} Isabella R. Lawrence,⁵ Emma M. Jenkinson,² Jessica L. Zambonin,⁴ Zeev Blumenfeld,¹⁶ Sergey Yalonetsky,^{13,17} Stephanie Oerum,¹⁸ Walter Rossmanith,¹⁹ Genomics England Research Consortium, Wyatt W. Yue,¹⁸ Johannes Zschocke,¹¹ Kevin J. Munro,^{20,21} Brendan J. Battersby,¹⁵ Thomas B. Friedman,¹² Robert W. Taylor,⁵ Raymond T. O'Keefe,^{2,*} and William G. Newman^{2,3,*}

Summary

Human mitochondrial RNase P (mt-RNase P) is responsible for 5' end processing of mitochondrial precursor tRNAs, a vital step in mitochondrial RNA maturation, and is comprised of three protein subunits: TRMT10C, SDR5C1 (HSD10), and PRORP. Pathogenic variants in *TRMT10C* and *SDR5C1* are associated with distinct recessive or x-linked infantile onset disorders, resulting from defects in mitochondrial RNA processing. We report four unrelated families with multisystem disease associated with bi-allelic variants in *PRORP*, the metallonuclease subunit of mt-RNase P. Affected individuals presented with variable phenotypes comprising sensorineural hearing loss, primary ovarian insufficiency, developmental delay, and brain white matter changes. Fibroblasts from affected individuals in two families demonstrated decreased steady state levels of PRORP, an accumulation of unprocessed mitochondrial transcripts, and decreased steady state levels of mitochondrial-encoded proteins, which were rescued by introduction of the wild-type PRORP cDNA. In mt-tRNA processing assays performed with recombinant mt-RNase P proteins, the disease-associated variants resulted in diminished mitochondrial tRNA processing. Identification of disease-causing variants in *PRORP* indicates that pathogenic variants in all three subunits of mt-RNase P can cause mitochondrial dysfunction, each with distinct pleiotropic clinical presentations.

Mitochondrial RNase P (mt-RNase P) is the endonuclease that processes the 5' end of mitochondrial tRNAs and thereby also releases adjacent mRNAs and rRNAs from the polycistronic primary transcripts.¹ In humans, the mt-RNase P complex is composed of three proteins, TRMT10C, SDR5C1 (HSD10), and PRORP (called MRPP1, MRPP2, and MRPP3, respectively), each encoded by the nuclear genome.^{2,3} Bi-allelic variants in *TRMT10C* (MIM: 615423) have been identified in two unrelated individuals

with a lethal childhood multisystem disorder, characterized by muscle hypotonia, sensorineural hearing loss (SNHL), metabolic acidosis, and multiple oxidative phosphorylation (OXPHOS) deficiencies (MIM: 616974).⁴ SDR5C1 (also known as HSD10, HADH2, MRPP2, or ABAD [MIM: 300256]), encoded by the X chromosome gene *HSD17B10*, is a moonlighting protein with involvement in multiple biochemical pathways, including isoleucine metabolism.^{3,5} Pathogenic variants in *HSD17B10*

¹Institute of Endocrinology, Diabetes, and Metabolism, Rambam Health Care Campus, Haifa 3109601, Israel; ²Division of Evolution, Infection, and Genomics, School of Biological Sciences, University of Manchester, Manchester M13 9PL, UK; ³Manchester Centre for Genomic Medicine, St Mary's Hospital, Manchester University NHS Foundation Trust, Manchester M13 9WL, UK; ⁴Department of Genetics, Children's Hospital of Eastern Ontario, Ottawa, ON K1H 8L1, Canada; ⁵Wellcome Centre for Mitochondrial Research, Clinical and Translational Research Institute, Faculty of Medical Sciences, Newcastle University, Newcastle upon Tyne NE2 4HH, UK; ⁶Royal National ENT and Eastman Dental Hospital, University College London Hospitals, London WC1E 6DG, UK; ⁷Neurometabolic Diseases Laboratory, Bellvitge Biomedical Research Institute, L'Hospitalet de Llobregat, and Center for Biomedical Research on Rare Diseases, 08908 Barcelona, Spain; ⁸Paediatric Neurology Unit, Hospital Universitari Germans Trias i Pujol, Universitat Autònoma de Barcelona, 08916 Barcelona, Spain; ⁹Catalan Institution for Research and Advanced Studies, 08010 Barcelona, Spain; ¹⁰Unit of Mitochondrial and Inherited Metabolic Diseases, Pediatric Department, University Hospital 12 de Octubre, National Reference Center, European Reference Network for Hereditary Metabolic Disorders, 28041 Madrid, Spain; ¹¹Institute of Human Genetics, Medical University Innsbruck, Innsbruck 6020, Austria; ¹²Laboratory of Molecular Genetics, National Institute on Deafness and Other Communication Disorders, National Institutes of Health, Bethesda, MD 20892-3729, USA; ¹³Department of Pediatrics, Children's Hospital of Eastern Ontario, University of Ottawa, Ottawa, ON K1H 8L1, Canada; ¹⁴The Royal London Hospital, Whitechapel Road, Whitechapel, London E1 1FR, UK; ¹⁵Institute of Biotechnology, University of Helsinki, 00790 Helsinki, Finland; ¹⁶Rappaport Faculty of Medicine, Technion - Israel Institute of Technology, Haifa 3109601, Israel; ¹⁷Department of Pediatric Cardiology, Rambam Health Care Campus, Haifa 3109601, Israel; ¹⁸Newcastle MX Structural Biology Laboratory, Newcastle University, Medical School, NUBI Framlington Place, Newcastle upon Tyne NE2 4HH, UK; ¹⁹Center for Anatomy and Cell Biology, Medical University of Vienna, 1090 Vienna, Austria; ²⁰Manchester Centre for Audiology and Deafness, School of Health Sciences, University of Manchester, Manchester M13 9PL, UK; ²¹Manchester University NHS Foundation Trust, Manchester M13 9WL, UK

²²These authors contributed equally

*Correspondence: rokeefe@manchester.ac.uk (R.T.O.), wiliam.newman@manchester.ac.uk (W.G.N.)
<https://doi.org/10.1016/j.ajhg.2021.10.002>.

© 2021

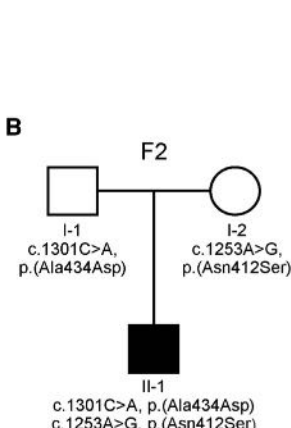
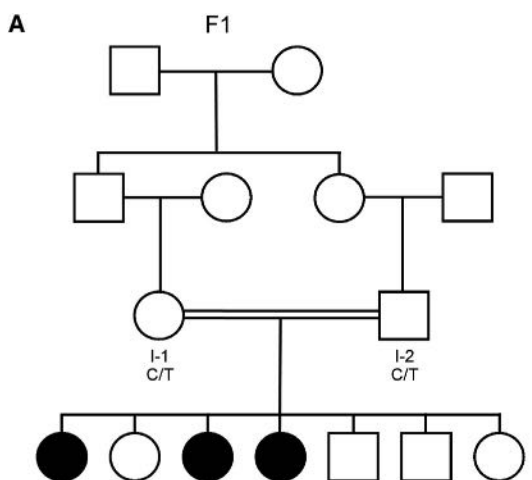


Figure 1. Variants in *PRORP* in four affected families result in pleiotropic clinical presentations

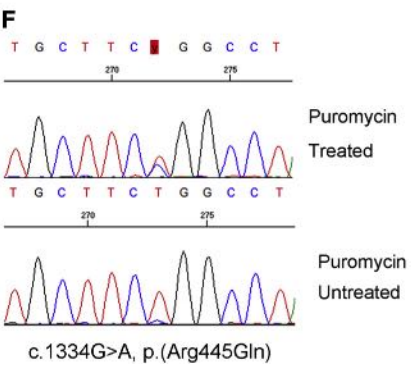
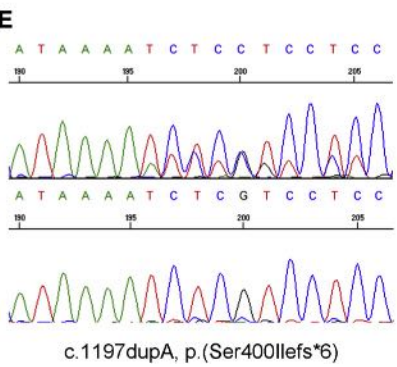
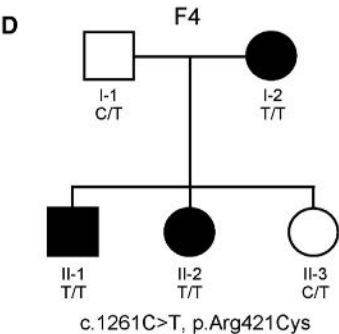
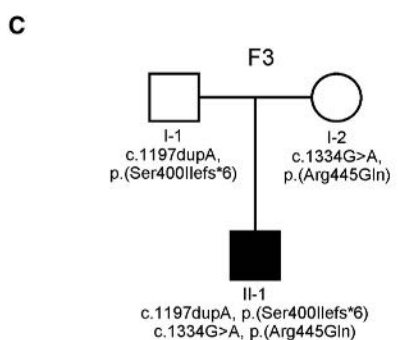
(A) The pedigree for a family (F1) with a variant in *PRORP*.

(B) The pedigree for the family F2.

(C) The pedigree for the family F3 and compound heterozygous variants in *PRORP*.

(D) The pedigree for a family (F4) with three affected individuals. Filled symbols indicate affected individuals.

(E and F) Sanger sequencing trace for the variants c.1197dupA and c.1334 G>A (highlighted in red) in the proband from F3 (II-1) with cDNA from puromycin treated and untreated fibroblasts. We display sequences in the reverse orientation to prevent masking of the missense variant by the frameshift variant. Sanger sequencing of the cDNA revealed that the frameshift c.1197dupA variant was present in the puromycin-treated cells, but not the untreated cells (E) and the missense variant c.1334G>A was present as a hemizygous change in the untreated samples (F), indicating that the frameshift transcript undergoes nonsense-mediated decay (E and F).



cause HSD10 disease (MIM: 300438), manifesting in males as a severe, infantile-onset neurodegenerative condition with cardiomyopathy.^{5,6} Both disorders are characterized by defects of mitochondrial tRNA processing.^{4,7,8}

PRORP (previously *KIAA0391* [MIM: 609947]) encodes the endonuclease subunit of the mt-RNase P complex. Here, we describe four families with overlapping phenotypes resulting from bi-allelic variants in *PRORP*. All individuals or their guardians provided written informed consent to participate in the gene discovery study in

accordance with local regulations (see [supplemental information](#)).

Affected individuals from two families, F1 and F2, presented with SNHL, which was accompanied in the affected females in F1 by primary ovarian insufficiency, consistent with a diagnosis of Perrault syndrome (MIM: 233400).⁹ In family F3, there was childhood onset of SNHL, lactic acidosis, and leukoencephalopathy, whereas affected individuals in family F4 presented with leukoencephalopathy. Recent reports of some individuals with variants in genes associated with Perrault syndrome have expanded the phenotypic spectrum to include presentations with childhood metabolic crises^{9,10} and leukoencephalopathy.^{9,11}

Family 1 (F1) is composed of three affected female siblings, two unaffected female siblings, two unaffected male siblings, and their unaffected parents (Figure 1A). At the last assessment the affected sisters were aged 30, 28, and 26 years of age. All three affected sisters presented with absent middle ear acoustic reflex, despite normal tympanometry, when tested in infancy and subsequent audiology examinations in each sister revealed profound bilateral SNHL (>90 dB hearing level at all frequencies) (Figure S1A). The three affected sisters each presented in their late teenage years with primary

amenorrhea, consistent with a diagnosis of Perrault syndrome (see "GeneReviews" in [web resources](#)). Pelvic ultrasound noted the absence of ovarian tissue in all three sisters. Hormonal profiles indicated hypergonadotropic hypogonadism ([Figure S1C](#)) with otherwise normal endocrine and biochemical tests and a 46, XX karyotype. The affected sisters were prescribed estrogen to induce puberty and are currently maintained on hormone replacement therapy. Each affected sibling has mild non-progressive intellectual disability (brain MR imaging has not been performed). Echocardiography for each of the affected sisters was normal. All other physical and neurological examinations were normal.

A homozygous variant in *PRORP*, c.1454C>T (p.Ala485Val) (GenBank: NM_014672.3), was identified in the affected individuals of F1 via autozygosity mapping and whole-exome sequencing. The variant segregated with the phenotype in the family.

Family 2 (F2) comprises a male proband and his unaffected, unrelated parents ([Figure 1B](#)). The proband (F2, II-1) was born at 40 + 4 weeks by emergency caesarean section for fetal tachycardia and meconium stained liquor. Hearing loss in the proband was first noted at 3 years of age but formally diagnosed at 5 years, at which age his brain magnetic resonance imaging (MRI) was normal. He was 9 years at last assessment and had bilateral mild to moderate SNHL ([Figure S1B](#)). His speech and language skills are delayed as a result of the hearing loss and he wears bilateral hearing aids. No behavioral or neurological issues have been noted and cardiovascular, respiratory, and abdominal system examinations have been unremarkable. A maternally inherited c.1235A>G (p.Asn412Ser) variant and a paternally inherited c.1301C>A (p.Ala434Asp) variant in *PRORP* were identified in the proband from whole genome sequence data generated through the 100,000 Genomes Project ([Figure 1B](#)).¹²

In family 3 (F3), a male proband (F3, II-1) of non-consanguineous unaffected parents ([Figure 1C](#)) was born by emergency caesarean section for failure to progress at 41 + 2 weeks gestation. Examination shortly after birth found appendicular hypertonia, more pronounced on the left-hand side, and mild dysmorphism (mild hypertelorism, bilateral epicanthal folds, thin vermillion of the lips, and microretrognathia). At 7 months of age, plasma lactic acid levels were increased at 5.6 mmol/L (reference 0.5–2.5 mmol/L) despite normal levels of plasma amino acids, urine organic acids, acylcarnitines, and free and total carnitine. Urine analysis and serum creatinine were normal. Repeat testing at 24 months revealed plasma lactic acid levels still raised at 3.0 mmol/L. Severe feeding difficulties resulted in the insertion of a gastrostomy tube at 15 months. An electroencephalogram (photic stimulation included) at 19 months revealed no evidence of seizure activity. At 20 months, he had severe global developmental delay, diffuse asymmetric hypertonia, acquired microcephaly (head circumference: 45.7 cm, <2nd percentile), and a mild scoliosis. Brain MRI at 13 months revealed peri-

ventricular nodular heterotopias, a dysplastic corpus callosum, diffuse sub-cortical white matter loss, and bilateral connatal cysts ([Figure S2](#)). Audiological tests were normal at 18 months, but at 3 years, an auditory brainstem response examination demonstrated evidence of auditory neuropathy spectrum disorder consistent with bilateral SNHL.

Microarray analysis performed on the proband (F3, II-1) detected no copy number variants. Whole-exome sequencing identified bi-allelic variants in *PRORP*, a maternally inherited missense variant c.1334G>A (p.Arg445Gln) (rs777185638) and a paternal frameshift variant c.1197dupA (p.Ser400Ilefs*6) (rs764714439), which was shown to result in nonsense-mediated decay of the transcript ([Figures 1E](#) and [1F](#)).

Family F4 is a family comprising three affected individuals, including a brother and sister and their affected mother ([Figure 1D](#)). The proband (F4, II-1) was 19 years of age at last assessment. He presented with a psychotic disorder, autistic traits, and learning disability at 7 years. At 8 years, he presented with brief generalized seizures consisting of loss of consciousness and generalized stiffening of the body and extremities. The EEG was normal, but he received treatment with levetiracetam with a good response. Recent physical examination showed obesity and genu and talus valgus. Fundoscopy displayed papillary pallor.

Brain MRI indicated bilateral multiple periventricular and subcortical T2 white matter hyperintense lesions with a posterior predominance that remain unchanged in successive controls ([Figure S2](#)). Spectroscopy was normal. Electromyogram and nerve conduction studies revealed no evidence of neuromuscular abnormalities. Ocular and auditory nerve response as assessed by visual evoked potential and auditory brainstem response were normal. Metabolic studies indicated increased lactate/pyruvate ratio with normal plasma lactate, plasma amino acids, and urine organic acids. The proband is currently treated with coenzyme Q10, vitamin B2, vitamin C, carnitine, and arginine.

The affected sister of the proband (F4, II-2) was aged 17 years at last assessment. F4, II-2 presented with intrauterine growth retardation, global developmental delay, and seizures in the first years of life. At the age of 15 years, she presented with tremor in her legs, migraines, and hyperglycemia. Lactate levels were normal. Her hearing is normal as are her electromyogram (EMG) and nerve conduction studies. Brain MRI displayed bilateral multiple periventricular and subcortical T2 white matter hyperintense lesions with a posterior predominance that remain unchanged in successive controls ([Figure S2](#)). Spectroscopy was normal. Like her brother, she is treated with coenzyme Q10, vitamin B2, vitamin C, and carnitine.

The mother (F4, I-2) of the proband presented with retrobulbar optic neuritis and tonic pupil (a dilated pupil that responded slowly to light) at 39 years of age. Subsequently, she presented with asthenia, myalgias, memory

Table 1. Analysis of variants in *PRORP* in four families with distinct clinical presentations

Family	F1	F2	F3	F4
Family details				
Family details	three affected female siblings	one affected male	one affected male	two affected siblings and their affected mother
Phenotype	Perrault syndrome	SNHL		
Variant details				
Variant	<i>PRORP</i> : c.1454C>T (p.Ala485Val)	<i>PRORP</i> : c.1235A>G (p.Asn412Ser)	<i>PRORP</i> : c.1301C>A (p.Arg444Gln)	<i>PRORP</i> : c.1197dupA (p.Ser400IlefsX6)
Location	Chr14(GRCh37): g.35739636C>T	Chr14(GRCh37): g.35649943A>G	Chr14(GRCh37): g.35735958C>A	Chr14(GRCh37): g.35649969C>T
dbSNP	not present	rs148259590	rs144536804	rs147065101
Zygosity	homozygous	heterozygous	heterozygous	homozygous
Inheritance	N/A	maternal	maternal	N/A
gnomAD	not present	0.0001382 (39 heterozygotes, 0 homozygotes)	0.0008385 (237 heterozygotes, 0 homozygotes)	0.0002475 (7 heterozygotes, 0 homozygotes)
MAF (count)				
Prediction tools				
SIFT	deleterious (0.0)	deleterious (0.0)	deleterious (0.0)	N/A
PolyPhen	probably damaging (1.0)	probably damaging (1.0)	benign (0.443)	probably damaging (1.0)
MutationTaster	disease causing (1.0)	disease causing (1.0)	disease causing (0.811)	disease causing (1.0)
VarCards	0.91 (extreme)	0.74(extreme)	0.39	0.83 (extreme)
CADD	34	26.4	28.2	34
Conservation	highly conserved	highly conserved	moderately conserved	highly conserved

(Continued on next page)

Table 1. Continued

Family	F1	F2	F3	F4
Effect on protein	Variant prediction may distort the active site	may interfere with the shape of the active site	reduce the stability of the protein	directly impact nuclease function loss of function this region is disordered in the structure so was not modeled
POLDX change	reduces stability ($\Delta\Delta G$ 3.97 kcal/mol)	slightly reduces stability ($\Delta\Delta G$ 1.61 kcal/mol)	slightly reduces stability ($\Delta\Delta G$ 1.66 kcal/mol)	N/A
tRNA processing (approximate % of wild-type)	82%	13%	86%	25% N/A 81%

All variants mapped to the PRORP transcript GenBank: NM_014672.3. SNHL, sensorineural hearing loss; MAF, minor allele frequency.

loss, and frequent headaches. She also had two episodes of left hemiparesis and hypoesthesia that resolved in 15 days without specific treatment and repetitive episodes of lower limb thrombophlebitis. Examination revealed afferent pupillary defect, nasal hemianopsia of the right visual field, and abnormal color perception. She also had distal weakness of the lower limbs, areflexia, and vibratory hypoesthesia of the left side of her body. Her hearing is normal, and she has no evidence of ovarian insufficiency. Routine blood tests and metabolic and thrombophilia studies were all normal. Specific genetic testing for metachromatic leukodystrophy, Krabbe disease, CADASIL, and Leber optic neuropathy were negative. Cerebrospinal fluid (CSF) oligoclonal bands and anti-MOG and anti-NMO antibodies were also negative. Visual evoked potentials displayed abnormal conduction in the right eye. EMG and nerve conduction studies were normal. Brain MRI indicated bilateral multiple periventricular and subcortical T2 white matter hyperintense lesions affecting both hemispheres, corpus callosum, pons, and cerebellum with no contrast enhancement and no changes in successive controls (Figure S2).

Whole-genome sequencing identified a homozygous c.1261C>T (p.Arg421Cys) *PRORP* variant in all three affected individuals. The father (F4, I-1) of the two affected children was a carrier for the variant, and subsequently, the family was confirmed to be consanguineous, consistent with the pseudo-dominant inheritance pattern. There was no evidence of any other putative disease-associated variants in the genome and exome datasets in the four families when the filtering steps were applied (supplemental information).

The altered residues in PRORP identified in the affected individuals from the four families are all highly conserved from vertebrates to fly (Figure S3). All of the variants are either absent from gnomAD¹³ or have a very low minor allele frequency and are not present as homozygous variants. All missense variants were predicted to be deleterious by multiple prediction software (Table 1). Of note, homozygous loss-of-function variants in *PRORP* are absent from publicly available databases and from a consanguineous cohort of >3,200 British Pakistani individuals.¹⁴

Mitochondrial tRNAs (mt-tRNAs) are processed at the 5' end by mt-RNase P¹ and at the 3' end by mt-RNase Z (encoded by *ELAC2* [MIM: 605367]).^{15,16} This tRNA cleavage also releases most of the RNA species from the polycistronic mitochondrial precursor transcripts according to the mitochondrial tRNA punctuation model.^{17,18} PRORP, as a subunit of mt-RNase P, catalyzes the Mg²⁺-dependent phosphodiester-bond cleavage of 5' extensions of mitochondrial tRNAs.^{2,19} The processing of mitochondrial tRNAs proceeds in a stepwise manner and 5' cleavage by mt-RNase P precedes tRNA 3' end processing.^{1,18}

We investigated the steady-state levels of the mt-RNase P subunits TRMT10C, SDR5C1, and PRORP in dermal fibroblasts available from affected individuals in families F1 and F3 by immunoblotting and detected a decrease in

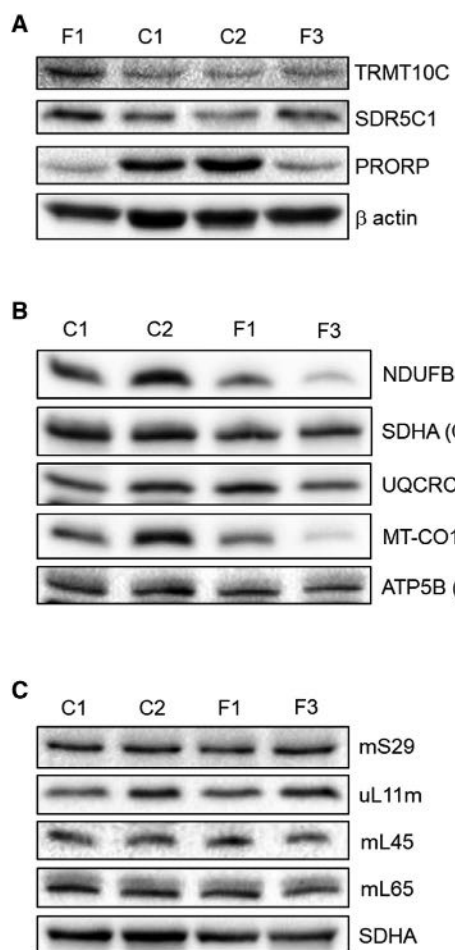


Figure 2. Fibroblasts from affected individuals F1, II-4 and F3, II-1 display reduction in subunits of mt-RNase P and reduced levels of mitochondrial DNA encoded-OXPHOS subunits but no reduction in mitochondrial ribosomal proteins

(A) Immunoblot analysis of mt-RNase P subunits TRMT10C, SDR5C1, and PRORP in fibroblasts from two healthy controls (C1 and C2); individual F1, II-4 with the p.Ala485Val variant in PRORP and the individual F3, II-1, who has compound heterozygous variants in PRORP ($n = 3$)

(B) Immunoblot analysis of proteins of the five oxidative phosphorylation complexes. Included are two control samples (C1 and C2) and two samples from affected individuals as detailed in (A) ($n = 3$).

(C) Immunoblot analysis of protein subunits of the mitochondrial ribosome. SDHA is included as a loading control. Samples for affected individuals and controls labeled as in (A) ($n = 3$).

PRORP levels in both affected individuals compared to controls (Figure 2A). The decrease in PRORP suggests that the variant p.Ala485Val is either less stable than the wild-type protein or downregulated in affected individuals from family F1. The decreased PRORP levels in F3, II-1 may partially result from absence of protein due to the allele that is subject to nonsense-mediated decay (Figures 1E and 1F). We also detected decreased steady-state levels of respiratory chain complex I (NDUFB8) and complex IV (COXI) subunits in fibroblasts from affected individuals compared to controls—both complexes contain mitochondrial DNA-encoded subunits. There was no change

of other OXPHOS components, most notably complex II, which is entirely nuclear encoded (Figure 2B). This profile is consistent with a generalized defect in mitochondrial translation. The decreased stability of complex I and IV subunits was more severe in subject F3, II-1, consistent with his more severe clinical phenotype. There was no noticeable difference in levels of several mitoribosomal proteins (MRPs) between the fibroblasts from affected individuals and controls (Figure 2C), indicating that any effect on translation most likely reflects a defect of transcript processing rather than a defect in the stability or assembly of the mitoribosome itself.

To determine the status of mitochondrial-encoded RNA transcripts in subject dermal fibroblasts, Northern blots were performed. We designed biotinylated strand-specific probes to detect transcripts from four different regions of the mitochondrial genome. An *MT-ND1* probe revealed the accumulation of a precursor RNA of approximately 2.5 kb in the samples from F1, II-4 and F3, II-1 (C1 and C2) (Figure 3), corresponding to unprocessed 16S rRNA-tRNALeu(UUR)-ND1 mRNA and apparently resulting from impaired 5' end processing of mt-tRNA^{Leu(UUR)}. This RNA species was previously termed RNA 19 and observed to be upregulated by the 3243A>G MELAS and other variants in mt-tRNA^{Leu(UUR)}.^{20–22} A larger RNA species was detected on a longer exposure for the *MT-ND1* probe, indicating that mt-tRNA^{Val} processing is also decreased. The *MT-ND2* and *MT-CO2* probes both detected multiple RNA species seen in affected individuals but not control samples. A *MT-ND6* probe detected a mitochondrial light strand transcript of approximately 2.3 kb in the F1, II-4 and F3, II-1 samples, which can be explained by impaired 5' processing of mt-tRNA^{Glu} (Figure 3). The presence of multiple large transcripts in the samples from the affected individuals, not seen in the control samples at the same intensity, indicates a deficiency in 5' processing across multiple mt-tRNA sites.

All disease-associated variants are located in the metallo-nuclease domain of PRORP (Figure S4A), as revealed by its crystal structure.²³ Residue Ala485 is situated close to four conserved aspartate residues implicated in metal-ion binding (Figure S4B).²³ Replacing the conserved alanine at residue 485 with the bulkier valine (F1) could distort the active site and impair catalysis by interfering with proper coordination of the metal ions, thereby reducing the endonucleolytic activity of PRORP. Residue Ala434 is surface exposed and the substitution Ala434Asp (F2) is predicted to slightly reduce the stability of PRORP but no structural change to the protein (Figure S4C). Residue Asn412 is located in the active site next to catalytic residue Asp409 (Figure S4D). Substitution Asn412Ser (also F2) results in no drastic structural changes but may interfere with the shape of the active site, thereby reducing the endonucleolytic activity of PRORP. Residue Arg445 forms stabilizing interactions with essential catalytic residues (e.g., Asp479, Asp478) (Figure S4E). It is likely that Arg445Gln (F3) would directly impact nuclease activity. In 150

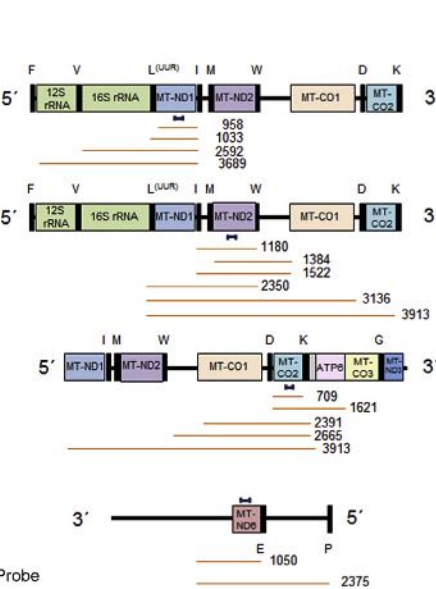
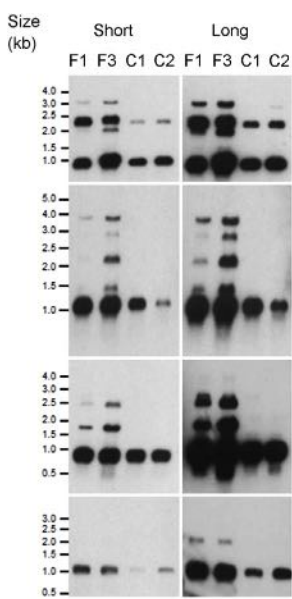


Figure 3. Fibroblasts from affected individuals display impaired mitochondrial RNA processing

(A) Northern blot assessment of RNA extracted from F1, II-4 and F3, II-1 fibroblasts and two control (C1 and C2) samples with strand specific probes designed to complement four different mitochondrial gene transcripts: *MT-ND1*, *MT-ND2*, *MT-CO2*, and *MT-ND6*. A long and short exposure of the blots are presented.

(B) Schematic representations of mitochondrial genome regions, the probes (red) and expected fragment sizes in bp (orange) are displayed to the right of each blot.

orthologs, the residue equivalent to Arg445 is invariably Arg (data not shown). The amino acid at residue 421 is highly variable and is disordered in the structure. During the review of this manuscript, the cryo-EM structure of PRORP in complex with tRNA, TRMT10C, and SDR5C1 was determined.²⁴ In addition to supporting the above interpretations of disease-associated variants, this structure reveals that PRORP residue Arg445 forms an interaction with the 5' end of the tRNA substrate, which will be broken by Arg445Gln (F3). Additionally, Arg421 becomes ordered in the context of the complex and forms stabilizing interactions with residue Glu429, which will be disrupted by Arg421Cys (F4). We investigated whether the disease-associated variants in *PRORP* affected the catalytic activity of the mt-RNase P complex. The three mt-RNase P complex wild-type proteins (TRMT10C, SDR5C1, and PRORP), and the PRORP variant proteins, were individually produced by recombinant expression in bacteria and purified. Recombinant mt-RNase P was reconstituted *in vitro* and 5' leader processing monitored with fluorescent labeled mt-pre-tRNA^{Leu}. All the amino acid variants in PRORP led to a reduction in mt-tRNA^{Leu} cleavage product compared to wild-type PRORP (Figure 4A). The fluorescence intensity of the mt-tRNA^{Leu} cleavage product was quantified. After 30 min from the start of the reaction, the mt-RNase P complexes with variants PRORP p.Arg445Gln (F3) and p.Asn412Ser (F2) displayed the most dramatic decreases in mt-tRNA^{Leu} cleavage products compared to wild-type of approximately 76% and 87%, respectively. The mt-RNase P complexes with variants PRORP p.Ala485Val (F1), p.Ala434Asp (F2), and p.Arg421Cys (F4) reduced 5' leader processing by approximately 19%, 15%, and 10%, respectively. The reductions in processing persisted after 60 min (Table 1). These data indicate that disease-associated PRORP variants reduce the RNase P activity of the complex *in vitro*. Of note, the greatest reduction of activity is seen in

the most severely clinically affected individual (F3, II-1), where a frame-shift resulting in loss of function is present in combination with PRORP p.Arg445Gln. However, there are insufficient data to define genotype-phenotype correlations because of the small number of affected individuals ascertained and investigated.

We performed rescue experiments to establish whether expression of wild-type *PRORP* could reduce the accumulation of unprocessed transcripts in the fibroblasts from an affected individual. Fibroblasts from individual F3, II-1 were transduced with a retroviral vector containing the wild-type *PRORP* cDNA or wild-type *TRMT10C* cDNA as a control. Expression of wild-type *PRORP* restored both the amount of PRORP and MT-CO1 protein, whereas *TRMT10C* and *SDHA* levels were unaffected (Figure 4B). This result indicates that increased levels of wild-type PRORP in the cells from the affected individual enhances the steady state levels of mitochondrial-encoded MT-CO1 but does not affect levels of nuclear-encoded SDHA. This effect is not seen with the empty vector or *TRMT10C* (Figure 4C). Transducing fibroblasts from the affected individual with *PRORP* also decreased the levels of unprocessed mitochondrial transcripts in the cells to near wild-type levels (Figure 4B). Again, this effect is not seen with the empty vector or the vector containing the coding sequence for *TRMT10C*. Taken together, these data indicate that the expression of wild-type *PRORP* in cells from an affected individual can rescue the molecular defects.

We undertook localization studies of PRORP in the mouse organ of Corti to understand why variants in *PRORP* may be associated with hearing loss (Figure S5). After the onset of hearing, which occurs in mice at postnatal day 12, PRORP is detected around the afferent and efferent synapses of the inner hair cells and the efferent synapses of the outer hair cells, indicating possible importance for synaptic functions after the onset of hearing.

PRORP partially co-localizes with a synaptic marker (SNAP25), indicating that it may not only be present in the mitochondria of efferent synapses but possibly also

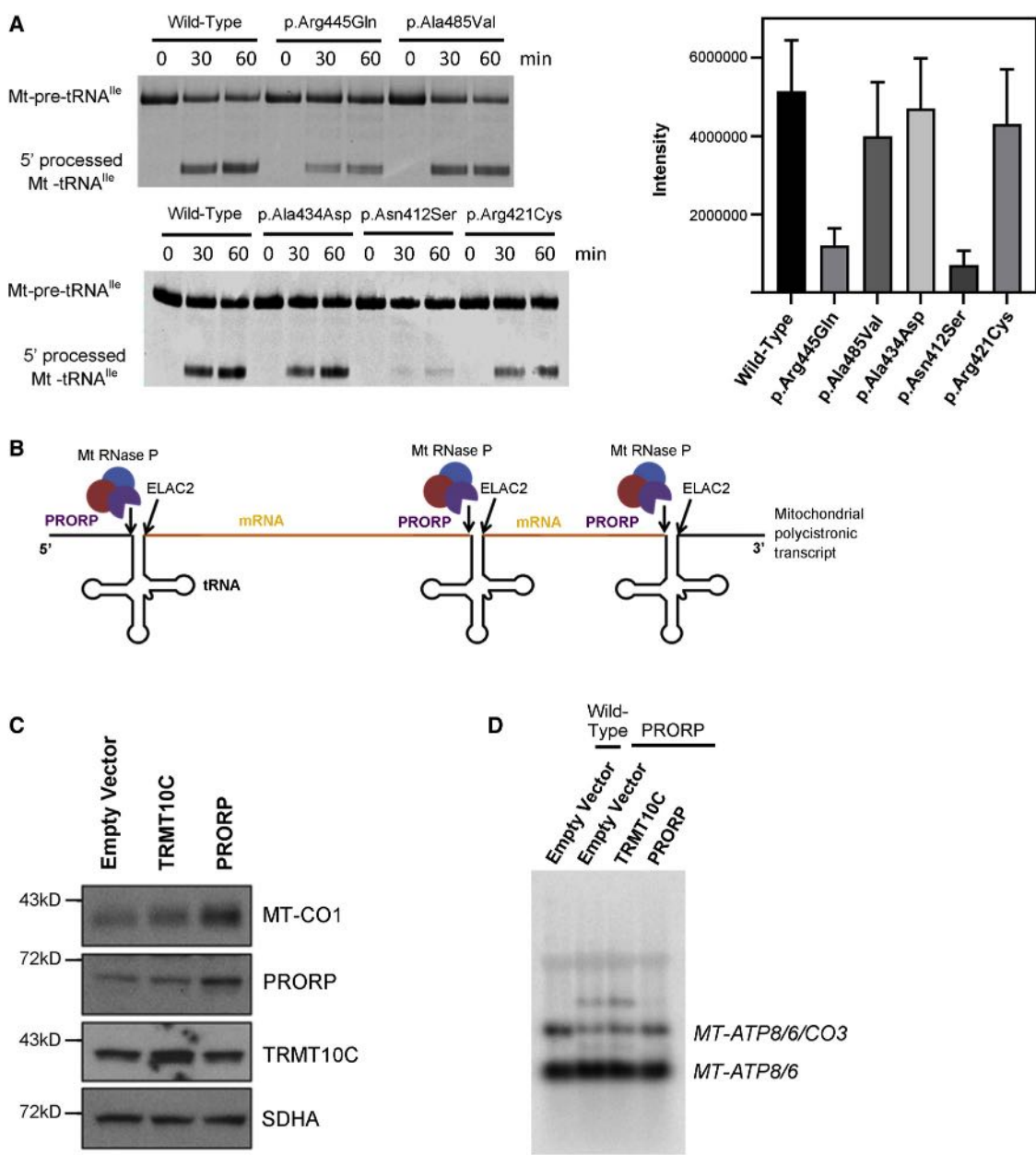


Figure 4. *In vitro* mt-RNase P processing assays reveal all variants produce less 5'-end-processed tRNA than wild-type PRORP; processing defects in subject F3 II-1 are rescued by wild-type KIAA0391

(A) Mitochondrial pre-tRNA^{lle} was cleaved by reconstituted recombinant mt-RNase P containing either wild-type or variant PRORP, as indicated, resulting in the release of the 5' leader sequence. Aliquots were taken from the reactions at the time points indicated and resolved by denaturing electrophoresis. Quantitative analysis of pre-tRNA^{lle} processing revealed an overall decrease in fluorescence intensity of the processed tRNA between wild-type and variants over three replicate experiments. Error bars indicate standard deviation. (B) Cartoon to illustrate the role of PRORP within the RNase P complex in 5' end cleavage of mitochondrial tRNA transcripts. (C) Immunoblotting of whole cell lysates from fibroblasts stably transduced with the indicated cDNAs. (C) Northern blotting of total RNA hybridized with a strand-specific oligonucleotide probe against MT-ATP8.

mitochondria of afferent synapses and nerve fibers around the inner hair cells. The pattern of PRORP staining does not entirely co-localize with mitochondrial marker TOM20. This lack of complete co-localization with TOM20 suggests that the high levels of PRORP found in a subset of mitochondria associated with the synapses and neurons of the organ of Corti hair cells reflect the increased demand for mitochondrial tRNA processing

and translation in these cells, which may be a characteristic of a particular type of mitochondria at these locations.^{25–27}

In summary, we present genetic and functional evidence that bi-allelic variants in *PRORP* are associated with pleiotropic clinical presentations and that *PRORP* should be considered another gene associated with the Perrault syndrome clinical spectrum. Such variability in clinical

presentation is not uncommon for mitochondrial disorders and is increasingly being shown for genes associated with Perrault syndrome.⁹ Bi-allelic hypomorphic variants in *CLPP*, for example, are associated with Perrault syndrome,²⁸ whereas more deleterious variants result in a more severe phenotype associated with SNHL, seizures, and brain white matter changes.¹¹ The clinical spectrum observed in individuals with different bi-allelic *PRORP* variants is consistent with this phenotypic range and most likely reflects altered mitochondrial dysfunction in different tissues at different time points. It is important to note that *PRORP* is ubiquitously expressed in the GTEx dataset. This is consistent with many disorders of mitochondrial function, which have specific clinical phenotypes despite these expression profiles. Notably in the families with multiple affected individuals (F1 and F4), the phenotypes were consistent, indicating that certain *PRORP* variants may result in specific phenotypes.

Similar OXPHOS defects to those seen in individuals with *PRORP* variants have been observed in individuals with pathogenic variants in the mt-RNase P genes *TRMT10C*⁴ and *HSD17B10*,²⁹ suggesting a common pathogenic mechanism in these disorders. Despite the similarities in defective mitochondrial tRNA processing, variants in the three subunits of mt-RNase P result in different clinical phenotypes. With our work, we demonstrate that bi-allelic variants in *PRORP* result in mitochondrial dysfunction and that all three subunits of mitochondrial RNase P have now been associated with mitochondrial disease, each with distinct pleiotropic clinical presentations.

Data and code availability

The *PRORP* variants were submitted to ClinVar (<https://www.ncbi.nlm.nih.gov/clinvar/>) (GenBank: NM_014672.4; accession numbers SCV001943322–SCV001943327). The exome and genome datasets supporting this study have not been deposited in a public repository because of ethical restriction but are available from the corresponding author on request.

Supplemental information

Supplemental information can be found online at <https://doi.org/10.1016/j.ajhg.2021.10.002>.

Acknowledgments

We would like to thank the families for their participation. Family F2 was ascertained via the 100,000 Genomes Project.¹² Families F3 and F4 were identified via GeneMatcher.³⁰ Further funding details are available in the supplemental information.

Declaration of interests

The authors declare no competing interests.

Received: August 24, 2021

Accepted: October 7, 2021

Published: October 28, 2021

Web resources

- dbSNP, <https://www.ncbi.nlm.nih.gov/projects/SNP/>
Exome Variant Server, <https://evs.gs.washington.edu/EVS/>
FoldX, <http://foldxsuite.crg.eu/>
GenBank, <https://www.ncbi.nlm.nih.gov/genbank/>
GeneMatcher, <https://genematcher.org/>
GeneReviews, Newman, W.G., Friedman, T.B., Conway, G.S., and Demain, L.A.M. (2018). Perrault Syndrome, <https://www.ncbi.nlm.nih.gov/books/NBK242617/>
gnomAD, <https://gnomad.broadinstitute.org/>
GTEx, <https://gtexportal.org/home/>
LOVD, <https://www.lovd.nl/>
MutationTaster, <http://www.mutationtaster.org/>
OMIM, <https://www.omim.org/>
PolyPhen-2, <http://genetics.bwh.harvard.edu/pph2/>
SIFT, <https://sift.bii.a-star.edu.sg/>

References

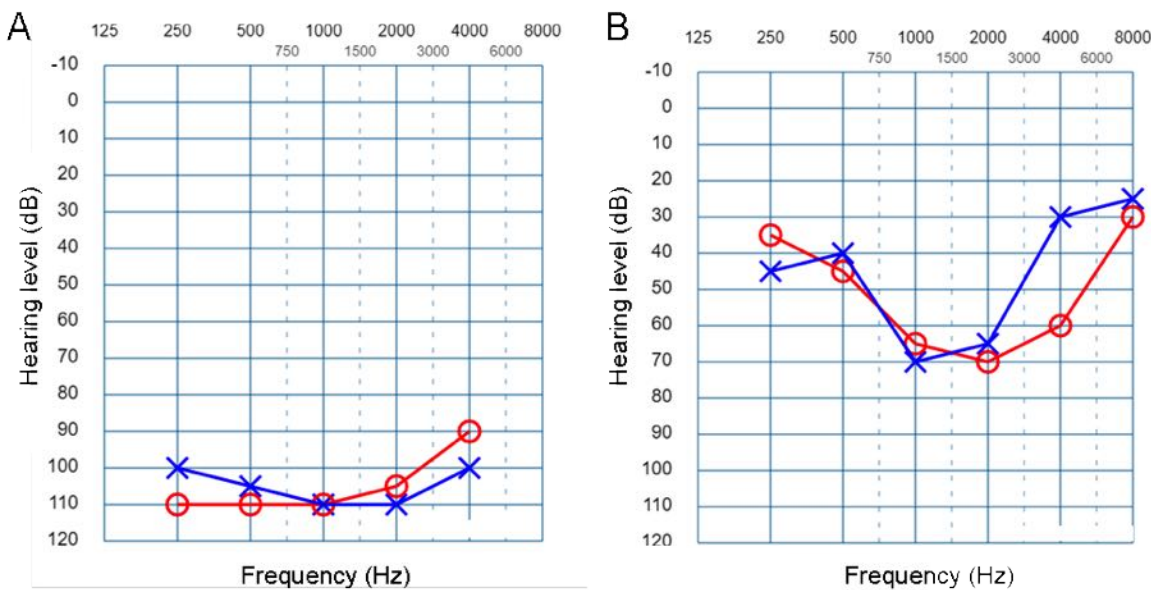
1. Rackham, O., Busch, J.D., Matic, S., Siira, S.J., Kuznetsova, I., Atanassov, I., et al. (2016). Hierarchical RNA processing is required for mitochondrial ribosome assembly. *Cell Rep.* **16**, 1874–1890.
2. Holzmann, J., Frank, P., Löffler, E., Bennett, K.L., Gerner, C., and Rossmanith, W. (2008). RNase P without RNA: identification and functional reconstitution of the human mitochondrial tRNA processing enzyme. *Cell* **135**, 462–474.
3. Vilardo, E., Nachbagauer, C., Buzet, A., Taschner, A., Holzmann, J., and Rossmanith, W. (2012). A subcomplex of human mitochondrial RNase P is a bifunctional methyltransferase-extensive moonlighting in mitochondrial tRNA biogenesis. *Nucleic Acids Res.* **40**, 11583–11593.
4. Metodiev, M.D., Thompson, K., Alston, C.L., Morris, A.A.M., He, L., Assouline, Z., et al. (2016). Recessive mutations in *TRMT10C* cause defects in mitochondrial RNA processing and multiple respiratory chain deficiencies. *Am. J. Hum. Genet.* **98**, 993–1000.
5. Zschocke, J. (2012). HSD10 disease: clinical consequences of mutations in the *HSD17B10* gene. *J. Inherit. Metab. Dis.* **35**, 81–89.
6. Ofman, R., Ruiter, J.P., Feenstra, M., Duran, M., Poll-The, B.T., Zschocke, J., Ensenauer, R., Lehnert, W., Sass, J.O., Sperl, W., and Wanders, R.J. (2003). 2-Methyl-3-hydroxybutyryl-CoA dehydrogenase deficiency is caused by mutations in the *HADH2* gene. *Am. J. Hum. Genet.* **72**, 1300–1307.
7. Deutschmann, A.J., Amberger, A., Zavadil, C., Steinbeisser, H., Mayr, J.A., Feichtinger, R.G., Oerum, S., Yue, W.W., and Zschocke, J. (2014). Mutation or knock-down of 17β-hydroxysteroid dehydrogenase type 10 cause loss of MRPP1 and impaired processing of mitochondrial heavy strand transcripts. *Hum. Mol. Genet.* **23**, 3618–3628.
8. Vilardo, E., and Rossmanith, W. (2015). Molecular insights into HSD10 disease: impact of SDR5C1 mutations on the human mitochondrial RNase P complex. *Nucleic Acids Res.* **43**, 5112–5119.
9. Faridi, R., Rea, A., Fenollar-Ferrer, C., O'Keefe, R.T., Gu, S., Munir, Z., Khan, A.A., Riazuddin, S., Hoa, M., Naz, S., et al. (2021). New insights into Perrault syndrome, a clinically and genetically heterogeneous disorder. *Hum. Genet.* **epub**. <https://doi.org/10.1007/s00439-021-02319-7>.
10. Riley, L.G., Rudinger-Thirion, J., Frugier, M., Wilson, M., Luig, M., Alahakoon, T.I., Nixon, C.Y., Kirk, E.P., Roscioli, T., Lunke,

- S., et al. (2020). The expanding LARS2 phenotypic spectrum: HLASA, Perrault syndrome with leukodystrophy, and mitochondrial myopathy. *Hum. Mutat.* *41*, 1425–1434.
11. Theunissen, T.E., Szklarczyk, R., Gerards, M., Hellebrekers, D.M., Mulder-Den Hartog, E.N., Vanoevelen, J., et al. (2016). Specific MRI abnormalities reveal severe Perrault syndrome due to CLPP defects. *Front. Neurol.* *7*, 203.
12. Turnbull, C., Scott, R.H., Thomas, E., Jones, L., Murugaesu, N., Pretty, F.B., Halai, D., Baple, E., Craig, C., Hamblin, A., et al. (2018). The 100 000 Genomes Project: bringing whole genome sequencing to the NHS. *BMJ* *361*, k1687.
13. Karczewski, K.J., Franciolini, L.C., Tiao, G., Cummings, B.B., Al-földi, J., Wang, Q., Collins, R.L., Laricchia, K.M., Ganna, A., Birnbaum, D.P., et al. (2020). The mutational constraint spectrum quantified from variation in 141,456 humans. *Nature* *581*, 434–443.
14. Narasimhan, V.M., Hunt, K.A., Mason, D., Baker, C.L., Karczewski, K.J., Barnes, M.R., Barnett, A.H., Bates, C., Bellary, S., Bockett, N.A., et al. (2016). Health and population effects of rare gene knockouts in adult humans with related parents. *Science* *352*, 474–477.
15. Brzezniak, L.K., Bijata, M., Szczesny, R.J., and Stepien, P.P. (2011). Involvement of human ELAC2 gene product in 3' end processing of mitochondrial tRNAs. *RNA Biol.* *8*, 616–626.
16. Rossmanith, W. (2011). Localization of human RNase Z isoforms: dual nuclear/mitochondrial targeting of the ELAC2 gene product by alternative translation initiation. *PLoS ONE* *6*, e19152.
17. Ojala, D., Montoya, J., and Attardi, G. (1981). tRNA punctuation model of RNA processing in human mitochondria. *Nature* *290*, 470–474.
18. Rossmanith, W. (2012). Of P and Z: mitochondrial tRNA processing enzymes. *Biochim. Biophys. Acta* *1819*, 1017–1026.
19. Reinhard, L., Sridhara, S., and Hällberg, B.M. (2015). Structure of the nuclease subunit of human mitochondrial RNase P. *Nucleic Acids Res.* *43*, 5664–5672.
20. Schon, E.A., Koga, Y., Davidson, M., Moraes, C.T., and King, M.P. (1992). The mitochondrial tRNA(Leu(UUR)) mutation in MELAS: a model for pathogenesis. *Biochim. Biophys. Acta* *1101*, 206–209.
21. Bindoff, L.A., Howell, N., Poulton, J., McCullough, D.A., Morten, K.J., Lightowers, R.N., Turnbull, D.M., and Weber, K. (1993). Abnormal RNA processing associated with a novel tRNA mutation in mitochondrial DNA. A potential disease mechanism. *J. Biol. Chem.* *268*, 19559–19564.
22. Koga, A., Koga, Y., Akita, Y., Fukiyama, R., Ueki, I., Yatsuga, S., and Matsuishi, T. (2003). Increased mitochondrial processing intermediates associated with three tRNA(Leu(UUR)) gene mutations. *Neuromuscul. Disord.* *13*, 259–262.
23. Howard, M.J., Lim, W.H., Fierke, C.A., and Koutmos, M. (2012). Mitochondrial ribonuclease P structure provides insight into the evolution of catalytic strategies for precursor-tRNA 5' processing. *Proc. Natl. Acad. Sci. USA* *109*, 16149–16154.
24. Bhatta, A., Dienemann, C., Cramer, P., and Hillen, H.S. (2021). Structural basis of RNA processing by human mitochondrial RNase P. *Nat. Struct. Mol. Biol.* *28*, 713–723.
25. Delgado, T., Petralia, R.S., Freeman, D.W., Sedlacek, M., Wang, Y.X., Brenowitz, S.D., Sheu, S.H., Gu, J.W., Kapogiannis, D., Mattson, M.P., and Yao, P.J. (2019). Comparing 3D ultrastructure of presynaptic and postsynaptic mitochondria. *Biol. Open* *8*, bio044834.
26. Wong, H.C., Zhang, Q., Beirl, A.J., Petralia, R.S., Wang, Y.X., and Kindt, K. (2019). Synaptic mitochondria regulate hair-cell synapse size and function. *eLife* *8*, e48914.
27. Freeman, D.W., Petralia, R.S., Wang, Y.X., Mattson, M.P., and Yao, P.J. (2017). Mitochondria in hippocampal presynaptic and postsynaptic compartments differ in size as well as intensity. *Matters (Zur)* *2017*. <https://doi.org/10.19185/matters.20171100009>.
28. Jenkinson, E.M., Rehman, A.U., Walsh, T., Clayton-Smith, J., Lee, K., Morell, R.J., Drummond, M.C., Khan, S.N., Naeem, M.A., Rauf, B., et al. (2013). Perrault syndrome is caused by recessive mutations in CLPP, encoding a mitochondrial ATP-dependent chambered protease. *Am. J. Hum. Genet.* *92*, 605–613.
29. Chatfield, K.C., Coughlin, C.R., 2nd, Friederich, M.W., Gallagher, R.C., Hesselberth, J.R., Lovell, M.A., Ofman, R., Swanson, M.A., Thomas, J.A., Wanders, R.J.A., et al. (2015). Mitochondrial energy failure in HSD10 disease is due to defective mtDNA transcript processing. *Mitochondrion* *21*, 1–10.
30. Sobreira, N., Schietecatte, F., Valle, D., and Hamosh, A. (2015). GeneMatcher: a matching tool for connecting investigators with an interest in the same gene. *Hum. Mutat.* *36*, 928–930.

Supplemental information

**Bi-allelic variants in the mitochondrial RNase P
subunit PRORP cause mitochondrial tRNA processing
defects and pleiotropic multisystem presentations**

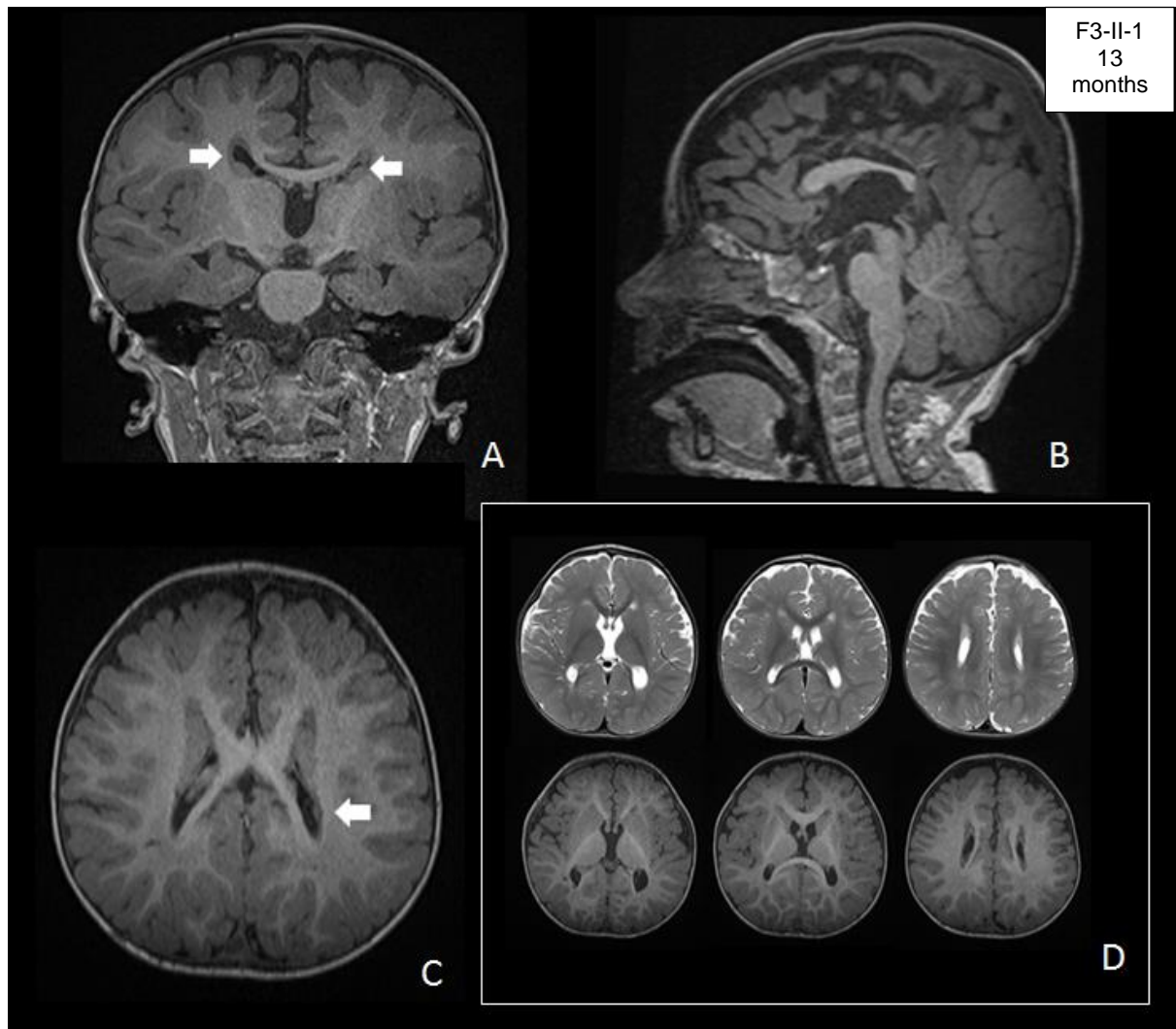
Irit Hochberg, Leigh A.M. Demain, Julie Richer, Kyle Thompson, Jill E. Urquhart, Alessandro Rea, Waheeda Pagarkar, Agustí Rodríguez-Palmero, Agatha Schlüter, Edgard Verdura, Aurora Pujol, Pilar Quijada-Fraile, Albert Amberger, Andrea J. Deutschmann, Sandra Demetz, Meredith Gillespie, Inna A. Belyantseva, Hugh J. McMillan, Melanie Barzik, Glenda M. Beaman, Reeya Motha, Kah Ying Ng, James O'Sullivan, Simon G. Williams, Sanjeev S. Bhaskar, Isabella R. Lawrence, Emma M. Jenkinson, Jessica L. Zambonin, Zeev Blumenfeld, Sergey Yalonetsky, Stephanie Oerum, Walter Rossmanith, Genomics England Research Consortium, Wyatt W. Yue, Johannes Zschocke, Kevin J. Munro, Brendan J. Battersby, Thomas B. Friedman, Robert W. Taylor, Raymond T. O'Keefe, and William G. Newman



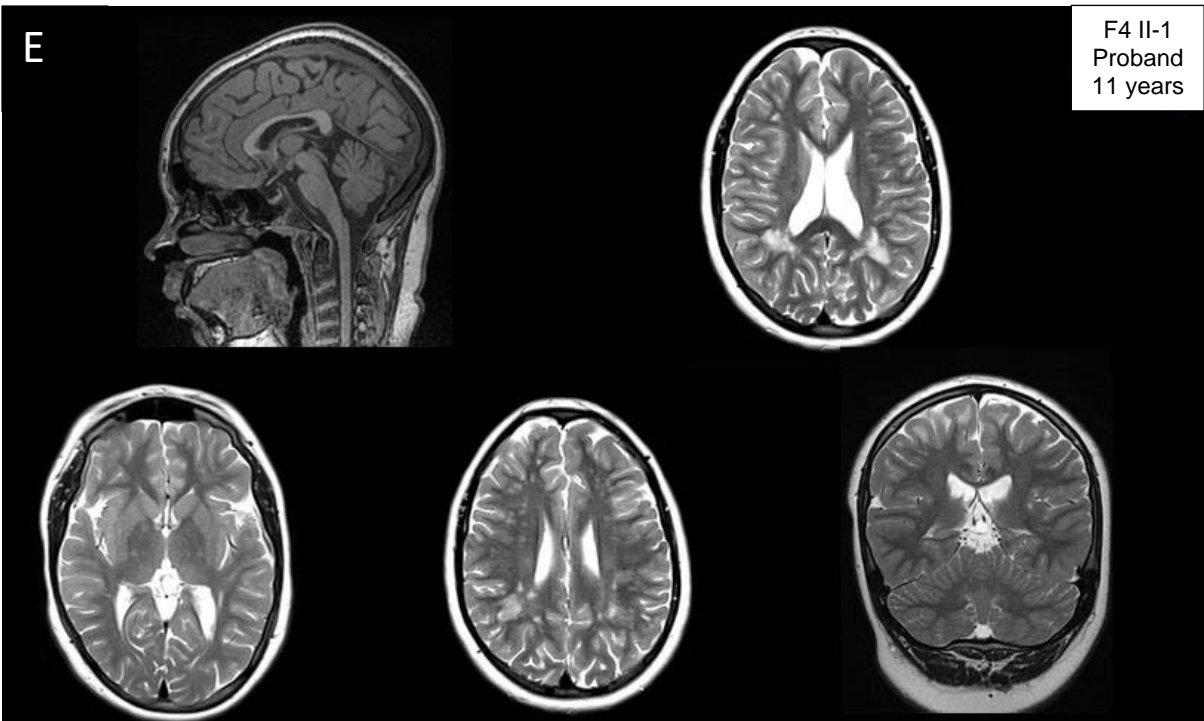
	II-1	II-3	II-4	Postmenopausal Reference Values
Follicle Stimulating Hormone (IU/l)	90.7	53.5	17.7	26.7 - 133.4
Luteinising Hormone (IU/l)	31.8	97.9	75.0	10.4 - 64.6
Estradiol (pmol/l)	14.2	37.3	12.0	36.7 - 102

Figure S1 – Affected individuals from family F1 and F2 have sensorineural hearing loss, and affected individuals from family F1 have hypergonadotropic hypogonadism

(A) Audiogram of affected individual F1 II-4. All three affected sisters show a similar audiometric configuration to F1-II-4, with profound hearing loss across all tested frequencies. (B) Audiogram of affected individual F2 II-1. The proband shows bilateral mild to moderate cookie-bite sensorineural hearing loss (SNHL). In both audiograms, the hearing level of the left ear is represented by the blue crosses and the right ear by red circles. The hearing threshold level of a normal adult is 0-20 dB.¹ Audiograms generated using AudGen software. (C) Hormone profiles for the three affected sisters in family F1, indicative of hypergonadotropic hypogonadism. Levels of follicle stimulating hormone, luteinising hormone and estrogen in the postmenopausal range are in bold.²

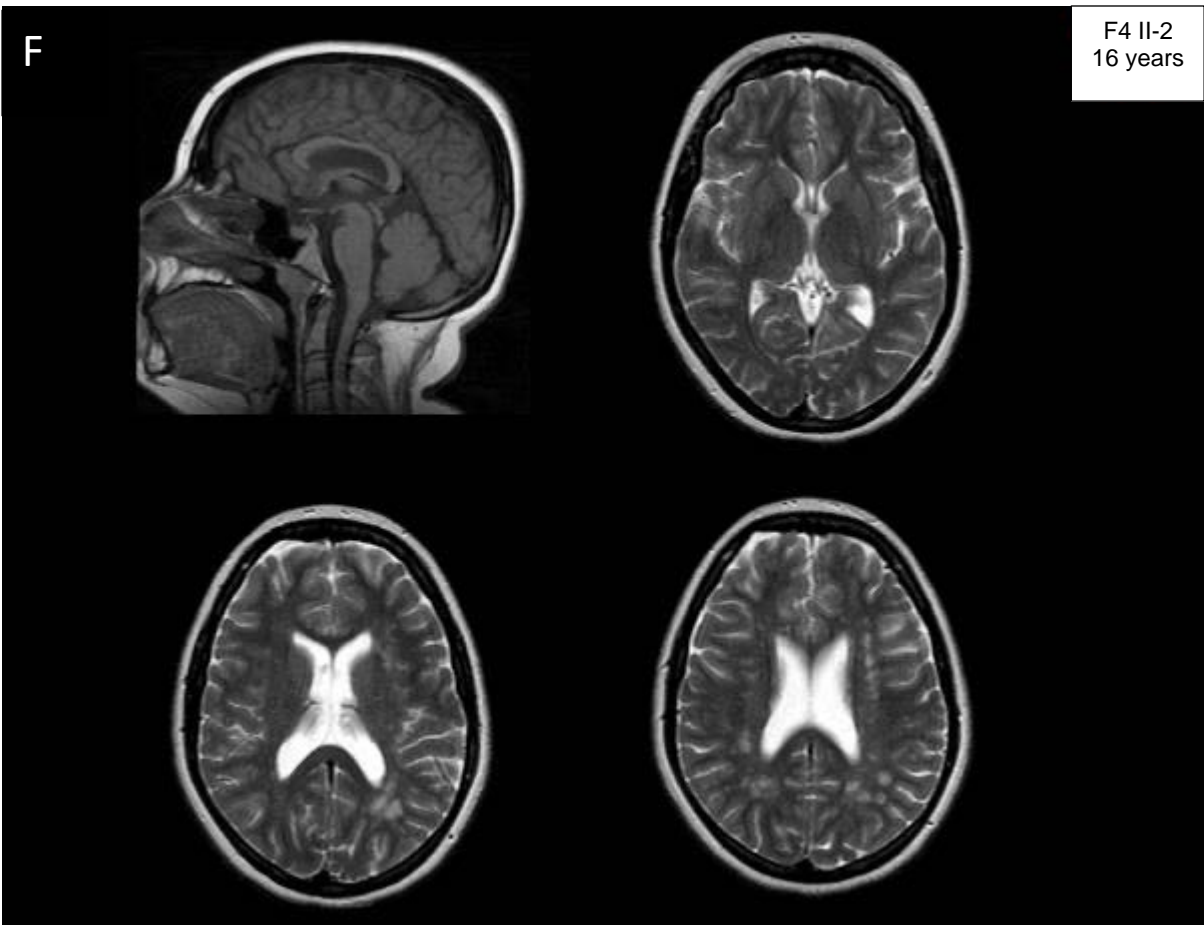


E



F4 II-1
Proband
11 years

F



F4 II-2
16 years

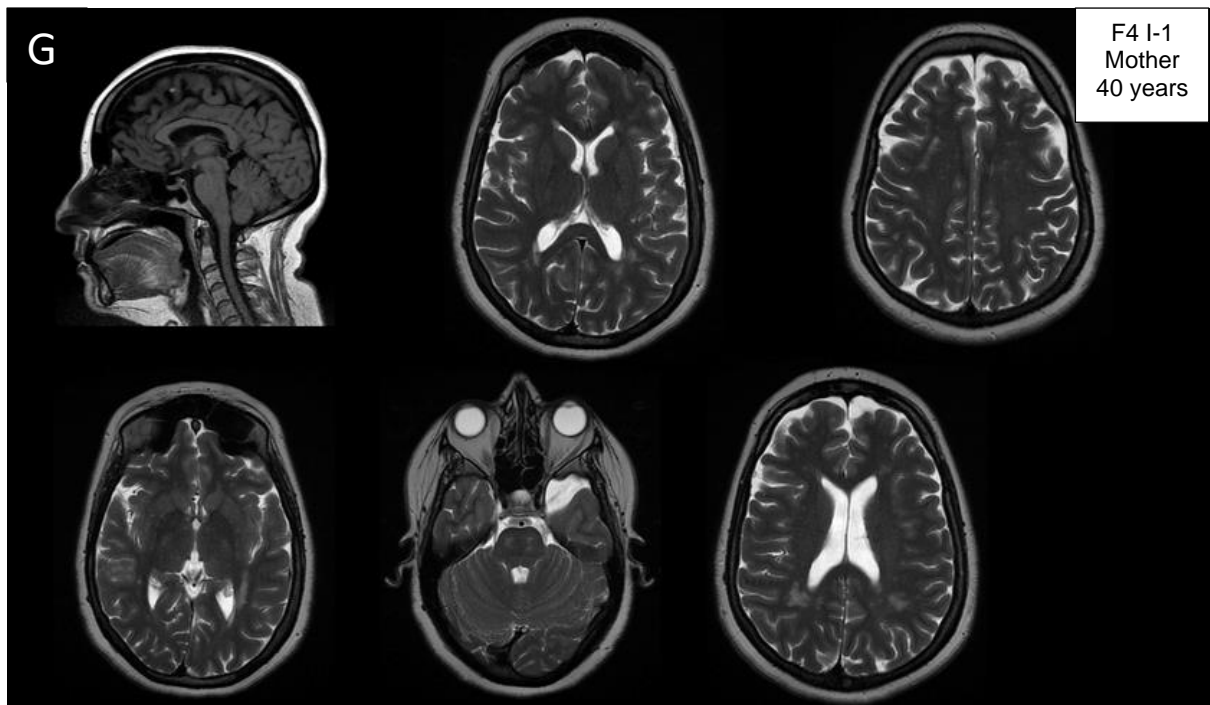


Figure S2 – Brain MRIs for affected individuals in F3 and F4

(A-D) Brain MRI at 13 months of age of individual F3-II-1. Note periventricular cysts – located just above body of lateral ventricles, consistent with connatal cysts (A), dysplastic corpus callosum (B), focal nodular thickening of the posterior horn of left lateral ventricle which may represent a focus of nodular heterotopia (C) and prominent 3rd & lateral ventricles with mild underdevelopment of white matter (D). (F-G) Brain MRI for affected individuals from family F4. Note bilateral multiple periventricular and subcortical T2 white matter hyperintense lesions with a posterior predominance in all affected individuals from this family. The affected mother shows hyper intense lesions involving also the pons (G; bottom right image). For all images age at time of assessment is noted in the white box in the upper right corner of the image.

	Asn412Ser Arg421Cys	
Human	IDGGDQYRKTTPQELKRFENFIKSRRPPFDVVIDGL	432
Chimpanzee	IDGGDQYRKTTPQELKRFENFIKSRRPPFDVVIDGL	432
Dog	IDGGDLYKKTTPQELERFQNFVKCCPPFDIVIDGL	431
Rat	IDGGDQYKKTTPQELKRFERFKSCPPFDIVIDGL	432
Mouse	IDGGDQYKKTTPQELKRFESFVNSCPPFDIVIDGL	429
Chicken	IHGTDTRKTTPQELKRFESFVNSCPPFDIVIDGL	437
Xenopus	IEGHDTFRKTTPQELQEFRQFVRSHPPYDIVDGL	411
Zebrafish	IEGGDVFNKSNPEELKSFKSFVKQRPFDIVIDGL	428
Tetraodon	IQGRDVFTKTTPEELERFRTFVGSQLAFDVVDGL	314
Fruitfly	LIRRDFVQRSTPEEVARFKKFVEKTAPYDCVIDGL	382
	Ala434Asp Arg445Gln	Ala485Val
Human	LAKRNLRLVLGRKHMLRRSSQWSRDEMEEVQKQASCFFADDISEDDPFLLY	492
Chimpanzee	LAKQNLRLVLGRKHMLRRSSQWSRDEMEEVQKQASCFFADDISEDDPFLLY	492
Dog	LAKQNLLELLVLGRKHMLTQHSRWRKDEMVKMQVKQASCFFADNISEDDPFLLY	491
Rat	LAQQNLQLLVLGRKHMLRPSSQWRKEEMEQVRKQAHCFADNISEDDPFLLY	492
Mouse	LAQQNLQLLVLGRKHMLRPSSQWRKEEMEQVRKQAHCFADNISEDDPFLLY	489
Chicken	LAKDYARLLVLGRKHMLTNSFNWKREVMKEMQNKADEFFFADNISEDDAFLY	497
Xenopus	LCGGGKRVVLVLGRKHMLQECSRWTQRRHMQLLQQRADCFPIDNTISEDDPFLLY	471
Zebrafish	LEQQSLNILVLGRKHMLRHSRNWDROQMSLIKQKAHCFFTTEIDISEDDPYLLY	488
Tetraodon	LQRRLGSVLVLGRKHMLRPSRSWPGRHMDLLQLKARCFFTENISEDDPFLLY	374
Fruitfly	FREQDKRVLVLGREHM---RNWSKQAMHYVHCNASLFTSNLSHDDPFLLY	438

Figure S3 - Conservation of PRORP with variant residues highlighted

The Conservation of PRORP across multiple species. The variant residues in the affected families are highlighted with blue boxes. Numbering relates to the human protein (GenPept: [NP_055487.2](#)). The multiple sequence alignments shown use the single letter abbreviations for amino acids while the variants use the three letter HGVS nomenclature. Sequences for each species are as follows; *P. troglodytes* UniProt: [H2Q865](#), *C. lupus familiaris* UniProt: [E2RMR1](#), *R. norvegicus* GenPept: [NP_001100200.1](#), *M. musculus* GenPept: [NP_079649.1](#), *X. tropicalis* UniProt: [F6QNJ3](#), *D. rerio* UniProt: [X1WBZ5](#), *T. nigroviridis* UniProt: [H3CE56](#), *D. melanogaster* GenPept: [NP_572309.2](#).

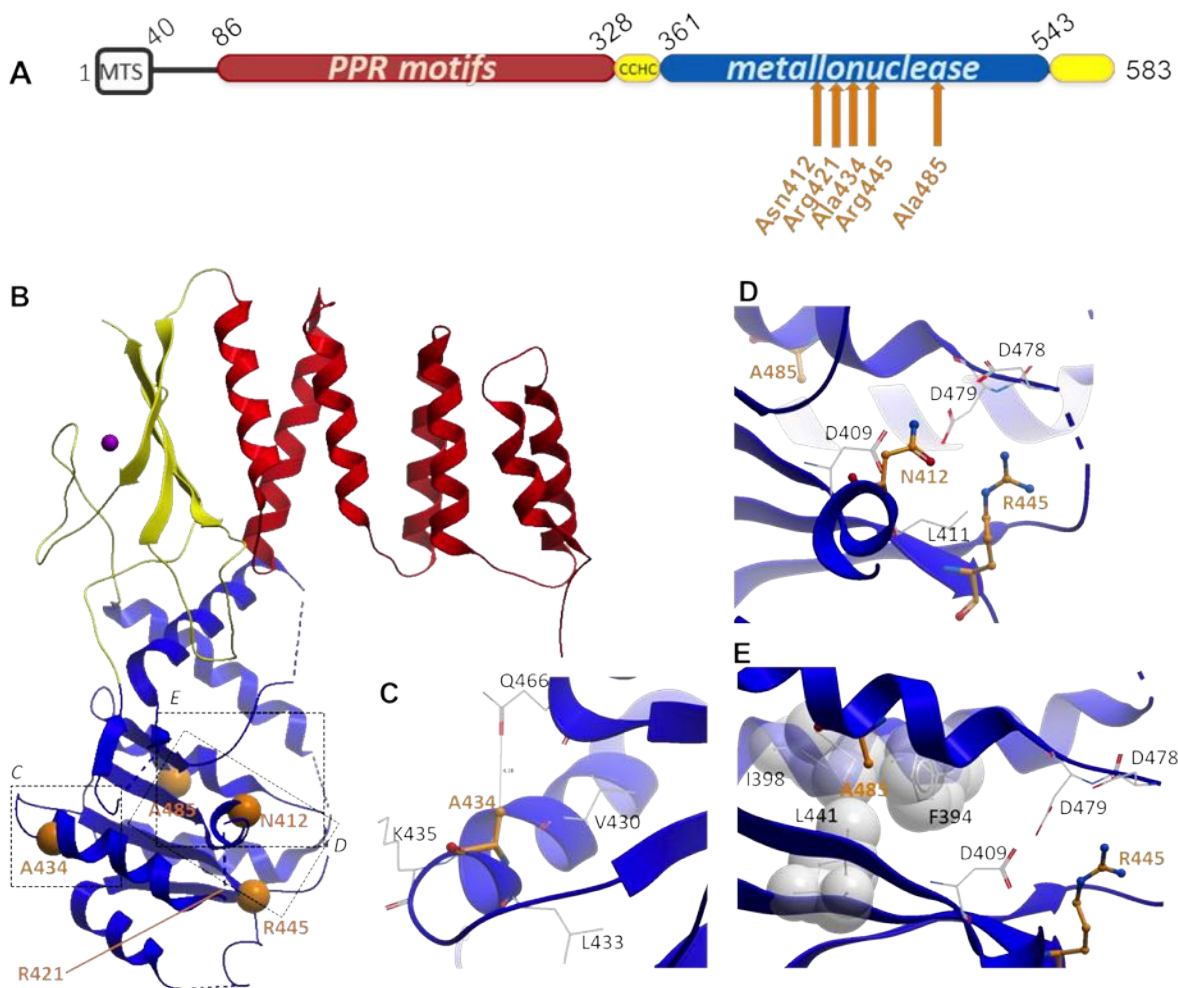


Figure S4 – Localisation of the variant residues in PRORP

(A) A schematic domain representation of human PRORP.³ The location of the variant residues (orange) is noted below the representation. Mitochondrial targeting sequence, MTS; pentatricopeptide repeat domain, PPR. The three letter HGVS nomenclature is used for amino acids **(B)** 3D schematic representation of the protein structure of human PRORP as a ribbon diagram; the enlarged region is part of the metallocnuclease domain. **(C, D, E)** The protein structure of human PRORP; the enlarged region is part of the metallocnuclease domain. Single letter abbreviations for amino acids are used. The variant amino acids in patients are depicted in orange. Amino acids with interactions with the variant residues are shown in black. The colour of each domain mirrors that of the schematic diagram in A.

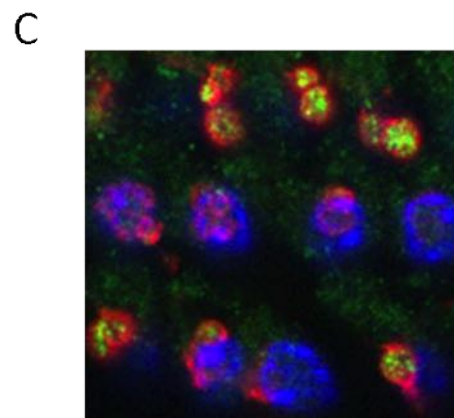
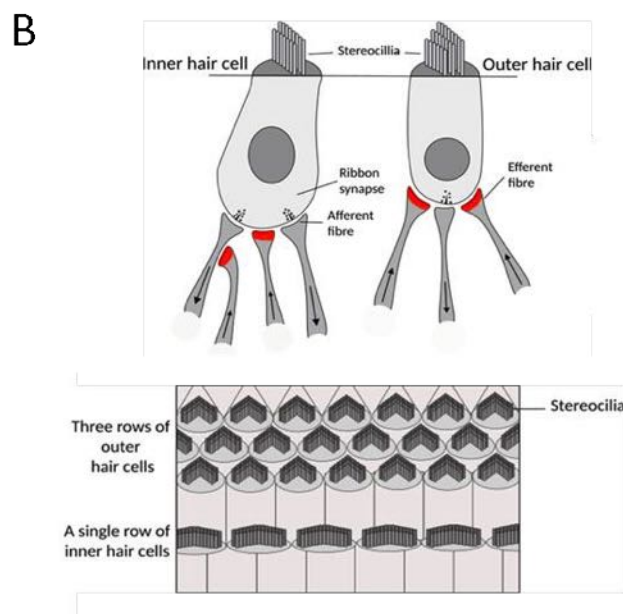
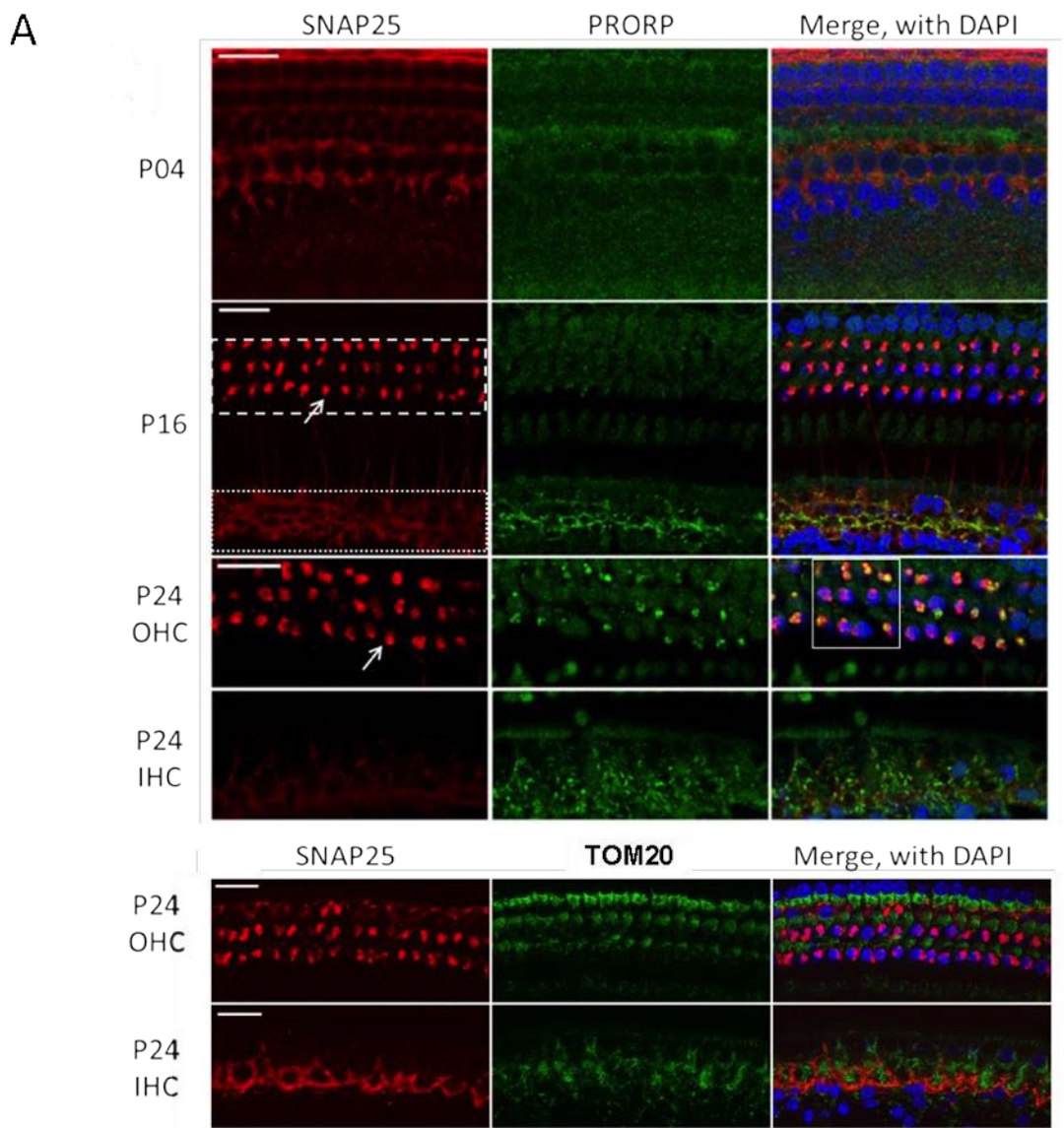


Figure S5 – Localisation in the mouse organ of Corti reveals high levels of PRORP in the synapses and nerve fibres of hair cells.

(A) Confocal fluorescence microscopy optical sections of the whole mount organ of Corti samples from C57/BJ6 mice at postnatal days 4, 16 and 24 (P04, P16 and P24, correspondingly) showing localization of PRORP protein (green). Samples were counterstained with DAPI (nuclear DNA marker, blue) to visualize the nuclei of hair cells and SNAP25 (presynaptic membrane marker, red) to stain efferent synapses at the base of OHCs and nerve fibres and synaptic buttons at the base and around IHCs. Samples at P24 were also stained with TOM20 (mitochondrial marker) as well as SNAP25 and DAPI to show generalized mitochondrial localisation. In the panels for P04, no high level of PRORP immunoreactivity is observed, while at P16, after the onset of hearing, the PRORP signal accumulates in the nerve fibres and at synaptic buttons at the base of IHCs and begins to accumulate at the efferent synaptic buttons of OHCs. The dashed white line outlines the area of the outer hair cell (OHC) efferent synapses, and the dotted white line outlines the area around the inner hair cell (IHC) nuclei and synaptic area. The white arrows point to one of the OHC efferent presynaptic buttons. The P24 panels represent two optical sections through the same organ of Corti sample at different focal plains to visualize OHC synaptic area (top) and IHC synaptic area (bottom). Note that by P24, in the fully mature organ of Corti, the PRORP signal concentrates in both OHC efferent synaptic buttons and in the afferent synaptic buttons of IHCs. The scale bar is 20 μ m. (B) Schematic representation of the hair cells of the organ of Corti. The top illustration displays the innervation of inner hair cells and outer hair cells during postnatal development. Arrows in the nerve fibres indicate the direction of transmission. The area of SNAP25 staining is shown in red. The lower panel illustration shows the arrangement of hair cells in the organ of Corti in the same orientation as shown in Panel A. (C) An enlarged view of the area inside the white box in Panel A showing a concentrated signal of PRORP (green) in the efferent buttons stained by SNAP25 (red); the OHC nuclei shown in blue.

Supplemental Web Resources

AudGen, <http://audism.com/audgen>

GenBank, <https://www.ncbi.nlm.nih.gov/genbank/>

UniProt, <https://www.uniprot.org/>

Materials and Methods

Ethical approval

All individuals or their guardians provided written informed consent in accordance with local regulations. Ethical approval for this study was granted by the National Health Service Ethics Committee (16/WA/0017), University of Manchester; the ethics committee of IDIBELL (CEIC n. PR076/14), and CHEO ethics committee for the Care4Rare Canada Study (ID: 1577), and Genomics England has approval from the HRA Committee East of England – Cambridge South (REC Ref 14/EE/1112).

Autozygosity mapping and whole exome sequencing

Autozygosity mapping was performed on six members of family F1 (II-1, II-2, II-3, II-4, II-6 and II-7) using the Affymetrix Genome-wide SNP6.0 arrays as previously described.⁴

Autozygosity mapping of the array data was performed using the AutoSNPa software.⁵

Whole exome sequencing was performed on DNA extracted from lymphocytes from individual F1-II-3. The Agilent SureSelect Human All Exon V5 Panel was used for library preparation and sequencing was performed on the HiSeq 2500 (Illumina) as previously described.⁶ Analysis of large deletions and copy number variations was performed on F3-II-1 using Affymetrix Cytoscan HD arrays with analysis via Affymetrix ChAS software (GRCh37/hg19). CNVs were assessed with comparison to databases including the Database of Genomic Variants (DGV). Pathogenic CNVs were identified with reference to databases, including Decipher, ClinVar and ClinGen (ISCA). Whole exome sequencing performed on genomic DNA from all three members of family F3 was performed as a service by GeneDx. Library preparation was performed using the GeneDx propriety technology and sequenced using an Illumina sequencer and using paired-end reads. Reads were aligned to the human genome build GRCh37/hg19 and variants identified using GeneDx software, XomeAnalyzer.

Identification of variants

Autozygosity mapping, performed on six siblings, identified three homozygous regions >2Mb shared between the affected individuals, but not with the unaffected individuals (chromosome 14: 34195478-37228220; chromosome 18: 10090808-12264512; and chromosome 22: 21317876-23416005, Genome build: Hg19). Whole exome sequencing was performed on one affected individual (F1, II-3). After sequence variants in the homozygous regions were filtered to remove variants seen more than once in >800 previously sequenced

exomes, and variants with a minor allele frequency above 1% in dbSNP or the Exome Variant Server (EVS)^{7;8} one variant remained, *PRORP* c.1454C>T; p.(Ala485Val) (Genbank: NM_014672.3).

The variants in family F2 were identified from whole genome sequence data generated through the 100,000 Genomes Project⁹ on the parents and affected child and accessed through the dedicated research portal. The trio genome dataset in this family was filtered initially to identify Tier 1 or 2 variants (i.e. rare or known pathogenic variants in genes known to be associated with sensorineural hearing loss). An agnostic approach consistent with an ultra-rare minor allele frequency ($<10^{-5}$) and recessive inheritance pattern revealed maternally inherited *PRORP* c.1235A>G, p.(Asn412Ser) and paternally inherited c.1301C>A, p.(Ala434Asp) variants.

For F3 whole exome sequencing of the family trio was undertaken by GeneDx. Exonic and flanking splice junctions were captured using a proprietary system developed by GeneDx and sequenced on an Illumina platform with 100bp or greater paired end reads. Reads were aligned to human genome build GRCh37/UCSC hg19, and analysed for sequence variants using a custom-developed analysis tool (Xome Analyzer). Mean depth of coverage 94X, quality threshold 98.7%. All available data files were run through the most recent iteration of our previously described bioinformatics pipeline.¹⁰ Family-based reanalysis was completed at the Children's Hospital of Eastern Ontario in collaboration with the referring clinical care team which included (Care4Rare study team members, including the local referring clinician, a clinical geneticist, a laboratory geneticist, genetic counsellor, and/or a post-doctoral fellow). Biallelic variants were identified in *PRORP*, a maternally inherited c.1334G>A p.(Arg445Gln) (rs777185638) and a paternal frameshift variant c.1197dupA p.(Ser400IlefsX6) (rs764714439) were identified.

For F4 genomic DNA was extracted from peripheral blood using standard methods. For WGS, a PCR-free library with 150-bp paired-end read sequences was generated on a HiSeq 2000-4000 platform (Illumina, Inc. USA) at Centre Nacional d'Anàlisi Genòmica (CNAG Barcelona, Spain). Sequences were aligned to hg19 by Burrows-Wheeler Aligner (BWA mem), and single nucleotide variants and small insertions/deletions (indels) were identified using GATK, applying GATK's best practices for germline SNP & indel discovery and annotated by ANNOVAR software. Copy number variants (CNVs) were analyzed by the R package ExomeDepth that uses read-depth data from targeted sequencing experiments and filtered with the Database of Genomic Variants that provides a comprehensive summary of structural variation in the human genome. A recessive model was applied and ultra-rare variants at a minor allele frequency of $<10^{-5}$ and CADD score >20 were filtered. The one candidate variant *PRORP* c.1261C>T, p.Arg421Cys was validated and tested for co-segregation in all family members by Sanger sequencing.

There was no evidence of any other putative disease associated variants in the genome and exome datasets in the four families.

Confirmation of variants

Variants were confirmed in family F1 via Sanger sequencing using the ABI big Dye v3.1 (ThermoFisher) sequencing technology. Primers used were *PRORP_exon7_FWD* (5'ACACTGTCCTCTGCCTCTTC3') and *PRORP_exon7_REV* (5'TCTAGGACCTGGCTAGTTCC3')

PRORP transcript analysis

Dermal fibroblasts from individual F3, II-1 were grown under standard conditions either in the presence of puromycin (200µg/ml) or without puromycin treatment. RNA was extracted using the Qiagen MiniprepRNA kit and RNA samples were DNase I treated on column. RNA was converted to cDNA using the Applied Biosystems RNA to cDNA kit. Samples were PCR amplified using primers that cross exon-exon borders and Sanger sequenced using ABI big Dye v3.1 (ThermoFisher) sequencing technology. Primers used were *PRORP_cDNA_Exon 5_Fwd* (5'CATGGTTGAGAGTGTCTGG3') and *PRORP_cDNA_Exon 5* (5'CTGAGAATACGCTGAAAGGTTAG3').

Assessment of protein and RNA levels in fibroblasts

Western blots for the subunits of mt-RNase P, respiratory chain complexes and mitoribosomal proteins (n=3 for each experiment) were performed using fibroblast cell lysates (F1 II-4 and F3 II-1). Cell lysates were incubated with sample dissociation buffer, separated by 12% SDS-PAGE and immobilized by wet transfer on to PVDF membrane (Immobilon-P, Millipore Corporation). Proteins of interest were bound by overnight incubation at 4°C with primary antibodies followed by HRP-conjugated secondary antibodies (Dako Cytomation) and visualized using ECL-prime (GE Healthcare) and BioRad ChemiDoc MP with Image Lab software. Antibodies used are as follows; TRMT10C (Sigma HPA036671), SDR5C1 (Sigma HPA001432), PRORP (Abcam ab185941), SDHA (Abcam ab14715), NDUFB8 (Abcam ab110242), MT-CO1 (ab14705), UQCRC2 (Abcam 14745), ATP5B (Abcam 14730), MT-CO1 (ab14705), and GAPDH (Abcam 8245) followed by HRP-conjugated secondary antibodies (Dako Cytomation).

Northern blot analysis was performed as previously described.¹¹ The NorthernMax kit from Ambion was used. Equal amounts of total RNA (2–5 µg range) from fibroblasts was separated on a 1% denaturing agarose gel. RNA was then transferred to nylon membrane (Hybond-N + Amersham, GE Healthcare) by capillary transfer, UV cross-linked and subjected to hybridization with biotinylated probes. Signals were detected using the BrightStar BioDetect kit (Ambion). A biotinylated RNA size marker (BrightStar RNA Millenium Marker, Ambion) was used to determine the size of RNA species. Probe sequences as previously described.¹¹

Preparation of the PRORP variant sequences for bacterial expression

The plasmid pET28-b(+) containing the coding sequence for PRORP (MRPP3)¹² was mutagenized as previously described¹³ with the synthetic oligonucleotides PRORP_p.A485V (5' GGAGTGCAGTGTG**A**CATACAGAAGGAATGG 3'), PRORP_p.R445Q (5'

CGTCTTAGCATGTGCTTCTGGCCTAGGACCAGCAGTCG 3'), PRORP_p.N412S (5' GGAAACATTTGGCAACACTGAGACCATCAATGACAAC 3'), PRORP_p.A434N (5' CAGTCGCAGATTCCGTTGTCTAGTTGAGAGACGACATT 3') and PRORP_p.R421C (5' CGACATTCAAGAGAAGTTGAGATTCACAAACTT~~AGGAAAC~~ATTTGGC 3') with the base altered from wild-type bold and underlined. The potential mutagenized plasmids were extracted using the GenElute HP Plasmid miniprep Kit (Sigma Aldrich) and the variant was confirmed by DNA sequencing.

Recombinant expression and purification of TRMT10C, SDR5C1 and PRORP

PRORP and PRORP variants, as described above, were expressed in *E.coli* Rosetta2 DE3 (Novagen) using Overnight Express TB medium (Novagen). Affinity chromatography of the His-tagged proteins was performed as previously described.¹² Purity was assessed by SDS-PAGE. Aliquots of purified proteins were dialysed overnight at 4°C in 20 mM Tris-Cl pH 7.4, 100 mM NaCl, 15% glycerol, then flash frozen and stored at -80°C. *TRMT10C* in pET28-b(+)¹² was subcloned into pET21d and co-expressed with SDR5C1 in pET28-b(+)¹² in *E.coli* Rosetta2 DE3 using Overnight Express TB medium at 19°C. Purified proteins were dialysed overnight at 4°C in 20 mM Tris-Cl pH 8, 200 mM NaCl, 2mM DTT, 15% glycerol, then flash frozen and stored at -80°C.

Preparation of mitochondrial pre-tRNA transcripts

The template for pre-tRNA^{Ile} (phiI2) was as described previously.¹² *In vitro* transcription was carried out with the T7 RiboMax Express system (Promega) according to the manufacturer's instructions with phiI2 linearized with XbaI and 2.5μM aminoallyl-UTP-ATTO-680 (Jena Biosciences). RNA was purified by ethanol precipitation.

Pre-tRNA processing assays

Pre-tRNA processing assays were performed as previously described.^{12,14} 6% (w/v) acrylamide 8M urea gels were used to resolve ATTO-680 labelled mt-tRNA substrate and cleavage products. Gels were visualised using the LI-COR Odyssey CLx imaging system and band quantitation carried out using the Image Studio software. Aliquots of the tRNA processing reactions were taken at the start of the reaction (0 minutes), after 30 minutes and 60 minutes from the start in three independent assays. Visible processed tRNA bands at time-points 30 minutes and 60 minutes were measured as a proxy for mt-RNase P activity. The relative intensities of tRNA processed by mt-RNase P with wild-type and PRORP variants from three independent assays were quantitated at 30 minutes and presented with standard deviation.

Rescue experiments

RNA isolation and northern blotting

Total RNA from cultured cells was isolated with the Monarch Total RNA Miniprep kit (NEB) according to the manufacturer's instructions. For northern blotting, 5 μg of total RNA

from each sample was separated through a 1.2% agarose-formaldehyde gel and transferred to HybondTM-N+ membrane (GE Healthcare) by neutral transfer. Using T4 Polynucleotide Kinase (NEB) and ATP (γ -³²P), an oligonucleotides probe (MT-ATP8, 5'-TGGGTGATGAGGAATAGTGTAAAGGAG) was radiolabeled for hybridisation (25% Formamide, 7% SDS, 1% BSA, 0.25M sodium phosphate pH 7.2, 1mM EDTA pH 8.0, 0.25M NaCl2) overnight at 37°C. Membranes were washed first with 2× SSC/0.1% SDS for 60 min, followed by 0.5× SSC/0.1% SDS for 60 min and finally in 0.1× SSC/0.1% SDS for 30 min. All washings were performed at 37°C. The membranes were dried, exposed to a Phosphoscreen (GE Healthcare) and scanned with Typhoon 9400 (GE Healthcare).

Retroviral expression

Full-length cDNAs of human TRMT10C and PRORP were generated by reverse transcription using Superscript IV (Invitrogen) with an oligo dT primer from total RNA isolated from wild-type cultured fibroblasts followed by PCR using specific primers with KAPA HiFi (Sigma-Aldrich) for Gateway cloning into pDONR201. Both cDNAs were verified by Sanger sequencing and sub-cloned into a Gateway-converted pBABE-puromycin retroviral vector. Retrovirus was generated following transfection of plasmids into the Phoenix packaging cell line, followed by transduction into immortalized wild-type and fibroblasts from an affected individual (F3, II-1). Transduced cells were selected with puromycin to select for stable cultures.

Immunoblotting

Cells were lysed in phosphate buffered saline, 1% dodecyl-maltoside (DDM), 1 mM PMSF (phenylmethylsulfonyl fluoride), and complete protease inhibitor (Thermo Fisher Scientific). Protein concentration of lysates was measured by the Bradford protein assay (BioRad) and equal amounts separated in 12% Tris-Glycine SDS-PAGE. Proteins were transferred to nitrocellulose membranes by semi-dry transfer. Membranes were blocked in TBST (Tris-buffered saline, 0.1% Tween 20) with 1% milk at room temperature for 1 hr. Primary antibodies (in 5% BSA/TBST) were incubated overnight at 4°C and detected the following day with secondary HRP conjugates (Jackson ImmunoResearch) using ECL (LumiGLO, Cell Signalling Technology) with film. The following primary antibodies were used for immunoblotting: Proteintech Group: MRPP3 (20959-1-AP, 1:3000); Abcam/Mitosciences: MT-CO1 (1D6E1A8, 1:500) and SDHA (C2061/ab14715, 1:10000); Santa Cruz: TOM40 (sc-11414, 1:5000) and Thermo Fisher Scientific: MRPP1 (A304-390A, 1:1000).

Immunohistochemistry

The NIH Animal Care and Use Committee approved protocol 1263-15 to T.B.F. for mice. C57/B6 mice at ages P04, P16 and P24 were euthanised, the cochleae were removed and fixed with 4% paraformaldehyde in PBS for 2 hours. The samples were microdissected and the organ of Corti was permeabilised with 0.5% Triton X-100 in PBS for 30 min followed by three 10 min washes with 1X PBS. Nonspecific binding sites were blocked with 5% normal goat serum and 2% BSA in PBS for 1 h at room temperature. Samples were incubated for 2 h

with rabbit polyclonal PRORP antibody (MRPP3, Proteintech, 20959-1-AP) at 1 μ g/ml and mouse monoclonal SNAP25 antibody (Santa Cruz, sc-136267) at 1 μ g/ml or rabbit polyclonal Tom20 antibody (Santa Cruz, sc-11415) at 2 μ g/ml and mouse monoclonal SNAP25 (Santa Cruz, sc-136267) at 1 μ g/ml followed by several rinses with PBS. Samples were incubated with goat anti-rabbit IgG Alexa Fluor 488 conjugated secondary antibody and goat anti mouse Alexa Fluor 568 conjugated secondary antibody (Molecular Probes) for 30 min. Samples were washed several times with PBS, with ProLongGold Antifade reagent with DAPI (Molecular Probes) and examined using an LSM780 confocal microscope (Zeiss Inc) equipped with 63X, 1.4 N.A. objective.

Acknowledgements

This study was supported by Action on Hearing Loss (S35); Action Medical Research (GN2494); NIHR Manchester Biomedical Research Centre ((IS-BRC-1215-20007); Wellcome Trust ISSF pump-prime award (097820/Z/11/B); the Wellcome Trust Centre for Mitochondrial Research (203105/Z/16/Z to RWT); the UK NHS Highly Specialised “Rare Mitochondrial Disorders of Adults and Children” Service (RWT); and The Lily Foundation (RWT); Austrian Science Fund (FWF) P25983 (WR); in part by the Intramural Research Program of the NIDCD at the NIH, (DC000039 to TBF); the Sigrid Juselius Foundation Senior Investigator Award (BJB; grants from the Hesperia Foundation; the Asociación Española contra las Leucodistrofias (ALE-ELA España), the PERIS program URD-Cat SLT002/16/00174); the Center for Biomedical Research on Rare Diseases (CIBERER) (ACCI19-759 to A.P); Fundació La Marató de TV3 (595/C/2020); Instituto de Salud Carlos III (FIS PI20/00758) (co-funded by European Regional Development Fund. ERDF, a way to build Europe); the Instituto de Salud Carlos III (Sara Borrell, CD19/00221 to E.V.), co-funded by European Social Fund; ESF investing in your future, and the Ministerio de Ciencia e Innovación y Universidades (Juan de la Cierva, FJCI-2016-28811 to E.V.). We also thank the CERCA Program/Generalitat de Catalunya for institutional support. This research was made possible through access to the data and findings generated by the 100,000 Genomes Project. The 100,000 Genomes Project is managed by Genomics England Limited (a wholly owned company of the Department of Health and Social Care). The 100,000 Genomes Project is funded by the National Institute for Health Research and NHS England. The Wellcome Trust, Cancer Research UK and the Medical Research Council have also funded research infrastructure. The 100,000 Genomes Project uses data provided by patients and collected by the National Health Service as part of their care and support. Thanks to Christie Boswell-Patterson for providing information from the Care4Rare Study. This work was performed under the Care4Rare Canada Consortium funded by Genome Canada and the Ontario Genomics Institute (OGI-147), the Canadian Institutes of Health Research, Ontario Research Fund, Genome Alberta, Genome British Columbia, Genome Quebec, and Children’s Hospital of Eastern Ontario Foundation.

References

1. Action on Hearing Loss. (2017). Levels of hearing loss. In. (Action on hearing loss).
2. Aiman, J., and Smentek, C. (1985). Premature ovarian failure. *Obstet Gynecol* 66, 9-14.
3. Reinhard, L., Sridhara, S., and Hallberg, B.M. (2015). Structure of the nuclease subunit of human mitochondrial RNase P. *Nucleic Acids Res* 43, 5664-5672.
4. Banka, S., Blom, H.J., Walter, J., Aziz, M., Urquhart, J., Clouthier, C.M., Rice, G.I., de Brouwer, A.P., Hilton, E., Vassallo, G., et al. (2011). Identification and characterization of an inborn error of metabolism caused by dihydrofolate reductase deficiency. *Am J Hum Genet* 88, 216-225.
5. Carr, I.M., Flintoff, K.J., Taylor, G.R., Markham, A.F., and Bonthron, D.T. (2006). Interactive visual analysis of SNP data for rapid autozygosity mapping in consanguineous families. *Hum Mutat* 27, 1041-1046.
6. Smith, M.J., Beetz, C., Williams, S.G., Bhaskar, S.S., O'Sullivan, J., Anderson, B., Daly, S.B., Urquhart, J.E., Bholah, Z., Oudit, D., et al. (2014). Germline mutations in SUFU cause Gorlin syndrome- associated childhood medulloblastoma and redefine the risk associated with PTCH1 mutations. *J Clin Oncol* 32, 4155-4161.
7. Sherry, S.T., Ward, M.H., Kholodov, M., Baker, J., Phan, L., Smigielski, E.M., and Sirotnik, K. (2001). dbSNP: the NCBI database of genetic variation. *Nucleic Acids Res* 29, 308-311.
8. NHLBI GO Exome Sequencing Project (ESP). Exome Variant Server. In. (Seattle, WA).
9. Turnbull, C., Scott, R.H., Thomas, E., Jones, L., Murugaesu, N., Pretty, F.B., Halai, D., Baple, E., Craig, C., Hamblin, A., et al. (2018). The 100 000 Genomes Project: bringing whole genome sequencing to the NHS. *BMJ* 361, k1687.
10. Kernohan, K.D., Hartley, T., Alirezaie, N., Care4Rare Canada Consortium, Robinson, P.N., Dyment, D.A., Boycott, K.M. (2018). Evaluation of exome filtering techniques for the analysis of clinically relevant genes. *Hum Mutat* 39:197-201.
11. Deutschmann, A.J., Amberger, A., Zavadil, C., Steinbeisser, H., Mayr, J.A., Feichtinger, R.G., Oerum, S., Yue, W.W., and Zschocke, J. (2014). Mutation or knock-down of 17beta-hydroxysteroid dehydrogenase type 10 cause loss of MRPP1 and impaired processing of mitochondrial heavy strand transcripts. *Hum Mol Genet* 23, 3618-3628.
12. Holzmann, J., Frank, P., Löffler, E., Bennett, K.L., Gerner, C., and Rossmanith, W. (2008). RNase P without RNA: identification and functional reconstitution of the human mitochondrial tRNA processing enzyme. *Cell* 135, 462-474.
13. Kunkel, T.A., Roberts, J.D., and Zakour, R.A. (1987). Rapid and efficient site-specific mutagenesis without phenotypic selection. *Methods Enzymol* 154, 367-382.
14. Rossmanith, W., Tullo, A., Potuschak, T., Karwan, R., and Sbisa, E. (1995). Human mitochondrial tRNA processing. *J Biol Chem* 270, 12885-12891.



Impairment of the mitochondrial one-carbon metabolism enzyme SHMT2 causes a novel brain and heart developmental syndrome

Àngels García-Cazorla^{1,2} · Edgard Verdura^{2,3} · Natalia Juliá-Palacios^{1,2} · Eric N. Anderson⁴ · Leire Goicoechea^{2,3} · Laura Planas-Serra^{2,3} · Enkhtuul Tsogtbaatar^{5,6,7} · Nikita R. Dsouza⁸ · Agatha Schlüter^{2,3} · Roser Urreizti^{2,9} · Jessica M. Tarnowski^{10,11} · Ralitza H. Gavrilova^{10,11} · SHMT2 Working Group · Montserrat Ruiz^{2,3} · Agustí Rodríguez-Palmero^{2,3,12} · Stéphane Fourcade^{2,3} · Benjamin Cogné¹³ · Thomas Besnard¹³ · Marie Vincent¹³ · Stéphane Bézieau¹³ · Clifford D. Folmes^{5,6,7} · Michael T. Zimmermann^{8,14} · Eric W. Klee^{10,15,16} · Udai Bhan Pandey⁴ · Rafael Artuch^{2,9} · Margot A. Cousin^{15,16} · Aurora Pujol^{2,3,17}

Received: 18 June 2020 / Revised: 31 August 2020 / Accepted: 31 August 2020 / Published online: 5 October 2020
© The Author(s) 2020

Keywords SHMT2 · Mitochondrial one-carbon metabolism · Congenital microcephaly · Perisylvian polymicrogyria · Cardiomyopathy

The members of SHMT2 Working Group are listed in the Acknowledgements section.

Àngels García-Cazorla and Edgard Verdura contributed equally to this study.

Margot A. Cousin and Aurora Pujol contributed equally to this study.

Electronic supplementary material The online version of this article (<https://doi.org/10.1007/s00401-020-02223-w>) contains supplementary material, which is available to authorized users.

Àngels García-Cazorla
agaricia@sjdhospitalbarcelona.org

Aurora Pujol
apujol@idibell.cat

¹ Neurometabolic Unit and Synaptic Metabolism Lab, Neurology Department, Institut Pediàtric de Recerca, Hospital Sant Joan de Déu, and MetabERN, 08950 Barcelona, Catalonia, Spain

² Centre for Biomedical Research on Rare Diseases (CIBERER), Instituto de Salud Carlos III, 28029 Madrid, Spain

³ Neurometabolic Diseases Laboratory, Bellvitge Biomedical Research Institute (IDIBELL), L'Hospitalet de Llobregat, 08908 Barcelona, Catalonia, Spain

⁴ Department of Pediatrics, Children's Hospital of Pittsburgh, University of Pittsburgh School of Medicine, Pittsburgh, PA 15224, USA

⁵ Department of Cardiovascular Medicine, Mayo Clinic, Scottsdale, AZ 85260, USA

⁶ Department of Biochemistry and Molecular Biology, Mayo Clinic, Scottsdale, AZ 85260, USA

⁷ Department of Molecular Pharmacology and Experimental Therapeutics, Mayo Clinic, Scottsdale, AZ 85260, USA

⁸ Bioinformatics Research and Development Laboratory, Genomic Sciences and Precision Medicine Center, Medical College of Wisconsin, Milwaukee, WI 53226, USA

⁹ Clinical Biochemistry Department, Institut de Recerca Sant Joan de Déu, and MetabERN, 08950 Barcelona, Catalonia, Spain

¹⁰ Department of Clinical Genomics, Mayo Clinic, Rochester, MN 55905, USA

¹¹ Department of Neurology, Mayo Clinic, Rochester, MN 55905, USA

¹² Department of Pediatrics, Paediatric Neurology Unit, University Hospital Germans Trias i Pujol, 08916 Badalona, Catalonia, Spain

¹³ Service de Génétique Médicale, CHU de Nantes, and INSERM, CNRS, Université de Nantes, l'Institut du Thorax, Nantes, 44000 Nantes, Pays de la Loire, France

¹⁴ Clinical and Translational Science Institute, Medical College of Wisconsin, Milwaukee, WI 53226, USA

¹⁵ Center for Individualized Medicine, Mayo Clinic, Rochester, MN 55905, USA

¹⁶ Department of Health Sciences Research, Mayo Clinic, Rochester, MN 55905, USA

¹⁷ Catalan Institution of Research and Advanced Studies (ICREA), 08010 Barcelona, Catalonia, Spain

Inborn errors of metabolism cause a wide spectrum of neurodevelopmental and neurodegenerative conditions [15]. A pivotal enzyme located at the intersection of the amino acid and folic acid metabolic pathways is SHMT2, the mitochondrial form of serine hydroxymethyltransferase. SHMT2 performs the first step in a series of reactions that provide one-carbon units covalently bound to folate species in mitochondria: it transfers one-carbon units from serine to tetrahydrofolate (THF), generating glycine and 5,10-methylene-THF [4, 11, 12].

Using whole exome sequencing (WES), we identified biallelic *SHMT2* variants in five individuals from four different families. All identified variants were located in conserved residues, either absent or extremely rare in control databases (gnomAD, ExAC), and cosegregated based on a recessive mode of inheritance ($p\text{Rec}=0.9918$ for this gene) (Supplementary Figs. 1–3, Supplementary Table 1). In family F1, a homozygous missense variant present in two affected siblings was located in a region without heterozygosity (~10 Mb, the only region >1 Mb shared by both siblings) in which no other candidate variants were found, providing a strong genetic evidence of causality for these variants. The missense/in-frame deletion nature of these variants, and the absence of loss-of-function homozygous individuals in control databases, combined with the fact that complete loss of SHMT2 is embryonic lethal in the mouse [18], suggested that these variants may cause hypomorphic effects. Using 3D molecular dynamics models of the SHMT2 protein, we concluded that these candidate variants probably alter the SHMT2 oligomerization process, and/or disrupt the conformation of the active site, thus inducing deleterious effects on SHMT2 enzymatic function (Supplementary Figs. 4–8, Supplementary Tables 2–3, Supplementary video) [8, 19].

All patients presented a similar phenotype, characterized by dysmorphic features including long palpebral fissures, eversion of lateral third of lower eyelids, arched eyebrows, long eyelashes, thin upper lip, long philtrum, short fifth finger, fleshy pads at the tips of the fingers, mild 2–3 toe syndactyly and low-set thumbs. All patients exhibited intellectual disability and motor dysfunction, in the form of spastic paraparesis, ataxia, and/or peripheral neuropathy. Also, four out of five patients showed hypertrophic cardiomyopathy or atrial-septal defects, which tend to progress over time. All of the patients showed congenital microcephaly; MRI revealed corpus callosum abnormalities in all patients and perisylvian polymicrogyria-like pattern in patients P1–P4 (Fig. 1a–c, Supplementary Figs. 9–11, Supplementary Table 4). Quadriceps muscle and myocardium biopsies from Patient 4 showed myopathic changes, and myocardium biopsy showed

the presence of “ragged red” fibers, suggestive of defective mitochondria (Fig. 1d, Supplementary Fig. 12).

To assess the pathogenicity of SHMT2 variants, we pursued functional testing with patient-derived primary fibroblasts. SHMT2 protein levels in fibroblasts were not significantly altered (Supplementary Fig. 13). While all metabolites were in the normal range in plasma, fibroblasts from affected individuals showed a significant decrease in glycine-serine ratios compared to controls. Folate metabolism was also impaired: 5-methyltetrahydrofolate levels were increased in patients in relation to total folate (Fig. 1e, f). The substrate of SHMT2 tetrahydrofolate (THF) was undetectable in mitochondria-enriched control fibroblast samples, but low levels of this molecule were detectable in extracts from patient fibroblasts (Supplementary Table 5). These data support the impairment of SHMT2 enzymatic function in these patients. Because folate and serine are required for proper mitochondrial translation [11, 12], we verified levels of mitochondrial OXPHOS complexes, which did not vary (Supplemental Fig. 14).

Next we analyzed bioenergetic and mitochondrial function in patients’ fibroblasts, which were described to be impaired in knockout human cancer cell lines [11, 12]. ATP measurements, as well as extracellular flux analysis in a Seahorse device, under glucose restriction conditions, indicated an impaired oxidative capacity in patients’ cells relative to controls (Fig. 1g, h, Supplementary Fig. 15). Mitochondrial membrane potential was found to be altered, as well as ROS levels (both total and mitochondrial), supporting mitochondrial redox metabolism malfunction (Supplementary Fig. 16).

In previous works, *Shmt2* knockout mice exhibited embryonic lethality, attributed to severe mitochondrial respiration defects in fetal liver, and ensuing inhibition of erythroblast differentiation resulting in anemia. Moreover, metabolic defects were not observed in brain tissue, possibly due to the preferential use of the glycine cleavage system to provide one-carbon units [17]. To investigate whether the patients’ neurological phenotype could be mediated by non-neuronal autonomous mechanisms, we knocked down *Shmt2* specifically in *Drosophila* motor neurons (~65% knockdown of *Shmt2* RNA as shown previously by qPCR) [3]. We analyzed the morphology of presynaptic terminals at neuromuscular junctions (NMJs), which reliably model excitatory synapses in the mammalian brain and spinal cord [2]. While no changes in the numbers of total boutons or mature boutons were observed in *Shmt2*-knockdown animals compared with eGFP controls, we found a significant increase in the numbers of satellite boutons, emerging from the main nerve terminal or budding excessively from primary boutons and

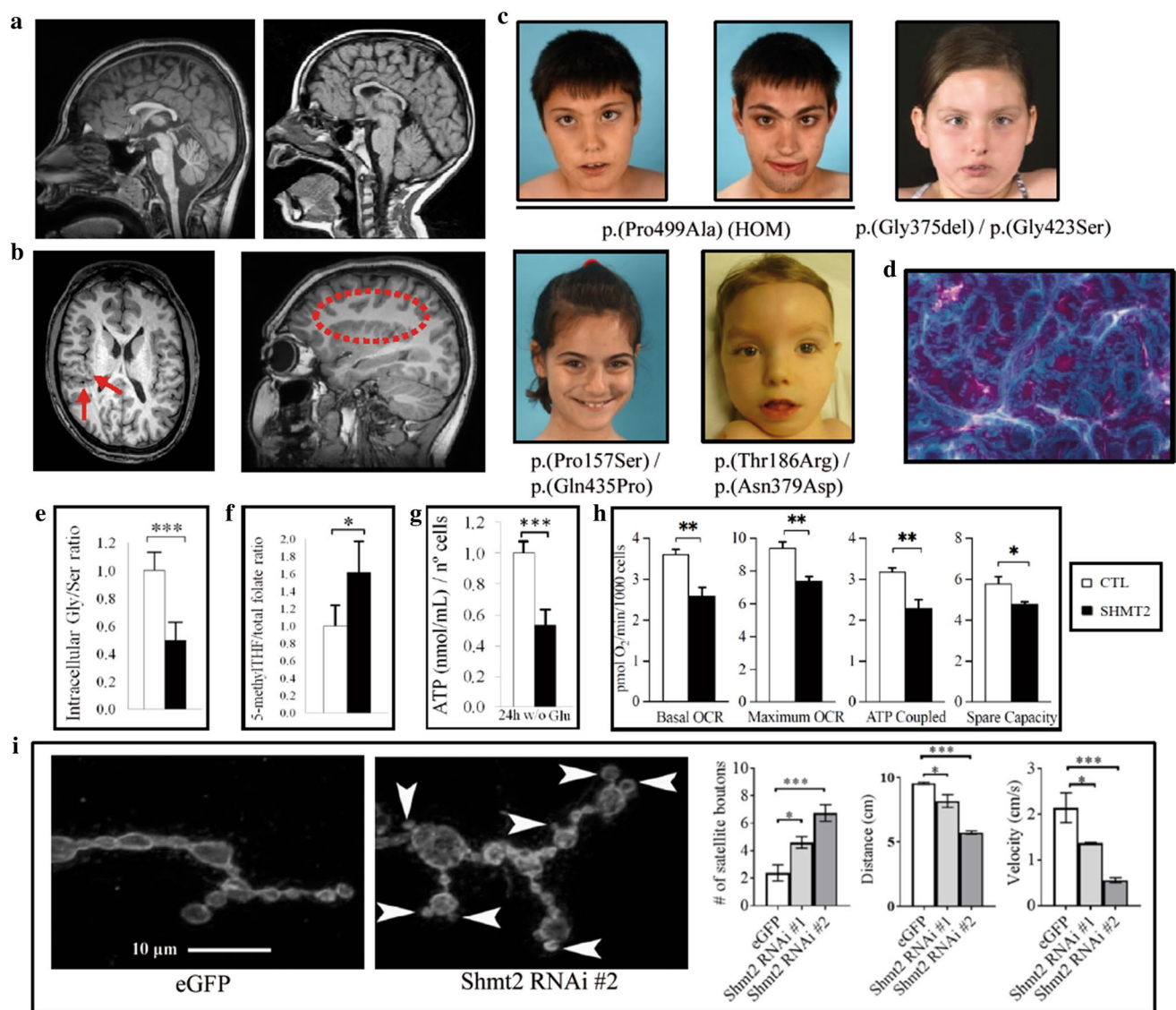


Fig. 1 SHMT2-mutated patients: phenotype and functional evaluation in fibroblasts. **a** Sagittal T1-weighted MRI planes showing corpus callosum hypoplasia in Patient P1 (left) and Patient P4 (right). **b** Axial T1-weighted MRI planes (left) in Patient P2 showing perisylvian polymicrogyria (PMG) visible around both Sylvian fissures and insulae (arrows) and right parasagittal T1-weighted MRI (dotted contour). Note the stippled gray-white boundary of the polymicrogyric cortex compared to the smooth gray-white boundary in normal cortical areas. **c** Dysmorphic features in Patients P1–P5. **d** Modified Gomori trichrome staining of Patient 4 myocardium biopsy sample showed the presence of “ragged red” fibers, consistent with a mitochondrial cytopathy. **e** Quantification of Gly/Ser ratio in fibroblasts from control individuals (CTL, $n=6$) and patients (SHMT2, $n=5$). **f** 5'-Methyl THF (tetrahydrofolate) normalized to total folate levels in fibroblasts from control individuals (CTL, $n=5$) and patients (SHMT2, $n=5$). **g** Measure of ATP concentration in control individuals (CTL, $n=6$) and patients (SHMT2, $n=5$) fibroblasts after 24-h incubation in a

medium without glucose. Values were normalized by number of cells. Quantification depicted as fold change to control fibroblasts. **h** Quantification of mitochondrial oxygen consumption rates (OCR, pmol O₂/min/1000 cells) in control individuals (CTL, $n=5$) and patients (SHMT2, $n=4$). **i** Shmt2 knockdown in motoneurons cause neuromuscular junction (NMJ) and motility defects in Drosophila. Left: immunofluorescence images of the neuromuscular junctions of muscle 4 segment A2–A3 stained with the presynaptic marker horseradish peroxidase (HRP, arrowhead). Right: quantification of the average number of satellite boutons, climbing distance and velocity in control (eGFP) and mutant (Shmt2 RNAi #1, #2) flies ($n=15$ –18 for boutons, $n=30$ for distance and velocity). In **e–h**, values are expressed as mean \pm SD, and two-tailed Student *t* tests were performed; in **i**, values are expressed as mean \pm SEM, and one-way ANOVA with Tukey’s multiple comparisons test was performed (* $p<0.05$, ** $p<0.01$, *** $p<0.001$)

forming clusters (Fig. 1i, Supplementary Fig. 17). Of note, previous studies have shown increased satellite boutons in *Drosophila* models for Amyotrophic Lateral Sclerosis and Spastic Paraplegia [7, 16]. Moreover, mutant flies showed reduced climbing distance and velocity compared to eGFP control animals (Fig. 1i). These results may reflect a role for human SHMT2 in the maintenance of presynaptic vesicles, and can be attributed to a selective decrease of Shmt2 in neurons, without any significant systemic interfering effects. Thus, these studies argue against non-cell autonomous mechanisms from the periphery causing neuronal malfunction in patients.

Interestingly, this novel rare disease entity corresponds faithfully to an intersection of diverse clinical manifestations associated with defects in metabolic pathways in which SHMT2 plays a crucial role, such as amino acid and folate metabolism and mitochondrial homeostasis [4, 11, 12]. SHMT2 impairment alters intracellular glycine/serine levels, which provides the main source of mitochondrial one-carbon units in proliferating cells, and thus probably contributes to microcephaly and polymicrogyria [9, 10, 13]. Microcephaly associated with hypomyelination is also seen in patients with loss of PYCR2, an enzyme of proline synthesis which interacts with SHMT2, causing hyperglycinemia, underscoring the impact of dysregulated glycine/serine levels on neurodevelopment [6]. SHMT2 malfunction also depletes a downstream product species, 5,10-methylTHF, required for nucleotide metabolism [1, 5]. Microcephaly, developmental delay/intellectual disability and cardiomyopathy have been extensively described in defects of folate metabolism [14]. In summary, we describe a novel neurodevelopmental, syndromic encephalopathy and movement disorder associated with cardiac defects. Despite a certain degree of variable severity, clinical manifestations were consistent in all individuals and thus establish a well-defined and recognizable clinical syndrome of defective folate and amino acid metabolism.

Acknowledgements We are indebted to the families who participated in this study. We thank CERCA Program/Generalitat de Catalunya for institutional support. We thank Cristina Guilera and Juanjo Martínez for excellent technical assistance at Neurometabolic Diseases Lab. We thank the Mayo Clinic Mitochondrial Disease Center for excellent support. This study was supported by the Centre for Biomedical Research on Rare Diseases (CIBERER) [ACCI14-759], [ACCI19-26], the URDCat program (PERIS SLT002/16/00174), the Fondo de Investigación Sanitaria FIS PI17/00916 (ISCIII) (co-funded by European Regional Development Fund. ERDF, a way to build Europe), the Hesperia Foundation, and the Secretary for Universities and Research of the Ministry of Business and Knowledge of the Government of Catalonia [2017SGR1206] to AP. AGC and NJP were funded by Fondo de Investigación Sanitaria (FIS) P118/00111 (Instituto de Salud Carlos III: ISCIII and “Fondo Europeo de desarrollo regional” FEDER). RA was funded by FIS PI17/00109 (ISCIII). EV was funded by grants from the Ministerio de Economía, Industria y Competitividad (Juan de

la Cierva program FJCI-2016-28811) and Instituto de Salud Carlos III (Sara Borrell program, CD19/00221). SF was funded by the Instituto de Salud Carlos III [Miguel Servet program CPII16/00016, co-funded by European Social Fund. ESF investing in your future]. MR was funded by CIBERER. LPS and AJP were funded by predoctoral grants from the Instituto de Salud Carlos III (PFIS, FI18/00141 and FI18/00253). EK and MC were funded by the Center for Individualized Medicine at Mayo Clinic. ET and CF were funded by a grant from the NIH (HL121079), the Anne Dash Weinman Fund in Cardiovascular Research Honoring Steven J. Lester, and the Nasser Al-Rashid Fund for Research in Cardiovascular Diseases. AP and EWK are members of the Undiagnosed Diseases Network International (UDNI). We are indebted to the “Biobanc de l’Hospital Infantil Sant Joan de Déu per a la Investigació” integrated in the Spanish Biobank Network of ISCIII for the sample and data procurement of patient 3. MZ and ND were supported in part by The Linda T. and John A. Mellowes Endowed Innovation and Discovery Fund and the Genomic Sciences and Precision Medicine Center of Medical College of Wisconsin.

SHMT2 Working Group: Alfonso Oyarzábal, Inés Medina, Aida Ormazábal, Jordi Muchart, Juan Manuel Carretero, Cristina Jou, Mireia del Toro, Andrés Nascimento, Abraham J. Paredes, Delia Yubero, Roser Colomé. Neurometabolic Unit and Synaptic Metabolism Lab, Neurology Department, Institut Pediàtric de Recerca, Hospital Sant Joan de Déu, and MetabERN, 08950, Barcelona, Catalonia, Spain: AlOy, IM, AiOr, JM, JMC, RC. Centre for Biomedical Research on Rare Diseases (CIBERER), Instituto de Salud Carlos III, 28029, Madrid, Spain: AlOy, AiOr, CJ, AJP, DY, RC. Pathology Department, Institut de Recerca Sant Joan de Déu, and MetabERN, 08950, Barcelona, Catalonia, Spain: CJ. Pediatric Neurology Department, Vall d’Hebron University Hospital, Universitat Autònoma de Barcelona, 08916, Barcelona, Spain: MdT. Neuromuscular Unit, Neurology Department, Institut Pediàtric de Recerca, Hospital Sant Joan de Déu, 08950, Barcelona, Catalonia, Spain: AN. Clinical Biochemistry and Genetics Departments, Institut de Recerca Sant Joan de Déu, and MetabERN, 08950, Barcelona, Catalonia, Spain: AJP, DY.

Author contributions Conceptualization: AGC, EV, MAC, and AP. Funding acquisition: AGC, SB, EWK, SF, UP, RA, MAC, and AP. Performed research and experiments: AGC, EV, NJP, ENA, LG, ET, NRD, AS, RU, LPS, JMT, RHG, SWG, MR, SF, ARP, BC, TB, MV, CF, MTZ, UP, and RA. Supervision: AGC, RA, MAC, and AP. Writing of the original draft: AGC, EVP, MAC, and AP. All authors contributed to revising the manuscript.

Compliance with ethical standards

Conflict of interest The authors have declared that no conflict of interest exists.

Open Access This article is licensed under a Creative Commons Attribution 4.0 International License, which permits use, sharing, adaptation, distribution and reproduction in any medium or format, as long as you give appropriate credit to the original author(s) and the source, provide a link to the Creative Commons licence, and indicate if changes were made. The images or other third party material in this article are included in the article’s Creative Commons licence, unless indicated otherwise in a credit line to the material. If material is not included in the article’s Creative Commons licence and your intended use is not permitted by statutory regulation or exceeds the permitted use, you will need to obtain permission directly from the copyright holder. To view a copy of this licence, visit <http://creativecommons.org/licenses/by/4.0/>.

References

1. Acuna-Hidalgo R, Schanze D, Kariminejad A, Nordgren A, Kariminejad MH, Conner P et al (2014) Neu-Laxova syndrome is a heterogeneous metabolic disorder caused by defects in enzymes of the L-serine biosynthesis pathway. *Am J Hum Genet* 95:285–293. <https://doi.org/10.1016/j.ajhg.2014.07.012>
2. Budnik V (1996) Synapse maturation and structural plasticity at Drosophila neuromuscular junctions. *Curr Opin Neurobiol* 6:858–867. [https://doi.org/10.1016/s0959-4388\(96\)80038-9](https://doi.org/10.1016/s0959-4388(96)80038-9)
3. Celardo I, Lehmann S, Costa AC, Loh SH, Martins LM (2017) DATF4 regulation of mitochondrial folate-mediated one-carbon metabolism is neuroprotective. *Cell Death Differ* 24:638–648. <https://doi.org/10.1038/cdd.2016.158>
4. Ducke GS, Rabinowitz JD (2017) One-carbon metabolism in health and disease. *Cell Metab* 25:27–42. <https://doi.org/10.1016/j.cmet.2016.08.009>
5. El-Hattab AW (2016) Serine biosynthesis and transport defects. *Mol Genet Metab* 118:153–159
6. Escande-Beillard N, Loh A, Saleem SN, Kanata K, Hashimoto Y, Altunoglu U et al (2020) Loss of PYCR2 causes neurodegeneration by increasing cerebral glycine levels via SHMT2. *Neuron* 107:82–94.e6. <https://doi.org/10.1016/j.neuron.2020.03.028>
7. Estes PS, Boehringen A, Zwick R, Tang JE, Grigsby B, Zarnescu DC (2011) Wild-type and A315T mutant TDP-43 exert differential neurotoxicity in a Drosophila model of ALS. *Hum Mol Genet* 20:2308–2321. <https://doi.org/10.1093/hmg/ddr124>
8. Giardina G, Brunotti P, Fiascarelli A, Cicalini A, Costa MG, Buckle AM et al (2015) How pyridoxal 5'-phosphate differentially regulates human cytosolic and mitochondrial serine hydroxymethyltransferase oligomeric state. *FEBS J* 282:1225–1241. <https://doi.org/10.1111/febs.13211>
9. De Koning TJ, Duran M, Dorland L, Gooskens R, Van Schaftingen E, Jaeken J et al (1998) Beneficial effects of L-serine and glycine in the management of seizures in 3-phosphoglycerate dehydrogenase deficiency. *Ann Neurol* 44:261–265. <https://doi.org/10.1002/ana.410440219>
10. De Koning TJ, Klomp LWJ (2004) Serine-deficiency syndromes. *Curr Opin Neurol* 17:197–204
11. Minton DR, Nam M, McLaughlin DJ, Shin J, Bayraktar EC, Alvarez SW et al (2018) Serine Catabolism by SHMT2 Is Required for Proper Mitochondrial Translation Initiation and Maintenance of Formylmethionyl-tRNAs. *Mol Cell* 69:610.e5–621.e5. <https://doi.org/10.1016/j.molcel.2018.01.024>
12. Morscher RJ, Ducke GS, Li SH, Mayer JA, Gitai Z, Sperl W, Rabinowitz JD (2018) Mitochondrial translation requires folate-dependent tRNA methylation. *Nature* 554:128–132. <https://doi.org/10.1038/nature25460>
13. Murtas G, Marcone GL, Sacchi S, Pollegioni L (2020) L-serine synthesis via the phosphorylated pathway in humans. *Cell Mol Life Sci*. <https://doi.org/10.1007/s00018-020-03574-z>
14. Pope S, Artuch R, Heales S, Rahman S (2019) Cerebral folate deficiency: analytical tests and differential diagnosis. *J Inherit Metab Dis* 42:655–672
15. Saudubray J-M, Baumgartner M, Walter J (2016) Inborn metabolic diseases, diagnosis and treatment, 2016th edn. Springer, New York
16. Sherwood NT, Sun Q, Xue M, Zhang B, Zinn K (2004) Drosophila spastin regulates synaptic microtubule networks and is required for normal motor function. *PLoS Biol*. <https://doi.org/10.1371/journal.pbio.0020429>
17. Tani H, Mito T, Velagapudi V, Ishikawa K, Umehara M, Nakada K et al (2019) Disruption of the mouse Shmt2 gene confers embryonic anaemia via foetal liver-specific metabolomic disorders. *Sci Rep* 9:16054. <https://doi.org/10.1038/s41598-019-52372-6>
18. Tani H, Ohnishi S, Shitara H, Mito T, Yamaguchi M, Yonekawa H et al (2018) Mice deficient in the Shmt2 gene have mitochondrial respiration defects and are embryonic lethal. *Sci Rep* 8:425. <https://doi.org/10.1038/s41598-017-18828-3>
19. Walden M, Tian L, Ross RL, Sykora UM, Byrne DP, Hesketh EL et al (2019) Metabolic control of BRISC–SHMT2 assembly regulates immune signalling. *Nature* 570:194–199. <https://doi.org/10.1038/s41586-019-1232-1>

Publisher's Note Springer Nature remains neutral with regard to jurisdictional claims in published maps and institutional affiliations.



POLR3A variants with striatal involvement and extrapyramidal movement disorder

Inga Harting¹ · Murtadha Al-Saady² · Ingeborg Krägeloh-Mann³ · Annette Bley⁴ · Maja Hempel⁵ · Tatjana Bierhals⁵ · Stephanie Karch⁶ · Ute Moog⁷ · Geneviève Bernard⁸ · Richard Huntsman⁹ · Rosalina M. L. van Spaendonk¹⁰ · Maaike Vreeburg¹¹ · Agustí Rodríguez-Palmero^{12,13} · Aurora Pujol^{12,14,15} · Marjo S. van der Knaap^{2,16} · Petra J. W. Pouwels¹⁷ · Nicole I. Wolf²

Received: 6 November 2019 / Accepted: 27 December 2019
© The Author(s) 2020

Abstract

Biallelic variants in *POLR3A* cause 4H leukodystrophy, characterized by hypomyelination in combination with cerebellar and pyramidal signs and variable non-neurological manifestations. Basal ganglia are spared in 4H leukodystrophy, and dystonia is not prominent. Three patients with variants in *POLR3A*, an atypical presentation with dystonia, and MR involvement of putamen and caudate nucleus (striatum) and red nucleus have previously been reported. Genetic, clinical findings and 18 MRI scans from nine patients with homozygous or compound heterozygous *POLR3A* variants and predominant striatal changes were retrospectively reviewed in order to characterize the striatal variant of *POLR3A*-associated disease. Prominent extrapyramidal involvement was the predominant clinical sign in all patients. The three youngest children were severely affected with muscle hypotonia, impaired head control, and choreic movements. Presentation of the six older patients was milder. Two brothers diagnosed with juvenile parkinsonism were homozygous for the c.1771-6C > G variant in *POLR3A*; the other seven either carried c.1771-6C > G ($n = 1$) or c.1771-7C > G ($n = 7$) together with another variant (missense, synonymous, or intronic). Striatal T2-hyperintensity and atrophy together with involvement of the superior cerebellar peduncles were characteristic. Additional MRI findings were involvement of dentate nuclei, hilus, or peridentate white matter (3, 6, and 4/9), inferior cerebellar peduncles (6/9), red nuclei (2/9), and abnormal myelination of pyramidal and visual tracts (6/9) but no frank hypomyelination. Clinical and MRI findings in patients with a striatal variant of *POLR3A*-related disease are distinct from 4H leukodystrophy and associated with one of two intronic variants, c.1771-6C > G or c.1771-7C > G, in combination with another *POLR3A* variant.

Keywords *POLR3A* · MRI · Basal ganglia · Striatum · Superior cerebellar peduncle · Inferior cerebellar peduncle · Brainstem · Hypomyelination

Introduction

RNA polymerase III (POLR3) transcribes genes encoding small, non-coding RNAs including tRNAs, 5S RNA, 7SK RNA, and U6 small nuclear RNA, which are involved in the regulation of transcription, RNA processing, and translation [1].

Electronic supplementary material The online version of this article (<https://doi.org/10.1007/s10048-019-00602-4>) contains supplementary material, which is available to authorized users.

✉ Nicole I. Wolf
n.wolf@amsterdamumc.nl

Extended author information available on the last page of the article

Disease-causing variants in genes coding for POLR3 subunits were first discovered in patients with hypomyelinating leukodystrophy. They are located in *POLR3A* [2] and *POLR3B* [1, 3], which encode the largest and second largest subunits of POLR3 forming the catalytic centre of the enzyme, as well as in *POLR1C* [4], a gene encoding a shared POLR1 and POLR3 subunit. The resulting 4H leukodystrophy (hypomyelination, hypodontia, hypogonadotropic hypogonadism) is characterized by hypomyelination in combination with early cerebellar and subsequent pyramidal signs (usually mild) and variable non-neurological manifestations, namely dental and endocrine features as well as myopia [5]. Ataxia is the predominant clinical finding in 4H leukodystrophy. Dystonia is an additional, common, and initially under-recognized feature in 4H leukodystrophy [6], but not

prominent at disease onset, and basal ganglia abnormalities as a potential correlate of dystonia have not been reported in 4H leukodystrophy. Clinical manifestations and hypomyelination in 4H leukodystrophy are more severe in patients with variants in *POLR3A* and *POLR1C* than in patients with variants in *POLR3B* [7, 8]; hypomyelination, however, is not obligatory, and manifestation without hypomyelination occurs in patients with variants in *POLR3A* or *POLR3B* [9].

During the last years, *POLR3A* variants without predominant ataxia have been reported: A striatal manifestation with predominant dystonia and MR involvement of putamen, caudate and red nucleus due to a homozygous founder variant in intron 13 was reported for three patients from two families with a Roma background [10]. In addition, biallelic *POLR3A* variants have been recognized as a cause of hereditary spastic ataxia [11, 12].

In order to characterize the striatal variant of *POLR3A*-related disease, we reviewed clinical, genetic, and MRI findings of nine patients with *POLR3A* variants and striatal changes.

Patients and methods

We retrospectively identified nine patients from eight families with biallelic *POLR3A* variants and striatal changes on MRI through the patient database at the Center for Childhood White Matter Disorders Amsterdam. Patients were referred to the Center for Childhood White Matter Disorders Amsterdam after identification of *POLR3A* variants, but without typical presentation for 4H leukodystrophy, for diagnostic evaluation. In all patients, *POLR3A* variants were identified by diagnostic whole exome sequencing, performed at different centres. Segregation analysis established their biallelic occurrence in all patients except patient 6, of whom only one parent was available for testing and carried one of the patient's two variants. No other variants were found explaining the movement disorder. NIW saw patients 1, 3, 7–9; IKM saw patient 5, AB patient 2, GB and RH patient 6, AR-P patient 4. Records were reviewed for clinical presentation and are summarized in Table 1; for case histories, see supplemental material.

The patients' 18 cranial MRI scans (age at examination 0.5–29 years, mean 9.1 years, median 4.8 years) were systematically reviewed in consensus by a pediatric neuroradiologist (IH) and pediatric neurologist (NIW). Axial T2-weighted (T2w) and T1-weighted (T1w) images were available for all MRI scans, sagittal T1w images for all but the follow-up MRI in patient 6 (sagittal 3D-T2w), diffusion-weighted imaging (DWI) with apparent diffusion coefficient (ADC) for at least one MRI in all patients (13/18 MRIs). MRI was assessed for presence and extent of T2w grey and white matter changes, in particular for involvement of deep grey matter and brainstem tracts, and for corresponding T1-signal changes. DWI and ADC-maps were inspected for restricted diffusion, namely

hyperintensity on DWI and corresponding low signal on ADC (below 60×10^{-5} mm 2 /s), or increased diffusion with high signal on ADC (above $100–110 \times 10^{-5}$ mm 2 /s, for basal ganglia and white matter, respectively [13–15]).

T2 gradient echo and susceptibility-weighted images, available for patient 9 and first MRIs of patients 1, 4, 5, and 6 (field strength 1.5 (2) or 3 Tesla(3)), were checked for hypointensities due to calcifications and/or blood degradation products; the cerebral CT scan available for patient 8 was checked for hyperdensities. Spinal MRIs were available for patients 1, 5, and 6.

For comparison of involvement of cerebellar peduncles and/or striatum in typical 4H leukodystrophy, we additionally reviewed 40 MRIs of 36 patients with 4H leukodystrophy and imaging between 2.8 and 40 years previously published [7].

Results

Patients

All patients except patient 5 had an extrapyramidal movement disorder. Onset of symptoms varied between neonatal period (patients 1–3), infancy (patients 4–6), and early childhood (patients 7–9). Initial symptoms in the patients with neonatal presentation comprised abnormal choreic movements, restlessness, poor visual contact, failure to thrive due to swallowing difficulties, and severe global developmental delay. In the patients with infantile presentation, there were developmental delay more of motor than of cognitive development and extrapyramidal signs with dystonic posturing and poor facial expression (excepting patient 5 who had only mild ataxia). In the patients with early childhood presentation, initial motor development was normal: All patients walked without support age 12–15 months, although at least in patient 9 there were always concerns of frequent falls. In these patients, both motor function and expressive speech deteriorated in childhood with resulting severe dysarthria/anarthria and dysphagia. For a detailed description, see supplemental case reports and Table 1.

Dentition was abnormal in six of nine patients. Of six patients tested, two had mild myopia (patients 5 and 9). Only three patients (7–9) were old enough to exclude delayed puberty due to hypogonadotropic hypogonadism. Clinical, genetic, and MRI findings are summarized in Tables 1, 2, and 3 with patients sorted for age at first MRI.

Genetic findings

All patients carried at least one of two intronic variants of *POLR3A*, c.1771-6C > G or c.1771-7C > G (Table 2; Fig. 1). While the two brothers were homozygous for c.1771-6C > G, all other patients were compound heterozygous: One patient

Table 1 Main clinical characteristics. BEAR brainstem evoked acoustic responses, F female, M male, mo month, n/a not applicable, yrs. years

	Patient 1	Patient 2	Patient 3	Patient 4	Patient 5	Patient 6	Patient 7	Patient 8	Patient 9
Gender	F	F	F	M	F	M	M	M	F
Current age	2 yrs	2 yrs	21 mo	7 yrs	7 yrs	6 yrs	22 yrs	26 yrs	29 yrs
Affected siblings	No	No	No	No	No	No	Yes, patient 8	Yes, patient 7	No
Consanguinity	No	No	First days of life	First year of life	Second year of life	13 months	4 years	Yes	No
Age at onset	2 months								14 months
Signs/symptoms at onset	No smiling, failure to thrive	No crying, absent visual contact	Abnormal movements, restlessness	Global developmental delay, poor facial expression	Mild motor delay	Abnormal gait	Psychomotor retardation	Mild delay in language acquisition	Abnormal gait, prone to falling
Age at last examination	17 mo	2 yrs.	16 mo	5 yrs	5 yrs	4 yrs.	21 yrs	26 yrs	29 yrs
Axial hypotonia	Yes	Yes, if relaxed.	Severe	No	No	Mild	No	No	No
Head balance	Suboptimal	Suboptimal	Suboptimal	Suboptimal at three mo	Normal	Normal	Normal	Normal	Normal
Ataxia	No	No intentional movements	No	Yes	Mild gait ataxia	Yes	No	No	Head titubation
Pyramidal signs	No	Yes	No	Yes	No	Yes	No	No	Mild pyramidal signs (legs)
Extrapyramidal signs	Yes, choreic movements and opisthotonus	Yes, choreic movements	Yes, choreic movements and opisthotonus	Yes, dystonia and bradykinesia	No	Yes, dystonia	Severe, compatible with Parkinsonism; in addition (rhythmic) tremor (3/s), increasing with action	Severe, compatible with Parkinsonism; in addition (rhythmic) tremor (3/s), increasing with action	Yes, (rhythmic) tremor (3/s), increasing with action
Eye movements	Saccadic pursuit	No fixation	Short periods of fixation	Normal	Normal	Saccadic pursuits	Saccadic pursuit and hypometric saccades	Saccadic pursuit	Saccadic pursuit
Highest motor achievement	Some head balance	Some head balance	Some head balance	Walks with posterior walker, manages to walk 20 steps without support	Walking without support	Walking without support	Walking without support	Walking without support	Walking without support (age 14 mo), wheelchair dependent from age 12 yrs
Swallowing problems	Mild	Severe	Severe (nasogastric tube)	Yes, especially with liquids (prone to aspiration)	No	No	No	Severe dysphagia	Yes
Speech and language	None	None	None	Delayed (uses about 20 words, difficult to understand)	Mild delay in language development, at age 4 yrs., stutter	Speech delay, dysarthria	Severe dysarthria	Language deterioration from age 5 yrs., now anarthric	Severe dysarthria
Cognition	Severe global delay	Severe global delay assumed	Severe global delay	Not formally tested but seems normal	Mild learning difficulties	Not formally tested but seems normal	Learning disability	Learning disability	Normal

Table 1 (continued)

	Patient 1	Patient 2	Patient 3	Patient 4	Patient 5	Patient 6	Patient 7	Patient 8	Patient 9
Epilepsy	Yes, myoclonic jerks from age 15 mo	No	No	No	No	seems normal	No	No	No
Dentition	Abnormal (lack of maxillary incisors)	Abnormal (delayed dentition, deciduous molars first teeth to erupt)	Abnormal (lack of maxillary incisors)	Abnormal (delayed eruption of maxillary incisors)	Normal	Normal	Abnormal (first teeth to erupt maxillary incisors, 2 persisting decidual teeth)	Abnormal (molars first to erupt, incisors erupted at 4y of age)	
Puberty development	n/a	n/a	n/a	n/a	n/a	Normal	Normal	Normal	Normal
Growth	Failure to thrive	Failure to thrive	Failure to thrive	Failure to thrive	Normal	n/a	Very low weight due to inadequate intake	Very low weight due to inadequate intake	Normal
Head circumference	Normal	Normal	Normal	Normal	Normal	Normal	Normal	Normal	Normal
Myopia	Not tested	Not tested	Not tested	Not tested	Mild myopia Not tested, clinically normal	No	No	Mild myopia Not tested, clinically normal	Mild myopia Not tested, clinically normal
Hearing loss	Not tested	Not tested	Not tested	Abnormal BEAR	BEAR normal	Not tested, clinically normal	Not tested, clinically normal	Not tested, clinically normal	Not tested, clinically normal
Other	n/a	Laboured breathing	Prone to respiratory tract infections; bacterial meningitis	n/a	n/a	n/a	n/a	n/a	n/a

Table 2 Genetic findings. Genetic variants for all patients

Patient	Variant 1	Variant 2
1	c.1771-7C>G p.(Glu548_Tyr637del) / p.(Pro591Metfs*9)	c.1048 + 5G > T p.(Glu350Glufs*27)
2	c.1771-7C>G p.(Glu548_Tyr637del) / p.(Pro591Metfs*9)	c.4025-1G > A p.?
3	c.1771-7C>G p.(Glu548_Tyr637del) / p.(Pro591Metfs*9)	c.2713G > A p.(Asp905Asn)
4	c.1771-7C>G p.(Glu548_Tyr637del) / p.(Pro591Metfs*9)	c.3387C > A p.(Leu1129Leu)
5	c.1771-7C>G p.(Glu548_Tyr637del) / p.(Pro591Metfs*9)	c.2809G > A p.(Glu937Lys)
6	c.1771-7C>G p.(Glu548_Tyr637del) / p.(Pro591Metfs*9)	c.1771-6C > G p.(Pro591Metfs*9)
7 & 8	c.1771-6C>G p.(Pro591Metfs*9)	c.1771-6C > G p.(Pro591Metfs*9)
9	c.1771-6C>G p.(Pro591Metfs*9)	c.2045G > A p.(Arg682Gln)

carried the variant c.1771-6C > G, and six carried the variant c.1771-7C > G in combination with another variant. These were an intronic variant at/close to a splice site ($n = 3$; including one with c.1771-6C > G), a synonymous variant predicted to affect splicing ($n = 1$), and missense variants ($n = 3$). The two missense variants were both located in the discontinuous cleft domain and had not yet been described in patients. The c.2045G > A variant (heterozygous) has been described in a patient with classic 4H leukodystrophy [5]. The c.1048 + 5G > T variant in a homozygous state has been described in a patient with Wiedemann-Rautenstrauch syndrome [16] and compound heterozygous with c.1771-7C > G in a patient classified as spastic ataxia [12]. The c.1771-7C > G variant has been found in patients classified as spastic ataxia, in combination with a frameshift variant [11, 12]. The c.1771-6C > G variant has been described in patients in homozygous form with basal ganglia involvement [10]. The c.4025-1G > A, previously not reported in literature, affects a canonical acceptor site and can be considered as a loss-of-function variant.

MRI findings

Basal ganglia

Symmetric, homogeneous, mild T2-hyperintensity and atrophy of putamen and caudate nucleus (*striatum*) were present in all patients (Fig. 2), with corresponding hyperintensity on ADC maps and increased ADC (range $110\text{--}120 \times 10^{-5} \text{ mm}^2/\text{s}$) in those with diffusion-weighted imaging. Among the five younger patients with first imaging until 2 years, the striatum was already T2-hyperintense and atrophic in two patients at 0.9 and 1.0 year. In the other three, the striatum was initially small or normal and had become T2-hyperintense and atrophic only by follow-up at 1.5, 4.8, and 2.9 years, respectively (patients 4, 1, and 5; Figs. 3 and 4). The four older patients imaged between 4 and 29 years all had striatal T2-hyperintensity and atrophy (Table 3). In contrast, the striatum was normal in the 36 patients with classic 4H leukodystrophy re-reviewed for comparison.

The *pallidum* was not abnormally T2-hyperintense in our patients. In those five patients with gradient echo/susceptibility-weighted images and in the CT scan of patient 8, there was no indication of abnormal calcification, iron deposition, or blood degradation products.

Cerebellum and brainstem

All patients had signal alterations of the superior cerebellar peduncle (SCP) in at least one MRI, involving the decussation in seven patients and reaching the red nucleus in two of these. Additional findings were involvement of the hilus of the dentate nuclei, the dentate nuclei, and/or the peridental white matter in six, three, and four patients, respectively, and of the inferior cerebellar peduncle (ICP) in five. The middle cerebellar peduncles (MCP) were involved in none. In contrast, MCP were T2-hyperintense in 29, decussation of SCP in two, and ICP was not involved in any of the 36 patients with classic 4H leukodystrophy re-reviewed for comparison.

T2-hyperintensity of SCP did not significantly change in patient 8 between 12 and 23 years, whereas it resolved in his brother between 13 and 19 years (Fig. 5). Similarly, T2-hyperintensity of SCP, hilus of dentate nuclei, peridental white matter, and ICP clearly decreased in patient 5 between 2 and 4.8 years (Fig. 4). Conversely, infratentorial changes increased in the youngest patient between 0.5 and 1.5 years: Only the decussation of SCP was hyperintense at 0.5 years, while, at follow-up, T2-hyperintensity involved the entire course of SCP as well as the hilus of the dentate nuclei, peridental white matter, and ICP (Fig. 5). Taken together, these findings suggest that signal alteration of SCP, ICP, and dentate area may be a transient phenomenon.

Supratentorial white matter

Signal of supratentorial white matter on T2w and T1w images was normal in three of the four older patients examined between 4 and 29 years (patients 6–9), while mild T2-hyperintensity of pyramidal tract in the centrum semiovale and subcortical white matter was present in patient 9. The

Table 3 Overview of MRI changes (sorted by age at first MRI). *AL/C* anterior limb of internal capsule, *CC* corpus callosum, *cor.rad.* corona radiata, *c.sem.* centrum semiovale, *decss.* SCP decussation of superior cerebellar peduncles, *dent. ncl.* dentate nucleus, *front.* frontal, *hilus hilus* of dentate ncl., *ICP inferior cerebellar peduncles*, *myel.* delay myelination delay, *pall.* pallidum, *perid.* periventricular white matter, *pyr.tr.* pyramidal tract, *resid.* residual, *SCP* superior cerebellar peduncles, *subcort.* subcortical, *suprat.* supratentorial white matter, *temp.* temporal, *vol.* volume, *yrs.* years, $\uparrow T2/\downarrow T1$ hyperintensity on T2/hypointensity on T1w images, \sim normal signal compared to controls

Patient	Age at MRI [yrs]	Basal ganglia		Brainstem/cerebellum						Supratent. wm			
		Striatum	Pall. red ncl.	decuss.	SCP	dent. ncl.	hilus	perid.	ICP	Abnormal	pyr. tract	Optic	Other radiation regions
1	0.5	\sim	\sim	\sim	$\uparrow T2, \downarrow T1$	\sim	\sim	\sim	\sim	yes	myel. delay: subcort., c.sem., corr.ad.	myel.	\sim
	1.5	$\uparrow T2, \downarrow vol.$	\sim	\sim	$\uparrow T2, \downarrow T1$	yes	$\uparrow T2$: subcort., c.sem., corr.ad.	$\uparrow T2$	$\uparrow T2$ c.sem., cor. rad.				
2	0.9	$\uparrow T2, \downarrow vol.$	\sim	$\uparrow T2$	$\uparrow T2, \downarrow T1$	yes	mild $\uparrow T2$: subcort., c.sem., corr.ad.	mild $\uparrow T2$	$\uparrow T2$ c.sem., cor. rad.				
3	1.0	$\uparrow T2, \downarrow vol.$	$\downarrow T2$	\sim	$\uparrow T2, \downarrow T1$	yes	mild $\uparrow T2$: subcort., c.sem., corr.ad.	mild $\uparrow T2$	$\uparrow T2$ c.sem., cor. rad.				
4	1.7	$\downarrow vol.$	\sim	\sim	$\uparrow T2, \downarrow T1$	yes	mild $\uparrow T2$: subcort., c.sem., corr.ad.	mild $\uparrow T2$	\sim				
	2.9	$\uparrow T2, \downarrow vol.$	$\downarrow T2$	\sim	$\uparrow T2, \downarrow T1$	yes	mild $\uparrow T2$: subcort., c.sem., corr.ad.	incr. $\uparrow T2$	new $\uparrow T2$ ILF				
5	2.0	\sim	$\downarrow T2$	$\uparrow T2$ (right)	$\uparrow T2, \downarrow T1$	yes	\sim	\sim	\sim				
	4.8	$\uparrow T2, \downarrow vol.$	$\downarrow T2$	\sim	residual	\sim	\sim	\sim	\sim	residual $\uparrow T2$	yes	\sim	\sim
6	4.0	$\downarrow vol.$	$\downarrow T2$	\sim	\sim	\sim	\sim	\sim	$\uparrow T2, \downarrow T1$	no	\sim	\sim	\sim
	4.9	$\downarrow vol.$	$\downarrow T2$	\sim	\sim	\sim	\sim	\sim	$\uparrow T2, \downarrow T1$	no	\sim	\sim	\sim
	7	$\uparrow T2, \downarrow vol.$	\sim	\sim	$\uparrow T2$	\sim	\sim	\sim	\sim	\sim	\sim	\sim	\sim
	13.6	$\uparrow T2, \downarrow vol.$	\sim	\sim	$\uparrow T2$	\sim	\sim	\sim	$\uparrow T2$	\sim	\sim	\sim	\sim
	18.5	$\uparrow T2, \downarrow vol.$	\sim	\sim	\sim	\sim	\sim	\sim	$\uparrow T2$	\sim	\sim	\sim	\sim
	12.1	$\uparrow T2, \downarrow vol.$	\sim	\sim	\sim	\sim	\sim	\sim	$\uparrow T2$	\sim	\sim	\sim	\sim
	14.9	$\uparrow T2, \downarrow vol.$	\sim	\sim	\sim	\sim	\sim	\sim	$\uparrow T2$	\sim	\sim	\sim	\sim
	18.5	$\uparrow T2, \downarrow vol.$	\sim	\sim	\sim	\sim	\sim	\sim	$\uparrow T2$	\sim	\sim	\sim	\sim
	23.5	$\uparrow T2, \downarrow vol.$	\sim	\sim	\sim	\sim	\sim	\sim	$\uparrow T2$	\sim	\sim	\sim	\sim
	9	$\uparrow T2, \downarrow vol.$	\sim	\sim	$\uparrow T2$	\sim	yes	mild $\uparrow T2$: subcort., c.sem., corr.ad	\sim				

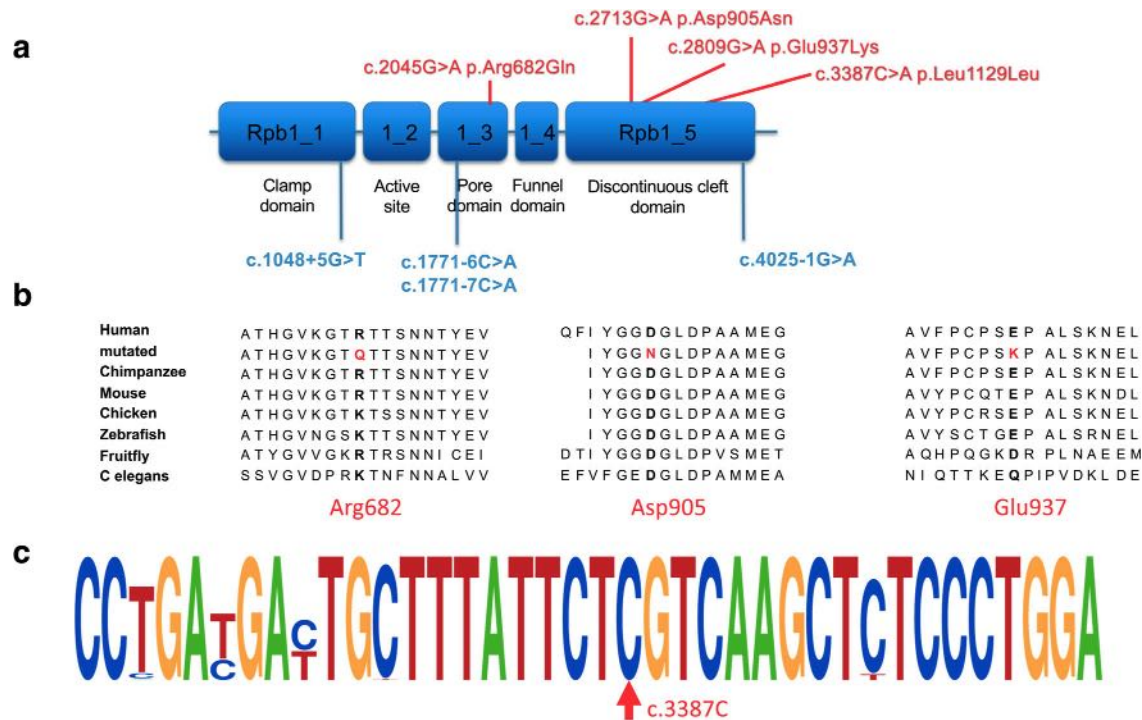


Fig. 1 Localisation of variants and conservation in *POLR3A*. This figure shows the localization of intronic variants (in blue) and exonic variants (in red) in *POLR3A*. **a** Two missense variants are both located in the discontinuous cleft domain, one in the pore domain. **b** denotes conservation of mutated amino acids across different species. **c** Motifs

of primary sequence conservation surrounding the c.3387C base pair based on alignment of 61 species using WebLogo, demonstrating the high conservation of the c.3387C base pair. The observed variant (c.3387C > A) does not lead to an amino acid change but is predicted to activate an exonic cryptic acceptor site in exon 26

optic radiation was well myelinated, with T2w hyperintense signal in the surrounding white matter.

In the five younger patients with first imaging up to the age of 2 years, myelination was delayed and/or inhomogeneous with progressing, more advanced, or normal myelination for age outside of pyramidal and visual tracts: In the youngest patient (patient 1), myelination was delayed at 0.5 years. By follow-up at 1.5 years, myelination in the central region had not progressed, and there was new T2-hyperintensity in centrum semiovale, corona radiata, and visual tract, whereas myelination was normal outside of pyramidal and visual tracts (Supplemental Fig. 1). T2-hyperintensity of pyramidal tract and/or optic radiation was also observed in patients 2–5, in patient 5 with incomplete myelination of subcortical white matter. Signal of the posterior limb of internal capsule, including the pyramidal tract, was normal in all patients and no patient had frank hypomyelination.

Pituitary gland, bulbi, atrophy, and spinal cord

The pituitary gland including T1-hyperintense signal of neurohypophysis was normally visualized on sagittal T1w images in all patients. No patients had clearly elongated bulbi as an indicator of myopia, often seen in classic 4H leukodystrophy. With regard to atrophy, corpus callosum was normal in eight patients on visual inspection and thin in one patient (patient 3).

Cerebellar atrophy was not observed. Spinal cord was normal in the three patients with spinal MRIs (patients 1, 5, and 6).

Discussion

We present nine patients with biallelic variants in *POLR3A* carrying at least one of two intronic variants (c.1771-6C > G or c.1771-7C > G), with predominantly extrapyramidal manifestations and characteristic MR changes of striatum, superior, and, often, inferior cerebellar peduncle. Their neurological presentation differs from classic 4H leukodystrophy, the initially described presentation of *POLR3A* variants. It also differs from a subform of spastic ataxia and the rare Wiedemann-Rautenstrauch syndrome (OMIM#264090), which have only recently been associated with *POLR3A*. Clinical presentation of these nine patients forms a continuum between a severe, extrapyramidal movement disorder with early onset at one end and juvenile parkinsonism with onset in childhood at the other end of the spectrum. Interestingly, six of the nine patients had abnormal dentition comparable with the abnormal dentition seen in 4H leukodystrophy. There was no evidence for endocrine involvement, although only three patients were old enough to exclude delayed puberty due to hypogonadotropic hypogonadism. Severe myopia, which occurs very frequently

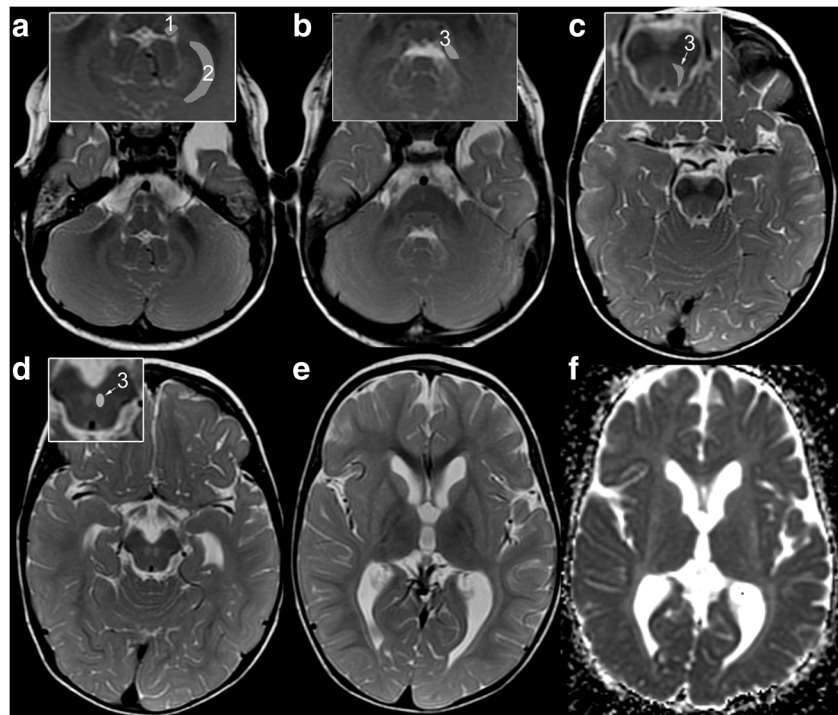


Fig. 2 Characteristic MRI pattern of striatal variant of POLR3A-related disease. MRI in patient 1 at 1.5 years demonstrates the characteristic combination of atrophic, T2-hyperintense striatum, and T2-hyperintense SCP (A-E: T2w; F: ADC-map; insets: 1 = ICP, 2 = peridentate white matter, 3 = SCP). **a** T2-hyperintensity of ICP (1) and peridentate white matter (2) are additional findings. **b** Further additional findings are T2-hyperintensity of tegmentum and intraparenchymal course of trigeminal nerve. T2-hyperintensity of SCP (3, insets in B-D) is seen along its course

from the cerebellum (**b**), dorsal mesencephalon (**c**) to the decussation in the anterior mesencephalon (**d**). **e, f**: Homogeneous, mild, and symmetric T2-hyperintensity of the striatum with volume loss and increased diffusion. NB the lateral medullary lamina between pallidum and putamen is commonly seen at this age due to its relative T2-hyperintensity compared with pallidum and putamen; increased conspicuity is due to T2-hyperintensity of putamen (**e**)

Fig. 3 Small striatum and infratentorial changes at first MRI of patient 4. At 20 months, the striatum is small (**e**, age-matched control image in (**f**) for comparison), but its signal does not exceed that of the cortex and is normal. Note involvement of ICP (**a**), dentate nuclei, hilus, and peridentate white matter (**b**), and of SCP including the decussation (**b-d**)

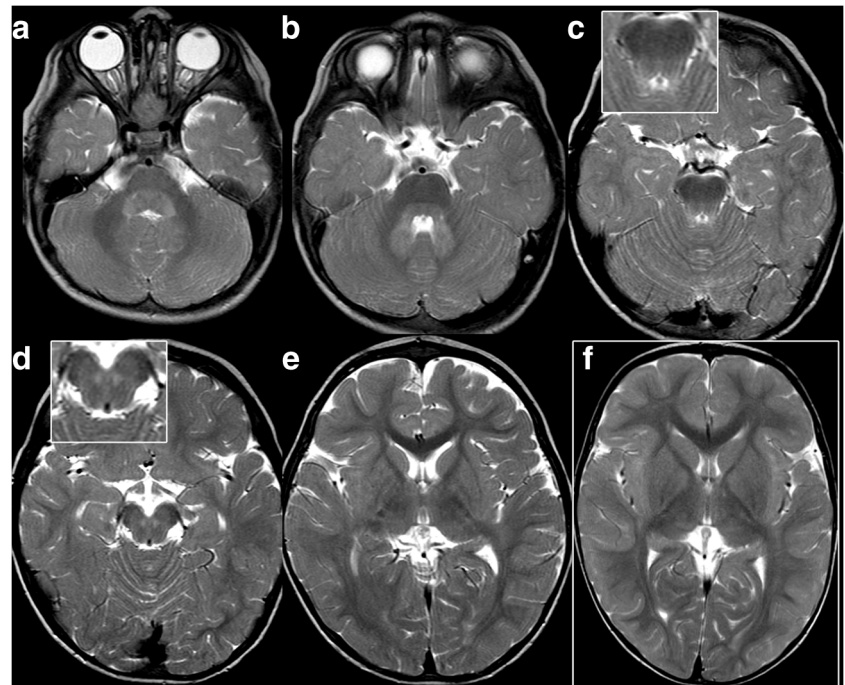
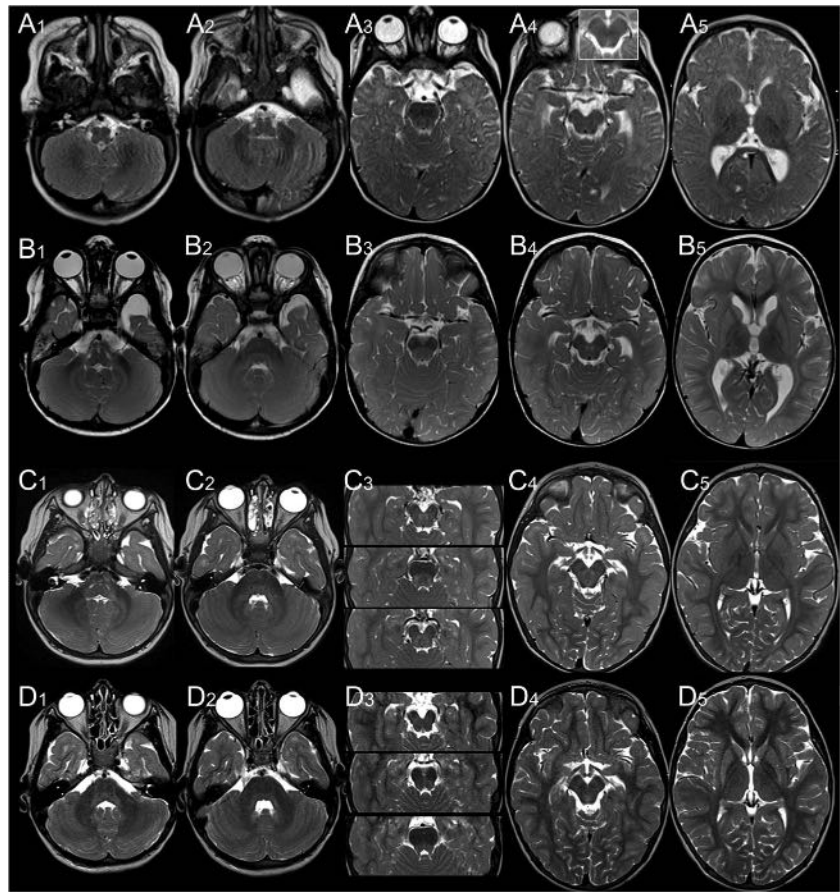


Fig. 4 Evolution of brainstem and striatal changes in patients 1 (A, B) and 5 (C, D). **A**, In patient 1 at 0.5 years, the decussation of SCP mildly hyperintense (A₄; inset: normal finding in age-matched control) and the striatum is normal (A₅). **B** At 2 years ICP (B₁), hila of dentate nuclei and peridentate white matter (B_{1,2}) are newly hyperintense, and SCP is now clearly hyperintense along its mesencephalic course (B₃) and in the decussation (B₄). The striatum is homogeneously T2-hyperintense and atrophic (B₅). **C** Patient 5 also has a normal striatum at 2 years (C₅). ICP (C₁), hila of dentate nuclei, peridentate white matter (C₂) and SCP (C₃), along to the red nucleus (C₄) are T2-hyperintense. At 4.8 years (**D**), infratentorial changes (D_{1–4}) are regressing whereas the striatum is newly T2-hyperintense and atrophic (D₅)



in children with 4H leukodystrophy and especially *POLR3B* variants, was not present.

Although our patients share variants with the spastic ataxia cohort (c.1771-7C>G; homozygous in several patients [12]), none was clinically classified as spastic ataxia. Interestingly,

the original description of the patients homozygous for this variant also mentions extrapyramidal features and early onset of disease. And, while striatal changes are not mentioned, FLAIR-hyperintensity along the superior cerebellar peduncles was noted in almost all patients with the c.1909 + 22G>A

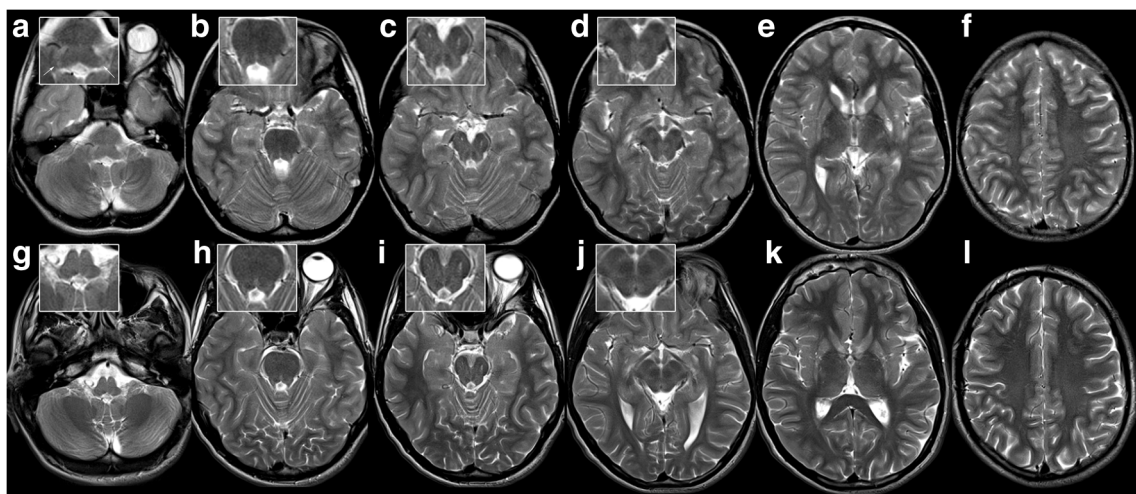


Fig. 5 Striatal injury, regressing infratentorial changes, and normal supratentorial white matter in patient 7 at 13.6 and 18.5 years. T2-hyperintensity of inferior cerebellar peduncle (**a**, arrows in inset) and outlining the mesencephalic course of superior cerebellar peduncles (**b**,

c; NB wide perivascular spaces in anterior mesencephalon) including their decussation (**d**) at 13.6 years (**a–f**). This has resolved by 18.5 years (**g–l**). The striatum is shrunken and T2-hyperintense (**k**), supratentorial white matter normal (including ADC, not depicted).

variant, but, interestingly, not in the two patients homozygous for the c.1771-7C>G variant [12]. They might thus also be classified as the striatal variant of *POLR3A*-associated disease. One variant seen in our cohort, c.1048 +5G > T, has also been found in spastic ataxia [12] and Wiedemann-Rautenstrauch syndrome [16]. However, our patient did not have the intrauterine and marked postnatal growth retardation, lipodystrophy, or distinctive facies characteristic of the progeroid syndrome of Wiedemann-Rautenstrauch [17].

The two brothers (patients 7 and 8) with the previously described, homozygous c.1771-6C>G variant [10], had a presentation similar to that of the three initially described patients [10] with onset in childhood and severe dysarthria, hypokinesia, and rigidity. A prominent, slow resting, and acting tremor, also sometimes called rubral tremor, in addition to severe dysarthria was seen in the older brother and in patient 9, who carried the c.1771-6C>G variant in combination with a missense variant.

The c.1771-6C>G variant was also described in one patient said to have spastic ataxia but also with dystonia [10, 11], without detailed MRI information. In a publication on atypical radiological findings in 4H leukodystrophy, one patient also carried this variant in heterozygous form, and, in retrospect, his last MRI showed small caudate and putamen with elevated T2 signal in addition to the signal abnormalities in the posterior limb of the internal capsule, fitting with his prominent extrapyramidal symptoms [9]. Recently, a young child with the c.1771-6C>G variant in trans with a frameshift variant has been published; the MRI shows the typical basal ganglia involvement described in this work, although this was not recognized as abnormal [18].

Among the other six patients, clinical manifestation varied despite sharing the c.1771-7C>G variant on one allele and the three youngest patients (patients 1–3) were much more severely affected than patients 4–6. The c.1048 +5G > T variant on the second allele in one severely affected patient has been predicted to cause a frameshift with premature stop of translation [16]. It can be classified as a loss-of-function variant, similar to the variant found in patient 2 (c.4025-1G > A). The c.1771-7C>G variant itself has been shown to lead to two aberrant transcripts in addition to the normal cDNA, interpreted as activating a leaky splice site with both wild-type and aberrant transcripts [12]. Similar results were obtained for the c.1771-6C>G variant, with skipping of exon 14 and a premature termination of a part of the transcripts, with the shorter transcript being subject to nonsense-mediated decay [10].

Findings at brain imaging reflect the prominent extrapyramidal movement disorder: T2-hyperintensity and atrophy of the striatum were present in all patients, either at first imaging or on follow-up. In one case, a small striatum preceded T2-hyperintensity. A normal striatum was not seen after onset of extrapyramidal movement

disorder. T2-hyperintensity was discrete and relatively inconspicuous compared with striatal injury, e.g. in glutaric aciduria type 1 or ischemia. Atrophy varied between mild and severe, e.g. in patients 1 and 7 (Figs. 2 and 5), similar to the initially described patients with striatal injury and homozygous c.1771-6C>G variant [10]. Extrapyramidal signs can also develop in classic 4H leukodystrophy [6], with visually normal basal ganglia on brain MRI.

The second characteristic MRI feature was involvement of SCP, which was present in all our patients. This included the dentate nucleus and/or its hilus as the starting point of the efferent neurons of SCP in six patients and the red nucleus as a relay station in two of these. ICP was additionally involved in six patients. Involvement of SCP in patients with *POLR3A* variants has previously been reported for the spasticataxia cohort [12] and in four of eight atypical patients [19]. It is also depicted in a report of a patient with hypomyelination and a previously unreported homozygous variant of c.2423G>A in exon 18 (Fig. 2a in [20]). Involvement of the red nucleus as a relay station of SCP was reported for the three patients homozygous for the c.1771-6C>G variant [10]. The symmetric, anterior mesencephalic T2-hyperintensity also reported might rather correspond to the superior mesencephalic course of SCP than the proposed intraparenchymal course of the oculomotor nerve [10].

Changes in SCP, dentate and red nuclei, and ICP were not clearly associated with striatal injury since they preceded striatal injury in two patients and were subsequent in one. Moreover, their decrease and disappearance in two patients suggest that they are a potentially transient phenomenon. While SCP involvement in the spasticataxia cohort was thought to represent the structural correlate of the cerebellar manifestation [12], contribution of SCP and ICP to the clinical picture in our patients is difficult to pinpoint. This is due to the predominantly extrapyramidal movement disorder, the infrequent ataxia, and the unchanged presentation in those patients with decreasing or resolving changes, although the prominent tremor in patients 8 and 9 is certainly compatible with the involvement of the striatum and the dentate outflow tract [21].

Compared with classic 4H leukodystrophy, infratentorial involvement was practically inverted in patients with the striatal variant of *POLR3A*-related disease: While MCP was normal in the striatal variant, T2-hyperintensity of MCP has been noted in reported cases of 4H leukodystrophy [22–24] and was present in 29 of the 36 the previously reported patients with classic 4H leukodystrophy [7] re-reviewed for comparison. SCP was involved in only two patients with classic

4H leukodystrophy, but in all patients with the striatal variant, ICP in none of the patients with classic 4H leukodystrophy and in six of nine patients with the striatal variant *POLR3A*-related disease. Moreover, T2-hyperintensity of cerebellar white matter with relatively T2-hypointense dentate nucleus and early cerebellar atrophy are common in 4H leukodystrophy [25], while cerebellar signal changes in patients with the striatal variant were restricted to dentate area, and cerebellar atrophy was absent. In addition, none of the 36 patients with classical 4H leukodystrophy re-reviewed for comparison had striatal T2-hyperintensity.

In 4H leukodystrophy, diffuse hypomyelination is a core finding, commonly with some myelination of the visual tract, the pyramidal tract in the posterior limb of the internal capsule, and the anterolateral thalamus [5, 25]. In contrast, myelination delay and white matter changes in our patients preferentially involved the optic radiation and pyramidal tracts, and none had frank hypomyelination. Thinning of corpus callosum, another common feature of 4H leukodystrophy, though somewhat less common in patients with carrying *POLR3A* variants [5], was only present in one of the nine patients with the striatal variant.

I

Recognition of the characteristic MRI pattern, including awareness of the potentially relatively mild T2-hyperintensity and atrophy of the striatum, should trigger genetic testing for *POLR3A* in patients with unexplained extrapyramidal movement disorders.

Acknowledgements We thank the patients and their parents for their support and participation in this study.

Author contributions I. Harting and N.I. Wolf designed the study and wrote the initial draft of the manuscript. Diffusion-MRI was interpreted by P.J.W. Pouwels and I. Harting. MRI was otherwise analyzed by I. Harting and N.I. Wolf. I. Harting and N.I. Wolf analyzed and interpreted the data; all authors examined patients and/or collected and interpreted data. All authors revised the manuscript and approved the submission.

Funding information AP was supported by the Centre for Biomedical Research on Rare Diseases (CIBERER), the URDCat program (PERIS SLT002/16/00174), the Hesperia Foundation, ‘La Marató de TV3’ Foundation 345/C/2014, and the Secretariat for Universities and Research of the Ministry of Business and Knowledge of the Government of Catalonia [2017SG R1206].

Compliance with ethical standards

Disclaimer AP is a member of the Undiagnosed Diseases Program International (UDNI). The following authors are members of the European Reference Network for Rare Neurological Disorders (ERN-RND), project ID 739510: I K-M, MSvdK and NIW.

Conflict of interest All authors declare no conflicts of interest in the publication of this manuscript.

Informed consent All procedures followed were in accordance with the ethical standards of the responsible committee on human experimentation (institutional and national) and with the Helsinki Declaration of 1975, as revised in 2000. The study was approved by institutional review board of VU University Medical Center (PhenoLD, 2018.300), and appropriate written informed consent obtained.

Open Access This article is licensed under a Creative Commons Attribution 4.0 International License, which permits use, sharing, adaptation, distribution and reproduction in any medium or format, as long as you give appropriate credit to the original author(s) and the source, provide a link to the Creative Commons licence, and indicate if changes were made. The images or other third party material in this article are included in the article's Creative Commons licence, unless indicated otherwise in a credit line to the material. If material is not included in the article's Creative Commons licence and your intended use is not permitted by statutory regulation or exceeds the permitted use, you will need to obtain permission directly from the copyright holder. To view a copy of this licence, visit <http://creativecommons.org/licenses/by/4.0/>.

References

1. Saitsu H, Osaka H, Sasaki M, Takanashi J, Hamada K, Yamashita A, Shibayama H, Shiina M, Kondo Y, Nishiyama K, Tsurusaki Y, Miyake N, Doi H, Ogata K, Inoue K, Matsumoto N (2011) Mutations in *POLR3A* and *POLR3B* encoding RNA polymerase III subunits cause an autosomal-recessive hypomyelinating leukoencephalopathy. Am J Hum Genet 89(5):644–651. <https://doi.org/10.1016/j.ajhg.2011.10.003>
2. Bernard G, Chouery E, Putorti ML, Tetreault M, Takanohashi A, Carosso G, Clement I, Boespflug-Tanguy O, Rodriguez D, Delague V, Abou Ghoch J, Jalkh N, Dorboz I, Fribourg S, Teichmann M, Megarbane A, Schiffmann R, Vanderver A, Brais B (2011) Mutations of *POLR3A* encoding a catalytic subunit of RNA polymerase Pol III cause a recessive hypomyelinating leukodystrophy. Am J Hum Genet 89(3):415–423. <https://doi.org/10.1016/j.ajhg.2011.07.014>
3. Tetreault M, Choquet K, Orcesi S, Tondutti D, Balottin U, Teichmann M, Fribourg S, Schiffmann R, Brais B, Vanderver A, Bernard G (2011) Recessive mutations in *POLR3B*, encoding the second largest subunit of Pol III, cause a rare hypomyelinating leukodystrophy. Am J Hum Genet 89(5):652–655. <https://doi.org/10.1016/j.ajhg.2011.10.006>
4. Thiffault I, Wolf NI, Forget D, Guerrero K, Tran LT, Choquet K, Lavallee-Adam M, Poitras C, Brais B, Yoon G, Sztriha L, Webster RI, Timmann D, van de Warrenburg BP, Seeger J, Zimmermann A, Mate A, Goizet C, Fung E, van der Knaap MS, Fribourg S, Vanderver A, Simons C, Taft RJ, Yates JR 3rd, Coulombe B, Bernard G (2015) Recessive mutations in *POLR1C* cause a leukodystrophy by impairing biogenesis of RNA polymerase III. Nat Commun 6:7623. <https://doi.org/10.1038/ncomms8623>
5. Wolf NI, Vanderver A, van Spaendonk RM, Schiffmann R, Brais B, Bugiani M, Sistermans E, Catsman-Berrevoets C, Kros JM, Pinto PS, Pohl D, Tirupathi S, Stromme P, de Grauw T, Fribourg S, Demos M, Pizzino A, Naidu S, Guerrero K, van der Knaap MS, Bernard G (2014) Clinical spectrum of 4H leukodystrophy caused by *POLR3A* and *POLR3B* mutations. Neurology 83(21):1898–1905. <https://doi.org/10.1212/WNL.0000000000001002>
6. Al Yazidi G, Tran LT, Guerrero K, Vanderver A, Schiffmann R, Wolf NI, Chouinard S, Bernard G (2019) Dystonia in RNA polymerase III-related leukodystrophy. Mov Disord Clin Pract 6(2):155–159. <https://doi.org/10.1002/mdc3.12715>

7. Vrij-van den Bos S, Hol J, La Piana R, Harting I, Vanderver A, Barkhof F, Cayami F, van Wieringen W, Pouwels P, van der Knaap M, Bernard G, Wolf N (2017) 4H leukodystrophy: a brain MRI scoring system. *Neuropediatrics* 48(3):152–160. <https://doi.org/10.1055/s-0037-1599141>
8. Gauquelin L, Cayami FK, Sztriha L, Yoon G, Tran LT, Guerrero K, Hocke F, van Spaendonk RML, Fung EL, D'Arrigo S, Vasco G, Thiffault I, Niyazov DM, Person R, Lewis KS, Wassmer E, Prescott T, Fallon P, McEntagart M, Rankin J, Webster R, Philippi H, van de Warrenburg B, Timmann D, Dixit A, Searle C, Thakur N, Kruger MC, Sharma S, Vanderver A, Tonduti D, van der Knaap MS, Bertini E, Goizet C, Fribourg S, Wolf NI, Bernard G (2019) Clinical spectrum of POLR3-related leukodystrophy caused by biallelic POLR1C pathogenic variants. *Neurol Genet* 5(6):e369. <https://doi.org/10.1212/nxg.0000000000000369>
9. La Piana R, Cayami FK, Tran LT, Guerrero K, van Spaendonk R, Ounap K, Pajusalu S, Haack T, Wassmer E, Timmann D, Mierzecka H, Poll-The BT, Patel C, Cox H, Atik T, Onay H, Ozkinalay F, Vanderver A, van der Knaap MS, Wolf NI, Bernard G (2016) Diffuse hypomyelination is not obligate for POLR3-related disorders. *Neurology* 86(17):1622–1626. <https://doi.org/10.1212/WNL.0000000000002612>
10. Azmanov DN, Siira SJ, Chamova T, Kaprelyan A, Guergueltcheva V, Shearwood AJ, Liu G, Morar B, Rackham O, Bynevelt M, Grudkova M, Kamenov Z, Svechtarov V, Tournev I, Kalaydjieva L, Filipovska A (2016) Transcriptome-wide effects of a POLR3A gene mutation in patients with an unusual phenotype of striatal involvement. *Hum Mol Genet* 25(19):4302–4314. <https://doi.org/10.1093/hmg/ddw263>
11. Rydning SL, Koht J, Sheng Y, Sowa P, Hjorthaug HS, Wedding IM, Erichsen AK, Hovden IA, Backe PH, Tallaksen CME, Vigeland MD, Selmer KK (2019) Biallelic POLR3A variants confirmed as a frequent cause of hereditary ataxia and spastic paraparesis. *Brain* 142(4):e12. <https://doi.org/10.1093/brain/awz041>
12. Minnerop M, Kurzwelly D, Wagner H, Soehn AS, Reichbauer J, Tao F, Rattay TW, Peitz M, Rehbach K, Giorgetti A, Pyle A, Thiele H, Altmuller J, Timmann D, Karaca I, Lennarz M, Baets J, Hengel H, Synofzik M, Atasu B, Feely S, Kennerson M, Stendel C, Lindig T, Gonzalez MA, Stirnberg R, Sturm M, Roeske S, Jung J, Bauer P, Lohmann E, Herms S, Heilmann-Heimbach S, Nicholson G, Mahanjah M, Sharkia R, Carloni P, Brustle O, Klopstock T, Mathews KD, Shy ME, de Jonghe P, Chinnery PF, Horvath R, Kohlhase J, Schmitt I, Wolf M, Greschus S, Amunts K, Maier W, Schols L, Nurnberg P, Zuchner S, Klockgether T, Ramirez A, Schule R (2017) Hypomorphic mutations in POLR3A are a frequent cause of sporadic and recessive spastic ataxia. *Brain* 140(6):1561–1578. <https://doi.org/10.1093/brain/awx095>
13. Helenius J, Soinne L, Perkiö J, Salonen O, Kangasmaki A, Kaste M, Carano RA, Aronen HJ, Tatlisumak T (2002) Diffusion-weighted MR imaging in normal human brains in various age groups. *AJNR Am J Neuroradiol* 23(2):194–199
14. van der Voorn JP, Pouwels PJ, Hart AA, Serrarens J, Willemse MA, Kremer HP, Barkhof F, van der Knaap MS (2006) Childhood white matter disorders: quantitative MR imaging and spectroscopy. *Radiology* 241(2):510–517. <https://doi.org/10.1148/radiol.2412051345>
15. Li MD, Forkert ND, Kundu P, Ambler C, Loher RM, Burns TC, Barnes PD, Gibbs IC, Grant GA, Fisher PG, Cheshier SH, Campen CJ, Monje M, Yeom KW (2017) Brain perfusion and diffusion abnormalities in children treated for posterior fossa brain tumors. *J Pediatr* 185(173–180):e173. <https://doi.org/10.1016/j.jpeds.2017.01.019>
16. Paolacci S, Li Y, Agolini E, Bellacchio E, Arboleda-Bustos CE, Carrero D, Bertola D, Al-Gazali L, Alders M, Altmuller J, Arboleda G, Beleggia F, Bruselles A, Ciolfi A, Gillessen-Kaesbach G, Krieg T, Mohammed S, Muller C, Novelli A, Ortega J, Sandoval A, Velasco G, Yigit G, Arboleda H, Lopez-Otin C, Wollnik B, Tartaglia M, Hennekam RC (2018) Specific combinations of biallelic POLR3A variants cause Wiedemann-Rautenstrauch syndrome. *J Med Genet* 55(12):837–846. <https://doi.org/10.1136/jmedgenet-2018-105528>
17. Paolacci S, Bertola D, Franco J, Mohammed S, Tartaglia M, Wollnik B, Hennekam RC (2017) Wiedemann-Rautenstrauch syndrome: a phenotype analysis. *Am J Med Genet A* 173(7):1763–1772. <https://doi.org/10.1002/ajmg.a.38246>
18. Wu S, Bai Z, Dong X, Yang D, Chen H, Hua J, Zhou L, Lv H (2019) Novel mutations of the POLR3A gene caused POLR3-related leukodystrophy in a Chinese family: a case report. *BMC Pediatr* 19(1):289–286. <https://doi.org/10.1186/s12887-019-1656-7>
19. Gauquelin L, Tetraault M, Thiffault I, Farrow E, Miller N, Yoo B, Barek E, Yoon G, Suchowersky O, Dupre N, Tarnopolsky M, Brais B, Wolf NI, Majewski J, Rouleau GA, Gan-Or Z, Bernard G (2018) POLR3A variants in hereditary spastic paraparesis and ataxia. *Brain* 141(1):e1. <https://doi.org/10.1093/brain/awx290>
20. Tewari VV, Mehta R, Sreedhar CM, Tewari K, Mohammad A, Gupta N, Gulati S, Kabra M (2018) A novel homozygous mutation in POLR3A gene causing 4H syndrome: a case report. *BMC Pediatr* 18(1):126. <https://doi.org/10.1186/s12887-018-1108-9>
21. Choi SM (2016) Movement disorders following cerebrovascular lesions in cerebellar circuits. *J Mov Disord* 9(2):80–88. <https://doi.org/10.14802/jmd.16004>
22. Jurkiewicz E, Dunin-Wasowicz D, Gieruszczak-Bialek D, Malczyk K, Guerrero K, Gutierrez M, Tran L, Bernard G (2017) Recessive mutations in POLR3B encoding RNA polymerase III subunit causing diffuse hypomyelination in patients with 4H leukodystrophy with polymicrogyria and cataracts. *Clin Neuroradiol* 27(2):213–220. <https://doi.org/10.1007/s00062-015-0472-1>
23. Muthusamy K, Sudhakar SV, Yoganathan S, Thomas MM, Alexander M (2015) Hypomyelination, hypodontia, hypogonadotropic hypogonadism (4H) syndrome with vertebral anomalies: a novel association. *J Child Neurol* 30(7):937–941. <https://doi.org/10.1177/0883073814541470>
24. Terao Y, Saitsu H, Segawa M, Kondo Y, Sakamoto K, Matsumoto N, Tsuji S, Nomura Y (2012) Diffuse central hypomyelination presenting as 4H syndrome caused by compound heterozygous mutations in POLR3A encoding the catalytic subunit of polymerase III. *J Neurol Sci* 320(1–2):102–105. <https://doi.org/10.1016/j.jns.2012.07.005>
25. Steenweg ME, Vanderver A, Blaser S, Bizzzi A, de Koning TJ, Mancini GM, van Wieringen WN, Barkhof F, Wolf NI, van der Knaap MS (2010) Magnetic resonance imaging pattern recognition in hypomyelinating disorders. *Brain* 133(10):2971–2982. <https://doi.org/10.1093/brain/awq257>

Publisher's note Springer Nature remains neutral with regard to jurisdictional claims in published maps and institutional affiliations.

Affiliations

Inga Harting¹  · Murtadha Al-Saady²  · Ingeborg Krägeloh-Mann³  · Annette Bley⁴  · Maja Hempel⁵  ·
Tatjana Bierhals⁵  · Stephanie Karch⁶  · Ute Moog⁷  · Geneviève Bernard⁸  · Richard Huntsman⁹  ·
Rosalina M. L. van Spaendonk¹⁰  · Maaike Vreeburg¹¹  · Agustí Rodríguez-Palmero^{12,13}  · Aurora Pujol^{12,14,15}  ·
Marjo S. van der Knaap^{2,16}  · Petra J. W. Pouwels¹⁷  · Nicole I. Wolf² 

- ¹ Department of Neuroradiology, University Hospital Heidelberg, Im Neuenheimer Feld 400, 69120 Heidelberg, Germany
- ² Department of Child Neurology, Center for Childhood White Matter Diseases, Emma Children's Hospital, Vrije Universiteit, and Amsterdam Neuroscience, Amsterdam University Medical Centers, Amsterdam, The Netherlands
- ³ Department of Paediatric Neurology and Developmental Medicine, University Children's Hospital Tübingen, Tübingen, Germany
- ⁴ University Children's Hospital, University Medical Center Hamburg Eppendorf, Hamburg, Germany
- ⁵ Institute of Human Genetics, University Medical Center Hamburg-Eppendorf, 20246 Hamburg, Germany
- ⁶ Division of Neuropaediatrics and Metabolic Medicine, Centre for Child and Adolescent Medicine, Clinic I, University Hospital Heidelberg, Im Neuenheimer Feld 430, 69120 Heidelberg, Germany
- ⁷ Institute of Human Genetics, Heidelberg University, Im Neuenheimer Feld 366, 69120 Heidelberg, Germany
- ⁸ Departments of Neurology and Neurosurgery, Paediatrics and Human Genetics, Department of Specialized Medicine, Division of Medical Genetics, McGill University Health Center, and Child Health and Human Development Program, Research Institute of the McGill University Health Centre, McGill University, McGill University, Montreal, Quebec, Canada
- ⁹ Division of Paediatric Neurology, University of Saskatchewan, Saskatoon, Saskatchewan, Canada
- ¹⁰ Department of Clinical Genetics, Vrije Universiteit, Amsterdam University Medical Centers, Amsterdam, The Netherlands
- ¹¹ Department of Clinical Genetics, Maastricht University Medical Center, Maastricht, The Netherlands
- ¹² Neurometabolic Diseases Laboratory, Bellvitge Biomedical Research Institute (IDIBELL), Hospitalet de Llobregat, Barcelona, Catalonia, Spain
- ¹³ Department of Pediatrics, Paediatric Neurology Unit, University Hospital Germans Trias i Pujol, Badalona, Barcelona, Catalonia, Spain
- ¹⁴ Centre for Biomedical Research on Rare Diseases (CIBERER), Institute Carlos III, Madrid, Spain
- ¹⁵ Catalan Institution for Research and Advanced Studies (ICREA), Barcelona, Spain
- ¹⁶ Department of Functional Genomics, Center for Neurogenomics and Cognitive Research, Vrije Universiteit Amsterdam, Amsterdam, The Netherlands
- ¹⁷ Department of Radiology and Nuclear Medicine, Vrije Universiteit, Amsterdam University Medical Centers, Amsterdam, The Netherlands



HNRNPH1-related syndromic intellectual disability: Seven additional cases suggestive of a distinct syndromic neurodevelopmental syndrome

Sara C. Reichert¹ | Rachel Li¹ | Scott A. Turner² | Richard H. van Jaarsveld³ | Maarten P.G. Massink³ | Marie-José H. van den Boogaard³ | Mireia del Toro⁴ | Agustí Rodríguez-Palmero⁵ | Stéphane Fourcade^{5,6} | Agatha Schlüter^{5,6} | Laura Planas-Serra^{5,6} | Aurora Pujol^{5,6,7} | Maria Iascone⁸ | Silvia Maitz⁹ | Lucy Loong¹⁰ | Helen Stewart¹⁰ | Elisa De Franco¹¹ | Sian Ellard¹² | Julie Frank¹³ | Raymond Lewandowski¹

¹Department of Human and Molecular Genetics, Clinical Genetics Services, VCU Health, Richmond, Virginia, USA

²Department of Pathology, VCU Health, Richmond, Virginia, USA

³Department of Genetics, University Medical Center Utrecht, Utrecht, The Netherlands

⁴Pediatric Neurology Department, Vall d'Hebron University Hospital, Universitat Autònoma de Barcelona, CIBERER, Barcelona, Spain

⁵Neurometabolic Diseases Laboratory, Bellvitge Biomedical Research Institute (IDIBELL), Hospital de Llobregat, Barcelona, Catalonia, Spain

⁶Centre for Biomedical Research on Rare Diseases (CIBERER), Institute Carlos III, Madrid, Spain

⁷Catalan Institution for Research and Advanced Studies (ICREA), Barcelona, Spain

⁸Laboratorio Genetica Medica, ASST Papa Giovanni XXIII, Bergamo, Italy

⁹Clinical Pediatric Genetic Unit, Pediatric Clinic, Fondazione MBBM, San Gerardo Hospital, Monza, Italy

¹⁰Oxford Centre for Genomic Medicine, Oxford University Hospitals NHS Foundation Trust, Oxford, UK

¹¹College of Medicine and Health, University of Exeter Medical School, Exeter, UK

¹²Genomics Laboratory, Royal Devon and Exeter NHS Foundation Trust, Exeter, UK

¹³Department of Pediatrics, University of Maryland School of Medicine, Baltimore, Maryland, USA

Correspondence

Sara C. Reichert, Department of Human and Molecular Genetics, Clinical Genetics Services, VCU Health, Richmond, VA 23298.
Email: sara.reichert@vcuhealth.org

Funding information

Centre for Biomedical Research on Rare Diseases, Grant/Award Number: ACCI14-759; GENE - Genomic analysis Evaluation NEtwork, Grant/Award Number: 2713 del 28/02/2018; Hesperia Foundation and the Secretariat for Universities and Research of the Ministry of Business and Knowledge of the Government of Catalonia, Grant/Award Number: 2017SGR1206; URDCat program, Grant/Award Number: PERIS SLT002/16/00174; Progetti di innovazione in ambito sanitario e socio sanitario Regione Lombardia

Abstract

Pathogenic variants in *HNRNPH1* were first reported in 2018. The reported individual, a 13 year old boy with a c.616C>T (p.R206W) variant in the *HNRNPH1* gene, was noted to have overlapping symptoms with those observed in *HNRNPH2*-related X-linked intellectual disability, Bain type (MRXSB), specifically intellectual disability and dysmorphic features. While *HNRNPH1* variants were initially proposed to represent an autosomal cause of MRXSB, we report an additional seven cases which identify phenotypic differences from MRXSB. Patients with *HNRNPH1* pathogenic variants diagnosed via WES were identified using clinical networks and GeneMatcher. Features unique to individuals with *HNRNPH1* variants include distinctive dysmorphic facial features; an increased incidence of congenital anomalies including cranial and brain abnormalities, genitourinary malformations, and palate abnormalities; increased incidence of ophthalmologic abnormalities; and a decreased incidence of epilepsy and

Peer Review

The peer review history for this article is available at <https://publons.com/publon/10.1111/cge.13765>.

cardiac defects compared to those with MRXSB. This suggests that pathogenic variants in *HNRNPH1* result in a related, but distinct syndromic cause of intellectual disability from MRXSB, which we refer to as *HNRNPH1*-related syndromic intellectual disability.

KEY WORDS

congenital abnormalities, *HNRNPH1* gene, intellectual disability, microcephaly, whole exome sequencing

1 | INTRODUCTION

The *HNRNPH1* [MIM 601035] and *HNRNPH2* [MIM 300986] genes produce the hnRNP H and hnRNP H' (also called hnRNP H2) proteins, respectively. These proteins belong to the heterogeneous nuclear ribonucleoprotein (hnRNP) family of RNA binding proteins which bind to pre-mRNA transcripts and assist in stabilizing, transporting, and targeting transcripts between the nucleus and cytoplasm for processing and alternative splicing prior to becoming mature mRNAs.¹ More than 20 hnRNPs have been identified, and hnRNP H and hnRNP H' share 96% homology. Both genes are ubiquitously expressed across multiple tissue types including the brain, eye, smooth muscle, small intestine, and stomach.² The functions of hnRNP H and H' on pre-mRNA processing include capping, splicing, polyadenylation, export, and translation and are mainly exerted within the nucleus.³

Given their central role in cellular function, it is not surprising that pathogenic variants affecting genes that code for hnRNPs are an emerging cause of disease. Altered expression of hnRNPs has been linked to tumorigenesis and germline variants in genes encoding hnRNPs have been implicated as a potential causes of adult-onset neurodegenerative conditions including frontotemporal dementia/amyotrophic lateral sclerosis, inclusion body myopathy with frontotemporal dementia (IBMPFM [MIM: 615424]), and Alzheimer disease.^{1,4} Whole exome sequencing (WES) has identified multiple HNRNP genes as novel causes of early-onset syndromic intellectual disability.⁵⁻⁷

In 2016, pathogenic variants in *HNRNPH2* were reported as a novel cause for an X-linked intellectual disability syndrome in females.⁶ This new syndrome, *HNRNPH2*-related X-linked intellectual disability, Bain type, (MRXSB [MIM: 300986]), was characterized by intellectual disability, dysmorphic features, feeding difficulties, seizures, and hypotonia. While originally thought that pathogenic variants would be lethal in males, three groups have reported four males with pathogenic variants in *HNRNPH2* and symptoms consistent with MRXSB.⁸⁻¹⁰ Among the 11 cases of MRXSB reported to date, seven have a common c.616C>T (p.R206W) variant, while another two have c.617G>A (p.R206Q) variants. The remaining two male cases carry c.626C>T (p.P209L) and c.340C>T (p.R114W) variants.

The first pathogenic variant in *HNRNPH1* was reported by Pilch et al in 2018.¹¹ In the reported individual, a 13-year-old boy, a de novo c.616C>T (p.R206W) variant in *HNRNPH1* was identified by WES. His phenotype included dysmorphic facial features,

microcephaly, hypermobile joints, hypotonia, non-verbal intellectual disability, and feeding difficulties.¹¹ Given the similar phenotypes, the conserved amino acid sequences at position 206 of hnRNP H and H', and the overall homology between these proteins, it was postulated that variants in *HNRNPH1* may represent an autosomal cause of MRXSB. However, some features reported by Pilch et al were not observed in the MRXSB cohort, including arched eyebrows, blepharophimosis, congenital microcephaly, and hip dislocations.

Here, we present an additional seven cases of de novo pathogenic variants in *HNRNPH1* to further characterize and expand the phenotype initially described by Pilch et al.

2 | MATERIALS AND METHODS

Seven individuals with *HNRNPH1* pathogenic variants were identified using GeneMatcher and clinical networks.¹² One individual resides in the United States, the remaining in the European Union. DNA extracted from peripheral blood was analyzed by WES on all individuals using standard technologies. Details on case specific WES can be found in Supporting Materials. This series was reviewed by the VCU Health IRB and not found to meet the definitions of human subjects research, and thus did not require IRB review or approval. Written informed consent was obtained for individuals whose photographs are included within this report. We characterized their phenotype retrospectively and contrasted them with features reported previously by Pilch et al as well as with individuals with MRXSB.

3 | RESULTS

The seven individuals range in age from a fetus at 30w4d to a 23-year-old. The five surviving cases have intellectual disability, ranging from moderate to severe. Congenital anomalies were observed in this cohort, with 7/7 having abnormalities identified on brain MRI, 4/7 having palate abnormalities, and 3/7 having genitourinary malformations. Other notable features observed include ophthalmological abnormalities (6/7), short stature (5/7), microcephaly (5/7), and hypotonia (4/7). Developmental regression is not observed in this cohort. 4/6 surviving individuals are non-verbal or have very limited speech. A complete phenotypic review can be found in Table 1. Dysmorphic features were also observed within our cohort, including medial

TABLE 1 Clinical characteristics of individuals with *HNRNPH1* variants (NM_005520.2) in comparison with individuals with *HNRNPH2*-related X-linked intellectual disability, Bain type (MRSXB)

	MRSXB (n = 11)	Pilch et al ¹¹	Case 1	Case 2	Case 3	Case 4	Case 5	Case 6	Case 7	<i>HNRNPH1</i> (n = 8)
Variant	c.616C>T (p.R206W) n = 7, c.617G>A (p.R206Q) n = 2, c.626C>T (p.P209L) n = 1, c.340C>T (p.R14W) n = 1	c.616C>T (p.R206W)	c.616C>T (p.R206W)	c.618dupG (p.Pro207fs)	178 977 572- duplication	c.617G>A (p.R206Q)	c.1116_1175del (p.Glu373- Tyr392del)	c.1240_1243dup (p.Q415s)	c.616C>T (p.R206W)	
Sex	7F, 4M	M	M	M	M	M	F	F	M	2F, 6M
Age		13y	14y	11y	14y	30w3d (d)	5 years	23 years	10.5 m (d)	30w3d-14y
Intellectual disability	+ (11/11)	+	+	+	+	+	+	+	+ global developmental delay	7/8
Verbal skills	Variable: nonverbal to short sentences	Non-verbal	Non-verbal	Non-verbal	Minimal	Minimal				3/8 nonverbal; 2/8 minimal verbal skills
Abnormalities of the cerebellar vermis	+ (2/11)	+	—	+	+	+	+	—	+	5/8
Other Brain Abnormalities	+ (1/11) Lipoma in the corpus callosum region; (1/11) white matter abnormalities	Anomaly of clivus and atlantooccipital joint	Tethered Cord, Anomaly of clivus and atlantooccipital joint	T2 periventricular white matter hyperintensities with cysts	Foramen magnum stenosis		White Matter Abnormalities	Dysmorphic midbrain, delayed myelination		6/8
Joint laxity	+ (3/11)	+	+	+	—	—	—	+		4/8
Short stature	+ (4/11)	+	+	+	+	+ (IUGR)	—	+		6/8
Skeletal Issues	+ (4/11) Scoliosis; (1/11) Pectus carinatum; (2/11) Pes Planus	Pectus carinatum, Scoliosis/Lordosis contractures	Scoliosis/Iordosis	Bilateral clubfoot, camptodactyly	Clenched fists, elbows and wrists flexed, toe walking	Prognathism	Bilateral Hip Dysplasia			6/8
Gastrointestinal abnormalities	+ (8/11) FTT, GERD, constipation, feeding difficulties	GERD	FTT, G-tube dependent, Hiatal hernia, constipation	Feeding difficulties, G-tube, GERD, constipation	—	—	—	Feeding difficulties, G-tube		4/8

(Continues)

TABLE 1 (Continued)

	MRXSB (n = 11)	Pilch et al ¹¹	Case 1	Case 2	Case 3	Case 4	Case 5	Case 6	Case 7	HNRNPH1 (n = 8)
Tone Abnormalities	+ (11/11) Hypotonia: (1/11)	+ Hypotonia	+ Hypotonia	+ Hypotonia	+ Hypertonia	+ Hypertonia	+ Hypotonia	+ Hypotonia	+ Hypotonia	6/8
Genitourinary anomalies	–	Hypospadias	Horseshoe kidney, hypospadias	–	Posterior urethral valves, Cryptorchidism	–	–	–	Cryptorchidism	4/8
Ophthalmologic findings	+ (1/11) exotropia, cortical visual impairment	Strabismus	Strabismus, Myopic astigmatism	Motility issue, retinal dystrophy/ RP?	Strabismus, nystagmus, Optic disk pallor	Left Squint	Hypermetropia, strabismus	Retinopathy of prematurity	7/8	
Movement disorder	+ (1/11) gait disturbance; (1/11) ataxia; (1/11) athetoid movements; (1/11) involuntary movements; (1/11) dystonic posturing	Non-ambulatory	Non-ambulatory	Non-ambulatory	Ataxia, tremor, wide-based gait, Dystonia	Dystonia	Dystonia	Dystonia	3/8 dystonia 1/8 ataxia	
Epilepsy	+ (5/11)	–	–	–	+	+	–	–	–	2/8

Abbreviations: d, deceased; FTI, failure to thrive; GERD, gastroesophageal reflux disease; (–), not present; (+), present; (+/–), mild.

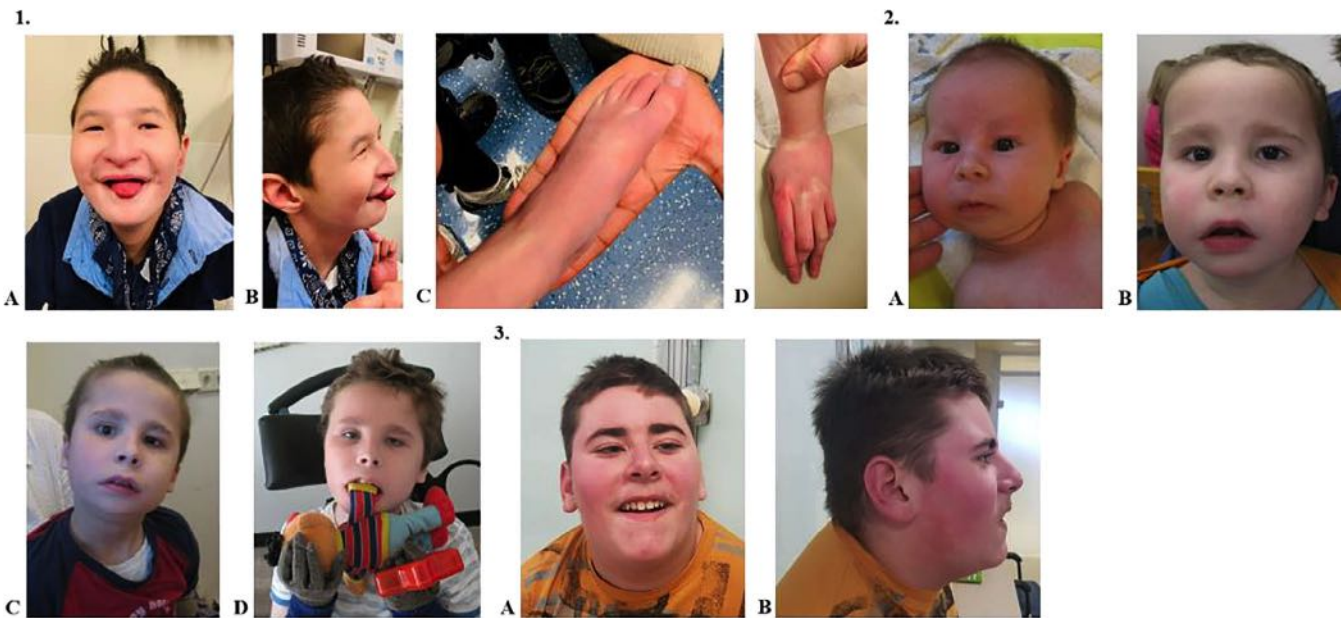


FIGURE 1 Dysmorphic features in affected individuals. Photographs of Case 1 at 14 years of age (1A-1D) with dysmorphic features including long face, hypotelorism, blepharophimosis, ptosis, downslanting palpebral fissures, medial arched eyebrows, long prominent nose with hypoplastic alae nasi and low hanging columella, small mouth, open bite, micrognathia, posteriorly rotated hypoplastic ears, arachnodactyly, clinodactyly, camptodactyly, and clubbed fingers. Photographs of Case 2 at 1 week, 3 years, 8 years, and 11 years of age respectively (2A-D) with dysmorphic features including blepharophimosis, ptosis, medial arched eyebrows, mild downslanting palpebral fissures, hypoplastic alae nasi, micrognathia, posteriorly rotated hypoplastic ears, and open bite. Case 2 was also noted to have clinodactyly (not shown). Photographs at Case 3 at 14 years of age (3A-B) with dysmorphic features including blepharophimosis, medial arched eyebrows, hypoplastic alae nasi, micrognathia, and posteriorly rotated ears [Colour figure can be viewed at wileyonlinelibrary.com]

arched eyebrows (4/7), blepharophimosis (3/7), ptosis (3/7), and hypotelorism (3/7). (Figure 1, Table S1). These features are similar to what was reported by Pilch et al.¹¹ Additional clinical history can be found in Supporting Materials.

Overlapping features with MRXSB include intellectual disability, microcephaly, and gastrointestinal abnormalities. However, our cohort has other anomalies not consistently reported among individuals with MRXSB. These include cerebellar anomalies, palate abnormalities, genitourinary abnormalities, micrognathia, and short stature. 3/7 individuals in this cohort were noted to have dystonia, vs 1/11 individuals with MRXSB. Individuals in this cohort were also more frequently observed to have ophthalmological abnormalities, most often strabismus. Epilepsy, reported in 5/11 individuals with MRXSB, was only observed in 2/7 individuals within our cohort. The constellation of dysmorphic facial features observed in this cohort also suggests a distinct phenotype when compared with MRXSB. Congenital microcephaly, blepharophimosis, ptosis, hypotelorism, posteriorly rotated hypoplastic ears, medial arched eyebrows, open bite, and syndactyly/clinodactyly are features observed in individuals with *HNRNPH1* pathogenic variants but not widely reported in MRXSB.

Six variants were identified in this cohort including two missense variants, two frameshift variants, an in-frame deletion, and an entire gene duplication (Figure 2). One variant, c.616C>T (p.R206W) identified in Cases 1 and 7, was previously described by Pilch et al.¹¹ Another, c.617G>A (p.R206Q) was identified in Case 4 and is analogous to the *HNRNPH2* variant described by Bain et al.⁶ The remaining

four variants have not been described in either *HNRNPH1* or *HNRNPH2* to date. These include two small duplications, c.618dupG (p.Pro207fs) and c.1240_1243dup (p.Q415fs) and one in-frame deletion, c.1116_1175del (p.Glu373-Tyr392del). The final variant is a large duplication encompassing both the *HNRNPH1* and *RUFY1* [MIM 610327] genes.

4 | DISCUSSION

The seven individuals reported in this series suggest a unique, but variable, phenotype due to pathogenic *HNRNPH1* variants. We hypothesize that much of the clinical variability observed among our cohort may be due to genotype/phenotype correlations. The hnRNP H and H' proteins have three highly homologous RNA recognition motifs that allow them to specifically bind to G-rich RNA.¹ In addition, they also have two glycine-rich domains, designated GYR and GY. A non-classical nuclear localization sequence (NLS) has been identified within the GYR region between amino acids 194 and 220 with amino acids 205 to 213 being highly conserved and required for nuclear transport.³ In vitro studies introducing point mutations into this NLS resulted in failure of these hnRNPs to shuttle from the cytoplasm to the nucleus, which is expected to compromise function.³

Individuals with missense variants affecting amino acids 206 to 208 appear to have a more severe clinical phenotype. This is probably because these variants are predicted to disrupt the NLS, thus

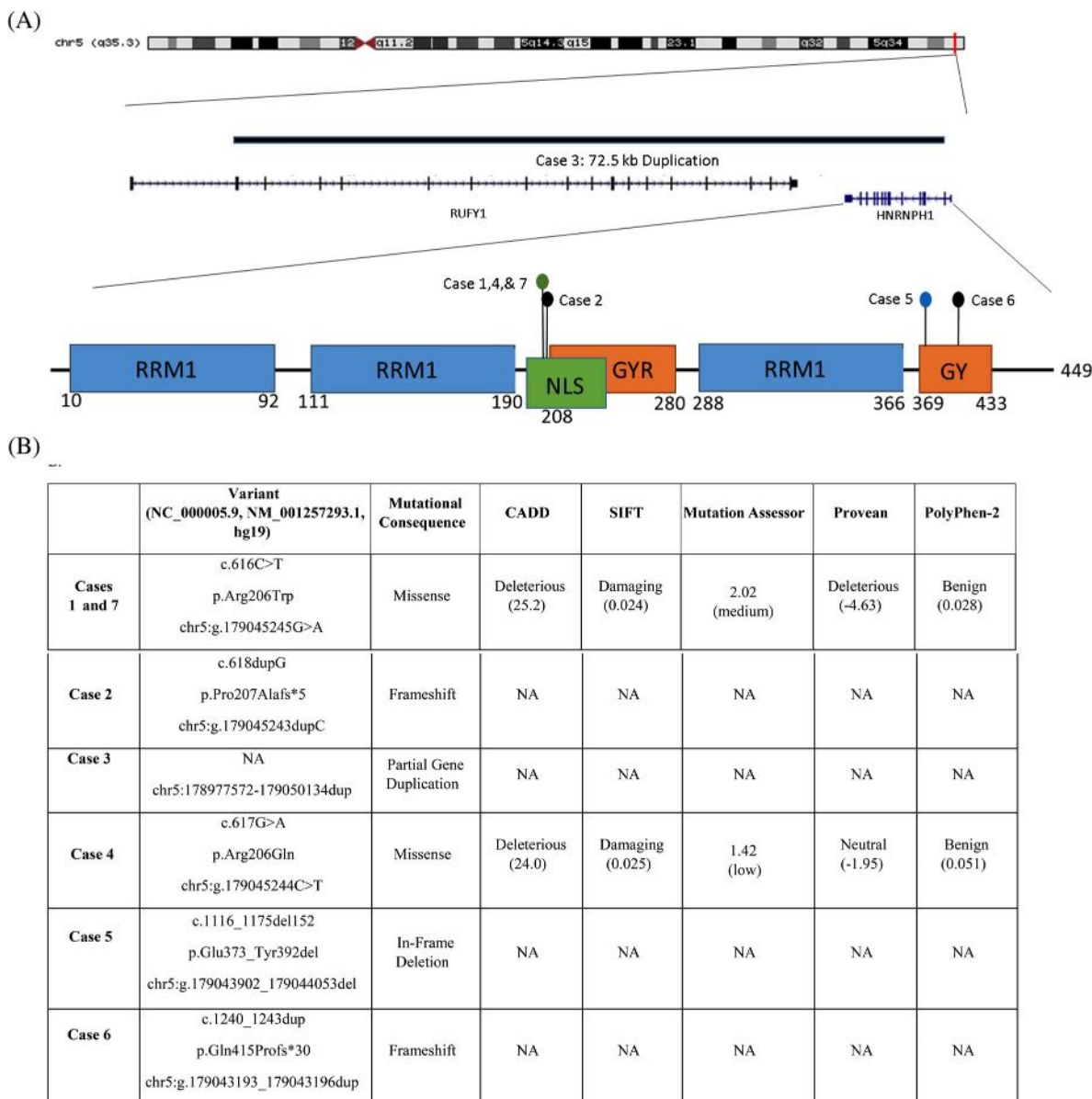


FIGURE 2 Characteristics of *HNRNPH1* pathogenic variants. A. Location of *HNRNPH1* pathogenic variants in the hnRNP H protein. B. Predicted pathogenicity and mutational consequence of *HNRNPH1* pathogenic variants [Colour figure can be viewed at wileyonlinelibrary.com]

impacting the overall function on the hnRNP H protein.^{6,11} Individuals observed with the recurrent c.616C>T and c.617G>A variants (Cases 1, 7, and 4) presented immediately following birth or prenatally with issues including microcephaly, respiratory distress, hypotonia, and congenital anomalies. This early-onset severe presentation further highlights the importance of the NLS sequence in the hnRNP H protein and suggests that disruption of this sequence has severe clinical consequences.

The two frameshift variants reported in this cohort, c.618dupG (p.P207fs) and c.1240_1243dup (p.Q415fs), are expected to result in either an abnormal, truncated protein or loss of protein from nonsense mediated mRNA decay. c.618dupG falls within the NLS and c.1240_1243dup in the GY domain. The discordant phenotypes of these two individuals with frameshift mutations may reflect the

severity of the frameshift on the overall protein structure. As c.618dupG (p.P207fs) lies within the NLS, it is predicted to produce a protein with a malfunctioning NLS. This supports the above suggestion that disruption of the NLS results in severe clinical consequences, as Case 2, found to have c.618dupG (p.P207fs), presented with hypotonia, respiratory distress, and congenital anomalies, similar to those with missense variants in the NLS. In contrast, Case 6, found to have c.1240_1243dup (p.Q415fs), has a less severe phenotype compared to cases 1, 2, 4, and 7. Case 6 did not come to medical attention in the neonatal period, is not noted to have microcephaly, and does not have palate abnormalities, short stature, or clinodactyly/syndactyly. Case 6 also has milder intellectual disability compared to other cases. Because c.1240_1243dup lies within the GY domain, it is predicted to impact the protein after the NLS, possibly resulting in an abnormal

protein that may have a functional NLS region, which may ameliorate the severity of the observed phenotype.

Of the remaining *HNRNPH1* variants, one falls in the GY domain, c.1116_1175del (p.Glu373-Tyr392del) (Case 5), and is expected to remove 19 amino acids. The function of the GY domain is not as well understood as the GYR domain, however it is thought to be important for protein-protein interactions and splicing.³ Thus, these pathogenic variants may have functional implications on protein/protein or protein/RNA interactions however it is difficult to say without additional functional studies. Case 5 has a less severe phenotype compared to those with pathogenic variants within the NLS, similar to Case 6 with a normal neonatal period, milder intellectual disability, and no microcephaly.

The final variant reported is an entire gene duplication of *HNRNPH1* and *RUFY1* (Case 3). This de novo 100.1 kb duplication was consistently identified by WES and whole genome sequencing (WGS) independently, with coordinates identified by three different CNV identification tools, ExomeDepth v1.1.10, XHMM and Conifer v0.2.2 (Figure S1). To confirm this duplication, a qPCR assay was run on fibroblasts from the proband and parents to confirm the de novo duplication (Figure S1). The *RUFY1* gene encodes the RUN and FYVE domain containing 1 protein, and is thought to be involved in early endosomal trafficking.¹³ To date, no human disease has been associated with the *RUFY1* gene. The impact of this *HNRNPH1* gene duplication on protein function is unclear, however given the overlap of features observed in other individuals with missense, frameshift, and small deletions within *HNRNPH1*, it is probably that it would result in abnormal hnRNP H function. It is also worth considering that a small rearrangement within the duplicated region cannot be ruled out, as it would go undetected by short read WES or WGS. Further functional studies are required to better understand the implications of this duplication on protein function. The clinical features of Case 3 are not as severe as those with pathogenic variants impacting the NLS, however they are more severe than those with pathogenic variants in the GY glycine rich domain. Specifically, Case 3 was found to have white matter and cerebellar abnormalities, dysmorphic features, short stature, genitourinary abnormalities, and microcephaly along with dysmorphic traits present in other reported cases. However, he has moderate intellectual disability, is verbal, and is ambulatory.

While limited due to a small number of individuals, these findings provide additional evidence that pathogenic variants in *HNRNPH1* cause a related, but unique syndrome from MRXSB. Given the observations presented in this report, genotype/phenotype correlation does appear to exist, because individuals with variants impacting the NLS have a more severe phenotype. Given the absence of predicted loss of function variants in healthy controls, haploinsufficiency is a probably pathogenic mechanism for variants in *HNRNPH1*. Future endeavors focusing on functional studies will provide insights into the pathological mechanisms of *HNRNPH1* variants.

Our findings suggest that pathogenic variants in *HNRNPH1* represent a related, but distinct, syndrome from MRXSB with unique dysmorphic features, increased incidence of congenital anomalies, and an increased incidence of ophthalmological abnormalities. Importantly,

identification of additional individuals with pathogenic *HNRNPH1* variants will continue to shape the observed phenotype and provide further insights into the potential genotype/phenotype correlation. While this represents a rare form of syndromic intellectual disability, given the severity observed in individuals with variants impacting the NLS, consideration of rapid-WES in critically ill newborns with microcephaly, congenital anomalies, and respiratory distress may identify pathogenic variants in *HNRNPH1*. Common features reported among the majority of individuals with *HNRNPH1* variants include short stature, microcephaly, intellectual disability, congenital anomalies, and dysmorphic features, specifically blepharophimosis, ptosis, hypotelorism, medial arched eyebrows, and micrognathia. We therefore propose that individuals with *HNRNPH1* pathogenic variants be described as having *HNRNPH1*-related syndromic intellectual disability.

ACKNOWLEDGEMENTS

We gratefully acknowledge all the individuals and their families. The work was funded by "Progetti di innovazione in ambito sanitario e socio sanitario Regione Lombardia, bando ex decreto n. 2713 del 28/02/2018" as part of the "GENE—Genomic analysis Evaluation NEtwork "project (MI). This work was supported by the Centre for Biomedical Research on Rare Diseases (CIBERER) [ACCI14-759], the URDCat program (PERIS SLT002/16/00174), the Hesperia Foundation and the Secretariat for Universities and Research of the Ministry of Business and Knowledge of the Government of Catalonia [2017SGR1206] to A.P. S.E. is a Wellcome Senior Investigator.

CONFLICTS OF INTEREST

There are no conflicts of interest to disclose among the authors included in the preparation and publication of this manuscript.

DATA AVAILABILITY STATEMENT

There are no other data associated with this manuscript.

ORCID

Sara C. Reichert  <https://orcid.org/0000-0002-0965-7506>

REFERENCES

1. Han SP, Tang YH, Smith R. Functional diversity of the hnRNPs: past, present and perspectives. *Biochem J.* 2010;430(3):379-392.
2. Honore B, Rasmussen HH, Vorum H, et al. Heterogeneous nuclear ribonucleoproteins H, H', and F are members of a ubiquitously expressed subfamily of related but distinct proteins encoded by genes mapping to different chromosomes. *J Biol Chem.* 1995;270(48):28780-28789.
3. Van Dusen CM, Yee L, McNally LM, McNally MT. A glycine-rich domain of hnRNP H/F promotes nucleocytoplasmic shuttling and nuclear import through an interaction with Transportin 1. *Mol Cell Biol.* 2010;30(10):2552-2562.
4. Geuens T, Bouhy D, Timmerman V. The hnRNP family: insights into their role in health and disease. *Hum Genet.* 2016;135(8):851-867.
5. Au PYB, You J, Caluseriu O, et al. GeneMatcher aids in the identification of a new malformation syndrome with intellectual disability.

- unique facial dysmorphisms, and skeletal and connective tissue abnormalities caused by *De novo* variants in HNRNPK. *Hum Mutat.* 2015;36(10):1009-1014.
6. Bain Jennifer M, Cho Megan T, Telegrafi A, et al. Variants in HNRNPH2 on the X chromosome are associated with a neurodevelopmental disorder in females. *Am J Hum Genet.* 2016;99(3):728-734.
 7. Bramswig NC, Lüdecke H-J, Hamdan FF, et al. Heterozygous HNRNPU variants cause early onset epilepsy and severe intellectual disability. *Hum Genet.* 2017;136(7):821-834.
 8. Harmsen S, Buchert R, Mayatepek E, Haack TB, Distelmaier F. Bain type of X-linked syndromic mental retardation in boys. *Clin Genet.* 2019;95(6):734-735.
 9. Jepsen WM, Ramsey K, Szelinger S, et al. Two additional males with X-linked, syndromic mental retardation carry *de novo* mutations in HNRNPH2. *Clin Genet.* 2019;96(2):183-185.
 10. Somashekar PH, Narayanan DL, Jagadeesh S, et al. Bain type of X-linked syndromic mental retardation in a male with a pathogenic variant in HNRNPH2. *Am J Med Genet A.* 2020;182(1):183-188.
 11. Pilch J, Koppolu AA, Walczak A, et al. Evidence for HNRNPH1 being another gene for Bain type syndromic mental retardation. *Clin Genet.* 2018;94(3-4):381-385.
 12. Sobreira N, Schiettecatte F, Valle D, Hamosh A. GeneMatcher: a matching tool for connecting investigators with an interest in the same gene. *Hum Mutat.* 2015;36(10):928-930.
 13. Yang J, Kim O, Wu J, Qiu Y. Interaction between tyrosine kinase Etk and a RUN domain- and FYVE domain-containing protein RUFY1: a possible role of Etk in regulation of vesicle trafficking. *J Biol Chem.* 2002;277(33):30219-30226.

SUPPORTING INFORMATION

Additional supporting information may be found online in the Supporting Information section at the end of this article.

How to cite this article: Reichert SC, Li R, A. Turner S, et al. HNRNPH1-related syndromic intellectual disability: Seven additional cases suggestive of a distinct syndromic neurodevelopmental syndrome. *Clin Genet.* 2020;98:91-98.
<https://doi.org/10.1111/cge.13765>

RESEARCH ARTICLE

A novel hypomorphic splice variant in EIF2B5 gene is associated with mild ovarioleukodystrophy

Agustí Rodríguez-Palmero^{1,2} , Agatha Schlüter^{1,3} , Edgard Verdura^{1,3} , Montserrat Ruiz^{1,3} , Juan José Martínez^{1,3}, Isabelle Gourlaouen^{4,5}, Chandran Ka^{4,5,6}, Ricardo Lobato⁷, Carlos Casasnovas^{1,3,8} , Gérald Le Gac^{4,5,6,9} , Stéphane Fourcade^{1,3} & Aurora Pujol^{1,3,10} 

¹Neurometabolic Diseases Laboratory, Bellvitge Biomedical Research Institute (IDIBELL), L'Hospitalet de Llobregat, 08908, Spain

²Pediatrics Department, University Hospital Germans Trias i Pujol, Badalona, 08916, Spain

³Center for Biomedical Research on Rare Diseases (CIBERER), ISCIII, Madrid, Spain

⁴INSERM U1078, Brest, France

⁵Laboratory of Excellence GR-Ex, Paris, France

⁶Laboratoire de Génétique Moléculaire et Histocompatibilité, CHRU de Brest, Hôpital Morvan, Brest, France

⁷Neurology Department, Hospital Universitario Infanta Sofía, San Sebastián de los Reyes, 28703, Spain

⁸Neuromuscular Unit, Neurology Department, Hospital Universitari de Bellvitge, L'Hospitalet de Llobregat, 08908, Spain

⁹Université Bretagne Loire, Université de Bretagne Occidentale, IBSAM, Brest, France

¹⁰Catalan Institution of Research and Advanced Studies (ICREA), Barcelona, Spain

Correspondence

Aurora Pujol, Neurometabolic Diseases
Laboratory, IDIBELL, Hospital Duran i Reynals,
Gran Via 199, 08908 L'Hospitalet de
Llobregat, Barcelona, Spain. Tel: +34
932607137; Fax: +34 932607414; E-mail:
apujol@idibell.cat

Funding Information

This study was supported by grants from the Hesperia Foundation, the Asociación Española contra las Leucodistrofias (ALE-ELA España), the Autonomous Government of Catalonia [SGR 2014SGR1430, 2017SGR1206], the PERIS Program [SLT002/16/00174] from the the Autonomous Government of Catalonia and the Center for Biomedical Research on Rare Diseases (CIBERER) [ACCI19-759] to A.P. This study has been funded by the Marató de TV3 [345/C/2014] as well as by Instituto de Salud Carlos III through the projects [FIS PI14/00581] to C.C. (Co-funded by European Regional Development Fund. ERDF, a way to build Europe), [Miguel Servet Program CPII16/00016 (Co-funded by European Social Fund. ESF investing in your future)] to S.F., [Sara Borrell program, CD19/00221 (Co-funded by European Social Fund. ESF investing in your future)] to E.V., and the Center for Biomedical Research on Rare Diseases (CIBERER) to M.R. CIBERER ER20P2AC759/2020, substituting the current CIBERER grant

Abstract

Objective: To identify the genetic cause in an adult ovarioleukodystrophy patient resistant to diagnosis. **Methods:** We applied whole-exome sequencing (WES) to a vanishing white matter disease patient associated with premature ovarian failure at 26 years of age. We functionally tested an intronic variant by RT-PCR on patient's peripheral blood mononuclear cells (PBMC) and by minigene splicing assay. **Results:** WES analysis identified two novel variants in the *EIF2B5* gene: c.725A > G (p.Tyr242Cys) and an intronic noncanonical mutation (c.1156 + 13G>A). This intronic mutation resulted into generation of various isoforms both in patient's PBMC and in the minigene splicing assay, showing that ~20% residual wild-type isoform is still expressed by the intronic-mutated allele alone, concordant with an hypomorphic effect of this variant. **Conclusion:** We report two novel variants in *EIF2B5*, one of them a noncanonical intronic splice variant, located at a +13 intronic position. This position is mutated only in 0.05% of ClinVar intronic mutations described so far. Furthermore, we illustrate how minigene splicing assay may be advantageous when validating splice-altering variants, in this case highlighting the coexistence of wild-type and mutated forms, probably explaining this patient's milder, late-onset phenotype.

Received: 5 June 2020; Accepted: 27 June 2020

doi: 10.1002/acn3.51131

Introduction

Vanishing white matter disease (VWMD; OMIM #603896) is a leukodystrophy caused by recessive mutations in any of the five genes encoding subunits of translation initiation factor EIF2B. Manifestations usually start between late infancy and early childhood, and mainly consist of pyramidal and cerebellar signs with mental decline and episodes of acute deterioration following stressors. However, 15% of cases are adult-onset forms associated with a more benign course and fewer decompressions.¹ Infrequently, VWMD can appear associated with premature ovarian failure (POF), a clinical syndrome that has been called ovarioleukodystrophy.² Although *EIF2B1-5* mutations are the main cause of leukodystrophy with POF, other genes have been described.³

More than 120 mutations have been reported in >250 patients with an EIF2B-related disorder, mostly in *EIF2B5* and *EIF2B2*.⁴ No mutational hotspots have been found, although some recurrent mutations seem to occur in paired cytosine/guanine (CpG) dinucleotides. The vast majority of pathogenic mutations are missense, whereas truncating mutations (frameshifts, nonsense, splice site mutations) are rare and have been reported only in compound-heterozygous state,⁵ indicating that total loss of function may be incompatible with life.

Here, we report a patient with an adult-onset ovarioleukodystrophy carrying two novel disease-causing variants in *EIF2B5* identified by WES, one of which is an intronic mutation leading to activation of a cryptic splice donor site. The impact of this rare, noncanonical splice variant on *EIF2B5* pre-mRNA processing was evaluated both in cDNA from patient's PBMC, and using minigene splicing reporter assays. These experiments revealed residual wild-type splicing, probably accounting for the mild late-onset clinical phenotype in this patient.

Methods

Participant and ethics

Blood was processed by centrifugation within 2 h of collection using a gradient of Histopaque to separate plasma, erythrocytes, and PBMC. Plasma and PBMC were stored at -80°C. The use of all samples was approved by the Clinical Research Ethics Committee of the Bellvitge University Hospital (PR076/14). Informed written consent was obtained from all patients and control individuals.

Exome sequencing and variant calling

In-solution exome capture was performed using the Seq-Cap EZ Human Exome Kit v3.0 (Roche Nimblegen,

USA) with 100-bp paired-end read sequences generated on a HiSeq2000 (Illumina, Inc. USA) in the Centro Nacional de Análisis Genómico in Barcelona (CNAG). Sequence processing was carried out with BWA aligner, the Genome Analysis Toolkit (GATK), SAMtools, and Picard Tools as previously described.⁶

More information regarding methods are detailed in the Data S1.

Results

Clinical findings

A 26-year-old woman was referred to the neurology department because of a leukoencephalopathy detected during the study of amenorrhea with hyperprolactinemia (108 ng/mL). She was born from nonconsanguineous parents and she had one asymptomatic sister. Physical exam showed right hand clumsiness, dystonic left foot postures, and generalized hyperreflexia in absence of cognitive, behavior or psychiatric symptoms. MRI evidenced T2 periventricular and pontine white matter hyperintensities with malacic areas in the frontal and atrial horns. Cortical-subcortical, spinal, and corpus callosum atrophy were also reported (Fig. 1A). Magnetic resonance spectroscopy was unremarkable. In the next 5 years, she developed unsteady gait, more evident pyramidal signs and lower limb paresthesia and cramps. Her cognitive level remained normal and she did not develop seizures. MRI performed four years after the initial one did not show significant changes. Routine hematology and clinical chemistry tests, as well as thyroid and adrenal function, were normal. Nerve conduction tests and electromyography were normal, whereas visual-evoked potentials showed bilateral latency enlargement of the P100 wave and somatosensory-evoked potentials exhibited bilaterally prolonged latencies with normal amplitudes.

WES analysis

Whole-exome sequencing (WES) revealed two suspicious novel variants in *EIF2B5*. The first one is a missense variant (NM_003907:c.725A > G; p.Tyr242Cys) referenced in dbSNP database as rs750767613, and has a frequency of 3,98.10e-6 in gnomAD database, with 0 homozygotes. This ultrarare missense mutation alters a highly conserved residue, and is predicted to be damaging by SIFT and PolyPhen-2. The second variant is intronic (NM_003907: c.1156 + 13G>A) and is predicted by different algorithms to increase the use of a cryptic donor splice site located at positions + 11/+12 (NNSplice, MaxEntScan, FS splice). Conversely, Human Splicing Finder and SpliceView did not predict a significant impact on splicing (Table S1).

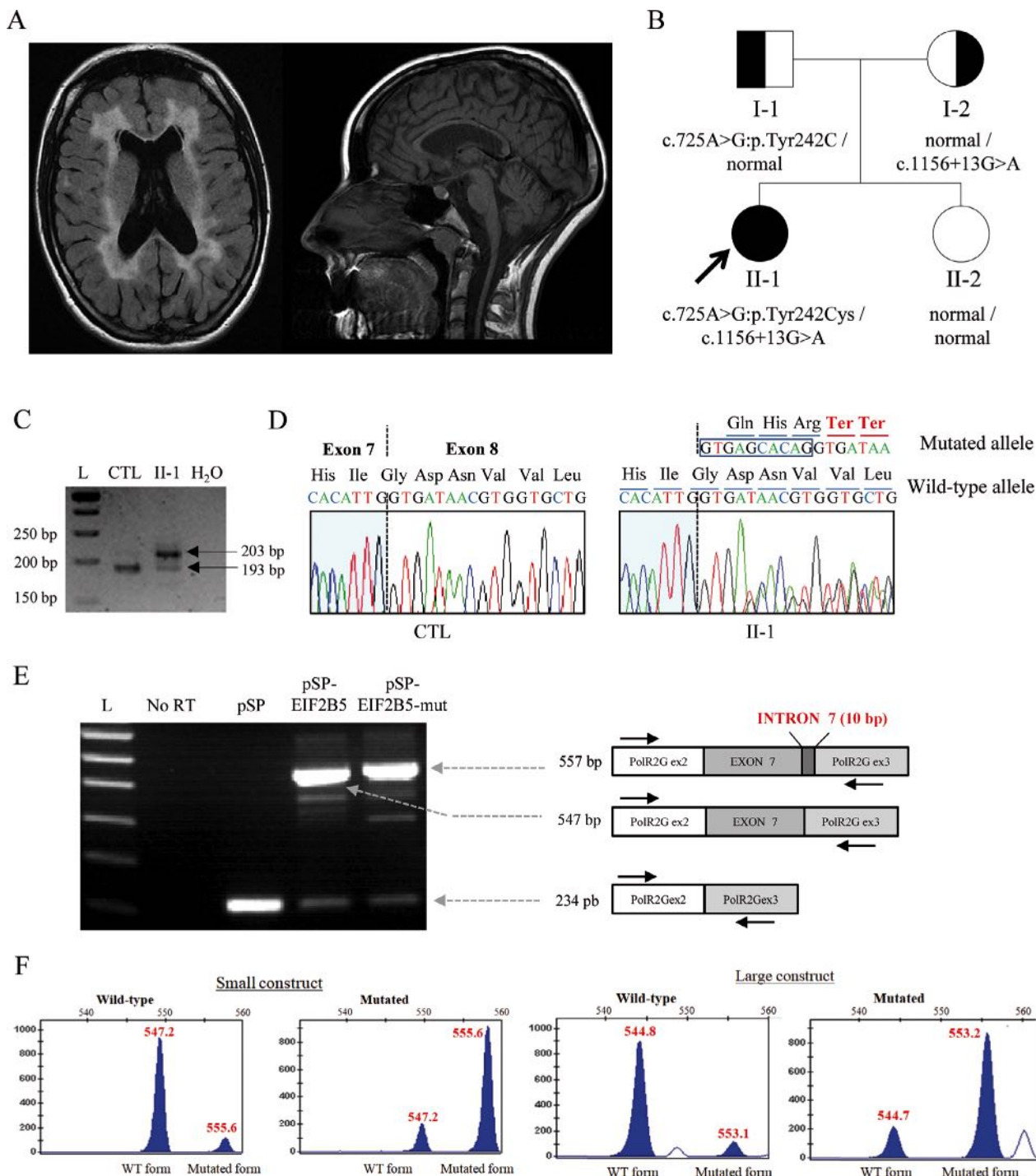


Figure 1. Clinical and genetic features. (A) Periventricular T2 white matter hyperintensities with small areas of cystic degeneration, and corpus callosum and mild cerebellar atrophy. (B) Family tree and cosegregation analysis of *EIF2B5* variants. (C) PCR amplified products of cDNA from II-1 and a healthy individual (CTL) resolved on a 4% agarose gel. L: Ladder (GeneRuler 50bp DNA ladder). (D) Partial sequence chromatograms of cDNA from CTL and II-1. Nucleotide and amino acid sequences of normal and mutated alleles are written above of each chromatogram. (E) RT-PCR from transfected HEK 293T17 and sequencing profiles of the products with retention of intron 7. Arrows indicate the relative positions of forward and reverse primers; the different constructs and sizes obtained are mentioned in the figure. L: Ladder; No RT: No Reverse Transcriptase; pSP: pSplicePOLR2G vector alone, pSP-*EIF2B5*: WT *EIF2B5* cloned into pSP and pSP-*EIF2B5*-mut: intronic variant of *EIF2B5* cloned into pSP. (F) Capillary electrophoresis of fluorescent RT-PCR products from wild-type and derived mutant minigenes, for the short and large constructs.

This variant is absent from gnomAD database. Cosegregation analysis revealed that the patient inherited these variants in *trans* (Fig. 1B). Despite their rare frequency, cosegregation, conservation of affected amino acids, *in silico* predictions for missense and splicing variants, and the patient's highly concordant phenotype, these variants were classified as variants of unknown significance (VUS) according to the ACMG/AMP (American College of Medical Genetics and Genomics) guidelines for variant evaluation.^{7,8}

In silico analysis of previously reported splicing variants

So far, 11998 single-nucleotide variants probably affecting splicing and considered as pathogenic or likely pathogenic are listed in the ClinVar database. Splice-site mutations are most commonly detected at the G(+1), T(+2), G(+5), A(-2), G(-1) canonical sequences of introns, as shown in Figure S1: +1 (4273 hits), -1 (2484), -2 (2181), +2 (1429), and +5 (551). Frequencies then decrease dramatically as distance from the acceptor/donor splice site increases. Only two variants have been reported in position +13: the A > G transition in intron 10 of the *MAPT* gene, associated with familial frontotemporal dementia with parkinsonism,⁹ and the C > T transition in *FGB* gene's intron 6, associated with congenital afibrinogenemia.¹⁰

Functional assays

Given c.1156 + 13G>A variant's absence from databases and the discordant results of splicing predictors, we evaluated the functional significance of this variant *in vitro*. Reverse-transcription PCR encompassing exons 7-8 of the *EIF2B5* mRNA produced a single 193 bp product from the control samples, whereas two bands (193 and 203 bp) were observed in the patient's sample. Sanger sequencing showed that the longest product included the first 10 nucleotides of intron 7. This 10-bp insertion creates two adjacent premature termination codons (TGA and TAA), leading to a truncated protein (Fig. 1C and D). To confirm the association between the c.1156 + 13G>A *EIF2B5* variant and partial retention of intron 7, we performed a minigene splicing assay. This technique consists of the construction of an expression vector containing a minimal gene fragment encompassing the variant sequence of interest along with flanking intronic sequences, and then is transfected into cultured cells in order to evaluate splicing patterns.^{11,12} This strategy allowed us to study the monoallelic effect of this *EIF2B5* variant compared to a wild-type situation, and to evaluate more precisely the influence of the G > A change on the use of the identified

donor cryptic splicing site. Two splicing reporter vectors were constructed in the background of the pSplice-POLR2G plasmid¹³: a small construction containing *EIF2B5*'s exon 7 and flanking intronic sequences (143 bp of intron 6202 bp of intron 7), and a large construction encompassing *EIF2B5*'s exons 7 and 8 and the whole intron 7 sequence. Both vectors, with either the wild-type or the mutated sequence, were transfected into HEK293T/17, U-251MG, and COS-7 cell lines. Results obtained from the smaller pSplicePOLR2G-*EIF2B5* construct in HEK293T cells show that the 10 intronic bp insertion was mainly, but not only, observed with the mutated c.1156 + 13G>A allele (Fig. 1E). Similar results were observed in U-251MG and COS7 cells (Fig. S2A-C). Semi-quantitative fluorescent RT-PCR revealed a normal/abnormal-splicing ratio of 0.9 for the wild-type allele and 0.2 for the mutated allele (547 bp peak area/557 bp peak area) (Fig. 1F). Similar results were obtained from the larger pSplice-POLR2G-*EIF2B5* construct. These results indicate that: (1) a cryptic donor splicing site is active in *EIF2B5* intron 7 and is moderately used by the splicing machinery in different cell types; and (2) this cryptic splicing site is significantly more active in the c.1156 + 13G>A *EIF2B5* pre-mRNA where it overcomes use of natural donor's splicing site.

In conclusion, we have identified a new intronic variant in the *EIF2B5* gene which activates acryptic 5' donor splice site of intron 7, probably leading to synthesis of a truncated protein (if not degraded by nonsense-mediated mRNA decay). This splicing variant is hypomorphic, as it leads to a residual 20% of WT splicing, and should be considered pathogenic after applying the ACMG criteria.^{7,8} In consequence, as VUS missense variant p.Tyr242Cys is *in trans* with the pathogenic intronic variant, this missense is reclassified as Likely Pathogenic^{7,8} and our case is solved.

Discussion

Splicing mutations represent approximately one-third of disease-causing mutations, most of them occurring in conserved consensus splice sites.¹⁴ However, the widespread use of high throughput technologies has increased the detection of variants in cryptic splice sites, which represent around 10% of total splicing mutations according to ClinVar data. In these cases, functional analysis is mandatory to confirm variant's pathogenicity since, as in the case here reported, splicing predictors may provide discordant results. Our case also underscores the importance of thorough clinical evaluation guiding the bioinformatic analysis, to uncover variants in intronic regions. As incomplete coverage of intron-exon boundaries in WES

studies may hamper detection of intronic variants, WGS may still be required to unravel some cases.

To the best of our knowledge, only four splicing variants have been reported in *EIF2B* genes so far,^{15–18} of which only one is noncanonical, although it was not functionally validated.¹⁵ Thus, our work is the first functional validation report of a novel, noncanonical splicing mutation in *EIF2B5* associated with ovarioleukodystrophy. In this case, the c.1156 + 13G>A hypomorphic mutation generates a novel splice site 10 bp beyond, that competes with the wild-type splicing donor site, therefore generating two coexisting populations of transcripts, the mutated, and the WT form. Our work has benefited from the capacity of the minigene assay to quantify the mRNA production in an allele-specific manner. Indeed, minigene splicing assays have several advantages, such as: (1) circumventing use of patient's RNA if sample is not available; (2) analysis and quantification of the splicing outcome of mutant alleles without interference of the wild-type allele; (3) high reproducibility of results; and (4) testing of variants located in any human disease gene, independently of gene expression. This approach allowed us to observe that the cryptic splice site activated by c.1156 + 13G>A is moderately functional in the wild-type allele, and also that the mutated allele expresses a residual amount of wild-type mRNA. Competition between the wild-type and the cryptic splice donor site could determine the expression of some degree of functional *EIF2B5* protein and consequently, the mild phenotype exhibited by the patient. Our finding of a partial mis-splicing is important in view of potential therapies since modulation of splice processes represents a therapeutic approach for some genetic diseases.¹⁹

Even if ovarioleukodystrophy seems to be an infrequent cause of pure premature ovarian failure (POF),²⁰ identification of hyperprolactinemia or amenorrhea should prompt both an exhaustive neurological examination and, possibly, the performance of a cranial MRI. If clinical and neuroimaging studies are suggestive, WES or even WGS are recommended to detect intronic mutations in *EIF2B* genes that could be responsible for mild phenotypes.

Acknowledgments

We thank CERCA Program / Generalitat de Catalunya for institutional support. We thank Peio Aristu, Cristina Guilera, and Laia Grau for technical assistance.

Conflict of Interest

The authors declare that this article was conducted in the absence of any commercial or financial relationships that could be construed as a potential conflict of interest.

References

- Hamilton EMC, van der Lei HDW, Vermeulen G, et al. Natural history of vanishing white matter. *Ann Neurol* 2018;84:274–288.
- Schiffmann R, Tedeschi G, Philip Kinkel R, et al. Leukodystrophy in patients with ovarian dysgenesis. *Ann Neurol* 1997;41:654–661.
- Dallabona C, Diodato D, Kevelam SH, et al. Novel (ovario) leukodystrophy related to AARS2 mutations. *Neurology* 2014;82:2063–2071.
- Maletkovic J, Schiffmann R, Gorospe RJ, et al. Genetic and clinical heterogeneity in eIF2B-related disorder. *J Child Neurol* 2008;23:205–215.
- Bugiani M, Boor I, Powers JM, et al. Leukoencephalopathy with vanishing white matter: a review. *J Neuropathol Exp Neurol* 2010;69:987–996.
- Pant DC, Boespflug-tanguy O, Pujol A, et al. Loss of the sphingolipid desaturase DEGS1 causes hypomyelinating leukodystrophy graphical abstract find the latest version. *J Clin Invest* 2019;129:1240–1256.
- Richards S, Aziz N, Bale S, et al. Standards and guidelines for the interpretation of sequence variants: a joint consensus recommendation of the American College of Medical Genetics and Genomics and the Association for Molecular Pathology. *Genet Med* 2015;17:405–424.
- Amendola LM, Jarvik GP, Leo MC, et al. Performance of ACMG-AMP variant-interpretation guidelines among nine laboratories in the clinical sequencing exploratory research consortium. *Am J Hum Genet* 2016;98:1067–1076.
- Hutton M, Lendon CL, Rizzu P, et al. Association of missense and 5'-splice-site mutations in tau with the inherited dementia FTDP-17. *Nature* 1998;393:702–705.
- Spena S, Duga S, Asselta R, et al. Congenital afibrinogenemia: First identification of splicing mutations in the fibrinogen Bβ-chain gene causing activation of cryptic splice sites. *Blood* 2002;100:4478–4484.
- Cooper TA. Use of minigene systems to dissect alternative splicing elements. *Methods* 2005;37:331–340.
- Gaildrat P, Killian A, Martins A, et al. Use of splicing reporter minigene assay to evaluate the effect on splicing of unclassified genetic variants. *Methods Mol Biol* 2010;653:249–257.
- Callebaut I, Joubrel R, Pissard S, et al. Comprehensive functional annotation of 18 missense mutations found in suspected hemochromatosis type 4 patients. *Hum Mol Genet* 2014;23:4479–4490.
- Sibley CR, Blazquez L, Ule J. Lessons from non-canonical splicing. *Nat Rev Genet* 2016;17:407–421.
- Fogli A, Schiffmann R, Bertini E, et al. The effect of genotype on the natural history of eIF2B-related leukodystrophies. *Neurology* 2004;63:1509–1517.
- Horzinski L, Gonthier C, Rodriguez D, et al. Exon deletion in the non-catalytic domain of eIF2Bε due to a

- splice site mutation leads to infantile forms of CACH/VWM with severe decrease of eIF2B GEF activity. *Ann Hum Genet* 2008;72(Pt 3):410–415.
17. Liu R, Van Der Lei HDW, Wang X, et al. Severity of vanishing white matter disease does not correlate with deficits in eIF2B activity or the integrity of eIF2B complexes. *Hum Mutat* 2011;32:1036–1045.
 18. Pronk JC, Van Kollenburg B, Scheper GC, Van Der Knaap MS. Vanishing white matter disease: a review with focus on its genetics. *Ment Retard Dev Disabil Res Rev* 2006;12:123–128.
 19. Spitali P, Aartsma-Rus A. Splice modulating therapies for human disease. *Cell* 2012;148:1085–1088.
 20. Fogli A, Gauthier-Barichard F, Schiffmann R, et al. Screening for known mutations in EIF2B genes in a large

panel of patients with premature ovarian failure. *BMC Womens Health* 2004;4:8.

Supporting Information

Additional supporting information may be found online in the Supporting Information section at the end of the article.

Data S1. In silico splicing predictors for variant c.1156+13G>A.

Figure S1. Single-nucleotide splicing variants annotated in ClinVar.

Figure S2. Mini-gene splicing analysis of *EIF2B5* c.1156 + 13 G> A variant.

